CONTENTS

Section Page

1.0 SCOPE/GENERAL REQUIREMENTS 1-1 **1/B11**
1.1 INTRODUCTION 1-1 **1/B11**
1.2 SATELLITE POWER SYSTEM CONCEPTS 1-3 **1/B13**
1.2.1 History of Study 1-3 **1/B14**
1.2.2 NASA Reference Satellite Concept 1-12 **1/C9**
1.2.3 Rockwell Alternative Satellite Concept (March 1979) 1-15 **1/C12**
1.2.4 Rockwell Reference Ground Receiving Station . 1-17 **1/C14**
1.2.5 Rockwell Concept Approaches (June 1980) . . 1-17 **1/C14**
1.2.6 Satellite Concept Summaries 1-22 **1/D6**
1.3 TRANSPORTATION SYSTEM 1-34 **1/E9**
1.4 PROGRAM GROUND RULES 1-35 **1/E10**
2.0 SYSTEM DESCRIPTION 2-1 **1/E11**
2.1 GENERAL 2-1 **1/E11**
2.1.1 System 2-1 **1/E11**
2.2 SATELLITE 2-9 **1/F7**
2.2.1 Reference System Definition 2-9 **1/F7**
2.2.2 Magnetron System Definition 2-16 **1/G1**
2.2.3 Solid State System Concepts 2-16 **1/G1**
2.3 GROUND RECEIVING STATION 2-26 **2/A3**
2.3.1 Introduction 2-26 **2/A3**
2.3.2 Rectenna 2-28 **2/A5**
2.3.3 Power Distribution 2-28 **2/A5**
2.4 OPERATIONS AND MAINTENANCE 2-29 **2/A6**
2.4.1 Satellite Operations 2-29 **2/A6**
2.4.2 Satellite Maintenance 2-46 **2/B9**
2.5 MASS PROPERTIES 2-51 **2/B14**
3.0 SUBSYSTEMS 3-1 **2/C2**
3.1 SATELLITE 3-1 **2/C2**
3.1.1 Introduction 3-1 **2/C2**
3.1.2 Power Generation 3-2 **2/C3**
3.1.3 Power Distribution 3-30 **2/E8**
3.1.4 Microwave Power Transmission 3-41 **2/F8**
3.1.5 Structure 3-84 **3/B12**
3.1.6 Attitude Control and Stationkeeping Subsystem . 3-101 **3/D3**
3.1.7 Thermal Control 3-112 **3/D14**
3.1.8 Communications and Data Management 3-131 **3/F6**
3.2 GROUND RECEIVING STATION 3-141 **3/G7**
3.2.1 Introduction 3-141 **3/G7**
3.2.2 Rectenna 3-141 **3/G7**
3.2.3 Power Distribution 3-150 **4/A4**
4.0 SUPPORT SYSTEMS 4-1 **4/A5**
4.1 GEO OPERATIONAL BASE 4-1 **4/A5**
4.2 MAINTENANCE AND REFURBISHMENT FACILITY 4-1 **4/A5**

Section Page

4.3 SPS TRANSPORTATION SYSTEM REQUIREMENTS (PRELIMINARY) . 4-1 **4/A5**
  4.3.1 Configuration and Mission Requirements . . 4-1 **4/A5**
  4.3.2 Heavy Launch Lift Vehicle(s) Requirements . . 4-2 **4/A6**
  4.3.3 Cargo Transfer Vehicle (COTV) 4-5 **4/A9**
  4.3.4 Personnel Orbital Transfer Vehicle (POTV) . . 4-6 **4/A10**
  4.3.5 Personnel Module (PM) 4-7 **4/A11**

MAY 2 0 1981

Item 830-H-14

NAS 1.26: 3399

ORIGINAL

COMPLETED

NASA Contractor Report 3399

Satellite Power Systems (SPS) Concept Definition Study (Exhibit D)

Volume VII - System/Subsystems Requirements Databook

G. M. Hanley

CONTRACT NAS8-32475
MARCH 1981

NASA

269

NASA Contractor Report 3399

Satellite Power Systems (SPS) Concept Definition Study (Exhibit D)

Volume VII - System/Subsystems Requirements Databook

G. M. Hanley
Rockwell International
Downey, California

Prepared for
Marshall Space Flight Center
under Contract NAS8-32475

National Aeronautics
and Space Administration

Scientific and Technical
Information Branch

1981

I

FOREWORD

Volume VII - *Systems/Subsystems Requirements Data Book*, of the SPS Concept Definition Study final report is submitted by Rockwell International through the Space Operations and Satellite Systems Division. All work was completed in response to NASA/MSFC Contract NAS8-32475, Exhibit D.

The SPS final report provides the NASA with additional information on the selection of a viable SPS concept, and furnishes a basis for subsequent technology advancement and verification activities. Other volumes of the final report are listed below.

Volume	Title
I	Executive Summary
II	Systems/Subsystems Analyses
III	Transportation Analyses
IV	Operations Analyses
V	Systems Engineering/Integration Analyses
VI	Cost and Programmatics

The SPS Program Manager, G. M. Hanley, may be contacted on any technical or management aspects of this report. He can be reached at 213/594-3911, Seal Beach, California.

BLANK PAGE

BLANK PAGE

CONTENTS

Section Page

1.0 SCOPE/GENERAL REQUIREMENTS 1-1
1.1 INTRODUCTION 1-1
1.2 SATELLITE POWER SYSTEM CONCEPTS 1-3
1.2.1 History of Study 1-3
1.2.2 NASA Reference Satellite Concept 1-12
1.2.3 Rockwell Alternative Satellite Concept (March 1979) 1-15
1.2.4 Rockwell Reference Ground Receiving Station . 1-17
1.2.5 Rockwell Concept Approaches (June 1980) . . 1-17
1.2.6 Satellite Concept Summaries 1-22
1.3 TRANSPORTATION SYSTEM 1-34
1.4 PROGRAM GROUND RULES 1-35
2.0 SYSTEM DESCRIPTION 2-1
2.1 GENERAL 2-1
2.1.1 System 2-1
2.2 SATELLITE 2-9
2.2.1 Reference System Definition 2-9
2.2.2 Magnetron System Definition 2-16
2.2.3 Solid State System Concepts 2-16
2.3 GROUND RECEIVING STATION 2-26
2.3.1 Introduction 2-26
2.3.2 Rectenna 2-28
2.3.3 Power Distribution 2-28
2.4 OPERATIONS AND MAINTENANCE 2-29
2.4.1 Satellite Operations 2-29
2.4.2 Satellite Maintenance 2-46
2.5 MASS PROPERTIES 2-51
3.0 SUBSYSTEMS 3-1
3.1 SATELLITE 3-1
3.1.1 Introduction 3-1
3.1.2 Power Generation 3-2
3.1.3 Power Distribution 3-30
3.1.4 Microwave Power Transmission 3-41
3.1.5 Structure 3-84
3.1.6 Attitude Control and Stationkeeping Subsystem . 3-101
3.1.7 Thermal Control 3-112
3.1.8 Communications and Data Management . . . 3-131
3.2 GROUND RECEIVING STATION 3-141
3.2.1 Introduction 3-141
3.2.2 Rectenna 3-141
3.2.3 Power Distribution 3-150
4.0 SUPPORT SYSTEMS 4-1
4.1 GEO OPERATIONAL BASE 4-1
4.2 MAINTENANCE AND REFURBISHMENT FACILITY 4-1

Section Page

4.3 SPS TRANSPORTATION SYSTEM REQUIREMENTS (PRELIMINARY) . 4-1
  4.3.1 Configuration and Mission Requirements . . 4-1
  4.3.2 Heavy Launch Lift Vehicle(s) Requirements . . 4-2
  4.3.3 Cargo Transfer Vehicle (COTV) 4-5
  4.3.4 Personnel Orbital Transfer Vehicle (POTV) . . 4-6
  4.3.5 Personnel Module (PM) 4-7

ILLUSTRATIONS

Figure Page

1.1-1 SPS Program Element Relationship . . . 1-2
1.1-2 Subsystem/Satellite System Relationship . . . 1-2
1.2-1 SPS Conceptual Configuration (November 1977) . . . 1-3
1.2-2 Solar Photovoltaic Satellite (CR-1) (November 1977) . . . 1-4
1.2-3 Solar Photovoltaic Satellite (CR-2) (November 1977) . . . 1-5
1.2-4 Solar Photovoltaic Satellite (CR-5) (November 1977) . . . 1-6
1.2-5 Solar Thermal Brayton (Boeing) 10 GW . . . 1-7
1.2-6 Solar Thermal—Rankine (November 1977) . . . 1-8
1.2-7 Nuclear—Brayton (November 1977) . . . 1-8
1.2-8 Solar Photovoltaic Satellite (CR-2) 5 GW (April 1978) . . . 1-11
1.2-9 Solar Thermal—Rankine (5 GW) (April 1978) . . . 1-12
1.2-10 Microwave Transmission Subsystem - Rectenna (April 1978) . . . 1-13
1.2-11 Rectenna Site Concept (April 1978) . . . 1-13
1.2-12 NASA Reference Configurations (October 1978) . . . 1-15
1.2-13 Alternate Satellite Concepts (March 1979) . . . 1-16
1.2-14 System Efficiency Chain (March 1979) . . . 1-18
1.2-15 Ground Receiving Station . . . 1-19
1.2-16 SPS Reference Configuration Single End-Mounted Tension Web Antenna—Klystron . . . 1-20
1.2-17 SPS Solid State Configuration—Dual End Mounted Antenna . . . 1-20
1.2-18 Solid-State Sandwich Satellite Point Design Concept . . . 1-21
1.2-19 System Efficient Chain—Reference Concept (April 1980) . . . 1-24
1.2-20 System Efficiency Chain Dual End-Mounted Concept (Solid State Antenna) (April 1980) . . . 1-27
1.2-21 System Efficiency Chain—Sandwich Concept (Solid-State Antenna) (April 1980) . . . 1-30
1.2-22 System Efficient Chain—Magnetron Concept (June 1980) . . . 1-32
1.3-1 SPS Transportation System—LEO Operations Operational Program . . . 1-34
2.1-1 SPS System Relationships . . . 2-2
2.1-2 Solar Power Satellite—Reference Configuration . . . 2-2
2.1-3 Solar Power Satellite Solid State Dual End Mounted Antenna . . . 2-3
2.1-4 Solid State Point Design Satellite Concept . . . 2-3
2.1-5 Ground Receiving Station Subassembly Relationships . . . 2-4
2.1-6 Operational Ground Receiving Facility (Rectenna) - Typical . . . 2-5
2.1-7 Eclipse Periods for Geosynchronous Circular Orbits . . . 2-7
2.1-8 Typical Photovoltaic Efficiency Chain . . . 2-8
2.2-1 Reference Configuration, Single End-Mounted Tension Web Antenna with Klystron Antenna . . . 2-10
2.2-2 Satellite Subsystems . . . 2-11
2.2-3 Subsystem IMCS Relationships . . . 2-12
2.2-4 Power Generation Subsystem . . . 2-12
2.2-5 Power Distribution Subsystem . . . 2-13
2.2-6 Microwave Transmission Subsystem . . . 2-14
2.2-7 Magnetron Satellite Power Distribution . . . 2-17

Figure Page

2.2-8 Magnetron Power Module Layout—Typical 2-18
2.2-9 Effect of Amplifier Efficiency on Antenna Power Density . 2-21
2.2-10 Dual SPS Solid-State Sandwich Satellite Concept . . . 2-22
2.2-11 Solar Power Satellite—PERSP Dual Solid-State Sandwich Configuration 2-23
2.3-1 Operational Ground Receiving Facility (Rectenna)—Typical . 2-28
2.3-2 Receiving Station Power Distribution Schematic—Preliminary. 2-29
2.4-1 SPS System 2-30
2.4-2 Ground Receiving Station—Rectenna Control Center Concept . 2-32
2.4-3 Area Control Center Concept 2-33
2.4-4 Manned Work Module, Free-Flying or Stationary 2-47
3.1-1 Total System 3-1
3.1-2 Simplified Integrated Block Diagram, Photovoltaic (CR-2) . 3-3
3.1-3 Assembly Tree—Power Generation 3-3
3.1-4 GaAs Solar Cell Blanket Cross Section 3-4
3.1-5 GaAs Solar Cell Voltage and Current Characteristics . . 3-4
3.1-6 Solar Array Dimensions and Panel Power Output 3-5
3.1-7 Radiation Dose Rates 3-6
3.1-8 Type-H Kapton 3-7
3.1-9 Solar Cell Damage Equivalent 1-MeV Electron Fluence Vs. Shield Density 3-8
3.1-10 Normalized Maximum Power Vs. 1-MeV Electron Fluence . . 3-9
3.1-11 Solar Array Configuration—Typical Segment (1 of 30) . . 3-13
3.1-12 Schematic Representation of Stacked Multiple-Bandgap Solar Cell 3-15
3.1-13 Dual-Junction Multi-Bandgap Solar Cell Blanket Cross Section 3-16
3.1-14 Current Vs. Voltage for a Cascade Cell Optimized for 475°K, Two Suns 3-16
3.1-15 Current Vs. Voltage for a Cascade Cell Optimized for 45°K, Five Suns 3-17
3.1-16 GaAlAs/GaAs Solar Array Dimensions for Reference Concept . 3-18
3.1-17 Solid-State Sandwich Concept, Power Distribution System to RF Devices 3-19
3.1-18 Solar Proton Model Environment 3-24
3.1-19 Solar Cell Damage-Equivalent 1-MeV Electron Fluence Vs. Shield Density 3-25
3.1-20 Normalized Maximum Power Vs. 1-MeV Electron Fluence . . 3-26
3.1-21 Relative Damage Coefficients for Space Proton Irradiation (Pmax) 3-27
3.1-22 Aluminum Spectral Reflectance Data 3-28
3.1-23 PDS Assembly Tree 3-31
3.1-24 Simplified Power Distribution System—Klystron 3-33
3.1-25 Simplified Power Distribution System—Magnetron . . . 3-34
3.1-26 Microwave Antenna—Power Distribution 3-38
3.1-27 Microwave Antenna Structure Selected Design Concept . . 3-42
3.1-28 Radiating Face of Power Module 3-43
3.1-29 Standard Subarray Size - Block 1 3-43
3.1-30 Standard Subarray Size - Block 2 3-44
3.1-31 Standard Subarray Size - Block 3 3-44

Figure Page

3.1-32 Gaussian Beam Microwave Antenna 3-45
3.1-33 Pattern Efficiency for Uniform Illumination (10 dB Taper) . 3-46
3.1-34 Klystron Power Module Waveguide Assembly 3-46
3.1-35 Collector Radiator 3-47
3.1-36 Microwave Antenna—Beam Generation and Control 3-49
3.1-37 Phase Conjugating Electronics 3-50
3.1-38 Monopulse Receiver 3-50
3.1-39 Array Reference Signal Distribution System 3-51
3.1-40 Reference Phase Distribution Servo 3-52
3.1-41 Electronic Servo Loop to Hold Feeder at Resonance . . . 3-53
3.1-42 Pilot Signal Regeneration Circuit 3-54
3.1-43 End-Mounted Antenna with Dipoles Over Ground Plane . . . 3-56
3.1-44 Spacetenna Total View (Bottom) 3-56
3.1-45 Spacetenna Total View (Top) 3-57
3.1-46 Mechanical Module Layout (Solid-State End-Mounted) . . . 3-58
3.1-47 Antenna Feeder Diagram (Solid-State End-Mounted) . . . 3-58
3.1-48 Dipole Amplifier Panel Configuration Solid-State End-Mounted (Preliminary) 3-59
3.1-49 Dipole Amplifier Assembly—Exploded View Solid-State End-Mounted (Preliminary) 3-59
3.1-50 Phase Reference Signal Distribution System 3-61
3.1-51 Reference Signal Control Loop 3-61
3.1-52 Pilot Beam Ground System Layout 3-63
3.1-53 Alternative Solid State Sandwich Concepts 3-64
3.1-54 Solid State Sandwich Concepts 3-65
3.1-55 Satellite Sandwich Solar Cell Configuration (Preliminary) . 3-68
3.1-56 Satellite Sandwich Antenna/Solar Cell Panel Configuration (Preliminary) 3-68
3.1-57 Dual Satellite Antenna/Solar Cell Panel Configuration Exploded View 3-69
3.1-58 Solid State Sandwich Concept—Stripline Corporate Feed System (Partial) (Preliminary) 3-69
3.1-59 High Power Density Power Module for Array Center . . . 3-72
3.1-60 Sectional View of Type 1 High Power Density Module . . . 3-72
3.1-61 Type 3, Lower Power Density Module 3-73
3.1-62 Two Examples of Subarray Formation (Type 6 at Left, Type 9 at Right) 3-75
3.1-63 Nine-Step Approximation to Hansen Aperture Distribution Truncated at -9.54 dB 3-76
3.1-64 Typical Magnetron Mounted on WR340 Waveguide 3-77
3.1-65 Primary Structure Evolution 3-84
3.1-66 End-Mounted Antenna/Yoke—Cross-Section 3-Trough Configuration 3-86
3.1-67 Slip Ring Structure Independent Fabrication 3-87
3.1-68 Reference Configuration Attach Fittings 3-88
3.1-69 Reference Configuration Details A and A' 3-88
3.1-70 Solar Power Satellite Sandwich Configuration, Deal Solar Reflectors 3-89
3.1-71 Primary Reflector Surface Compression Frame I 3-90
3.1-72 Primary Reflector Surface Compression Frame II 3-91

Figure Page

3.1-73 Secondary Reflector Surface Compression Frame III 3-91
3.1-74 Space Frame Antenna Configuration 3-92
3.1-75 Microwave Antenna Structure Design Condition 3-93
3.1-76 Analysis Model and Parameter Variations 3-95
3.1-77 Microwave Antenna Operational Scenario 3-96
3.1-78 Structural Analysis Methodology 3-97
3.1-79 Basic Frame/Array Loading Equations 3-97
3.1-80 Hexagon Frame Stability Considerations 3-98
3.1-81 Hexagonal Frame Comparison Stability Criteria 3-98
3.1-82 Hexagonal Frame Mass Variation (Size and Surface Deviation) 3-99
3.1-83 Hexagonal Frame Mass Vs. Surface Deviation Δ 3-99
3.1-84 Orbit Selection Trade 3-101
3.1-85 Solar Pressure Model 3-102
3.1-86 Some Alternative Configurations Considered 3-103
3.1-87 ACSS Equipment Locations 3-104
3.1-88 Attitude Control Propellant and Reaction Wheel Mass (Y-POP, X-IOP) 3-104
3.1-89 Control Bandwidth Requirement 3-107
3.1-90 Solid-State Concepts 3-108
3.1-91 Impact of Solar Pressure 3-109
3.1-92 Thruster Configuration 3-111
3.1-93 Photovoltaic Structure Model 3-113
3.1-94 Photovoltaic Structural Configuration Temperatures (Graphite Composite) 3-113
3.1-95 Power Distribution Component Thermal Control—Switch Gear 3-115
3.1-96 Antenna Frame/Web Model 3-116
3.1-97 Frame Temperature Variation with Solar Orientation (BOL) 3-117
3.1-98 Frame Temperature Variation with Solar Orientation (EOL) 3-117
3.1-99 Klystron Radiator Configuration (Rear Mounted 3-119
3.1-100 Related Design Configurations 3-120
3.1-101 Collector Radiator 3-120
3.1-102 Rear Surface Cavity Radiator Thermal Response 3-122
3.1-103 Power Distribution Component Thermal Control—HV Converters 3-122
3.1-104 Klystron Radiator Configuration—Radiation from Both Sides 3-123
3.1-105 Revised Thermal Profile—Klystron Antenna 3-123
3.1-106 Model for Thermal Analysis of Magnetron Heat Dissipation 3-124
3.1-107 End-Mounted Concept 3-126
3.1-108 Thermal Model for End-Mounted Concept 3-127
3.1-109 Sandwich Configuration 3-128
3.1-110 Thermal Model for Sandwich Configuration 3-129
3.1-111 SPS IMCS Top-Level Block Diagram 3-132
3.1-112 IMCS—MW Antenna 3-134
3.1-113 IMCS-Attitude Control 3-135
3.1-114 IMCS—Power Distribution (Solar Array and Yoke) 3-136
3.1-115 Assembly Tree—IMCS 3-137
3.2-1 Operational Ground Receiving Facility (Rectenna)—Typical 3-141
3.2-2 Rectenna Panel Assembly and Installation 3-143
3.2-3 Rectifier OPerating Proficiency 3-143
3.2-4 Rectenna Power Density Pattern (34°N Latitude) 3-144
3.2-5 Panel Alternative/Rectenna Concepts 3-146

Figure Page

3.2-6 Billboard Feed—Stripline 3-147
3.2-7 Cluster Interconnect 3-148
3.2-8 Rectenna Array Support Structure 3-149
3.2-9 Receiving Station Power Distribution Schematic—Preliminary. 3-150

TABLES

Table Page

1.2-1 Solar Photovoltaic Weight Summary (GaAlAs Solar Cells) (November 1977) 1-9
1.2-2 Solar Thermal Weight Summary (November 1977) 1-10
1.2-3 Nuclear Reactor Concept Weight Summary (November 1977) . . 1-10
1.2-4 Photovoltaic (CR-2) Satellite Mass Statement - Point Design (April 1978) 1-14
1.2-5 Solar Thermal Satellite Mass Statement - Point Design (April 1978) 1-14
1.2-6 NASA Reference Satellite Mass Properties (October 1978) . 1-16
1.2-7 Mass Properties—Rockwell Alternate Concepts (March 1979) . 1-19
1.2-8 Satellite System Summaries—Alternate Concepts (June 1980) . 1-23
1.2-9 Mass Properties—Reference Concept (April 1980) . . . 1-25
1.2-10 Recommended End Mounted Solid State Antenna Concept Characteristics 1-26
1.2-11 Mass Properties, Dual End-Mounted Solid-State Antenna . . 1-28
1.2-12 Nominal Characteristics of Sandwich Concepts 1-29
1.2-13 Mass Properties, Dual Sandwich Solid-State Antenna . . . 1-31
1.2-14 Mass Properties—Magnetron Antenna (April 1980) . . . 1-33
1.4-1 Program Ground Rules 1-35
1.4-2 General Requirements Describing Overall SPS Program . . 1-35
2.1-1 Point Design Solar Array Functional Requirements . . . 2-5
2.1-2 Point Design Solar Array Functional Requirements—Operations 2-6
2.2-1 Satellite Reference Design Summary (GaAs) 2-15
2.2-2 Magnetron Satellite Design Summary (GaAs) 2-19
2.2-3 Solid-State Sandwich (Dual) Design Summary 2-25
2.2-4 End-Mounted Solid-State Antenna Based Satellite Design Summary 2-27
2.4-1 Annual Spares Requirements for Each Satellite 2-49
2.5-1 Mass Properties Summary (May 1980) 2-52
3.1-1 Reflectivity 3-6
3.1-2 Solar Photovoltaic Power Conversion Mass (GaAs) . . . 3-10
3.1-3 GaAs Solar Cell and Blanket Design and Performance Characteristics 3-11
3.1-4 SPS Reflector Design and Performance Characteristics for Planar Configurations 3-12
3.1-5 SPS Reflector Design and Performance Characteristics for the Sandwich Configuration 3-12
3.1-6 Multi-Bandgap Solar Cell Technology Assessment 3-17
3.1-7 Solar Cell Voltage Characteristics 3-18
3.1-8 MBG Solar Cell and Blanket Preliminary Specification . . 3-20
3.1-9 SPS Reflector Preliminary Specification (Klystron or End-Mounted Solid State) 3-21
3.1-10 Efficiency Chain Comparison—Satellite Concepts . . . 3-22
3.1-11 Total 1-MeV Equivalent Fluence (e^-/cm^2)—30 Years . . . 3-25

Table Page

3.1-12 Temperature Limitation on GaAs Solar Cell 3-29
3.1-13 PDS Functional Requirements 3-31
3.1-14 Planar Array Power Distribution—Voltage and Power Summary 3-32
3.1-15 Power Distribution Interface Requirements 3-32
3.1-16 System Sizing 3-35
3.1-17 Slip Ring Design Characteristics 3-37
3.1-18 PDC Subsystem Mass Summary 3-40
3.1-19 Point Design Microwave Power Transmission System (MPTS) Satellite Antenna Characteristics 3-42
3.1-20 Klystron Mass Estimate 3-48
3.1-21 Mass Properties—Reference MWPT 3-54
3.1-22 End-Mounted Solid-State Concept Characteristics 3-55
3.1-23 Pilot System Link Budget 3-62
3.1-24 Pilot Ground System Summary 3-62
3.1-25 Mass Properties—Solid-State End-Mounted MW Electronics (Dual) 3-63
3.1-26 Solid State Sandwich Concept Comparison of 0 dB and 10 dB Antenna Power Taper 3-65
3.1-27 Recommended Solid-State Sandwich Concept Characteristics 3-66
3.1-28 Nominal Characteristics of Sandwich Concept 3-66
3.1-29 Preliminary Mass Properties of Recommended Solid-State Sandwich Concept ($CR_E = 5.2$) 3-67
3.1-30 Nine Basic Power Module/Panel Configurations 3-74
3.1-31 Spacetenna Characteristics 3-82
3.1-32 Rectenna Characteristics (Magnetron Transmitter) 3-82
3.1-33 Mass Breakdown for Subarrays 3-83
3.1-34 Mass Breakdown for Spacetenna 3-83
3.1-35 Solar Array and Rotary Joint Tribeam Girder Characteristics 3-85
3.1-36 Frame Structural Characteristics 3-90
3.1-37 Frame Buckling Coefficient, η^* (Variation with Ratio of GI/EI) 3-92
3.1-38 Antenna Structure Elements Physical and Mechanical Properties 3-94
3.1-39 Mass Properties—Structures 3-100
3.1-40 Stationkeeping Perturbation Sources 3-102
3.1-41 Attitude Control System Concept Comparison 3-105
3.1-42 ACSS Mass Summary 3-106
3.1-43 RCS Requirements 3-110
3.1-44 ACSS Mass Summary 3-112
3.1-45 Maximum Estimated Temperatures (Graphite Composite) 3-114
3.1-46 Reflector Thermo-Optical Properties 3-115
3.1-47 Reflector Predicted Temperatures 3-115
3.1-48 Space Frame Configuration Limitations of Low Temperature Composites 3-118
3.1-49 Collector Radiator Analysis 3-121
3.1-50 50-kW Klystron Radiator Thermal Levels 3-122
3.1-51 Results of Thermal Analysis 3-125
3.1-52 Thermal Calculation Assumptions 3-127
3.1-53 Maximum Microwave Output for End-Mounted Configuration 3-128
3.1-54 Sandwich Antenna Thermal Model Assumptions 3-130

Table Page

3.1-55 Node Temperatures and Energy Flow for Sandwich Configuration (GaAs Cells) 3-130
3.1-56 Node Temperature and Energy Flow for Sandwich Configuration (Multi-Bandgap Cells) 3-131
3.1-57 Preliminary Data Interface Summary—Photovoltaic (CR-2) Configuration 3-137
3.1-58 Preliminary Control Interface Summary—Photovoltaic (CR-2) Configuration 3-137
3.1-59 Hardware Summary—IMCS 3-139
3.1-60 Mass/Power/Volume Summary—IMCS 3-140
3.1-61 IMCS Mass Properties—Summary (Partial) 3-140
3.2-1 Ground Receiving Station Area Requirements 3-142
3.2-2 Billboard Summary 3-144
3.2-3 Polarization Characteristics 3-149

XVI

GLOSSARY

A	Ampere
Å	Angstrom
ac	Alternating current
ACSS	Attitude control and stationkeeping system
AMO	Air mass zero
ARDS	Attitude reference determination system

$\bar{B}$	Billions of dollars
B_eO	Beryllium oxide (Berlox)
BCD	Binary coded decimal
BCU	Bus control units
BOL	Beginning of life
BT	Battery tie contactor

°C	Degree centigrade
C_e	Cesium
cm	Centimeter
CMD	Command
COTV	Cargo orbital transfer vehicle
CPU	Central processing unit
CR	Concentration ratio
CR_E	Effective concentration ratio
CVD	Controlled vapor deposit

D/A	Digital to analog
dB	Decibel
dc	Direct current
DOE	Department of Energy
DVM	Digital voltmeter

EBS	Electron beam semiconductor
E_g	Bandgap energy
EMI	Electromagnetic interference
EOL	End of life
EOTV	Electric orbital transfer vehicle
EVA	Extra-vehicular activity
f	Frequency
°F	Degree Fahrenheit
FEP	Adhesive material
FET	Field-effect transistor
FOC	Final operational capability
f_p	Pilot frequency
f_r	Reference signal frequency
f_T	Transmitted frequency
G	Giga- (10^9)
G	Gear, switch
GaAlAs	Gallium aluminum arsenide
GaAs	Gallium arsenide
GEO	Geosynchronous, equatorial orbit
GHz	Gigahertz
GPS	Global Positioning System
GRS	Ground receiving station
GW	Gigawatt
HLLV	Heavy-lift launch vehicle
HPWB	Half-power-point beamwidth
HV	High voltage
Hz	Hertz
IB	Interface bus
IBM	International Business Machines Corp.
IMCS	Information management and control system
IMS	Information management system (see IMCS)

IOC	Initial operations capability
IOP	In-orbit plane
IOTV	Inter-orbit transfer vehicle
IUS	Inter-orbit utility stage
k	Kilo (10^3)
K	Potassium
°K	Degree Kelvin
km	Kilometer (1000 meters)
kN	Kilonewton
KSC	Kennedy Space Flight Center
kV	Kilovolts
LED	Light-emitting diode
LEO	Low earth orbit
LH_2	Liquid hydrogen
LOX	Liquid oxygen
LPE	Liquid phase epitaxal
LRB	Liquid rocket booster
LRU	Line replaceable unit
LSST	Large space structures technology
m	Meter
M	Mega- (10^6)
MBG	Multi-bandgap
MC-ABES	Multi-cycle airbreathing engine system
MeV	Millions of electron volts
μp	Microprocessor
MPCA	Master phase reference control amplifier
MPTS	Microwave power transmission system
MSFC	Marshall Space Flight Center
MTBF	Mean time between failure
MTTF	Mean time to failure
MW	Megawatt
MW	Microwave

MW_e	Megawatt—electrical
MWM	Manned work modules
MW_T	Megawatt—thermal
M_x	Disturbance torque along X-axis
N	Newton
NaK	Sodium-potassium
NASA	National Aeronautics and Space Administration
N-S	North-South
O&M	Operations and maintenance
OTV	Orbit transfer vehicle
PDS	Power distribution system
PLV	Personnel launch vehicle
PM	Personnel module
POP	Perpendicular to orbit plane
POTV	Personnel orbital transfer vehicle
psi	Pounds per square inch
RAC	Remote acquisition and control
R&D	Research and development
R&T	Research and technology
RCA	Radio Corporation of America
RCI	Replacement cost investment
RCR	Resonant cavity radiator
RCS	Reaction control system
RF	Radio frequency
RFI	Radio frequency interference
RTE	Real-time evaluation
S/A	Solar array
SCB	Space construction base
SG	Switch gear
Si	Silicon

SIT	Static induction transistor
SM	Sub-multiplexer
SOC	Space Operations Center
SPS	Satellite Power Systems
SRB	Solid rocket booster
STS	Space Transportation System
T	Temperature
TBD	To be determined
T&E	Test and evaluation
TFU	Theoretical first unit
TT&C	Telemetry, tracking, and communications
TWT	Traveling wave tubes
UI	Utility interface
V	Volt
VHF	Very high frequency
VSWR	Voltage standing wave ratio
VTO	Vertical take-off
W	Watt
Wh	Watt-hour
X,Y,Z	Coordinate axes of satellite

Symbols

ε	Error signals
λ	Wavelength of frequency f (Hertz)
μ	Micro-
η	Efficiency
ϕ	Phase
φ	Coordinate axis angle—Phi
θ	Coordinate axis (angle)—Theta

1.0 SCOPE/GENERAL REQUIREMENTS

1.1 INTRODUCTION

This volume of Satellite Power Systems (SPS) Concept Definition Study final report summarizes the basic requirements used as a guide to systems analysis and is a basis for the selection of candidate SPS point designs. Initially, these collected data reflected the level of definition resulting from the evaluation of a broad spectrum of SPS concepts. As the various concepts matured these requirements were updated to reflect the requirements identified for the projected satellite system/subsystem point designs. Earlier studies (reported in Volumes I—VII, SD 78-AP-0023, dated April 1978) established two candidate concepts which were presented to the NASA for consideration. NASA, in turn, utilizing these and other concepts developed under the auspices of other contracts, established a baseline or reference concept which was to be the basis for future evaluation and point design.

A revised Rockwell candidate was defined and reported in Volumes I—VI (SSD 79-0010, dated March 1979) at the end of the period specified in Exhibit C of contract NAS8-32475.

This volume presents an updated version of the March 1979 Rockwell concept utilizing Klystrons as the specific microwave power amplification approach as well as a more indepth definition, analysis and preliminary point design on two concepts based upon the use of advanced solid-state technology to accomplish the task of high power amplification of the 2.45 GHz transmitted power beam to the earth receiver. Finally, a preliminary definition of a concept utilizing magnetrons as the microwave power amplifiers is presented. Included are the preliminary identification of subsystem/system requirements, alternate configurations considered, in-depth discussions of the selected (recommended) alternatives as well as alternate approaches which may have potential for improved operation or fabrication/installation.

The rectenna system described in this document essentially remains the same as described at the conclusion of the Exhibit C activity although it was determined that variations due to alternate beam shaping techniques applied may cause a variation in the overall rectenna and ground receiving station dimensions. Where appropriate the alternate rectenna dimensions will be noted but the effects of the altered dimensions are not evaluated in detail.

Figure 1.1-1 establishes the relationship of the satellite system with the other elements of the SPS program.

Figure 1.1-2 identifies the various satellite subsystems and the functions that may apply on the satellite. Equivalent functions are applicable to the ground receiving station (rectenna) system and will not be expanded here. A limited discussion of ground receiving station subsystem functions will be found in Section 3.4.

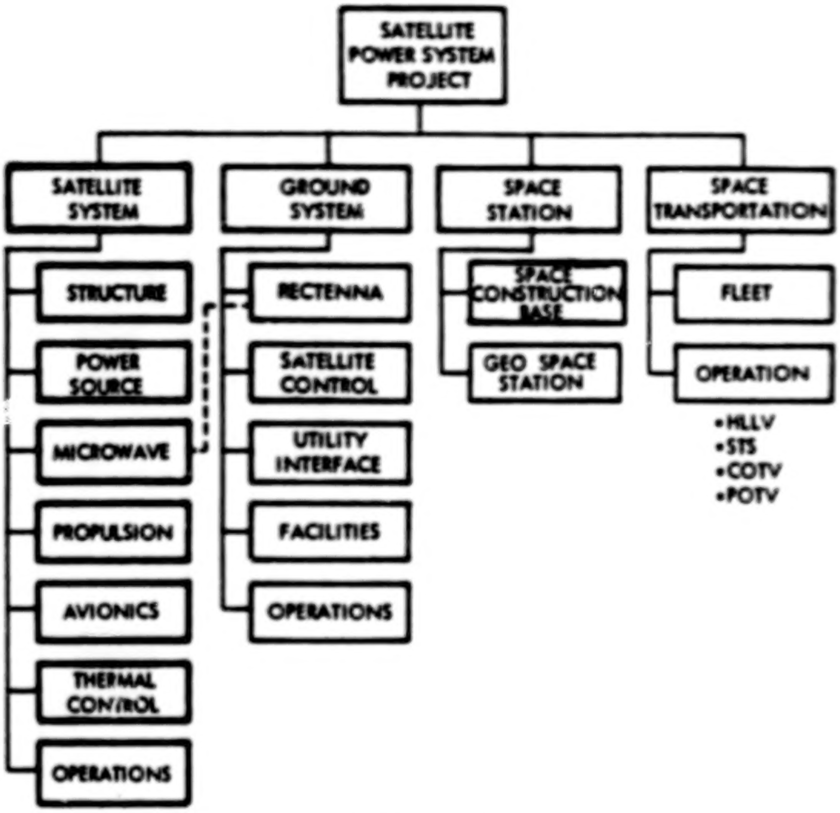
SATELLITE POWER SYSTEM PROJECT
SATELLITE SYSTEM
GROUND SYSTEM
SPACE STATION
SPACE TRANSPORTATION
STRUCTURE
POWER SOURCE
MICROWAVE
PROPULSION
AVIONICS
THERMAL CONTROL
OPERATIONS
RECTENNA
SATELLITE CONTROL
UTILITY INTERFACE
FACILITIES
OPERATIONS
SPACE CONSTRUCTION BASE
GEO SPACE STATION
FLEET
OPERATION
•HLLV
•STS
•COTV
•POTV

Figure 1.1-1. SPS Program Element Relationship

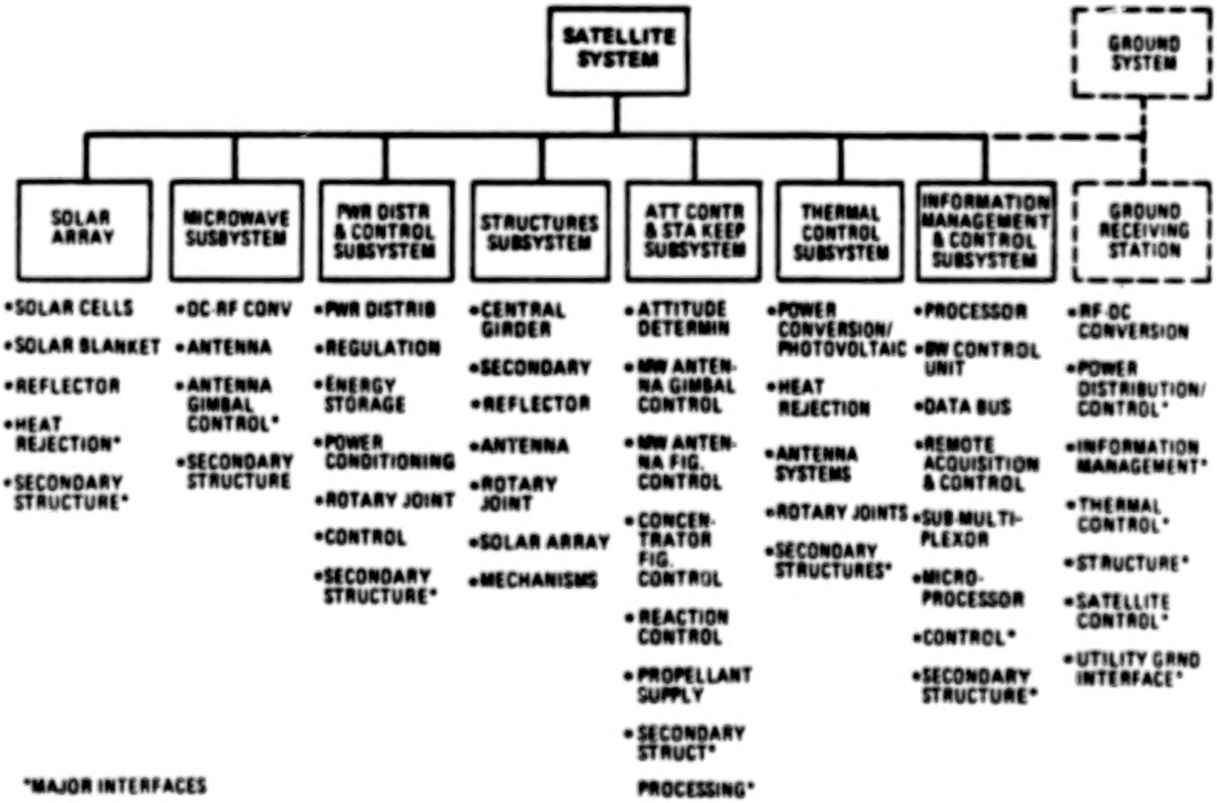
SATELLITE SYSTEM
GROUND SYSTEM
SOLAR ARRAY
MICROWAVE SUSBYSTEM
PWR DISTR & CONTROL SUBSYSTEM
STRUCTURES SUBSYSTEM
ATT CONTR & STA KEEP SUBSYSTEM
THERMAL CONTROL SUBSYSTEM
INFORMATION MANAGEMENT & CONTROL SUBSYSTEM
GROUND RECEIVING STATION
•SOLAR CELLS
•SOLAR BLANKET
•REFLECTOR
•HEAT REJECTION*
•SECONDARY STRUCTURE*
•DC-RF CONV
•ANTENNA
•ANTENNA GIMBAL CONTROL*
•SECONDARY STRUCTURE
•PWR DISTRIB
•REGULATION
•ENERGY STORAGE
•POWER CONDITIONING
•ROTARY JOINT
•CONTROL
•SECONDARY STRUCTURE*
•CENTRAL GIRDER
•SECONDARY
•REFLECTOR
•ANTENNA
•ROTARY JOINT
•SOLAR ARRAY
•MECHANISMS
•ATTITUDE DETERMIN
•MW ANTENNA GIMBAL CONTROL
•MW ANTENNA FIG. CONTROL
•CONCENTRATOR FIG. CONTROL
•REACTION CONTROL
•PROPELLANT SUPPLY
•SECONDARY STRUCT*
PROCESSING*
•POWER CONVERSION/PHOTOVOLTAIC
•HEAT REJECTION
•ANTENNA SYSTEMS
•ROTARY JOINTS
•SECONDARY STRUCTURES*
•PROCESSOR
•BW CONTROL UNIT
•DATA BUS
•REMOTE ACQUISITION & CONTROL
•SUB-MULTIPLEXOR
•MICROPROCESSOR
•CONTROL*
•SECONDARY STRUCTURE*
•RF-DC CONVERSION
•POWER DISTRIBUTION/CONTROL*
•INFORMATION MANAGEMENT*
•THERMAL CONTROL*
•STRUCTURE*
•SATELLITE CONTROL*
•UTILITY GRND INTERFACE*
*MAJOR INTERFACES

Figure 1.1-2. Subsystem/Satellite System Relationship

The ground receiving station functions are identified in Figure 1.1-2 and is shown to have an indirect (dotted) relationship to the orbiting satellite. Major assemblies comprising each subsystem are identified. Unique factors such as elements of one subsystem that are integrated with another (for example, thermal radiators, subsystem control, etc.) are also identified. This document will also identify supporting subsystems, including the transportation system and SPS related ground facilities where these elements have been identified and evaluated.

1.2 SATELLITE POWER SYSTEM CONCEPTS

1.2.1 HISTORY OF STUDY

Initial Candidate Concepts

Many candidate system concepts have been considered since the inception of this study program. Six satellite concepts were identified for consideration in November 1977. These concepts are shown in Figure 1.2-1. A single ground receiving station (rectenna) concept was assumed to be applicable to all satellite concepts.

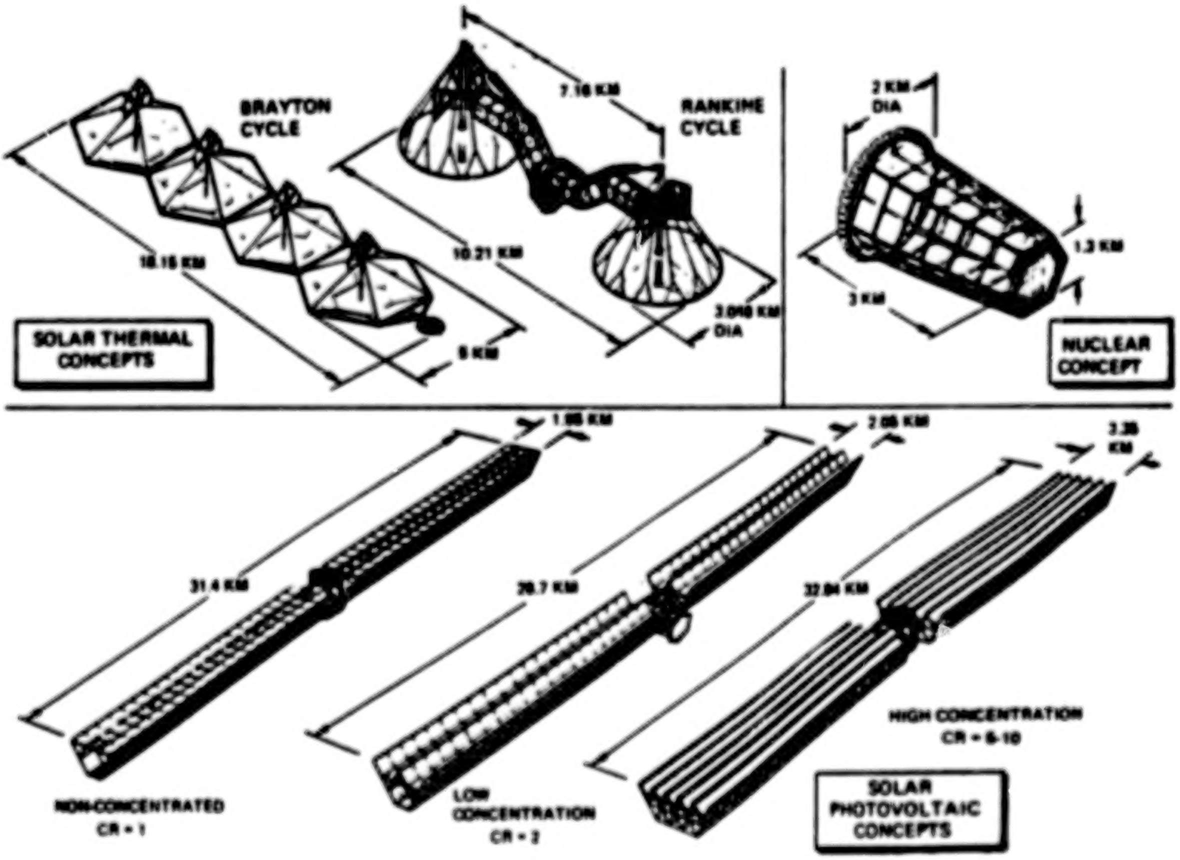
BRAYTON
CYCLE
16.15 KM
5 KM
SOLAR THERMAL
CONCEPTS
7.16 KM
RANKINE
CYCLE
10.21 KM
3.040 KM
DIA
2 KM
DIA
1.3 KM
3 KM
NUCLEAR
CONCEPT
1.85 KM
31.4 KM
NON-CONCENTRATED
CR = 1
2.05 KM
20.7 KM
LOW
CONCENTRATION
CR = 2
3.20
KM
32.04 KM
HIGH CONCENTRATION
CR = 6-10
SOLAR
PHOTOVOLTAIC
CONCEPTS

Figure 1.2-1. SPS Conceptual Configuration
(November 1977)

Solar Photovoltaic (CR-1)

Figure 1.2-2 illustrates the solar photovoltaic (CR-1) satellite power system concept. The CR-1 system was a planar array and had an overall planform dimension of 2.0x28.58 km. The depth of the satellite was 1.17 km. This system required 48.99 km^2 of deployed solar cell area and had a total mass of 37.3x10^6 kg, including a 30.7 percent growth factor. The major advantages of the CR-1 configuration were its simplicity of design; it did not require reflectors; and its relative insensitivity to misorientation angles of as much as ±3 degrees. The CR-1 configuration would have had the largest solar cell area and mass in orbit.

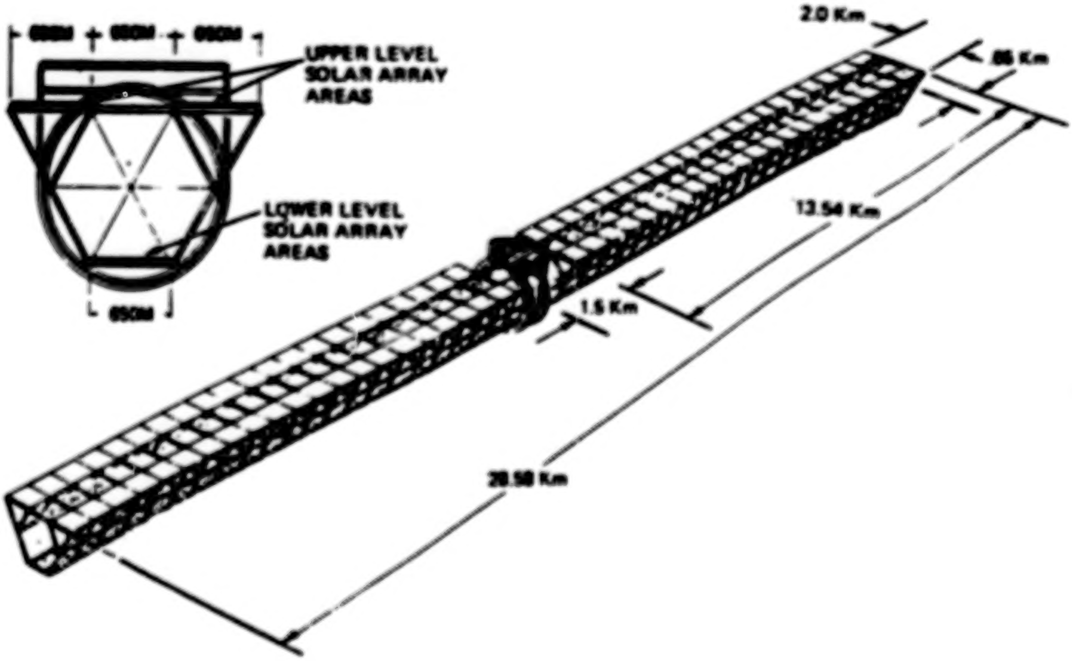

Figure 1.2-2. Solar Photovoltaic Satellite (CR-1)
(November 1977)

Solar Photovoltaic (CR-2)

Figure 1.2-3 illustrates the solar photovoltaic (CR-2) satellite power system concept. The CR-2 system used reflector membranes to concentrate solar energy on the cells. The satellite had two "Vee" troughs per wing. The overall planform dimensions were 2.75x27.16 km, and the depth was 1.2 km. This system required 23.76 km^2 of deployed solar cell area and had a total mass of 33.7x10^6 kg, including a 30-percent growth factor. The major advantages of the CR-2 configuration were the reduced requirement for solar cells and low weight which reduced overall cost. The disadvantages were the planform of the satellite was higher than for CR-1 and the system was sensitive to misorientation. A ±1 degree misorientation of the solar array required an additional 7.9 percent of reflector surface area. The reflective membranes for the GEO environment was not available, and reflectivities of 90 percent at the beginning of life and 72 percent at the end of life were used in the design.

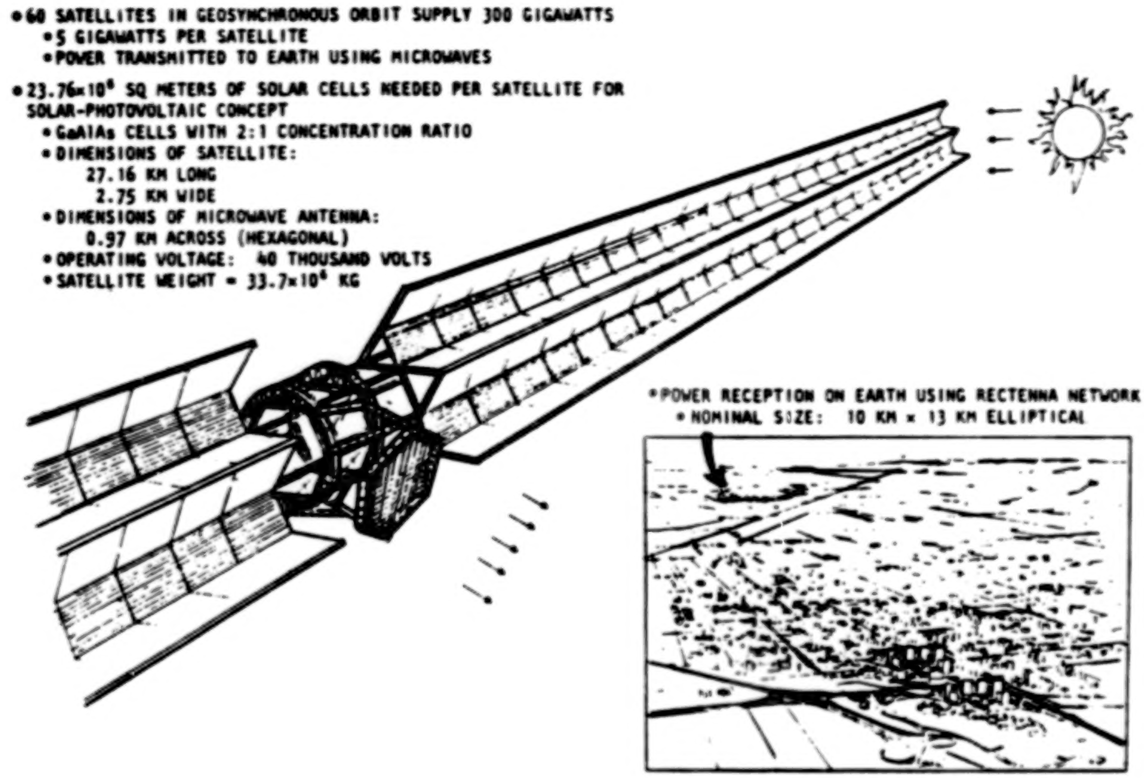
•60 SATELLITES IN GEOSYNCHRONOUS ORBIT SUPPLY 300 GIGAWATTS
•5 GIGAWATTS PER SATELLITE
•POWER TRANSMITTED TO EARTH USING MICROWAVES
•23.76×10⁶ SQ METERS OF SOLAR CELLS NEEDED PER SATELLITE FOR SOLAR-PHOTOVOLTAIC CONCEPT
•GaAlAs CELLS WITH 2:1 CONCENTRATION RATIO
•DIMENSIONS OF SATELLITE:
27.16 KM LONG
2.75 KM WIDE
•DIMENSIONS OF MICROWAVE ANTENNA:
0.97 KM ACROSS (HEXAGONAL)
•OPERATING VOLTAGE: 40 THOUSAND VOLTS
•SATELLITE WEIGHT = 33.7×10⁶ KG
•POWER RECEPTION ON EARTH USING RECTENNA NETWORK
•NOMINAL SIZE: 10 KM × 13 KM ELLIPTICAL

Figure 1.2-3. Solar Photovoltaic Satellite (CR-2)
(November 1977)

Solar Photovoltaic (CR-5)

Figure 1.2-4 illustrates the solar photovoltaic (CR-5) satellite power system concept. The CR-5 system had two troughs per wing and used reflector membranes to concentrate solar energy on the cells. The satellite had the overall planform dimension of 3.12×32.84 km and the depth was 1.4 km. This system required 10.4 km^2 of deployed solar cell area and had a total mass of 37.4×10^6 kg, including a 31.2-percent growth factor. The CR-5 system required the lowest solar cell area. The CR-5 configuration was very sensitive to misorientation angles of only ±1 degree. At a geometric concentration ratio of 5, an increase in reflector surface of 43 percent was required to compensate for a misorientation of ±1 degree.

Solar Thermal—Brayton

Figure 1.2-5 shows one Boeing concept for a 10-GW solar thermal SPS. It used four concentrator modules, each composed of thousands of planar facets which reflect sunlight into a cavity absorber. Ceramic tubing in the absorber heated pressurized helium to 1379°C (2514°F) which was supplied to a Brayton cycle power module comprised of a turbine, regenerator, cooler, compressor, and electrical generator. Heat rejected from the cycle was dissipated by means of a NaK loop to a heat pipe/fin radiator. Microwave power was transmitted from a single antenna at the end of the satellite.

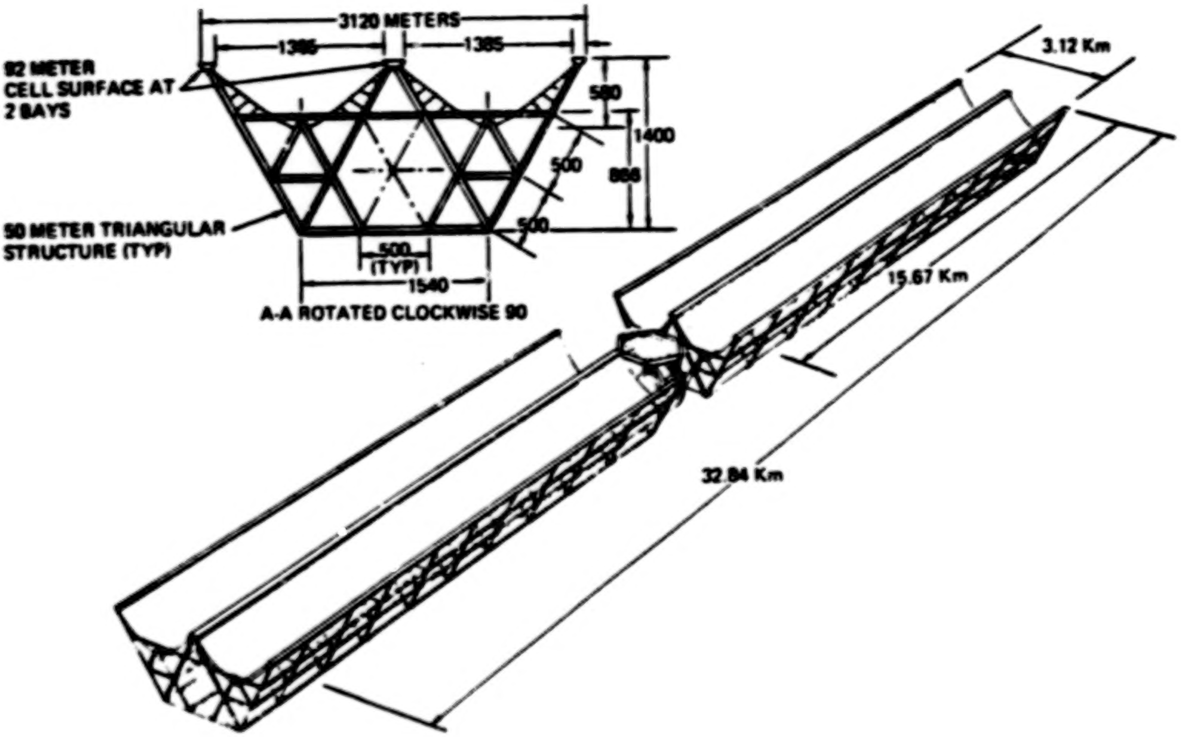

Figure 1.2-4. Solar Photovoltaic Satellite (CR-5)
(November 1977)

Solar Thermal—Rankine

Figure 1.2-6 shows a Rockwell concept for a 5-GW solar thermal SPS using a cesium Rankine cycle. The two concentrators were inflatable, using aluminized plastic film with a transparent canopy. Sunlight was concentrated on an open-disc absorber (cesium boiler) which provides cesium vapor at 1038 C (1900 F) to cesium turbines. Exhaust from the cesium turbines was condensed at 400 F in a tube/fin radiator. Each of the concentrator modules was hinged to permit seasonal tracking of the sun without imposing gravity gradient torques on the satellite. The beam connecting the two modules was offset to locate the rotary joint at the satellite center of gravity.

Nuclear—Brayton

Figure 1.2-7 illustrates the nuclear-powered satellite power system concept. The nuclear Brayton powered SPS consisted of 26 power modules configured in a circular array 2 km in diameter. The antenna was separated by a distance of 3 km from the power modules. In this manner, reactor shadow shielding and reactor-close plane separation distance were combined to reduce nuclear radiation at the antenna to a level acceptable to maintenance personnel. Each power module generated 344 MW_e to provide the required power at the distribution bus as well as its own housekeeping requirements. Brayton cycle waste heat was rejected by a square radiator measuring 227 meters (750 feet) on each side (26 required). Each power module was approximately 40 feet in diameter and 144 feet in length, and contained one nuclear reactor with shadow shield, fuel reprocessing assembly, and two closed Brayton cycle power conversion units. The power module could be removed from the radiator for replacement by remotely operated equipment.

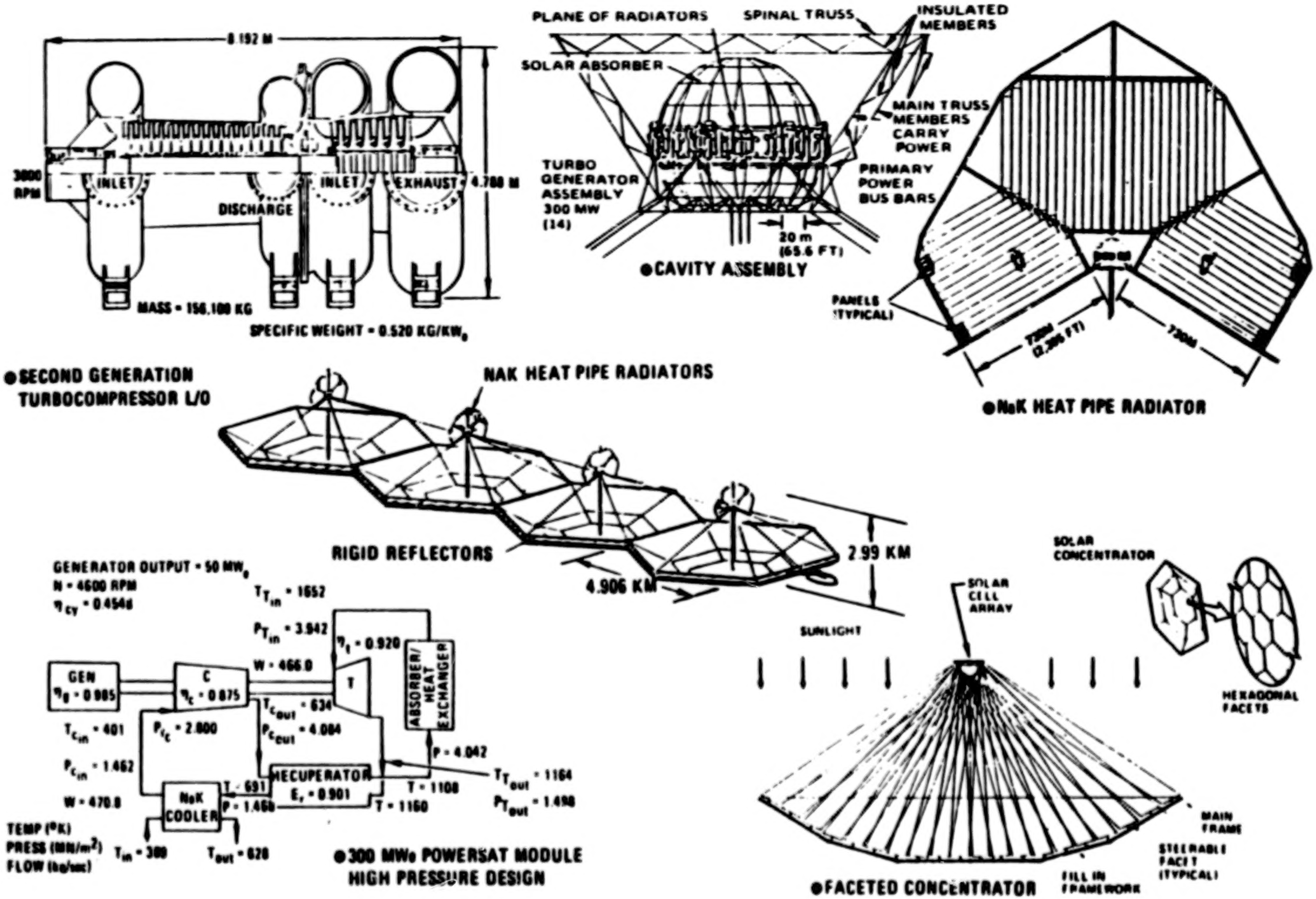
8.192 M
3600 RPM
INLET
DISCHARGE
INLET
EXHAUST
4.788 M
MASS = 156,100 KG
SPECIFIC WEIGHT = 0.520 KG/KW$_e$
●SECOND GENERATION TURBOCOMPRESSOR L/O
PLANE OF RADIATORS
SPINAL TRUSS
INSULATED MEMBERS
SOLAR ABSORBER
MAIN TRUSS MEMBERS CARRY POWER
TURBO GENERATOR ASSEMBLY 300 MW (14)
PRIMARY POWER BUS BARS
20 m (65.6 FT)
●CAVITY ASSEMBLY
PANELS (TYPICAL)
720M (2,366 FT)
720M
●NaK HEAT PIPE RADIATOR
NAK HEAT PIPE RADIATORS
RIGID REFLECTORS
2.99 KM
4.906 KM
GENERATOR OUTPUT = 50 MW$_e$
N = 4600 RPM
η_{cy} = 0.4548
$T_{T_{in}}$ = 1652
$P_{T_{in}}$ = 3.942
η_t = 0.920
W = 466.0
GEN
η_g = 0.985
C
η_c = 0.875
T
ABSORBER/ HEAT EXCHANGER
$T_{c_{out}}$ = 634
$P_{c_{out}}$ = 4.084
$T_{c_{in}}$ = 401
P_{r_c} = 2.800
$P_{c_{in}}$ = 1.462
P = 4.042
RECUPERATOR
E_r = 0.901
T = 691
P = 1.466
T = 1108
T = 1160
$T_{T_{out}}$ = 1164
$P_{T_{out}}$ = 1.498
W = 470.8
NaK COOLER
TEMP (°K)
PRESS (MN/m^2)
FLOW (kg/sec)
T_{in} = 389
T_{out} = 628
●300 MWe POWERSAT MODULE HIGH PRESSURE DESIGN
SOLAR CONCENTRATOR
HEXAGONAL FACETS
SOLAR CELL ARRAY
SUNLIGHT
MAIN FRAME
STEERABLE FACET (TYPICAL)
FILL IN FRAMEWORK
●FACETED CONCENTRATOR

Figure 1.2-5. Solar Thermal Brayton (Boeing) 10 GW

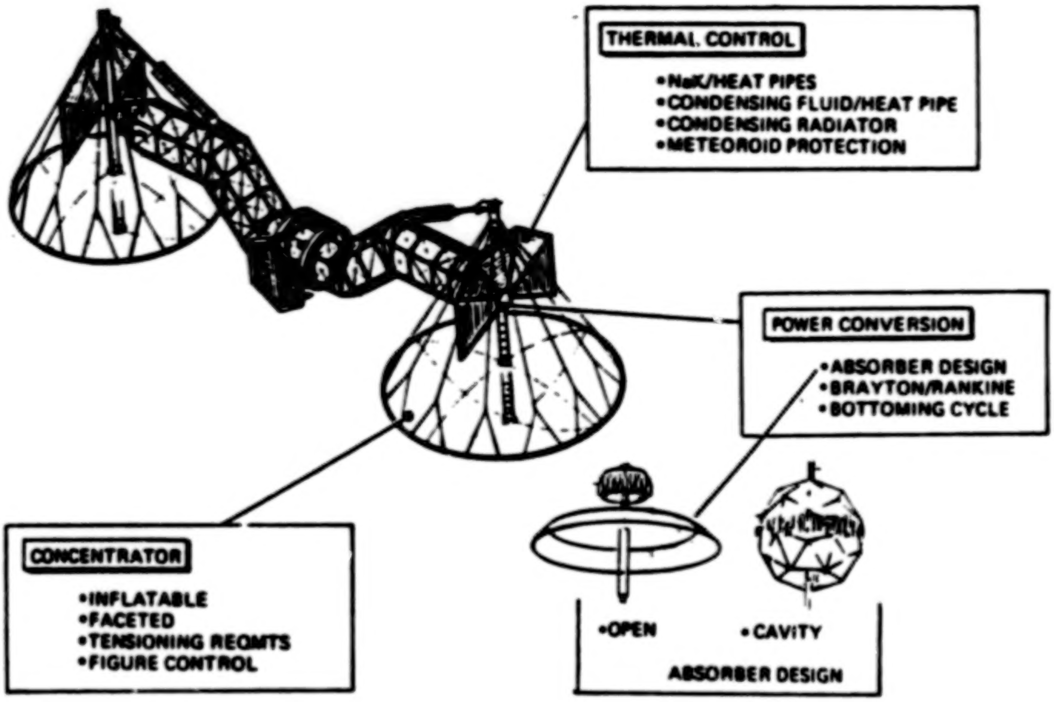
THERMAL CONTROL
•NaK/HEAT PIPES
•CONDENSING FLUID/HEAT PIPE
•CONDENSING RADIATOR
•METEOROID PROTECTION
POWER CONVERSION
•ABSORBER DESIGN
•BRAYTON/RANKINE
•BOTTOMING CYCLE
CONCENTRATOR
•INFLATABLE
•FACETED
•TENSIONING REQMTS
•FIGURE CONTROL
•OPEN
•CAVITY
ABSORBER DESIGN

Figure 1.2-6. Solar Thermal—Rankine
(November 1977)

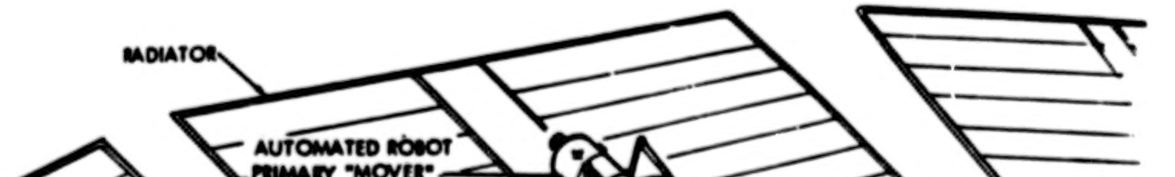
RADIATOR
AUTOMATED ROBOT PRIMARY "MOVER"
MANNED SHIELDED AUXILIARY "MOVER"
2 KM DIA
1 KM ANT.
3 KM
•PREFERRED CONFIG
REMOVEABLE NUCLEAR POWER MODULE
INTERNALLY SHIELDED
344 MWe (26 REQD)
40FT X 144 FT

Figure 1.2-7. Nuclear—Brayton
(November 1977)

Satellite Mass Properties

Tables 1.2-1 through 1.2-3 present the summary weights for the six initial candidate satellite concepts. The solar thermal weight summary illustrates the known weight elements for both potassium-(K) and cesium-(Ce) based Rankine thermal cycles.

Table 1.2-1. Solar Photovoltaic Weight Summary
(GaAlAs Solar Cells) (November 1977)

CONCENTRATION RATIO	CR = 5 10^6 KG	CR = 2 10^6 KG	CR = 1 10^6 KG	GROWTH %
COLLECTOR ARRAY (NON ROT.)	(18.383)	(15.486)	(18.379)	(38.3)
PRIM./SEC. STRUCT./MECH.	9.308	3.983	2.806	25.0
ATTITUDE CONTROL	.300	0.212	.375	30.0
SOLAR CELLS	3.297	5.980	12.343	24.7
REFLECTORS	2.182	2.052	N/A	15.0
POWER CONDIT.	.387	.387	.387	50.0
WIRE HARNESS/SLIP RING	2.891	2.891	2.469	97.0
ANTENNA (ROTATING)	(9.794)	(9.794)	9.794	(23.1)
PRIM./SEC. STRUCT./MECH.	.268	SAME	SAME	25.0
COOLING	.200			50.0
PWR CONVERTERS	5.690			20.0
WIRING/SLIP RING	.098			94.0
WAVEGUIDES	3.540			20.0
IMS EQMT/CABLING	.240	.240	.240	88.0
PROPELLANT/YEAR	.100	.100	.100	0
SUBTOTAL SATELLITE SYST.	28.497	25.599	28.513	
GROWTH ALLOWANCE	8.891	7.987	7.960	31.2
TOTAL SATELLITE SYST.	37.388	33.586	36.473	

COMPARABLE SILICON CR = 1
WEIGHT = 48.589 X 10^6 KG

Rectenna

The ground receiver or rectenna transforms the transmitted radio frequency energy to dc current for distribution into the utility network. The area covered by a 5-gigawatt (GW) delivered power rectenna rate is shown for a typical city (Figure 1.2-3). The rectenna formed an ellipse that is approximately 10×13 km at 34°N latitude.

First Candidate Selection (April 1977)

The two concepts selected for further evaluation and definition at the end of the initial study in April 1978 were a photovoltaic (CR-2) approach and a variation of the proposed Rockwell Solar Thermal satellite. A summary description of the two selected point designs are given in the following two paragraphs. Both these concepts are described in greater detail in Volume II of Final Report SD 78-AP-0023, dated April 1978.

In addition the selected ground receiving station point design which differs slightly from the previous concept is briefly described below and in more expanded form in Section 3.4 of this volume.

Table 1.2-2. Solar Thermal Weight Summary
(November 1977)

CONVERSION CONCEPT	BRAYTON (10^6 KG)	RANKINE POTASSIUM (10^6 KG)	 CESSIUM (10^6 KG)	 GROWTH %
COLLECTOR ARRAY (NON-ROT)	(22.848)	(31.178)	(22.559)	
PRIM./SEC. STRUCT./MECH.	2.217	2.217	2.139	25.0
ATTITUDE CONTROL	.200	.200	.200	30.0
SOLAR COLLECTOR	.878	1.200	1.109	24.4
SOLAR ABSORBER	2.000	.230	.230	30.0
TURBO-EQUIP./GEN.	4.980	14.100	5.650	30.0
POWER CONDIT.	1.830	1.830	1.839	50.0
WIRE HARNESS/SLIP RING	1.282	1.282	1.262	100
RADIATORS	8.880	10.130	10.130	30.0
ANTENNA (ROT.)	9.794	9.794	9.794	23.1
IMS EQMT/CABLING	.240	.240	.240	75.0
PROPELLANT/YEAR	.100	.100	.100	0
SUBTOTAL SATELLITE SYST.	32.980	41.312	32.693	
GROWTH ALLOWANCE	10.182	12.566	10.087	30.8
TOTAL SATELLITE SYST.	43.162	53.878	42.780	

Table 1.2-3. Nuclear Reactor Concept Weight Summary
(November 1977)

	(10^6 KG)		GROWTH %
PRIMARY STRUCTURE	0.381		25.0
SEC. STRUCT.	1.112		25.0
ATTITUDE CONTROL	0.20	20.92*	30.0
SHEILDING	0.54		30.0
REACTORS (28)	2.08		30.0
FUEL PROCESSING	1.01		30.0
TURBO-EQUIPMENT	3.34		30.0
GENERATORS	1.83		30.0
RADIATORS	11.94		30.0
POWER CONDIT.	1.830		50.0
WIRE HARDNESS	0.80		100
ANTENNA	9.88'		23.1
IMS EQUIP.	0.081		50.0
IMS CABLING ITS	0.179		100
PROPELLANT/YEAR	0.10		0
SUBTOTAL	35.052		-
GROWTH ALLOWANCE	10.411		29.6
TOTAL SATELLITE SYST.	45.463		

CONCEPT WEIGHT COMPARISONS			
POWER CONVERSION CONCEPT	BASE WEIGHT (10^6 KG)	GROWTH (%)	TOTAL WEIGHT (10^6 KG)
CR = 1	28.513	30.7	37.270
2	25.599	31.7	33.714
5	28.497	31.2	37.379
RANKINE CS/STEAM	26.386	31.2	34.605
NUCLEAR	35.056	29.6	45.465

*GASEOUS CORE REACTOR/MHD COULD POTENTIALLY REDUCE THIS TO 1.99 X 10^6 KG – REFERENCE: 8TH IECEC PAPER 739018, 1973

RADIATOR OPTIMIZATION COULD POTENTIALLY REDUCE THIS TO 14.95 X 10^6KG · CONDENDING STEAM RADIATOR (LOWER TEMPERATURE)

Solar Photovoltaic (CR-2) (April 1978)

The GaAlAs photovoltaic point design satellite power system concept is shown in Figure 1.2-8. The system utilizes aluminized reflector membranes to concentrate the solar energy on the cells. The satellite solar reflectors produce a concentration ratio of CR-2. The satellite employs the "V-trough" configuration that has three troughs per wing. The system has an overall efficiency of 6.08% and delivers 5 GW of electrical energy to the utility company on the ground. The overall planform dimensions are 3.85x21.3 km, and the depth is 1.69 km. The satellite has a mass of 36.56×10^6 kg which includes a 30% growth factor for the mass. The system requires 30.6×10^6 m^2 of solar cells and 61.2×10^6 m^2 of reflector surface. The solar cells for the point design are GaAlAs cells rated at 20% efficiency at AMO and 28°C. The solar array blanket mass is 0.252 kg/m .

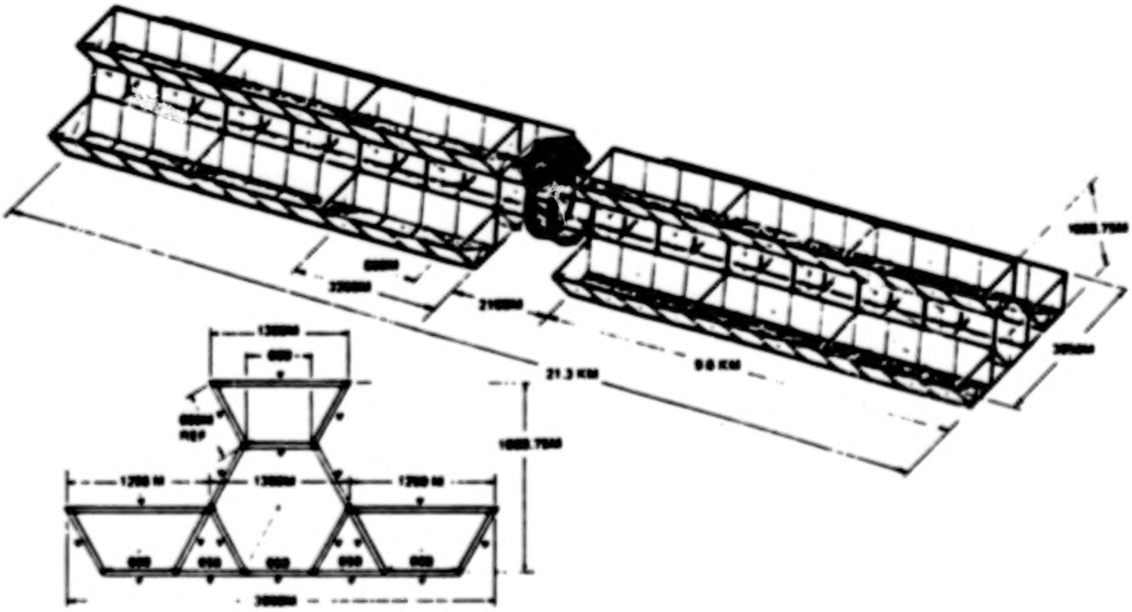

Figure 1.2-8. Solar Photovoltaic Satellite (CR-2) 5 GW (April 1978)

Solar Thermal—Rankine (April 1978)

Figure 1.2-9 shows the Rockwell point design concept of a 5-GW solar thermal SPS using a cesium/steam Rankine cycle. The two concentrators are of an inflatable design, using aluminized plastic film with a transparent canopy. Sunlight is concentrated on an open-disc absorber (cesium boiler) which provides cesium vapor at 1260°C (2300°F) to cesium turbines. Exhaust from the cesium turbines is condensed at 593°C (1100°F) on the outside of steam boiler tubes which produce steam at 538°C (1000°F) and 16.6 kN/m^2 (2400 psia) to a bottoming steam turbine. Exhaust from the steam turbines is condensed at 204°C (400°F) in a tube/heat pipe/fin radiator.

Each of the concentrator modules is hinged to permit seasonal tracking of the sun without imposing gravity gradient torques on the satellite. The beam connecting the two modules is offset to locate the rotary joint at the satellite

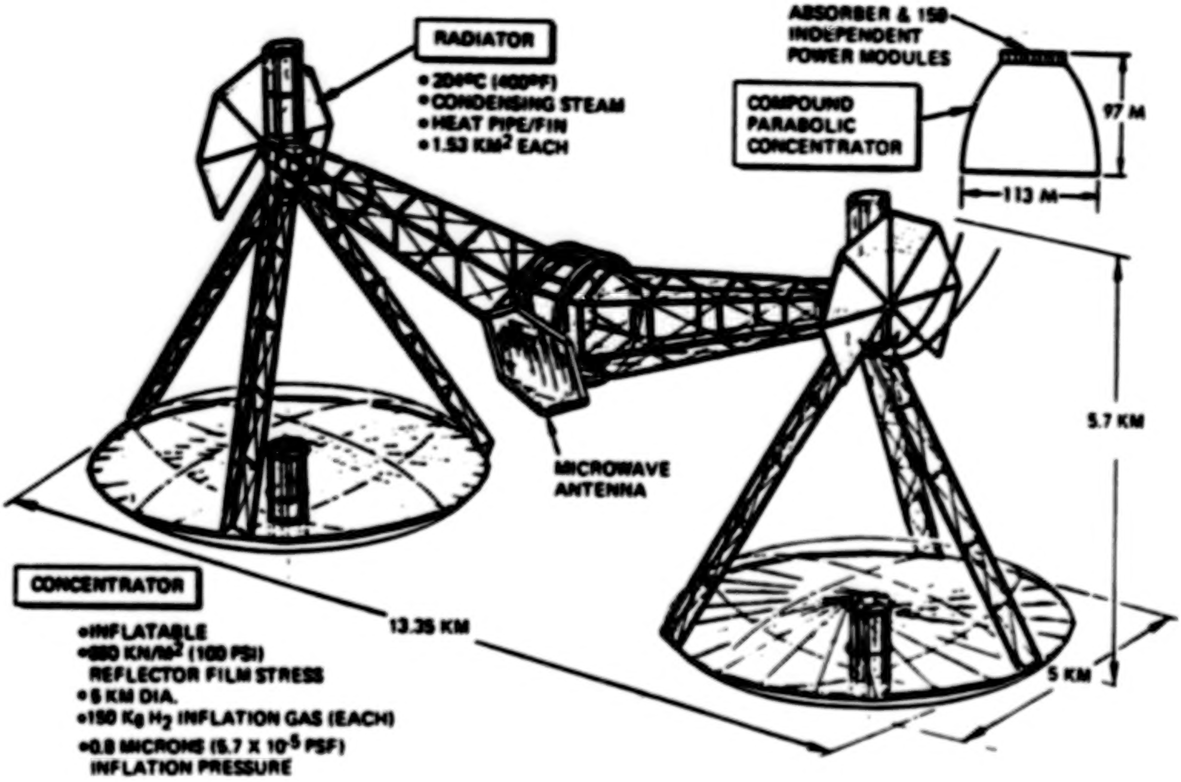
RADIATOR
• 204°C (400°F)
• CONDENSING STEAM
• HEAT PIPE/FIN
• 1.53 KM² EACH
ABSORBER & 150 INDEPENDENT POWER MODULES
COMPOUND PARABOLIC CONCENTRATOR
97 M
113 M
MICROWAVE ANTENNA
5.7 KM
CONCENTRATOR
• INFLATABLE
• 690 KN/M² (100 PSI) REFLECTOR FILM STRESS
• 5 KM DIA.
• 150 Kg H₂ INFLATION GAS (EACH)
• 0.8 MICRONS (5.7 X 10⁻⁵ PSF) INFLATION PRESSURE
13.35 KM
5 KM

Figure 1.2-9. Solar Thermal—Rankine (5 GW)
(April 1978)

center of gravity. This permits mounting of thrusters on the rotary joint and facilitates their orientation during LEO/GEO orbital transfer.

Ground Receiving Station

The ground receiving station (rectenna) concept selected for further definition is illustrated in Figure 1.2-10. The receiving antenna forms an eclipse with major and minor axis of 13 km and 10 km respectively. The major axis is aligned along the N-S geographic line. Figure 1.2-11 illustrates the general site concept recommended by the study in April 1978.

Mass Properties

Table 1.2-4 and 1.2-5 present a summary of the estimated weight for the two point design concepts as of April 1979.

1.2.2 NASA REFERENCE SATELLITE CONCEPT

In October 1978, NASA established a baseline (Reference) concept to be used in subsequent design and feasibility analysis. The primary approach selected consisted of solar blankets installed on a multi-trough, plannar structure with a microwave transmission system for power transfer to Earth located sites. The initial concept proposed a primary solar conversion approach utilizing Silicon solar cells with a concentration ratio of one (CR-1) and an alternate approach using GaAlAs with a concentration ratio of two (CR-2).

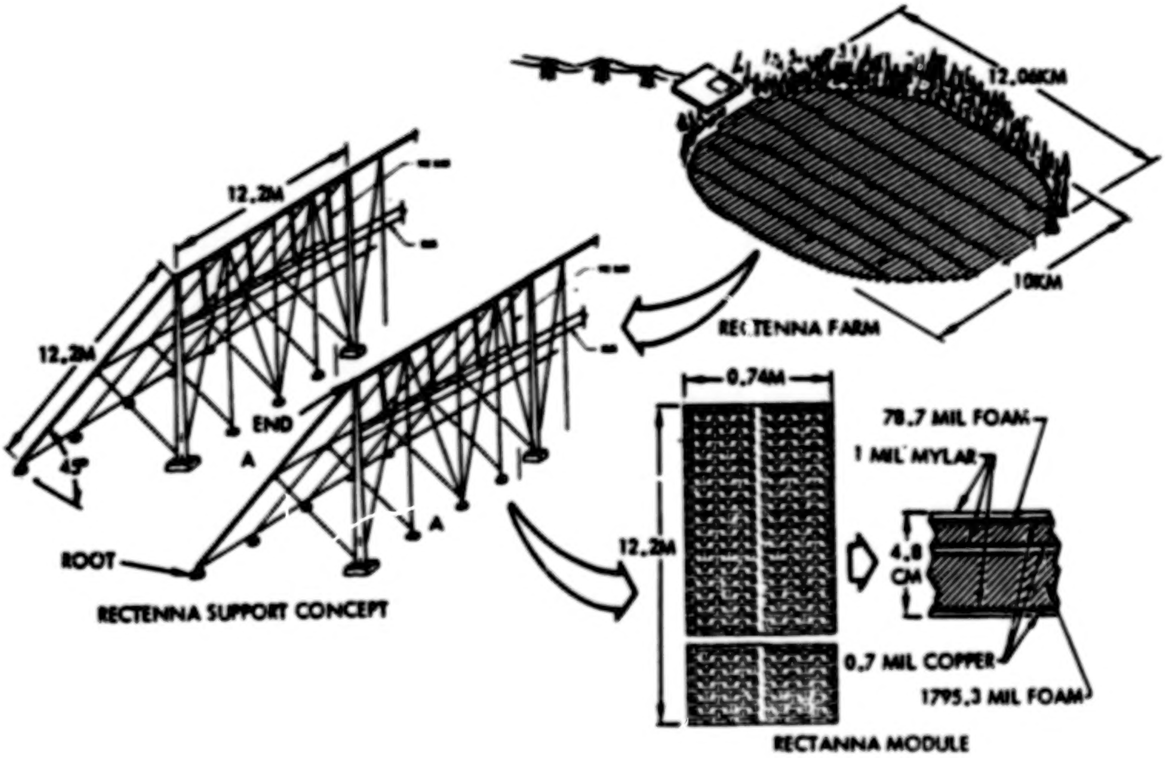
12.06KM
10KM
RECTENNA FARM
12.2M
12.2M
45°
END
A
A
ROOT
RECTENNA SUPPORT CONCEPT
0.74M
12.2M
78.7 MIL FOAM
1 MIL MYLAR
4.8 CM
0.7 MIL COPPER
1795.3 MIL FOAM
RECTANNA MODULE

Figure 1.2-10. Microwave Transmission Subsystem - Rectenna (April 1978)

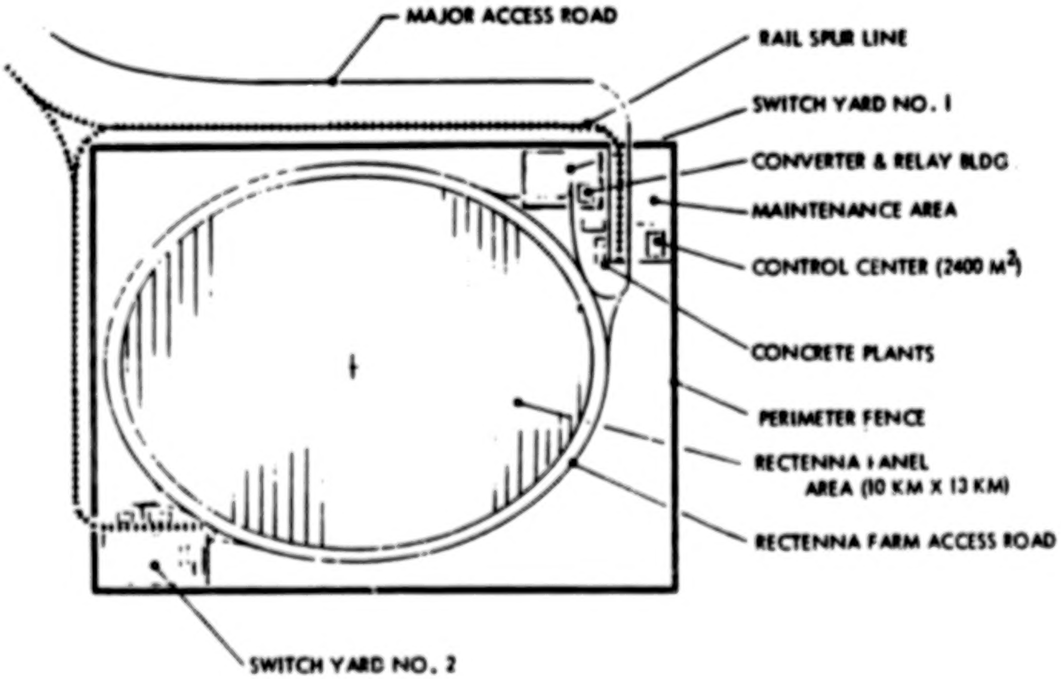
MAJOR ACCESS ROAD
RAIL SPUR LINE
SWITCH YARD NO. 1
CONVERTER & RELAY BLDG
MAINTENANCE AREA
CONTROL CENTER (2400 M²)
CONCRETE PLANTS
PERIMETER FENCE
RECTENNA PANEL AREA (10 KM X 13 KM)
RECTENNA FARM ACCESS ROAD
SWITCH YARD NO. 2

Figure 1.2-11. Rectenna Site Concept (April 1978)

Table 1.2-4. Photovoltaic (CR-2) Satellite Mass Statement - Point Design (April 1978)

SUBSYSTEM	WEIGHT (MILLION KG)
COLLECTOR ARRAY	
STRUCTURE AND MECHANISMS	3.777
POWER SOURCE	8.831
POWER DISTRIBUTION AND CONTROL	1.166
ATTITUDE CONTROL	0.095
INFORMATION MANAGEMENT AND CONTROL	0.050
TOTAL ARRAY (DRY)	(13.919)
ANTENNA SECTION	
STRUCTURE AND MECHANISMS	1.685
THERMAL CONTROL	1.408
MICROWAVE POWER	7.012
POWER DISTRIBUTION AND CONTROL	3.469
INFORMATION MANAGEMENT AND CONTROL	0.630
TOTAL ANTENNA SECTION (DRY)	(14.204)
TOTAL SPS DRY WEIGHT	28.123
GROWTH (30%)	8.437
TOTAL SPS DRY WEIGHT WITH GROWTH	36.560
PROPELLANT PER YEAR	0.040

Table 1.2-5. Solar Thermal Satellite Mass Statement - Point Design (April 1978)

SUBSYSTEM	WEIGHT (MILLION KG)
COLLECTOR ARRAY	
STRUCTURE AND MECHANISMS	1.661
POWER SOURCE	3.120
POWER DISTRIBUTION AND CONTROL	4.304
ATTITUDE CONTROL	0.095
THERMAL CONTROL	8.786
INFORMATION MANAGEMENT AND CONTROL	0.050
TOTAL ARRAY (DRY)	(18.016)
ANTENNA SECTION	
STRUCTURE AND MECHANISMS	1.685
THERMAL CONTROL	1.408
MICROWAVE POWER	7.012
POWER DISTRIBUTION AND CONTROL	3.469
INFORMATION MANAGEMENT AND CONTROL	0.630
TOTAL ANTENNA SECTION	(14.204)
TOTAL SPS DRY WEIGHT	32.220
GROWTH (30%)	9.666
TOTAL SPS DRY WEIGHT WITH GROWTH	(41.986)
PROPELLANT PER YEAR	0.040

The Silicon cell based concept consisted of 8 cell troughs each containing 16 bays. The GaAlAs concept consisted of 5 troughs by 20 bays. Both concepts utilized an end mounted, 1 km (nominal) microwave antenna. Both concepts were normally 5.3×10.4 km, with the Silicon concept containing a greater mass, (51×10^6 kg) compared with GaAlAs (34×10^6 kg). Figure 1.2-12 illustrates the GaAlAs version of the reference satellite. Overall system efficiency for the Silicon based concept is estimated to be 7.06%, while for GaAlAs the efficiency is estimated to be 6.97%. Power output for these concepts (at utility interface) is estimated at 5.0 GW.

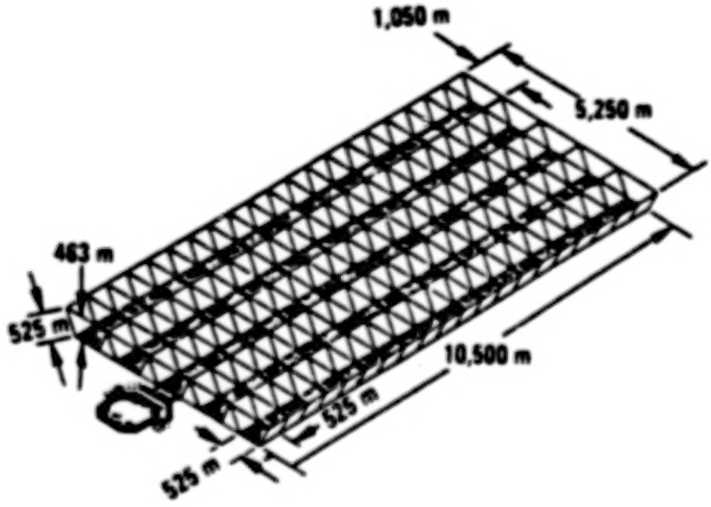

Figure 1.2-12. NASA Reference Configurations (October 1978)

Mass Properties

Table 1.2-6 presents a summary of the estimated mass for the two NASA reference concepts. Note that the growth allowance has changed from 30% to the present 25%.

1.2.3 ROCKWELL ALTERNATIVE SATELLITE CONCEPT (MARCH 1979)

The Rockwell satellite concepts as of March 1979 are presented in Figure 1.2-13. Figure 1.2-13(a) illustrates the rockwell end-mounted antenna, while Figure 1.2-13(b) depicts a satellite with a center-mounted antenna concept. Both approaches consist of a 3-bay by 10-bay structure containing the solar arrays and reflectors. The 30-bay structure is sized to dimensions of 3900 m by 16,000 m. The center, antenna mounting, structure adds 1900 m to the overall length of the center-mounted antenna satellite. The end-mounted antenna concept adds 1850 m to the overall dimensions. The end-mounted antenna dry mass is greater by approximately 2.3×10^6 kg because of the added average length of the main power buses.

The solar array panel is 600 m wide × 750 m long. Two of these panels make up a voltage string (45.7 kV). The 600 m width consists of 24 rolls each 25 m wide. Sizing of the array is based on a solar constant at summer solstice (1311.5 W/m^2), an end of life concentration ratio of 1.83, an operating temperature of 113°C and the design factors listed in the figure. A design margin

Table 1.2-6. NASA Reference Satellite Mass Properties (October 1978) (10^6 kg)

SUBSYSTEM	GAALAS CR = 2 OPTION		SILICON CR = 1 OPTION	
SOLAR ARRAY		13.798		27.258
PRIMARY STRUCTURE	4.172		3.388	
SECONDARY STRUCTURE	0.581		0.436	
SOLAR BLANKETS	6.896		22.051	
CONCENTRATORS	0.955		—	
POWER DISTRIBUTION & CONDITIONING	1.144		1.134	
INFORMATION MANAGEMENT & CONTROL	0.050		0.050	
ANTENNA		13.382		13.382
PRIMARY STRUCTURE	0.250		0.250	
SECONDARY STRUCTURE	0.786		0.786	
TRANSMITTER SUBARRAYS	7.178		7.178	
POWER DISTRIBUTION & CONDITIONING	2.189		2.189	
THERMAL CONTROL	2.222		2.222	
INFORMATION MANAGEMENT & CONTROL	0.630		0.630	
ATTITUDE CONTROL	0.128		0.128	
ARRAY/ANTENNA INTERFACES*		0.147		0.147
PRIMARY STRUCTURE	0.094		0.094	
SECONDARY STRUCTURE	0.003		0.003	
MECHANISMS	0.033		0.033	
POWER DISTRIBUTION	0.017		0.017	
SUBTOTAL		27.327		40.787
CONTINGENCY (25%)		6.832		10.197
TOTAL		34.159		50.984

* ROTARY JOINT, SLIP RINGS, ANTENNA YOKE

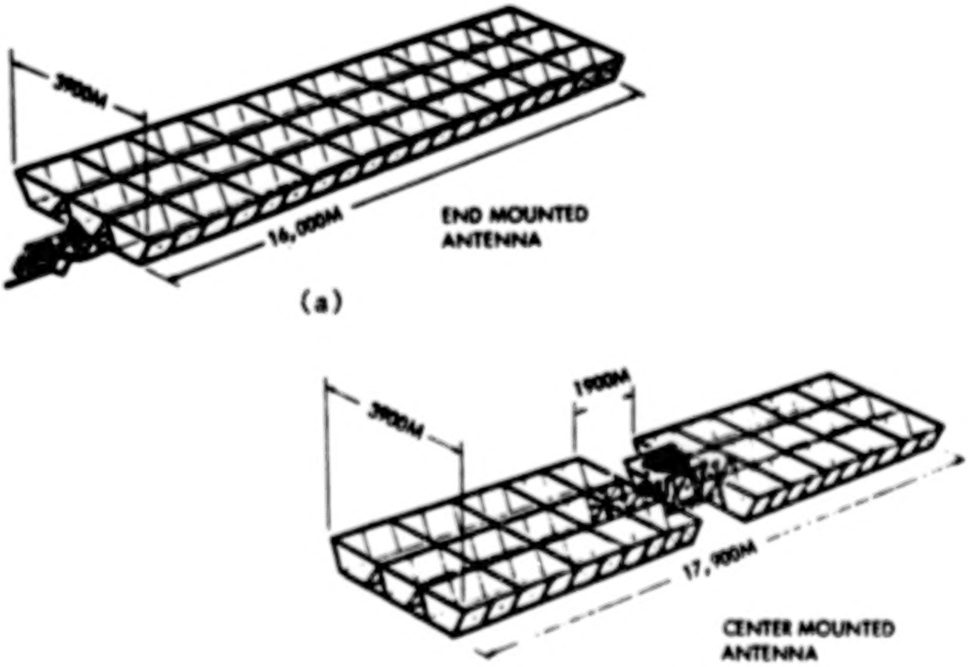

(a)

(b)

Figure 1.2-13. Alternate Satellite Concepts (March 1979)

factor of 0.975 is used to match the available area of 27×10^6 m². Total power at the array output is 9.52 GW. Total transmitted power is 6.79 GW. System efficiency factors for the satellite as indicated in Figure 1.2-14.

Mass Properties

Table 1.2-7 presents a summary of the mass for the two alternate concepts of March 1979.

1.2.4 ROCKWELL REFERENCE GROUND RECEIVING STATION

The various elements of the initially defined Ground Receiving Station (GRS) are shown in Figure 1.2-15. The major elements shown include the basic receiving/rectifying panels (rectenna), the power distribution and power conversion elements, as well as the various supporting elements (maintenance, facilities, land, etc.). The estimated efficiency of the various links of the ground system power chain is shown in Figure 1.2-14.

The rectenna panels are located in the center of the receiving station and covers a ground area of approximately 100 km² (approximately 25,000 acres). An additional 32 km² (approximately 10,000 acres) is required for the distribution and conversion stations plus a security perimeter. Received power is approximately 6.15 GW (at 2.45 GHz). Power available at the utility interface is approximately 5 GW ac.

1.2.5 ROCKWELL CONCEPT APPROACHES (JUNE 1980)

Satellite

The present concepts suggested by Rockwell are illustrated in Figures 1.2-16, 1.2-17, and 1.2-18. The first concept (Figure 1.2-16) consists of a three trough planar solar cell array with a CR_E of 1.83 and utilizing klystrons (or magnetrons) for powering the microwave power transmission array. The klystron variation is essentially an updated version of the end-mounted concept depicted in March 1979.

Figures 1.2-17 and 1.2-18 depict the Rockwell alternate concepts that are predicated on the use of advanced technology, solid-state microwave power amplifiers as the means of generating the microwave transmission power beam. The concept in Figure 1.2-17 illustrates a concept similar to the baseline (Klystron) reference concept. The solar array in this case remains a three trough, planar configuration with a CR_E of 1.83. Two antennas are required, one at each end to overcome the lower transmission power (3.68 GW) available at each antenna, and the solar array area is increased to compensate for the lower overall system efficiency. All planar configurations utilize a modified 10-dB Gaussian beam taper to minimize beam side lobe losses.

Figure 1.2-18 represents a major deviation from the planar concepts most often considered for solar photovoltaic power generation satellites. The depicted approach utilizes a CR_E of 5.2 with the solar cell blanket and microwave antenna array forming the outer layer of a "sandwich". The inner layers provide for interconnection and thermal isolation since the desired operating

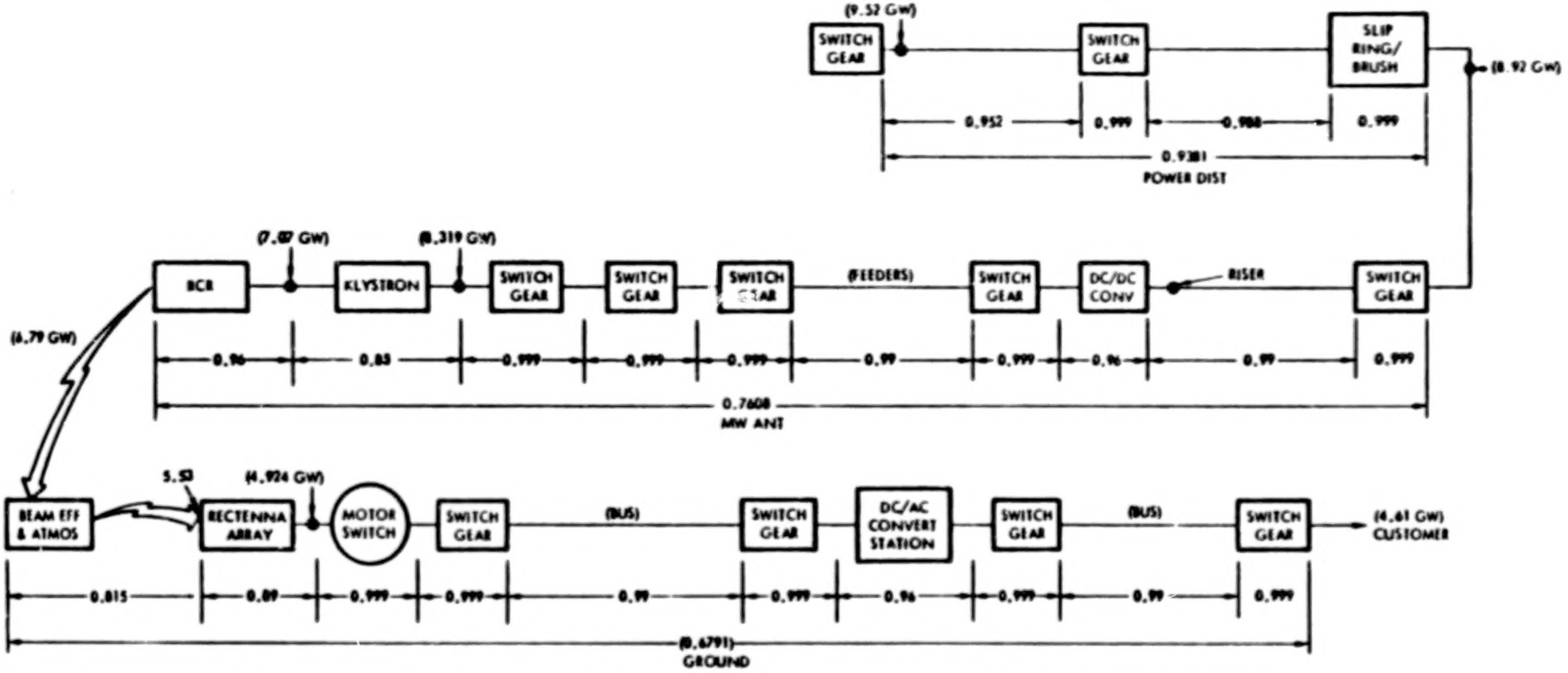
(9.52 GW)
SWITCH GEAR
SWITCH GEAR
SLIP RING/ BRUSH
(8.92 GW)
0.952
0.999
0.988
0.999
0.9381
POWER DIST
(7.07 GW)
(8.319 GW)
BCR
KLYSTRON
SWITCH GEAR
SWITCH GEAR
SWITCH GEAR
(FEEDERS)
SWITCH GEAR
DC/DC CONV
RISER
SWITCH GEAR
0.96
0.83
0.999
0.999
0.999
0.99
0.999
0.96
0.99
0.999
0.7608
MW ANT
(6.79 GW)
5.53
(4.924 GW)
BEAM EFF & ATMOS
RECTENNA ARRAY
MOTOR SWITCH
SWITCH GEAR
(BUS)
SWITCH GEAR
DC/AC CONVERT STATION
SWITCH GEAR
(BUS)
SWITCH GEAR
(4.61 GW) CUSTOMER
0.815
0.89
0.999
0.999
0.99
0.999
0.96
0.999
0.99
0.999
(0.6791)
GROUND

= POWER GEN. X POWER DIST. X MW ANT. X GROUND

(13.35%) (93.81%) (76.08%) (67.91%)

6.47%

(5.6% BASED ON TOTAL INTERCEPTED AREA)

η SG = $.999^{14}$ = .986

NOTE $.995^{14}$ = .932

Figure 1.2-14. System Efficiency Chain
(March 1979)

Table 1.2-7. Mass Properties—Rockwell Alternate Concepts (March 1979)*

SUBSYSTEM	END-MOUNTED	CENTER-MOUNTED
SOLAR ARRAY	(11.884)	(10.025)
PRIMARY STRUCTURE	.702	.702
SECONDARY STRUCTURE & MECH.	.558	.420
SOLAR BLANKETS	6.818	6.818
CONCENTRATORS	1.037	1.037
POWER DISTRIBUTION & CONDITIONING	2.603	0.882
INFORMATION MANAGEMENT & CONTROL	0.050	0.050
ATTITUDE CONTROL	0.116	0.116
ANTENNA	(14.532)	(14.532)
PRIMARY STRUCTURE	0.120	0.120
SECONDARY STRUCTURE	0.857	0.857
TRANSMITTER SUBARRAYS	7.012	7.012
POWER DISTRIBUTION & CONDITIONING	4.505	4.505
THERMAL CONTROL	1.408	1.408
INFORMATION MANAGEMENT & CONTROL	0.630	0.630
SUBTOTAL	26.416	24.557
CONTINGENCY (25%)	6.604	6.137
TOTAL	33.020	30.694

*10^6 kg

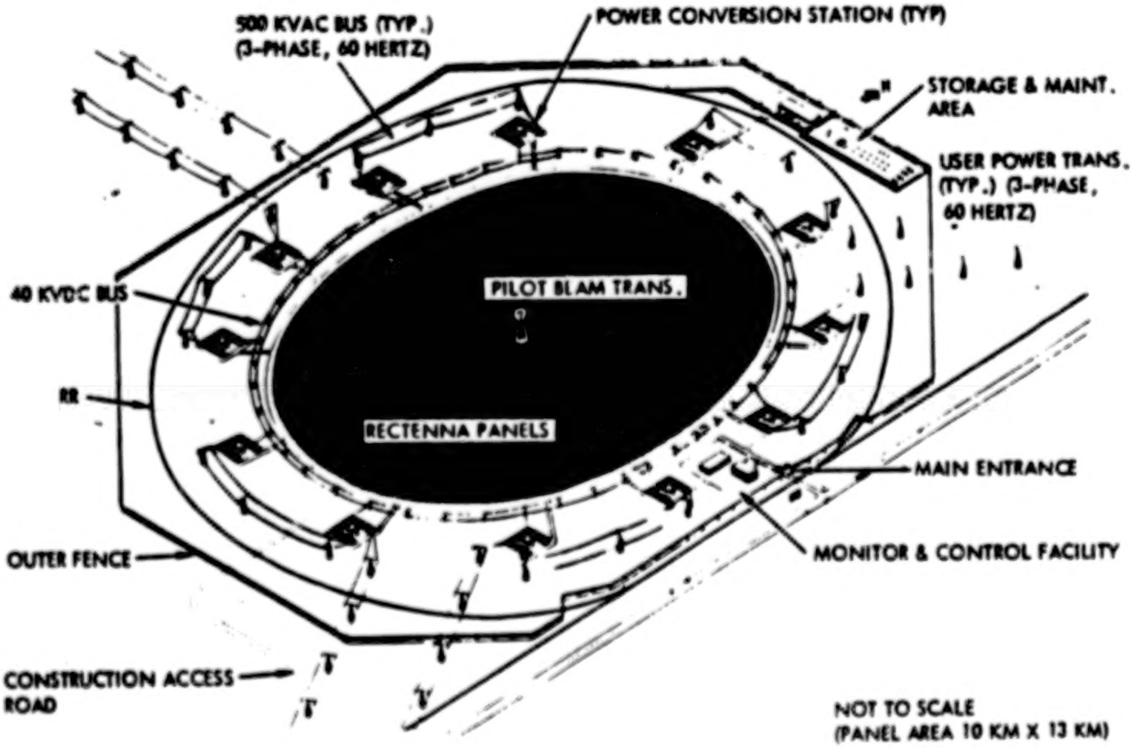
500 KVAC BUS (TYP.)
(3-PHASE, 60 HERTZ)
POWER CONVERSION STATION (TYP)
STORAGE & MAINT. AREA
USER POWER TRANS. (TYP.) (3-PHASE, 60 HERTZ)
PILOT BEAM TRANS.
40 KVDC BUS
RR
RECTENNA PANELS
MAIN ENTRANCE
MONITOR & CONTROL FACILITY
OUTER FENCE
CONSTRUCTION ACCESS ROAD
NOT TO SCALE
(PANEL AREA 10 KM X 13 KM)

Figure 1.2-15. Ground Receiving Station

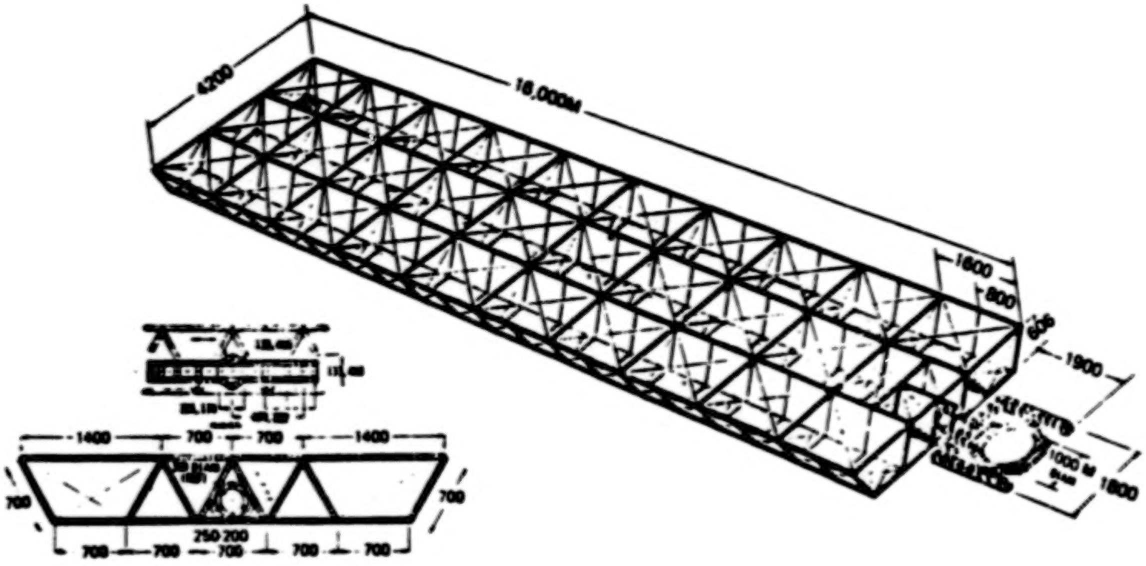
4200
18,000M
1600
800
600
1900
1000 M DIAM
1800
1400
700
1400
700
700
700
250 200
700
700
700
700
700

Figure 1.2-16. SPS Reference Configuration Single End-Mounted Tension Web Antenna—Klystron

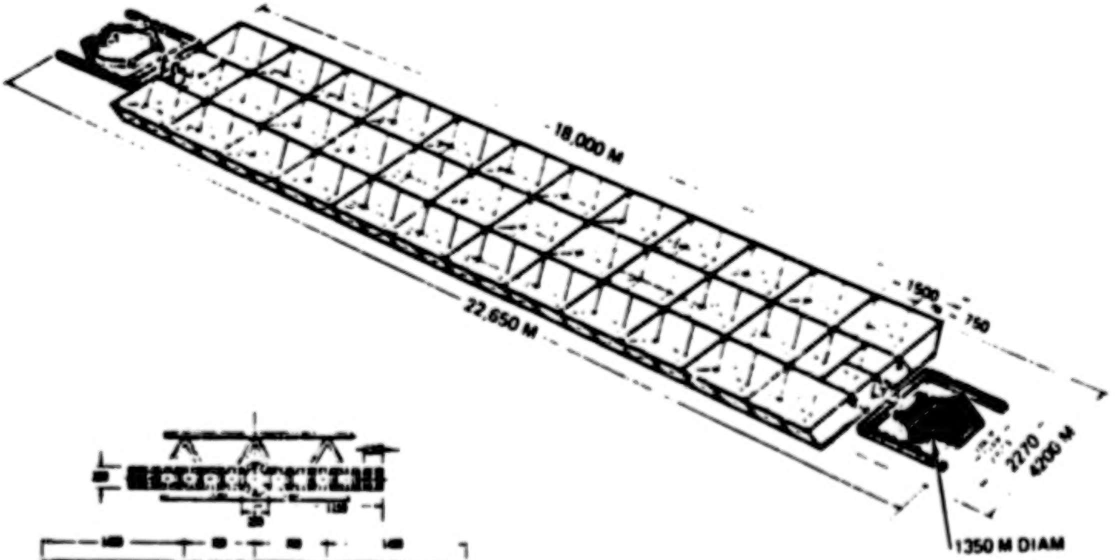
18,000 M
22,650 M
1500
750
2270
4200 M
1350 M DIAM

Figure 1.2-17. SPS Solid State Configuration—Dual End Mounted Antenna

temperature (estimated) for the solar cell and microwave amplifiers are 200°C and 125°C respectively. The satellite reflector system consists of a large planar mirror array that may be adjusted relative to sun and a relatively flat but adjustable secondary mirror to maintain a focused solar image on the solar blanket.

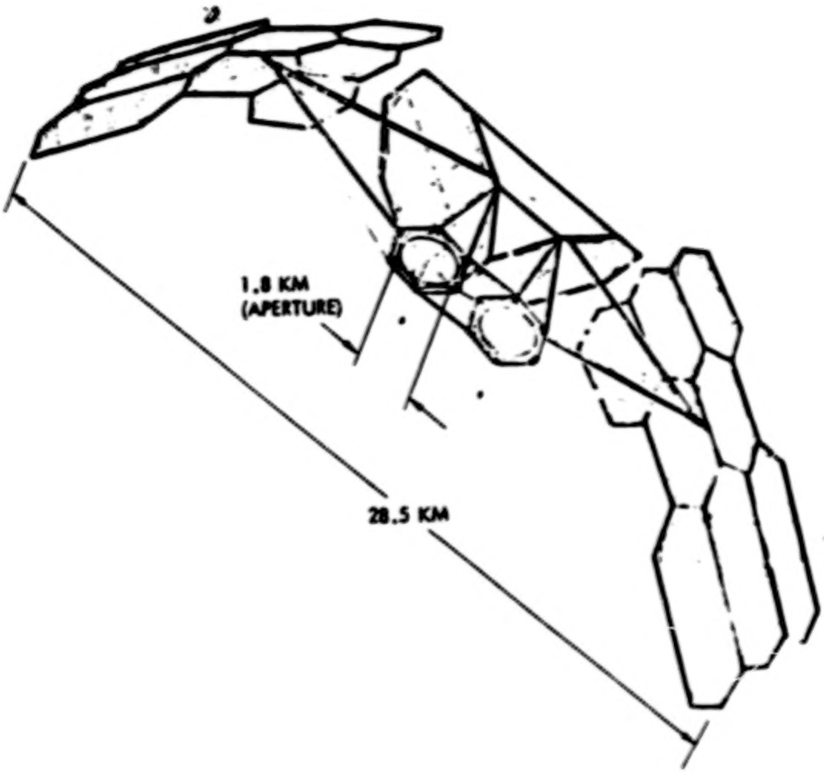

Figure 1.2-18. Solid-State Sandwich Satellite Point Design Concept

A major advantage of the "sandwich" configuration is the co-location of the microwave system and the solar power generation elements and therefore the elimination of the need for a high power rotary joint. It thus becomes possible to generate voltages directly at levels appropriate to solid state device operation, eliminating the need for large masses of HV-to-LV dc-dc converters.

Ground Receiving Station

The Ground Receiving Station (GRS) conceptually remains identical to the concept described earlier in Section 1.2.4. The only factor which is subjected to change are the base dimensions of the rectenna. For example the rectenna dimensions for the March 1979 system was stated to be 10 km (minor axis) and 13 km (major axis). For the reference system update (Klystron) the minor and major axis dimensions remain the same although the alternate configuration will require smaller rectenna area.

Preliminary analysis of the power beam footprint for the solid-state reference concept (Figure 1.2-17) (2 required), and the "sandwich" concept (Figure 1.2-18), (2 required), have indicated that the minor axis dimensions are 7.45 km and 4.87 km respectively (for the single junction GaAs solar cell configuration). The major axis dimensions are 1.31 times the above figures.

1.2.6 SATELLITE CONCEPT SUMMARIES

At the present time seven alternate configurations have been identified in detail. Of these five have been considered for costing and transportation analysis. The seven configurations are summarized in Table 1.2-8 and consist of the klystron and solid state antenna configurations utilizing the GaAs and GaAlAs/GaAs solar cells and a magnetron antenna configuration considering GaAs solar cells only. An eighth alternate magnetron antenna with GaAlAs/GaAs cells has been tentatively defined but details are not included to any depth in this document.

Klystron Microwave Antenna

The recommended satellite concept utilizing a klystron microwave power amplifier is shown in Figure 1.2-16. The illustrated concept consists of an end-mounted microwave power transmission system and a GaAs based three-trough, planar solar array. The array length is 16,000 m for a GaAs single junction cell and 11,000 m for an array based upon a GaAlAs/GaAs dual junction (multi-bandgap) solar cell. The antenna array adds 1900 m to the overall length.

The solar array panels are 730 m long and 650 m wide. Two of these panels make up a voltage string (43.3 kV) when using a single junction cell. A single panel is capable of providing the necessary 43.3 kV when a multi-bandgap cell is used. The 650 m width consists of 26 strips, each 25 m wide. Sizing of the array is based on a solar constant at summer solstice (1311.5 W/m^2), and an end of life concentration ratio of 1.83, an operating temperature of 113°C and the design factors shown in Figure 1.2-19 (efficiency chain). The installed solar panel area is defined as 28.47×10^6 m^2 for the standard GaAs cell and 18.47×10^6 m^2 for the MBG cell. Total power from the solar array output is estimated to be 9.94 GW. Total transmitted power is 7.14 GW. System efficiency factors for both satellite configurations are indicated in Figure 1.2-19 (only the cell efficiency differs).

Table 1.2-9 presents a summary of the satellite mass for the two concepts.

End-Mounted Solid-State Antenna

The satellite concept utilizing end-mounted solid state antennas is shown in Figure 1.2-17. The basic characteristics are summarized in Table 1.2-10. The illustrated concept consists of a solar array, consisting of either single or dual junction solar cells, and dual solid-state microwave power transmitting antenna. In essence the satellite configuration consists of two end-mounted satellites, each providing one-half the total output, joined together in a back-to-back configuration, sharing a common central crossbeam structure. Overall dimensions of the array are 4200 m wide by 18,000 m long (12,000 m MBG), exclusive of antenna. Each antenna installation adds 2325 m. Thus the overall length is 22,650 m (16,650 m for MBG).

Blanket dimensions are 650 m wide by 690 m long (650×465 m for MBG cells). Total area is 32.3×10^6 m^2 for the single junction cell configuration and 21.2×10^6 m^2 for the dual junction (MBG) cell configuration. The antennas shown both utilize a 10 dB Gaussian shaped beam pattern to minimize side lobe power levels. Total power output from each half of the area is estimated as 5.73 GW. Total power transmitted from each antenna is estimated to be 3.68 GW. Total

Table 1.2-8. Satellite System Summaries—Alternate Concepts (June 1980)

	GaAs SOLAR CELL				GaAlAs/GaAs SOLAR CELL			
	REFERENCE	DUAL END-MOUNTED	DUAL SANDWICH	MAGNETRON	REFERENCE	DUAL END-MOUNTED	DUAL SANDWICH	MAGNETRON
SATELLITE								
TYPE	PLANAR	PLANAR	COMPOUND	PLANAR	PLANAR	PLANAR	COMPOUND	PLANAR
CR_E	1.83	1.83	5.2	1.83	1.83	1.83	5.2	1.83
DIMENSION (METERS)	4200 × 16,000	4200 × 18,000	6600 × 28,500	4200 × 15,000	4200 × 11,000	4200 × 12,000	TBD	4200 × 10,000
MASS ($\times 10^6$ KG)	31.63	39.97	20.53	26.80	25.97	35.57	16.39	21.533
SOLAR ARRAY/ANTENNA	DECOUPLED	DECOUPLED	SANDWICH	DECOUPLED	DECOUPLED	DECOUPLED	SANDWICH	DECOUPLED
NUMBER OF BAYS	30	36	-	30	30	36	-	30
SOLAR ARRAY								
NUMBER OF PANELS	60	72	-	60	58	70	-	60
PANEL DIMENSION (METERS)	650W×730L	650W×690L	1.83D (×2)	650W×700L	650L×490L	650W×465L	1.63D (×2)	650W×470L
AREA ($\times 10^6$ M^2)	28.47	32.29	5.26	27.3	18.47	21.16	4.17	18.33
GEN. POWER (GW)	9.94	11.46	4.82	9.8	9.94	11.46	6.11	9.8
ANTENNA								
TYPE	KLYSTRON	SOLID STATE	SOLID STATE	MAGNETRON	KLYSTRON	SOLID STATE	SOLID STATE	MAGNETRON
POWER OUTPUT (GW)	7.14	7.36	3.66	8.00	7.14	7.36	4.64	8.0
ILLUMINATION	10 dB GAUS.	10 dB GAUS.	UNIFORM	10 dB HANSEN	10 dB GAUS.	10 dB GAUS.	UNIFORM	10 dB HANSEN
APERTURE (KM)	~1.0	1.35	1.83 (×2)	0.92	~1.0	1.35	1.63 (×2)	0.92
UTILITY INTERFACE POWER (GW)	5.07	5.22	2.42	5.6	5.07	5.22	3.06	5.6
NO. OF SATELLITES ($P_T \lesssim 300$ GW)	60	58	125	54	60	58	98	54
MASS DENSITY (KG/KW_{UI})*	6.24	7.66	8.52	4.79	5.12	6.81	5.35	3.85

$^*KW_{UI}$ = KILOWATTS AT UTILITY INTERFACE NETWORK

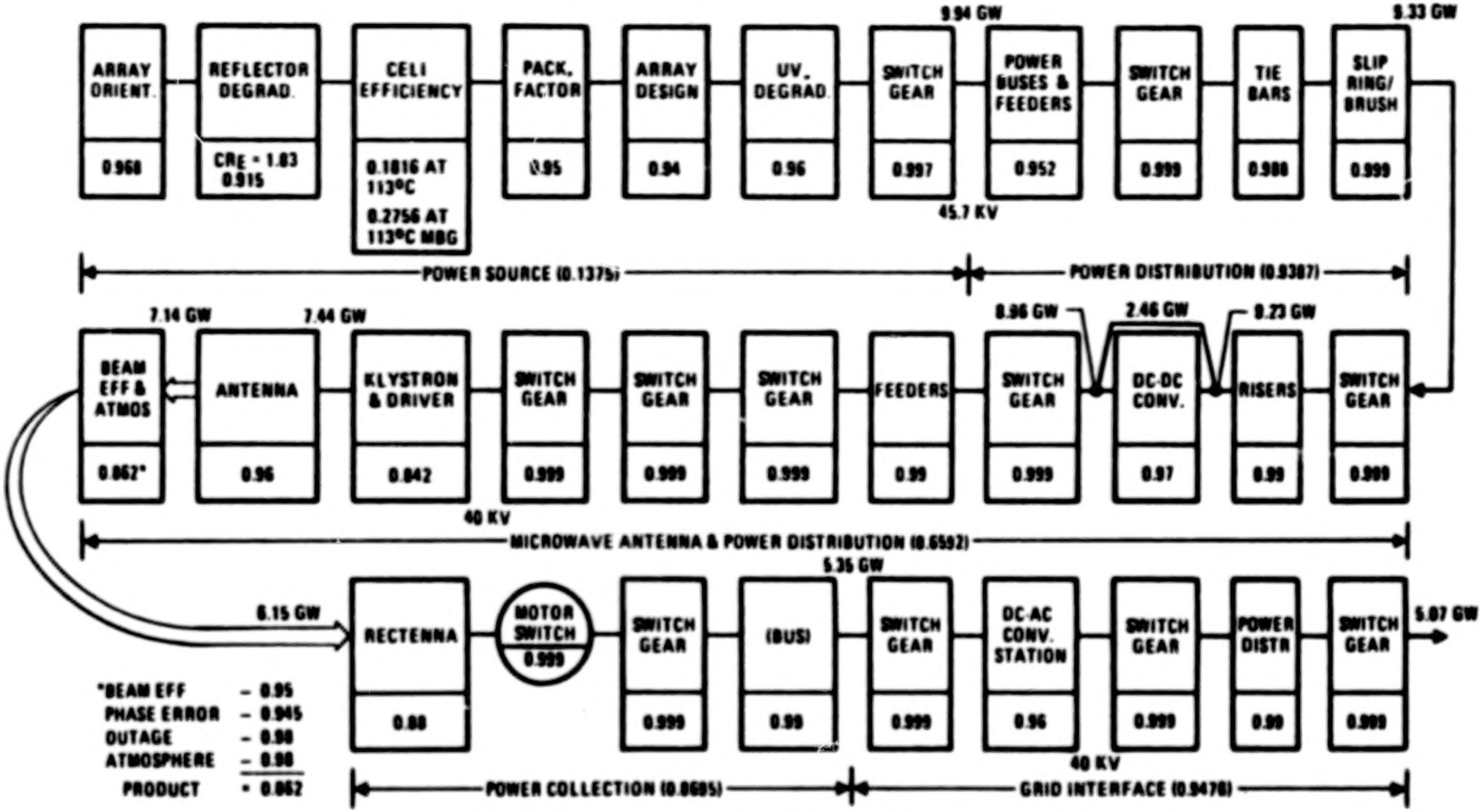
ARRAY ORIENT.
0.968
REFLECTOR DEGRAD.
CR_E = 1.83
0.915
CELL EFFICIENCY
0.1816 AT 113°C
0.2756 AT 113°C MBG
PACK. FACTOR
0.95
ARRAY DESIGN
0.94
UV. DEGRAD.
0.96
SWITCH GEAR
0.997
9.94 GW
45.7 KV
POWER BUSES & FEEDERS
0.952
SWITCH GEAR
0.999
TIE BARS
0.988
SLIP RING/ BRUSH
0.999
9.33 GW
POWER SOURCE (0.1375)
POWER DISTRIBUTION (0.9387)
7.14 GW
7.44 GW
BEAM EFF & ATMOS
0.862*
ANTENNA
0.96
KLYSTRON & DRIVER
0.842
SWITCH GEAR
0.999
SWITCH GEAR
0.999
SWITCH GEAR
0.999
FEEDERS
0.99
8.96 GW
2.46 GW
9.23 GW
SWITCH GEAR
0.999
DC-DC CONV.
0.97
RISERS
0.99
SWITCH GEAR
0.999
40 KV
MICROWAVE ANTENNA & POWER DISTRIBUTION (0.6592)
5.35 GW
6.15 GW
RECTENNA
0.88
MOTOR SWITCH
0.999
SWITCH GEAR
0.999
(BUS)
0.99
SWITCH GEAR
0.999
DC-AC CONV. STATION
0.96
SWITCH GEAR
0.999
POWER DISTR
0.99
SWITCH GEAR
0.999
5.07 GW
*BEAM EFF – 0.95
PHASE ERROR – 0.945
OUTAGE – 0.98
ATMOSPHERE – 0.98
PRODUCT = 0.862
40 KV
POWER COLLECTION (0.8695)
GRID INTERFACE (0.9476)

η_T = POWER SOURCE X POWER DIST. X MW ANT X POWER COLLECTION X GRID INTERFACE

13.75% 93.87% 65.92% 86.95% 94.76%

= 7.00%

Figure 1.2-19. System Efficient Chain—Reference Concept (April 1980)

Table 1.2-9. Mass Properties—Reference Concept
(April 1980)*

		STANDARD CELL GaAs	MBG CELL GaAlAs/GaAs
1.1.1	ENERGY CONVERSION (SOLAR ARRAY)		
	STRUCTURE	1.514	1.133
	PRIMARY	(0.928)	(0.804)
	SECONDARY	(0.586)	(0.329)
	MECHANISMS	0.070	0.070
	CONCENTRATOR	1.030	0.648
	SOLAR PANEL	7.174	4.804
	POWER DISTRIBUTION & CONTROL	2.757	1.388
	PWR COND. EQUIP. & BATT.	(0.319)	(0.206)
	POWER DISTRIBUTION	(2.438)	(1.182)
	THERMAL	NONE	NONE
	MAINTENANCE	0.092	0.063
1.1.3 (PARTIAL)	INFORMATION MANAGEMENT & CONTROL	0.050	0.050
	DATA PROCESSING	(0.021)	(0.021)
	INSTRUMENTATION	(0.029)	(0.029)
1.1.4 (PARTIAL)	ATTITUDE CONTROL	0.116	0.116
	SUBTOTAL	12.803	8.272
1.1.2	POWER TRANSMISSION (ANTENNA)		
	STRUCTURE	0.838	0.838
	PRIMARY	(0.023)	(0.023)
	SECONDARY	(0.815)	(0.815)
	MECHANISM	0.002	0.002
	SUBARRAY	7.050	7.050
	POWER DISTRIBUTION & CONTROL	2.453	2.453
	POWER COND. & BATT.	(1.680)	(1.680)
	POWER DISTRIBUTION	(0.773)	(0.773)
	THERMAL	0.720	0.720
	ANTENNA CONTROL ELECTRONICS	0.170	0.170
	MAINTENANCE	0.107	0.107
1.1.3 (PARTIAL)	INFORMATION MANAGEMENT & CONTROL	0.640	0.640
	DATA PROCESSING	(0.380)	(0.380)
	INSTRUMENTATION	(0.260)	(0.260)
1.1.4 (PARTIAL)	ATTITUDE CONTROL	NEGLIGIBLE	NEGLIGIBLE
	SUBTOTAL	11.980	11.980
1.1.6	INTERFACE		
	STRUCTURE	0.170	0.170
	PRIMARY	(0.136)	(0.136)
	SECONDARY	(0.034)	(0.034)
	MECHANISMS	0.033	0.033
	POWER DISTRIBUTION & CONTROL	0.288	0.288
	POWER DISTRIBUTION	(0.271)	(0.271)
	SLIP RING BRUSHES	(0.017)	(0.017)
	THERMAL	NONE	NONE
	MAINTENANCE	0.032	0.032
	COMMUNICATION	TBD	TBD
	SUBTOTAL	0.523	0.523
	SPS TOTAL (DRY)	25.306	20.775
	GROWTH (25%)	6.326	5.194
	TOTAL SPS (DRY) WITH GROWTH	31.632	25.969
	SATELLITE POWER @ UTILITY INTERFACE (GW)	5.07	5.07
	SATELLITE DENSITY, KG/KW$_{UI}$	6.24	5.12

* 10^6 kg

Table 1.2-10. Recommended End Mounted Solid State Antenna Concept Characteristics

- GaAs SOLAR ARRAY
- GEOMETRIC CR = 2.0
- DUAL END-MOUNTED MICROWAVE ANTENNAS
- AMPLIFIER BASE TEMPERATURE = 125°C
- AMPLIFIER EFFICIENCY = 0.8
- ANTENNA POWER TAPER = 10 dB
- ANTENNA DIAMETER = 1.35 km
- POWER AT UTILITY INTERFACE = 2.61 GW PER ANTENNA (5.22 GW TOTAL)
- RECTENNA BORESIGHT DIAMETER = 7.45 km PER RECTENNA

transmission power from the satellite is therefore 7.76 GW. System efficiencies for these configurations is shown in Figure 1.2-20.

Table 1.2-11 presents a summary of the mass properties for these configurations.

Sandwich Concept Solid-State Antenna

The solid-state sandwich antenna system concept is illustrated in Figure 1.2-18. The system consists of dual mirror configurations focusing solar energy upon the rear mounted solar cell blankets of the dual integrated solar cell/power transmitting antenna (sandwich). The primary mirror is pivoted and may be rotated about the reflected solar axis so that antenna will remain locked to the antenna/rectenna boresight while maintaining solar pointing during the 24 hour earth rotation and the ±23.5° variation in the solar/equatorial plane.

Characteristics of the single and multi-junction based antenna sandwich are summarized in Table 1.2-12. Total solar cell area of 2.63×10^6 m^2 and 2.09×10^6 m^2 is available. In this configuration solar cell area and antenna aperture area is the same. System efficiencies for these configurations is shown in Figure 1.2-21.

Table 1.2-13 presents a summary of the mass properties of both solar cell variations of the dual sandwich configuration.

Magnetron Concept

The satellite concept using magnetrons as microwave power amplifiers on the antenna is physically similar to the klystron based concept and therefore has the same general configuration as the reference concept (Figure 1.2-16). The array length of the concept, based upon a 20-kV (nominal) solar array voltage is 15,000 m (10,000 m MBG). Overall length including the antenna is 16,900 m (11,900 m MBG).

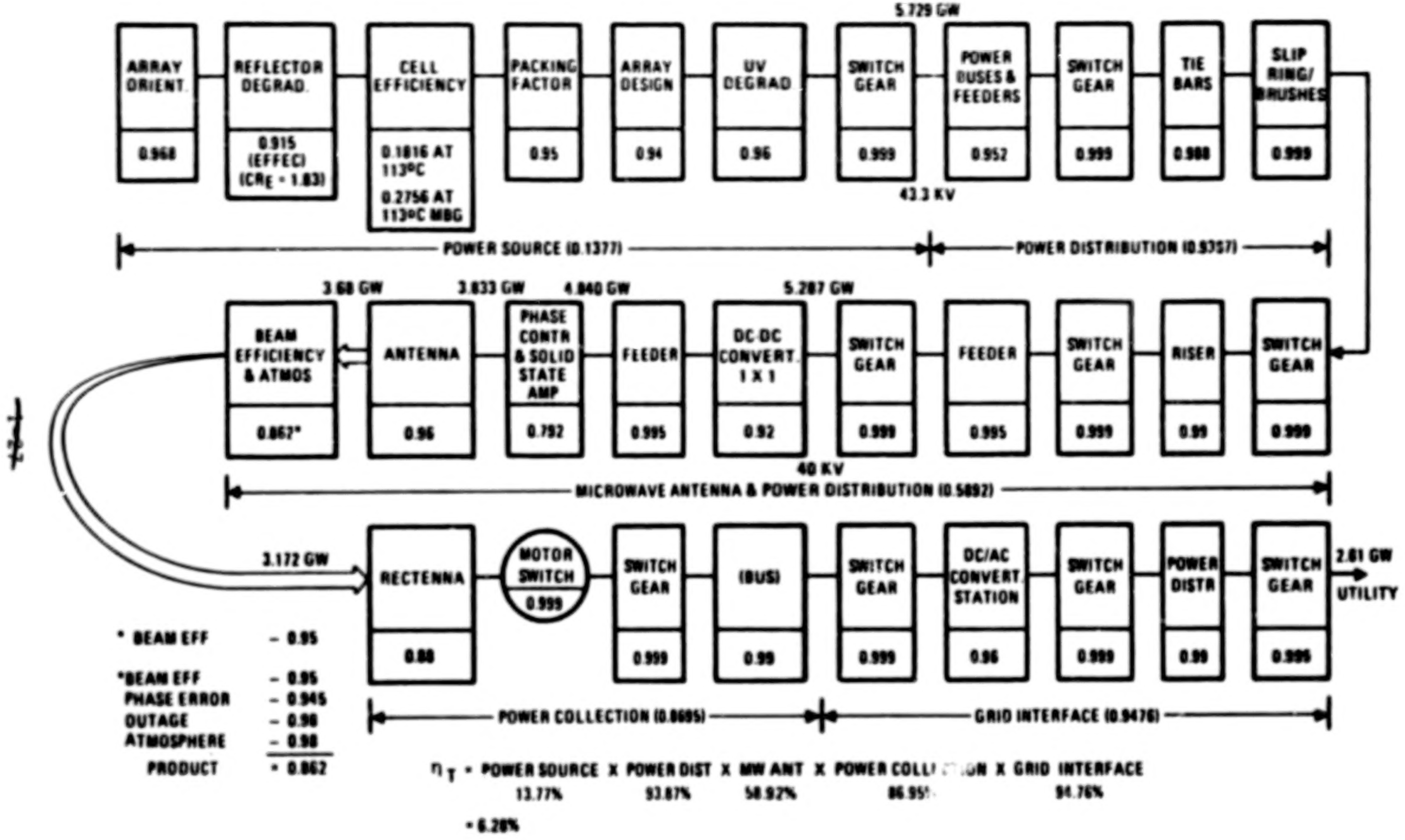
5.729 GW
ARRAY ORIENT.
0.968
REFLECTOR DEGRAD.
0.915 (EFFEC) (CR$_E$ = 1.83)
CELL EFFICIENCY
0.1816 AT 113°C
0.2756 AT 113°C MBG
PACKING FACTOR
0.95
ARRAY DESIGN
0.94
UV DEGRAD.
0.96
SWITCH GEAR
0.999
POWER BUSES & FEEDERS
0.952
SWITCH GEAR
0.999
TIE BARS
0.988
SLIP RING/ BRUSHES
0.999
43.3 KV
POWER SOURCE (0.1377)
POWER DISTRIBUTION (0.9757)
3.68 GW
3.833 GW
4.840 GW
5.287 GW
BEAM EFFICIENCY & ATMOS
0.862*
ANTENNA
0.96
PHASE CONTR & SOLID STATE AMP
0.792
FEEDER
0.995
DC-DC CONVERT. 1 X 1
0.92
SWITCH GEAR
0.999
FEEDER
0.995
SWITCH GEAR
0.999
RISER
0.99
SWITCH GEAR
0.999
40 KV
MICROWAVE ANTENNA & POWER DISTRIBUTION (0.5892)
3.172 GW
RECTENNA
0.88
MOTOR SWITCH
0.999
SWITCH GEAR
0.999
(BUS)
0.99
SWITCH GEAR
0.999
DC/AC CONVERT. STATION
0.96
SWITCH GEAR
0.999
POWER DISTR
0.99
SWITCH GEAR
0.995
2.81 GW
UTILITY
POWER COLLECTION (0.8695)
GRID INTERFACE (0.9476)
* BEAM EFF - 0.95
*BEAM EFF - 0.95
PHASE ERROR - 0.945
OUTAGE - 0.98
ATMOSPHERE - 0.98
PRODUCT = 0.862
η_T = POWER SOURCE X POWER DIST X MW ANT X POWER COLL[illegible]ION X GRID INTERFACE
13.77% 93.87% 58.92% 86.95[illegible] 94.76%
= 6.28%

Figure 1.2-20. System Efficiency Chain Dual End-Mounted Concept (Solid State Antenna) (April 1980)

Table 1.2-11. Mass Properties, Dual End-Mounted Solid-State Antenna*

		STD CELL GaAs	MBG CELL GaAlAs/GaAs
1.1.1	ENERGY CONVERSION (SOLAR ARRAY)		
	STRUCTURE	1.496	1.233
	PRIMARY	(1.077)	(0.902)
	SECONDARY	(0.419)	(0.331)
	MECHANISMS	0.087	0.078
	CONCENTRATOR	1.169	0.766
	SOLAR PANEL	8.138	5.607
	POWER DISTRIBUTION AND CONTROL	1.112	0.846
	POWER COND. EQUIP. & BATT.	(0.102)	(0.222)
	POWER DISTRIBUTION	(1.010)	(0.624)
	THERMAL	NONE	NONE
	MAINTENANCE	0.104	0.056
1.1.3 (PARTIAL)	INFORMATION MANAGEMENT AND CONTROL	0.057	0.057
	DATA PROCESSING	(0.024)	(0.024)
	INSTRUMENTATION	(0.033)	(0.033)
1.1.4 (PARTIAL)	ATTITUDE CONTROL	0.116	0.116
	SUBTOTAL	12.279	8.759
1.1.2	POWER TRANSMISSION (ANTENNA)		
	STRUCTURE	1.409	1.409
	PRIMARY	(0.094)	(0.094)
	SECONDARY	(1.315)	(1.315)
	MECHANISM	0.004	0.004
	SUBARRAY	10.561	10.561
	POWER DISTRIBUTION AND CONTROL	4.405	4.405
	POWER CONDITIONING & BATT.	(2.164)	(2.164)
	POWER DISTRIBUTION	(2.241)	(2.241)
	THERMAL	NONE	NONE
	ANTENNA CONTROL ELECTRONICS	0.340	0.340
	MAINTENANCE	0.448	0.448
1.1.3 (PARTIAL)	INFORMATION MANAGEMENT AND CONTROL	1.622	1.662
	DATA PROCESSING	(1.385)	(1.385)
	INSTRUMENTATION	(0.237)	(0.237)
1.1.4 (PARTIAL)	ATTITUDE CONTROL	NEGLIG.	NEGLIG.
	SUBTOTAL	18.789	18.789
1.1.6	INTERFACE		
	STRUCTURE	0.236	0.236
	PRIMARY	(0.168	(0.168)
	SECONDARY	(0.068)	(0.068)
	MECHANISMS	0.072	0.072
	POWER DISTRIBUTION AND CONTROL	0.538	0.538
	POWER DISTRIBUTION	(0.487)	(0.487)
	SLIP RING BRUSHES	(0.051)	(0.051)
	THERMAL	NONE	NONE
	MAINTENANCE	0.064	0.064
	COMMUNICATION	TBD	TBD
	SUBTOTAL	0.910	0.910
	SPS TOTAL (DRY)	31.978	28.458
	GROWTH (25%)	7.995	7.114
	TOTAL SPS (DRY) WITH GROWTH	39.973	35.572
	SATELLITE POWER @ UTILITY INTERFACE (GW)	5.22	5.22
	SATELLITE DENSITY, KG/KW_{UI}	7.66	6.81

$^*10^6$ kg

Table 1.2-12. Nominal Characteristics of Sandwich Concepts

	GaAs	GaAlAs/GaAs
UNIFORM ILLUMINATION EFFECTIVE (CR_E)	(0 dB TAPER) 5.2	(0 dB TAPER) 5.2
SOLAR CELL TEMPERATURE	200°C	200°C
SOLAR CELL EFFICIENCY	0.1566	0.2506
AMPLIFIER EFFICIENCY	0.8	0.8
AMPLIFIER BASE TEMPERATURE	125°C	125°C
ANTENNA OHMIC EFFICIENCY	0.96	0.96
SOLAR CELL PACKING FACTORS	0.8547	0.8547
POWER TRANSMITTED/UNIT AREA	778.9 W/m^2	1242 W/m^2
ANTENNA DIAMETER	1.83 km	1.63 km
ANTENNA AREA	2.63 km^2	2.09 km^2
TOTAL TRANSMITTED POWER	3.66 GW	4.64 GW
POWER AT UTILITY INTERFACE (EA.)	1.21 GW	1.53 GW
RECTENNA AXIS (EACH)	4.87×5.99 km	5.47×7.16 km
RECTENNA AREA (EACH)	23.2 km^2	31.3 km^2
ANTENNA DETAIL		
TYPE—DIPOLE WITH DIPOLE-MOUNTED AMPLIFIERS		
• ELEMENT SPACING	7.32 cm	7.81 cm
• NUMBER OF ELEMENTS/SQUARE METER	164	164
• OUTPUT POWER/DEVICE	4.24 W	6.77 W
• HEAT DISSIPATED DEVICE	1.06 W	1.69 W
• GROUND PLANE TO DIPOLE LENGTH	3.05 cm	3.05 cm
• BERLOX DISC DIAMETER	4.46 cm	6.09 cm
• BERLOX DISC AREA	15.62 cm^2	29.1 cm^2
• BERLOX DISC THICKNESS	0.0254 cm	0.0254 cm
• BERLOX DISC VOLUME	0.397 cm^3	0.740 cm^3

The solar array panels are 700 m long and 650 m wide, and generate 21.85 kV at the switch gear output. The solar array panels with MBG cells are 470 m long. As was the case with the klystron concept, the 650-m width consists of 26 strips, each 25 m wide. Total power from the solar array output is estimated to be 9.8 GW. Total transmitted power is calculated to be 8.00 GW. System efficiency factors for this configuration are indicated in Figure 1.2-22.

Table 1.2-14 summarizes the satellite mass properties.

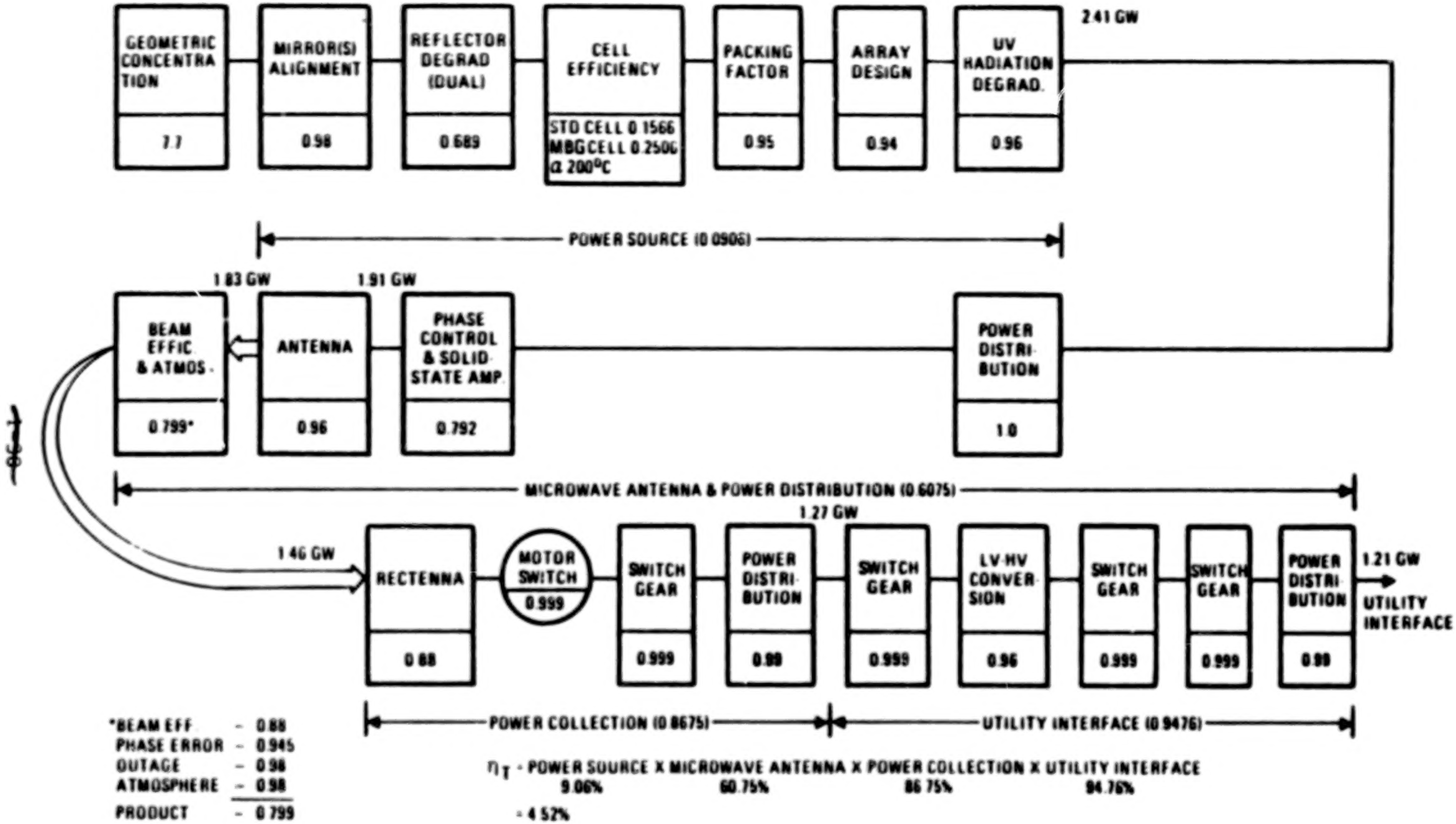
GEOMETRIC CONCENTRATION
7.7
MIRROR(S) ALIGNMENT
0.98
REFLECTOR DEGRAD (DUAL)
0.689
CELL EFFICIENCY
STD CELL 0.1566
MBG CELL 0.2506
@ 200°C
PACKING FACTOR
0.95
ARRAY DESIGN
0.94
UV RADIATION DEGRAD.
0.96
2.41 GW
POWER SOURCE (0.0906)
1.83 GW
1.91 GW
BEAM EFFIC & ATMOS.
0.799*
ANTENNA
0.96
PHASE CONTROL & SOLID STATE AMP.
0.792
POWER DISTRIBUTION
1.0
MICROWAVE ANTENNA & POWER DISTRIBUTION (0.6075)
1.27 GW
1.46 GW
RECTENNA
0.88
MOTOR SWITCH
0.999
SWITCH GEAR
0.999
POWER DISTRIBUTION
0.99
SWITCH GEAR
0.999
LV-HV CONVERSION
0.96
SWITCH GEAR
0.999
SWITCH GEAR
0.999
POWER DISTRIBUTION
0.99
1.21 GW
UTILITY INTERFACE
POWER COLLECTION (0.8675)
UTILITY INTERFACE (0.9476)
*BEAM EFF - 0.88
PHASE ERROR - 0.945
OUTAGE - 0.98
ATMOSPHERE - 0.98
PRODUCT - 0.799
η_T = POWER SOURCE X MICROWAVE ANTENNA X POWER COLLECTION X UTILITY INTERFACE
9.06% 60.75% 86.75% 94.76%
= 4.52%

Figure 1.2-21. System Efficiency Chain—Sandwich Concept (Solid-State Antenna) (April 1980)

Table 1.2-13. Mass Properties, Dual Sandwich Solid-State Antenna†

		STD CELL	MBG CELL
		GaAs	GaAlAs/GaAs
1.1.1	ENERGY CONVERSION (SOLAR ARRAY)		
	STRUCTURE	3.412	2.411
	PRIMARY	(3.026)	(2.138)
	SECONDARY	(0.386)	(0.273)
	MECHANISMS	0.027	0.019
	CONCENTRATOR	2.075	1.646
	SOLAR PANEL	0.076*	0.076*
	POWER DISTRIBUTION AND CONTROL	0.015	0.015
	POWER COND. EQUIP. & BATT.	(0.013)	(0.013)
	POWER DISTRIBUTION	(0.002)	(0.002)
	THERMAL	NONE	NONE
	MAINTENANCE	0.100	0.100
1.1.3	INFORMATION MANAGEMENT AND CONTROL	0.033**	0.033**
(PARTIAL)	DATA PROCESSING	(0.014)	(0.014)
	INSTRUMENTATION	(0.019)	(0.019)
1.1.4	ATTITUDE CONTROL	0.103	0.103
(PARTIAL)			
	SUBTOTAL	5.841	4.403
1.1.2	POWER TRANSMISSION (ANTENNA)		
	STRUCTURE	0.729	0.649
	PRIMARY	(0.161)	(0.143)
	SECONDARY	(0.568)	(0.506)
	MECHANISM	NONE	NONE
	SUBARRAY	8.821	7.053
	POWER DISTRIBUTION AND CONTROL	INCLUDED	INCLUDED
	THERMAL	NONE	NONE
	ANTENNA CONTROL ELECTRONICS	0.340	0.340
	MAINTENANCE	0.436	0.408
1.1.3	INFORMATION MANAGEMENT & CONTROL	0.256***	0.256***
(PARTIAL)	DATA PROCESSING	(0.152)	(0.152)
	INSTRUMENTATION	(0.104)	(0.104)
1.1.4	ATTITUDE CONTROL	NEGLIG.	NEGLIG.
(PARTIAL)			
	SUBTOTAL	10.582	8.706
1.1.6	INTERFACE		
	STRUCTURE	N/A	N/A
	PRIMARY		
	SECONDARY		
	MECHANISMS	N/A	N/A
	POWER DISTRIBUTION AND CONTROL	N/A	N/A
	POWER DISTRIBUTION		
	SLIP RING BRUSHES		
	THERMAL	N/A	N/A
	MAINTENANCE	-	-
	COMMUNICATION	TBD	TBD
	SUBTOTAL	-	-
	SPS TOTAL (DRY)	16.423	13.109
	GROWTH (25%)	4.106	3.277
	TOTAL SPS (DRY) WITH GROWTH	20.529	16.386
	SAT. PWR @ UTILITY INTERFACE (GW)	2.41	3.06
	SAT. DENSITY, KG/KW_{UI}	8.52	5.35

*AUXILIARY POWER ONLY

**TWO-THIRDS MASS OF REFERENCE CONCEPT

***20% REF. MASS PER ANTENNA

†10^6 kg

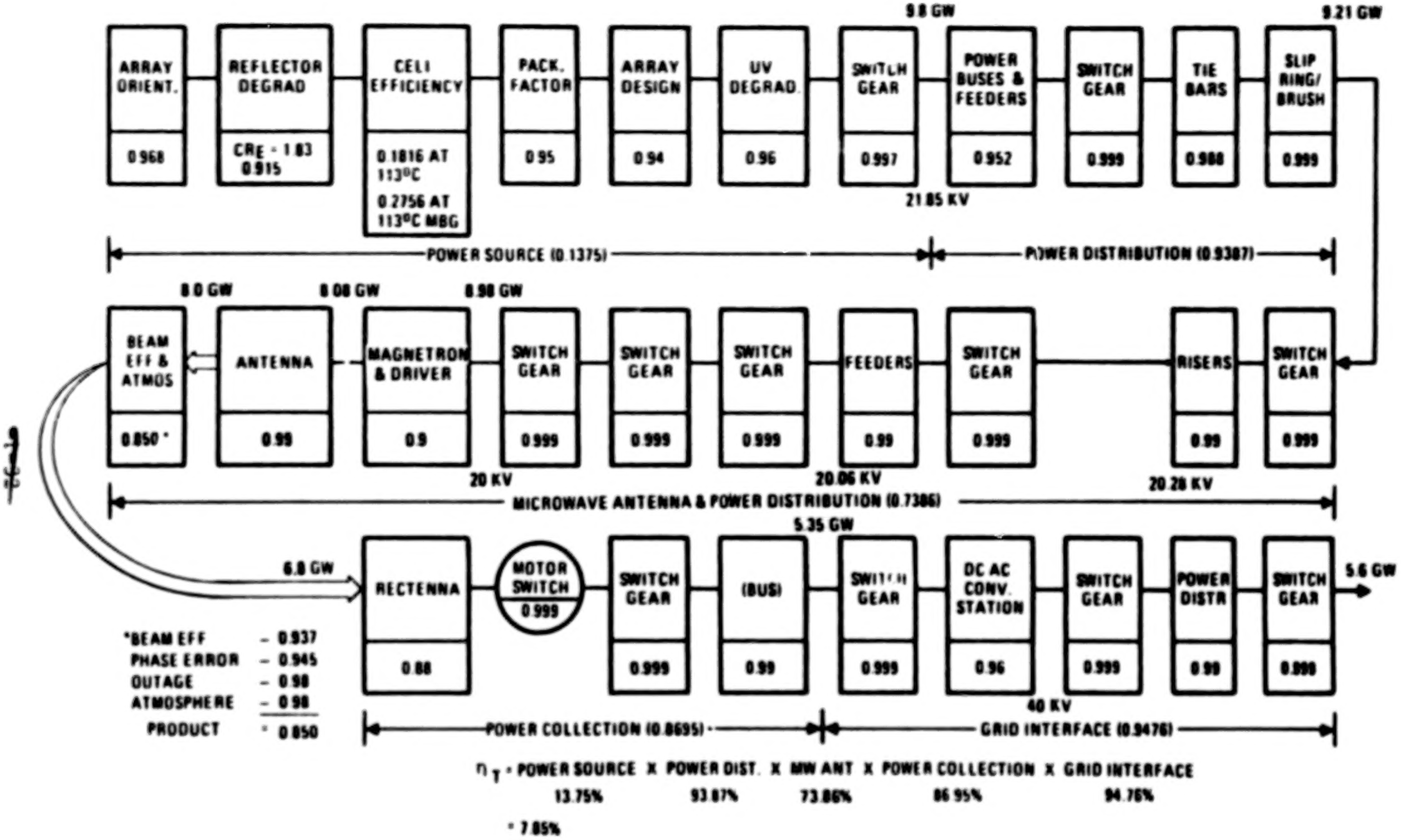
ARRAY ORIENT.
0.968
REFLECTOR DEGRAD
CR_E = 1.83
0.915
CELL EFFICIENCY
0.1816 AT 113°C
0.2756 AT 113°C MBG
PACK. FACTOR
0.95
ARRAY DESIGN
0.94
UV DEGRAD.
0.96
9.8 GW
SWITCH GEAR
0.997
21.85 KV
POWER BUSES & FEEDERS
0.952
SWITCH GEAR
0.999
TIE BARS
0.988
9.21 GW
SLIP RING/ BRUSH
0.999
POWER SOURCE (0.1375)
POWER DISTRIBUTION (0.9387)
8.0 GW
8.08 GW
8.98 GW
BEAM EFF & ATMOS
0.850 *
ANTENNA
0.99
MAGNETRON & DRIVER
0.9
SWITCH GEAR
0.999
SWITCH GEAR
0.999
SWITCH GEAR
0.999
FEEDERS
0.99
SWITCH GEAR
0.999
RISERS
0.99
SWITCH GEAR
0.999
20 KV
20.06 KV
20.28 KV
MICROWAVE ANTENNA & POWER DISTRIBUTION (0.7386)
5.35 GW
6.8 GW
RECTENNA
0.88
MOTOR SWITCH
0.999
SWITCH GEAR
0.999
(BUS)
0.99
SWITCH GEAR
0.999
DC AC CONV. STATION
0.96
SWITCH GEAR
0.999
POWER DISTR
0.99
SWITCH GEAR
0.999
5.6 GW
40 KV
*BEAM EFF – 0.937
PHASE ERROR – 0.945
OUTAGE – 0.98
ATMOSPHERE – 0.98
PRODUCT = 0.850
POWER COLLECTION (0.8695)
GRID INTERFACE (0.9476)
η_T = POWER SOURCE X POWER DIST. X MW ANT X POWER COLLECTION X GRID INTERFACE
13.75%
93.87%
73.86%
86.95%
94.76%
= 7.85%

Figure 1.2-22. System Efficient Chain—Magnetron Concept
(June 1980)

Table 1.2-14. Mass Properties—Magnetron Antenna (April 1980)

	STD CELL GaAs	MBG CELL GaAlAs/GaAs
	**	**
1.1.1 ENERGY CONVERSION (SOLAR ARRAY)		
STRUCTURE	1.601	1.245
PRIMARY	(0.904)	(0.565)
SECONDARY	(0.697)	(0.680)
MECHANISMS	0.070	0.070
CONCENTRATOR	0.988	0.663
SOLAR PANEL	6.880	4.619
POWER DISTRIBUTION & CONTROL	4.146	2.874
POWER COND. EQUIP. & BATT.	(0.319)	(0.319)
POWER DISTRIBUTION	(3.827)	(2.555)
THERMAL	NONE	NONE
MAINTENANCE	0.092	0.092
1.1.3* INFORMATION MANAGEMENT & CONTROL	0.050	0.050
DATA PROCESSING	(0.021)	(0.021)
INSTRUMENTATION	(0.029)	(0.029)
1.1.4* ATTITUDE CONTROL	0.116	0.116
SUBTOTAL	13.943	9.729
1.1.2 POWER TRANSMISSION (ANTENNA)		
STRUCTURE	0.547	0.547
PRIMARY	(0.023)	(0.023)
SECONDARY	(0.524)	(0.524)
MECHANISM	0.002	0.002
SUBARRAY	3.320	3.320
POWER DISTRIBUTION & CONTROL	1.515	1.515
POWER CONDITIONING & BATT.	(0.346)	(0.346)
POWER DISTRIBUTION	(1.169)	(1.169)
THERMAL	NONE	NONE
ANTENNA CONTROL ELECTRONICS	0.170	0.170
MAINTENANCE	0.107	0.107
1.1.3* INFORMATION MANAGEMENT AND CONTROL	0.320	0.320
DATA PROCESSING	(0.190)	(0.190)
INSTRUMENTATION	(0.130)	(0.130)
1.1.4* ATTITUDE CONTROL	NEGLIG.	NEGLIG.
SUBTOTAL	5.981	5.981
1.1.6 INTERFACE		
STRUCTURE	0.257	0.257
PRIMARY	(0.136)	(0.136)
SECONDARY	(0.121)	(0.121)
MECHANISMS	0.033	0.033
POWER DISTRIBUTION & CONTROL	1.194	1.194
POWER DISTRIBUTION	(1.177)	(1.177)
SLIP RING BRUSHES	(0.017)	(0.017)
THERMAL	NONE	NONE
MAINTENANCE	0.032	0.032
COMMUNICATION	TBD	TBD
SUBTOTAL	1.516	1.516
SPS TOTAL (DRY)	21.44	17.226
GROWTH (25%)	5.36	4.307
TOTAL SPS (DRY) WITH GROWTH	26.8	21.533
SAT. PWR @ UTILITY INTERFACE (GW)	5.6	5.6
SATELLITE DENSITY, KG/KW$_{UI}$	4.79	3.85

*PARTIAL **10^6 kg

1.3 TRANSPORTATION SYSTEM

Figure 1.3-1 illustrates the Rockwell Reference Transportation flight operations designed to deliver cargo and personnel to geosynchronous (GEO) orbit for SPS construction. Three SPS unique elements of the system are: the Heavy Lift Launch Vehicle (HLLV), the Electric Orbit Transfer Vehicle (EOTV), and the Personnel Orbit Transfer Vehicle (POTV). The HLLV is a two stage parallel burn launch vehicle utilizing LOX/RP in the first stage and LOX/LH_2 in the second stage. Second stage propellants are crossfed from the first stage during first stage burn. These stages take off from a vertical position and land horizontally in a manner similar to that of the Shuttle transportation system. Each HLLV launch can transport a 0.227×10^6 kg (0.500×10^6 lb) payload to low earth orbit (LEO).

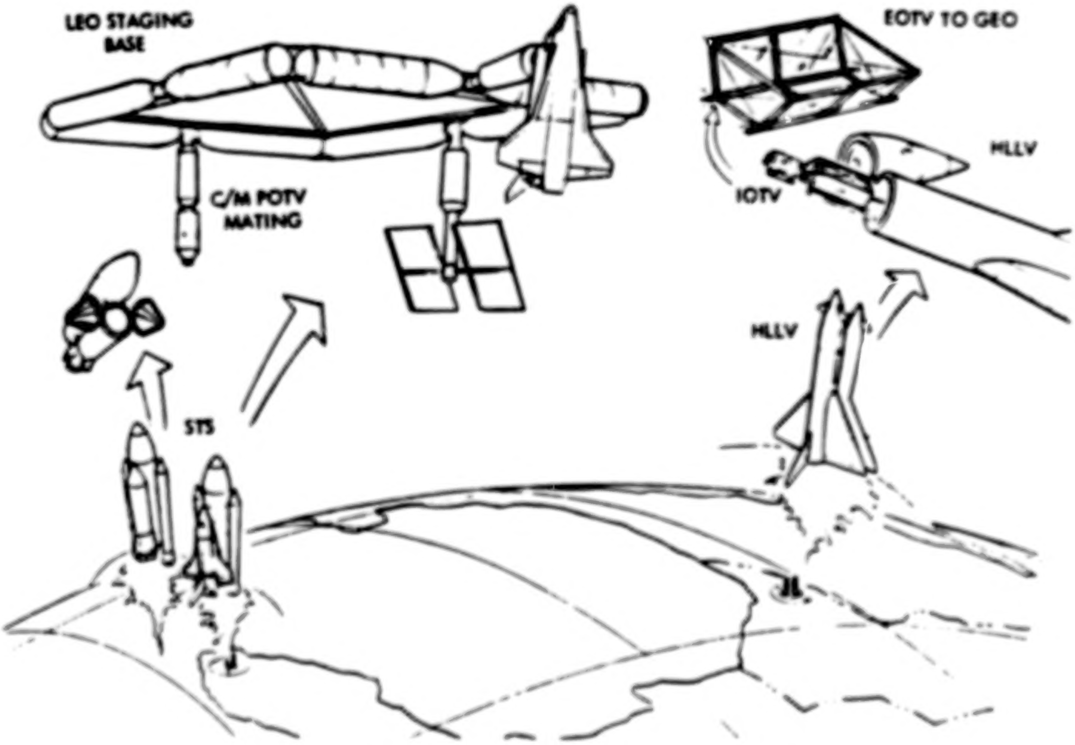

Figure 1.3-1. SPS Transportation System—LEO Operations Operational Program

A second major transportation element is the LEO-to-GEO cargo transfer vehicle, the EOTV. The EOTV consists of a basic solar array structure and electric (ion) thruster arrays by which as much as 6.86×10^6 kg of cargo can be transferred to a GEO—located construction site. A maximum EOTV load would therefore require approximately 25 HLLV missions. The same EOTV configuration has been retained for all satellite options.

A third vehicle is designed to transport personnel from the LEO staging area to and from the GEO site. The vehicle consists of a single chemical propulsion stage and a separable crew module. The propulsion element is refueled in GEO for return to LEO. Acceleration and operation restrictions are similar to those imposed for manned space vehicles.

Detail descriptions of the transportation elements are contained in Volume III.

1.4 PROGRAM GROUND RULES

Table 1.4-1 shows the program ground rules that affected the development of requirements. Table 1.4-2 shows the general requirements describing the overall SPS program.

Table 1.4-1. Program Ground Rules

IOC DATE: 2000
PROGRAM SIZE: 2030—300 GW (10 GW/YR)
SYSTEM LIFE: 30 YEARS
COSTS: 1979 CONSTANT DOLLARS (7.5% DISCOUNT RATE)
TECHNOLOGY BASE: 1990
SYSTEMS AVAILABLE IN THE 1980'S: SHUTTLE, IUS, & OTV

Table 1.4-2. General Requirements Describing Overall SPS Program

Programmatic	Technology
ENERGY SOURCE—Solar *CAPACITY*—Assume 2 units/year after initial buildup (300 GW Total) *LIFETIME*—30 years with minimum planned maintenance (should be capable of extended life beyond 30 years with replacement) *IOC*—2000 *BUILDUP*—Provide 10 GW (nominal)/year power buildup rate to utility interface *OPERATIONS*—Geosynchronous orbit; 0-degree inclination, circular (35,786-km altitude) *RESOURCES*—Minimum use of critical resources *COMMERCIALIZATION*—Compatible with U.S. utility networks *DEVELOPMENT*—Evolutionary, with provisions for incorporating later technology	*OUTPUT POWER*—Power level is defined as constant power level (except during solar eclipse) at utility interface (5 GW, nominal) *MAXIMUM RADIATION LEVELS*—Maximum radiation level at rectenna is 23 mW/cm^2; maximum radiation level at perimeter fence line is 1 mW/cm^2 *WEIGHT GROWTH*—25% *TOTAL WEIGHT*—All summary weight (totals) will be in term of kg/kW$_e$ *ENERGY STORAGE*—To support on-board satellite system operations only *CONSTELLATION*—Satellite space, 3 degrees *FAILURE CRITERIA*—No single point failure may cause total loss of SPS function *STORAGE*—One year on-board consumables storage without resupply *CONSTRUCTION*—Structural material to be graphite composite. *STARTUP/SHUTDOWN*—TBD

2.0 SYSTEM DESCRIPTION

2.1 GENERAL

The Satellite Power Systems (SPS) concept is based upon a large photovoltaic power collection satellite located in a Geosynchronous, Equatorial Orbit (GEO) utilizing a microwave power transmission concept to transmit the collected energy to Ground Receiving Stations (GRS) located at selected sites within or near the continental United States. The ground receiving sites then convert the received energy to a form compatible with local utility power networks where the available energy will contribute to the base load power capability of the network.

The basic features of the Rockwell satellites is the use of Gallium Arsenide solar cells at various concentration ratios to convert solar energy into its electrical equivalent; and klystron, magnetron or solid state power amplifiers as the means of developing the high power microwave beam necessary for the efficient transfer of energy from GEO. The ground system utilizes microstrip concepts to fabricate the ground-based receiving antenna (rectenna); uses a high power ground-based low-voltage dc to high-voltage ac or dc conversion concept based upon an existing utility system[1] located in Sylmar, California; and uses conventional utility company-type ground switching techniques.

2.1.1 SYSTEM

The system relationship of the total Satellite Power System is depicted in Figure 2.1-1. This document discusses only the first two elements; the satellite and ground systems.

A summary of the primary program ground rules followed in development of the various versions of the photovoltaic satellite is as follows:

- IOC Date: 2000
- Program Size: 300 GW by 2030 (10 GW per year, average)
- System Life: 30 years

The satellite may be considered to be made up of a solar pointing section, (associated with the conversion of solar energy to electrical energy), and an earth pointing section, (concerned with the conversion of electrical energy into its RF equivalent and the transmission of the RF to the associated ground receiver). The ground receiving station is treated as a single unit.

The point design photovoltaic reference and the baseline alternative concepts are shown in Figures 2.1-2 through 2.1-4. The planar SPS concepts (Figures 2.1-2 and 2.1-3) consist of a three trough configuration having reflective membranes at a a 60° slant angle. It has a single microwave antenna (magnetron or klystron), located at one end of the configuration, or two antennas (solid state), located at each end of the solar array.

---

[1] Southern California Edison

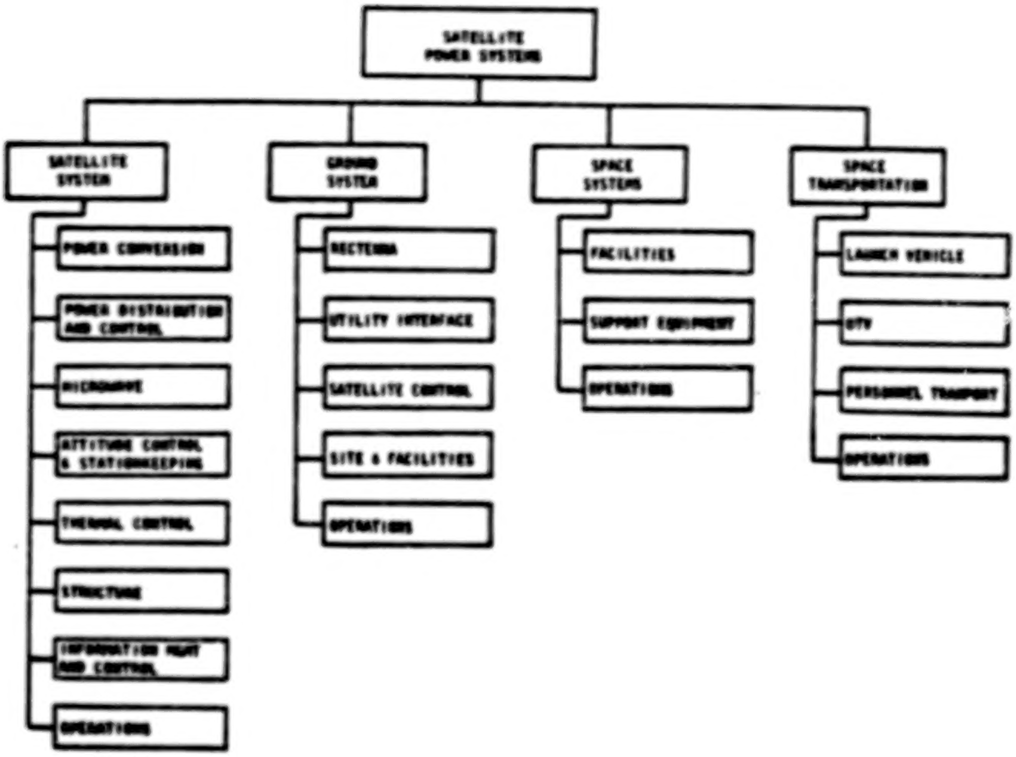
SATELLITE POWER SYSTEMS
SATELLITE SYSTEM
GROUND SYSTEM
SPACE SYSTEMS
SPACE TRANSPORTATION
POWER CONVERSION
POWER DISTRIBUTION AND CONTROL
MICROWAVE
ATTITUDE CONTROL & STATIONKEEPING
THERMAL CONTROL
STRUCTURE
INFORMATION MGMT AND CONTROL
OPERATIONS
RECTENNA
UTILITY INTERFACE
SATELLITE CONTROL
SITE & FACILITIES
OPERATIONS
FACILITIES
SUPPORT EQUIPMENT
OPERATIONS
LAUNCH VEHICLE
OTV
PERSONNEL TRANSPORT
OPERATIONS

Figure 2.1-1. SPS System Relationships

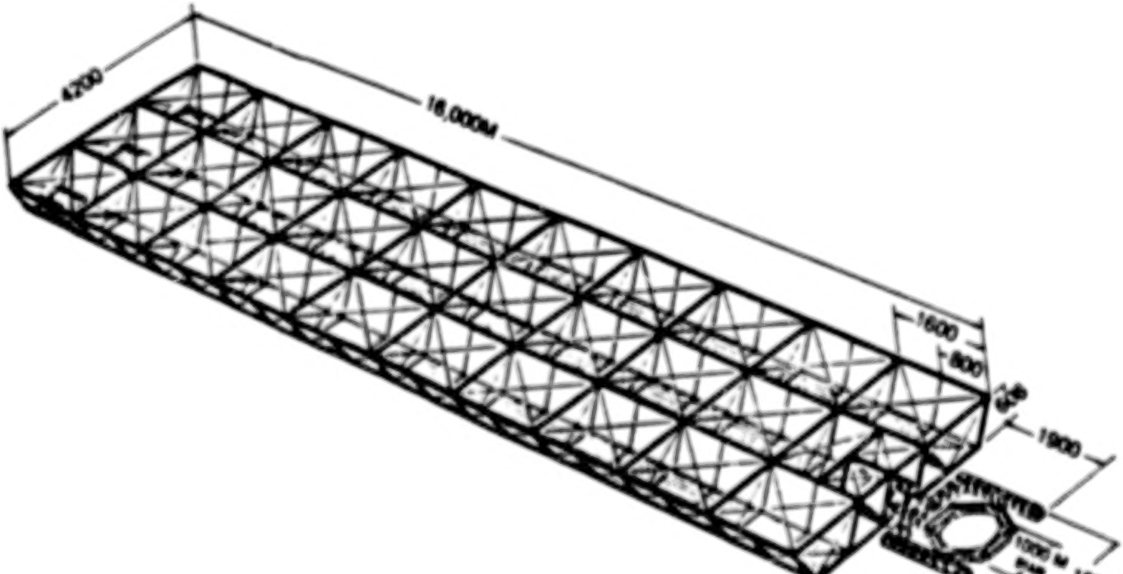
4200
18,000M
1600
800
600
1900
1000 M DIAM
1800

Figure 2.1-2. Solar Power Satellite—Reference Configuration

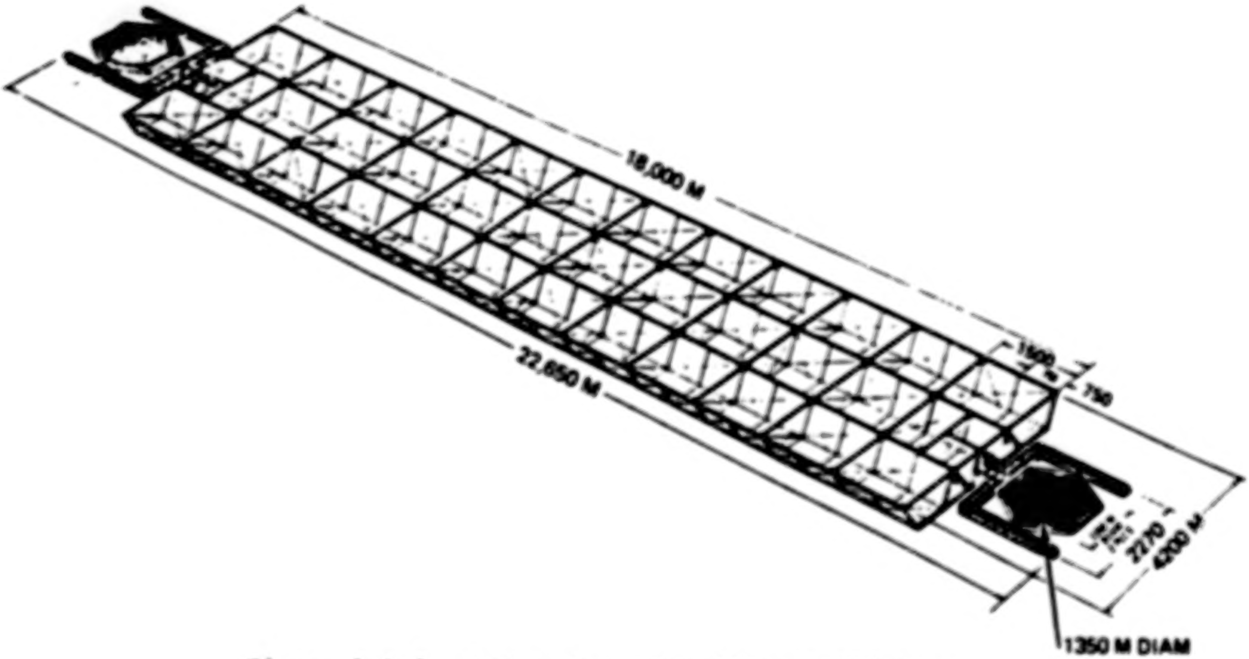
18,000 M
22,650 M
1500
750
2270
4200 M
1350 M DIAM

Figure 2.1-3. Solar Power Satellite Solid State Dual End Mounted Antenna

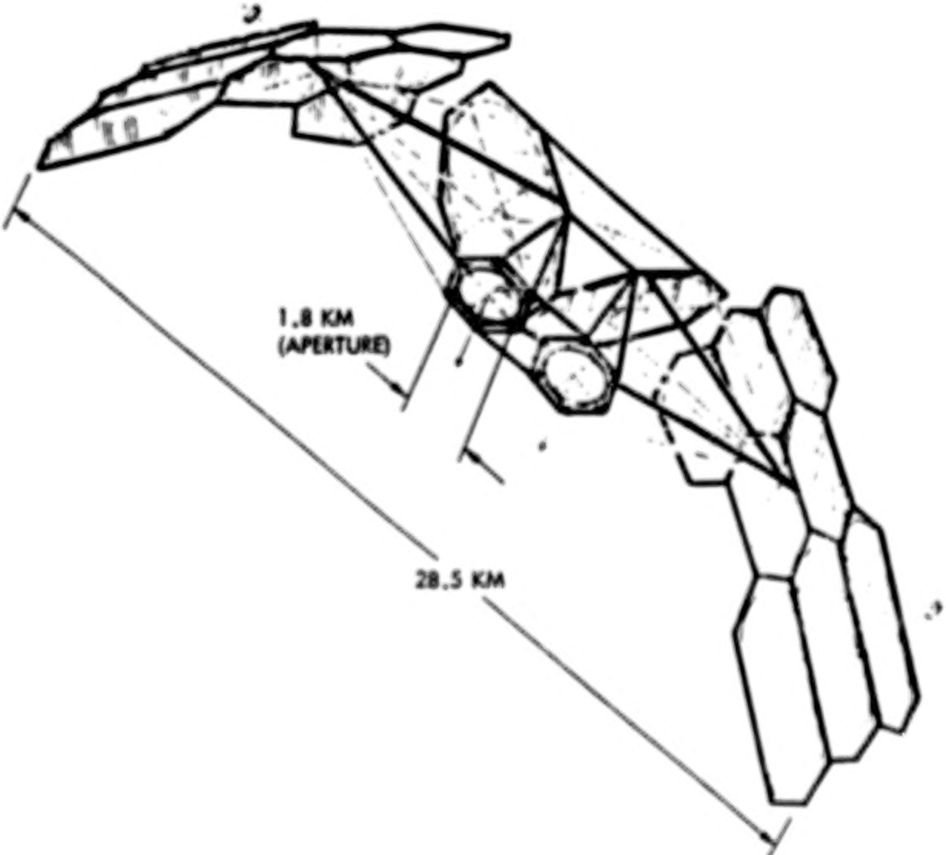
1.8 KM
(APERTURE)
28.5 KM

Figure 2.1-4. Solid State Point Design Satellite Concept

In geosynchronous orbit the longitudinal axis of the SPS is oriented perpendicular to the orbital plane. The reference design is based on construction in GEO.

The ground receiving station (GRS) consists of two major system elements and several additional supporting subsystems (Figure 2.1-5). The first is the receiving antenna/rectifier circuit (rectenna) portion of the Microwave Power Transmission System. A second major element consists of the power distribution subsystems required to collect, switch, converter, and transfer and received/rectifier power to the associated utility power network.

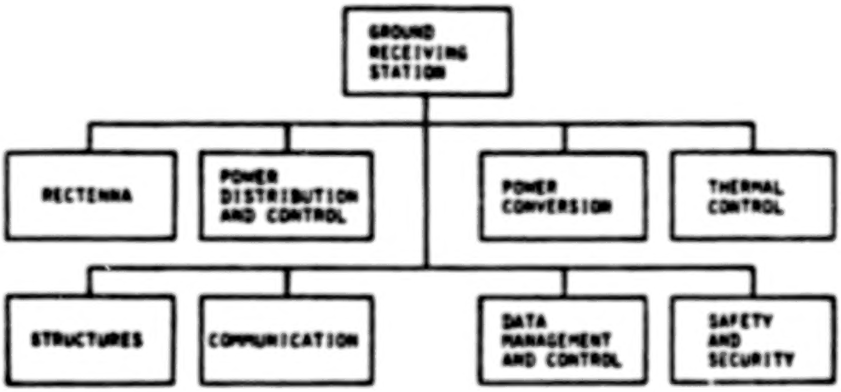

Figure 2.1-5. Ground Receiving Station
Subassembly Relationships

Each rectenna is designed to accept power from a single satellite and provide 1-5 GW (nominal) at the interface to the power distribution subsystem. As shown in Figure 2.1-6, the typical GRS site located at 34° N latitude includes an elliptical rectenna area, oriented with the major axis in the N-S direction. The overall GRS (for the reference concept) would utilize approximately 35,000 acres. The rectenna area consists of approximately 25,200 acres or 72% of the total acreage. The area surrounding the inner ellipse is utilized for maintenance facilities, access roads, converter stations and the two peripheral rows of towers which support the intermediate (40 kV dc) and high voltage (500 kV ac) transmission wires.

While communications have not been specifically studied in this preliminary analysis, a number of implications have been drawn. The satellite must be capable of maintaining continuous contact with the GRS control center. This includes voice, data, video, and commands in both directions. In addition, the uplink pilot beam from the GRS is crucial to acquisition and fine pointing. The high EMI environment in the near vicinity of the satellite imposes difficult conditions for communications. This requires primary emphasis and special design considerations.

Functional requirements for the photovoltaic SPS are summarized in Table 2.1-1. Primary operational requirements are summarized in Table 2.1-2.

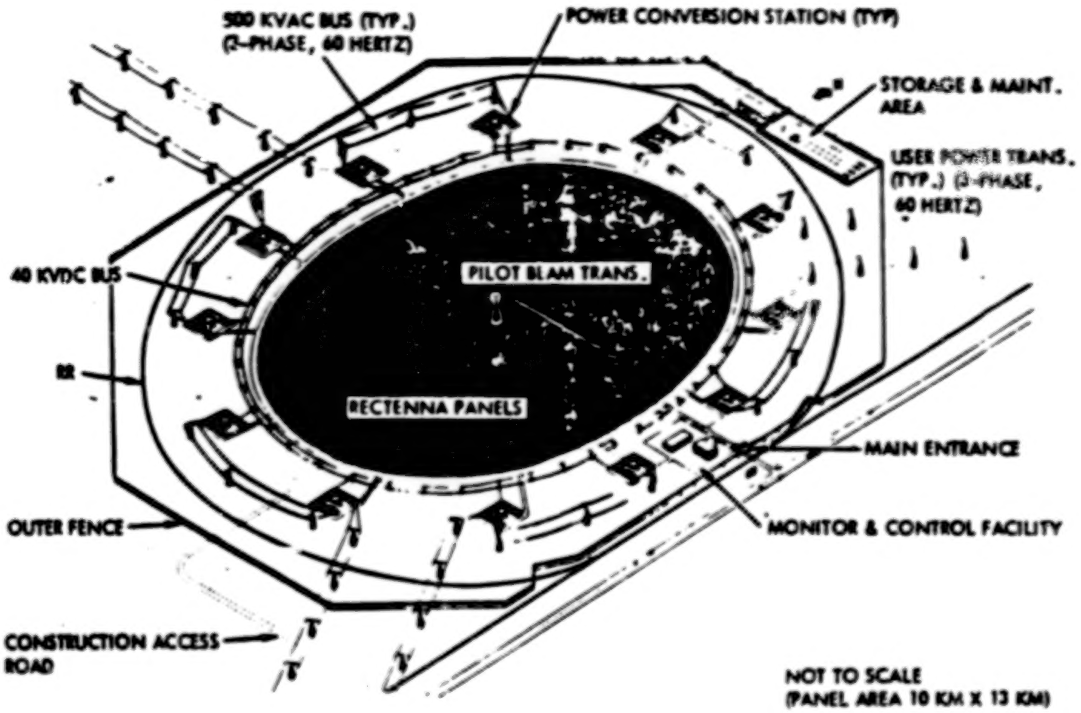
500 KVAC BUS (TYP.)
(3-PHASE, 60 HERTZ)
POWER CONVERSION STATION (TYP)
STORAGE & MAINT. AREA
USER POWER TRANS. (TYP.) (3-PHASE, 60 HERTZ)
40 KVDC BUS
PILOT BEAM TRANS.
RR
RECTENNA PANELS
MAIN ENTRANCE
MONITOR & CONTROL FACILITY
OUTER FENCE
CONSTRUCTION ACCESS ROAD
NOT TO SCALE
(PANEL AREA 10 KM X 13 KM)

Figure 2.1-6. Operational Ground Receiving Facility (Rectenna) - Typical

Table 2.1-1. Point Design Solar Array Functional Requirements

PROGRAMMATIC	
ENERGY SOURCE	SOLAR
CAPACITY	5 GW DELIVERED TO UTILITY NETWORKS
LIFETIME	30 YEARS WITH MINIMUM PLANNED MAINTENANCE (SHOULD BE CAPABLE OF EXTENDED LIFE BEYOND 30 YEARS WITH REPLACEMENT)
IOC DATE	2000
OPERATIONS	GEOSYNCH ORBIT; 0-DEG INCLIN, CIRCULAR (35,786 km ALTITUDE)
RESOURCES	MINIMUM USE OF CRITICAL RESOURCES
COMMERCIALIZATION	COMPATIBLE WITH U.S. UTILITY NETWORKS
DEVELOPMENT	EVOLUTIONARY WITH PROVISIONS FOR INCORPORATING LATER TECHNOLOGY
TECHNOLOGY	
OUTPUT POWER	POWER LEVEL IS DEFINED AS CONSTANT POWER LEVEL (EXCEPT DURING SOLAR ECLIPSE
WEIGHT GROWTH	25%
ENERGY STORAGE	TO SUPPORT ON-BOARD SATELLITE SYSTEM OPERATIONS ONLY
FAILURE CRITERIA	NO SINGLE POINT FAILURE MAY CAUSE TOTAL LOSS OF SPS FUNCTION
ENERGY PAYBACK	LESS THAN 3 YR
COST	COMPETITIVE WITH GRND-BASED PWR GENERATION WITHIN LIFETIME OF SPS PROJECT
STORAGE	ONE YEAR ON-BOARD CONSUMABLE STORAGE WITHOUT RESUPPLY

Table 2.1-2. Point Design Solar Array
Functional Requirements—Operations

MODE	ASSEMBLY	FUNCTIONS
CONSTRUCTION	SUBSYSTEM	NONE
INTER-ORBIT TRANSFER	SUBSYSTEM	NONE
OPERATIONS	SUBSYSTEM REFLECTOR	STEADY STATE OPERATION SIZED FOR EOL POWER RATING
ECLIPSE	SUBSYSTEM	SHUT DOWN BEFORE ENTERING ECLIPSE STANDBY (ZERO POWER) TURN ON AFTER LEAVING ECLIPSE AND ARRAYS REACH EQUILIBRIUM TEMPERATURE
	BATTERIES	SUPPLY POWER FOR ESSENTIAL FUNCTIONS
FAILURE/MAINTENANCE	SUBSYSTEM	REDUNDANT OPERATION, AUTO SHUTDOWN, MANUAL STARTUP
	POWER MODULE*	SHUT DOWN AND ISOLATE FAILED MODULE, REPLACE SOLAR CELL BLANKET AND/OR REFLECTOR
CHECKOUT	SUBSYSTEM	FAIL-SAFE CHECKS; CONTROL RESPONSE

*SOLAR CELL/BLANKET/REFLECTOR MODULE

A factor which must be considered when evaluating operational requirements are the solar eclipses which occur during the spring and autumn and last for up to 1.2 hours. Figure 2.1-7 shows the expected ecliptic periods and their duration as a function of the calendar year. For rectenna sites in the northern hemisphere the eclipses will be centered about midnight.

Figure 2.1-8 presents a typical efficiency chain for the overall SPS and indicates the relative efficiencies of each of the major sub-elements of the system.

Mass Properties

Satellite mass properties are summarized in Section 2.5.

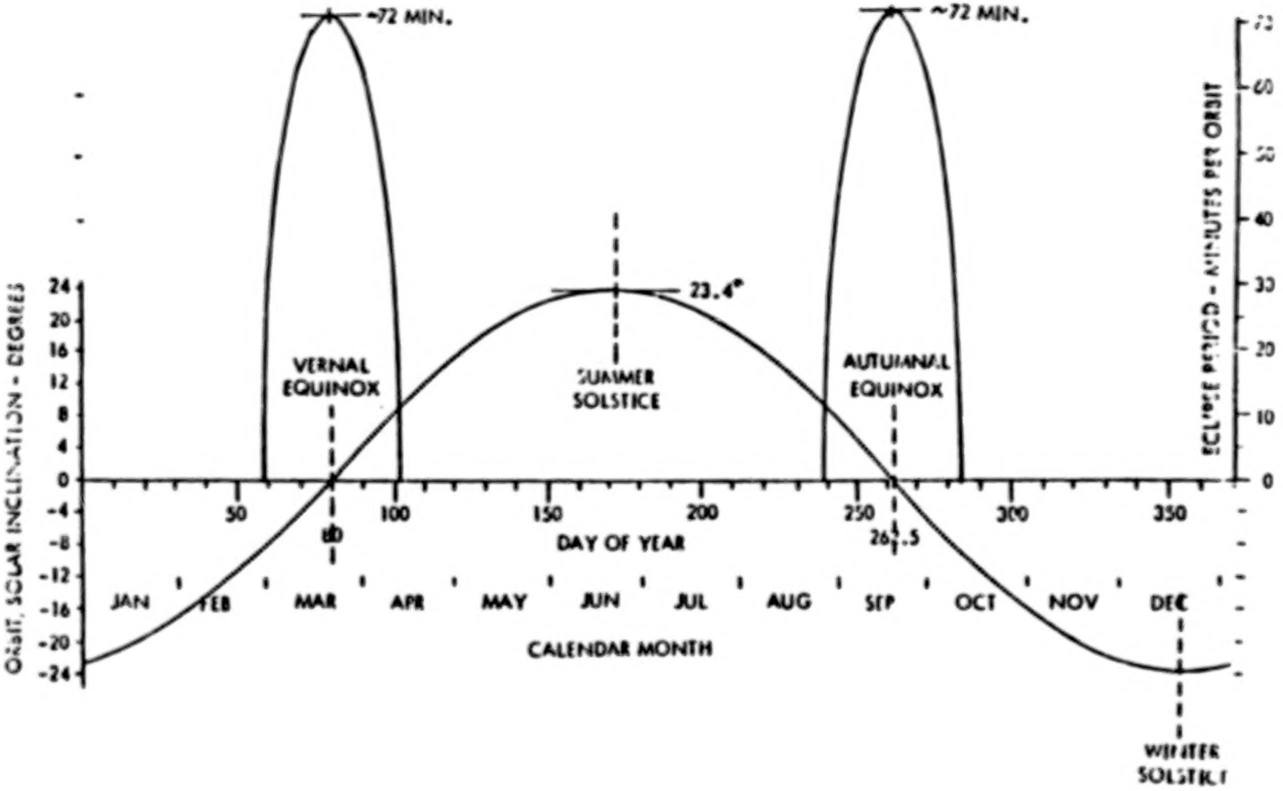

Figure 2.1-7. Eclipse Periods for Geosynchronous Circular Orbits

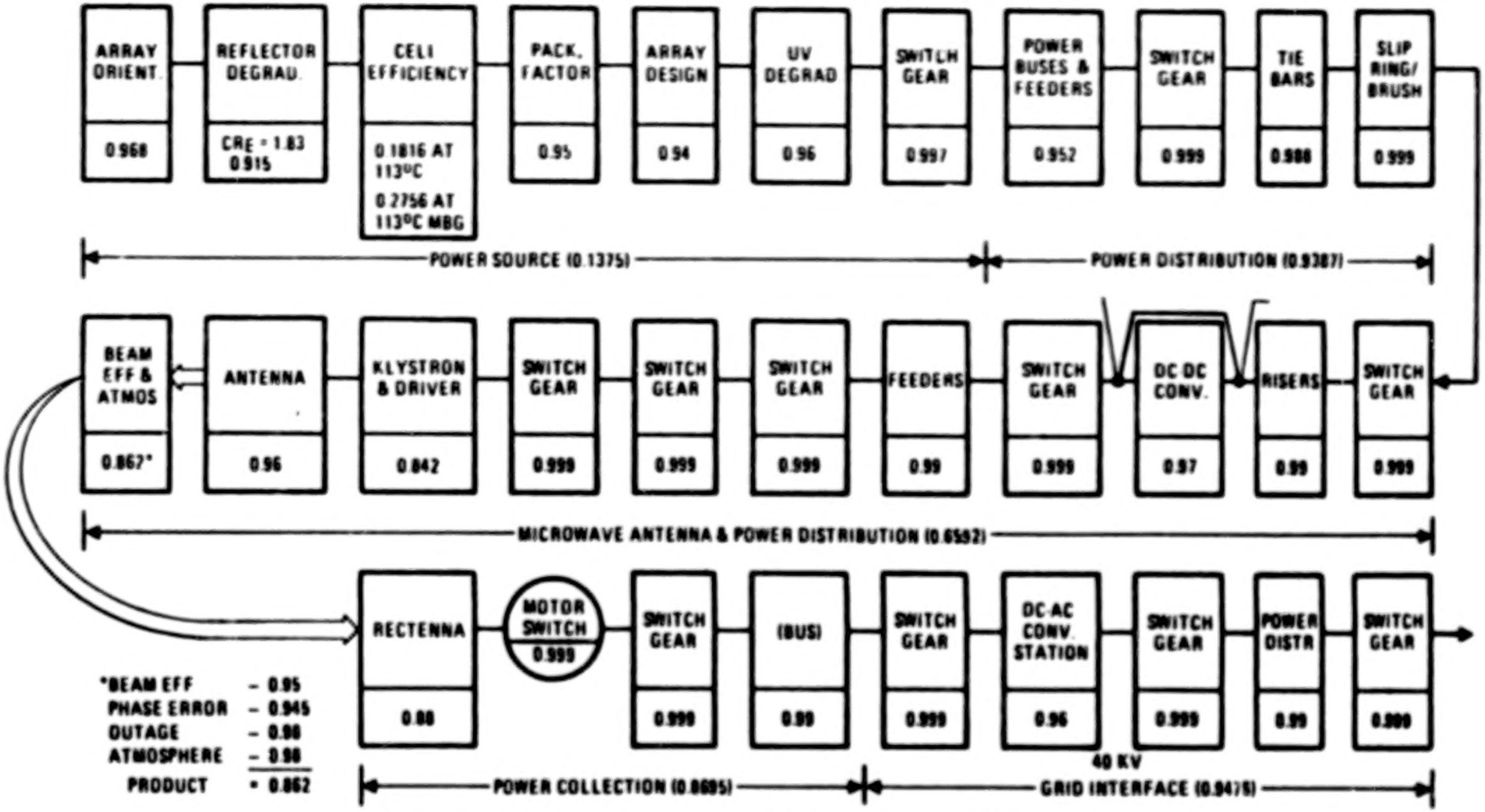
ARRAY ORIENT.
0.968
REFLECTOR DEGRAD.
CR$_E$ = 1.83
0.915
CELL EFFICIENCY
0.1816 AT 113°C
0.2756 AT 113°C MBG
PACK. FACTOR
0.95
ARRAY DESIGN
0.94
UV DEGRAD
0.96
SWITCH GEAR
0.997
POWER BUSES & FEEDERS
0.952
SWITCH GEAR
0.999
TIE BARS
0.988
SLIP RING/ BRUSH
0.999
POWER SOURCE (0.1375)
POWER DISTRIBUTION (0.9387)
SWITCH GEAR
0.999
RISERS
0.99
DC-DC CONV.
0.97
SWITCH GEAR
0.999
FEEDERS
0.99
SWITCH GEAR
0.999
SWITCH GEAR
0.999
SWITCH GEAR
0.999
KLYSTRON & DRIVER
0.842
ANTENNA
0.96
BEAM EFF & ATMOS
0.862*
MICROWAVE ANTENNA & POWER DISTRIBUTION (0.6592)
RECTENNA
0.88
MOTOR SWITCH
0.999
SWITCH GEAR
0.999
(BUS)
0.99
SWITCH GEAR
0.999
DC-AC CONV. STATION
0.96
SWITCH GEAR
0.999
POWER DISTR
0.99
SWITCH GEAR
0.999
40 KV
POWER COLLECTION (0.8695)
GRID INTERFACE (0.9476)

*BEAM EFF - 0.95
PHASE ERROR - 0.945
OUTAGE - 0.98
ATMOSPHERE - 0.98
PRODUCT = 0.862

η_T = POWER SOURCE X POWER DIST. X MW ANT X POWER COLLECTION X GRID INTERFACE
13.75% 93.87% 65.92% 86.95% 94.76%
= 7.00%

Figure 2.1-8. Typical Photovoltaic Efficiency Chain

2.2 SATELLITE

The satellite concepts developed by Rockwell International all consist of large-area photovoltaic energy converters located in a geosynchronous equatorial orbit (GEO), and utilize a microwave power transmission concept to transmit the collected energy to ground receiving stations (GRS) located at selected sites within or near the continental United States. Laser systems have been examined to determine their adaptability to the power transmission function[1], but for the present the microwave approach remains the selected concept.

Three basic system approaches for satellite implementation have been considered—all based upon the means by which the low-level RF reference signals are amplified to produce the high-power microwave transmission beams. These three approaches consider (1) klystrons, (2) magnetrons, and (3) solid-state amplifiers. The third approach (solid-state amplification) is further divided into (1) an approach that assumes power is collected independently of the microwave antenna, and (2) an approach that combines the solar photovoltaic energy conversion and the microwave antenna into a single back-to-back or "sandwich" configuration.

As part of the overall satellite evaluation, the analyses also included the analysis of the effects of using a more sophisticated solar cell as the means of collecting solar energy. In this study, this took the form of considering a two-junction GaAlAs/GaAs solar cell as well as the standard single-junction GaAs solar cell.

The following sections of this report describe these approaches in greater detail.

2.2.1 REFERENCE SYSTEM DEFINITION

General

The basic features of the Rockwell reference satellite are the use of gallium arsenide solar cells at a concentration ratio of 2 (CR-2) (nominal) to convert solar energy into its electrical equivalent, and 50-kW (nominal) klystron power amplifiers as the means of developing the high-power microwave beam necessary to the efficient transfer of energy from GEO.

The major satellite subsystems indicated in Figure 2.1-1 are briefly discussed in the following paragraphs and in more detail in Section 3.0.

The satellite may be considered to be made up of a solar pointing section (associated with the conversion of solar energy to electrical energy) and an earth pointing section (concerned with the conversion of electrical energy into its RF equivalent and the transmission of the RF to the associated ground receiver).

The reference (GaAs) photovoltaic concept is shown in Figure 2.2-1; it has been designed to supply 5 GW (nominal) of electrical power to the utility grid on the ground. The SPS is a three-trough configuration having reflective membranes at a 60-degree slant angle. It has a single microwave antenna, located at the end of the configuration. The overall dimensions of the SPS troughs are approximately: (1) length, 16.0 km; (2) width, 4.2 km; and (3) depth, 0.606 km. The mass is estimated to be 31.6×10⁶ kg, and includes a 25% growth factor.

---

[1] *SPS Laser Studies*, SSD 80-0119, Volumes I and II, Rockwell International, August 1980.

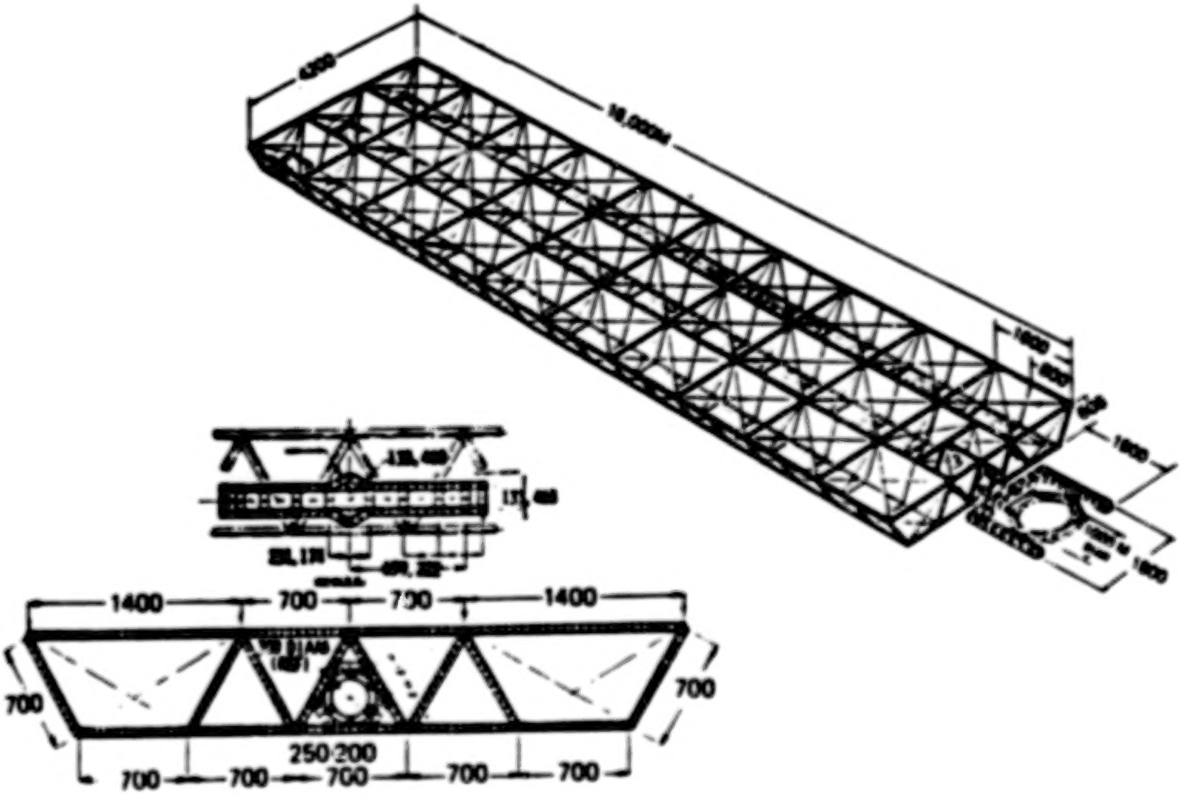

Figure 2.2-1. Reference Configuration, Single End-Mounted Tension Web Antenna with Klystron Antenna

The satellite length of the variation using dual-junction (MBG) solar cells is reduced to 11,000 m. Vehicle mass is estimated as 26×10⁶ kg, including the 25% growth allowance.

In geosynchronous orbit, the longitudinal axis of the SPS is oriented perpendicular to the orbital plane. The reference design is based on construction in GEO.

Figure 1.2-19 presents the basic efficiency of the overall reference SPS concept and indicates the relative efficiencies of each of the major subelements of the system. Overall efficiency of the reference system is shown to be approximately 7.0%.

A detailed satellite mass property summary for the reference configuration is shown in Section 2.5.

Reference Satellite Subsystems

The reference satellite is comprised of seven major subsystems, as shown in Figure 2.2-2. Attitude control directly affects power generation efficiency and includes satellite-rectenna pointing. Power generation, distribution and transmission are dominant functions, while thermal control is essential to dissipation of the large amounts of waste heat. Coordination of satellite functions and operations is performed by the information management and control subsystem (IMCS) as shown in Figure 2.2-3.

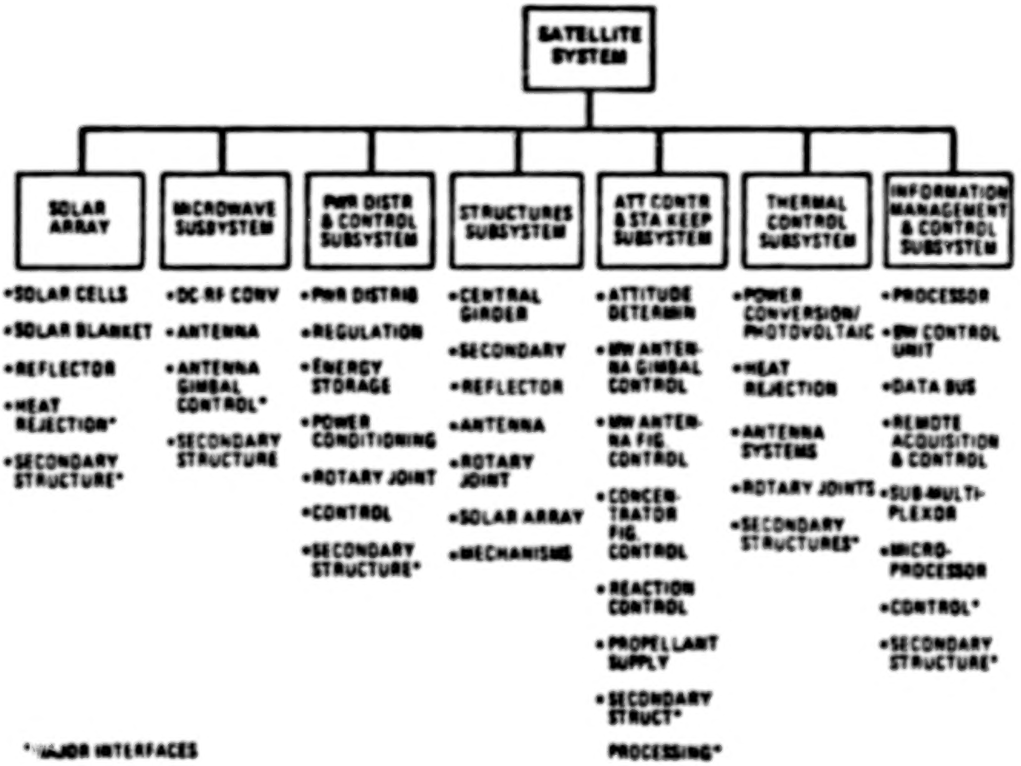
SATELLITE SYSTEM
SOLAR ARRAY
MICROWAVE SUBSYSTEM
PWR DISTR & CONTROL SUBSYSTEM
STRUCTURES SUBSYSTEM
ATT CONTR & STA KEEP SUBSYSTEM
THERMAL CONTROL SUBSYSTEM
INFORMATION MANAGEMENT & CONTROL SUBSYSTEM
•SOLAR CELLS
•SOLAR BLANKET
•REFLECTOR
•HEAT REJECTION*
•SECONDARY STRUCTURE*
•DC-RF CONV
•ANTENNA
•ANTENNA GIMBAL CONTROL*
•SECONDARY STRUCTURE
•PWR DISTRIB
•REGULATION
•ENERGY STORAGE
•POWER CONDITIONING
•ROTARY JOINT
•CONTROL
•SECONDARY STRUCTURE*
•CENTRAL GIRDER
•SECONDARY
•REFLECTOR
•ANTENNA
•ROTARY JOINT
•SOLAR ARRAY
•MECHANISMS
•ATTITUDE DETERMIN
•MW ANTENNA GIMBAL CONTROL
•MW ANTENNA FIG. CONTROL
•CONCENTRATOR FIG. CONTROL
•REACTION CONTROL
•PROPELLANT SUPPLY
•SECONDARY STRUCT*
PROCESSING*
•POWER CONVERSION/ PHOTOVOLTAIC
•HEAT REJECTION
•ANTENNA SYSTEMS
•ROTARY JOINTS
•SECONDARY STRUCTURES*
•PROCESSOR
•MW CONTROL UNIT
•DATA BUS
•REMOTE ACQUISITION & CONTROL
•SUB-MULTIPLEXOR
•MICRO-PROCESSOR
•CONTROL*
•SECONDARY STRUCTURE*
*MAJOR INTERFACES

Figure 2.2-2. Satellite Subsystems

All subsystems support the mission functions of power generation, distribution, and transmission. Electrical power output from the solar panels is fed via switch gears into feeder buses and then into main distribution buses to the antenna (Figures 2.2-4 and 2.2-5). Power is also distributed to batteries so that critical functions, such as IMCS and thermal support, can be provided through solar eclipses.

The microwave power transmission subsystem (MPTS), Figure 2.2-6, consists of a reference system and high-power amplifier devices which feed an array antenna. Phasing control is maintained by use of a pilot beam originating at the rectenna and received at the satellite antenna.

A reasonable way to view the satellite system is to consider the entire satellite as being made up of two major on-orbit assemblies with a connecting

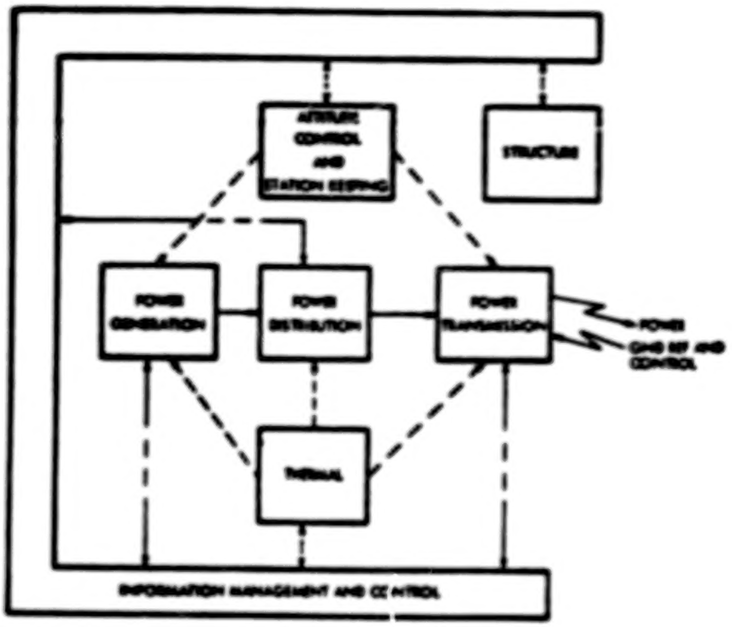
ATTITUDE CONTROL AND STATION KEEPING
STRUCTURE
POWER GENERATION
POWER DISTRIBUTION
POWER TRANSMISSION
POWER
GND REF AND CONTROL
THERMAL
INFORMATION MANAGEMENT AND CONTROL

Figure 2.2-3. Subsystem IMCS Relationships

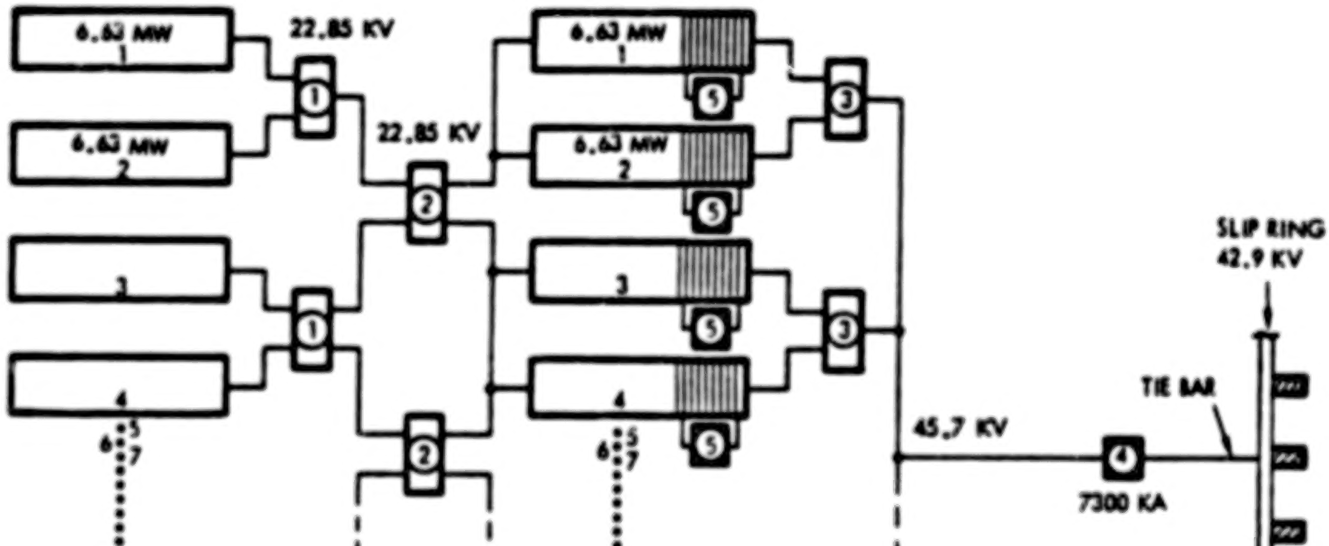
6.63 MW 1
6.63 MW 2
3
4
5
6
7
22
23
24
25
26
22.85 KV
22.85 KV
①
②
③
④
⑤
45.7 KV
7300 KA
TIE BAR
SLIP RING 42.9 KV
①②③④ SWITCH GEAR
④ SELF TRIP SWITCH GEAR
⑤ REGULATOR

Figure 2.2-4. Power Generation Subsystem

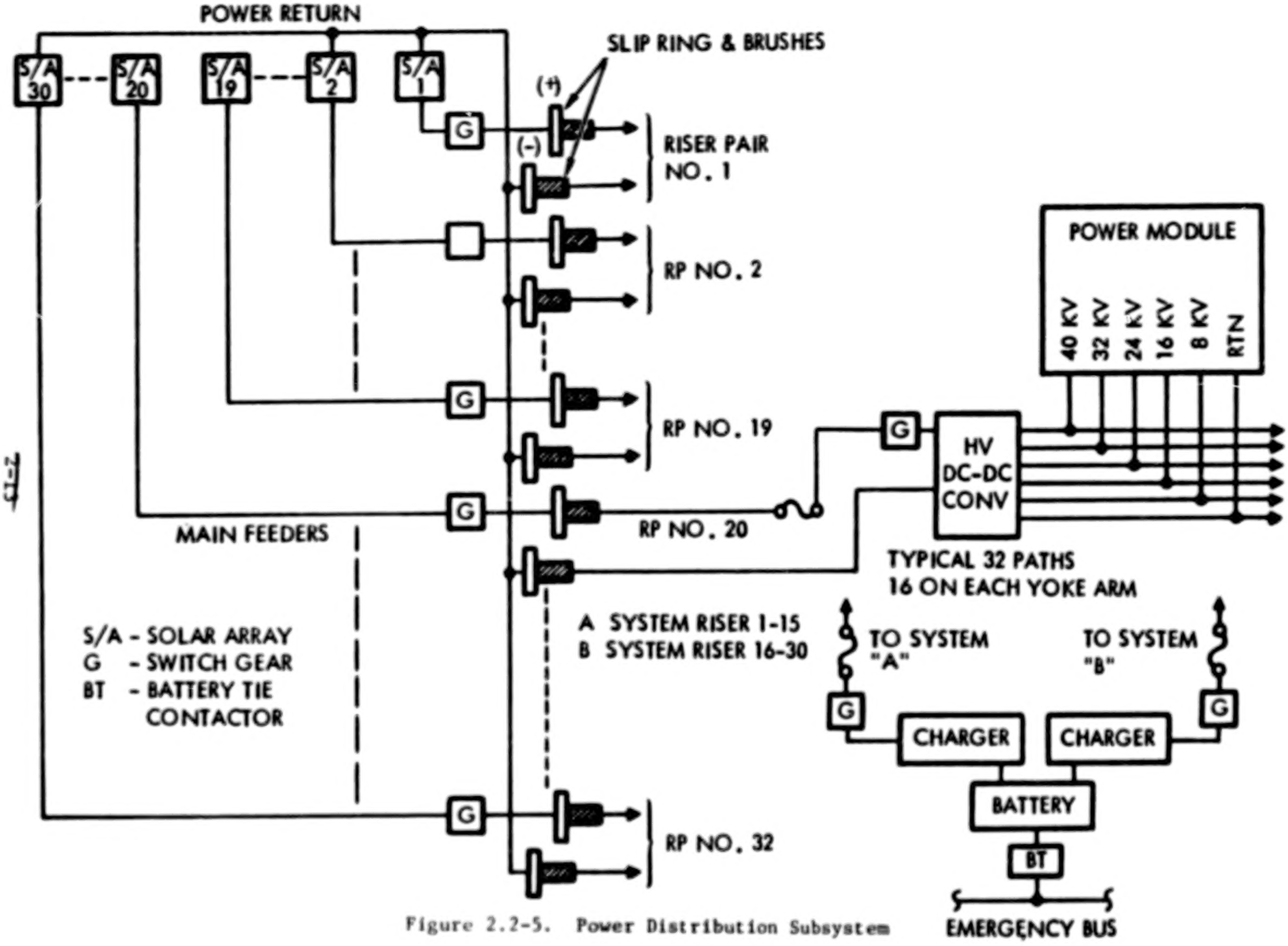
POWER RETURN
S/A 30
S/A 20
S/A 19
S/A 2
S/A 1
SLIP RING & BRUSHES
(+)
(-)
G
RISER PAIR NO. 1
RP NO. 2
RP NO. 19
RP NO. 20
RP NO. 32
MAIN FEEDERS
POWER MODULE
40 KV
32 KV
24 KV
16 KV
8 KV
RTN
HV DC-DC CONV
TYPICAL 32 PATHS
16 ON EACH YOKE ARM
A SYSTEM RISER 1-15
B SYSTEM RISER 16-30
S/A - SOLAR ARRAY
G - SWITCH GEAR
BT - BATTERY TIE CONTACTOR
TO SYSTEM "A"
TO SYSTEM "B"
CHARGER
CHARGER
BATTERY
BT
EMERGENCY BUS

Figure 2.2-5. Power Distribution Subsystem

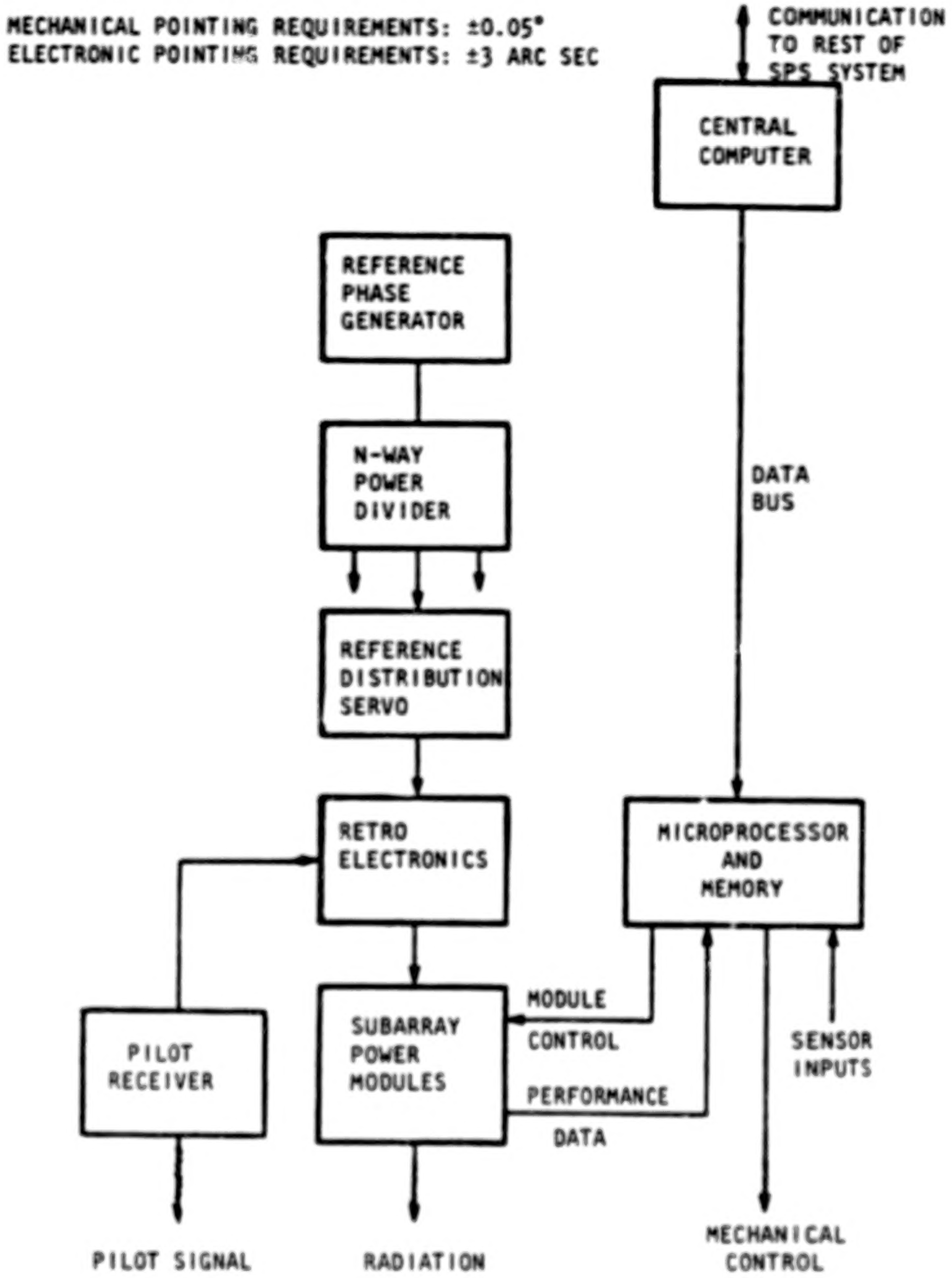
MECHANICAL POINTING REQUIREMENTS: ±0.05°
ELECTRONIC POINTING REQUIREMENTS: ±3 ARC SEC
COMMUNICATION TO REST OF SPS SYSTEM
CENTRAL COMPUTER
REFERENCE PHASE GENERATOR
N-WAY POWER DIVIDER
DATA BUS
REFERENCE DISTRIBUTION SERVO
RETRO ELECTRONICS
MICROPROCESSOR AND MEMORY
MODULE CONTROL
PILOT RECEIVER
SUBARRAY POWER MODULES
SENSOR INPUTS
PERFORMANCE DATA
PILOT SIGNAL
RADIATION
MECHANICAL CONTROL

Figure 2.2-6. Microwave Transmission Subsystem

interface assembly operating in concert at GEO. These on-orbit assemblies are the sun pointing solar arrays and the earth pointing power antenna.

The solar array consists of the GaAs solar cells and the supporting subsystems required to operate the satellite in a sun-oriented mode. Included in this subelement are information management and control subsystem assemblies required to monitor and control the power generation devices; and the power distribution network, as well as all remaining subsystem functions. The solar panels are grouped in 60 independent panels. The power supplied totals 9.94 GW at 45.7 kV over 30 independent (two panels in series) main feeders (Figure 2.2-5).

The antenna consists of the antenna primary and secondary structure, the microwave conversion and transmission assemblies, and the elements of the various supporting subsystems required to operate the microwave transmission system.

A summary of the satellite reference (GaAs) design is provided in Table 2.2-1.

Table 2.2-1. Satellite Reference Design Summary (GaAs)

Basic		
Frequency	2.45 GHz	
Power density of rectenna		
Center	23 mW/cm^2	
Edge	1 mW/cm^2	
Location	GEO	
Transmission technique	10 dB Gaussian/microwave	
Power generation	Photovoltaic GaAs or GaAlAs/GaAs $CR_E = 1.83$	
System	GaAs	GaAlAs/GaAs
Power at utility interface	5 GW	5 GW
Solar array configuration	Planar	Planar
Number of troughs	3	3
Antenna location	End	End
Planform Area	4200 m (W)×16,000 m (L) (67.2 km^2)	4200 m (W)×11,000 m (L) (46.2 km^2)
Solar panel area	28.47×10^6 m^2	18.13×10^6 m^2
Reflector array area	56.94×10^6 m^2	36.26×10^6 m^2
MW dc-RF converter type	Klystron	Klystron
Number of tubes	142,902	142,902
Transmitted power	7.14 GW	7.14 GW
Overall efficiency	7.2%	16.0%
Overall satellite mass (with 25% growth)	31.6×10^6 kg	25.96×10^6 kg

2.2.2 MAGNETRON SYSTEM DEFINITION

General

The magnetron system as defined by Rockwell International consists of a solar collection array similar in concept to the reference concept, but with the antenna design based upon the use of a magnetron cavity resonator rather than the klystron as a power amplifier. In general appearance, the satellite is similar to the configuration depicted in Figure 2.2-1.

The basic system generates and transmits microwave power at a level sufficient to provide 5.6 GW at the utility interface. The overall dimensions for the magnetron based satellite are: (1) length, 15.0 km; (2) width, 4.2 km; and (3) depth, 0.564 km. The mass is estimated to be 26.7×10^6 kg and includes a 25% growth factor.

The satellite length of the variation using dual-junction (MBG) solar cells is reduced to 10,000 m. Vehicle mass is estimated as 21.5×10^6 kg, including the 25% growth allowance.

Figure 1.2-22 presents the efficiency of the SPS system utilizing the magnetron power amplifier. Overall efficiency is shown to be approximately 7.9 percent.

A detailed satellite mass property summary for the magnetron based system is shown in Section 2.5.

Magnetron Satellite Subsystems

The magnetron satellite concept is comprised of seven major subsystems as shown in Figure 2.2-2. Power generation, distribution, and transmission remains the dominant mission function, while the need for thermal control is virtually eliminated. Coordination of satellite functions and operations remains the province of the information and control subsystem (IMCS) as shown in Figure 2.2-3.

The solar array supplies 9.8 GW at 21.85 kV over 30 independent (two panels in parallel) main feeders (Figure 2.2-7).

The microwave power transmission subsystem consists of a microwave phase reference generator, an RF distribution network, and more than 2.35×10^6 magnetrons used as power amplifiers to drive a resonant cavity radiator antenna. The layout of a typical segment of the antenna is shown in Figure 2.2-8. A summary of the satellite magnetron (GaAs) design is presented in Table 2.2-2. A more detailed description of each major subsystem is provided in Section 3.0.

2.2.3 SOLID STATE SYSTEM CONCEPTS

Introduction

The reference satellite concept utilizes high voltage (HV) klystron dc-RF converters to convert the dc power to 2.45 GHz microwave. The power for the RF converters is transferred from the solar array at 40 kV dc (nominal) across

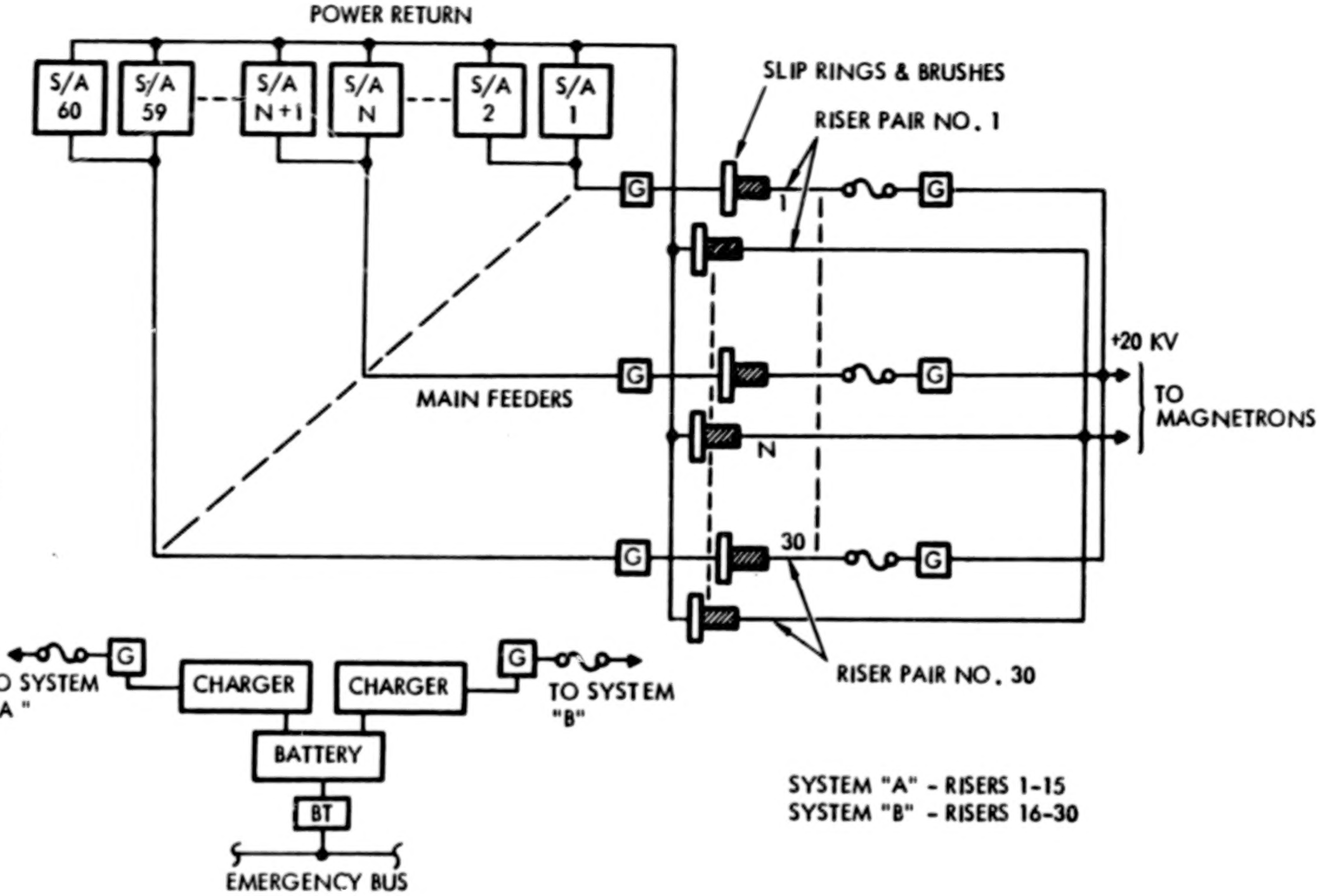
POWER RETURN
S/A 60
S/A 59
S/A N+1
S/A N
S/A 2
S/A 1
SLIP RINGS & BRUSHES
RISER PAIR NO. 1
G
1
MAIN FEEDERS
+20 KV
TO MAGNETRONS
N
30
RISER PAIR NO. 30
TO SYSTEM "A"
CHARGER
CHARGER
TO SYSTEM "B"
BATTERY
BT
EMERGENCY BUS
SYSTEM "A" - RISERS 1-15
SYSTEM "B" - RISERS 16-30

Figure 2.2-7. Magnetron Satellite Power Distribution

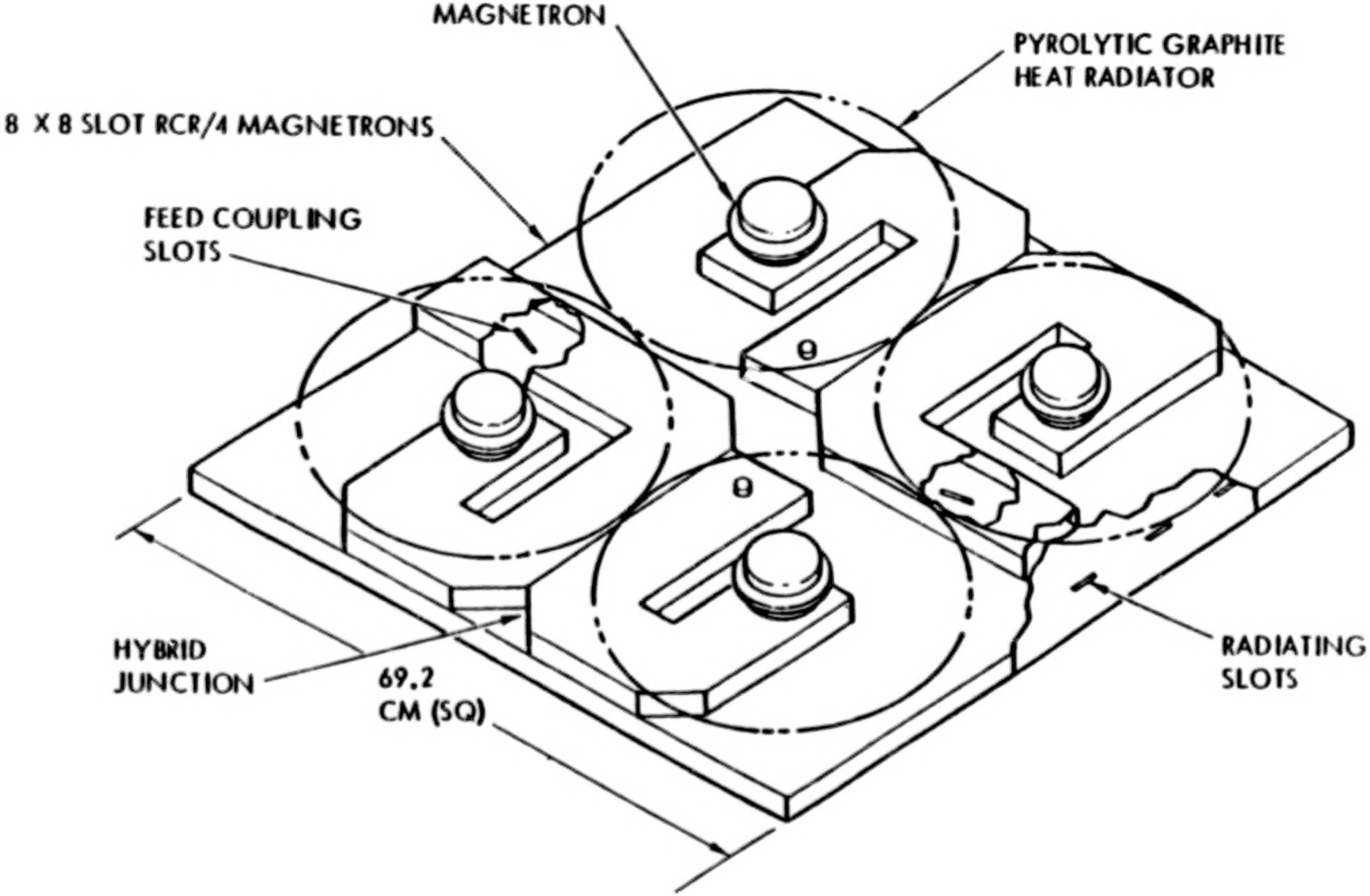
MAGNETRON
PYROLYTIC GRAPHITE
HEAT RADIATOR
8 X 8 SLOT RCR/4 MAGNETRONS
FEED COUPLING
SLOTS
θ
θ
HYBRID
JUNCTION
69.2
CM (SQ)
RADIATING
SLOTS

Figure 2.2-8. Magnetron Power Module Layout—Typical

Table 2.2-2. Magnetron Satellite Design Summary
(GaAs)

Basic		
Frequency	2.45 GHz	
Power density at rectenna	23 mW/cm^2 (center) 1 mW/cm^2 (edge)	
Location	GEO	
Transmission technique	Microwave	
Power generation	Photovoltaic GaAs or GaAlAs/GaAs $CR_E = 1.83$	
System	**GaAs**	**GaAlAs/GaAs**
Power at utility interface	5.6 GW	5.6 GW
Solar array configuration	Planar	Planar
Number of troughs	3	3
Antenna location	End	End
Planform Area	4200 m (W) × 15,000 m (L) (63 km^2)	4200 m (W)×10,000 m (L) (42 km^2)
Solar panel area	27.3 km^2	18.3 km^2
Reflector area	54.6 km^2	56.6 km^2
Microwave antenna type	Magnetron tube	Magnetron tube
Number of tubes	2.3×10^6	2.3×10^6
Transmitted power	8 GW	8 GW
Overall efficiency	7.9%	11.9%
Overall satellite mass (with 25% growth)	26.8×10^6 kg	21.5×10^6 kg

the antenna slip rings, coverted to five selected HV dc voltages, and utilized by the klystrons. A major study goal has been to devise satellite approaches that use low-voltage solid-state devices on the satellite for conversion from dc to RF. The desire to replace the klystrons with solid-state devices is driven by their potential for highly improved satellite reliability; klystrons would probably have to be replaced at least two and perhaps three times during the 30-year operational period. Solid-state microwave design drivers are identified as having maximum breakdown voltage limits of 10 to 70 V dc, junction temperatures of <200°C, output power limits of <100 W, and circuit efficiencies of 78% to 90%. Solid-state dc-RF amplifiers require a low input voltage (present Rockwell design indicates an input voltage of approximately 10 V dc). If the appropriate low voltage is generated at the source, power conductor mass becomes excessive and the current-carrying capability of the rings need to be very large. Efforts were made to provide module designs with a very low loss means of combining the output of solid-state power amplifiers and increasing the dc power input requirements.

Two primary approaches were considered during the design phase of the study: (1) a concept that considered simple replacement of the klystron microwave power modules with a transistorized equivalent, and (2) a totally new approach considering the characteristics of the solid-state power amplifier. The second approach integrated the photovoltaic solar cells and the microwave power elements into a "sandwich" (back-to-back) configuration eliminating the requirement for dc-dc conversion in the power path. Figures 1.2-17 and 1.2-18 illustrate these two different solid-state approaches. The concept shown in Figure 1.2-17 has two antennas, each antenna having twice the area and approximately half the power of the reference klystron concept. The concept shown in Figure 1.2-18 uses a new sandwich approach that has solar cells on one side, an RF radiator on the other side, and solid-state dc/RF converters sandwiched between. Solar energy is directed on the solar cells by a rotating primary reflector and a fixed secondary reflector.

The most significant parameter was determined to be antenna power density. It is possible to increase power density for the sandwich concept by using higher efficiency solar cells (multi-bandgap cells), raising the allowable surfact emperatures (solar cell and RF elements and/or use of optical filters), and improved dc-RF converter efficiency. The thermal barrier between solar cells and RF elements must be controlled to permit balanced surface temperatures; otherwise, the RF element allowable surface temperature (125°C) would be reached before reaching the allowable solar cell temperature (200°C), resulting in a significant penalty in RF power density. Power distribution wiring mass was not considered a major consideration in the sandwich concept analysis.

Antenna power density is also an important sizing parameter for the end-mounted solid-state antenna concept. Since heat rejection for this configuration is accomplished from both sides of the antenna, higher power density is achieved. Figure 2.2-9 shows a plot of power density as a function of phase control/amplifier efficiency. The design point ($\eta_R = 0.792$) results in a power density of 6638 W/m^2. (Note: The klystron reference design is 21,000 W/m^2.) In the actual design, a power density factor of approximately 6580 W/m^2 was used.

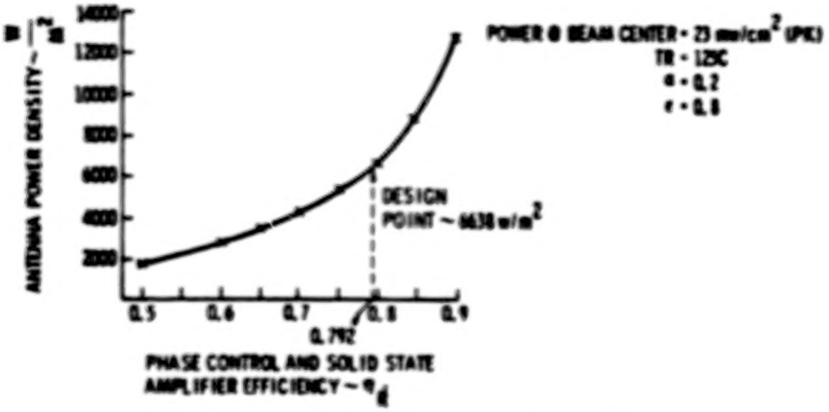

Figure 2.2-9. Effect of Amplifier Efficiency on Antenna Power Density

Solid-State Sandwich Concept

General

The solid-state sandwich concept is based on the use of a combination solar cell/microwave transmitter-antenna panel, thus eliminating the large high-power, main conducting cables, and the corresponding high-power slip rings required in the baseline reference configuration. The Rockwell International satellite configuration is shown in Figure 1.2-18.

The satellite configuration consists of two smaller satellite configurations joined together so as to provide a "balanced" configuration relative to certain attitude control considerations. The major advantage is that solar pressure moments will be reduced (when compared to those developed by two independent satellites maintained in a stationkeeping mode), resulting in lowered propellant requirements.

The major features of the solid-state sandwich configuration are a large mirror (reflector) system consisting of an eight-segment primary mirror and a single secondary mirror (Figure 2.2-10) delivering an effective concentration ratio (CR_E) of approximately 5.2, and a "coupled" solar cell/microwave antenna panel. The microwave system is made up of approximately 4.3×10^8 solid-state amplifiers/antennas (3.4×10^8 amplifiers with MBG solar cell approach) located on 7.81-cm centers.

The primary mirror planes are angled with respect to each other, as shown in Figure 2.2-11, to attain the desired focus on the secondary mirror. Additionally, the primary mirrors are suspended on a rotatable joint, as indicated, to permit adjustment for the seasonal variations of the sun. The reflecting surface of all reflectors consists of aluminized kapton attached to the frame by catenaries which maintain the proper degree of tension.

The secondary reflector is an octagonal frame arrangement which is rigid with respect to the antenna and which transmits the solar energy received from the primary reflectors to the solar cells mounted on the face of the antenna. The antenna itself consists of a hexagonal frame with tension-web cabling

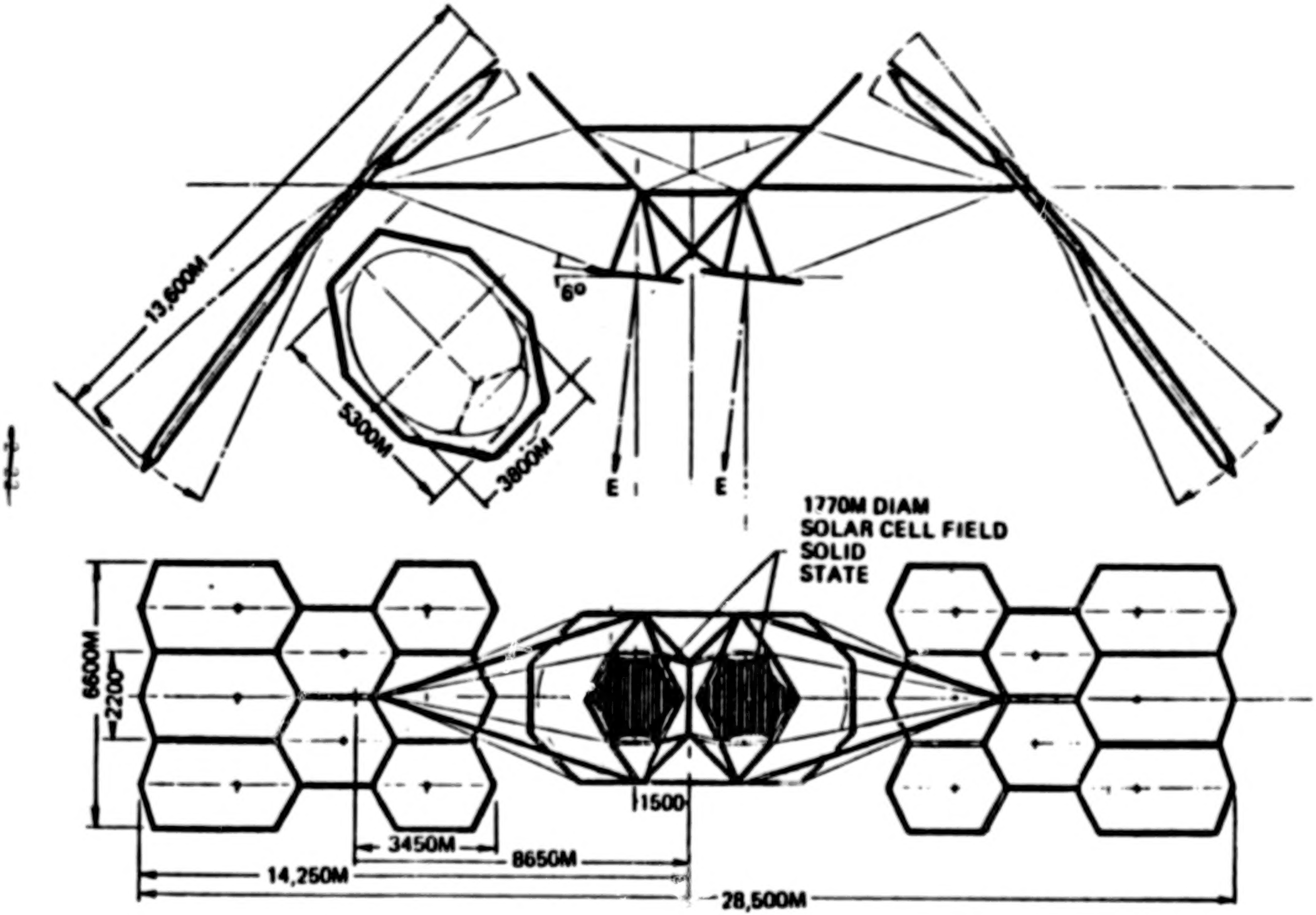
13,600M
5300M
3800M
6°
E
E
1770M DIAM
SOLAR CELL FIELD
SOLID
STATE
6600M
2200
1500
3450M
8650M
14,250M
28,500M

Figure 2.2-10. Dual SPS Solid-State Sandwich Satellite Concept

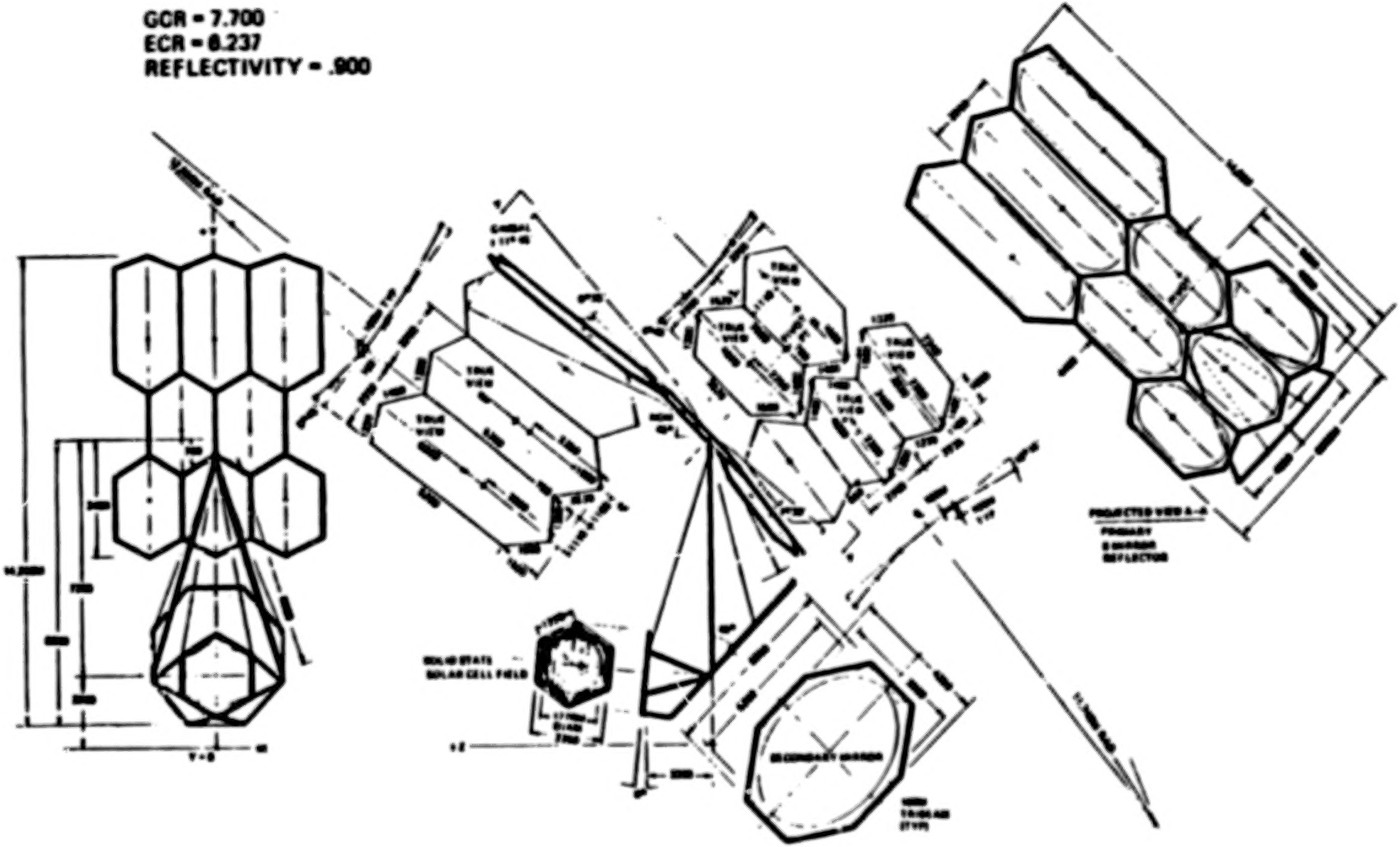
GCR = 7.700
ECR = 6.237
REFLECTIVITY = .900
SOLID STATE SOLAR CELL FIELD
SECONDARY MIRROR
PROJECTED VIEW A-A
PRIMARY MIRROR REFLECTOR
TRUE VIEW

Figure 2.2-11. Solar Power Satellite—PEKSP Dual Solid-State Sandwich Configuration

which provides the support for the solid-state panels. Solar cells are mounted on one side of the panels and the solid-state devices utilized for transmission on the other side.

The mass is estimated to be 20.5×10^6 kg (16.39×10^6 kg for MBG variation) and includes a 25% growth factor. In geosynchronous orbit, the longitudinal axis of the SPS is oriented perpendicular to the orbital plane. The reference design is based on construction in GEO.

While communications have not been specifically studied in this preliminary analysis, a number of implications have been drawn. The satellite must maintain continuous contact with the GRS control center. This includes voice, data, video, and commands in both directions. In addition, the uplink pilot beam from the GRS is crucial to acquisition and fine pointing. The high EMI environment in the near vicinity of the satellite imposes difficult conditions for communications. This requires primary emphasis and special design considerations.

Figure 1.2-21 presents the basic efficiency of the overall SPS and indicates the relative efficiencies of each of the major subelements of the system. Overall efficiency of the solid-state sandwich system is shown to be approximately 4.5%. A detailed satellite mass property summary is given in Section 2.5.

Subsystems

The solid-state concept is also comprised of seven major subsystems although the relative impact of certain ones is significantly less. For example, the power and distribution subsystem is limited to those elements necessary to control and route the power required to operate the supporting subsystems only. The major portion of the energy developed by the power generation elements (the photovoltaic solar cells) needed for the primary function of the satellite is generated in very small segments (<6 W) and located in very close proximity (<5 cm) to the individual power amplifiers on the antenna. The impact of the interconnecting wiring is, therefore, accounted for within the subarray definition. A second major deviation from the power distribution and control concept utilized in the reference concept is the removal of all power control elements (switch gears) in the power path. Basic beam diffusion (beam cutoff) would be attained by removing either the pilot beam signal or the RF reference signal from the amplifier. If a repair activity must be accomplished on the antenna, the necessary procedure would require the rotation of the primary mirror so as to eliminate the illumination of the solar cell field.

The basic concepts utilized in the attitude control and data management and control concepts remain the same although scale factors do change. For example, because of the lack of control requirements on the antenna, the data management subsystem in this element is reduced to 20% of the equivalent system on the reference system and is restricted to the monitoring of basic structure and a very limited monitoring of the basic antenna area by indirect (spectral observation) means.

A summary of the satellite sandwich design is given in Table 2.2-3. A more rigorous description of the various subsystems is presented in Section 3.0.

Table 2.2-3. Solid-State Sandwich (Dual) Design Summary

Basic	
Frequency	2.45 GHz
Power density at rectenna	23 mW/cm^2 (center), 1 mW/cm^2 (edge)
Location	GEO
Transmission technique	Microwave
Number of antennas	2
Power generation	Photovoltaic GaAs or GaAlAs/GaAs CR_g = 5.2

System	GaAs	GaAlAs/GaAs
Power at utility interface	2.42 GW	3.06 GW
Solar array configuration	Back of antenna	Back of antenna
Solar panel area	5.26×10^6 m^2	4.17×10^6 m^2
Reflector area	2.29×10^8 m^2	1.81×10^8 m^2
Microwave antenna type	Solid state	Solid state
Number of amplifiers (total)	$\sim850\times10^6$	1.07×10^9
Transmitted power	3.66 GW	4.64 GW
Overall efficiency	4.52%	7.23%
Overall satellite mass (with 25% growth)	20.3×10^6 kg	16.4×10^6 kg

Solid-State End-Mounted Configuration

General

The solid-state end-mounted antenna configuration combines the relative simplicity of the basic planar solar array and a microwave power transmission concept that utilizes monolithic solid-state power amplifiers to develope the high-power-level microwave beam. The Rockwell International satellite configuration is shown in Figure 1.2-17.

The total satellite may be considered to consist of two satellites joined at the solar array end opposite to their respective antennas. This approach has been selected to increase the amount of SPS power that originates from a particular sector or "slot" of the GEO assigned to the satellite. The two antennas operate with two separate ground receiving stations, not necessarily co-located in the continental United States.

CONTENTS

Section Page

1.0 SCOPE/GENERAL REQUIREMENTS 1-1 1/B11
  1.1 INTRODUCTION 1-1 1/B11
  1.2 SATELLITE POWER SYSTEM CONCEPTS 1-3 1/B13
    1.2.1 History of Study 1-3 1/B14
    1.2.2 NASA Reference Satellite Concept 1-12 1/C9
    1.2.3 Rockwell Alternative Satellite Concept (March 1979) 1-15 1/C12
    1.2.4 Rockwell Reference Ground Receiving Station . 1-17 1/C14
    1.2.5 Rockwell Concept Approaches (June 1980) . . 1-17 1/C14
    1.2.6 Satellite Concept Summaries 1-22 1/D6
  1.3 TRANSPORTATION SYSTEM 1-34 1/E9
  1.4 PROGRAM GROUND RULES 1-35 1/E10
2.0 SYSTEM DESCRIPTION 2-1 1/E11
  2.1 GENERAL 2-1 1/E11
    2.1.1 System 2-1 1/E11
  2.2 SATELLITE 2-9 1/F7
    2.2.1 Reference System Definition 2-9 1/F7
    2.2.2 Magnetron System Definition 2-16 1/G1
    2.2.3 Solid State System Concepts 2-16 1/G1
  2.3 GROUND RECEIVING STATION 2-26 2/A3
    2.3.1 Introduction 2-26 2/A3
    2.3.2 Rectenna 2-28 2/A5
    2.3.3 Power Distribution 2-28 2/A5
  2.4 OPERATIONS AND MAINTENANCE 2-29 2/A6
    2.4.1 Satellite Operations 2-29 2/A6
    2.4.2 Satellite Maintenance 2-46 2/B9
  2.5 MASS PROPERTIES 2-51 2/B14
3.0 SUBSYSTEMS 3-1 2/C2
  3.1 SATELLITE 3-1 2/C2
    3.1.1 Introduction 3-1 2/C2
    3.1.2 Power Generation 3-2 2/C3
    3.1.3 Power Distribution 3-30 2/E8
    3.1.4 Microwave Power Transmission 3-41 2/F8
    3.1.5 Structure 3-84 3/B12
    3.1.6 Attitude Control and Stationkeeping Subsystem . 3-101 3/D3
    3.1.7 Thermal Control 3-112 3/D14
    3.1.8 Communications and Data Management 3-131 3/F6
  3.2 GROUND RECEIVING STATION 3-141 3/G7
    3.2.1 Introduction 3-141 3/G7
    3.2.2 Rectenna 3-141 3/G7
    3.2.3 Power Distribution 3-150 4/A4
4.0 SUPPORT SYSTEMS 4-1 4/A5
  4.1 GEO OPERATIONAL BASE 4-1 4/A5
  4.2 MAINTENANCE AND REFURBISHMENT FACILITY 4-1 4/A5

Section Page

4.3 SPS TRANSPORTATION SYSTEM REQUIREMENTS (PRELIMINARY) . 4-1 **4/A5**
  4.3.1 Configuration and Mission Requirements . . 4-1 **4/A5**
  4.3.2 Heavy Launch Lift Vehicle(s) Requirements . . 4-2 **4/A6**
  4.3.3 Cargo Transfer Vehicle (COTV) 4-5 **4/A9**
  4.3.4 Personnel Orbital Transfer Vehicle (POTV) . . 4-6 **4/A10**
  4.3.5 Personnel Module (PM) 4-7 **4/A11**

Major features of the end-mounted configuration are the use of 40-kV (nominal) main feeders and dc-dc voltage conversion to 640 dc (nominal) at the antenna dc feed points. The solid-state power amplifiers are then interconnected in a series-parallel configuration to allow each amplifier to operate at approximately 10 V dc. In this configuration, it has been assumed that any bias voltages required for amplifier operation will be developed internal to each individual amplifier.

The antenna is developed assuming a nominal 10-dB Gaussian distribution pattern with dipole elements at the center delivering 40 W, and elements at the antenna perimeter handling less than 5 W. Approximately 8×10^8 solid-state amplifiers are utilized on each antenna with the dipole spacing set at 7.81 cm on each axis.

The satellite mass is estimated to be 40×10^6 kg (16.4×10^6 kg for the MBG solar cell concept), including a 25% growth allowance. In geosynchronous orbit, the longitudinal axis of the SPS is oriented perpendicular to the orbital plane.

Figure 1.2-20 presents the overall efficiency of the SPS system; overall efficiency is approximately 6.3%. A detailed mass property summary is shown in Section 2.5.

Subsystem

The end-mounted antenna configuration utilizes a solar collection array of the general type described for the klystron based reference satellite concept. Therefore, the general arrangements for the solar panels and the array power distribution remain the same. The interface elements (antenna yoke) also retains the general configuration used on the reference concept.

The antenna proper thus becomes the only area where a significant deviation from the reference satellite occurs. Figure 2.2-10 illustrates, in simplified format, the essential features of the portion of the power distribution system located on the antenna. Total power developed in the solar array is equal to 11.46 GW. A summary of the satellite design is provided in Table 2.2-4. A more rigorous description of each subsystem is presented in Section 3.0.

2.3 GROUND RECEIVING STATION

2.3.1 INTRODUCTION

The microwave power transmission system (MPTS) consists of two major elements: (1) the orbiting transmission antenna, and (2) the ground receiving antenna (rectenna). The ground receiving station (GRS) consists of the ground element of the MPTS (the rectenna), and the power distribution, power conversion, data management, and other supporting subsystems required to collect, convert, and route power to the utility interface tie lines.

The following subsections address the rectenna and power distribution subsystems only. The other subsystems are not considered, but may be evaluated in future studies.

Table 2.2-4. End-Mounted Solid-State Antenna Based Satellite Design Summary

Basic		
Frequency	2.45 GHz	
Power density of rectenna	23 mW/cm (center) 1 mW/cm (edge)	
Location	GEO	
Transmission technique	10-dB Gaussian/microwave	
Power generation	Photovoltaic GaAs or GaAlAs/GaAs (MBG)	
Number of antennas	2	
System	**GaAs**	**MBC**
Power at utility interface (ea. antenna)	2.61 GW	2.61 GW
Solar array configuration	Planar	Planar
Number of troughs	3	3
Antenna location	One at each end	One at each end
Planform Area	4200 m (W)×18,000 m (L) (75.6 km^2)	4200 m (W)×12,000 m (L) (50.4 km^2)
Solar panel area	32.29 km^2	21.16 km^2
Reflector area	64.58 km^2	42.32 km^2
Microwave amplifier type	Solid state	Solid state
No. amplifiers @ 4.5 W each	1.7×10^9	1.7×10^9
Transmitted power	7.36 GW	7.36 GW
Overall efficiency	6.3%	9.5%
Satellite mass (with 25% growth)	40×10^6 kg	35.6×10^6 kg

2.3.2 RECTENNA

The GRS site for the reference satellite requires approximately 35,000 acres. The rectenna site for the magnetron associated site will increase to about 42,000 acres, while the siting requirement for the solid-state system is expected to be less than 20,000 acres. Figure 2.3-1 shows a layout of a reference system site. The inner ellipse containing the rectenna panels (10×13 km) is about 20,000 acres, or 72% of the total acreage. The rectenna dimensions for the magnetron, end-mounted, and sandwich solid-state concept are 10.95 km ×14.34 km, × 7.45 km × 9.76 km, and 4.87 km × 6.38 km, respectively. The area surrounding the inner ellipse is utilized for maintenance facilities, access roads, converter stations, and the two peripheral rows of towers which support the 40-kV dc and 500-kV ac cables. The outer perimeter of the area is fenced for security reasons. The towers which support the 500-kV ac cables are constructed of steel girders footed in concrete and are approximately 230 ft (70 m) high. The inner towers are each comprised for four tapered steel columns 60 ft (18.3 m) tall. Fifty-four of the larger towers and 401 of the smaller towers are required; the latter figure translating into 1604 tubular members because of the configuration.

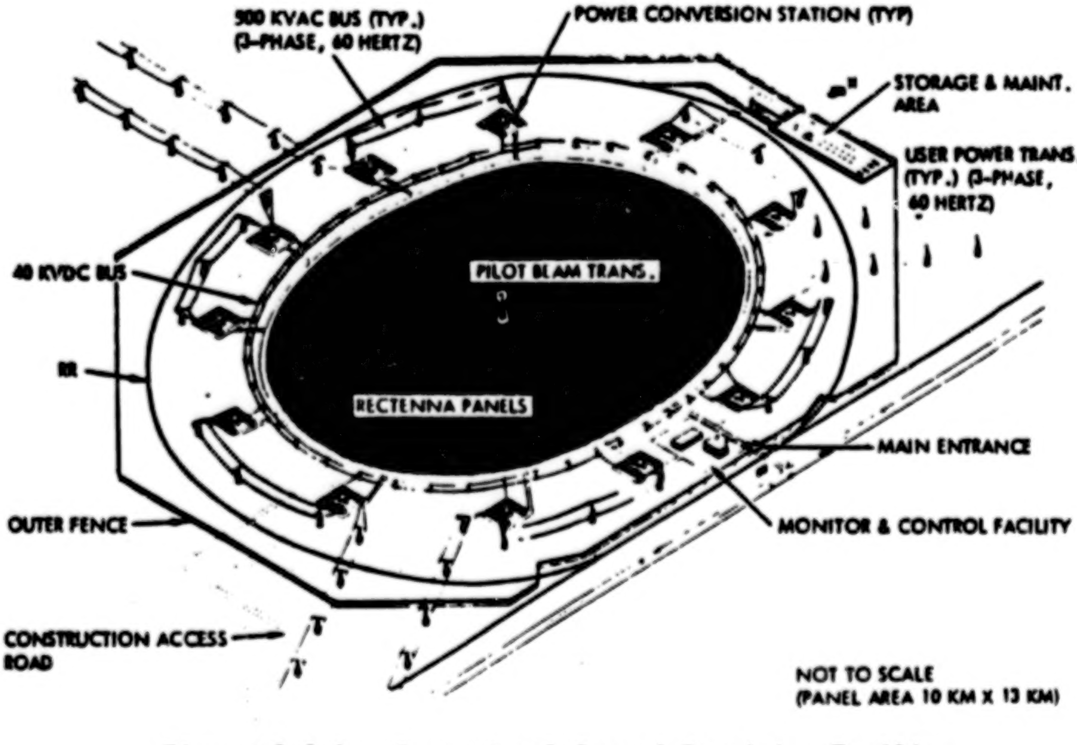
500 KVAC BUS (TYP.)
(3-PHASE, 60 HERTZ)
POWER CONVERSION STATION (TYP)
STORAGE & MAINT. AREA
USER POWER TRANS. (TYP.) (3-PHASE, 60 HERTZ)
40 KVDC BUS
PILOT BEAM TRANS.
RR
RECTENNA PANELS
MAIN ENTRANCE
OUTER FENCE
MONITOR & CONTROL FACILITY
CONSTRUCTION ACCESS ROAD
NOT TO SCALE
(PANEL AREA 10 KM X 13 KM)

Figure 2.3-1. Operational Ground Receiving Facility (Rectenna)—Typical

2.3.3 POWER DISTRIBUTION

The power available from each "voltage string" on the rectenna panels must now be collected and distributed to various feeders and buses. From there, the power is routed through interface converters and eventually converted to utility inter-ties. Figure 2.3-2 represents a simplified schematic of the basic station distribution subsystem.

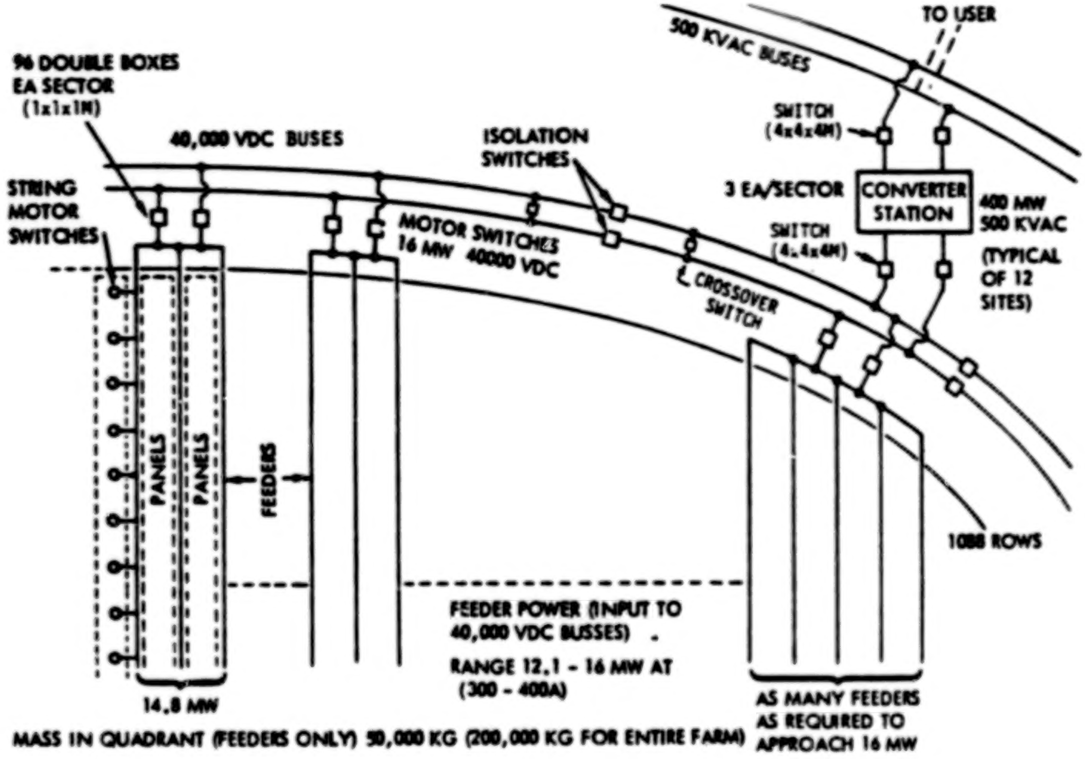
TO USER
500 KVAC BUSES
96 DOUBLE BOXES
EA SECTOR
(1x1x1M)
40,000 VDC BUSES
ISOLATION
SWITCHES
SWITCH
(4x4x4M)
STRING
MOTOR
SWITCHES
3 EA/SECTOR
CONVERTER
STATION
400 MW
500 KVAC
MOTOR SWITCHES
16 MW 40000 VDC
SWITCH
(4x4x4M)
(TYPICAL
OF 12
SITES)
℄ CROSSOVER
SWITCH
PANELS
PANELS
FEEDERS
1088 ROWS
FEEDER POWER (INPUT TO
40,000 VDC BUSSES) .
RANGE 12.1 - 16 MW AT
(300 - 400A)
14.8 MW
AS MANY FEEDERS
AS REQUIRED TO
APPROACH 16 MW
MASS IN QUADRANT (FEEDERS ONLY) 50,000 KG (200,000 KG FOR ENTIRE FARM)

Figure 2.3-2. Receiving Station Power Distribution Schematic—Preliminary

2.4 OPERATIONS AND MAINTENANCE

2.4.1 SATELLITE OPERATIONS

Introduction

The satellite power system consists of a large solar power collecting and conversion satellite, located in a stable geosynchronous equatorial orbit (GEO), that transmits this energy in microwave form to a dedicated collecting/conditioning ground receiving station located at designated sites throughout the U.S. Each of the orbiting satellites transmits (beams) the microwave power to a single, specific, rectenna location. The ultimate SPS program may consist of many of the satellite/rectenna combinations. The following discussion was based upon the use of a reference concept configuration, but may be adapted to the magnetron concept as well.

It was the intent of this activity to identify and analyze the operating functions of the satellite and the rectenna system to determine the control characteristics of a single satellite/rectenna combination, and to also consider the relationship with other satellite/rectenna systems in the total program. Because of the level of system and subsystem definition, the scope of this study focused on the identification of probable operating functions in an attempt to determine the existence of critical operation paths, and to determine specific areas where other definitions would be most effective.

The majority of the work on operations was accomplished by IBM Federal Systems Division personnel under contract (M7M8BNS-890163M) to the Space Operations and Satellite Systems Division (SO&SSD) of Rockwell International.

Scope

Satellite/ground functional analysis is constrained to startup and nominal operations because of the limited time and because of the limited subsystem/system data available. The satellite functions identified and evaluated primarily address the major subsystems to generate and transfer the energy obtained during the primary satellite mission. The ground portion of this study included the space-ground interface, the primary rectenna, GRS-utility interfaces, the GRS control center, and (if required) an area control center. Emphasis is on all but the area control center. The reference satellite/rectenna configuration is shown in Figure 2.4-1, although the selection of any alternate configuration utilizing klystron or magnetron microwave amplifiers will not substantially alter the following discussion.

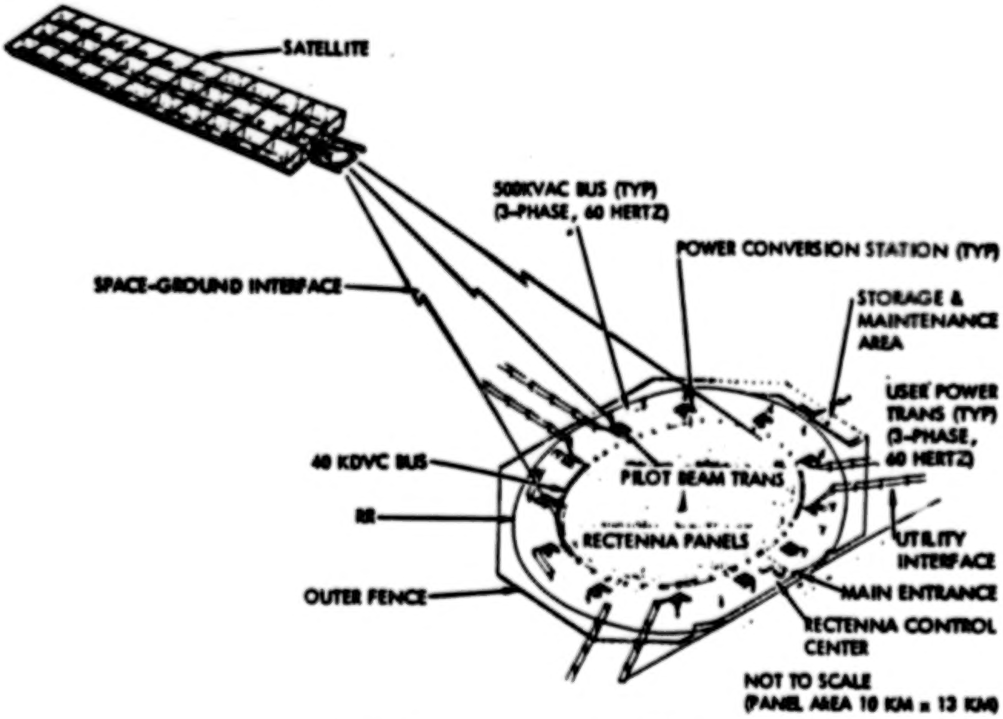
SATELLITE
500KVAC BUS (TYP)
(3-PHASE, 60 HERTZ)
POWER CONVERSION STATION (TYP)
SPACE-GROUND INTERFACE
STORAGE & MAINTENANCE AREA
USER POWER TRANS (TYP) (3-PHASE, 60 HERTZ)
40 KDVC BUS
PILOT BEAM TRANS
RR
RECTENNA PANELS
UTILITY INTERFACE
OUTER FENCE
MAIN ENTRANCE
RECTENNA CONTROL CENTER
NOT TO SCALE
(PANEL AREA 10 KM x 13 KM)

Figure 2.4-1. SPS System

The ground control facility is used to monitor and control the satellite from the ground. Included in this activity is the activities associated with telemetry, tracking, communications, monitoring of microwave beam characteristics, computing gross plan corrections, and providing frequency standard signals for the satellite. Concurrently, the ground facility will control and monitor the collected electrical power through required conversion and distribution to the designated utility interfaces.

Approach

Satellite control has been functionally analyzed from two perspectives: (1) nominal satellite and antenna control, and (2) startup and shutdown operations. These are then considered in a logical time/subsystem ordered sequence to facilitate development of a comprehensive operations scenario.

A chronological sequence is followed from pre-start and startup to steady-state functions. Subsystems are considered as they logically become involved in providing any necessary support, e.g., command/control, communications, information processing, power conversion, distribution, switching, environmental control, etc. Since startup operations are critical to establishing systems operations within the bounds established by the effects of large power transients, to establish accurate beam pointing and to produce minimum utility power transients, these functions are scrutinized more closely than are the steady-state operations.

Overall functional flows and system performance information is not included pending more detailed subsystems designs. Nevertheless, these preliminary scenarios provide some significant cross-checks to concept feasibility by helping identify any conflicts or lack of identified support requirements (space or ground). These studies also provide a basis for future functional flow chart definition, help identify (to the subsystem designers) those areas requiring increased definition, and help clarify (to program management) how the system may be cohesively integrated into operational reality.

Systems

The Satellite Power System (SPS) major elements consist of a power satellite placed in a geosynchronous equatorial orbit and a dedicated companion element, the ground receiving station (GRS), located at a selected site within the continental United States.

Critical Operations

Microwave control and solar eclipses are two major areas of consideration because they are critical to SPS operations. Beam control is initiated from the GRS through the pilot beam, which is used in a conjugation scheme to provide phase-control signals for fine pointing. The involvement of ground support, coupled with a large number of measurements and commands on the antenna, suggests the need for the operations analysis to focus on antenna functions. Solar eclipses occur during the spring and autumn and can last for up to 1.2 hours. These cause power outages which can complicate operations (Figure 2.1-7).

Ground Systems

The earth-based power receiving element, the rectenna, has been conceptually defined and some hardware technology investigations have been completed; but, the control center which is generally acknowledged to be necessary to satellite-GRS operations has not been conceptually defined/designed. In addition, if many solar power satellites are deployed, area control centers may be required to coordinate satellite logistics and utility power distribution.

General assumptions are made as to the architecture of GRS and area control centers. Several GRS are assumed to be under the control of an area control center. The GRS may be geographically widely separated, e.g., several hundred miles apart. The area center also might be collocated with a GRS control center, or might be independently sited on the basis of utility switching center locations, or its location may be determined by other criteria.

The functional allocations assumed are that power routings are established within the GRS/utility interfaces. Operational procedures are assumed to be established within the GRS control centers. Also, operational requirements including scheduling, logistics, and related requirements are established at the area level.

GRS-Utility Interfaces

The GRS and utility interfaces are designed to effectively emulate existing power generation sources such as hydro-electric, thermal, or nuclear plants which are presently used. The fact that the electrical power is first converted from solar sources in space is irrelevant to the utility companies. The rectenna receiving panels and other elements of the GRS, which cover 20 to 30 square miles, are treated as if they are merely another type of power source with the ability to adapt to signals from the utility that controls frequency, phase, and power factor.

Ground Control Center

The ground control center at the GRS site will control the uplink pilot beams, provided status and control of the GRS power distribution network and utility interfaces, as well as providing primary satellite control support. It is anticipated that it will be located at the GRS site in a separate building which also would house administrative personnel, management and maintenance workers, as well as displays, computers, and controls.

The computer architecture concept is shown in Figure 2.4-2, and projects the use of multi-processing units which interface to the satellite through communications processors and control/status operations through a common bus and terminal equipment. Real-time displays and related keyboard control/entry equipment would be incorporated into the design.

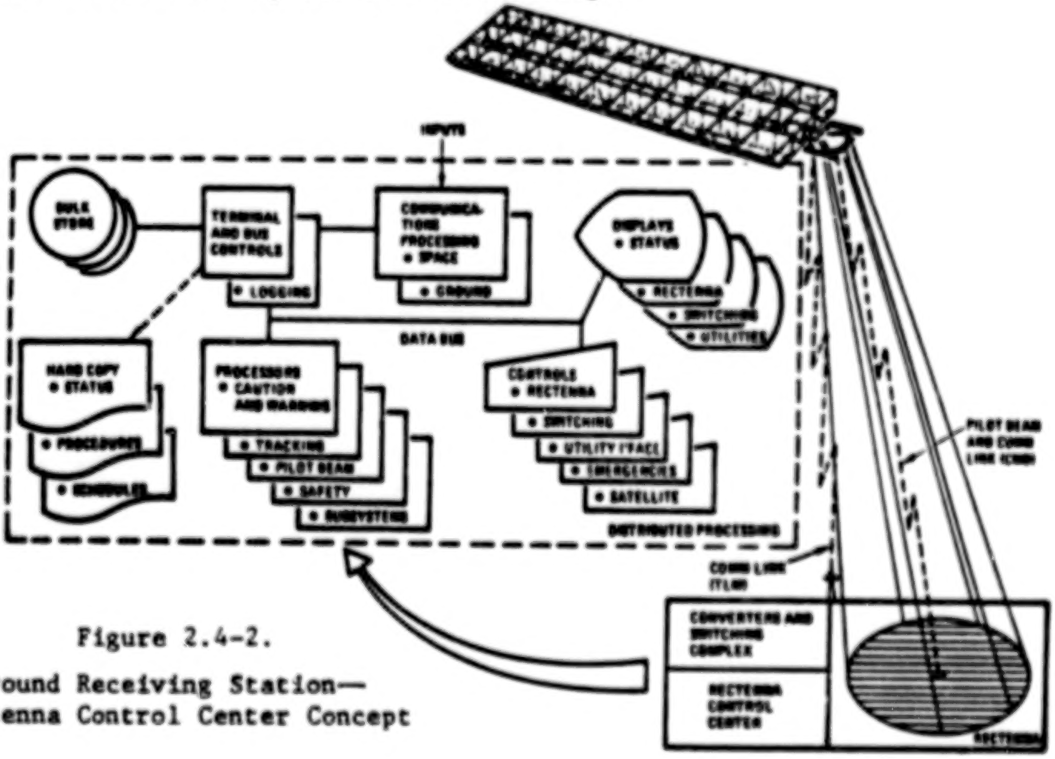
INPUTS
BULK STORE
TERMINAL AND BUS CONTROLS
• LOGGING
COMMUNICATIONS PROCESSING
• SPACE
• GROUND
DISPLAYS
• STATUS
• RECTENNA
• SWITCHING
• UTILITIES
DATA BUS
HARD COPY
• STATUS
• PROCEDURES
• SCHEDULES
PROCESSORS
• CAUTION AND WARNING
• TRACKING
• PILOT BEAM
• SAFETY
• SUBSYSTEMS
CONTROLS
• RECTENNA
• SWITCHING
• UTILITY I'FACE
• EMERGENCIES
• SATELLITE
DISTRIBUTED PROCESSING
PILOT BEAM AND COMM LINK
COMM LINK (TLM)
CONVERTERS AND SWITCHING COMPLEX
RECTENNA CONTROL CENTER
RECTENNA

Figure 2.4-2.

Ground Receiving Station—
Rectenna Control Center Concept

The ground control center's functions and their allocations are beyond the scope of this introductory study. Some of the basic functions anticipated include:

- Operating system
- Data base control
- Data logging/storage
- Pilot beam control
- Satellite status monitoring
- Satellite control
- Power beam monitoring

Rectenna site safety
- Intrusion control
- Telemetry control
- Rectenna power distribution
- Converter station status/control
- Emergency shutdown
  - Satellite
  - Rectenna
- Utility interface control/monitoring

Area Control Center

A conceptual area control center is shown in Figure 2.4-3. It would be differentiated from the ground control facility by a higher functional level. Whereas the local centers are procedurally implementing controls based on instrumentation and telemetry inputs, the area center accepts computer data from the various local centers and then establishes a schedule of GRS satellite support requirements. The local centers could then define a compatible procedural performance of, say, logistical, maintenance, power distribution, or load shifting requirements.

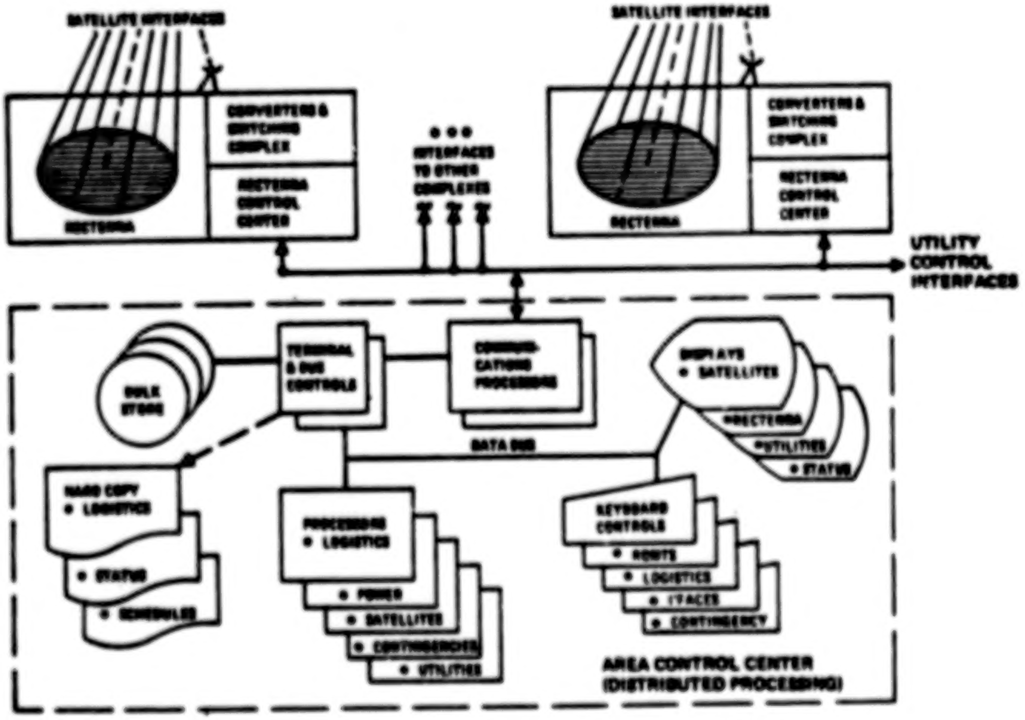
SATELLITE INTERFACES
CONVERTERS & SWITCHING COMPLEX
RECTENNA CONTROL CENTER
RECTENNA
• • •
INTERFACES TO OTHER COMPLEXES
SATELLITE INTERFACES
CONVERTERS & SWITCHING COMPLEX
RECTENNA CONTROL CENTER
RECTENNA
UTILITY CONTROL INTERFACES
BULK STORE
TERMINAL & BUS CONTROLS
COMMUNI-CATIONS PROCESSORS
DISPLAYS
• SATELLITES
• RECTENNA
• UTILITIES
• STATUS
DATA BUS
HARD COPY
• LOGISTICS
• STATUS
• SCHEDULES
PROCESSORS
• LOGISTICS
• POWER
• SATELLITES
• CONTINGENCIES
• UTILITIES
KEYBOARD CONTROLS
• ROUTS
• LOGISTICS
• I'FACES
• CONTINGENCY
AREA CONTROL CENTER (DISTRIBUTED PROCESSING)

Figure 2.4-3. Area Control Center Concept

The area center idea has only been conceptually postulated and has not received further study consideration nor design definition. Future studies should examine the need and functional allocations of such a center. It may evolve as the only effective interface to coordinate the SPS ground power sites and the existing utility networks. Analysis also might show that this function is best served by integrating the area functions into existing utility network command/control centers.

A generalized multi-processing architecture is shown in Figure 2.4-3 as one concept for meeting support demands, Again, a separate study is needed to define architecture and performance requirements as well as functional and siting needs. A centralized dedicated control architecture may be adequate with use of large computers, or perhaps only partial support is needed at a utility network command center using multi-programming.

Operations

The SPS has at least three distinct time phases of operations: (1) test and evaluation (T&E), (2) initial operational capability (IOC) including start-up, and (3) final operational capability (FOC). As the SPS capability passes through these time phases there will be an evolutionary change from semi-automated control and validation to a more automated system. The ultimate level of automation will reflect the highest degree of system performance commensurate with required safety standards. It is assumed that the initial test phase (e.g., T&E) has been successfully completed and that start-up procedures are to be initiated.

Initial discussions will address the satellite with ground operations considered later. This section will conclude with a brief discussion of expected nominal operational requirements.

Satellite Operations

The operations analysis begins with preliminary preparations for power generation and traces the power flow, enabling commands, and system controls across the satellite-rectenna/control center interfaces. The satellite is assumed to have been assembled and to have completed basic individual subsystems checkout. At this point it is expected to be ready for startup operations during which each subsystem is brought on line and integrated with other elements in logical order.

Startup

Startup operations are divided between the solar array portions of the satellite and its antenna.

- *Solar Array*

Five major areas of satellite operations have been identified:

- Status checking of all system components
- Attitude control to enable solar power conversion
- Power distribution to and through the antenna rotary joint (on concepts having rotary joints)
- Voltage regulation to account for losses and aging

Status

Prior to startup, all satellite subsystems must be checked for ready status. These include structure, attitude control, solar blankets, power distribution, thermal control, and the information management and control system (IMCS). A status check command or request would be expected to be received from the rectenna control center, indicating that the ground systems are ready for operations and that status of the satellite must now be checked.

The IMCS is a central element in the checkout of all satellite subsystems. It is assumed to already be in an ON status since it is required at all times for satellite operations, such as attitude control. However, it may be in a standby mode with only essential support functions operative. Control support to power generation, distribution, and microwave transmission may be in an OFF or STANDBY status. Whatever the existing IMCS configuration and operational condition, the IMCS must be checked out. IMCS operative portions are placed into automatic sequencing checks and nonoperating portions are brought on line and similarly status-checked.

After IMCS checkout is complete, measurements data are accepted from the attitude control, structural, thermal, solar blanket, and power distribution subsystems and verified. These include temperatures, positions, pressures, voltages, etc. Next, limited control actions are issued to the various subsystems to check control loops and operating modes. Even though measurements and controls, as compared to the antenna, are relatively limited on the solar array, they still represent a hundred thousand or more data points which are sampled a number of times. Similarly, over 10,000 control points are exercised. Such checkout sequences will be automatically implemented with human monitoring of test results on the ground in the GRS control center. The time duration of such status checks may well be established by subsystem stabilization time constants rather than the actual time to automatically sequence through the various functions.

Attitude Control

Once all systems are checked out, the satellite must concurrently be oriented to its solar inertial attitude for power generation. For example, it may have been allowed to drift several degrees in attitude during the time since completion of assembly and basic checkout. Such drift errors must be corrected prior to initiation of power generation. Since stationkeeping is included in this function, the geographic location of the satellite centroid must be verified in relation to the rectenna location. Any undesirable drift must be eliminated and the satellite's longitude location refined.

The physical pointing angle of the microwave antenna is also controlled by this subsystem. Once the satellite achieves its proper solar orientation and longitude location with residual drift errors eliminated, the antenna gimbal drives are controlled to bring the antenna within boresight of the rectenna. This is likely to be a process that will take a significant period of time because of the large masses involved. Both support from the rectenna site to assist boresighting, and power support from the solar blankets to the gimbal drives will be required.

Solar Blankets

The solar blankets are brought on line by closing switch gears between pairs of adjacent bay segments. The two segments are connected so as to provide flexibility for current control and panel outages. Bay segment pairs are sequentially brought on line from all 30 bays until the power demands are met.

Power Distribution

Bay bus switch gears isolate each bay segment pair from the bay buses. As each bay panel pair is connected, it is tied to the main buses through closure of the related switch gear. During this connection process, bus temperatures and current measurements must be monitored to detect any shorts throughout the vast bus runs of the satellite so that controlled emergency disconnects can occur under IMCS or local breaker control to avoid catastrophic effects. During the startup sequence (as well as during nominal operations), it will be necessary to monitor ground power flows because of their possible influence on satellite procedures.

Voltage Regulation

Voltage regulation is obtained by selecting module segments within the panels. During the solar blanket connection process, voltage levels of each bay segment pair are monitored continuously to assure proper matching between outputs and the main antenna summing bus.

- *Antenna*

Antenna startup operations are divided into status checking, power distribution, power storage, pointing initialization, thermal stabilization, acquisition of the rectenna, and fine-pointing including focus.

Status

The electronic and pointing status of the microwave antenna must be verified prior to power distribution for space-ground transmission. For example, the previously verified boresight of the antenna to the rectenna may have drifted so that updating may be required. This type of boresight support, from the rectenna control center, may be required on a continuous basis.

Concurrently with the boresight verification, the power distribution, thermal, and phase control electronics must be checked. The switch gears on the antenna must be verified for proper positioning and functioning. The ability of the thermal control system to provide both heating and cooling is confirmed. Finally, the phase control electronics are activated to ensure that all components are properly functioning. The reference phase generator is energized and the reference distribution system is exercised to confirm that it is operating properly. Retro-electronics are activated so that the pilot beams from the rectenna can be received and processed through the phase control subsystem.

Power Distribution

If the satellite is experiencing a solar eclipse, internal battery power is utilized to energize the satellite emergency distribution buses. The main power module switch gears are opened while switches at the subarray, mechanical module, and bus levels may be left closed to provide power to antenna electronics for checkout and thermal stabilization.

If the satellite is leaving an eclipse, antenna electronic phase control must be reactivated and power fed to the klystrons for transmission to earth. The satellite's power distribution system is reenergized and stabilized; the antenna ring brush switch gears are closed, allowing power to be distributed to the dc-dc central converters. Switch gears are then closed, allowing the power to enter the primary and secondary feeders, where additional sets of switches determine whether one or both secondary feeders may be activated (redundantly). In the same manner, the switch gears at the mechanical and power module levels are sequentially closed until power flows through the klystrons and is transmitted to earth.

Power Storage

Prior to the satellite entering an eclipse, the batteries are checked and brought up to full storage capacity to ensure IMCS, thermal, attitude control, communications, and other vital functions when photovoltaic power is lost. Closed-loop control of the charging process is maintained through the IMCS until the batteries are fully charged.

When the satellite enters the eclipse, the photovoltaic supply buses are shut down and the emergency buses provide subsystem power. Prior to this time, the klystron power modules are switched off. Nonessential subsystems are shut down or placed in a standby mode to preserve power during the up to 1.2 hours of eclipse time. GRS control center support is used to update orbit predictions for eclipses and generally support scheduling of satellite operations prior to predictable power outages.

Initialization

Initialization of antenna operations begins with activation of the reference frequency module and computation of coarse phase angles by the beam programmers, which command the digital diode phase shifters. Pilot signals are fed through the retro-electronics to initiate the phase conjugation process. Cathode heater power was applied during initial startup to bring the klystrons up to a stabilized temperature for accurate phase control. This heater power is maintained through all eclipses and other scheduled standby situations.

Under IMCS control, the amount of power fed to the klystron is increased while monitoring phase and pointing stability. All scheduled klystrons are brought on line simultaneously with this gradual process to first establish pointing and then the required power levels. Klystron operation is carefully monitored and local arc detection circuits/circuit breakers disconnect any power module which malfunctions.

Thermal Stabilization

Thermal stabilization of klystron cathode temperatures is extremely important to accurate phase control and fine pointing. Phase control and fine pointing are achieved using pilot beam and reference phase comparisons through the phase control system. Phase error signals are provided for correcting the coarse phase angle which was computed at startup.

During eclipses, when excessive cooling would occur, the battery storage subsystem provides cathode heating capability to prepare the system for restart as the satellite emerges from the eclipse.

Conversely, antenna array temperatures on the back side, where control electronics are mounted, must remain less than 100°C. The IMCS continuously monitors component temperatures and adjusts power levels or heater input power (if required) to maintain required temperatures consistent with the passive heat pipe cooling system used on the antenna.

Phasing

Once the MPTS acquires the rectenna by locking on the pilot signals, the antenna must also be phased (focused) so that all down-linked power remains within the confines of the rectenna and is within given safe power levels. The phase control system computes a phase gradient to be applied across each subarray. This, in turn, is locked to the reference phase which is generated at the reference subarray.

After lock-on to the rectenna is achieved, phase gradient corrections begin to achieve the required beam pattern. Signal strength is also monitored at the rectenna and transmitted to the satellite to provide independent confirmation of beam location and focus.

Ground Operations

The organization of the ground operations scenario parallels that of the satellite scenario. Operations begin with status confirmation and proceed to startup and steady-state phases. The satellite and ground systems are assumed to have been completely assembled, integrated, manned, and checked out and placed in standby status.

Display and Control Terminal—Human Interface

The SPS ground system requires a high degree of adaptability in its ground operations center to meet the varying demands of the system. The operating scenario discussed herein has been oriented toward providing a basic representative understanding of the operator-machine interfaces.

In the initial system startup, man will interface with the system primarily in order to validate or stop system operations. The basic information that will be presented to the human will involve status and operational checks of all ground subsystems and a countdown to system startup. In addition, status summaries of all satellite subsystems will also be presented.

The system initiation sequence will involve the utilization of both voice and displayed messages. These will be properly validated and authenticated.

The focal point of human decision-making and control is the display and control terminal. Augmenting this interface are:

- Communications
  - Voice
  - Teletype
  - Computer-to-computer
  - Written with manual transmission
- Management
  - Organization
  - Operating policies and rules

Manual Operations
- Space/ground on-site

Prior to startup of the satellite or GRS, the configuration and status of the local control center must be determined by operations personnel. Displays will be assigned to various functions, e.g., communications, computer operations, satellite, and rectenna. Each of these consoles might be sequenced through various types of display formats and information content to assess the status of:

- Display electronics
- Keyboard functions
- Related data buses and external communications
- Supporting computer(s) and software
- Data files
- Operating modes

Upon system startup, all power levels, beam focusing, beam dispersion, etc., will be monitored and checked to assure that they are within predetermined levels. For elements of the system that will require switching or shut down faster than human reaction time, the system will operate in an automated mode in order to prevent damage to any system elements and to maintain safety requirements. When time and policy permit, human intervention will be able to start, stop, validate, override, or branch any machine function.

Upon receipt of a requirements schedule and startup command from a higher echelon of authority, i.e., area control center director, the aforementioned make-ready status assessment would be performed. Next, the GRS control center is ready to extend its information input and command authority to other interfaces, i.e., GRS and satellite.

Satellite Interfaces

Communications, telemetry, command, and pilot beam control interfaces to the satellite must now be exercised to ensure control integrity. Data links to and from the satellite are exercised with test messages to ensure functional readiness. Satellite computer (and backup primary instrumentation) data telemetry streams would be sampled to confirm high-speed downlink digital data functions as well as reported subsystem status. Ground-based pilot beam transmitter status is next checked. This scenario assumes that a spaceborne crew has completed satellite assembly and checkout, and placed the satellite into a standby systems mode; i.e., only computer controls, communications, and environmental systems activated.

The GRS pilot transmitters are now activated, and radiated power and pointing angles verified. On the satellite, pilot receivers are turned on in response to enabling commands from the GRS control center. Downlink telemetry further verifies reception of the pilot beam signals and boresight.

Those elements of the detailed schedule of required operations, logistical support and power demands, which are needed by the spaceborne control center, are transmitted by high-speed uplinks. These data are assumed to be prepared in the area control center on a generalized basis, and are refined as a detailed scheduled at the ground control facility.

GRS-Utility Interfaces

The GRS and its utility interfaces must be configured to receive the power which is converted and transmitted form the satellite. Rectenna panel status must be checked through instrumentation inputs related to temperature, mechanical integrity, and electrical continuity. Maintenance status must be reviewed to ascertain which panels are inoperative and to reroute any affected interconnections. Personnel must be notified and cleared from exposed areas within the rectenna site.

Power distribution to the utility interface is next configured. Feeder lines and bus switches are configured to route the scheduled power to the proper customer interfaces. The various groups of panels are appropriately interconnected on the dc buses to provide the required degree of isolation. All bus connections, including backups, and breakers are checked. Orders are automatically issued to yard crews to establish correct switch positions for manual maintenance disconnect switches.

Status and control is next sequenced to dc-to-ac converter subsystems. The huge size, redundancy needs, and system complexity of the converter stations dictate that they incorporate their own dedicated computerized controls. Within this assumption it is also presumed that digital data buses connect converter and rectenna control centers so that converter station-ready status is automatically determined. Status is, of course, displayed to rectenna center control personnel who may sequence their displays to examine in increased depth any specific areas of concern.

Converter stations are sent enabling commands to allow local control to turn on electronics to standby mode. Automatic sequencers and input power detectors are assumed to switch each converter station to operating mode as power is received from the satellite.

Finally, the ac bus switches are monitored for their status, and appropriate commands are issued to establish the required distribution configuration. At this point, the ground systems are checked out and placed in standby or operating mode, as appropriate.

Next, area control center and the utility distribution network control centers are sent standby status signals. Similarly, the satellite is also sent pre-start "make ready" warning signals and appropriate enabling commands. Encryption is utilized for communications and command to ensure security against intrusions or takeover.

Area Control Center

As stated previously, it is uncertain whether an area center is required to coordinate several rectenna sites. It may be that coordination of each rectenna only with its respective utility network center is needed. Even these separate centers might be eliminated if they could be integrated into a single location by the utility company. Design trade studies are needed to investigate these possible ramifications.

In this preliminary study, an area control center is assumed. Its primary purpose is development of schedules for required operations, while the rectenna center would define the procedural accommodation of such requirements.

The area center would maintain archival records of system problems and recommended schedules for logistical resupply and maintenance. It would also review past history for unique needs or difficulties in the SPS-utility interfaces, load leveling, contingency outages, etc. Based on these experiences, operational directives could be developed to impose policy, procedural, and contingency response requirements. These could ensure improvements in overall system safety, efficiency, coordination of operations, and power output-to-load matching.

Scheduling of requirements for GRS site and satellite maintenance could also be the function of the regional center. These would be based on site operational logs and would be provided to GRS and on-board satellite control centers, where they would be translated into detailed schedules and procedures.

System Operation

Satellite Pre-Start "Make Ready"

The ground control facility is assumed to control the satellite through the master control center which is located on the satellite. Control is effected through the satellite's distributed computer control and information management system. This results in a higher level of control on the ground, i.e., enabling and scheduling of spaceborne activities in contrast to direct telemetered control.

The spaceborne computerized control system must be polled to determine subsystem status. The ground center would also be expected to issue enabling commands, adjustments to performance levels, requests for specific pointing angles, system configurations, etc. Status polling would include structure, attitude control, colar panel conditions, power distribution, environmental control, and the spaceborne information management and control system. The latter would include operating modes of the various distributed computers, data bus ready condition, terminal equipment, software configuration, and data base contents. Any updates to the data bases would be provided from the ground control center. Such updates might include maintenance schedules, logistics planning, control system parameters, ephemeris updates, etc.

Status pre-start operations would also include providing to the satellite systems various ground-based systems status data. These might include pilot beam status and pointing parameters to facilitate acquisition and boresight.

Status checking would include issuance of enabling command to the satellite IMCS to begin automatic sequencing checks. These would also bring non-operating segments on line to achieve the required configuration of the various subsystems. When checkout is complete, a formal data logging command would be issued to record a sequential subsystems summary of satellite status into the ground center logs.

Where questionable status exists in various areas, the ground center might command prestored limited control actions on the satellite to test, debug, or verify system conditions. Pre-start status and configuration operations involve hundreds of thousands of control and data points, requiring significant processing time even with automatic sequencing. Satellite attitude refinement may involve long time delays and the integration of space-ground pre-start operations may amplify any such time delays. Special studies are needed to quantify these potential impacts on SPS operations.

Startup control functions for satellite power production and transmission are automatically sequenced by the spaceborne computers. The ground control center does not plan a direct role unless the on-board control system fails. In this event, direct ground control would be limited to performing emergency shutdown using separate control links in critical systems' areas.

Whether this would be implemented through separate, direct telemetry command linkes, which bypass the on-board IMCS, is undetermined. Special operations impact and design feasibility studies are needed in this area to clarify this situation.

The ground control center would monitor startup sequencing in order to provide any necessary ground support to the satellite. This includes antenna boresighting, pilot beam control and initiation of power reception, and conversion and distribution to the utility customer interfaces. Special coordination functions may be needed from the ground center to avoid power surges and to provide load leveling. Emergency shutdown of satellite operations may also be required if a major ground system failure occurs.

Ground center support to satellite startup will generally parallel satellite systems sequencing. Ground center support to boresight and ephemeris updates based on precision observations are major elements of this type of ground support. This may include revised satellite antenna gimbal angles to be inputted into the spaceborne data base. Attitude stationkeeping and boresight functions are expected to be long-term repetitive operations which extend into steady-state operations.

Once boresight is achieved, the solar panels can be brought on line. This operation is automatically sequenced by on-board computers. Ground center personnel would merely issue enabling commands once prerequisite spaceborne functional modes and system configurations are achieved and verified. Similarly, power distribution from the solar panels to the antenn is automatically implemented by on-board computers; this is also true of the voltage regulation process. Operations are only monitored on the ground. Preemptive ground support is required only if the on-board IMCS fails.

Antenna operations do require additional ground support because of boresight, alignment, and pilot beam functions. The mechanical pointing status of the antenna is verified during the earlier status checking phase. However, this must be continuously rechecked during startup to ensure safety and efficiency of power transmission.

Subsequent to boresight confirmation, enabling commands are sent to the satellite to turn on the reference phase frequency generator and related retro control electronics. This enables processing of the received pilot signals and initiation of power transmission. Earlier data base updates ensure insertion of the correct data to the phase control system.

Power beam monitors are located throughout the GRS site to provide an independent assessment of power beam pointing. Outputs of these monitors are computer polled and processed. Any residual pointing errors are translated into phase angle corrections and telemetered to the satellite for use by the beam programmers within the retro-electronic control system. Beam location and drift rate are monitored for possible emergency shutdown of satellite operations if error boundaries are exceeded.

If the satellite startup is coincident with termination of a solar eclipse, the ground center must confirm that battery recharging operations are initiated. If the satellite is projected to enter an eclipse, battery status must be verified. Use of klystrons for power transmission requires ample power for thermal stabilization, i.e., cathode heating, during eclipse periods.

Two operational considerations should be investigated, both relating to klystron activation. For example, if all klystrons are powered up simultaneously there will be possible power surges injected into the utility network. Therefore, simultaneous klystron energization is assumed to begin at low output levels with power output gradually raised so that the ground power station can gradually come on line to full power output to the utility network. Coordination between the rectenna, area, and utility network control center is needed to ensure smooth load time history changes.

Secondly, if klystrons were to be activated to full power with a large number of klystrons activated at a time, the impact on rectenna power output must be ascertained. Problems may result in coordination of panel grouping, conversion, and distribution. Unstable beam patterns could cause power output transients to utility customers, distribution surges with undesired bus breaker activations, and unstable dc-to-ac conversion processes.

In any event, power startup operations between space and ground systems must be closely coordinated to ensure smooth power delivery. Excessive transients in the satellite and rectenna/utility interfaces must be avoided. Any unusual situations will be displayed to rectenna center operations in real time. Emergency conditions must be relayed to any area and utility network command centers.

Nominal Operations—Satellite

At this point, the satellite has reached stabilized power production and transmission of that power to the rectenna. Power demands are constantly monitored at the GRS and transmitted to the satellite so that system surges can be mitigated and scheduled maintenance can be planned. For example, as midnight is reached at the users' locations, power demands reduce. Solar blankets, antenna components, or other related power production elements may be removed from the line.

Satellite status is constantly monitored so that any unscheduled power production or distribution changes can be accommodated. Constant communications, data, and commands are required between the satellite and the ground control center to achieve effective coordination.

Progressive maintenance checks are performed on the satellite to ensure reliable operation. The IMCS is constantly monitoring the status of components. As out-of-tolerance conditions are noted, the affected element is scheduled for repair or replacement. As a statistical basis is developed for predicting problem conditions, inspections and replacement are pre-scheduled at convenient times before the problem occurs. The GRS control center is expected to provide support through logistical scheduling and data base maintenance.

Scheduled outages occur during solar eclipses. These time periods can be utilized for minor repairs and replacements. Prior to each eclipse, coordinated planning occurs between the satellite and ground control center crews to develop a master maintenance schedule. Since an eclipse may last for a maximum of 1.2 hours, careful planning is needed to capitalize on this time for component replacements. Once replacement parts are installed and safe conditions are verified, selective activation of the affected subsystems is implemented to check out replaced parts in preparation for startup subsequent to the eclipse.

Nominal Operations—Ground

In this phase the satellite and GRS have reached stabilized power conversion and transmission to the utility network. The GRS center will receive periodic updates of scheduled power requirements from the utility network control center. These load schedules are translated by the GRS center into satellite power output schedules which take into account RF transmission, rectenna conversion, dc-to-dc conversion efficiencies, and related factors. This scheduling facilitates matching of generated power to load levels.

If for some reason the entire utility network or a dedicated customer drops off the line, the SPS power output may be shut down, adjusted, or switched to other loads. The GRS center must accommodate these and other contingencies, such as problems in rectenna dc-to-ac conversion and distribution. Emergency shutdowns or load adjustments require authenticated commands, rather than enabling messages, to be transmitted to the satellite.

Progressive maintenance schedules and procedures are prepared by the GRS center for rectenna, coverter, and distribution maintenance. Similar schedules and procedures are prepared for satellite. The control center personnel would convert such inputs from the GRS center into the required detailed form.

Satellite tracking and ephemeris refinement functions are performed by the supporting rectenna satellite tracking subsystem. Eclipse and related systems schedules are then prepared based on these schedules which include space-ground system startup, shutdown, and logistical support.

Several other safety, security, and environmental monitoring functions are performed during startup and steady-state operations. Safety will be of continuous concern. Prior to startup, maintenance and other types of workers must be evacuated from exposed radiation or high-power switching areas. Equipment must be properly configured and adjusted to avoid or investigate accidents or incidents. Particularly, close monitoring must be maintained and safety shutdown possibilities must be preserved during startup due to the presence of rapid and large power transients. Required safety functions must be defined along with supporting caution and warning instrumentation and controls.

Security perimeters must be defined so that the GRS site, control center, and switching yards are protected from intruders. This includes personal, command, and other forms of physical intrusion. Accidental or intentional intrusion of people must be prevented by automatic detector, entry controls, and guard personnel. Command links must be encrypted and physically protected from accidental or intentional interference or takeover. Arrangements must be made with appropriate authorities to avoid beam interruption by overflights which might cause power transients in various portions of the rectenna, confuse beam location monitoring equipment, or interrupt the pilot beam.

Environmental monitoring will also take place during all phases of system operation. For example, radio receivers which are located within the neighborhood of the GRS (e.g., 30-mile radius) will scan the radio spectrum for possible interference to radio, television, and other forms of radio frequency interference (RFI). Inputs to the GRS control center may allow identification of malfunctioning SPS equipment to resolve any RFI problems. The SPS system design must minimize environmental impacts to acceptable community levels. Electromagnetic interference (EMI) must also be monitored.

Communications

While communications have not been specifically studied in this preliminary analysis, a number of implications have been drawn. The satellite must maintain continuous contact with the ground control center. This includes data and commands in both directions. In addition, the uplink pilot beam from the rectenna is crucial to acquisition and fine pointing. The high EMI environment in the near vicinity of the satellite imposes potentially difficult conditions for communications; this requires primary emphasis and special design considerations to eliminate this possibility.

Intra-satellite communications are highly dependent upon optical data buses to avoid the EMI problem.

Space-ground communications may have to be encrypted to avoid command intrusions and interference. Data compression may be required if data traffic becomes too heavy due to large data base updates, significant amounts of video traffic, or excessive interference.

2.4.2 SATELLITE MAINTENANCE

Introduction

Satellite maintenance operations will vary, depending on the type and configuration of the satellite. The Rockwell reference concept, which utilizes klystrons in the antenna, can be expected to require considerable more maintenance than in the case of the solid-state satellite, which employs solid-state devices characterized by much higher reliability than the klystrons. For these reasons, the maintenance concept for the klystron-equipped satellite entails a permanent crew at each satellite, while the solid-state satellite will be maintained through periodic visits by maintenance personnel. The overall concepts for each type of satellite are summarized below.

Rockwell Reference Concept

The permanent satellite maintenance base is located on the first frame which is adjacent to the rotary joint, since the bulk of the maintenance activity is anticipated to be on antenna concepts (Figure 2.1-2). (For a center-mounted antenna configuration, the base would be located on one of the two center frames.) Spares are transported to GEO via EOTV's and delivered to specific satellites by IOTV's.

Antenna

Klystron maintenance is anticipated to be a major portion of the overall maintenance effort. The population of approximately 143,000 klystrons is life-limited and also can be expected to experience a higher number of random failures. Currently, mean time to failures (MTTF) of over 150,000 hours is being projected for TWT's, which are somewhat similar to klystrons. The primary life-limiting factor is the cathodes. Even if klystrons reflecting SPS requirements can be developed with similar MTTF's, a virtually total replacement would be required over a 30-year period. An alternative would be to develop a klystron design which would permit changing the cathodes without removing the klystron.

Because of the thermal interface between the klystrons and heat pipes, it is not clear at present as to what constitutes an LRU. Preferably, it would consist of a klystron cathode or klystron, but could be a power module or higher assembly. Regardless of LRU definition, means for removal and replacement of either the entire klystron or the cathode element alone will be provided by the gantries or cable-mounted antenna platforms which provide access to both sides of the antenna. These platforms will be equipped with the special equipment needed to perform maintenance on both the face and the underside of the antenna. Since shutdown will be required during maintenance, it is anticipated that degradation to a predetermined point would be tolerated and that a nonoperating period of several days might be required for complete restoration of functions.

Power Distribution System (PDS)

The components comprsing the PDS (e.g., switch gears) generally are more reliable and fewer in number than the klystrons, but random failures can be expected. (PDS elements on the back side of the antenna are accessible to the antenna gantry.) Because of the locations of these components in the bottom crossbeams of the troughs, the distance of a failed component from the maintenance base could approach 16,000 m for an end-mounted antenna configuration. Removal and replacement of PDS components, then, will require either an extensive track system or a free-flying facility with the capability of a manned work module (MWM) plus space for components. Since maintenance operations would be sporadic, and would occur at various locations, a free-flying concept appears to be preferable to an extensive track system which would have to provide access to every crossbeam throughout the length of the satellite, as well as to other areas.

A version of the free-flying concept could consist of an arrangement similar to the vehicle shown in Figure 2.4-4. The module would be equipped with special grabber arms for attaching to a 2-m beam and providing a measure of stability during the operation. Sections of the solar array will be deactivated during maintenance periods. However, temperatures of 125°C or higher may be encountered at the bottom of the trough. Depending on detailed design characteristics and the type of materials used in construction relating to thermal control, it may be necessary to work from the underside of the crossbeam rather than the top. This would slightly restrict the access, but the operations still could be accomplished.

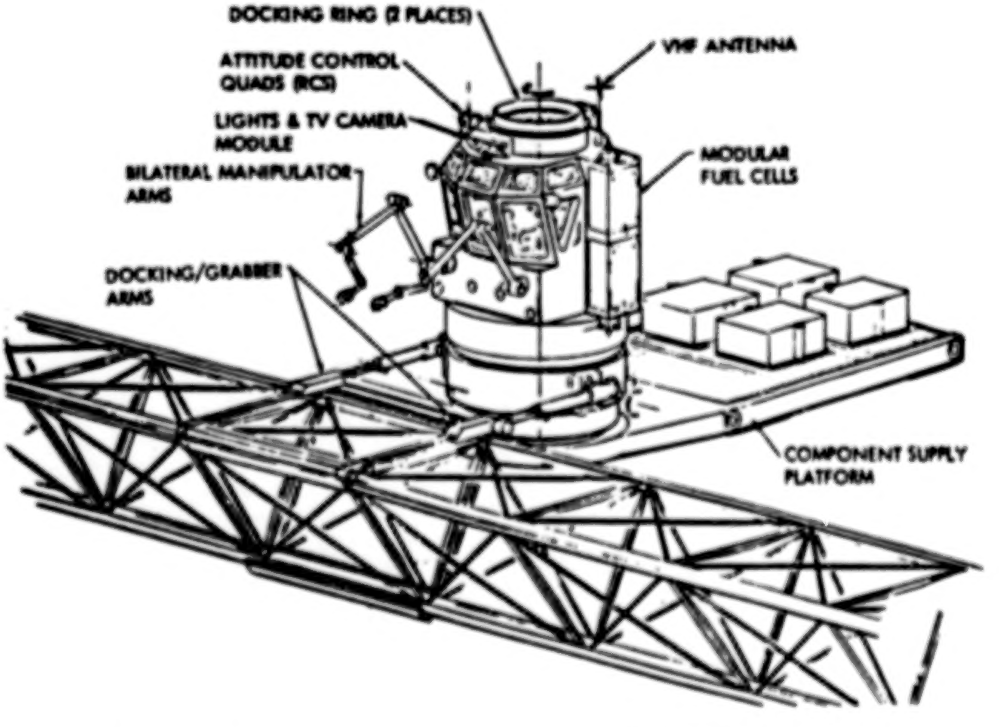
DOCKING RING (2 PLACES)
VHF ANTENNA
ATTITUDE CONTROL QUADS (RCS)
LIGHTS & TV CAMERA MODULE
MODULAR FUEL CELLS
BILATERAL MANIPULATOR ARMS
DOCKING/GRABBER ARMS
COMPONENT SUPPLY PLATFORM

Figure 2.4-4. Manned Work Module, Free-Flying or Stationary

Solar Blanket/Reflector

The design and sizing of these elements are predicated on the degradation expected over 30 years, including meteoroid penetration. To effectively immobilize a large section of the solar blanket would require some kind of catastrophic event (e.g., large meteor, collision, etc.). The isolation, removal, and replacement of small solar blanket sections with the many interconnects do not appear feasible at this time. Replacement of an entire 25×730-m strip by utilization of free-flyers also does not appear practical. The alternative of using permanently installed equipment mounted on tracks or cables would require an installation in each bay of each trough, totaling 60 sets; most of these installations probably would not be used during the satellite life because of the low probability of catastrophic events. Therefore, the current design accepts the predicted degradation and does not provide for blanket strip replacement.

The same rationale applies in general to the reflector sheets which are considerably larger. However, in the event of a large perforation or tear in the reflector, it may be possible, by use of free-flyers, to treat the edges of the perforation in some manner to avoid propagation.

Attitude Control

Servicing and maintenance of the reaction control system, including thruster replacement and propellant replenishment, will be accomplished by the same type of vehicle (beam-grabbing MWM) utilized for the PDS.

Summary

With the exception of solar blanket and reflector replacement, maintenance of the satellite subsystems is feasible. Partial or complete satellite shutdown will be required for conducting maintenance in some areas. More detailed design information for both satellite subsystem installations and manned manipulators will be required before maintenance operations can be defined in any great detail, timelines established, and satellite downtime assessed.

Solid-State Satellite

The maintenance concept developed for the SPS satellite defined in Exhibit C (April 1979) entailed stationing of a maintenance crew at each satellite (or at a maintenance base) on a full-time basis. The large number of klystrons utilized for each satellite antenna together with the expected klystron life of ten years or less, plus anticipated maintenance activities in support of the PDS, rotary joint, etc., would be expected to generate a requirement for maintenance operations sufficient to justify this permanent, satellite maintenance base. The solid-state satellite concept (Figure 2.1-4), which substitutes solid-state amplifiers for klystrons, will reflect a substantial increase in expected antenna reliability. Given a successful post-assembly checkout, the antenna (solar cells and solid-state devices) is expected to operate unmaintained for a 30-year period with minimum degradation. Therefore, the current maintenance scenario does not include replacement or repair of antenna panel modules as either a scheduled or unscheduled operation.

It is recognized that further development of the high-power solid-state amplifiers and accumulation of test data may dictate a change in this policy to allow for periodic maintenance. In any event, the characteristics and configuration of the solid-state satellite concept should require substantially less maintenance than its klystron-equipped counterpart. For this reason, maintenance personnel will not be based at each satellite, but instead will be stationed at one of the two satellite construction fixtures and will also be utilized to maintain construction fixture equipment when not involved in satellite maintenance operations.

Spares Requirements

Table 2.4-1 contains an estimate of the annual spares required for each dual satellite configuration. The solar cell spares are for the special arrays which provide power for remotely located electric ion thrusters. It can be seen that the propellants for attitude control and stationkeeping comprise the bulk of the mass and must be replenished yearly, regardless of other maintenance requirements. The remainder of the equipment listed in the table was estimated as a percentage of the subsystem mass, since the design detail required for a more precise evaluation is not now available. An exception is thruster grids which must be replaced periodically; however, the number of thrusters and weight invovled (4 kg/grid) constitute a relatively insignificant percentage of the overall mass.

Table 2.4-1. Annual Spares Requirements for Each Satellite

ELEMENT	DATA BASE MASS FOR COMPLETE SATELLITE	EST. SPARES REQMTS (%)	SPARES MASS (kg×10^{-6})
• MECHANISMS	0.031	1.0	NEG
• PWR DIST. AND CONDITIONING	0.007	2.0	NEG
• INFORMATION MGMT AND CONTROL	0.161	2.0	0.003
• ATT. CONT. HDWR	0.232	-	NEG*
• SOLID STATE ANT. DEV.	4.674	NO SPARES	-
• SOLAR CELLS	0.089	0.5	NEG
• ATT. CONTROL ELECTRONICS	0.172	2.0	0.003
		+25% GROWTH	0.066

*PRIMARILY THRUSTER GRIDS @ 4 kg/GRID

ATT. CONT. PROPELLANT/YR = 0.164
10% FOR TANKAGE .016
0.180×10^6 kg
SPARES 0.066
TOTAL 0.246×10^6 kg

Operations

The annual maintenance mass for each satellite is transported to LEO via HLLV's and then to the satellite construction fixture in GEO by EOTV's. Because of the close proximity of the two construction fixtures to each other, one fixture would be designated as the maintenance control center for storing and dispensing the supplies. However, the maintenance crews could be somewhat equally divided between the two fixtures for more efficient utilization in other tasks when not engaged in a maintenance sortie.

Because of the number of satellites which eventually will be operational, it will be necessary to establish a maintenance control center on one of the satellite construction fixtures which will remain in operation as long as satellites are still in commission. The center will store data received from the information management and control systems of each operating satellite, either by direct reception, update link from the ground, or a combination of both in order to maintain a satellite "health" status relevant to hardware anomalies. Prior to planning a maintenance sortie to one or more satellites, satellite data would be evaluated to determine the type and number of necessary spares and maintenance support equipment/tool requirements; e.g., free-flying manned work module or cherry picker (Figure 2.4-4), special removal/installation tools, etc. This is in addition to ACSS propellant replenishment which is scheduled on an annual basis.

Following maintenance data analysis and loading of the IOTV with the ACSS cryogenic propellant tanks and other equipment, the IOTV would proceed to the satellite to be maintained. A crew module providing habitat for the maintenance crew would be carried in a separate IOTV. After rendezvous with the satellite, a number of dockings at the various RCS locations would be accomplished where, under human remote control, the full propellant tanks would be inserted by quick-disconnects into the propellant manifold and the partially empty tanks removed for ultimate return to earth. Concurrently, other required maintenance operations would be conducted as required. All manned activities would utilize protected modules—no EVA is planned except in case of emergency.

The size of the maintenance crew will vary, depending on the scope of required activities and the distance to the satellite, which could result in utilization of multiple shifts. For overall planning purposes, an average crew size of 24 men has been postulated. It has been assumed that one dual satellite configuration can be serviced per sortie from the base, and that each crew ill visit four dual satellites during their 90-day orbital tour.

The requirement for a protected environment and the probable need for mobile cherry pickers at each satellite during maintenance operations generate the ingredients of an operational and cost trade study. A possible approach is to station selected habitat and maintenance modules at each satellite on a permanent basis, to be activated as required during the maintenance visit. This concept reduces the propellant needed to transit between the base and the satellites because of reduced mass, but increases the material cost because of duplication of facilities and equipment. Moreover, any required maintaining of equipment can be accomplished more effectively at a central location. No definite conclusions regarding the preferred approach have been reached; the alternative concepts should be the subject of further study.

End-Mounted Solid-State Antenna

The maintenance concept developed for the end-mounted solid-state antenna essentially is a hybrid of the concepts discussed in the previous sections. The satellite (Figure 1.2-17) consists of a solar collection array similar to that required for the reference satellite concept, and an antenna which replaces the klystron tube power amplifier with a version utilizing solid-state power amplifiers. Thus, the maintenance requirements would fall between the two concepts already discussed.

2.5 MASS PROPERTIES

A summary of the mass properties for the eight satellite concepts considered during Exhibit D of this contract is provided in Table 2.5-1. The estimated satellite mass, including a 25-percent growth factor, varies from 16.386×10^6 kg for the MBG version of the solid-state sandwich configuration, to 39.973×10^6 kg for the solid-state end-mounted configuration.

The best density in kilograms per kilowatt at the utility interface (kg/kW_{UI}) is obtained for the MBG magnetron concept with a value of 3.85 kg/kW_{UI}. The worst density occurs on the standard cell solid-state sandwich concept with a value of 8.52 kg/kW_{UI}.

Table 2.5-1. Mass Properties Summary (Aug. 1980)
(10^6 kg)

	CONCEPTS							
	REFERENCE		MAGNETRON		SOLID-STATE END-MOUNTED		SOLID-STATE SANDWICH	
	STD CELL GaAs	HBG CELL GaAlAs/GaAs	STD CELL GaAs	HBG CELL GaAlAs/GaAs	STD CELL GaAs	HBG CELL GaAlAs/GaAs	STD CELL GaAs	HBG CELL GaAlAs/GaAs
1.1.1 ENERGY CONVERSION (SOLAR ARRAY)								
STRUCTURE	1.514	1.133	1.601	1.245	1.496	1.233	3.412	2.411
PRIMARY	(0.928)	(0.804)	(0.904)	(0.565)	(1.077)	(0.902)	(3.026)	(2.138)
SECONDARY	(0.586)	(0.429)	(0.697)	(0.680)	(0.419)	(0.331)	(0.386)	(0.273)
MECHANISMS	0.070	0.070	0.070	0.070	0.087	0.078	0.027	0.019
CONCENTRATOR	1.030	0.648	0.988	0.663	1.169	0.766	2.075	1.646
SOLAR PANEL	7.174	4.804	6.880	4.619	8.138	5.607	0.076(a)	0.076(a)
POWER DISTRIBUTION AND CONTROL	2.757	1.388	4.146	2.874	1.112	0.846	0.015	0.015
PWR COND. EQUIPMENT & BATT.	(0.319)	(0.206)	(0.319)	(0.319)	(0.102)	(0.222)	(0.013)	(0.013)
POWER DISTRIBUTION	(2.438)	(1.182)	(3.827)	(2.555)	(1.010)	(0.624)	(0.002)	(0.002)
THERMAL	NONE	NONE	NONE	NONE	NONE	NONE	NONE	NONE
MAINTENANCE	0.092	0.063	0.092	0.092	0.104	0.056	0.100	0.100
1.1.3 (P) INFORMATION MANAGEMENT AND CONTROL	0.050	0.050	0.050	0.050	0.057	0.057	0.033(b)	0.033(b)
DATA PROCESSING	(0.021)	(0.021)	(0.021)	(0.021)	(0.024)	(0.024)	(0.014)	(0.014)
INSTRUMENTATION	(0.029)	(0.029)	(0.029)	(0.029)	(0.033)	(0.033)	(0.019)	(0.019)
1.1.4 (P) ATTITUDE CONTROL	0.116	0.116	0.116	0.116	0.116	0.116	0.103	0.103
SUBTOTAL	12.803	8.272	13.943	9.729	12.279	8.759	5.841	4.403
1.1.2 POWER TRANSMISSION (ANTENNA)								
STRUCTURE	0.838	0.838	0.547	0.547	1.409	1.409	0.729	0.649
PRIMARY	(0.023)	(0.023)	(0.023)	(0.023)	(0.094)	(0.097)	(0.161)	(0.143)
SECONDARY	(0.815)	(0.815)	(0.524)	(0.524)	(1.315)	(1.315)	(0.568)	(0.506)
MECHANISM	0.002	0.002	0.002	0.002	0.004	0.004	NONE	NONE
SUBARRAY	7.050	7.050	3.320	3.320	10.561	10.561	8.821	7.053
POWER DISTRIBUTION AND CONTROL	2.453	2.453	1.515	1.515	4.405	4.405	INCLUDED	INCLUDED
PWR COND. EQUIPMENT & BATT.	(1.680)	(1.680)	(0.346)	(0.346)	(2.164)	(2.164)		
POWER DISTRIBUTION	(0.773)	(0.773)	(1.169)	(1.169)	(2.241)	(2.241)		
THERMAL	0.720	0.720	NONE	NONE	NONE	NONE	NONE	NONE
ANTENNA CONTROL ELECTRONICS	0.170	0.170	0.170	0.170	0.340	0.340	0.340	0.340
MAINTENANCE	0.107	0.107	0.107	0.107	0.448	0.448	0.436	0.408
1.1.3 (P) INFORMATION MANAGEMENT AND CONTROL	0.640	0.640	0.320	0.320	1.627	1.662	0.258(c)	0.258(c)
DATA PROCESSING	(0.380)	(0.380)	(0.190)	(0.190)	(1.385)	(1.385)	(0.152)	(0.152)
INSTRUMENTATION	(0.260)	(0.260)	(0.130)	(0.130)	(0.237)	(0.237)	(0.104)	(0.104)
1.1.4 (P) ATTITUDE CONTROL	NEGLIG.	NEGLIG.	NEGLIG.	NEGLIG.	NEGLIG.	NEGLIG.	NEGLIG.	NEGLIG.
SUBTOTAL	11.980	11.980	5.981	5.981	18.789	18.789	10.582	8.705
1.1.6 INTERFACE								
STRUCTURE	0.170	0.170	0.257	0.257	0.236	0.236	N/A	N/A
PRIMARY	(0.136)	(0.136)	(0.136)	(0.136)	(0.168)	(0.168)		
SECONDARY	(0.034)	(0.034)	(0.121)	(0.121)	(0.068)	(0.068)		
MECHANISMS	0.033	0.033	0.033	0.033	0.072	0.072	N/A	N/A
POWER DISTRIBUTION AND CONTROL	0.288	0.288	1.194	1.194	0.538	0.538	N/A	N/A
POWER DISTRIBUTION	(0.271)	(0.271)	(1.177)	(1.177)	(0.487)	(0.487)		
SLIP RING BRUSHES	(0.017)	(0.017)	(0.017)	(0.017)	(0.051)	(0.051)		
THERMAL	NONE	NONE	NONE	NONE	NONE	NONE	N/A	N/A
MAINTENANCE	0.032	0.032	0.032	0.032	0.064	0.064	-	-
COMMUNICATION	TBD	TBD	TBD	TBD	TBD	TBD	TBD	TBD
SUBTOTAL	0.523	0.523	1.516	1.516	0.910	0.910	-	-
SPS TOTAL (DRY)	25.306	20.775	21.44	17.226	31.978	28.458	16.423	13.108
GROWTH (25%)	6.326	5.194	5.36	4.307	7.995	7.114	4.106	3.277
TOTAL SPS (DRY) WITH GROWTH	31.632	25.969	26.8	21.533	39.973	35.572	20.529	16.386
SATELLITE PWR & UTILITY INTERFACE (GW)	5.07	5.07	5.6	5.6	5.22	5.22	2.41	3.06
SATELLITE DENSITY, KG/KW$_{UI}$	6.24	5.12	4.79	3.83	7.66	6.81	8.52	5.35

NOTES: (a) AUXILIARY POWER ONLY
(b) TWO-THIRDS MASS OF REFERENCE CONCEPT
(c) 20% REF. MASS PER ANTENNA

(P) = PARTIAL

MICROFILMED FROM
BEST AVAILABLE COPY

3.0 SUBSYSTEMS

3.1 SATELLITE

3.1.1 INTRODUCTION

This section presents in some detail the selected subsystem concepts and characteristics of the various major satellite subsystems. The approach taken emphasizes the subsystem design appropriate to the reference satellite concept with the variations appropriate to the other configurations treated as deltas. Where the selected subsystem concept differs significantly from the reference concept, the subsystem will be discussed in each appropriate section. The detailed subsystems are (1) power generation, (2) power distribution and control, (3) microwave antenna, (4) information management and control, (5) attitude control and stationkeeping, (6) structures, and (7) thermal control.

Additional functional areas such as communications, safety, security, etc., have not been defined as of this time and, therefore, although they are considered of major importance, are not included.

The relationships of the various subsystem elements onboard the satellite are shown in Figure 3.1-1.

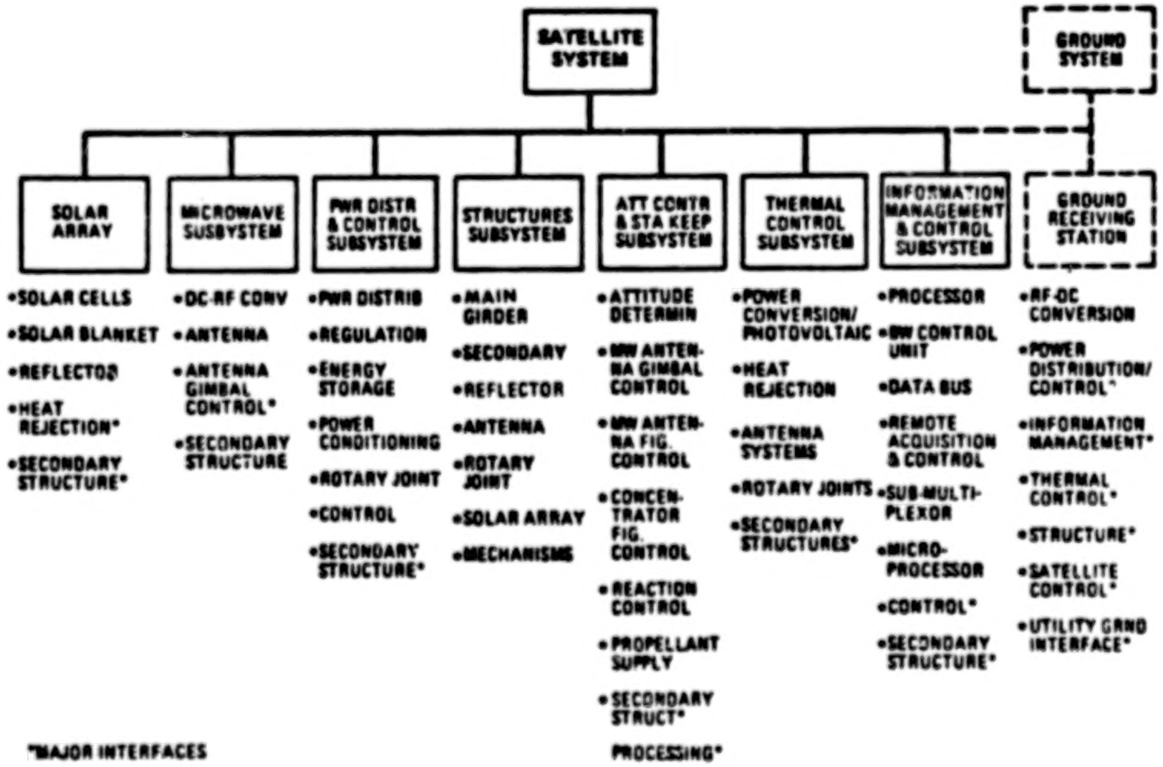
SATELLITE SYSTEM
GROUND SYSTEM
SOLAR ARRAY
MICROWAVE SUBSYSTEM
PWR DISTR & CONTROL SUBSYSTEM
STRUCTURES SUBSYSTEM
ATT CONTR & STA KEEP SUBSYSTEM
THERMAL CONTROL SUBSYSTEM
INFORMATION MANAGEMENT & CONTROL SUBSYSTEM
GROUND RECEIVING STATION
•SOLAR CELLS
•SOLAR BLANKET
•REFLECTOR
•HEAT REJECTION*
•SECONDARY STRUCTURE*
•DC-RF CONV
•ANTENNA
•ANTENNA GIMBAL CONTROL*
•SECONDARY STRUCTURE
•PWR DISTRIB
•REGULATION
•ENERGY STORAGE
•POWER CONDITIONING
•ROTARY JOINT
•CONTROL
•SECONDARY STRUCTURE*
•MAIN GIRDER
•SECONDARY
•REFLECTOR
•ANTENNA
•ROTARY JOINT
•SOLAR ARRAY
•MECHANISMS
•ATTITUDE DETERMIN
•MW ANTENNA GIMBAL CONTROL
•MW ANTENNA FIG. CONTROL
•CONCENTRATOR FIG. CONTROL
•REACTION CONTROL
•PROPELLANT SUPPLY
•SECONDARY STRUCT*
PROCESSING*
•POWER CONVERSION/ PHOTOVOLTAIC
•HEAT REJECTION
•ANTENNA SYSTEMS
•ROTARY JOINTS
•SECONDARY STRUCTURES*
•PROCESSOR
•MW CONTROL UNIT
•DATA BUS
•REMOTE ACQUISITION & CONTROL
•SUB-MULTIPLEXOR
•MICRO-PROCESSOR
•CONTROL*
•SECONDARY STRUCTURE*
•RF-DC CONVERSION
•POWER DISTRIBUTION/ CONTROL*
•INFORMATION MANAGEMENT*
•THERMAL CONTROL*
•STRUCTURE*
•SATELLITE CONTROL*
•UTILITY GRND INTERFACE*
*MAJOR INTERFACES

Figure 3.1-1. Total System

3.1.2 POWER GENERATION

GaAs Solar Cells

Introduction

The solar photovoltaic power subsystem on the reference satellite consists of the solar cells, blankets, attachment devices, and includes the reflector membranes and attachment devices. Gallium arsenide (GaAs) cells have been selected as the point-design solar cell. The cell is fastened to a thin-film Kapton substrate with an FEP adhesive. The photovoltaic power conversion subsystem is designed for a geometric concentration ratio of 2.

All of the various satellite configurations, with the exception of the dual solid-state sandwich configuration, use similar configuration to generate their required power. Accordingly, the discussion will focus upon the reference configuration with the differences being described as appropriate. The sandwich configuration, of the other hand, is radically different in that (1) the solar cell is bonded directly to the back of the microwave subarray, and (2) the reflector system is a two-element steerable array with an effective concentration ratio (CR_E) of 5.2.

The reflector concept will be discussed in this section, but the basic configuration of the sandwich subarray will be discussed in Section 3.1.3. It is sufficient to say, at this time, that the solar panel portion of the subarray is assumed to be identical to the solar panel described here.

The functional requirements for the photovoltaic power subsystems were listed in Tables 2.1-1 and 2.1-2. The system efficiency block diagram was shown in Figure 2.1-2. Shown in the figure are power levels, efficiencies, temperatures, degradation factors, and solar cell area requirements. A simplified integrated block diagram for the CR-2 point-design concept is presented in Figure 3.1-2. The major assemblies and components that are required for the photovoltaic subsystem are shown in Figure 3.1-3.

Solar Cells

The solar cell used in the SPS design is a GaAs cell having an efficiency of 18.16% at air mass zero (AMO) and 113°C. The cell consists of the GaAs junction, GaAlAs window, cover/substrate, current collectors and an antireflection coating. The basic cell design is the inverted GaAs/sapphire design having a weight of 0.252 kg/m^2. The selected design is shown in Figure 3.1-4. The point-design cell has a 20-μm sapphire substrate upon which is grown a 5-μm junction. The voltage and current characteristics of the cell as a function of operating temperature are shown in Figure 3.1-5.

Solar Panel

The solar panel for the planar configuration consists of a 25-μm Kapton membrane upon which the cells are fastened with a thermosetting FEP adhesive. Also included in the panel are the interconnects, transparent thermal coating required for thermal control, attachments, tensioning devices, and sensors.

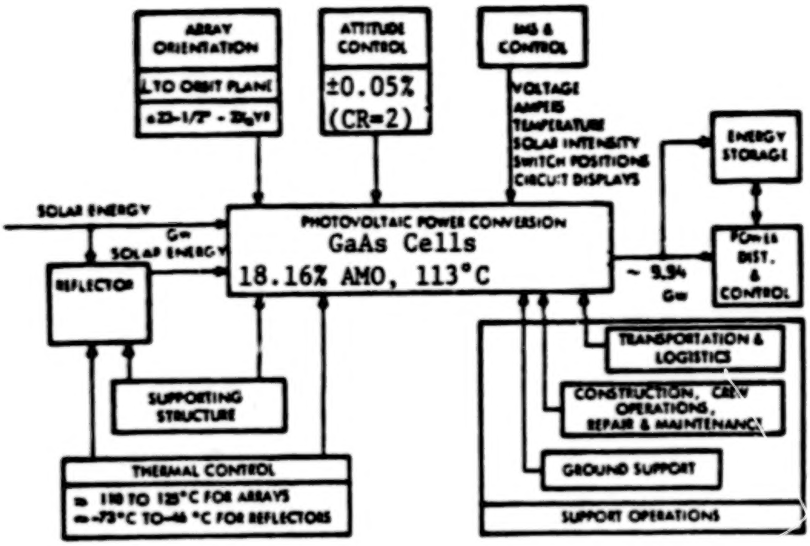
ARRAY ORIENTATION
⊥ TO ORBIT PLANE
±23-1/2° - 2V
ATTITUDE CONTROL
±0.05%
(CR=2)
IMS & CONTROL
VOLTAGE
AMPERS
TEMPERATURE
SOLAR INTENSITY
SWITCH POSITIONS
CIRCUIT DISPLAYS
ENERGY STORAGE
SOLAR ENERGY
Gw
SOLAR ENERGY
PHOTOVOLTAIC POWER CONVERSION
GaAs Cells
18.16% AMO, 113°C
~ 9.94 Gw
POWER DIST. & CONTROL
REFLECTOR
SUPPORTING STRUCTURE
THERMAL CONTROL
≈ 110 TO 125°C FOR ARRAYS
≈ -73°C TO -46 °C FOR REFLECTORS
TRANSPORTATION & LOGISTICS
CONSTRUCTION, CREW OPERATIONS, REPAIR & MAINTENANCE
GROUND SUPPORT
SUPPORT OPERATIONS

Figure 3.1-2. Simplified Integrated Block Diagram, Photovoltaic (CR-2)

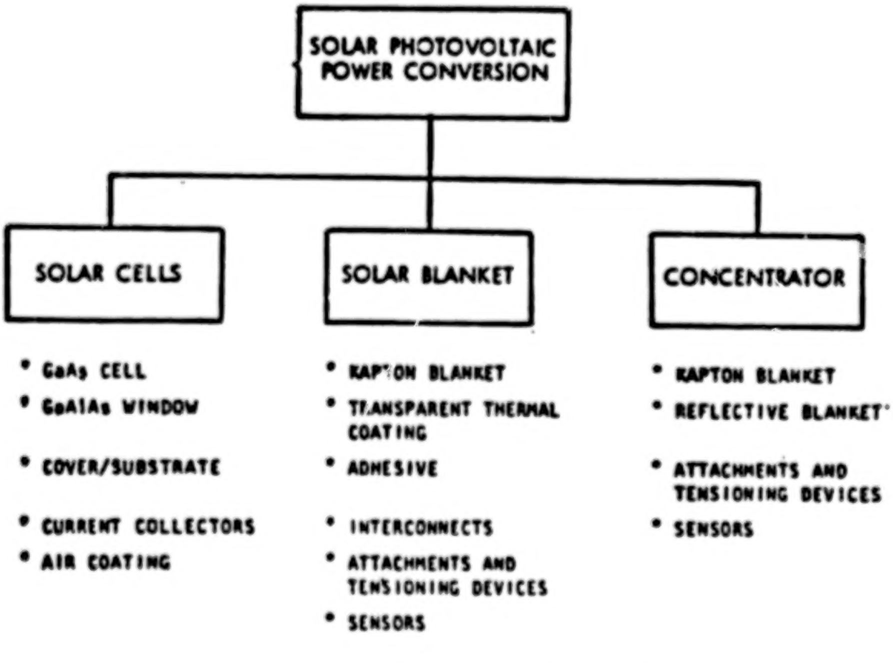
SOLAR PHOTOVOLTAIC POWER CONVERSION
SOLAR CELLS
SOLAR BLANKET
CONCENTRATOR
• GaAs CELL
• GaAlAs WINDOW
• COVER/SUBSTRATE
• CURRENT COLLECTORS
• AIR COATING
• KAPTON BLANKET
• TRANSPARENT THERMAL COATING
• ADHESIVE
• INTERCONNECTS
• ATTACHMENTS AND TENSIONING DEVICES
• SENSORS
• KAPTON BLANKET
• REFLECTIVE BLANKET
• ATTACHMENTS AND TENSIONING DEVICES
• SENSORS

Figure 3.1-3. Assembly Tree—Power Generation

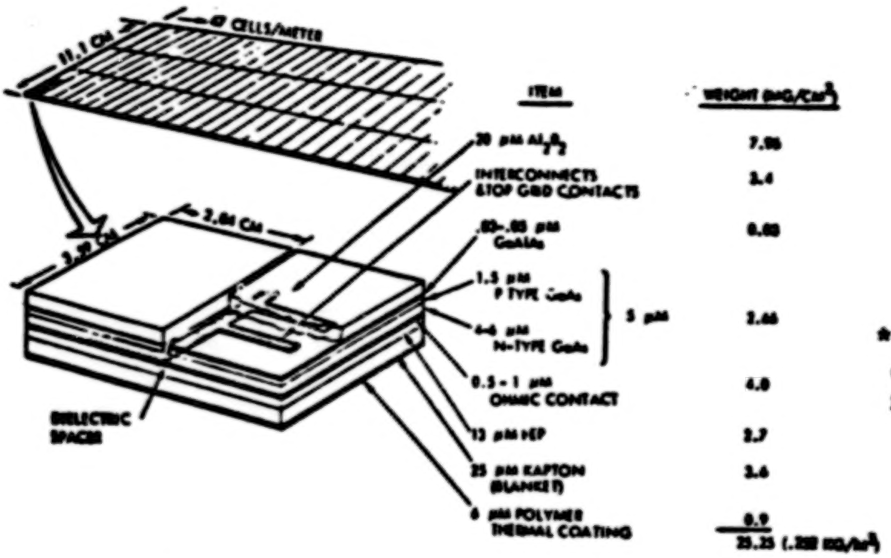
47 CELLS/METER
11.1 CM
2.04 CM
3.59 CM
DIELECTRIC SPACER
ITEM
WEIGHT (MG/CM²)*
20 µM Al2O3
7.95
INTERCONNECTS & TOP GRID CONTACTS
3.4
.03-.05 µM GaAlAs
0.03
1.5 µM P TYPE GaAs
4-6 µM N-TYPE GaAs
5 µM
2.66
0.5-1 µM OHMIC CONTACT
4.0
13 µM FEP
2.7
25 µM KAPTON (BLANKET)
3.6
6 µM POLYMER THERMAL COATING
0.9
25.25 (.253 KG/M²)

*Includes contingency factor

Figure 3.1-4. GaAs Solar Cell Blanket Cross Section

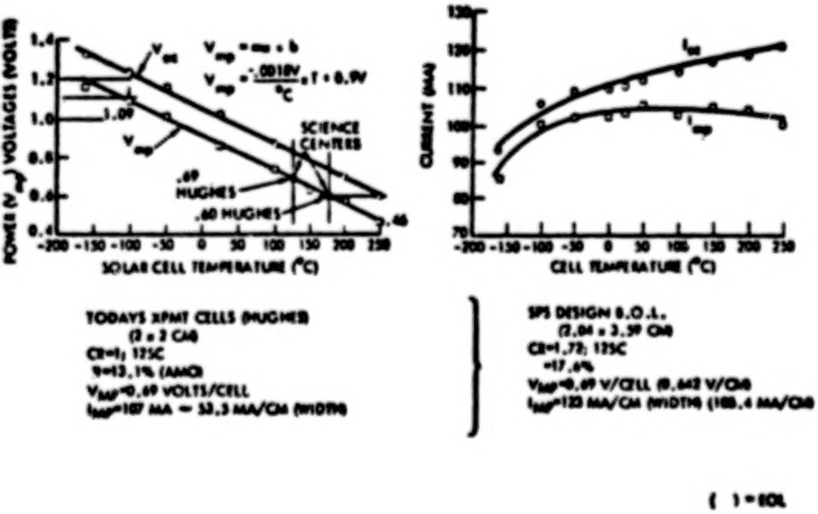

Figure 3.1-5. GaAs Solar Cell Voltage
and Current Characteristics

The solar cell assemblies will be manufactured in panel form and the solar cells attached. This assembly will then be rolled up on a drum-type canister. It is postulated that the panels will be 25 m wide by approximately 750 m in length for the reference concept. The magnetron and solid-state end-mounted concept panels are 700 m and 690 m, respectively. The canisters are then transported to orbit where the panels are deployed via a rollout deployment-type operation.

The solar array layout for the GaAs reference configuration is shown in Figure 3.1-6. The solar array in each trough (effective cell area) measures

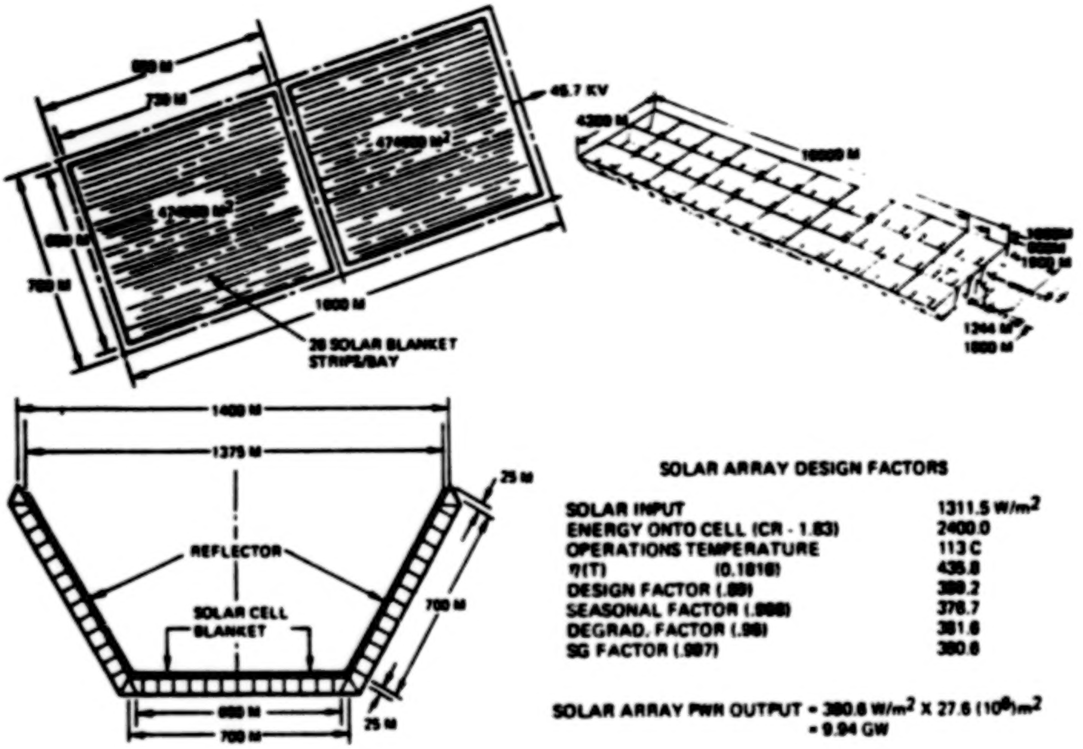

SOLAR ARRAY DESIGN FACTORS

SOLAR INPUT	1311.5 W/m²
ENERGY ONTO CELL (CR - 1.83)	2400.0
OPERATIONS TEMPERATURE	113 C
η(T) (0.1816)	435.8
DESIGN FACTOR (.89)	388.2
SEASONAL FACTOR (.970)	376.7
DEGRAD. FACTOR (.96)	361.6
SG FACTOR (.997)	360.6

SOLAR ARRAY PWR OUTPUT = 360.6 W/m² X 27.6 (10⁶)m²
= 9.94 GW

Figure 3.1-6. Solar Array Dimensions and Panel Power Output

650×730 m for 474,500 m^2. Twenty-six 25-m panels are required for the troughs. Two solar arrays are in series to provide the required 45.7 kV. The total deployed solar area for the reference SPS is 28.47×10^6 m^2. The usable area considering regulation, sun angle, etc., is approximately 27.6×10^6 m^2. The basic building block is in a 1-m^2 module configuration and the cells are connected together in a series parallel arrangement. The module output is calculated to be 361 W/m^2 (nominal, worst case) at the end of life (EOL) with a nominal concentratio ratio of 2. The cell characteristics and cell design factors used to form a submodule for the solar blanket are also shown in Figure 3.1-6.

The solar panel power segment for the solid-state sandwich configuration is unique in that the solar cells and the microwave power segments are combined into a back-to-back or "sandwich" array (Figure 3.1-56). The basic solar panel, e.g., the cells, interconnects, and supporting membrane, are manufactured in a manner identical to that described above for the planar concepts.

The solar panel mass used to generate the system primary power is accounted for in the microwave antenna mass summary. Subsystem and auxiliary power source photovoltaic panels are accounted for as a separate item. The total area of the auxiliary panels is estimated as 0.302 km^2, for a total mass of 0.076×10^6 kg.

Reflectors

Thin reflector membranes are used on the SPS to reflect the sun onto the solar cell surfaces and obtain a nominal concentration ratio of 2. The reflector is made of 12.5-µm (0.5-mil) aluminized Kapton. Reflectivity of the reflector was taken at 0.87 BOL and 0.83 EOL. The reflector membrane has a mass of 0.018 kg/m², while the aluminum coating adds an additional 96 kg/km² (500 Å thick). The reflective membranes are mounted on the structure using attachments and tensioning devices. Tensioning based on structural limit of the existing beam design (with safety factor of 1.5) indicates that tensioning of up to 50-75 psi can be used.

Reflectivity values for coated metal reflectors and thin-film membranes are illustrated in Table 3.1-1. The thin-film membranes, utilizing an aluminum coating, have the potential of low weight and cost with high reflectivity. The table indicates that an aluminized film of at least 200 Å is required for a reflectivity of 0.87. In the study, a 500 Å coating was used on the Kapton film. The radiation dose rates for a geosynchronous orbit are illustrated in Figure 3.1-7. Long-term and on-orbit testing is required to verify the actual

Table 3.1-1. Reflectivity

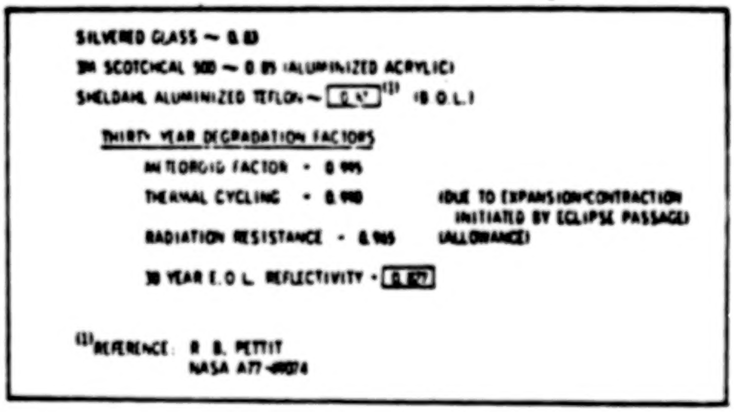
SILVERED GLASS ~ 0.83
3M SCOTCHCAL 500 ~ 0.85 (ALUMINIZED ACRYLIC)
SHELDAHL ALUMINIZED TEFLON ~ $\boxed{0.9[illegible]}$ (1) (B.O.L.)

THIRTY YEAR DEGRADATION FACTORS
METEOROID FACTOR = 0.995
THERMAL CYCLING = 0.990 (DUE TO EXPANSION/CONTRACTION INITIATED BY ECLIPSE PASSAGE)
RADIATION RESISTANCE = 0.985 (ALLOWANCE)
30 YEAR E.O.L. REFLECTIVITY = $\boxed{0.87}$

(1) REFERENCE: R. B. PETTIT
NASA A77-[illegible]

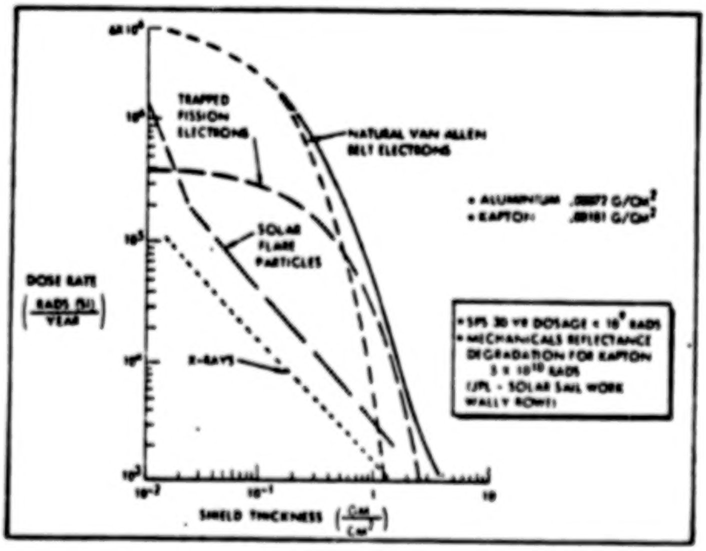

Figure 3.1-7. Radiation Dose Rates

reflectivity values used for the design of the SPS reflectors. The Kapton film properties such as ultimate strength, coefficient of thermal expansion, and dielectric strength as a function of temperature are shown in Figure 3.1-8.

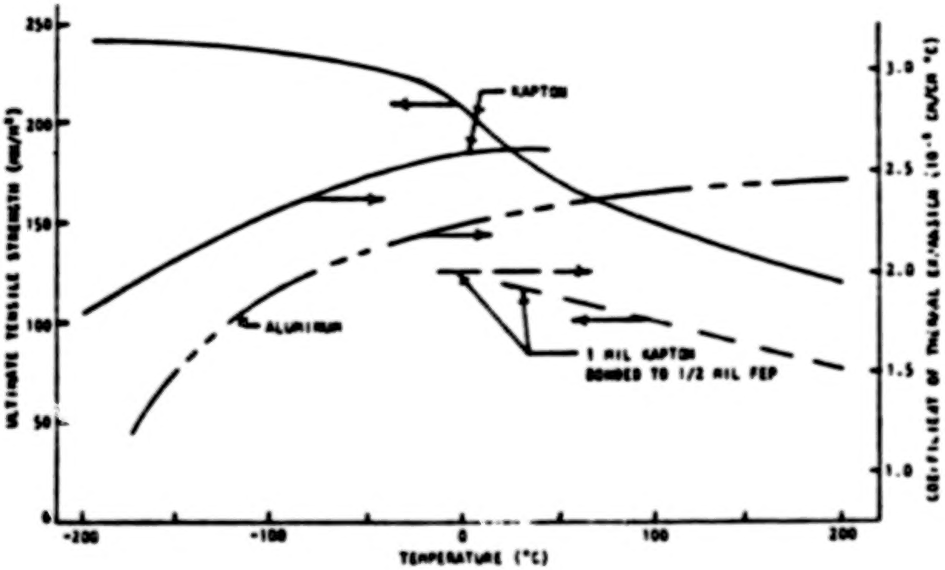

(b) Dielectric Strength

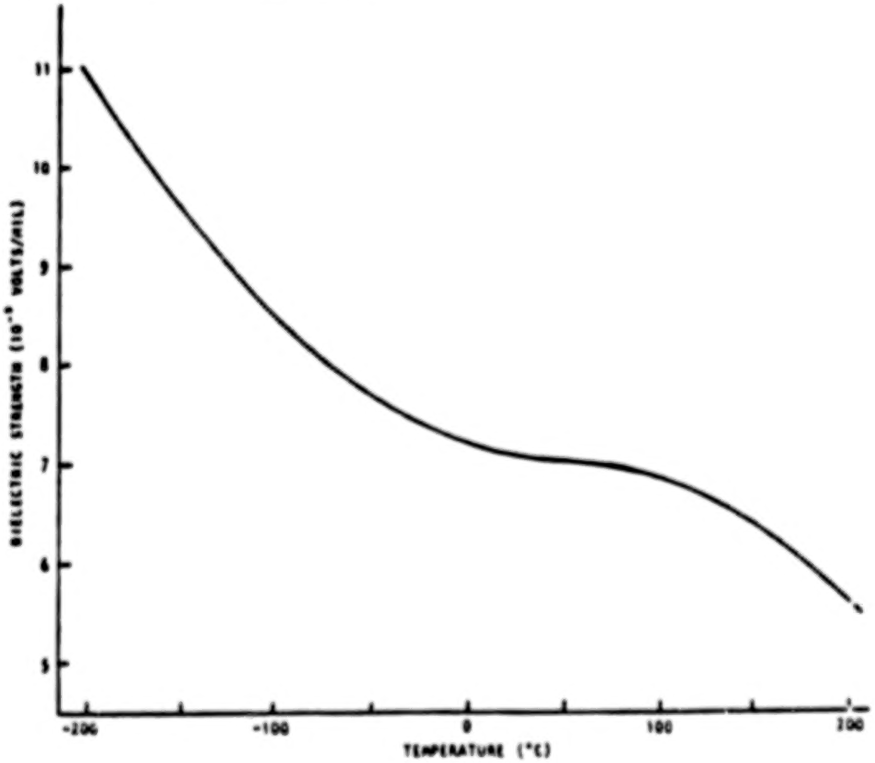

Figure 3.1-8. Type-H Kapton

The selected design concept for the point design is the 60° V-trough configuration. Weight, cost, on-orbit assembly, and fabrication and design complexity were used in the selection of the 60° V-trough point-design configuration. Weight comparisons showed that penalties for ±1° misorientation in reflector oversizing at concentration ratios of 5, and penalties for 1000-psi tensioning, are prohibitive. It appears that attitude control errors are controllable and that high membrane tensioning may not be a real requirement. Preliminary radiation tests indicate insignificant reflectivity degradation for aluminized thin-film Kapton, e.g., MSFC tests at 10^{15} proton/cm^2 (2 MeV) and Rockwell tests at 10^{15} protons/cm (0.7 MeV). The point-design solar array sizing model allows for 18% reflectivity degradation over 30 years which, in view of some of the newer test data, appears to be extremely conservative.

Radiation Degradation

The solar array electrical output is affected by the on-orbit environment which includes trapped particle radiation, solar flare proton radiation, ultraviolet radiation, and the temperature cycling associated with eclipse seasons. A composite 30-year GEO environment model is shown in Figure 3.1-9.

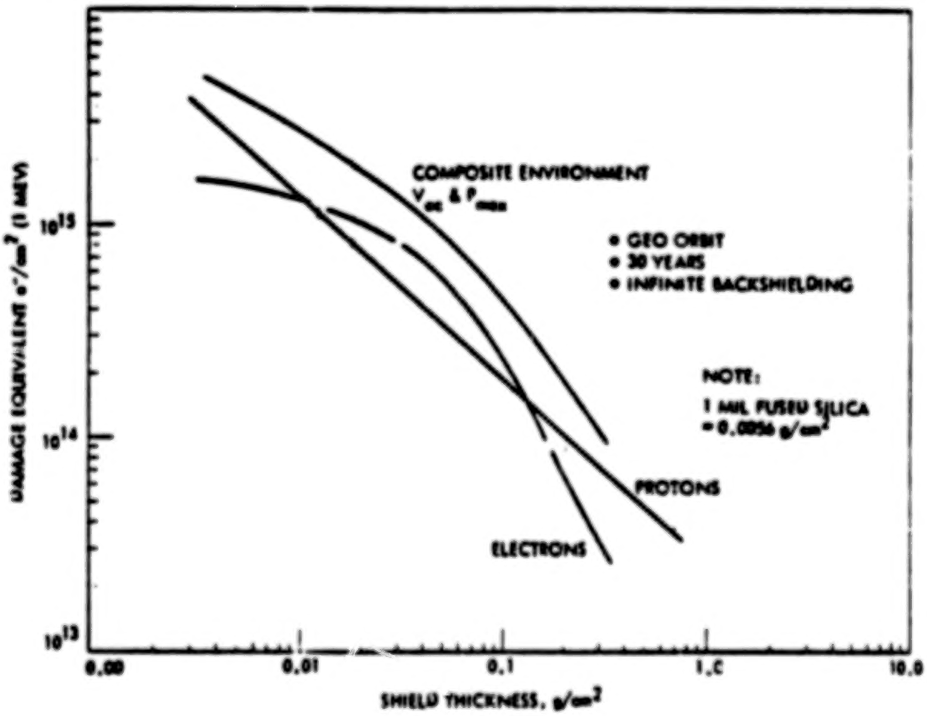

Figure 3.1-9. Solar Cell Damage Equivalent 1-MeV Electron Fluence Vs. Shield Density

A major contributor to the environmental model is solar flare protons. Estimated values were obtained by averaging the integral flux values for the five worst years of the 19th and 20th solar cycles and multiplying by 1.35 to allow for six quiet years of the solar cycle. The values for an 11-year cycle are then multiplied by a factor of 3 to obtain a 30-year model. The natural trapped particle radiation environment was obtained from the *Solar Cell Radiation Handbook*, TRW Report 21945-6001-RV-00. The values for damage equivalent

1-MeV electrons are taken from *A Proposal for Global Positioning Satellite Electrical Power Subsystem*, General Electric, Space Division Proposal N-30065, dated February 28, 1974.

The normalized maximum power of GaAs and Si solar cells versus 1-MeV electron radiation fluence is shown in Figure 3.1-10. The data indicate significant differences between the reference sources. In the solar cell comparisons at Rockwell, the curve identified for 50-μm silicon extrapolated JPL—the Solar Cell Radiation Handbook was used. These data are taken from several references and represent the mean behavior of n-p silicon solar cell production in the U.S. Solar cells produced with significantly different compositions may not show the same radiation loss. The significance of the data is that thinner silicon solar cells, percentagewise, show less radiation degradation than thicker cells. GaAs solar cells do provide more radiation hardening than the Si cells.

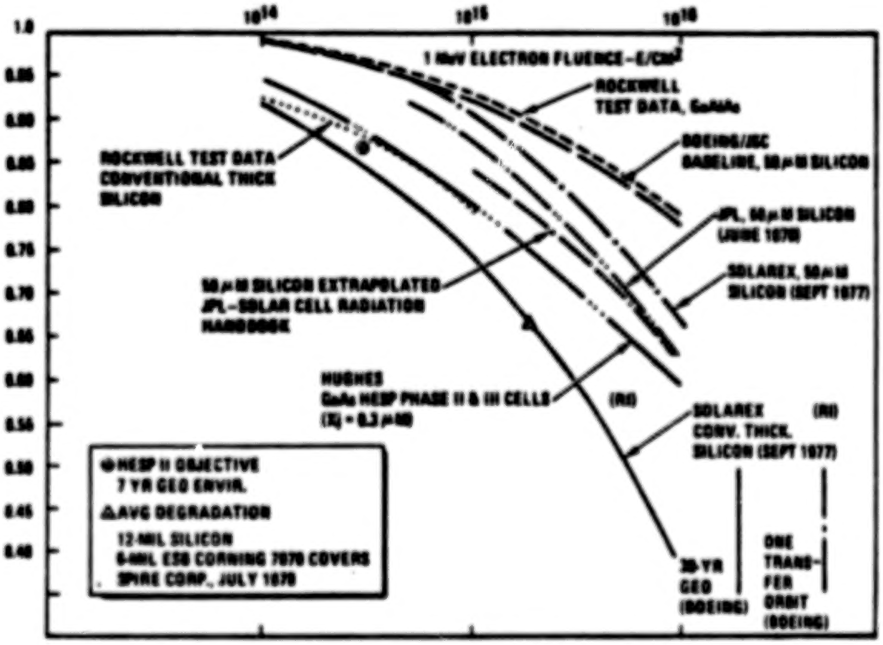

Figure 3.1-10. Normalized Maximum Power Vs. 1-MeV Electron Fluence

Solar Array Physical Characteristics

The SPS solar array efficiency chains are shown in Figures 1.2-19, 1.2-20, and 1.2-22.

The mass of the solar cells, solar blanket, and concentrator for the SPS configurations are shown in Table 3.1-2. The mass of each component of the three major assemblies is defined; the total mass of the reference concept is 8.14×10^6 kg.

Table 3.1-2. Solar Photovoltaic Power Conversion Mass (GaAs)

	Mass×10^6 kg		
	Reference	Magnetron	End-Mount
Solar Cells			
Component			
GaAs cell	0.754	0.723	0.855
GaAlAs window	0.007	0.007	0.008
Sapphire (cover/substrate)	2.260	2.167	2.563
Current collectors	1.706	1.637	1.936
Air coating	0.002	0.002	0.002
Subtotal	4.729	4.536	5.364
Solar Blanket			
Kapton panel	1.025	0.983	1.163
Transparent polymer-thermal coating	0.257	0.246	0.291
Adhesives	0.768	0.737	0.872
Interconnects	0.395	0.378	0.448
Subtotal	2.445	2.344	2.774
Concentrator			
Kapton panel	1.025	0.983	1.163
Reflective material	0.005	0.005	0.006
Subtotal	1.030	0.988	1.169
Total mass	8.204	7.868	9.307

The array design parameters, efficiencies, materials of construction, area requirements, and mass are presented in Table 1.1-3. The reflector design parameters, operating temperatures, area, and mass in the various planar configurations are presented in Table 3.1-4. The design parameters for the sandwich configurations are presented in Table 3.1-5.

Solar Array Configuration

Figure 3.1-11 illustrates the electrical flow diagram of a typical solar cell bay. Switching devices ①, ②, and ③ operate the satellite power system. These devices may be used as switching devices or fault isolation. Switching device ⑤ is used to regulate the voltage output of the array. The power network is entirely under the control of the on-board data processing system. Switching device ④ is the final switch gear of the solar cell bay at the summing bus. This device may incorporate current overload detection. The device may be used to isolate the bay and may not be incorporated in the data processing system. The outputs of the bays are routed to the appropriate summing bus and slip ring pair.

Table 3.1-3. GaAs Solar Cell and Blanket Design and Performance Characteristics

ITEM	CHARACTERISTIC		
	REFERENCE	MAGNETRON	END-MOUNTED
CELL η AT 28°C, AMO	20.6%	→	→
CELL η AT 113°C, AMO	18.15%	→	→
ARRAY OUTPUT TO DISTRIB. BUS EOL	9.94 GW	9.8 GW	5.73 GW
ARRAY OUTPUT VOLTAGE	45.7 kV	21.85 kV	43.3 kV
CELL OUTPUT VOLTAGE AT 113°C	0.7 V	→	→
CELLS IN SERIES	65,300	31,200	61,900
SOLAR CELL SUBPANEL SIZE	650×730 m	650×700 m	650×690 m
NUMBER OF BAYS PER SPS	60	60	72
ARRAY DESIGN FACTOR	89.3%	→	→
REFLECTIVITY AND DEGRADATION	0.87 BOL, 0.83 EOL	→	→
CONCENTRATION RATIO			
GEOMETRIC	2	→	→
BOL	1.87	→	→
EOL	1.83	→	→
SOLAR CELL CONSTRUCTION			
COVER	20 μm SAPPHIRE	→	→
WINDOW	0.05 GaAlAs	→	→
CELL	5 μm GaAs	→	→
INTERCONNECT	12.5 μm SILVER MESH EQUIV.*	→	→
SUBSTRATE			
ADHESIVE	12.5 μm FEP	→	→
FILM	25 μm KAPTON	→	→
TRANSPARENT THERMAL COATING	6 μm POLYMER	→	→
SPECIFIC WEIGHT	0.2525 kg/m^2 (0.0516 lb/ft^2)	→	→
DEPLOYED CELL & BLANKET AREA PLANFORM	67.2 km^2	63.0 km^2	75.6 km^2
SOLAR CELL AREA	28.5 km^2	27.3 km^2	32.3 km^2
REFLECTOR SURFACE AREA	56.9 km^2	54.6 km^2	64.6 km^2
MASS			
SOLAR PANELS	7.174×10^6 kg	6.880×10^6 kg	8.138×10^6 kg
REFLECTORS	1.030×10^6 kg	0.988×10^6 kg	1.169×10^6 kg
TOTAL MASS	8.204×10^6 kg	7.868×10^6 kg	9.307×10^6 kg

*SUBSTITUTE ALUMINUM OR COPPER (NOBLE METAL SHOULD NOT BE USED)

Table 3.1-4. SPS Reflector Design and Performance Characteristics for Planar Configurations

ITEM	REFERENCE	END-MOUNTED SOLID-STATE
MATERIAL	ALUMINIZED KAPTON	SAME
KAPTON THICKNESS	12.5 μm (0.5 MIL)	
KAPTON SPECIFIC GRAVITY	1.42 (0.018 kg/m^2)	
ALUMINIZED COATING THICKNESS	500 ANGSTROM UNITS	
WEIGHT OF ALUMINIZED COATING	96 kg/km^2	
REFLECTOR SURFACE PROTECTIVE FILM COATING	QUARTZ OR CALCIUM FLUORIDE	
REFLECTOR SUBPANEL SIZE	550×730 m	650×690 m
NUMBER OF REFLECTOR PANELS	120	144
REFLECTOR/REFLECTIVITY/DEGRAD.	0.87 BOL, 0.83 EOL	SAME
CONCENTRATION RATIO	1.9 BOL, 1.83 EOL	
REFLECTOR SLANT ANGLE FROM HORIZ.	60 DEG.	
OPERATING TEMPERATURE		
TOP REFLECTORS	-52°C	
INBOARD BOTTOM REFLECTORS	-46°C	
OUTBOARD BOTTOM REFLECTORS	-73°C	
TOTAL AREA OF REFLECTORS	56.9×10^6 m^2	64.6×10^6 m^2
TOTAL WEIGHT OF REFLECTORS	1.030×10^6 kg	0.648 10 kg

Table 3.1-5. SPS Reflector Design and Performance Characteristics for the Sandwich Configuration

MATERIAL	ALUMINIZED KAPTON
KAPTON THICKNESS	12.5 μM (0.5 mil)
KAPTON SPECIFIC GRAVITY	1.42 (0.018 kg/m^2)
ALUMINIZED COATING THICKNESS	500 ANGSTROM UNITS
WEIGHT OF ALUMINIZED COATING	96 kg/km^2
REFLECTOR SURFACE PROTECTIVE COATING	QUARTZ OR CALCIUM FLUORIDE
REFLECTOR NUMBER AND NOMINAL SHAPE	
PRIMARY	8 OVAL
SECONDARY	1 OVAL
REFLECTOR REFLECTIVITY/DEGRADATION	0.84 BOL, 0.83 EOL
SYSTEM CONCENTRATION RATIO (GEOMETRIC)	7.6
CONCENTRATION RATIO	5.8 BOL, 5.2 EOL
OPERATING TEMPERATURE	
PRIMARY	-52°C
SECONDARY	186°C
AREA OF REFLECTORS	GaAs CONFIGURATION
PRIMARY	66.6×10^6 m^2
SECONDARY	48.1×10^6 m^2
MASS OF REFLECTORS	
PRIMARY	1.21×10^6 kg
SECONDARY	0.87×10^6 kg

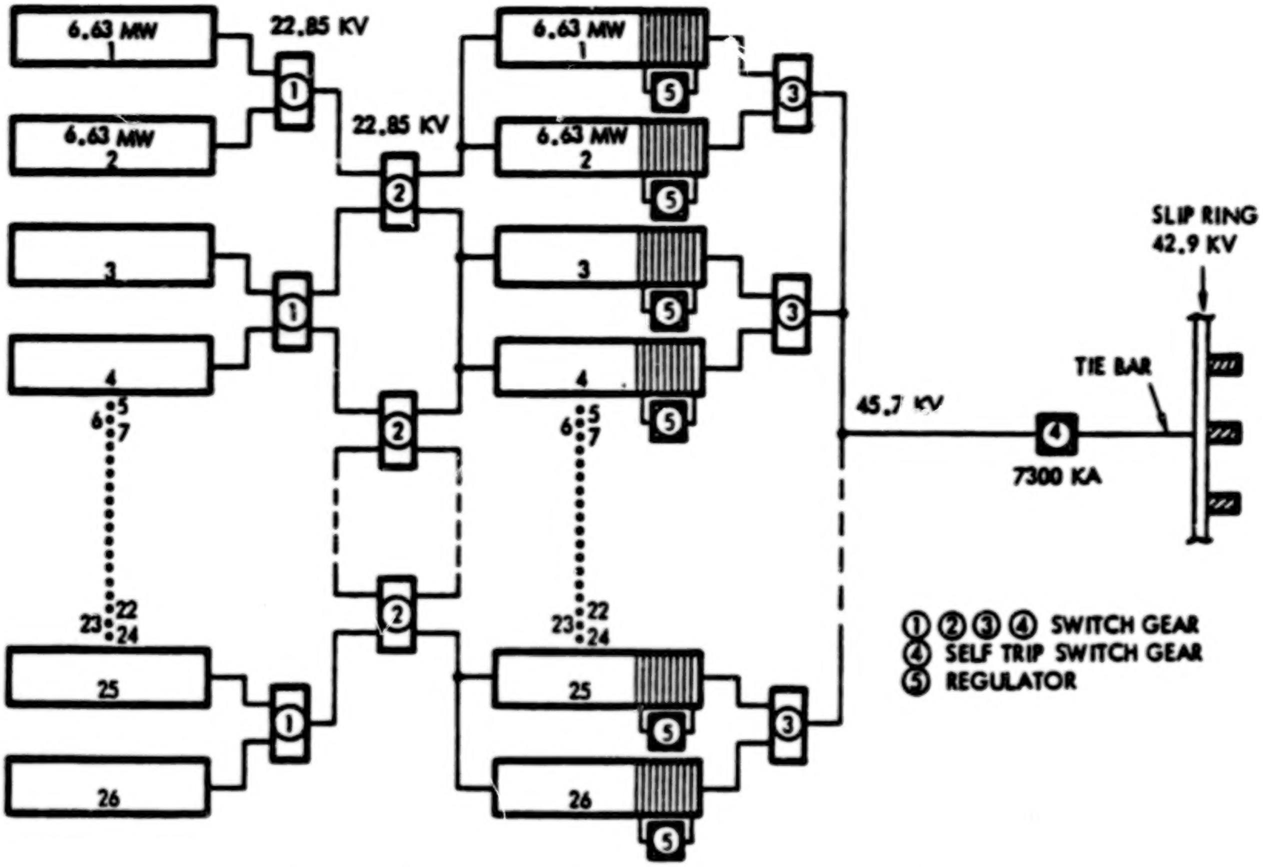
6.63 MW
1
6.63 MW
2
3
4
5
6
7
22
23
24
25
26
22.85 KV
22.85 KV
①
②
③
⑤
45.7 KV
④
7300 KA
TIE BAR
SLIP RING
42.9 KV
①②③④ SWITCH GEAR
④ SELF TRIP SWITCH GEAR
⑤ REGULATOR

Figure 3.1-11. Solar Array Configuration—Typical Segment
(1 of 30)

The output of the configuration shown in Figure 3.1-11 (40 kV nominal) is appropriate for the klystron and end-mounted solid-state concepts. The magnetron voltage output is specified at 20 kV (nominal). Voltage regulation of the solar array, power output, and BOL excess power dissipation will be controlled by selective switching of isolation/regulation switch gears on array submodules. Optimum power output will be assured at all times by proper sizing and design of the submodules, their associated switch gear, and IMCS control of the switching—in addition to control of the various loads. Voltages and currents being handled by the switch gears will be monitored by the IMC to determine their status and to establish a need for the opening and closing of these switches.

The power source for the solid-state sandwich configuration is included as part of the microwave subarray analysis. The auxiliary power solar panel area requirements have, at this time, only been roughly estimated at 0.30 km^2, but with no specific definition as to form factor or degree of segmentation. This lack of detail definition also extends to the interconnect and switching components of the subsystem.

Multi-Bandgap (GaAlAs/GaAs) Solar Cells

Introduction

The Rockwell SPS reference design used (for cost purposes) is based on a GaAs technology having a cell performance of 20.6% efficiency at AMO and 28°C. Although this cell is believed to offer the highest AMO conversion efficiency of all the single-crystal photovoltaic cells developed at this time, it is essential for a long-term project of the magnitude and importance of the SPS to be planned so that future technology developments having a significant positive impact on its performance and cost can be incorporated with minimum delay and technological complication. The cell conversion efficiency under orbital operating conditions is a critical performance parameter that, in turn, affects essentially all other design aspects of the SPS. The prospect of a dramatic increase in cell operating efficiency—even with respect to the present high value of 20.6 percent—is offered by the concept of the tandem, multiple-bandgap solar cell.

Theoretical analyses by various investigators (presented in detail in Volume II of this final report) have shown that the maximum conversion efficiency for the solar spectrum, that can be expected from any open p-n junction type of photovoltaic cell operating at its maximum power point (at ~25°C), is in the 20 to 25% range; the specific theoretical maximum depending primarily upon the bandgap energy E_g of the particular semiconductor involved.

The most efficient response of p-n junction cell is to photons of energy just exceeding the bandgap energy, so if two or more solar cells of differing bandgap energy (and thus of different composition) could be arranged appropriately to "share" the solar spectrum, with each operating on that portion of the spectrum to which it is most responsive, a combination converter of overall power efficiency exceeding that of the individual cells used separately in the full solar spectrum could quite possibly be realized.

There are two principal embodiments of this concept. One involves interposing dichroic mirrors or filters (i.e., "beam splitters") in the incident beam of solar radiation so that selected radiation of a portion of the spectrum is diverted to a solar cell whose properties [mainly bandgap energy (E_{g1})] allow it to make relatively efficient use of that selected band of radiation, while allowing the remainder of the spectrum to pass on to a second filter/mirror, which again selects a portion of the spectrum to direct onto a second cell of bandgap energy E_{g2}, while transmitting the remainder to a third cell (or a third filter/mirror), and so on.

The other multiple-cell concept—and the one with potential major impact on the SPS—can now seriously be considered for practical applications, primarily because of the remarkable progress made in thin-film photovoltaic material technologies in the past several years. This version involves two or more solar cells of differing composition (and thus differing bandgap energies) used optically in series, in a monolithic tandem, or stacked arrangement. The cell of largest bandgap energy E_{g1} receives the full solar spectrum incident on its front surface, coverting what it can of the absorbed photons of energy greater than E_{g1} and transmitting the radiation of energy $<E_{g1}$ onto

the second cell of bandgap E_{g2}, which utilizes the narrowed band of energies to generate photovoltage and photocurrent consistent with its photovoltaic properties and transmits the remaining radiation of energy $<E_{g2}$ onto a third cell, if used, and so on. This configuration of the tandem or stacked multiple-bandgap solar cell is shown schematically in Figure 3.1-12.

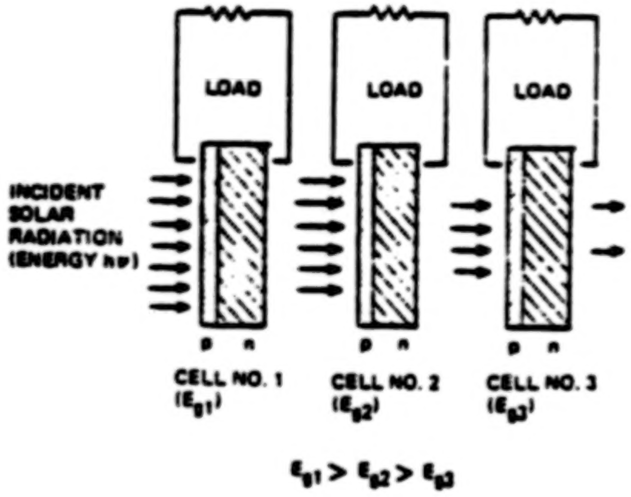

Figure 3.1-12. Schematic Representation of Stacked Multiple-Bandgap Solar Cell

Solar Cell

The monolithic stacked multi-bandgap approach has simple integrated form (both optical and electrical) and will have less weight. The preliminary SPS study has selected the GaAlAs/GaAs dual junction cell as the baseline multi-bandgap cell. The cell structure is shown in Figure 3.1-13 with a panel weight of 0.265 kg/m^2. The cell has an AMO efficiency of 30% at 28°C. The cell structure parameters such as junction depth, layer thicknesses, and doping concentration have not been optimized for the cell operating temperature. Rockwell SPS design has calculated two solar cell operating temperatures: (1) an operating temperature of 113°C for the CR = 2 design, and (2) an operating temperature of 200°C for the effective concentration ratio (CR_E) = 5.2 design. The projected cell performance data through computer modeling simulation is presented in Figures 3.1-14 and 3.1-15 for the GaAlAs/GaAs (CR = 2, CR = 5) multi-bandgap solar cells. As expected, the current increases linearly and voltage logarithmically as sollar illumination (or CR) increases. The selected dual-junction solar cell has a cell efficiency temperature coefficient of about 0.285%/°C, which is twice that of Si cells, because of the larger bandgap that allows higher temperature operation of the junction. Also, these multi-bandgap solar cells typically have low minority carrier lifetimes, diffusion lengths, and steep optical absorption edge; therefore, they are less susceptible to radiation damage and capable of low temperature self-annealing characteristics. Based on Rockwell SPS design goals and technology assessments by Research Triangle Institute, a comparison of the cell efficiency, temperature coefficient, equivalent radiation degradation, and mass was made and is shown in Table 3.1-6.

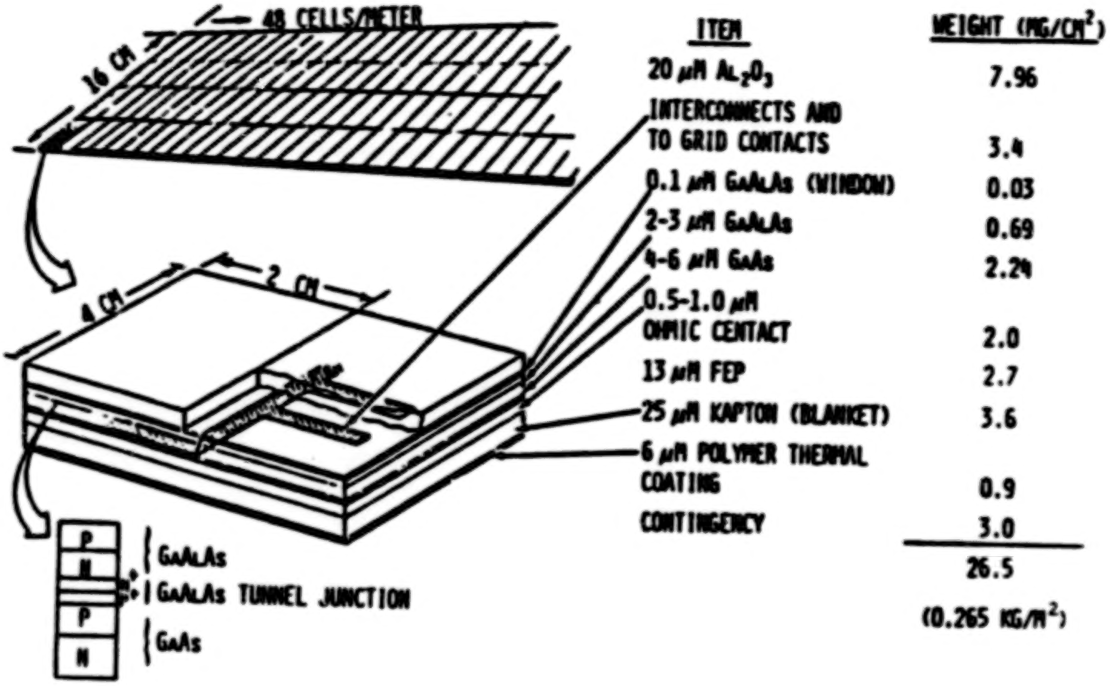
48 CELLS/METER
16 CM
4 CM
2 CM
P
N
P
N
GAALAS
GAALAS TUNNEL JUNCTION
GAAS

ITEM	WEIGHT (MG/CM^2)
20 μM AL_2O_3	7.96
INTERCONNECTS AND TO GRID CONTACTS	3.4
0.1 μM GAALAS (WINDOW)	0.03
2-3 μM GAALAS	0.69
4-6 μM GAAS	2.24
0.5-1.0 μM OHMIC CONTACT	2.0
13 μM FEP	2.7
25 μM KAPTON (BLANKET)	3.6
6 μM POLYMER THERMAL COATING	0.9
CONTINGENCY	3.0
	26.5
	(0.265 KG/M^2)

Figure 3.1-13. Dual-Junction Multi-Bandgap Solar Cell Blanket Cross Section

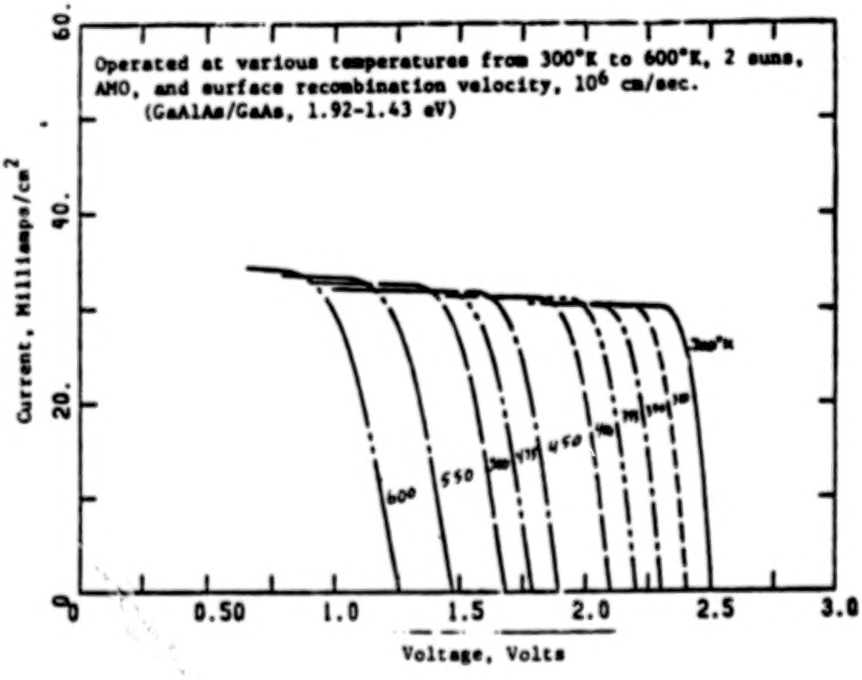

Figure 3.1-14. Current Vs. Voltage for a Cascade Cell Optimized for 475°K, Two Suns

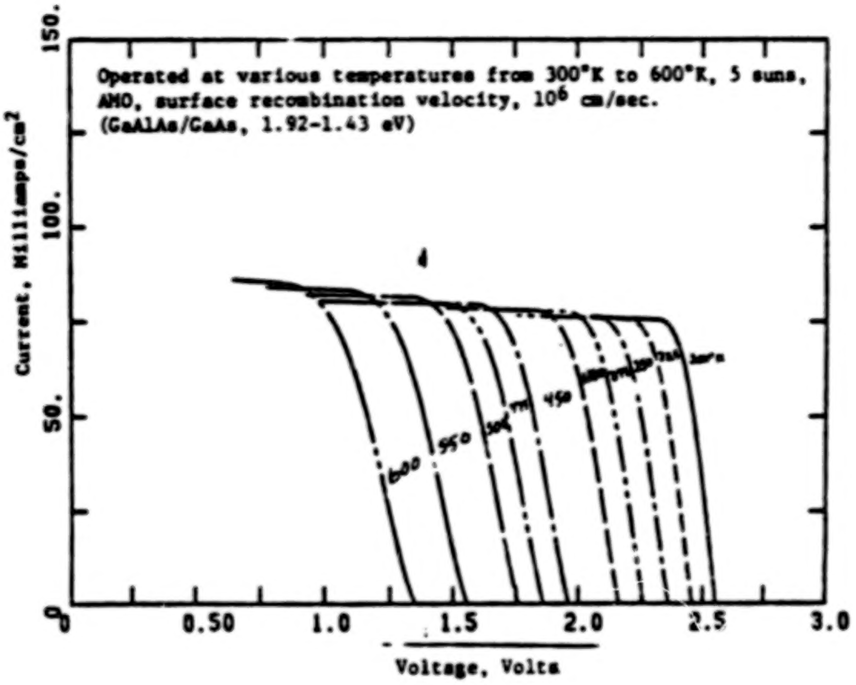

Figure 3.1-15. Current Vs. Voltage for a Cascade Cell Optimized for 45°K, Five Suns

Table 3.1-6. Multi-Bandgap Solar Cell Technology Assessment

Parameter	SPS Design (Goals)	Technology Assessment*
AMO efficiency	30 (28°C) 23.9 (200°C)	32 (28°C) 19 (200°C)
Temperature coefficient	Comparable to GaAs (-0.0015/°C)	-0.0027/°C for GaAlAs/GaInAs cell
Equivalent radiation degradation	4% (30 years)	Under study
Mass (kg/m^2)	0.265 (5% higher than GaAs baseline cell)	Same

*Research Triangle Institute technology assessment based on a two-junction GaAlAs/GaInAs multi-bandgap solar cell.

Solar Array Design and Comparison

One of the main factors to design and size the solar array is the solar cell voltage characteristics. In the SPS design concept, klystron and solid-state devices result in extreme voltage requirements. The magnetron configuration was not resized for the multi-bandgap (MBG) solar cell. Furthermore, the klystron device has a very high voltage (8-40 kV), whereas the voltage of the individual solid-state device is only 4-10 volts. The cell voltage outputs are listed in Table 3.1-7. The basic GaAlAs/GaAs solar array design for the klystron and solid-state end-mounted CR = 2 concepts are shown in Figure 3.1-16. In order to utilize the high-voltage output per each multi-bandgap solar cell in every solar array string, the size of the cell is dependent on its thermal and RF devices spacing limitation. A concept of laying down the multi-bandgap solar array for the sandwich concept is shown in Figure 3.1-17, which also shows the 7.8×7.8-cm spacing limitation requirement for each RF device, and that each RF device requires +10 V and -4 V.

Table 3.1-7. Solar Cell Voltage Characteristics

Cell Material		Op. Temp. (°C)	Initial[1] Cell Voltage (V)	EOL Cell Voltage (V)	Voltage[2] per meter (V)
Single Junction	GaAs	113 200	0.69 (0.85) 0.575 (0.85)	0.657 0.547	31.48 26.26
Dual Junction	GaAlAs/ GaAs	113 200	2.05 (2.2) 1.92 (2.2)	1.952 1.82	93.7 40.04

[1] Cell temperature coefficient = 0.00175 V/°C, ( ) = 28°C value.

[2] 48 cells in series, each 2.04 cm length × 3.59 cm width for single jct. cell
22 cells in series, ea. 2.5 cm length × 4.44 cm width for GaAlAs/GaAs cell at 200°C
48 cells in series, ea. 2.0 cm length × 4.0 cm width for GaAlAs/GaAs cells at 113°C.

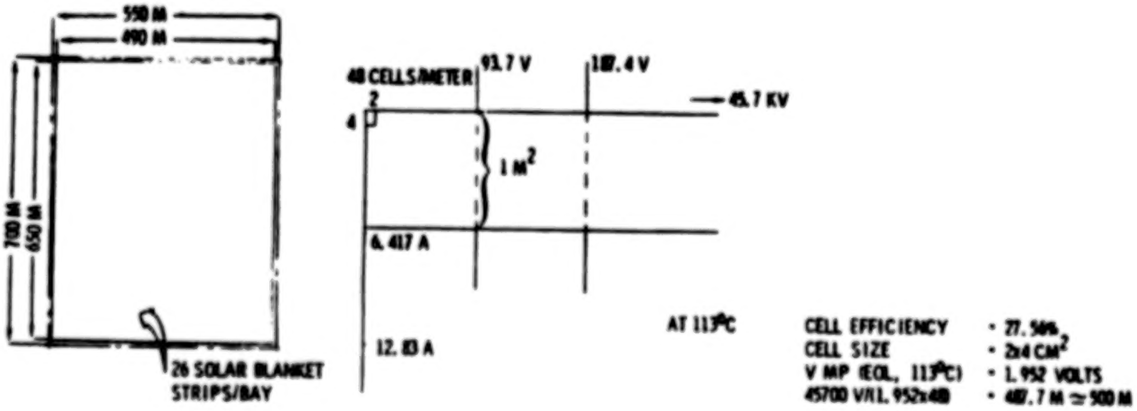
550 M
490 M
700 M
650 M
26 SOLAR BLANKET STRIPS/BAY
48 CELLS/METER
2
4
93.7 V
187.4 V
45.7 KV
1 M²
6.417 A
12.83 A
AT 113°C
CELL EFFICIENCY = 27.5%
CELL SIZE = 2x4 CM²
V MP (EOL, 113°C) = 1.952 VOLTS
45700 V/(1.952x48) = 487.7 M ≃ 500 M

Figure 3.1-16. GaAlAs/GaAs Solar Array Dimensions for Reference Concept

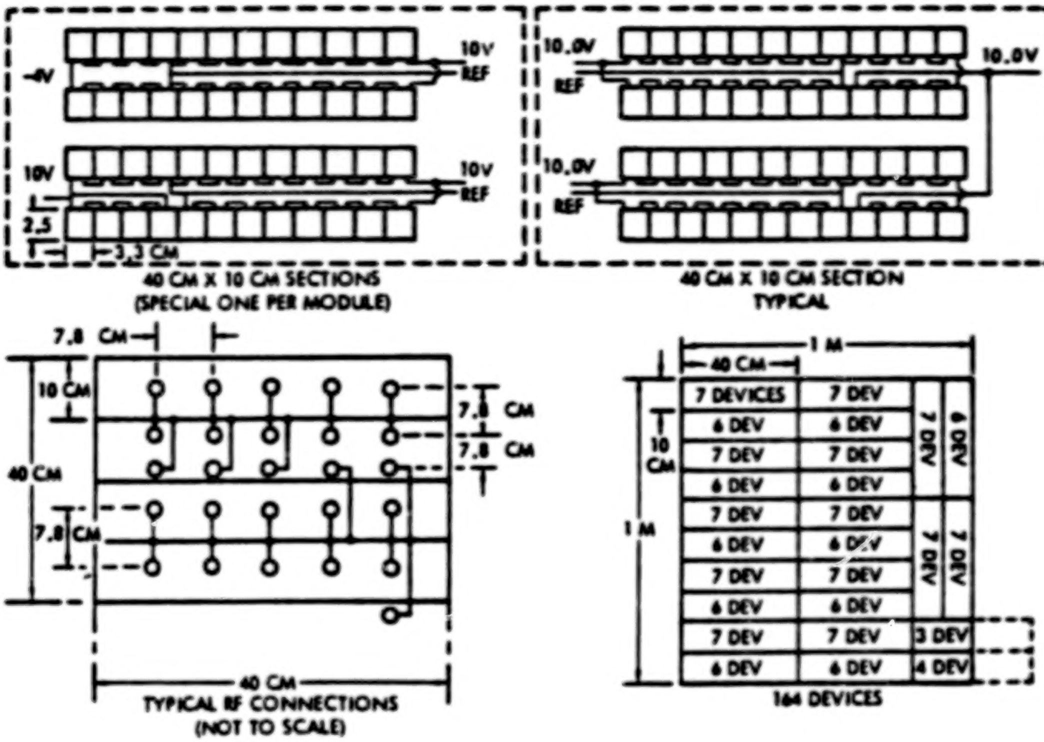
10V
-4V
REF
10V
10V
REF
2.5
3.3 CM
40 CM X 10 CM SECTIONS
(SPECIAL ONE PER MODULE)
10.0V
REF
10.0V
10.0V
REF
40 CM X 10 CM SECTION
TYPICAL
7.8 CM
10 CM
40 CM
7.8 CM
7.8 CM
7.8 CM
40 CM
TYPICAL RF CONNECTIONS
(NOT TO SCALE)
1 M
40 CM
10 CM
1 M
7 DEVICES
7 DEV
6 DEV
3 DEV
4 DEV
164 DEVICES

Figure 3.1-17. Solid-State Sandwich Concept, Power Distribution System to RF Devices

Design and Performance Characteristics

The design and performance characteristics of the photovoltaic system are presented in Tables 3.1-8, 3.1-9, and 3.1-10. Operational parameters, materials of construction, deployed and planform areas and weights are presented for the subsystem.

The power output requirement for the solar array is directly proportional to its design system efficiency. The relative efficiencies for each item in the efficiency chain for the reference concept using klystrons on the antenna are compared to the two basic solid-state antenna satellite approaches (Table 3.1-10). Overall power at the solar array output varies from 6.82 GW for the dual, standard cell, solid-state "sandwich" configuration to [illegible] GW for the dual, end-mounted solid-state concept.

Environmental Impacts and Annealing

Introduction

The environmental degradation of the SPS energy conversion system resulting from a 30-year space mission lifetime has great impact on the future of the SPS program. The solar array electrical output is affected by the on-orbit environment which includes trapped particle radiation, solar flare proton radiation, ultraviolet radiation, and the temperature cycling associated with the eclipse seasons. The high degradation factors of solar cells and reflectors

Table 3.1-8. MBG Solar Cell and Blanket Preliminary Specification

ITEM	CR = 2, KLYSTRON	CR = 2, SOLID-STATE*	CR = 7.7, DUAL SANDWICH
ARRAY INTERCEPTED ENERGY	69 GW	39.78 GW	34.18 GW
CELL η AT 28°C, AMO	30%	30%	30%
CELL η AT 113°C, AMO	27.56%	27.56%	25.06% (AT 200°C)
ARRAY OUTPUT TO DIST. BUS EOL	9.94 GW	5.73 GW	4.678 GW
ARRAY OUTPUT VOLTAGE	45.7 kV	45.7 kV	10 V
CELL OUTPUT VOLT. (113°C OR 200°C)	1.45 OR 2.05 V	1.45 OR 2.05 V	1.32 OR 1.92 V
CELLS IN SERIES	33,100 OR 23.450	33,100 OR 23,450	8 OR 6
SOLAR CELL SUBPANEL SIZE	650×490 m	650×465 m	10×10 m
NUMBER OF BAYS PER SPS	39	35	49,200
ARRAY DESIGN FACTOR	89%	89%	91.8%
REFLECTIVITY & DEGRADATION	0.87 BOL, 0.83 EOL	0.87 BOL, 0.83 EOL	0.87 BOL, 0.83 EOL
CONCENTRATION RATIO			
• GEOMETRIC	2	2	7.7
• BOL	1.87	1.87	5.828
• EOL	1.83	1.83	5.3
SOLAR CELL CONSTRUCTION			
• COVER	20 μm SAPPHIRE	20 μm SAPPHIRE	20 μm SAPPHIRE
• CELL	5 μm GaAlAs/GaInAs OR GaAlAs/GaAs	5 μm GaAlAs/GaInAs OR GaAlAs/GaAs	5 μm GaAlAs/GaInAs OR GaAlAs/GaAs
• INTERCONNECT	12.5 μm SILVER MESH OR EQUIVALENT	12.5 μm SILVER MESH OR EQUIVALENT	12.5 μm SILVER MESH OR EQUIVALENT
• SUBSTRATE			
- ADHESIVE	12.5 μm FEP →	→	→
- FILM	25 μm KAPTON →	→	→
- TRANSP. THERMAL COATING	6 μm POLYMER →	→	→
• SPECIFIC WEIGHT	0.265 kg/m² →	→	→
DEPLOYED CELL & BLANKET AREA PLANFORM	46.2 km²	25.2 km²	6.3 km²
SOLAR CELL AREA	18.13 km²	10.6 km²	4.92 km²
REFLECTOR SURFACE AREA	36.3 km²	21.2 km²	114.8 km²
MASS			
• SOLAR CELLS	4.804×10⁶ kg	2.804×10⁶ kg	1.105×10⁶ kg**
• REFLECTORS	0.648×10⁶ kg	0.363×10⁶ kg	2.075×10⁶ kg
TOTAL MASS	5.552×10⁶ kg	3.187×10⁶ kg	3.18×10⁶ kg

*HALF OF THE TOTAL SOLAR ARRAY

**PRIMARY POWER ONLY

Table 3.1-9. SPS Reflector Preliminary Specification
(Klystron or End-Mounted Solid State)

ITEM	CHARACTERISTIC
MATERIAL	ALUMINIZED KAPTON
KAPTON THICKNESS	12.5 μm
KAPTON SPECIFIC GRAVITY	1.42 (0.018 kg/m^2)
ALUMINIZED COATING THICKNESS	400 ANGSTROM UNITS
WEIGHT OF ALUMINIZED COATING	96 kg/km^2
REFLECTOR SURFACE PROTECTIVE FILM COATING	QUARTZ OR CALCIUM FLUORIDE
REFLECTOR SUBPANEL SIZE	650×400 m OR 650×465 m
NUMBER OF REFLECTOR PANELS	78 OR 140
REFLECTOR REFLECTIVITY/DEGRADATION	0.87 BOL, 0.83 EOL
CONCENTRATION RATIO, GEOMETRIC	2.0
CONCENTRATION RATIO	1.87 BOL, 1.83 EOL
REFLECTOR SLANT ANGLE FROM HORIZONTAL	60 DEGREES
OPERATING TEMPERATURE	
TOP REFLECTORS	-52°C
INBOARD BOTTOM REFLECTORS	-46°C
OUTBOARD BOTTOM REFLECTORS	-73°C
TOTAL AREA OF REFLECTORS	36.3-42.3 km^2
TOTAL WEIGHT OF REFLECTORS	0.648 OR 0.766×10^6 kg

Table 3.1-10. Efficiency Chain Comparison—Satellite Concepts

	REFERENCE—KLYSTRON & MAGNETRON		REF—ARRAY/S-S ANTENNA		DUAL SANDWICH	
	STD	MBG	STD	MBG	STD	MBG
POWER SOURCE						
CELL EFFICIENCY	0.1816	0.2756	0.1816	0.2756	0.1566	0.2506
EFFECTIVE REFLECTOR EFFICIENCY	0.915	0.915	0.915	0.915	0.689	0.689
POINTING/SEASONAL FACTOR	0.968	0.968	0.968	0.968	0.98	0.98
DESIGN FACTOR	0.893	0.893	0.893	0.893	0.893	0.893
UV DEGRADATION	0.96	0.96	0.96	0.96	0.96	0.96
SWITCH GEAR	0.997	0.997	0.999	0.999	-	-
					-	-
TOTAL	(0.1375)	(0.2086)	(0.1377)	(0.2091)	(0.0906)	(0.145)
POWER DISTRIBUTION						
BUSES	0.9405	0.9405	0.9405	0.9405	-	-
SWITCH GEAR	0.999	0.999	0.999	0.999	-	-
SLIP RING BRUSHES	0.999	0.999	0.999	0.999	-	-
TOTAL	(0.938)	(0.938)	(0.938)	(0.938)	(-)	(-)
SOLAR ARRAY POWER OUTPUT (GW)	9.94		11.46		4.82	6.11

result in increased sizing of the SPS with additional weight and cost penalties. This section presents the definition of the environment for the 30-year GEO mission and the orbit transfer (OTV). The subject of the degradation effect on the solar cell and reflector will be presented theoretically and experimentally, while the self-annealing property of the GaAs solar cell will be addressed. The projected solar cell and reflector degradation value has been estimated to the be SPS design point.

Definition of Environment for 30-Year GEO

Solar Flare Proton

For the past 20 years men have been recording meaningful data on the energetic particle emission from the sun, but only in the energy range from 10 to 100 MeV. The observed data have been extrapolated to energies lower than 10 MeV and form the basis for predicting the flux for solar events.

For SPS application at geosynchronous orbit, solar flare proton radiation is one of the major environments that degrades the solar array electrical output. Therefore, it is sensitive to the selection of the solar flare proton model for the SPS solar array design. Different solar proton models are presented in Figure 3.1-18. One major difference in models is the technique for predicting the low energy portion of solar flares. (It has the major effect of converting to a 1-MeV electron equivalent damage of the solar cell.) A conservative extrapolation assumes a power law spectrum at low energies and a more optimistic assumption is that the exponential rigidity spectral description holds below 10 MeV. Since the SPS program spans a total of 60 years, it did not seem reasonable to impose a penalty for superimposing continuous solar flare peak years. The Rockwell SPS solar flare proton model is obtained by using the Aerospace model with a safety factor of 1.0 (Dr. R. G. Pruett, Aerospace Corporation). The values for an 11-year cycle are them multiplied by a factor of 3 to obtain a 30-year model. A comparison of 1-MeV electron fluence for 30 years for different solar flare proton models is tabulated below.

Solar Flare Proton Model	NASA 77 Model	GPS Phase 3 Aerospace Model	TADA Model	Rockwell SPS Model	1972 Single Event
Silicon 3-mil cover 2-mil back Substrate	2.22×10^{16}	2.25×10^{15}	9.5×10^{14}	2.05×10^{15}	5.5×10^{13}

Trapped Electron and Proton

At geosynchronous orbit altitude, the energy spectrum is so soft that practically no protons with energy greater than two MeV exist. The effect on the SPS solar array performance of the trapped proton particles is negligible. The trapped electrons' 1-MeV electron damage was calculated from the appropriate volumes of NASA-3024, "Model of the Trapped Radiation Environment." The trapped electrons are based on the AE-4 model of the outer radiation zone

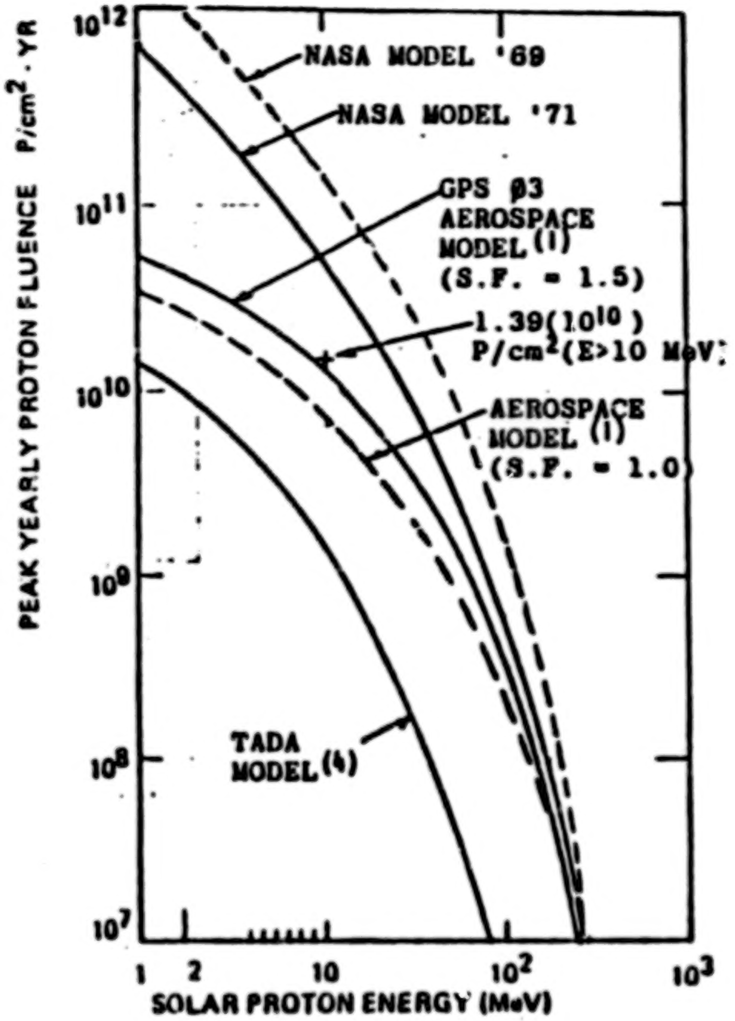

SOLAR CYCLE NO.	PERIOD OF CYCLE	DURATION OF MAXIMUM ACTIVITY
19	1953-1964	1955-1961
20	1964-1975	1965-1972
21	1975-1986	1977-1983

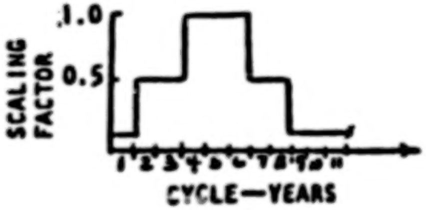

REFERENCES:

1. R. G. PRUETT—AEROSPACE CORP.
2. DR. B. E. ANSPAUGH—JPL
3. DR. A. MEULENBERG, JR—COMSAT
4. H. Y. TADA—TRW

Figure 3.1-18. Solar Proton Model Environment

electron environment. The damage value for 30 years, GEO, is $2.35\times10^{15}\ e^-/cm^2$. Solar cell damage-equivalent 1-MeV electron fluence versus shield density with various radiation models for 30 years in GEO is shown in Figure 3.1-19 and Table 3.1-11.

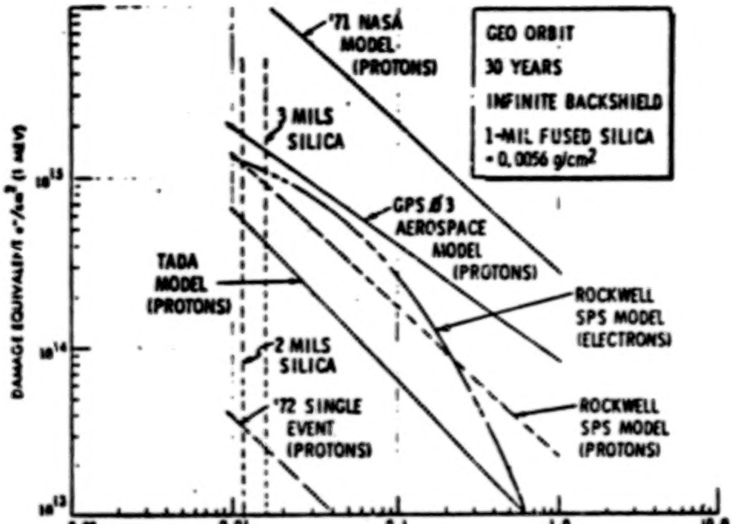

Figure 3.1-19. Solar Cell Damage-Equivalent 1-MeV Electron Fluence Vs. Shield Density

Table 3.1-11. Total 1-MeV Equivalent Fluence (e^-/cm^2) —30 Years

SOLAR FLARE PROTON MODEL	NASA '71 MODEL	GPS PHASE 3 AEROSPACE MODEL	TADA MODEL	ROCKWELL SPS MODEL
SILICON 3-MIL COVER 2-MIL BACK SUBSTRATE	2.55×10^{16}	5.6×10^{15}	3.3×10^{15}	$\boxed{4.4 \times 10^{15}}$

(1) INCLUDES 2.35×10^{15} FOR GEO TRAPPED ELECTRON 1-MeV EQUIVALENT FOR 30 YEARS

(2) BOEING MODEL PREDICTS 2×10^{16} 1-MeV ELECTRON EQUIV/cm² USING CONSERVATIVE EXTRAPOLATION ASSUMING POWER LAW SPECTRUM AT LOW PROTON ENERGIES (<10 MeV). THE MORE OPTIMISTIC ASSUMPTION OF EXPONENTIAL RIGIDITY SPECTRAL YIELDS 2.5×10^{15} 1-MeV ELECTRON EQUIV/cm². BOEING STATES 30 YR ELECTRON FLUENCE = 2.9×10^{14} e/cm² (Phase 1 Final Briefing, Volume VII, December 1978)

(3) HUGHES MODEL PREDICTS 5.2×10^{15} 1-MeV ELECTRON EQUIV/cm², 30 YEARS GEO Reference: (AlGaAs-GaAs Solar Cell Study for Rockwell International, L. J. Goldhammer, R. Knechtli, S. Kamath, and R. Loo; Final Report, November 1977. Note: 3-mil cover, 2-mil Kapton substrate.

Space Plasma

Large numbers of solar cells would be connected in series to produce high voltage (~45.7 kV) for operating the klystron device. The high electric fields or time-varying magnetic field near synchronous orbit drive out the cold (1 eV) component, and it is replaced by a hot (10 to 20 keV) plasma. Severe electrostatic charging may build up at the exposed surface of the satellite and develop loss of power by current leaking through the surrounding plasma.

No significant flight test data are available on plasma current leakage. K. L. Kennerud predicted that in low earth orbits a small solar cell array could not produce 16 kV because at that voltage the leakage current would exceed the generated current[1]. His prediction was based on the experimental plasma chamber analysis results. The plasma leakage current in the 95 electrons per cm^3 environment of geosynchronous orbit might be varied several orders of magnitude by simple estimation methods; therefore, no reliable answer can be reached. Up to the present time, this is an open issue with experimental confirmation of the leakage current predictions needed.

Solar Cell Degradation

Figure 3.1-20 shows the effects of 1-MeV electron radiation on solar cell power output. The data indicate significant differences between the reference sources. In the solar cell comparisons at Rockwell, the curve identified for 50-µm silicon extrapolated JPL—the Solar Cell Radiation Handbook was used. These data are taken from several references and represent the mean behavior of n-p silicon solar cell production in the United States. The signifiance of the data is that thinner silicon solar cells, percentage-wise, show less radiation degradation than thicker cells.

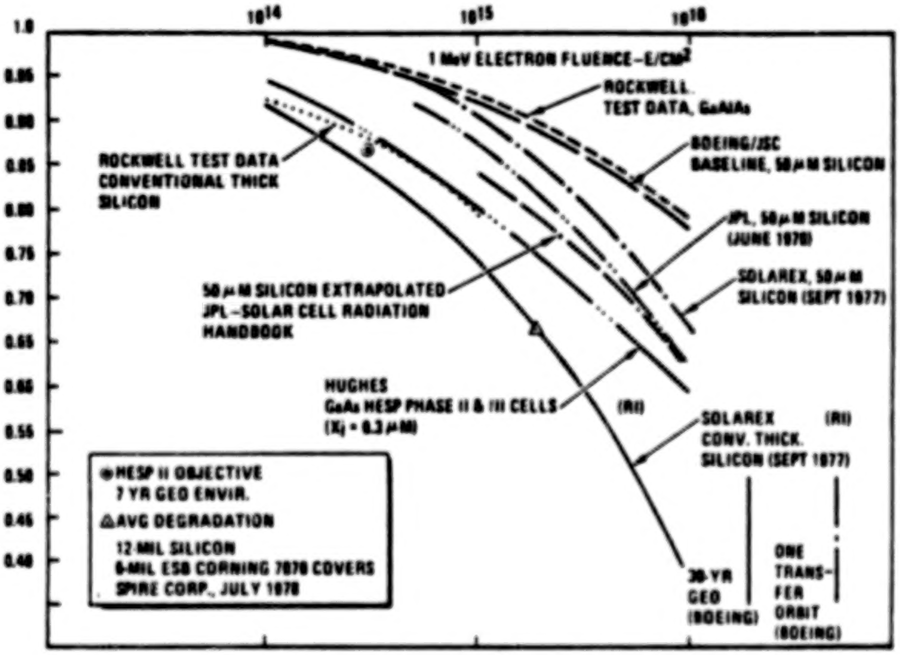

Figure 3.1-20. Normalized Maximum Power Vs. 1-MeV Electron Fluence

---

[1] Kennerud, K.L., *High-Voltage Solar Array Experiments*, NASA-Lewis, Document CR-121280

The results of several studies of proton damage have been summarized in terms of relative silicon solar cell damage as a function of proton energy. These relative damage results (normalized to 10-MeV proton damage) are shown in Figure 3.1-21 (taken from JPL Publication 77-56, Solar Cell Radiation Handbook). Results for several coverslide thicknesses are also shown. The dashed line is the result of GaAs solar cell test data at Rockwell. The equivalent 1-MeV fluence for gallium arsenide solar cells cannot be determined at this time. Only when radiation tests are conducted in which the damage coefficients for both electrons and protons are determined can the equivalent 1-MeV fluence be calculated for gallium arsenide solar cells.

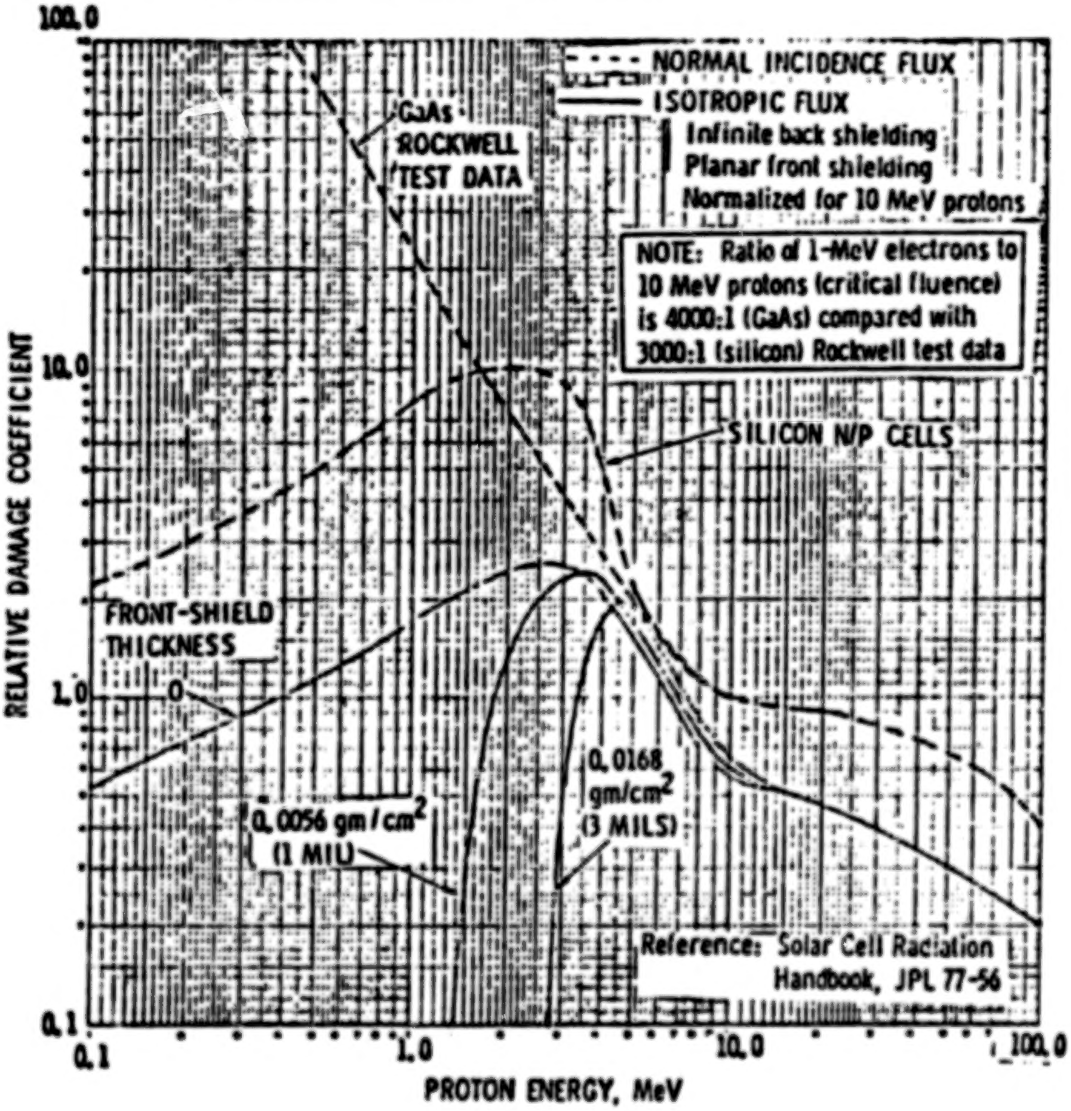

Figure 3.1-21. Relative Damage Coefficients for Space Proton Irradiation (P_{max})

For the present, we are assuming that the equivalent 1-MeV electron fluence for gallium arsenide is reasonably close to silicon for the energy levels of interest (above the cutoff levels with shielding).

The possibility of thermal annealing of radiation damage is of critical importance. Heavier protective cover and solar array substrate thicknesses soon lead to unacceptable weight penalties which can be avoided if thermal annealing is found to be sufficiently effective.

Reflector Degradation

The present Rockwell SPS reflector design had selected the 0.5-mil Kapton with 500-angstrom aluminum as the reflector material. Since GaAs solar cell has used it for the photovoltaic power generation source, a more appropriate concentrator reflectivity can be derived from measured data in the conversion band of GaAs.

Figure 3.1-22 exhibits the optical reflectance of aluminum as presented by Toulnkian et al., in the *Thermophysical Properties of Matter* series. It shows the reduction in reflectance of evaporated films in the peak conversion wavelength region of GaAlAs, which results in decreased reflection of desired solar radiation from the concentrators. Data measured at Sandia for aluminized Teflon indicate a beginning-of-life (BOL) magnitude of 0.87. This value has been applied to the SPS reflectors. Lifetime deterioration estimates also have been recomputed. A math model of the meteoroid exposure levels has been

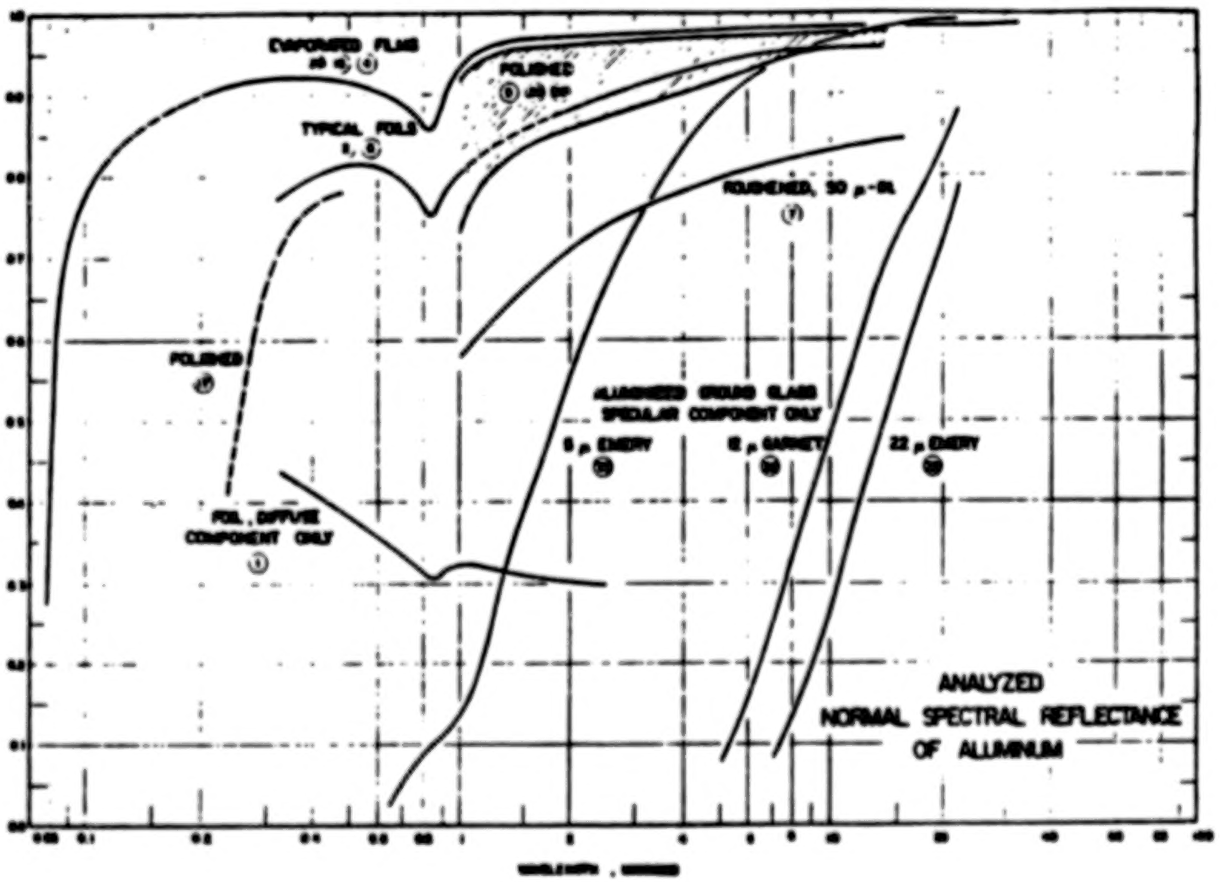

Figure 3.1-22. Aluminum Spectral Reflectance Data

developed. The model indicates that a loss of about one half of one percent can be expected. Because of the relatively low temperatures of the reflectors, thermal cycling degradation due to eclipse passage should be slight and is estimated to be one percent. The reflector radiator resistance has been increased from earlier estimates because it has been shown that the test data used as a basis for predicting radiation losses greatly exceeded the operation spacecraft environmental exposure. Consideration of these factors has led to the selection of an end-of-life (EOL) value of 0.827.

Thermocycling of the Solar Array Components

The temperature limitation factors for GaAs, silicon, and multi-bandgap solar cells have been given a preliminary evaluation. In view of cell material and device area, the GaAs cell may be usable and reliable at temperatures above 300°C, whereas silicon solar cells will be limited in performance at temperatures about 200°C. Delamination of cell from substrate and cell junction temperature in the array elements may be the critical failure factor of the solar array as high temperatures are reached (Table 3.1-12). Further investigation of heat dissipation at the converter will be necessary to evaluate these effects. Multi-bandgap cells broaden the spectral response and thereby more energy is converted to electrical power, resulting in less waste heat generation in the cell than lower-efficiency single-crystal cells. Temperature coefficient and radiation hardening are the key issues in determining the application of the multi-bandgap solar cell, as well as its availability and cost by the technology readiness date.

Table 3.1-12. Temperature Limitation on GaAs Solar Cell

Characteristics	Failure Temperature Range
Debonding of soldered leads	300°C to 460°C
Delamination of cell from substrate*	180°C to 400°C (melting, bubbling, and darkening)
Degradation of cover adhesive	300°C to 520°C
Degradation of cell electrical parameter*	220°C to 520°C (based on Si data)
Degradation of cell cover	>430°C

*Further investigation needed.

NOTE: GaAs solar cells may be usable and stable at temperatures up to 300°C—Long-term metallurgic effects are unknown at this time.

GaAs Solar Cell Self-Annealing

One of the major advantages of GaAs cells over Si solar cells for the SPS application is the relatively greater radiation damage resistance of the GaAs cell. Gallium arsenide is a promising material for thin-film solar cells. Because of its sharp absorption edge and large absorption coefficient, solar radiation with energy in excess of the energy gap is essentially all absorbed within a few micrometers of the surface, and a relatively short minority carrier lifetime can be tolerated.

Previous investigations of the radiation damage properties of single-crystal high-efficiency GaAs cells, grown by LPE* techniques on GaAs substrates, at the Rockwell Science Center have shown that such cells are approximately an order of magnitude less susceptible to radiation damage than are single-crystal Si cells and, furthermore, that in some of the devices, the radiation damage can be largely removed by annealing at temperatures as low at ~125°C. For the same reasons, e.g., the advantage of the short carrier lifetime, thin active GaAs materials are required.

The GaAs cells are, however, more sensitive to low-energy proton damage than are Si cells. This is to be expected since all of the photovoltaic conversion process in GaAs cells takes place in about the first 3 μm of the material below the surface, while in Si cells the effective active volume extends to depths approaching 100 μm. Most of the low-energy protons can, fortunately, be stopped by a relatively thin cover slide or other protection applied over the cell.

Test results showed only a 15% and 25% degradation following 10^{16} 1-MeV equivalent electrons/cm^2. The 10-MeV proton flux for comparable degradation was 6×10^{12} proton/cm , which is substantially harder than now possible with high-efficiency Si cells. It was also determined, as a result of these tests, that the degradations under proton and electron bombardment varied strongly with depth and uniformity of the active region.

3.1.3 POWER DISTRIBUTION

Introduction

The power distribution and control subsystem (PDS) receives power from the power conversion subsystem, and provides the regulation and switching required to deliver power for distribution to the satellite power users. During the ecliptic periods, batteries will be utilized to supply the minimum required power to the various subsystems. Figure 3.1-23 illustrates the major assemblies comprising the PDS; functional requirements are shown in Table 3.1-13. The power distribution consists of main feeders, secondary feeders, tie bars, summing buses, circuit breakers, manually operated switches, slip rings, brushes, and subsystem cabling.

The major requirements are to deliver power at specified voltages and levels on a continuous basis throughout the solar seasons for a duration of 30 years. To assure 5 GW (nominal) at the utility interface, the reference concept solar array will generate and deliver 9.94 GW EOL at the power distribution and control interfaces. Each reference concept solar array module is designed for 45.7 kV output. The total array produces 217,000 A. Power delivered to the klystrons (major power user) through power distribution is 8.69 GW, requiring 9.32 GW transferred across the rotary slip ring power interface.

**liquid-phase epitaxial*

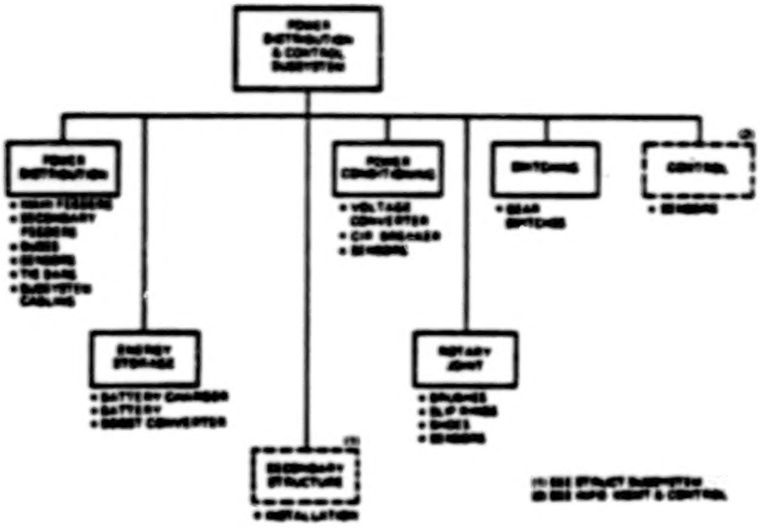
POWER DISTRIBUTION & CONTROL SUBSYSTEM
POWER DISTRIBUTION
ENERGY STORAGE
SECONDARY STRUCTURE
POWER CONDITIONING
ROTARY JOINT
SWITCHING
CONTROL

Figure 3.1-23. PDS Assembly Tree

Table 3.1-13. PDS Functional Requirements

• Lifetime	30 years with minimum planned maintenance
• Operations	Geosynch. orbit; 0° incl., circular (35,786 km alt.)
• Commercialization	Compatible with U.S. utility networks
• Output power	Steady-state operation, 42.9 kV @ 217 kA at slip ring interface; 5 GW at utility interface
• Weight growth	25%
• Total weight	Satellite power distrib. approx.<1.5 kg/kW
• Energy storage	Batteries included to support on-board satellite system operations only during ecliptic periods (~ 42 MW-hr)
• Failure criteria	No single-point failure may cause total loss of SPS functions
• Development	Evolutionary with provisions for incorporating later technology
• Resources	Minimum use of critical resources
• Subsystem checkout	Continuity, insulation resistance, functional switching of switch gears

The other planar satellite concepts accommodate similar voltages with the exception of the magnetron concept, which operates at 20 kV nominal. The voltage and power requirements for all of the planar array concepts are summarized in Table 3.1-14.

Table 3.1-14. Planar Array Power Distribution
—Voltage and Power Summary

	Klystron		S-S End Mounted		Magnetron
	GaAs	GaAlAs/ GaAs	GaAs	GaAlAs/ GaAs	GaAs
Total power generated, GW	9.94	9.94	11.46	11.46	9.8
Voltage at power source, kV	45.7	45.7	43.3	43.3	28.85
Total current, kA	217.5	217.5	264.7	264.7	448.5
Power at slip rings, GW	9.34	9.34	10.77	10.77	9.22
Power delivered to amplifiers, GW	8.84	8.84	9.68	9.68	8.98

Operations of the system are to be in geosynchronous orbit, and the ground rectenna power delivered at the utility interface compatible with U.S. utility networks. The design is to be such that no single-point failure may cause total loss of SPS functions.

Functional Description

SPS power distribution interfaces are presented in Table 3.1-15 for the solar photovoltaic point-design concepts.

Table 3.1-15. Power Distribution Interface Requirements

Thermal/PDS	50°C to 68°C for regulators and converters
PDS/IMS	1 kW, dc/dc converter with 28-V output
IMS/PDS	Monitor and control functions
Structural PDS	Approximately 10% of PDS mass for support structure, brackets, clamps, etc.
PDS/solar array	Switch gear, array summing buses, regulation
PDS/attitude and stationkeeping	DC/DC conversion
PDS/klystron	DC/DC conversion: 40 kV, 32 kV, 24 kV, 16 kV, 8 kV
PDS/magnetron	No dc/dc conversion, 20 kV
Solid-state/end-mounted	DC/DC conversion, 640 V

Figure 3.1-24 shows a simplified solar array power distribution system for the solar photovoltaic three-trough end-mounted klystron antenna concept. The magnetron concept is illustrated in Figure 3.1-25. The interties transfer the power from the solar array to the main feeders. The on-board data processing system performs the required switching of the submodules to maintain the bus regulation as required for the satellite power system. The power from the main feeders is transferred via switchgear to tie buses which then

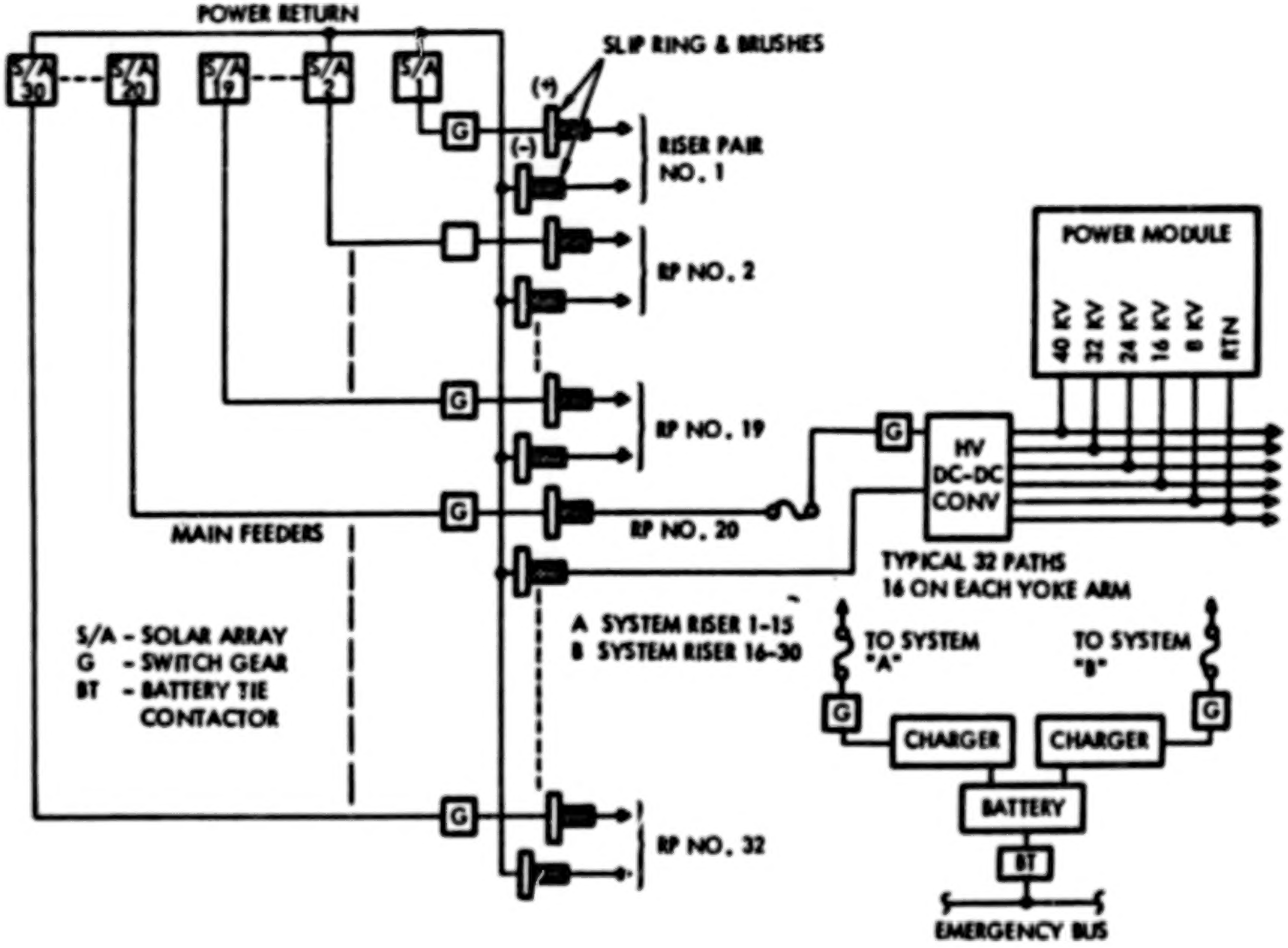
POWER RETURN
S/A 30
S/A 20
S/A 19
S/A 2
S/A 1
SLIP RING & BRUSHES
(+)
(-)
G
RISER PAIR NO. 1
RP NO. 2
RP NO. 19
RP NO. 20
RP NO. 32
MAIN FEEDERS
POWER MODULE
40 KV
32 KV
24 KV
16 KV
8 KV
RTN
HV DC-DC CONV
TYPICAL 32 PATHS 16 ON EACH YOKE ARM
A SYSTEM RISER 1-15
B SYSTEM RISER 16-30
S/A - SOLAR ARRAY
G - SWITCH GEAR
BT - BATTERY TIE CONTACTOR
TO SYSTEM "A"
TO SYSTEM "B"
CHARGER
CHARGER
BATTERY
BT
EMERGENCY BUS

Figure 3.1-24. Simplified Power Distribution System—Klystron

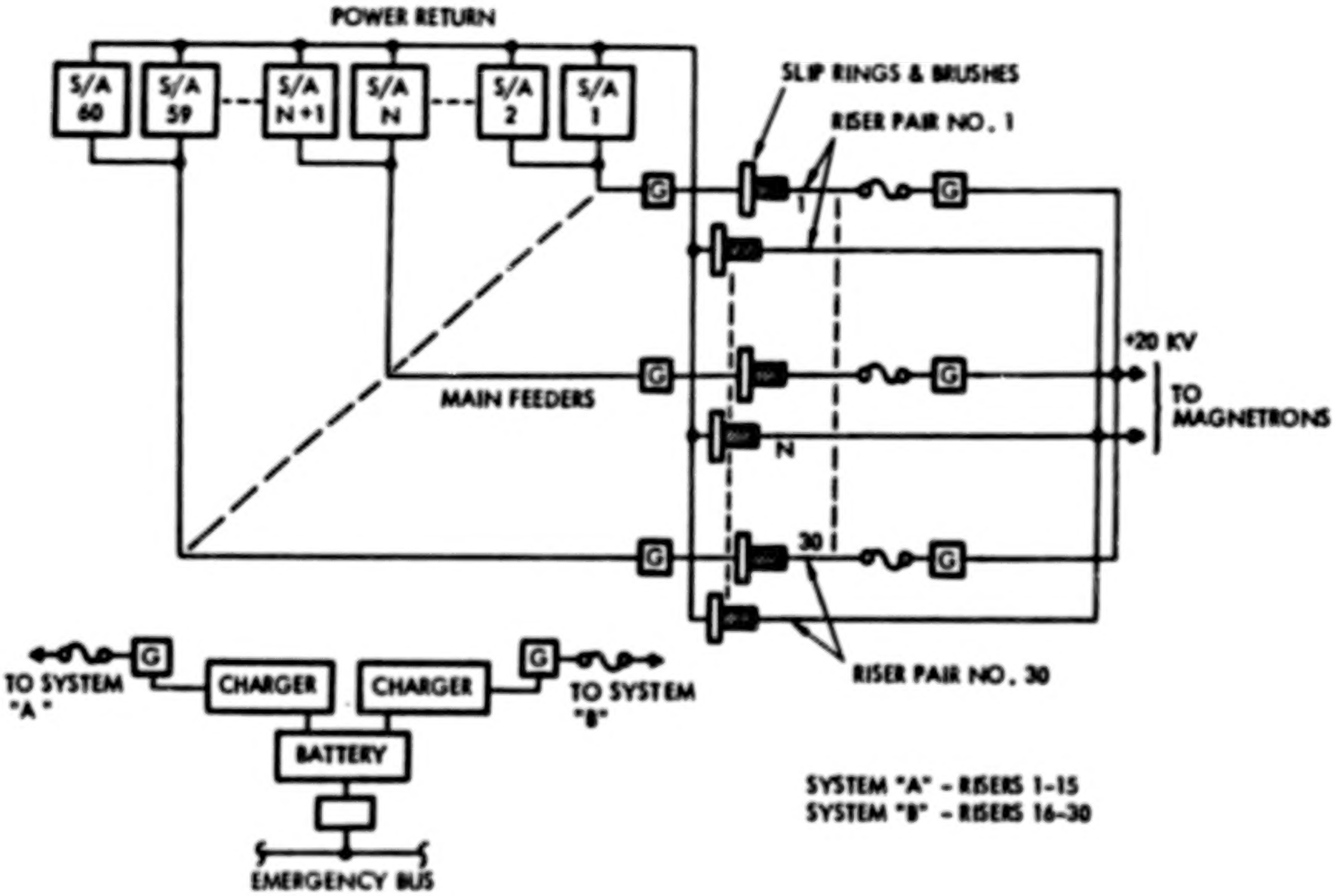
POWER RETURN
S/A 60
S/A 59
S/A N+1
S/A N
S/A 2
S/A 1
SLIP RINGS & BRUSHES
RISER PAIR NO. 1
G
1
N
30
+20 KV
TO MAGNETRONS
MAIN FEEDERS
RISER PAIR NO. 30
TO SYSTEM "A"
TO SYSTEM "B"
CHARGER
CHARGER
BATTERY
EMERGENCY BUS
SYSTEM "A" - RISERS 1-15
SYSTEM "B" - RISERS 16-30

Figure 3.1-25. Simplified Power Distribution System—Magnetron

connect the available power to the slip rings. A pair of slip rings per main feeders (3) provides system redundancy in case of a partial power failure on the array. A battery and battery charging system is provided to maintain power to provide for required housekeeping tasks during the eclipse periods.

Sizing

A continuous review of subsystem efficiencies has been maintained in order to provide updated efficiency factors for sizing the SPS. The efficiencies of major components on the nonrotating solar array wing were shown in Figures 1.2-19, 1.2-20, and 1.2-22. The major consideration for sizing the PDS is the power level (voltage and current) and line loss allowables. This subsystem was sized to handle EOL power levels as shown in Table 3.1-16.

Table 3.1-16. System Sizing

	Reference	Magnetron	Solid-State End Mounted
Power input (GW)	9.94	9.8	5.729*
Voltage input (kV)	45.7	21.85	43.3

*each half

Conductors

The power distribution subsystem utilizes flat aluminum (6101/T6) feeders. These flat conductors are not considered part of the main structure and will normally be passively cooled by radiation to free space. Main feeders are sized to an average transmission efficiency of 94% (determined to be optimum on a cost basis), with a standard thickness of 0.1 cm and ranging in width from 5.0 m to 40.0 m.

The configurations selected for the klystron and magnetron antenna and the solid-state end-mounted antenna concepts were shown in Figures 2.1-2 and 2.1-3. The magnetron concept is identical to the klystron system, except that the overall length is reduced to 15 km and the bay lengths are reduced to 1500 m.

Analysis

The electrical power distribution subsystem is configuration-dependent. Basic elements of the solar array power distribution subsystem are: secondary feeders, main feeders, summing bus, tie bar, and insulation. Similarly, basic elements of the antenna are risers, summing bus, main feeders, and secondary feeders. An examination of the formulae for calculating the conductor weight shows that the weight is increased by the square of the length of the conductor. The formula for determining the conductor cross-section is:

$$A = \frac{\gamma I L}{\Delta V}$$

The formula for weight is:

$$\omega = \rho AL$$

where A = cross-section area
I = amperes flowing
γ = resistivity of wire
L = length of conductor
ΔV = voltage drop in conductor
ω = conductor mass
ρ = density

Therefore,

$$= \frac{\gamma IL}{\Delta V} (\rho L) = \frac{\rho \gamma IL^2}{\Delta V}$$

It is seen that conductor mass varies as the square of its length. Examining the main elements of the power distribution subsystem, it appears that the main feeders, tie bars, and risers are impacted the most by a long, narrow configuration, while the summing bus favors a narrow configuration. The secondary feeders are not impacted, to a large extent, by the aspect ratio of the configuration. The insulation weight is impacted by both the length of the conductor and its shape, i.e., flat or round. Round conductors require less insulation, being more compact. The round conductor also will have the lesser cooling surface for passive cooling and, therefore, will become hotter or require a greater cross-section to operate at the same temperature.

Rotary Joint

The rotary joint is utilized to transfer energy through slip rings and brushes from the satellite fixed member to the satellite rotating member upon which the microwave antenna is located. The rotary joint assembly design characteristics are given in Table 3.1-17.

Antenna

A schematic of the power distribution system for the rotating antenna on the reference satellite is shown in Figure 3.1-26. Risers from the brushes are routed on the antenna supporting yoke, across the antenna pivot, with a loop, to the dc/dc centralized converters. Switch gears are provided to allow isolation when performing maintenance. Power from the dc/dc converters are tied to a multi-conductor summing bus for delivering the necessary voltages to the klystrons. Each slip ring feeds 16 centralized dc/dc converters situated near the antenna pivot. The multi-conductor summing bus runs along the two sides of the antenna adjacent to the pivot. The other slip ring supplies power similarly to 16 dc/dc converters on the opposite side of the antenna along with its accompanying summing bus. Thirty-three feeders, isolated by switch gear at the summing buses, are interconnected between the summing buses. Mechanical modules of klystrons are then powered from adjacent feeders and are isolated with each feeder by switch gear. The feeder interconnect from the summing buses and the mechanical module feeder between adjacent feeders are

Table 3.1-17. Slip Ring Design Characteristics

	Klystron (GaAs)	Klystron (MBG)	Magnetron	End Mount. (Dual)
TOTAL ASSEMBLY				
Operating voltage (kV)	42.9	42.9	20.5	40.7
Amps/ring assembly (A)	7300	7300	14,900	4400
Total mass ($\times10^6$ kg)	0.060	0.060	0.060	0.120
SLIP RINGS (PAIRS)	32	32	60	
Core	← aluminum →			
Cladding	← coin-silver →			
Core size (cm^2)	← 104.9 (cross-section) →			
Diameter (m)	← 6 →			
Length (m)	← 18.85 →			
SHOE BRUSH				
Number of shoes per ring	← 3 →			
Material	← 75% MoS_2, 25 Mo + Ta →			
Shoe size (cm)	← 20.3W×25H×152L →			
Current (A/cm^2)	← 7.75 →			
Contact area (cm^2)	← 825.9 →			
Quantity (brushes/shoe)	← 32 →			
GROUNDING				
Single-point aluminum bus	———→			

Note: All rings are sized to handle 15,000 A

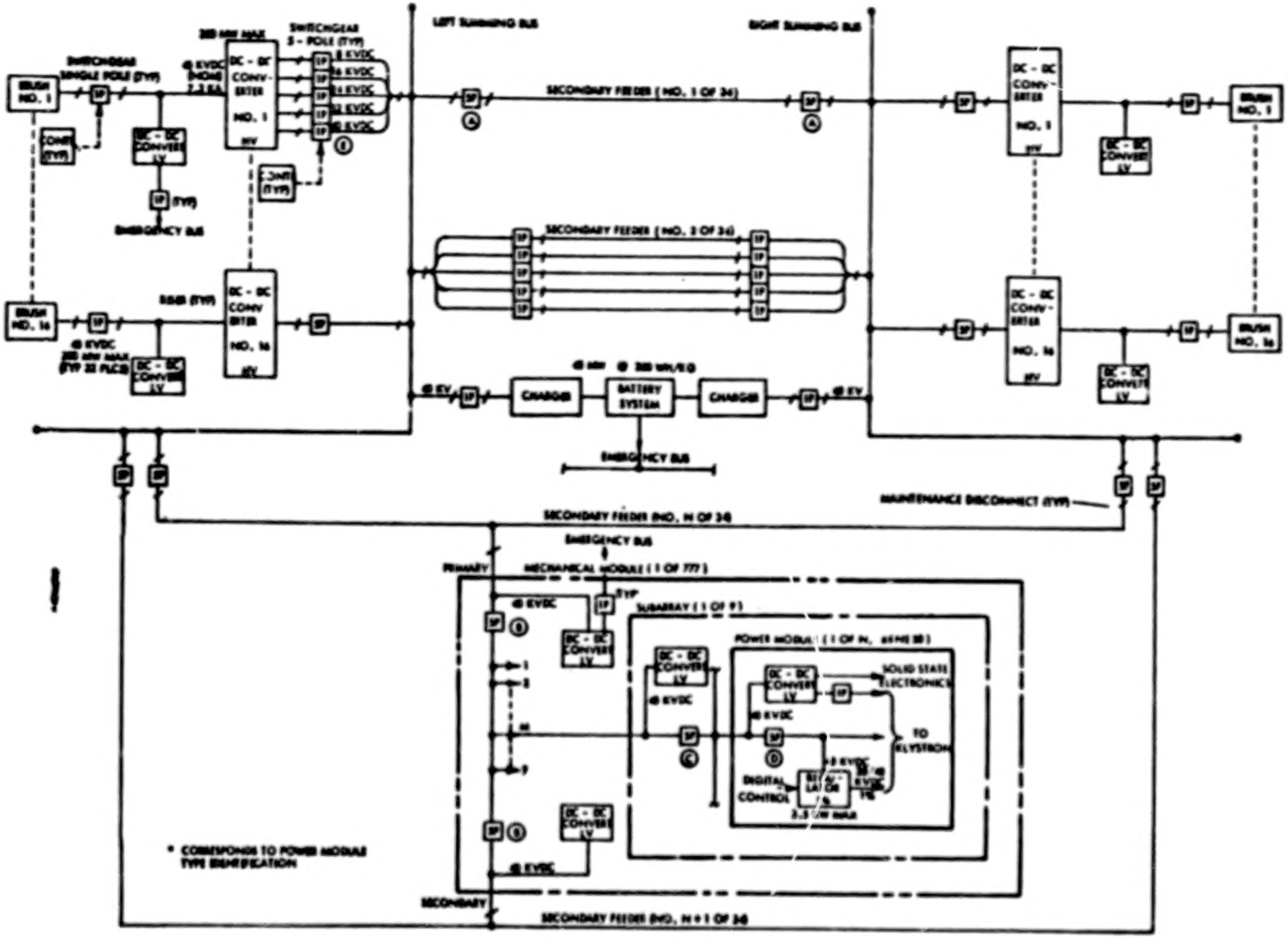
LEFT SUMMING BUS
RIGHT SUMMING BUS
BRUSH NO. 1
SWITCHGEAR SINGLE POLE (TYP)
CONT (TYP)
DC - DC CONVERTER LV
SP (TYP)
EMERGENCY BUS
40 KVDC (NOM) 7.3 KA
300 MW MAX
DC - DC CONVERTER NO. 1 HV
SWITCHGEAR 5 - POLE (TYP)
8 KVDC
16 KVDC
24 KVDC
32 KVDC
40 KVDC
E
CONT (TYP)
SECONDARY FEEDER (NO. 1 OF 36)
A
SECONDARY FEEDER (NO. 2 OF 36)
BRUSH NO. 16
RISER (TYP)
40 KVDC 300 MW MAX (TYP 32 PLCS)
DC - DC CONVERTER NO. 16 HV
40 KV
CHARGER
BATTERY SYSTEM
40 MW @ 300 MW/EQ
EMERGENCY BUS
SP
MAINTENANCE DISCONNECT (TYP)
SECONDARY FEEDER (NO. N OF 36)
EMERGENCY BUS
PRIMARY
MECHANICAL MODULE (1 OF 777)
40 KVDC
TYP
B
SUBARRAY (1 OF 9)
POWER MODULE (1 OF N, ≤N≤ 30)
1
2
N
9
SOLID STATE ELECTRONICS
TO KLYSTRON
C
D
DIGITAL CONTROL
REGULATOR
3.5 KW MAX
SECONDARY
SECONDARY FEEDER (NO. N + 1 OF 36)
* CORRESPONDS TO POWER MODULE TYPE IDENTIFICATION

Figure 3.1-26. Microwave Antenna—Power Distribution

for redundancy in the event of faults. The IMCS controls the power flow to each mechanical module so that a combination of one summing bus and one feeder is supplying power at any one time. There are 777 mechanical modules on the antenna. Each mechanical module has nine subarrays, and each subarray is isolated through switch gear.

The magnetron-based antenna concept differs from the klystron version in two instances. The first is that high-voltage dc/dc converters are not utilized; and second, the distribution system need accommodate only one voltage (20 kV, nominal). With these two exceptions, the distribution concept implemented for the magnetron antenna is similar to that proposed for the reference antenna. The total number of isolatable subarrays in the magnetron array is estimated at 37,500 units.

The solid-state end-mounted concept also uses a distribution scheme similar to the reference concept, except that the dc/dc converter reduces the voltage to a single level (640 V). The subsequent reduction in voltage to the 10 V dc required by the solid-state amplifiers is accomplished by series-parallel interconnections on the basic subarray. Switch gear isolation is provided only at the subarray (640 V) level.

The power distribution scheme proposed for the sandwich concept results in a major departure from the approach suggested for all of the planar satellite concepts. Because the solar array segments are an integral part of the microwave sandwich combination, the power distribution of each segment is also dedicated. The power distribution concept was illustrated in Figure 3.2-16. Note that no provision is made to interrupt the power through outside intervention through the use of switch gear components. Power shutdown can only be achieved by either covering the solar cells with an opaque material or by turning the primary mirror away from the sun. Beam turn-off is attained by removing either the pilot signal or the reference signal input.

Although direct switching of the main power path is not included in the sandwich configuration, more conventional switching operations are included for the independent power generated for support subsystem operation on the antenna. The source of the energy for the subsystem will be independent solar panels located at various locations on the antenna structure, operating at a concentration ratio of 1.0. The question of generated voltage level has not been explored, although it has been assessed that the subsystem will nomenally operate at voltage levels in the 20 to 100 V region.

Energy Storage

Batteries will be utilized during solar eclipses to provide 2-40 MW/hour energy. The batteries will be a sodium-chloride type and have a density of at least 200 Wh/kg. The 40-MW/hour sizing is only required for the cathode heaters on the klystron power amplifier. The magnetron and other concepts will require less than 2 MW/hour of stored energy.

Subsystem Mass Summary

A mass breakdown for the PD subsystem in each of the selected concepts is given in Table 3.1-18. The related mass included in the secondary structure area has been included to show the full mass impact of the PDS.

Table 3.1-18. PD Subsystem Mass Summary

	REFERENCE		SOLID-STATE END MOUNTED (DUAL)		MAGNETRON		SOLID-STATE * SANDWICH (DUAL)	
($\times 10^6$ kg)	GaAs	GaAlAs/ GaAs	GaAs	GaAlAs/ GaAs	GaAs	GaAlAs/ GaAs	GaAs	GaAlAs/ GaAs
SOLAR ARRAY								
SECONDARY & PANEL FEEDERS	0.048	0.047	0.0282	0.325	0.100	0.100	0.002	0.002
MAIN FEEDERS	2.020	0.765	0.0622	0.230	3.318	2.074	--	--
TIE BARS	0.043	0.043	0.048	0.048	0.086	0.086	--	--
AC THRUSTER CABLES	0.005	0.005	0.005	0.011	0.005	0.005	--	--
INSULATION	0.032	0.032	0.021	0.010	0.028	0.032	NEGL.	NEGL.
SWITCH GEAR	0.304	0.192	0.072	0.192	0.304	0.304	NEGL.	NEGL.
LOW VOLT. DC-DC CONV.	0.009	0.008	0.018	0.018	0.009	0.009	0.001	0.001
CONDUCTOR TERMINALS	0.247	0.247	--	--	0.247	0.247	--	--
SLIP RINGS	0.043	0.043	0.032	0.032	0.043	0.043	--	--
SECONDARY STRUCTURE	0.305	0.153	0.105	0.060	0.420	0.293	NEGL.	NEGL.
SUBTOTAL	3.056	1.535	1.205	0.926	4.560	0.193	0.003	0.003
ANTENNA ARRAY								
SUMMING BUS	0.326	0.326	0.256	0.256	0.684	0.684	--	--
FEEDERS	0.311	0.311	0.420	0.420	0.343	0.343	NEGL.	NEGL.
MODULE CABLE	0.125	0.125	1.455	1.455	0.125	0.125	--	--
INSULATION	0.011	0.011	0.110	0.110	0.017	0.017	NEGL.	NEGL.
SWITCH GEAR	0.343	0.343	0.079	0.079	0.343	0.343	NEGL.	NEGL.
HIGH VOLT. DC-DC CONV.	1.334	1.334	2.081	2.081	--	--	--	--
LOW VOLTAGE DC-DC CONV.	0.003	0.003	0.003	0.003	0.003	0.003	NEGL.	NEGL.
SECONDARY STRUCTURE	0.245	0.245	0.657	0.657	0.117	0.117	--	--
SUBTOTAL	2.698	2.698	5.061	5.061	1.632	1.632	NEGL.	NEGL.
INTERFACE								
RISERS & INSULATION	0.271	0.271	0.487	0.487	1.177	1.177	--	--
SLIP RING BRUSHES	0.017	0.017	0.051	0.051	0.017	0.017	--	--
SECONDARY STRUCTURE	0.031	0.031	0.054	0.054	0.118	0.118	--	--
SUBTOTAL	0.319	0.319	0.592	0.592	1.312	1.312	--	--
TOTAL	6.073	4.552	6.858	6.579	7.504	6.137	0.003	0.003
DELIVERED PWR @ U.I. (GW)	5.07	5.07	5.22	5.22	5.6	5.6	2.42	5.06
SP DENSITY (kg/kW_{UI})	1.20	0.90	1.31	1.26	1.34	0.001	0.001	0.001

*NOTE: NUMBERS SHOWN ARE FOR AUXILIARY SUBSYSTEM SUPPORT ONLY. MAIN POWER DISTRIBUTION IS INCLUDED IN SUBARRAY MASS.

3.1.4 MICROWAVE POWER TRANSMISSION

Introduction

The microwave power transmission system (MPTS) deals with the need to transmit large amounts of power from geosynchronous equatorial orbit (GEO) to a receiving station located within or near the continental United States. The MPTS is basically made up of the energy conversion (to microwave energy at 2.45 GHz) and transmission element (antenna) on the satellite, the retrodirective phase control system, and the ground receiving antenna (the rectenna). The first two elements of the MPTS are discussed in this section. The rectenna (and its associated support subsystems), are discussed in Section 3.2.

Four alternate antenna concepts were evaluated. The initial concept, termed the Rockwell reference concept, utilizes klystrons as the primary microwave power amplification element.

Two concepts utilizing the solid state amplifiers were considered. The first considered the "replacement" of the klystron based microwave antenna system with a solid state equivalent. The planar photovoltaic energy conversion concept was retained. The second approach utilized a completely different approach wherein the microwave transmission system and the solar conversion systems were "married" into a hybrid "sandwich". As the total area of the solar array was limited by the required antenna aperture it becomes necessary to use higher solar concentration ratios to provide more realistic power levels.

The fourth approach considered utilized magnetron crossed field amplifiers to provide the microwave power signal.

Reference Concept

The reference concept satellite, Figure 2.1-16, consists of a solar array, a yoke structure (interface) and the antenna section utilizing klystrons as power amplifiers. The antenna is nominally 1200 m in diameter with a 1 km diameter aperture or active area. A large number of power modules with high power (nominal) klystrons are mounted on the array structure. The klystrons serve as microwave power amplifiers and the microwave energy is beamed to an antenna array located on the earth's surface as part of the ground receiving station (GRS). Table 3.1-19 presents a summary of the MPTS and satellite antenna point design characteristics. The basis for the antenna analysis was a transmission capability of 7.14 GW. An assessed maximum klystron output of 52 kW (each) was established.

The microwave controlled segments or subarrays are mounted on a hexagonal tension web/compression frame configuration depicted in Figure 3.1-27. A discussion of the structure and its important parameters is provided in Section 3.1-5.

Subarray

The 50 kW klystrons, selected as power converters, are mounted on waveguide radiators as shown in Figure 3.1-28. This assembly is defined as a

Table 3.1-19. Point Design Microwave Power Transmission System (MPTS) Satellite Antenna Characteristics

MPTS System (Gaussian Beam)	
Frequency (GHz)	2.45
Maximum satellite array power density (kw/m^2)	21
Power density at ionosphere (mW/cm^2)	23
MPTS efficiency (includes ionosphere and atmospherics), %	59.3
DC input power to MPTS from solar array (GW)	9.94
DC output power to utility (GW)	5.07
Satellite MPTS Antenna Array	
Size (transmitting diameter), km	1
- Area (km^2)	0.785
Weight (kg)	11.98×10^6
Number of mechanical modules	777
Number of subarrays	6933
Number of klystron power modules	142,902

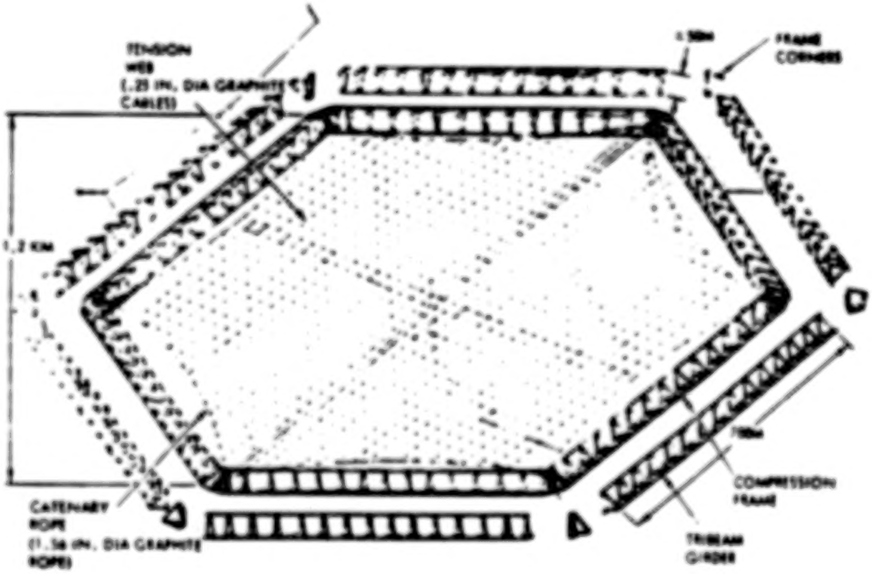
TENSION WEB (.25 IN. DIA GRAPHITE CABLES)
FRAME CORNERS
1.2 KM
CATENARY ROPE (1.56 IN. DIA GRAPHITE ROPE)
COMPRESSION FRAME
TRIBEAM GIRDER

Figure 3.1-27. Microwave Antenna Structure Selected Design Concept

power module. Its area varies so as to set the radiated power densities required over the array surface. There are nine density steps and corresponding module designs. These modules are assembled to form nine subarray types.

When the klystrons are removed from their mounts, the subarray power modules can be stacked in a compact form for transport. The nine point-design subarray configurations and the dimensions of the stacked packages are shown in Figures 3.1-29, 3.1-30, and 3.1-31. The parameters associated with each subarray type are also given. The subarray coding is keyed to the coding of Figure 3.1-32 showing the total array.

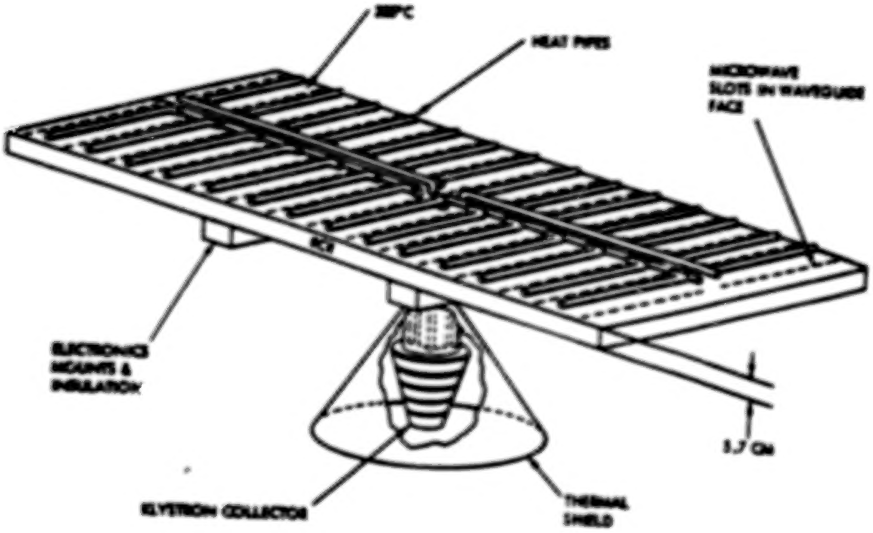
300°C
HEAT PIPES
MICROWAVE
SLOTS IN WAVEGUIDE
FACE
RCS
ELECTRONICS
MOUNTS &
INSULATION
3.7 CM
KLYSTRON COLLECTOR
THERMAL
SHIELD

Figure 3.1-28. Radiating Face of Power Module

TYPE PWR DENSITY	1. 21.82 KW/M²	2. 17.80 KW/M²	3. 15.16 KW/M²
NO. OF KLYSTRONS/ SUBARRAY & ARRANGEMENT • PWR MOD SIZE • HINGED CONFIG	50 10 × 5 1.02 × 2.33 10.20 × 2.33	42 7 × 6 1.46 × 1.94 10.2 × 2.33	36 9 × 4 1.13 × 2.91 10.2 × 2.91
	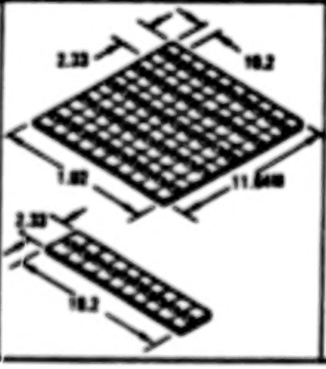	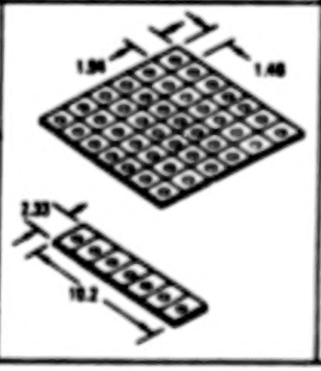	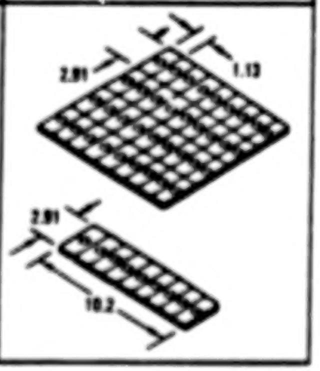

2.33
10.2
1.02
11.640
2.33
10.2
1.94
1.46
2.33
10.2
2.91
1.13
2.91
10.2

Figure 3.1-29. Standard Subarray Size - Block 1

A subarray is defined as a portion of the total antenna array which has the same phase over its radiating surface. This definition will be modified where the subarray beam is steered to point in the direction of the pilot beam. In this case, the center of the subarray has a phase, set by a single retroelectronics assembly. In addition, there may be phase variation across the array face to steer the subarray antenna pattern.

The subarray size selected is 11.64×10.2 m. Sets of nine subarrays are then supported by a secondary structure to form a 34.92×30.6 m mechanical module. The module is supported by connections to the antenna tension web cabling.

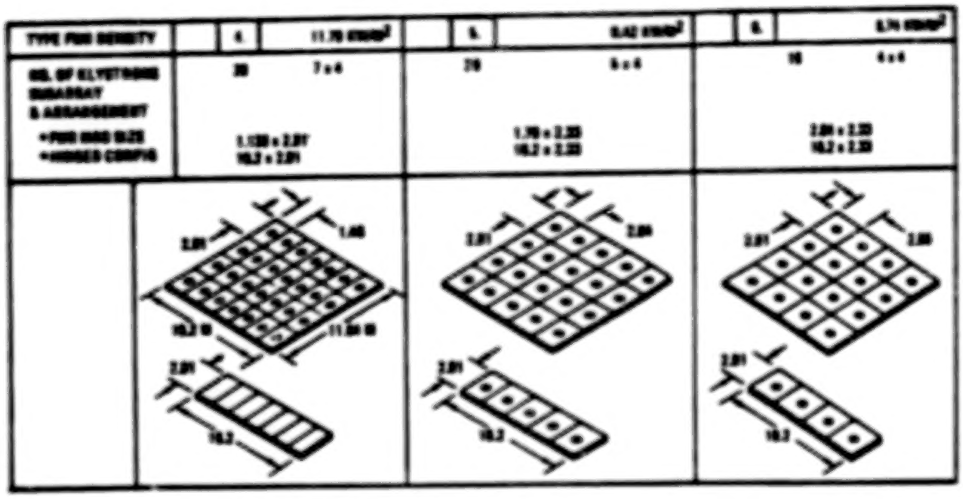

Figure 3.1-30. Standard Subarray Size - Block 2

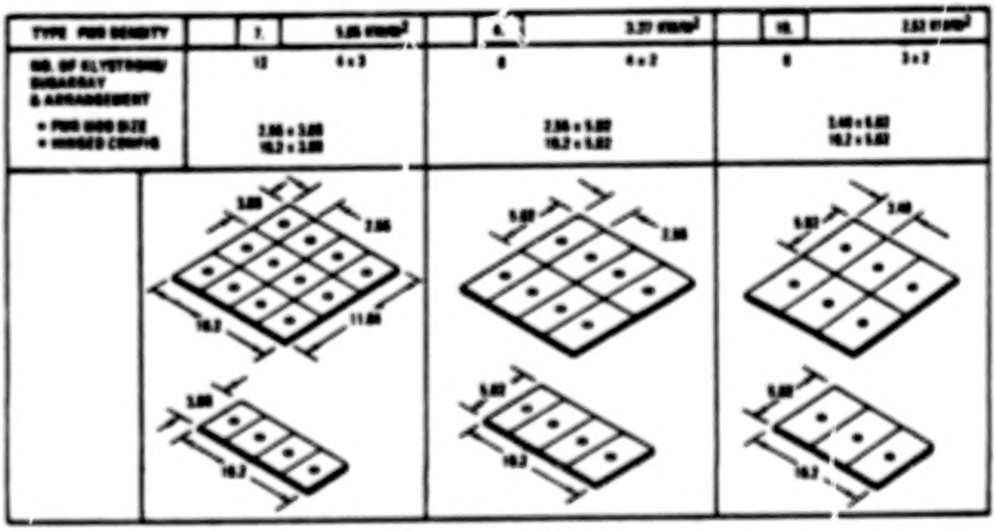

Figure 3.1-31. Standard Subarray Size - Block 3

In order to keep costs down and make fabrication easy it is desirable that the subarray radiators be made of metal. However, neither the total mechanical module nor the subarrays can be a single metal structure due to thermal effects. As an example, for aluminum with an expansion coefficient of $2.5\times10^{-5}/°C$ and an operating temperature range of 100°C, the change in dimension for the mechanical module is 7.5 cm and for a subarray 2.5 cm. The resulting deviation from uniform spacing of the radiating elements in the subarray surfaces is too great.

The subarrays are made up of power modules, each fed by a single microwave amplifier. These modules vary from about 1.0 m to 6.0 m on a side. The corresponding thermal dimension changes are ±0.13 cm to ±0.76 cm or $\pm0.010\ \lambda$

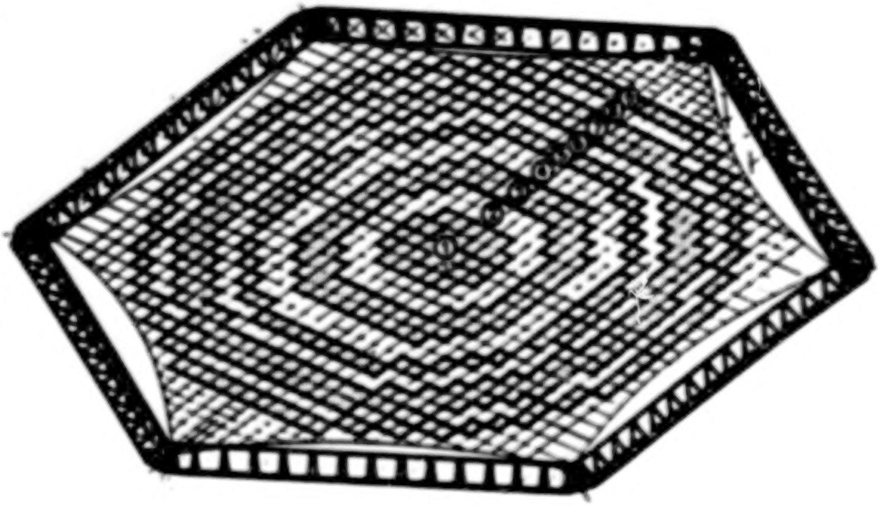

TYPE	NO. OF MECH MOD	Kw/M² PWR DENSITY
1	31	21.05
2	[illegible]	17.69
3	84	15.2
4	110	11.70
5	60	8.42
6	[illegible]	6.74
7	104	5.05
8	[illegible]	3.37
9	[illegible]	2.52

Figure 3.1-32. Gaussian Beam Microwave Antenna

to 0.062 λ around a design configuration. This is felt to be an upper limit on movement of the radiator elements. Therefore, the tension web cabling will be graphite-epon. Since the expansion coefficient of graphite-epon is an order of magnitude less than metals, only very small gaps between the mechanical modules are needed to accommodate thermal expansion.

The power level of all module amplifiers is the same. The size of the module radiating surface is varied to vary the power density weighting over the total array area. For instance, if 50-kW klystrons are used and the weighting is Gaussian, the number of modules per 11.96x10.2-m subarray varies from 50 at the array center to 6 at the array edge in the case of a 5-GW SPS system with a 1-km-diameter array. The module area then varies from 2.38 m^2 to 19.79 m^2. The layout of the nine subarray designs needed for a 9-step approximation to the Gaussian taper is shown in Figures 3.1-29 through 3.1-32. A nine-step quantization of a 10 dB taper (Figure 3.1-33) was chosen.

Antenna

The reference concept antenna is a basic slotted-waveguide radiator assembly. The power module antenna combines a number of 6x10 cm (nominal) waveguides and a transverse feeder waveguide as shown in Figure 3.1-34.

Klystron Amplifiers

Klystrons with an efficiency of 85.86% have been suggested for the reference concept microwave power transmitting antenna. The reference klystron is based on the performance of the various VKS-7773, 50 kW, 2.45 GHz klystron previously built which obtained an efficiency of 74.4% without a depressed collector. Addition of a depressed collector with 55% beam power recovery

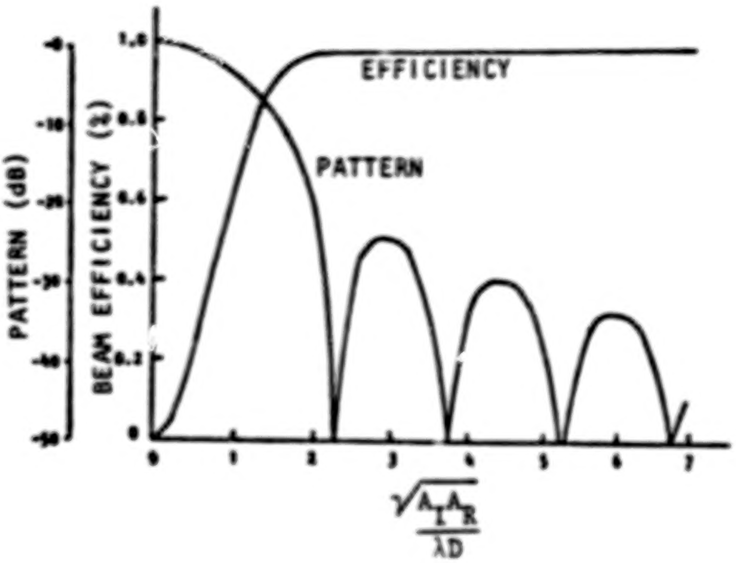

Figure 3.1-33. Pattern Efficiency for
Uniform Illumination (10 dB Taper)

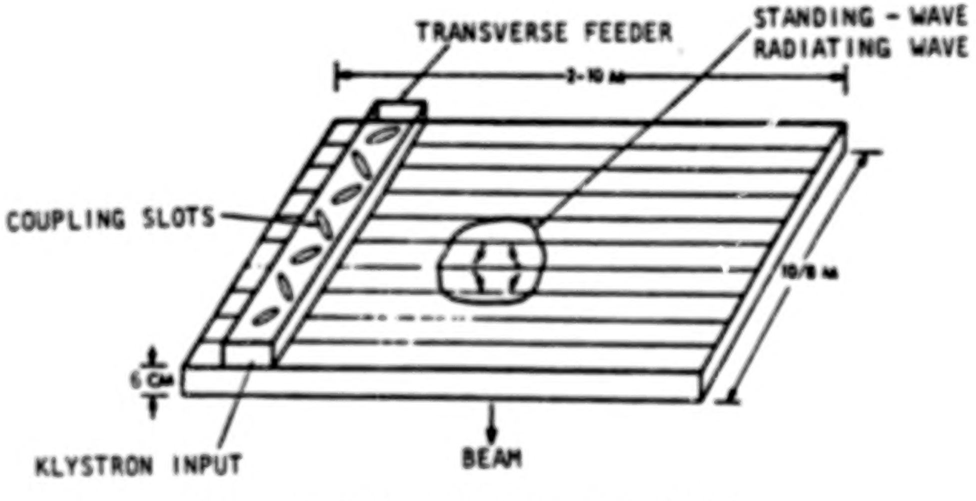
TRANSVERSE FEEDER
STANDING - WAVE
RADIATING WAVE
2-10 M
COUPLING SLOTS
10/8 M
6 CM
KLYSTRON INPUT
BEAM

Figure 3.1-34. Klystron Power Module
Waveguide Assembly

efficiency plus other minor changes leads to an 80% efficiency. Taking into account cathode heater and solenoid power, a final efficiency of 85% is used in the point design calculations.

The major drawback to the use of klystrons is the large number of electrode voltages which are required. The depressed collector design selected requires five low regulation voltages. In addition, two regulated power supplies (1%) are required to supply body current and establish the potential of the module anode, which controls beam current. The present point design generates all these voltages from a single 40 kV (nominal) bus by means of dc-dc converters plus precision regulators, where required.

The collector can be run very hot and radiate directly to space, if it is made of a refractory material. Figure 3.1-35 shows that in such a collector assembly, made of pyrolytic graphite, the body cannot radiate directly to space as the collector can. The body cooling method selected is the use of heat pipes embedded in the klystron body walls and output drift tube. The heat-carrying pipes leave the klystron and carry heat to a set of pipes lying between the microwave slot radiators of the waveguide face. This permits the disposal of klystron body waste heat downward toward earth and away from the satellite.

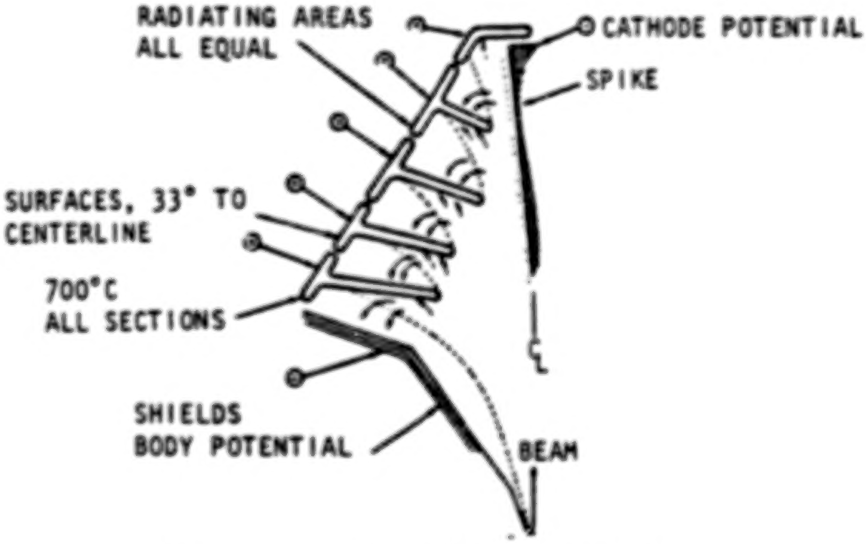

Figure 3.1-35. Collector Radiator

Heat is permitted to radiate from both front and rear surfaces of the antenna waveguides. The electronics devices required to provide phase control and maintain the MPTS during operation are mounted on isolation standoffs and thermally shielded to maintain a base temperature equal to or less than 100°C.

In the array center there are 42 klystrons per 100 m^2 subarray. The radiator area per tube is then 4.74 m^2, if the microwave array structure is also used to radiate heat. The array face temperature is about 200°C for a power density of 25 kW/m^2.

Analysis of the latest efficiency chain, Figure 1.2-19, has indicated a need for a transmission power level of 7.14 GW.

The mass properties of the individual klystron are provided in Table 3.1-20 without including any uncertainty of growth factor.

Phase Array System—Eclectic Conjugate

The reference phase distribution system is a modification of the system proposed by Seyl and Leopold of JSC. An overall block diagram is given in Figure 3.1-36. It used a group of traveling wave feeders which distribute the reference source to a set of array regions. These feeders are servoed to produce the same phase at all outputs by means of signals fed back to the

Table 3.1-20. Klystron Mass Estimate

COMPONENTS	MASS (kg)
PPM Magnet	2.0
Magnetic Poles	6.5
Electromagnet	13.0
Collector Assembly	5.5
Collector Heat Shield	0.1
Body Heat Shield	0.8
Copper Cavities	0.4
Heat Pipes in Tube	2.1
Electron Gun	0.6
TOTAL	31.0 kg
Specific Mass	0.62 kg/kW

feeder inputs. The amplifiers in a given region are excited by a local feeder distribution system using resonant feeder elements.

The pilot phase regeneration system is based on the JPL design. However, the transmitter signal is used as the local oscillator. This signal is of very high amplitude. It was feared that if the transmitter signal is not incorporated into the phase regeneration loop, it would produce so many spurious signals the design may fail. Elimination of transmitter phase noise forces us to a multiplier arrangement such as JPL used.

A pair of reference signals are used symmetrically placed around the operating frequency in order to eliminate ionospheric phase errors and errors due to filter detuning. The reference signal and the regenerated pilot are fed into the phase conjugating circuit shown in Figure 3.1-37.

Note that the output is $(2f_p - f_p)$. This is of the correct form to produce phase conjugation. If $f_r = f_p$, $f_T = f_p$; this is the most desirable condition. The only drawback is possible leakage of the high power transmitted signal into the phase reference distribution system. This is controlled by distribution of a reference at a frequency of $f_r/2$ which is converted to f_r by doubling at the point of usage.

The phase-conjugated signal, f_T, (which is what we wish to transmit) is fed to a transistor preamp and then to a power divider where the signal is distributed to the klystron amplifiers. The divider outputs are fed through analog phase shifters to the klystrons, where power generation occurs. The klystron outputs are used to drive the standing wave arrays which comprise the subarray.

The same subarray is receiving the pilot signals coming up from the earth station. Diplexers allow the klystron signals to flow into the standing wave radiators, while diverting the pilot signal coming from the cavity into a power combining network which feeds a monopulse bridge. Since the pilot signals are equally displaced from the transmitted signal, the 180°C change in phase needed in the diplexer occurs for both pilots. Alternately the standing waveguide

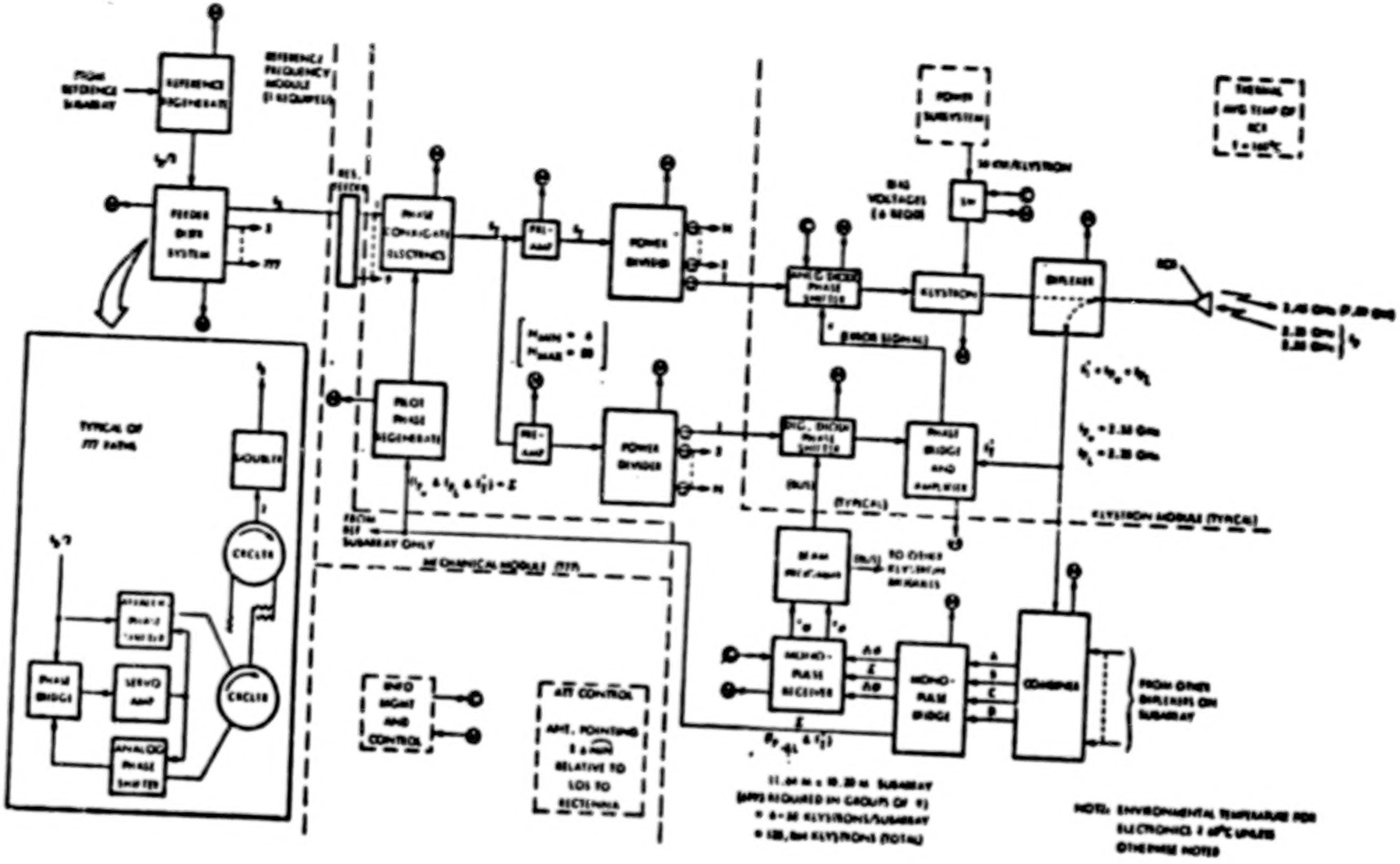
FROM REFERENCE SUBARRAY
REFERENCE REGENERATE
REFERENCE FREQUENCY MODULE (1 REQUIRED)
FEEDER DIST SYSTEM
REF. FEEDER
PHASE CONJUGATE ELECTRONICS
PRE-AMP
POWER DIVIDER
N
2
TYPICAL OF FFF PATHS
DOUBLER
CIRCLTR
PHASE BRIDGE
SERVO AMP
ANALOG PHASE SHIFTER
PILOT PHASE REGENERATE
FROM REF SUBARRAY ONLY
MECHANICAL MODULE (TYP)
INFO MGMT AND CONTROL
ATT CONTROL
ANT. POINTING RELATIVE TO LOS TO RECTENNA
POWER SUBSYSTEM
BIAS VOLTAGES (4 REQD)
SW
DIG. DIODE PHASE SHIFTER
KLYSTRON
ERROR SIGNAL
DIPLEXER
RCI
2.45 GHz
2.33 GHz
2.33 GHz
PHASE BRIDGE AND AMPLIFIER
(TYPICAL)
KLYSTRON MODULE (TYPICAL)
(BUS)
BEAM PROCESSOR
TO OTHER KLYSTRON MODULES
MONO-PULSE RECEIVER
MONO-PULSE BRIDGE
COMBINER
A
B
C
D
Δφ
Σ
Δθ
FROM OTHER DIPLEXERS ON SUBARRAY
THERMAL AVG TEMP OF RCI
(APPS REQUIRED IN GROUPS OF 9)
KLYSTRONS/SUBARRAY
KLYSTRONS (TOTAL)
NOTE: ENVIRONMENTAL TEMPERATURE FOR ELECTRONICS UNLESS OTHERWISE NOTED

Figure 3.1-36. Microwave Antenna—Beam Generation and Control

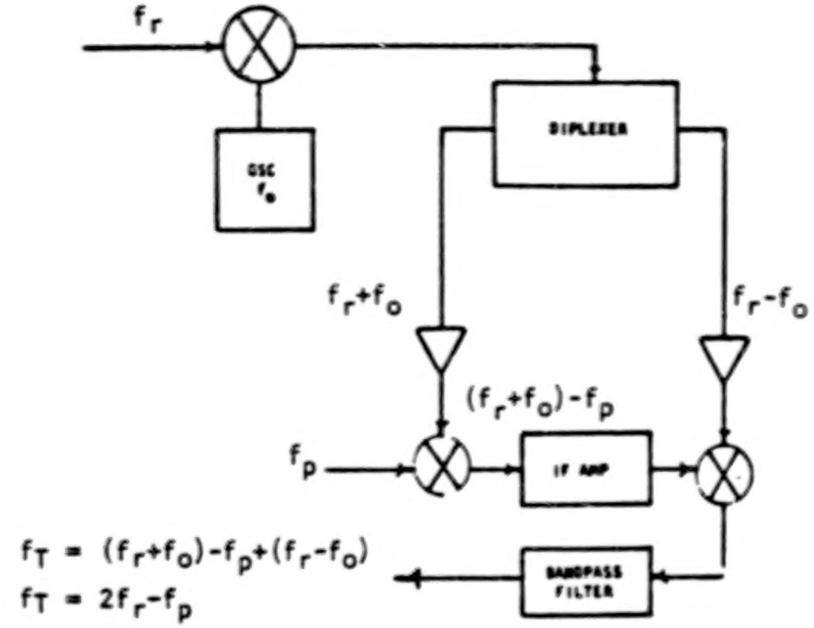
f_r
OSC
f_o
DIPLEXER
f_r+f_o
f_r-f_o
$(f_r+f_o)-f_p$
f_p
IF AMP
BANDPASS FILTER
$f_T = (f_r+f_o)-f_p+(f_r-f_o)$
$f_T = 2f_r-f_p$

Figure 3.1-37. Phase Conjugating Electronics

assembly or cavity can be fed from a separate feeder. The klystron signal at the bridge input is reduced by about 30 dB. The pilot signals are about 1 mW at this point. The pilot signals are then fed to a monopulse bridge. The sum signal is fed to the pilot phase regeneration circuitry. This sum signal and also the difference signals are fed to a monopulse receiver as shown in Figure 3.1-38. Just as in the pilot phase regeneration circuits, the transmitted signal is used as the local oscillator.

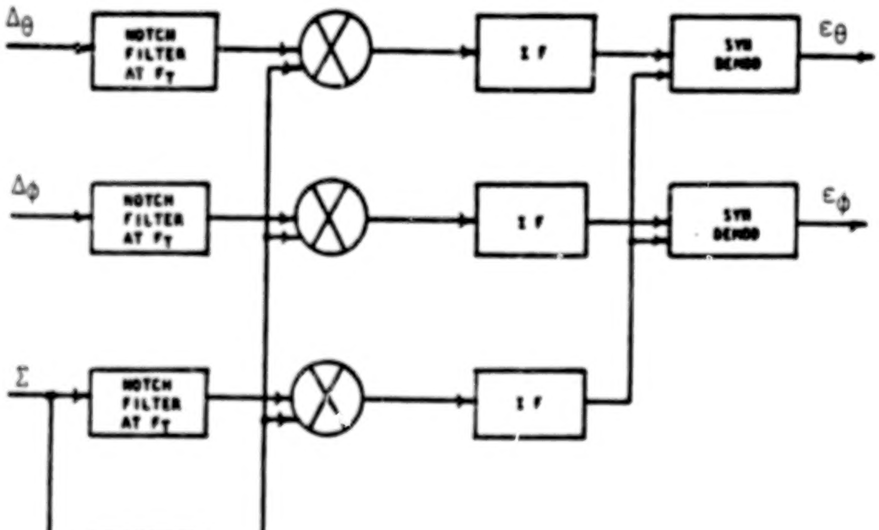
Δ_θ
NOTCH FILTER AT f_T
IF
SYN DEMOD
ϵ_θ
Δ_ϕ
NOTCH FILTER AT f_T
IF
SYN DEMOD
ϵ_ϕ
Σ
NOTCH FILTER AT f_T
IF
LIMITER

Figure 3.1-38. Monopulse Receiver

The monopulse receiver outputs $\epsilon\theta$ and $\epsilon\phi$ are a measure of the angular deviation of the direction of reception of the subarray from the direction of arrival of the pilot beam. The same signal f_T which was fed to the klystrons is fed to a second power divider. The outputs of this divider are fed through a set of phase shifters to an array of phase bridges.

The other set of inputs to these bridges is from taps which sample each klystron output in the standing wave radiators fed by the klystrons which comprise the subarray. These signals would be f_T, except that they have suffered phase shifts in the klystrons. They will be called f'_T. The first input to the phase bridges is f_T at the center bridge corresponding to the center of the subarray. The other members of this set are F_T shifted by the phase shifters so as to point the subarray pattern in the direction of arrival of the pilot beam. The phase shifters are set by a beam programmer which uses $\epsilon\theta$ and $\epsilon\phi$ from the monopulse receiver to make the correction. The phase bridge outputs are amplified and used to control the analog phase shifters at the klystron inputs. These servo loops then remove phase shift errors caused by the klystrons and introduce a phase gradient across the subarray face which corrects for subarray tilt.

At the edge of the array, subarrays will have only about six klystrons. As a result the subarray beam can only be steered about one beamwidth before the rms phase error of the subarray becomes too great. However, even angular control of one beamwidth greatly reduces the angular tolerances in mechanical orientation of the subarrays.

Reference Frequency Distribution

The basic organization of this distribution system is shown in Figure 3.1-39. Since each region supplied by a primary feeder is fed directly from the phase reference system, there is no buildup of phase error due to repeated processing at the primary feeder output points. A feedback servo is used to hold the phase of the feeder outputs with respect to the source to a fixed value. This servo is shown in Figure 3.1-40.

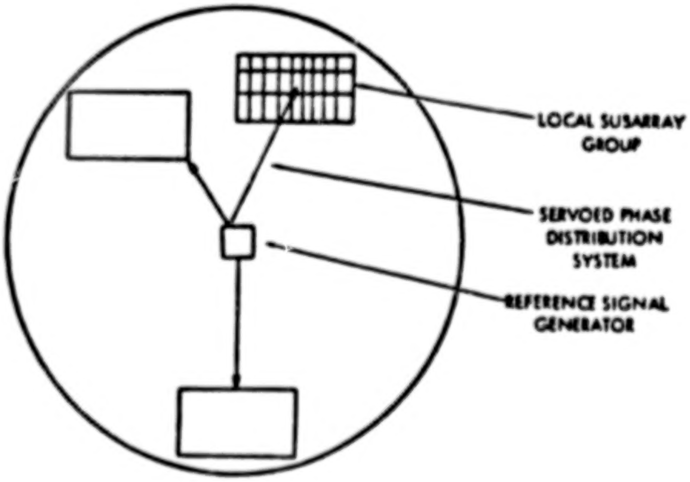

Figure 3.1-39. Array Reference Signal Distribution System

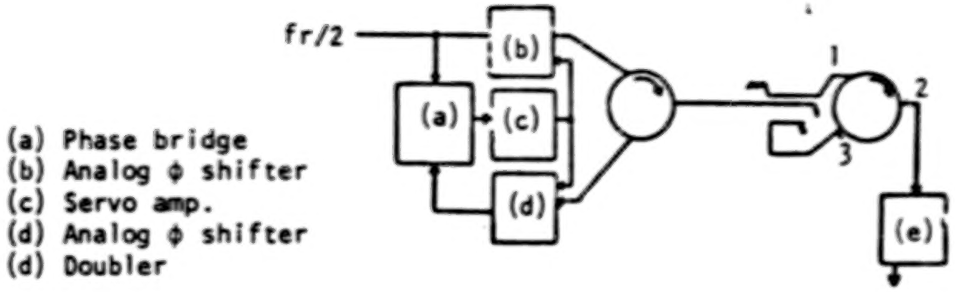

Figure 3.1-40. Reference Phase Distribution Servo

The reference source is at half the actual reference frequency. This signal enters the feeder through a diode phase shifter and a circulator. After reflection from the short at the other end of the feeder, it arrives back at the input and directed by the circulator into the output port. It then passes through a second phase shifter to a phase bridge. The other input to the bridge is the original reference signal.

The phase bridge output is an error signal which changes the phase shifter settings until the input to the feeder and the reflected signal from the feeder are in phase. The path delay through the shifters and feeder is then an integral number of wavelengths, since the forward and backward path delays are of equal length. Since the forward and return paths are of equal length, the forward path is an integral number of halfwaves long. This forward-path signal is sampled by the directional coupler/circulator arrangement. At port 2 of the circulator part of the signal is reflected back to the central station and part is fed to the doubler. When the signal is doubled to form f_r in the harmonic multiplier driven by the probe the doubler output phase delay with respect to f_r at the source will be twice the phase delay of $f_r/2$ or an integral number of full wavelengths. Therefore, the phase of the doubler output is the same as the phase of the source.

Each coax feeder serves an array region which is small enough to use a phase distribution system based on resonant feeders. Such regions are shown in Figure 3.1-39, designated as local subarray groups. The resonant feeder distribution concept depends on the fact that the phase at all points in a resonant cavity is approximately the same. The phase variation from point to point depends on the attenuation a wave experiences in traveling across the cavity. If the resonant feeder cavity is not too long, the cavity can be trapped along its length at the standing wave loops to obtain the reference phase. The accuracy with which the signals tapped from the feeder reproduce the reference phase depends on the total loss in the feeder.

If the resonant feeders are made of graphite-epox coated with metal or thin-wall invar, their thermal expansion coefficient can be of the order of 10^{-6} per °C or 10^{-4} for a 100°C change. The elongation is 2.4×10^{-3} m for a 25 m feeder. The corresponding change in electrical length at 2.45 GHz or 0.122 m wavelength is 7°. This small change will not destroy resonance, so it is felt that a servo to hold resonance is not required.

A servo to maintain resonance is required, if guide materials with larger expansion coefficients are used. An error signal for such a servo can be obtained by use of a loop and a dipole probe in the guide. At resonance, the electric and magnetic fields are in exact phase quadrature. These fields are sampled with a probe and a loop respectively and compared in a phase bridge to generate an off-resonance error signal. This signal can then be used to change effective length of the line till it is exactly in resonance. Figure 3.1-41 shows such an arrangement.

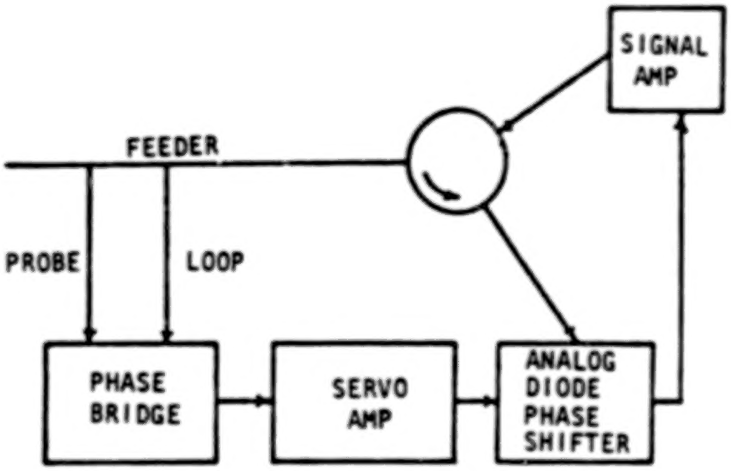

Figure 3.1-41. Electronic Servo Loop to Hold Feeder at Resonance

Since the signal is removed from the feeder and then reinserted, it can be amplified to make up for losses in the phase shift loop and some of the guide losses.

Pilot Signal Regeneration

The pilot signal required should be at the same frequency as the transmitted signal. However, it could not be detected in the presence of the very high power transmitted signal, if it were at the same frequency. Therefore, it must be offset in frequency. It turns out that in order to control phase errors due to filtering and the ionosphere it is best to have two pilot signals displaced by equal amounts upward and downward from the transmitter frequency. Also since the transmitted signal is at such a high power level, transmitter phase noise can be the dominant noise in pilot signal reception, if the pilot regeneration system is not planned with this in mind. The transmitter signal can also cause spurious frequencies by beating with other signals which can cause trouble.

The solution appears to be to include the transmitter signal in the regeneration process in such a way it cannot cause harm, rather than suffer its presence as an extraneous signal. This is done in the regeneration circuit shown in Figure 3.1-42. Since the output of the frequency quadrupler is the basic

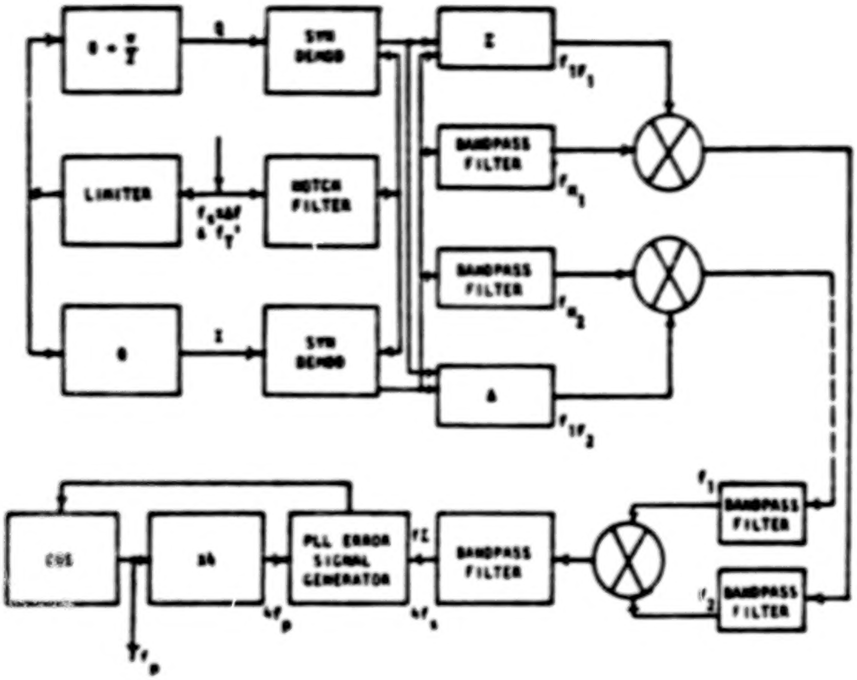
θ + π/2
Q
SYN DEMOD
Σ
f_{IF_1}
BANDPASS FILTER
f_{R_1}
LIMITER
NOTCH FILTER
$f_0 \pm \Delta f$ & f_T'
BANDPASS FILTER
f_{R_2}
θ
I
SYN DEMOD
Δ
f_{IF_2}
f_1
BANDPASS FILTER
f_2
BANDPASS FILTER
BANDPASS FILTER
PLL ERROR SIGNAL GENERATOR
fI
$4f_p$
$4f_s$
x4
f_p

Figure 3.1-42. Pilot Signal Regeneration Circuit

quantity, any change in phase in the multiplier will be divided by four. The multiplier should be two halfwave rectifier frequency doublers, rather than high efficiency multipliers using snap-back diodes. This will reduce phase errors due to the multiplier.

Mass Properties

The mass properties of the space portions of the MPTS system is summarized in Table 3.1-21.

Table 3.1-21.
Mass Properties—Reference MPTS (Spacetenna)

Subarray	7.050
Thermal	0.720
Antenna phase control	0.170
Total	7.940×10^6 kg

Solid State Antenna System

Two concepts utilizing the solid state amplifiers have been considered. The first considers the "replacement" of the klystron based microwave antenna system with a solid state equivalent. The planar photovoltaic energy conversion concept is retained. The second approach utilizes a completely different approach wherein the microwave transmission system and the solar conversion systems are "married" into a hybrid "sandwich". As the total area of the solar array is limited by the required antenna aperture it becomes necessary to use higher solar concentration ratios to provide more realistic power levels.

End-Mounted Solid-State Array System

The end-mounted space system layout is shown in Figure 2.1-3 and its preliminary characteristics are summarized in Table 3.1-22. Figure 3.1-43 shows a dipole/amplifier detail of the array aperture. Only one amplifier housing is shown but if the thermal conductivity of a ground-plane of sufficient thickness (16 mils perhaps not being strong enough) is not high enough to allow transverse condition of waste heat so that it can be uniformly radiated from the ground-plane, then two or more housings may be required, with a corresponding increase in signal and dc distribution complexity. The output from the single amplifier will be unbalanced against the ground-plane, and a balun will be incorporated into the dipole feed. For two amplifier housings, the two can be driven 180° out of phase and the balun is eliminated.

Table 3.1-22. End-Mounted Solid-State Concept Characteristics

- GaAs SOLAR ARRAY
- GEOMETRIC CR = 1.83
- DUAL END-MOUNTED MICROWAVE ANTENNA
- AMPLIFIER BASE TEMPERATURE = -100°C
- AMPLIFIER EFFICIENCY = 0.8
- ANTENNA POWER TAPER = 10 dB GAUSSIAN
- ANTENNA DIAMETER = 1.35 km
- POWER AT UTILITY INTERFACE = 2.61 GW PER ANTENNA (5.22 GW TOTAL)
- RECTENNA BORESIGHT DIAMETER = 7.51 km PER RECTENNA

A solar concentrator trough system is used with a geometric concentration ratio of 2 ($CR_e = 1.83$), yielding higher power output per unit area. A 40-kW voltage is transmitted through the rotary joints to supply the dc power to the amplifiers in the two arrays. The transmitted voltage is stepped down to the low voltage required by each amplifier by converters immediately behind the amplifier in the array structure.

System

The solid state arrays are subdivided into square subarrays of approximately 5 m by 5 m each. This subarray size is sufficiently small to keep the gain (efficiency) loss due to main beam wander within the subarray pattern to less than two percent maximum. This implies a mechanical antenna attitude control accuracy of ±3 minutes of arc, or a total swing of 6 minutes of arc, or 0.1°. It is expected that overall, major axis fluctuations can be controlled to this accuracy, with average values below that peak value, using conventional star sensor and earth-edge sensor plus inertial attitude control systems; with

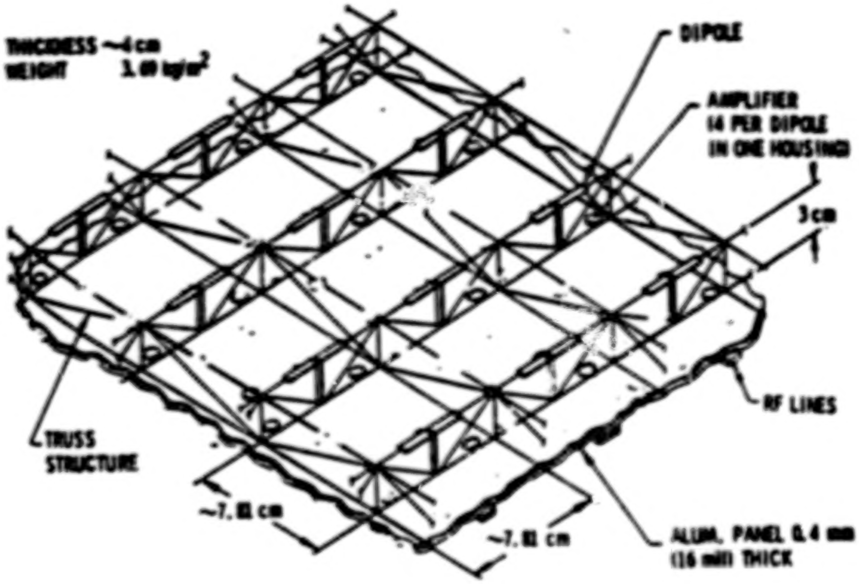
THICKNESS ~4 cm
WEIGHT 3.00 kg/m²
DIPOLE
AMPLIFIER
(4 PER DIPOLE
IN ONE HOUSING)
3 cm
RF LINES
TRUSS
STRUCTURE
~7.81 cm
~7.81 cm
ALUM. PANEL 0.4 mm
(16 mil) THICK

Figure 3.1-43. End-Mounted Antenna with Dipoles Over Ground Plane

ion thrusters providing the required impulses. All amplifiers within the 5×5 m subarray are controlled as a group, i.e., in phase. A diagramatic view from the bottom of the solid state arrays is illustrated in Figure 3.1-44. We see power dipoles radiating downward in the "power beam", and a high-gain (in this case a yagi) pilot antenna receives a pilot beam coming from the ground. The received pilot beam signal is then processed to direct the power beam. An alternate pilot antenna is shown in the square insert.

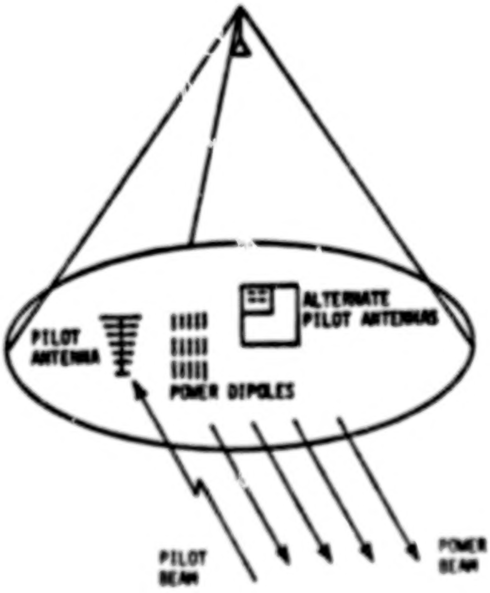
PILOT
ANTENNA
POWER DIPOLES
ALTERNATE
PILOT ANTENNAS
PILOT
BEAM
POWER
BEAM

Figure 3.1-44. Spacetenna Total View (Bottom)

The pilot beam and phase reference signal receiver antenna are always orthogonally polarized to the power dipoles to avoid interference from the power signal. The pilot signal received by the antenna is simplified, filtered, and then processed in a phase conjugation circuit which gets a phase reference signal from the rear of the array (see Figure 3.1-45). A reference signal transmitter is located somewhere near the center of the array, and sufficiently above to allow reception with a high-gain reference signal receiver antenna. An approximate range of reference transmitter heights is indicated also in Figure 3.1-45. One would like to mount the transmitter as low as possible, but gain variations at the receiving point are also of some concern. All circuits should be identical, to minimize fabrication costs.

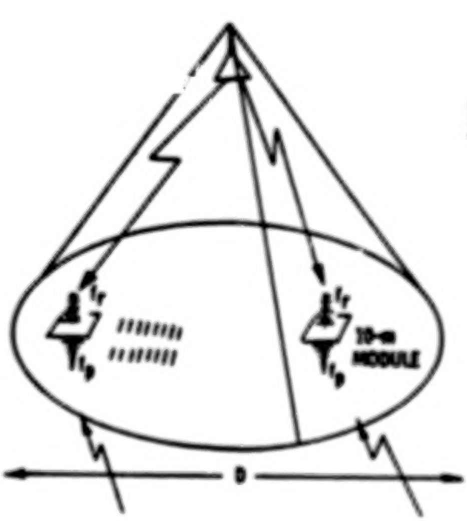

Figure 3.1-45. Spacetenna Total View (Top)

The antenna mechanical module layout is given in Figure 3.1-46. Dipole amplifiers are series-paralleled in the manner shown with each dipole requiring 10 V dc and up to nine power amplifiers paralleled per dipole. A total of 64 dipoles are series connected for a 640 V input requirement. These series connected dipoles are made up into subarrays, each 5 m × 5 m, installed into mechanical modules, each 30 m × 30 m. Each mechanical module has four dc converters to provide the 640 V to the series connected dipoles. Input voltage to the dc converters is 40 kV. The antenna feeder layout is shown in Figure 3.1-47. There are 1588 mechanical modules on the antenna. One fourth of the antenna section is shown (i.e., 397 mechanical modules).

Configuration details of the dipole amplifier are shown in Figures 3.1-48 and 3.1-49.

Each dipole is spaced 7.81 cm on center as shown in Figure 3.1-48. Power output per dipole is 40.5 W (maximum) to satisfy a Gaussian 10-dB taper illumination beam. The specific mass of the antenna cross section is 3.68 kg/m^2.

Trade study results show that for the solid-state end-mounted antenna concept a high voltage power transmission system is desired. High efficiency and lightweight dc converters are critical to the design concept. A 10-dB Gaussian power beam was selected for the solid-state end-mounted antenna to

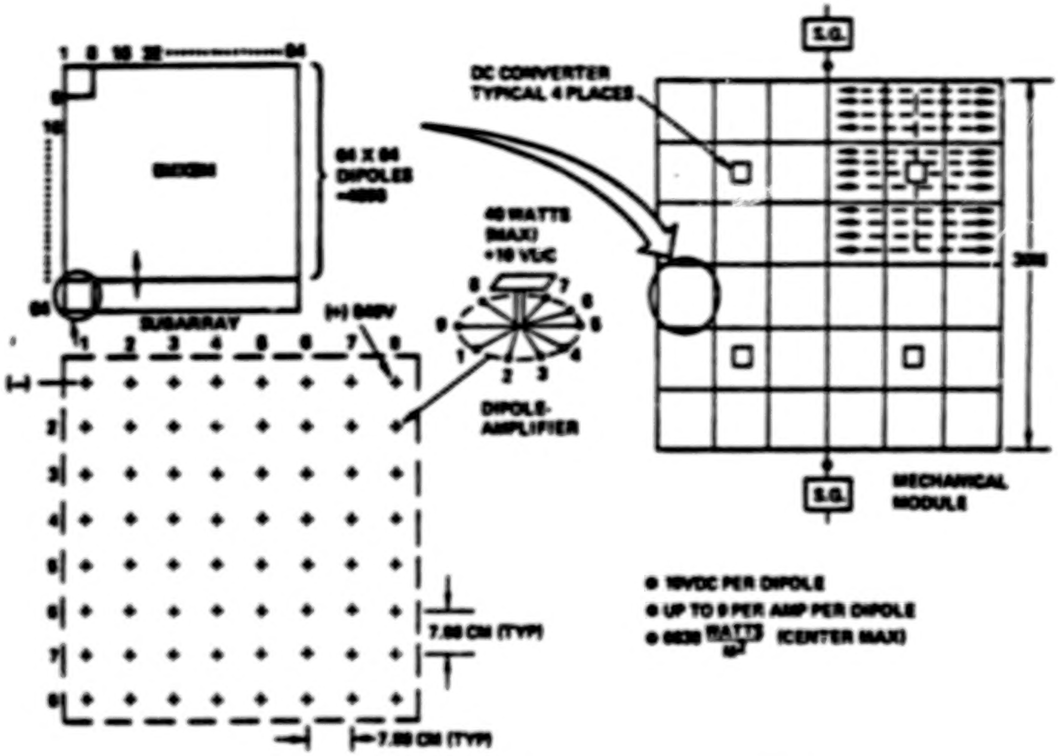
1 8 16 32 64
64 X 64
DIPOLES
=4096
SUBARRAY
(+) 840V
40 WATTS
(MAX)
+10 VDC
DIPOLE-
AMPLIFIER
7.50 CM (TYP)
7.50 CM (TYP)
DC CONVERTER
TYPICAL 4 PLACES
S.G.
30M
S.G.
MECHANICAL
MODULE
● 10VDC PER DIPOLE
● UP TO 9 PER AMP PER DIPOLE
● 6630 WATTS/M² (CENTER MAX)

Figure 3.1-46. Mechanical Module Layout
(Solid-State End-Mounted)

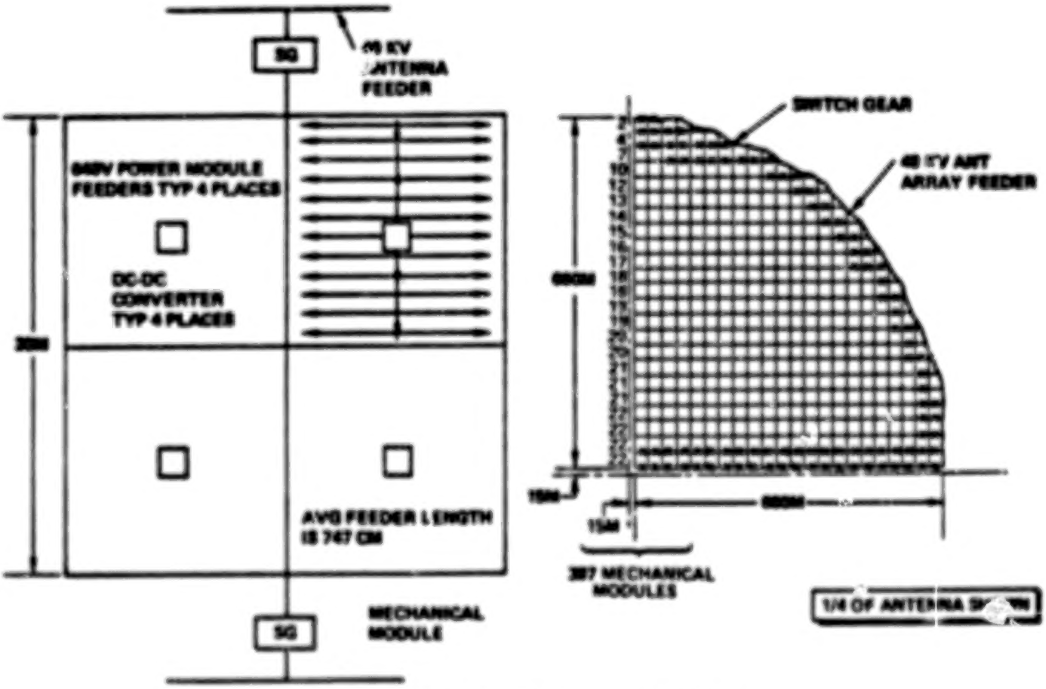
SG
40 KV
ANTENNA
FEEDER
840V POWER MODULE
FEEDERS TYP 4 PLACES
DC-DC
CONVERTER
TYP 4 PLACES
30M
AVG FEEDER LENGTH
IS 747 CM
SG
MECHANICAL
MODULE
SWITCH GEAR
40 KV ANT
ARRAY FEEDER
690M
15M
690M
15M
397 MECHANICAL
MODULES
1/4 OF ANTENNA SHOWN

NOTE: THERE ARE 1588 MECHANICAL MODULES 30 M X 30M EACH. FEEDERS OVERSIZED BY FACTOR 1.07 FOR FAULT OVERLOAD

Figure 3.1-47. Antenna Feeder Diagram
(Solid-State End-Mounted)

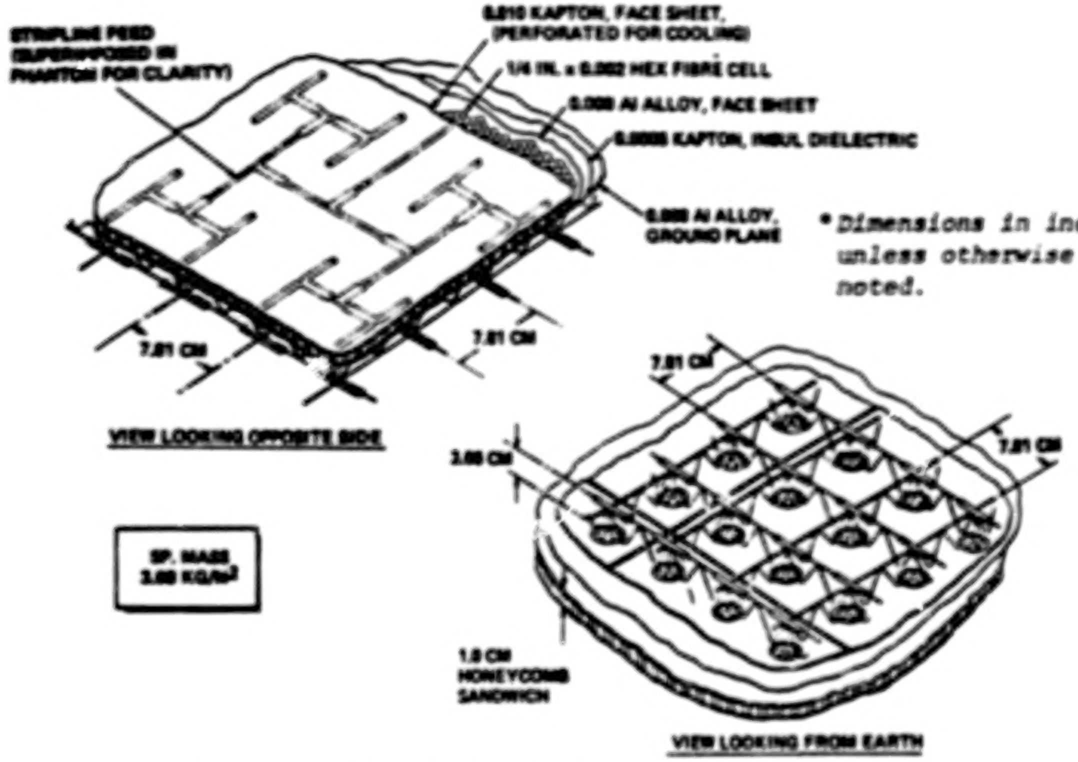
STRIPLINE FEED (SUPERIMPOSED IN PHANTOM FOR CLARITY)
0.010 KAPTON, FACE SHEET, (PERFORATED FOR COOLING)
1/4 IN. x 0.002 HEX FIBRE CELL
0.008 Al ALLOY, FACE SHEET
0.0005 KAPTON, INSUL DIELECTRIC
0.008 Al ALLOY, GROUND PLANE
7.81 CM
7.81 CM
VIEW LOOKING OPPOSITE SIDE
SP. MASS 3.00 KG/M²
7.81 CM
3.00 CM
7.81 CM
1.0 CM HONEYCOMB SANDWICH
VIEW LOOKING FROM EARTH

*Dimensions in inches unless otherwise noted.

Figure 3.1-48. Dipole Amplifier Panel Configuration
Solid-State End-Mounted (Preliminary)

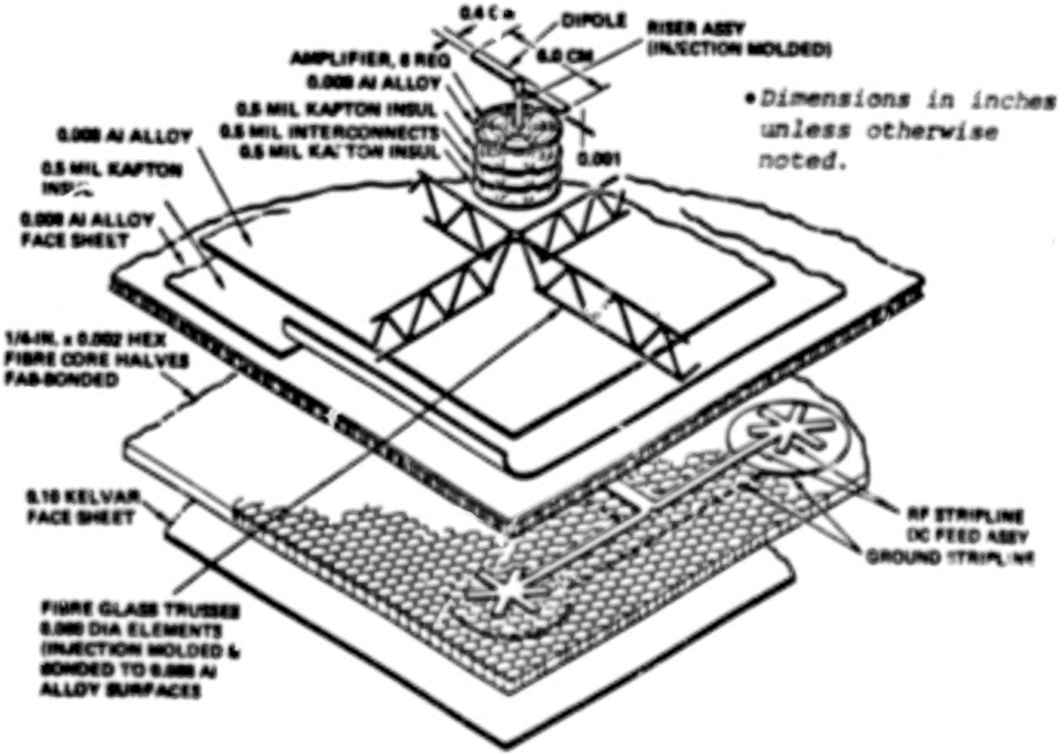
0.4 Cm
DIPOLE
RISER ASSY (INJECTION MOLDED)
AMPLIFIER, 8 REQ
6.0 CM
0.008 Al ALLOY
0.5 MIL KAPTON INSUL
0.5 MIL INTERCONNECTS
0.5 MIL KAPTON INSUL
0.001
0.008 Al ALLOY
0.5 MIL KAPTON INSUL
0.008 Al ALLOY FACE SHEET
1/4-IN. x 0.002 HEX FIBRE CORE HALVES FAB-BONDED
0.10 KELVAR FACE SHEET
RF STRIPLINE
DC FEED ASSY
GROUND STRIPLINE
FIBRE GLASS TRUSSES 0.080 DIA ELEMENTS (INJECTION MOLDED & BONDED TO 0.008 Al ALLOY SURFACES

•Dimensions in inches unless otherwise noted.

Figure 3.1-49. Dipole Amplifier Assembly—Exploded View
Solid-State End-Mounted (Preliminary)

reduce side lobes. The sandwich concept favors a uniform distribution beam, thereby increasing the antenna radiative power capability per satellite. Multi-bandgap solar cells with higher efficiencies (~30%) greatly benefit the sandwich concept by increasing antenna power densities. For the solid-state end-mounted antenna, a power amplifier module voltage of 640 V dc was selected to reduce module wiring mass. More study is required of the losses associated with series-paralleling solid-state amplifiers to meet this voltage requirement.

Reference Phase Distribution

While several systems characteristics are generic for a solid-state approach, one selected feature of the beam control is common to all Rockwell systems, with the exception of the "Reference Concept", i.e., one consisting of klystron-powered sub-modules. (The reference concept beam control system will be converted to the common approach at a future time.) This is the way in which the reference phase signal is distributed over the on-board antenna, or spacetenna aperture. Figure 3.1-45 illustrates this method in a very general way, giving a perspective view of the top of a circular aperture. (An actual aperture will have steps in the boundary, of course). Two important features are illustrated: (1) the phase reference signal originates from a single transmit location at the rear of the aperture; and (2) the phase reference and pilot antennas are orthogonally polarized with respect to the power dipoles. This is necessary in order to avoid feedback loops. Also shown in Figure 3.1-44 is an alternate pilot antenna layout using a broadside array of dipoles instead of an endfire (e.g., "Cigar") array. Both configurations are not only possible but practical, and shall be considered in more detail in future studies. The reference pick-up antenna can utilize an array as well.

The broadside array of antenna dipoles need only be placed over approximately a 0.31×0.31 m portion within a 5×5 m subarray. (A logical place for this portion will be shown later.) No constraints exist for such an array for the reference phase pick-up, except for the sandwich, when it has to be integrated with, or placed over the solar cells. For the end-mounted approach, locations have to be found where the dc distribution system causes no interference, but this should pose no problem.

Figure 3.1-50 explains in detail how the phase reference signal is distributed.

From the shaped-beam illuminator antenna the RF signal is distributed over a cone with a 90° (maximum) beamwidth. The illuminator may be a courrugated, phase-corrected horn or a synthetic-beam array using multiple weighted generating beams. The latter approach has the advantage of very tight control over the amplitude function, so that all reference pick-up antennas see the same signal strength, and of very high reliability because a large number of distributed transmitters is used, with built-in redundancy, so that only the local oscillators and driver amplifiers need to be made redundant. Current plans call for a structural integrity of the array aperture to within ±18 cm flatness. The phase at each subarray pick-up point is normalized with respect to a perfectly flat uniform aperture by means of a servo, as loop shown in Figure 3.1-51. For each subarray center location, a phase delay differential ("reference standard") is computed, which occurs for the two generating frequencies f_{R1} and f_{R2} if the receiving antenna is located on a perfect plane.

CONTENTS

Section Page

1.0 SCOPE/GENERAL REQUIREMENTS 1-1 1/B11
1.1 INTRODUCTION 1-1 1/B11
1.2 SATELLITE POWER SYSTEM CONCEPTS 1-3 1/B13
1.2.1 History of Study 1-3 1/B14
1.2.2 NASA Reference Satellite Concept 1-12 1/C9
1.2.3 Rockwell Alternative Satellite Concept (March 1979) 1-15 1/C12
1.2.4 Rockwell Reference Ground Receiving Station 1-17 1/C14
1.2.5 Rockwell Concept Approaches (June 1980) 1-17 1/C14
1.2.6 Satellite Concept Summaries 1-22 1/D6
1.3 TRANSPORTATION SYSTEM 1-34 1/E9
1.4 PROGRAM GROUND RULES 1-35 1/E10
2.0 SYSTEM DESCRIPTION 2-1 1/E11
2.1 GENERAL 2-1 1/E11
2.1.1 System 2-1 1/E11
2.2 SATELLITE 2-9 1/F7
2.2.1 Reference System Definition 2-9 1/F7
2.2.2 Magnetron System Definition 2-16 1/G1
2.2.3 Solid State System Concepts 2-16 1/G1
2.3 GROUND RECEIVING STATION 2-26 2/A3
2.3.1 Introduction 2-26 2/A3
2.3.2 Rectenna 2-28 2/A5
2.3.3 Power Distribution 2-28 2/A5
2.4 OPERATIONS AND MAINTENANCE 2-29 2/A6
2.4.1 Satellite Operations 2-29 2/A6
2.4.2 Satellite Maintenance 2-46 2/B9
2.5 MASS PROPERTIES 2-51 2/B14
3.0 SUBSYSTEMS 3-1 2/C2
3.1 SATELLITE 3-1 2/C2
3.1.1 Introduction 3-1 2/C2
3.1.2 Power Generation 3-2 2/C3
3.1.3 Power Distribution 3-30 2/E8
3.1.4 Microwave Power Transmission 3-41 2/F8
3.1.5 Structure 3-84 3/B12
3.1.6 Attitude Control and Stationkeeping Subsystem 3-101 3/D3
3.1.7 Thermal Control 3-112 3/D14
3.1.8 Communications and Data Management 3-131 3/F6
3.2 GROUND RECEIVING STATION 3-141 3/G7
3.2.1 Introduction 3-141 3/G7
3.2.2 Rectenna 3-141 3/G7
3.2.3 Power Distribution 3-150 4/A4
4.0 SUPPORT SYSTEMS 4-1 4/A5
4.1 GEO OPERATIONAL BASE 4-1 4/A5
4.2 MAINTENANCE AND REFURBISHMENT FACILITY 4-1 4/A5

Section Page

4.3 SPS TRANSPORTATION SYSTEM REQUIREMENTS (PRELIMINARY) . 4-1 **4/A5**
  4.3.1 Configuration and Mission Requirements . . 4-1 **4/A5**
  4.3.2 Heavy Launch Lift Vehicle(s) Requirements . . 4-2 **4/A6**
  4.3.3 Cargo Transfer Vehicle (COTV) 4-5 **4/A9**
  4.3.4 Personnel Orbital Transfer Vehicle (POTV) . . 4-6 **4/A10**
  4.3.5 Personnel Module (PM) 4-7 **4/A11**

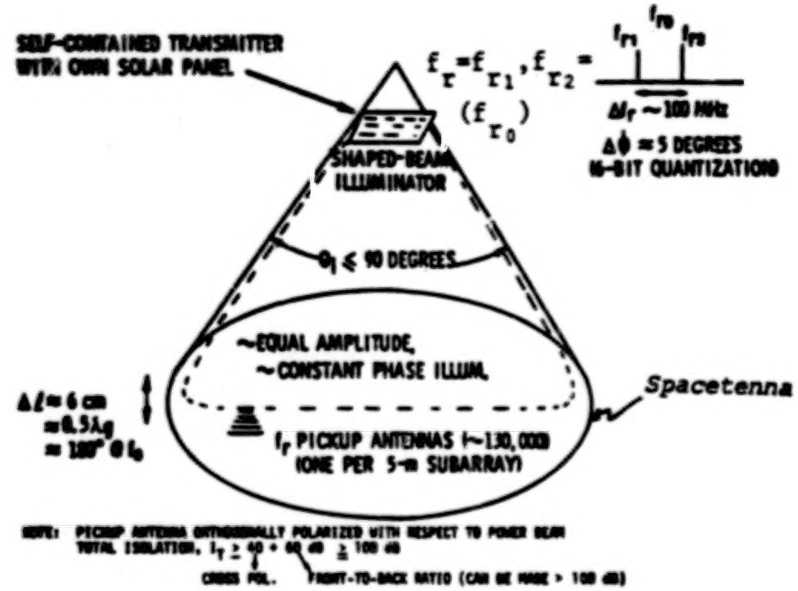
SELF-CONTAINED TRANSMITTER
WITH OWN SOLAR PANEL
$f_r = f_{r1}, f_{r2} =$
(f_{r0})
f_{r1}
f_{r0}
f_{r2}
$\Delta f_r \sim 100$ MHz
$\Delta\phi = 5$ DEGREES
6-BIT QUANTIZATION
SHAPED-BEAM
ILLUMINATOR
$\theta_1 \leq 90$ DEGREES
~EQUAL AMPLITUDE,
~CONSTANT PHASE ILLUM.
$\Delta\ell \approx 6$ cm
$\approx 0.5\lambda_g$
$\approx 180° @ f_0$
Spacetenna
f_r PICKUP ANTENNAS (~130,000)
(ONE PER 5-m SUBARRAY)
NOTE: PICKUP ANTENNA ORTHOGONALLY POLARIZED WITH RESPECT TO POWER BEAM
TOTAL ISOLATION, $I_T \geq 40 + 60$ dB ≥ 100 dB
CROSS POL.
FRONT-TO-BACK RATIO (CAN BE MADE > 100 dB)

Figure 3.1-50. Phase Reference Signal Distribution System

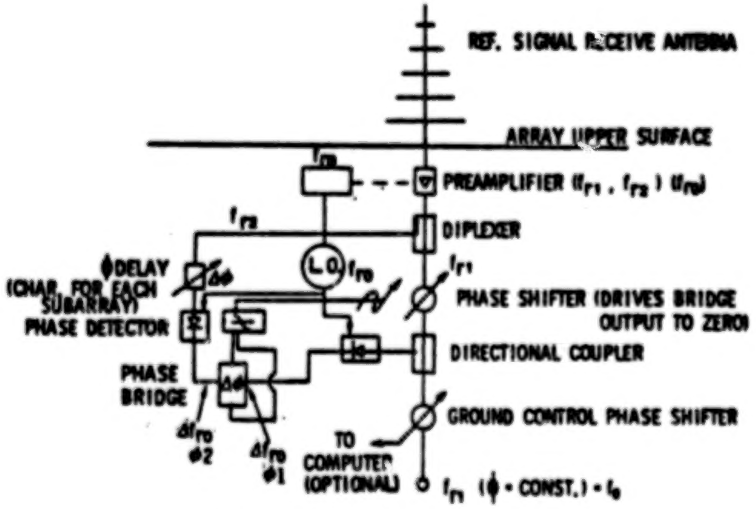
REF. SIGNAL RECEIVE ANTENNA
ARRAY UPPER SURFACE
f_{r0}
PREAMPLIFIER (f_{r1}, f_{r2}) (f_{r0})
f_{r2}
DIPLEXER
ϕDELAY
(CHAR. FOR EACH
SUBARRAY)
$\Delta\phi$
L.O.
f_{r0}
f_{r1}
PHASE SHIFTER (DRIVES BRIDGE
OUTPUT TO ZERO)
PHASE DETECTOR
DIRECTIONAL COUPLER
PHASE
BRIDGE
$\Delta\phi$
GROUND CONTROL PHASE SHIFTER
Δf_{r0}
$\phi 2$
Δf_{r0}
$\phi 1$
TO
COMPUTER
(OPTIONAL)
f_{r1} (ϕ = CONST.) = t_0

Figure 3.1-51. Reference Signal Control Loop

These delays can be calculated and tuned in the lab to fractions of a degree. The output of the phase bridge then drives a phase shifter until the path delay differential equals that of the reference standard. Since this circuit is used at every subarray, the subarray center points are electrically normalized to show $\phi = \phi_0$ constant across the entire array. This provides the conjugation circuit with the required reference phase.

The retrodirective control circuit which compensates for pilot-generated beam shifts (without ionospheric effects) shown in Figure 3.1-48 is a modified Chernoff circuit with additional isolation added by (1) separating the pilot and power frequency paths, (2) using orthogonally polarized radiating elements; and (3) providing the remaining isolation in separate bandpass filters. The total required filter isolation is 70 dB, according to pilot system calculations presented in Table 3.1-23.

Table 3.1-23. Pilot System Link Budget

•GROUND SIGNAL ERP	100 dBW	
•SPACE LOSS	-192 dB	
•POWER AT SPACETENNA	- 92 dBW	
•PILOT ANTENNA RECEIVE GAIN	80 dB	-74 dBW
•ISOLATION TO POWER DIPOLE	20 dB	(INCLUDES DIPOLE GAIN)
•POWER DIPOLE OUTPUT	-10 dBW	
•CROSS POLARIZATION ATTENUATION	30 dB	
•PILOT TO POWER SIGNAL RATIO	-34 dB	
•NOTCH FILTER ATTENUATION (RELATIVE TO TWO PILOT SIGNALS SYMMETRICAL TO CARRIER)	+70 dB	
•NET PILOT SIGNAL TO POWER SIGNAL RATIO	+36 dB	
•PILOT-TO-THERMAL NOISE RATIO (ASSUMING 3 dB NOISE FIGURE AND 3 dB NOTCH FILTER LOSS)	≈+37 dB	(THERMAL NOISE ≈-117 dBW FOR 500 MHz PILOT WIDTH)

The pilot system (ground) is based on having available at least 100 dBW pilot power. The proposed implementation of this pilot system consists of a circular array (one or more rings) of low to medium-gain elements placed at the periphery of the rectenna, on top of utility poles if necessary to avoid interference from the power collection and transmission system. The characteristics of this pilot transmit system are summarized in Table 3.1-24 and the pilot array layout is compared with a dish type in Figure 3.1-52.

Table 3.1-24. Pilot Ground System Summary

- CIRCULAR ARRAY OF LOW-GAIN ELEMENTS AT 3.14 METER (≈25 λ) SPACING; ELEMENTS FED IN PHASE
- 10,000 PILOT ARRAY ELEMENTS OF 10 dB GAIN EACH
- MINIMUM 50 dB ARRAY GAIN
- 10 WATT SOLID-STATE TRANSMITTER AT EACH ELEMENT
- PHASE DISTRIBUTION USING FIBER OPTICS
- BEAM STEERED TO SATELLITE LOCATION BY TIME DELAY COMPENSATION AT EACH ELEMENT
- TOTAL ERP: 100 dBW

The system provides vastly improved reliability over a single-dish concentrated amplifier pilot system, and also has such a wide beamwidth when the beam enters the ionosphere that certain ionospheric effects will be mitigated.

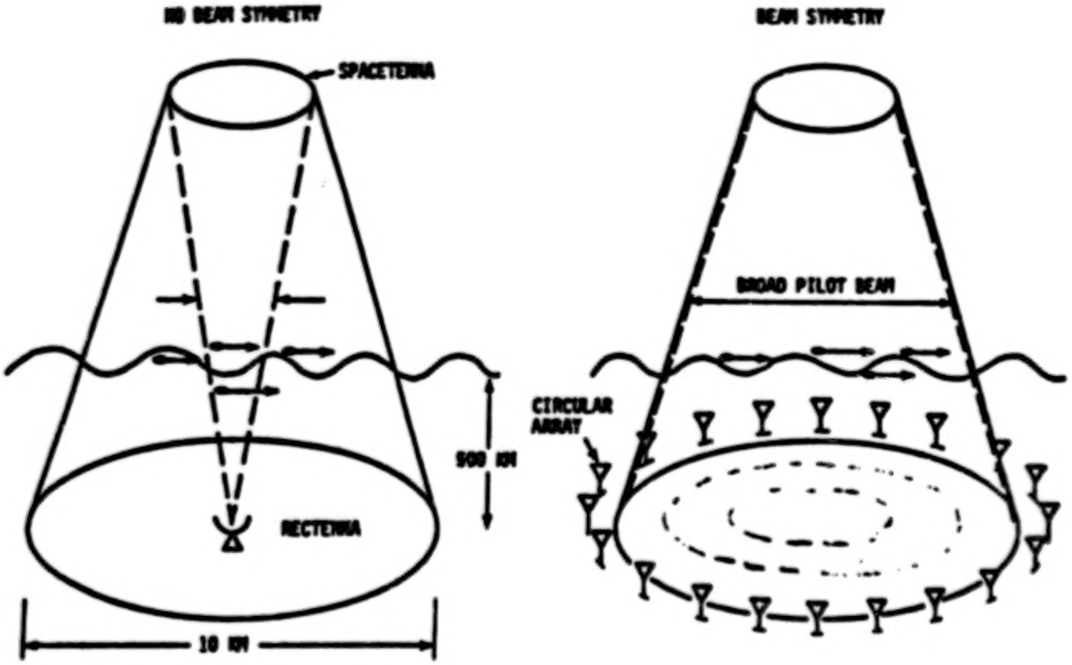

Figure 3.1-52. Pilot Beam Ground System Layout

It must be noted that neither the exact design of the ground pilot array, nor that of the on-board pilot receiver antenna is available at this point.

Mass Properties

The mass properties of the end-mounted space antenna MPTS system is summarized in Table 3.1-25.

Table 3.1-25. Mass Properties—Solid-State End-Mounted MW Electronics (Dual)

SUBARRAY	10.561
THERMAL	NONE
ANTENNA CONTROL	0.340
TOTAL	10.901×10^6 kg

Solid-State "Sandwich" Configuration

A number of "sandwich" concepts have been investigated in order to find the solution best suited for the overall goal, i.e., minimum life cycle cost of energy. The major alternative configurations are summarized in Figure 3.1-53. The one presently favored because of less overall volume and best control features, is similar to concept number 5, although with only two transmitting antenna. This approach is based upon attaching two concept 2 type configurations into a rigid configuration thus sharing a common location in GEO

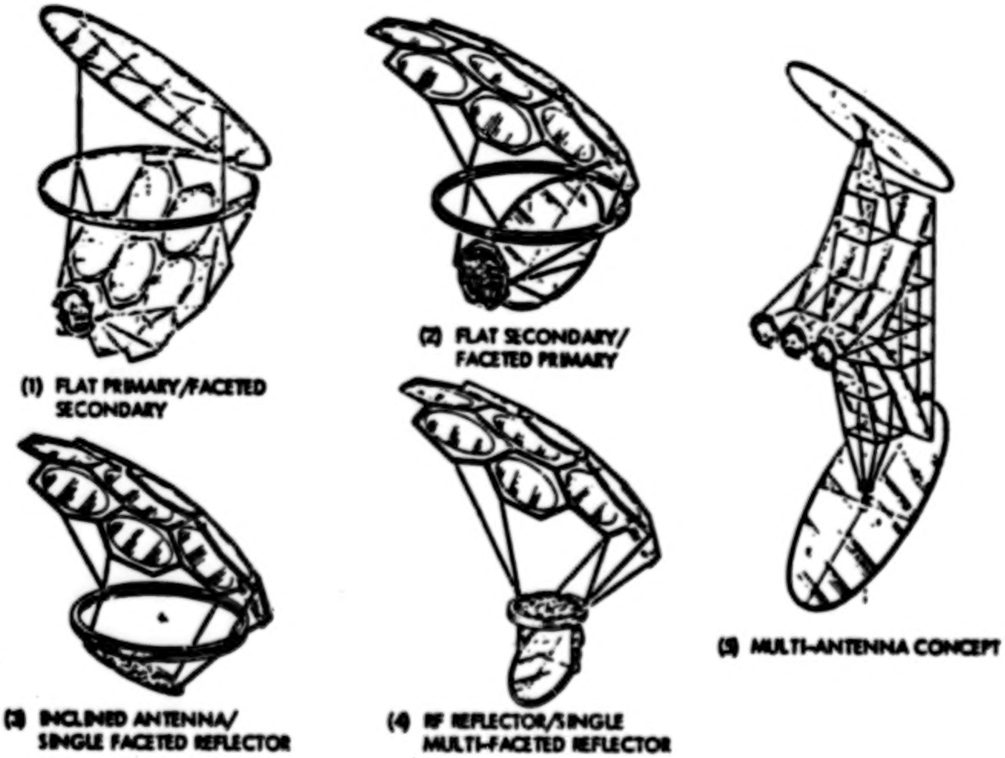

(1) FLAT PRIMARY/FACETED SECONDARY

(2) FLAT SECONDARY/ FACETED PRIMARY

(3) INCLINED ANTENNA/ SINGLE FACETED REFLECTOR

(4) RF REFLECTOR/SINGLE MULTI-FACETED REFLECTOR

(5) MULTI-ANTENNA CONCEPT

Figure 3.1-53. Alternative Solid State Sandwich Concepts

(Figure 3.1-54). The "sandwich" microwave antenna arrays were assumed to be identical for all of the various configurations shown in Figure 3.1-53.

The use of low level solid-state microwave power amplifiers also led to a re-examination of the microwave antenna illumination pattern or taper. Unlike the reference concept, where very high power sources (~50 kW) are used, and a sloping taper is a natural feature (in addition to the high beam efficiency affected by such a taper), in the case of a solid-state sandwich the main idea is to have as large a number of identical components as possible, and to minimize the size of the space segment at the same time. A comparison of a 10 dB (Gaussian) and zero dB (uniform) taper is thus in order. For the latter, of course, all amplifiers carry the same power level, and the spacetenna diameter is a minimum for a given beam width. As a first-order comparison, Table 3.1-26 shows the salient features of a typical 0-dB sandwich with a 10 dB-tapered-sandwich. (Multi-bandgap solar cells are assumed, in this study summary, but the chart is for comparison purposes only.) The rectenna size was increased somewhat, but the space segment drives the total system cost, resulting in a substantially higher total installation cost for the 10 dB taper. Table 3.1-27 compares the characteristic of a standard GaAs based sandwich with a multi-bandgap cell alternative.

System

The selected GaAs sandwich concept has the nominal characteristics described in Table 3.1-28 with a final $CR_e = 5.2$.

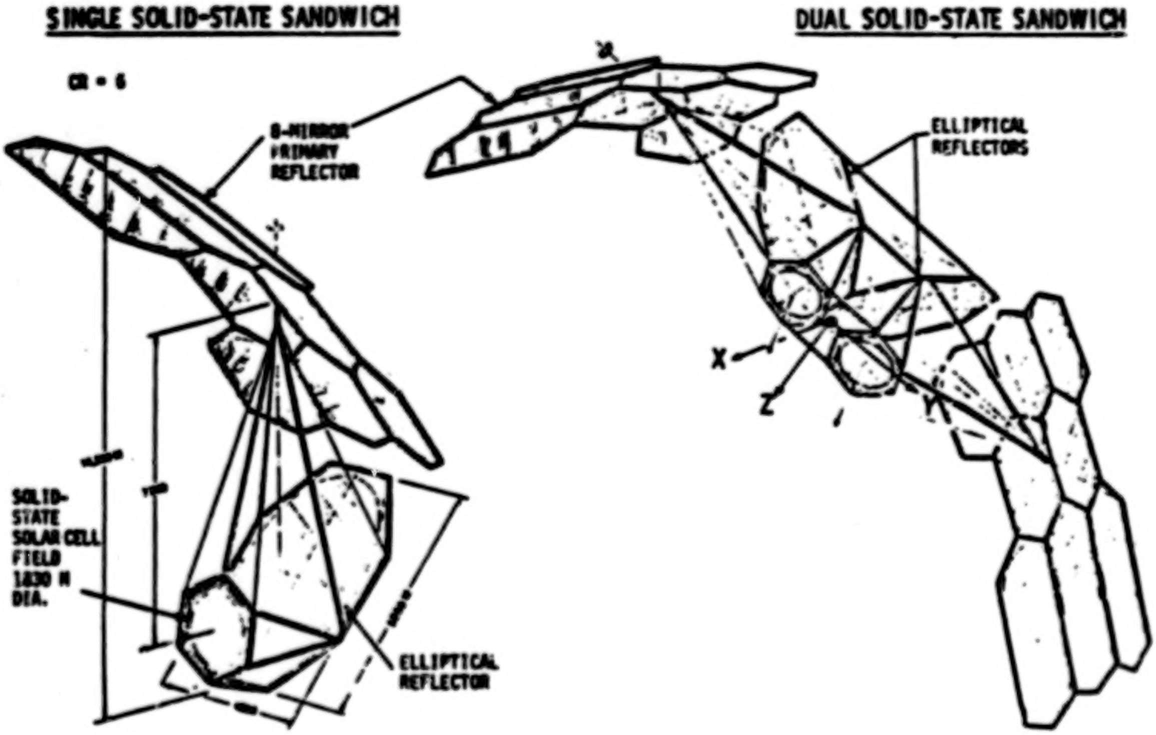
SINGLE SOLID-STATE SANDWICH
CR = 6
8-MIRROR PRIMARY REFLECTOR
SOLID-STATE SOLAR CELL FIELD 1830 M DIA.
ELLIPTICAL REFLECTOR
DUAL SOLID-STATE SANDWICH
ELLIPTICAL REFLECTORS
X
Y
Z

Figure 3.1-54. Solid State Sandwich Concepts

Table 3.1-26. Solid State Sandwich Concept
Comparison of 0 dB and 10 dB Antenna Power Taper

	0 dB	10 dB
TYPE OF SOLAR ARRAY	MBG	MBG
MAXIMUM EFFECTIVE CONCENTRATION RATIO	6.0	6.0
AMPLIFIER EFFICIENCY	0.8	0.8
MAX. ANTENNA POWER DENSITY (W/m^2)	1,235	1,235
ANTENNA DIAMETER (km)	1.578	2,049
TOTAL TRANSMITTED POWER (GW)	2.418	1.588
POWER AT UTILITY INTERFACE (GW)	1.591	1.127
RECTENNA BORESIGHT DIAMETER (km)	5.600	4.929
TOTAL SATELLITE MASS (10^6 kg)	10.13	13.30
COST DATA(\$$\overline{B}$)		
• SATELLITE	0.796	0.963
• CONSTRUCTION OPERATIONS	0.079	0.096
• TRANSPORTATION	0.598	0.798
• RECTENNA	0.985	0.763
• TOTAL COST (INCL. MGMT & CONTINGENCY)	2.789	3.030
INSTALLATION COST (\$/kW)$_{UI}$	1,759	2,689

Table 3.1-27. Recommended Solid-State Sandwich Concept Characteristics

CHARACTERISTIC	SECONDARY	PRIMARY
SOLAR ARRAY TYPE	MULTI-BANDGAP	GaAs
EFFECTIVE CR	5.2	5.2
SOLAR ARRAY TEMPERATURE (°C)	200	200
AMPLIFIER BASE TEMPERATURE (°C)	125	125
AMPLIFIER EFFICIENCY	0.8	0.8
ANTENNA TAPER RATIO (dB)	0	0
ANTENNA DIAMETER (km)	1.63	1.83
POWER AT UTILITY INTERFACE (GW)	1.53	1.21
RECTENNA BORESIGHT DIAMETER (km)	5.5	4.87

Table 3.1-28. Nominal Characteristics of Sandwich Concept

	GaAs	GaAlAs/GaAs
UNIFORM ILLUMINATION EFFECTIVE (CR_e)	5.2	5.2
SOLAR TEMPERATURE	200°C	200°C
SOLAR CELL EFFICIENCY	0.1566	0.2506
AMPLIFIER EFFICIENCY	0.8	0.8
AMPLIFIER BASE TEMPERATURE	125°C	125°C
ANTENNA OHMIC EFFICIENCY	0.96	0.96
SOLAR CELL PACKAGING FACTORS	0.8547	0.8547
POWER TRANSMITTED/UNIT AREA	695.8 W/m^2	1110 W/m^2
ANTENNA DIAMETER	1.83 km	1.63 km
ANTENNA AREA	2.63 km^2	2.09 km^2
TOTAL TRANSMITTED POWER	1.83 GW	2.32 GW
POWER AT UTILITY INTERFACE	1.21 GW	1.53 GW
RECTENNA DIA. (MINOR AXIS)	4.87 km	5.47 km
RECTENNA AREA	24.85 km^2	31.37 km^2

The preliminary mass properties of such a system are summarized in Table 3.1-29. It should be noted that, higher amplifier base temperatures are permitted(125° versus 100°) in the sandwich concept, because the amplifiers in the sandwich are relatively small (6 to 5 W), and can be cooled by their own beryllium oxide radiator discs, whereas the end-mounted array amplifiers use high power levels in the center of the array (in analogy with the reference system) and hence have a rely on cooling by the array surface itself. The temperature gradient between the amplifier base and the critical part (the actual junction or channel) can be expected to be larger for the high-power-density end-mounted amplifier designs.

Table 3.1-29. Preliminary Mass Properties of Recommended Solid-State Sandwich Concept (CRg = 5.2)

Subsystem (10^6 kg)	GaAs	GaAlAs/GaAs
Primary and secondary structure	4.168	3.079
Microwave array and solar cells	9.161	7.393
Reflectors	2.075	1.646
Support subsystems	1.019	0.991
25% contingency	4.106	3.277
TOTAL	20.529	16.386

Detailed sections of the point design sandwich antenna dipole configuration is shown in Figure 3.1-55 through 3.1-58. Figure 3.1-55 shows the sandwich solar cell configuration. Each dipole amplifier requires +10 V dc and a -4 V dc bias. The solar array is configured with 18 cells in series to provide the +10 V and a specially designed end group of cells with 7 cells in series to provide the -4 V bias. The power required by the dipole amplifier is matched to that available from the solar cells, i.e., the RF beam has a uniform distribution and each 7.81×7.81 cm solar cell patch supports a single dedicated dipole. The sandwich antenna/solar cell panel configuration is shown in Figure 3.1-56. This shows the dipoles located on 7.81 cm centers and a typical configuration of dipoles being a subarrays of 5×5 m with 4096 dipoles per subarray. Each dipole subassembly includes a power amplifier and berlox radiator. An exploded view of the antenna/solar cell panel configuration is shown in Figure 3.1-57. This shows riser assembly, structure and solar cells with power distribution +10 V lead strips and -4 V leads feeding into dc power strips. A prefabricated honeycomb section and an open truss structure provide the necessary structural stiffness. The open truss provides requires spacing and allows good heat transfer (heat leak) through the cross section. A stripline corporate feed system layout is shown in Figure 3.1-58.

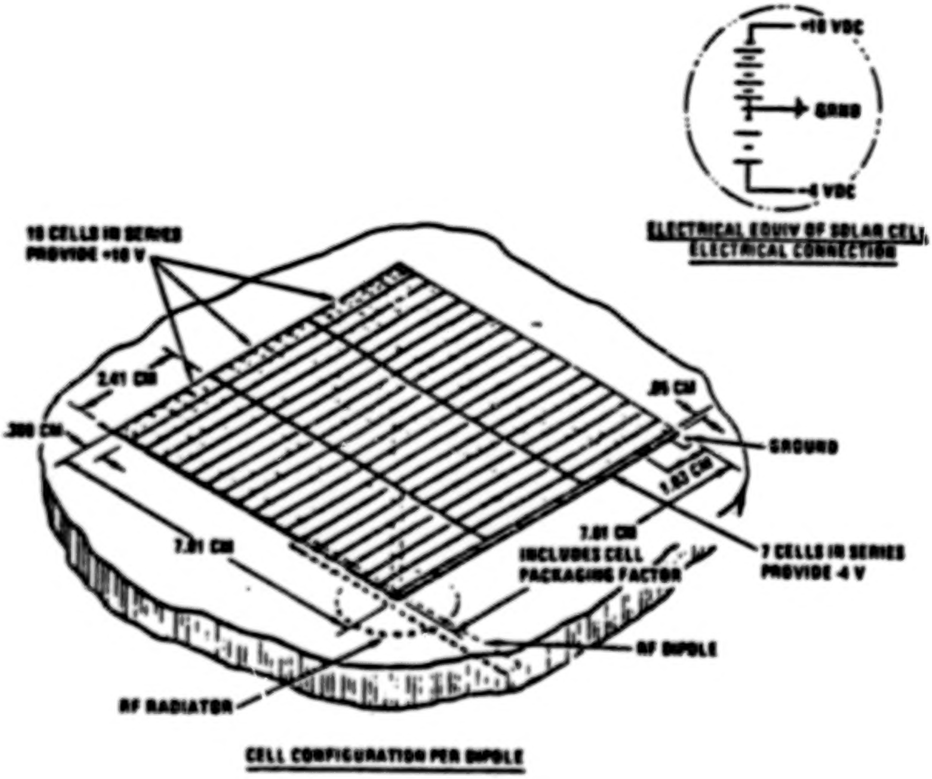
+10 VDC
GRND
-4 VDC
ELECTRICAL EQUIV OF SOLAR CELL, ELECTRICAL CONNECTION
10 CELLS IN SERIES PROVIDE +10 V
2.01 CM
.300 CM
.05 CM
GROUND
7.01 CM
7.01 CM INCLUDES CELL PACKAGING FACTOR
7 CELLS IN SERIES PROVIDE -4 V
RF DIPOLE
RF RADIATOR
CELL CONFIGURATION PER DIPOLE

Figure 3.1-55. Satellite Sandwich Solar Cell Configuration (Preliminary)

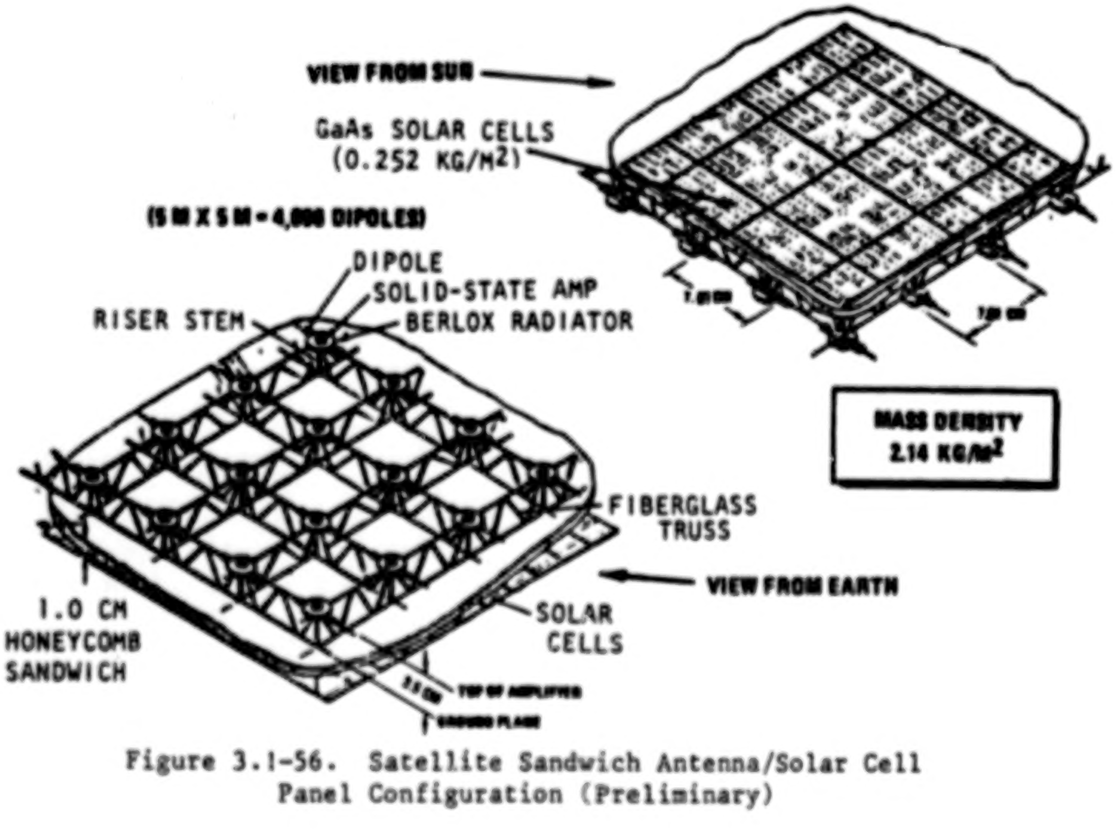
VIEW FROM SUN
GaAs SOLAR CELLS (0.252 KG/M²)
(5 M X 5 M = 4,000 DIPOLES)
DIPOLE
SOLID-STATE AMP
RISER STEM
BERLOX RADIATOR
7.01 CM
7.01 CM
MASS DENSITY 2.14 KG/M²
FIBERGLASS TRUSS
VIEW FROM EARTH
1.0 CM HONEYCOMB SANDWICH
SOLAR CELLS
TOP OF AMPLIFIER
GROUND PLANE

Figure 3.1-56. Satellite Sandwich Antenna/Solar Cell Panel Configuration (Preliminary)

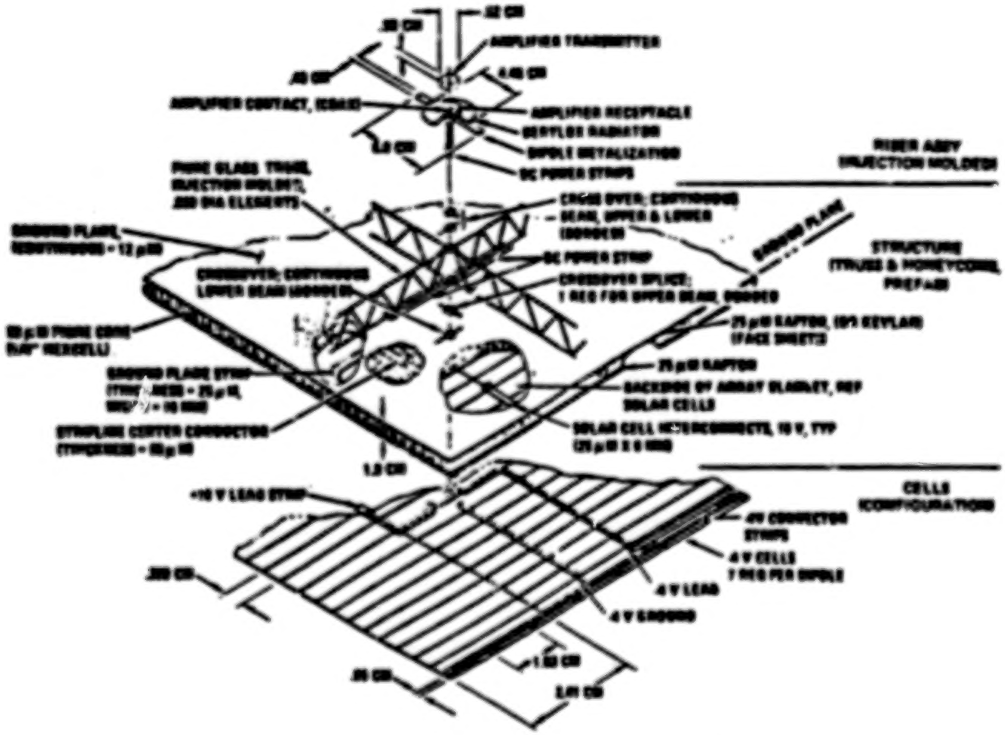
.12 CM
.30 CM
AMPLIFIER TRANSMITTER
4.40 CM
.30 CM
AMPLIFIER CONTACT, (COAX)
AMPLIFIER RECEPTACLE
BERYLOX RADIATOR
DIPOLE METALIZATION
DC POWER STRIPS
FIBER ASSY (INJECTION MOLDED)
FIBRE GLASS TRUSS, (INJECTION MOLDED), .330 DIA ELEMENTS
CROSS OVER; CONTINUOUS BEAM, UPPER & LOWER (BONDED)
GROUND PLANE
STRUCTURE (TRUSS & HONEYCOMB, PREFAB)
GROUND PLANE, (CONTINUOUS) - 12 µM
CROSSOVER; CONTINUOUS LOWER BEAM (BONDED)
DC POWER STRIP
CROSSOVER SPLICE; 1 REQ FOR UPPER BEAM, BONDED
25 µM KAPTON, (OR KEVLAR) (FACE SHEETS)
25 µM KAPTON
GROUND PLANE STRIP
BACKSIDE OF ARRAY BLANKET, REF SOLAR CELLS
STRIPLINE CENTER CONDUCTOR
SOLAR CELL INTERCONNECTS, 10 V, TYP
1.0 CM
CELLS (CONFIGURATION)
+10 V LEAD STRIP
4V CONNECTOR STRIPS
4 V CELLS 1 REQ PER DIPOLE
4 V LEAD
4 V GROUND
.300 CM
1.50 CM
.30 CM
3.01 CM

Figure 3.1-57. Dual Satellite Antenna/Solar Cell Panel Configuration Exploded View

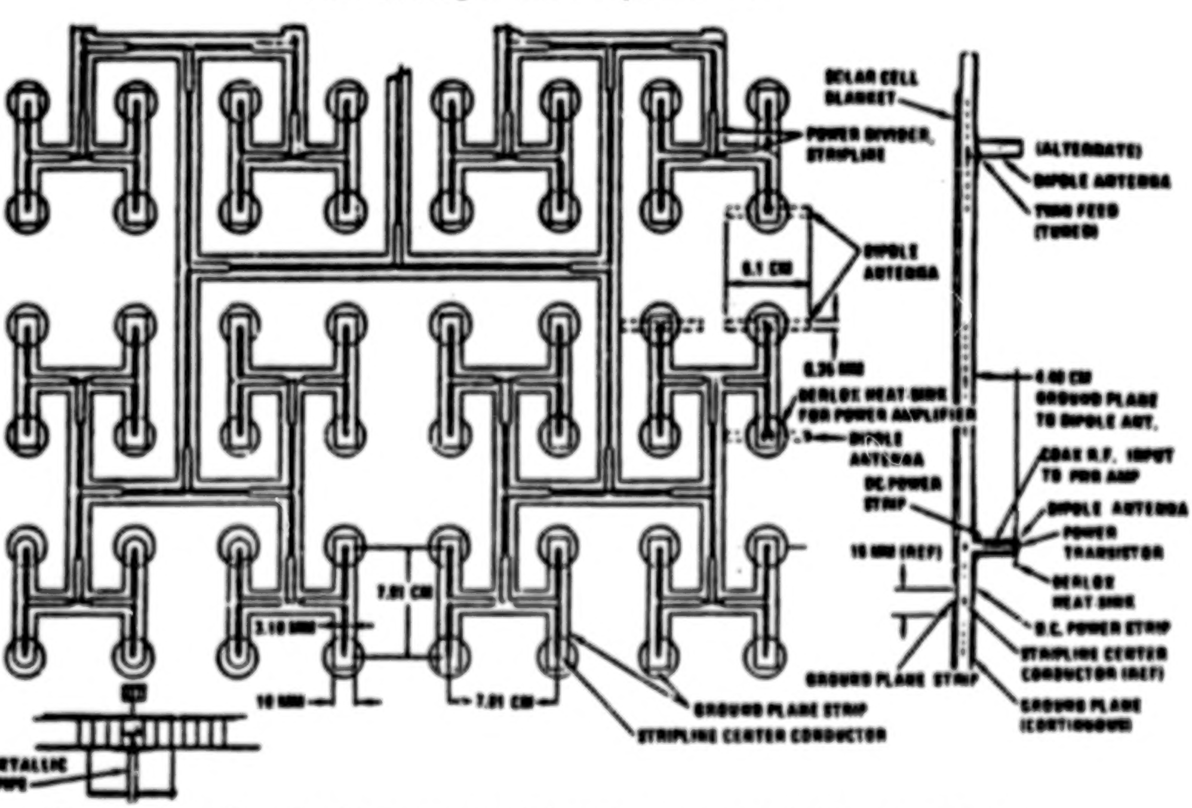
SOLAR CELL BLANKET
POWER DIVIDER, STRIPLINE
(ALTERNATE)
DIPOLE ANTENNA
TWIN FEED (TUNED)
DIPOLE ANTENNA
6.1 CM
6.35 MM
4.40 CM GROUND PLANE TO DIPOLE ANT.
BERLOX HEAT SINK FOR POWER AMPLIFIER
DIPOLE ANTENNA
COAX R.F. INPUT TO PWR AMP
DC POWER STRIP
DIPOLE ANTENNA
POWER TRANSISTOR
10 MM (REF)
BERLOX HEAT SINK
D.C. POWER STRIP
STRIPLINE CENTER CONDUCTOR (REF)
GROUND PLANE STRIP
GROUND PLANE (CONTINUOUS)
7.01 CM
3.10 MM
10 MM
7.01 CM
GROUND PLANE STRIP
STRIPLINE CENTER CONDUCTOR
NON-METALLIC HEAT PIPE

Figure 3.1-58. Solid State Sandwich Concept—Stripline Corporate Feed System (Partial) (Preliminary)

MICROFILMED FROM
BEST AVAILABLE COPY

Reference Phase Distribution

The reference phase distribution concept proposed for the sandwich configuration is identical to that discussed in the section dealing with the end-mounted solid state antenna.

Magnetron-Powered SPS Antenna

Cross-field tubes have long been considered potential candidates for use as dc to RF conversion devices in the SPS system. Indeed, early studies, circa 1969, pre-supposed the use of the amplitron tube, chiefly because of its high conversion efficiency. However, perhaps because of its low gain (5 to 10 dB) and reputation for having a noisy output spectrum, the amplitron lost out to the linear beam klystron, despite the latter's lower efficiency.

In 1978, Brown (see Volume II for full study discussion) made two discoveries that catapulted the crossed-field device back into contention for SPS use. He found that noise in the output spectrum of a conventional microwave oven magnetron was dramatically reduced when the tube was operated with no cathode heater power, its emission temperature being maintained only by back bombardment of electrons in the tube. The other finding was that, under these circumstances, the low cathode temperature could be expected to lead to a cathode lifetime of many tens of years.

Injection Locked Magnetron Amplifier

The conventional magnetron is a single port device which normally functions as a free-running oscillator at a frequency determined by anode voltage, magnetic field and RF load reflection coefficient. Because all power converter devices used in the SPS antenna array must operate at exactly the same frequency with precisely controlled output phases, a free-running oscillator cannot be used as such. What is needed, of course, is a two-port amplifying device to which a master control signal can be applied so that all the devices may be slaved to a single reference. There are two principal ways in which a one-port device may be converted to a two-port. In the case of the magnetron, both of these techniques make use of the fact that the magnetron cannot distinguish between an applied input signal and a reflection of its own output from a load impedance.

Basic Power Module and Subarray Design

The two-magnetron technique with 3 dB hybrid combiner has been selected for implementation. There are numerous types of 3 dB hybrid in waveguide, coaxial and strip transmission line forms. For SPS purposes a waveguide form is preferred because of its compatibility with a slotted waveguide radiator. The two basic waveguide forms are the magic-Tee, which requires internal matching ports and irises, and the short-slot coupler which needs no tuning devices and has a very compact form. There are two variants of this latter hybrid device, one called a top-wall coupler, the other a side-wall coupler. It is the sidewall coupler which has been chosen for this application since it is structurally the most compatible with a slotted waveguide planar array.

The basic building blocks for constructing the very large space antenna are power modules comprising a slotted waveguide planar array excited by one or more pairs of magnetrons whose outputs are combined in a 3 dB short-slot, side-wall coupler and fed to a short length of waveguide feed line. Alternatively it may be a Resonant Cavity Radiator (RCR) as described in previous Rockwell reports, and also at the January 1980 Microwave Workshop at JSC. The RCR has been chosen as the basic radiating element because of its lesser mass and lower ohmic loss, both of which result from the elimination of internal common waveguide walls.

Nine different power module configurations, having different dimensions and/or numbers of magnetrons, have been designed in such a way that standard subarrays, all square and having identical dimensions, can be formed from the power modules of any one of the nine different types. As a result, the complete spacetenna can be built from these standard size subarrays and since there are nine types of subarrays, differing only in numbers of magnetron tubes, it is possible to create a nine-step approximation to any desired power distribution across the array aperture. It is emphasized that all magnetrons, wherever used in the array, are identical and have the same power output levels. The change in power density across the array is created by the varying numbers of tubes associated with each of the nine types of subarrays.

High Power Density Module, Type 1

Highest RF power density occurs at the array center, consequently the power module for this region will require the greatest number of magnetron tubes per unit area. A design for this module, which will be termed a type 1 power module, is shown in Figure 3.1-59. Its aluminum RCR has 8×8 = 64 slots and dimensions of 8 by 8.65 cm = 69.2 cm^2. A symmetrical arrangement of two pairs of magnetrons is used which maximizes the surface area of the pyrolytic graphite heat radiating discs which are attached to each magnetron. These discs are made as large in diameter as possible, so that adjacent discs touch one another, in order to dissipate as much waste heat as possible from each tube. A thermal analysis, to be discussed in Section 3.1.7, has shown that each magnetron may then operate at a 3.5 kW RF output level, if its dc to RF conversion efficiency is 90%. The area of this RCR's radiating surface is $(0.692)^2 = 0.479$ m so that with four 3.5-kW tubes, the radiated RF power density is theoretically 29.2 kW/m^2.

The two short slot hybrid couplers and feed waveguides are also constructed of aluminum whose internal dimensions are $a = 8.65$ cm, $b = 2.0$ cm. Aluminum wall thickness is 0.25 mm (.010 in) for the RCR, hybrid couplers and feed guides. Figure 3.1-60 is a schematic sectional view through the power module which indicates the locations of the radiating slots in the lower face of the RCR and the coupling slots in the upper face of the RCR which forms a common wall with the feed waveguides. The radiating slots are displaced, longitudinal, shunt elements in which slot displacements are staggered alternately across the center lines in order to obtain successive phase shifts of π radians from slot to slot. Coupled with the π radians shift due to the $\lambda g/2$ spacing, this means that all slots are in phase and the RCR radiates a broadside beam. The feed, or coupling slots, are inclined series elements in the broad wall of the feed waveguide. The total of six coupling slots, located as shown, are sufficient to ensure that only the desired $TE_{8,8,0}$ cavity mode is excited within the RCR.

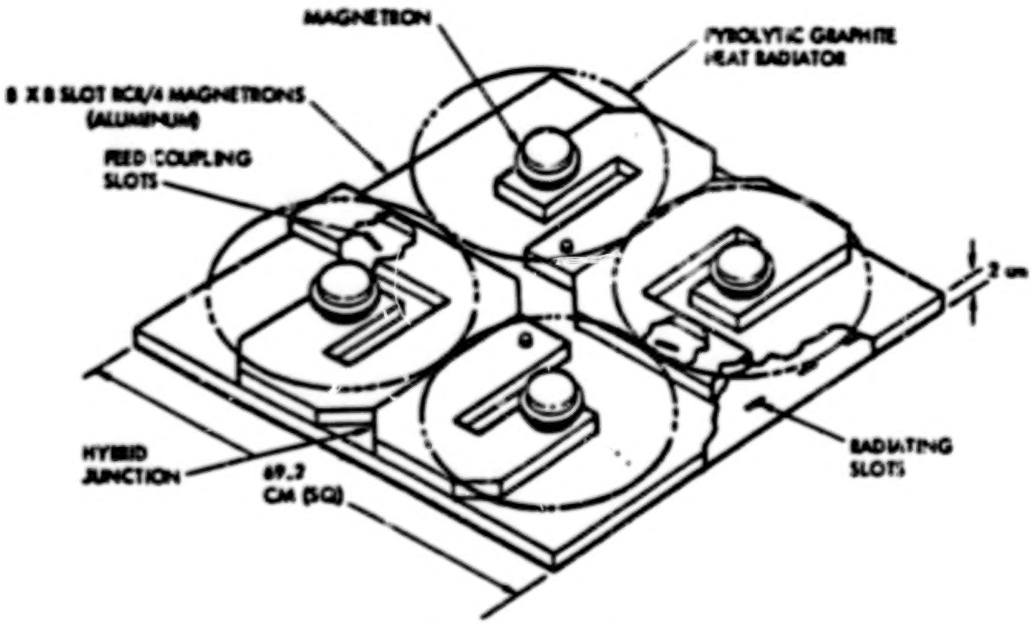
MAGNETRON
PYROLYTIC GRAPHITE HEAT RADIATOR
8 X 8 SLOT RCR/4 MAGNETRONS (ALUMINUM)
FEED COUPLING SLOTS
2 cm
HYBRID JUNCTION
69.2 CM (SQ)
RADIATING SLOTS

Figure 3.1-59. High Power Density Power Module for Array Center

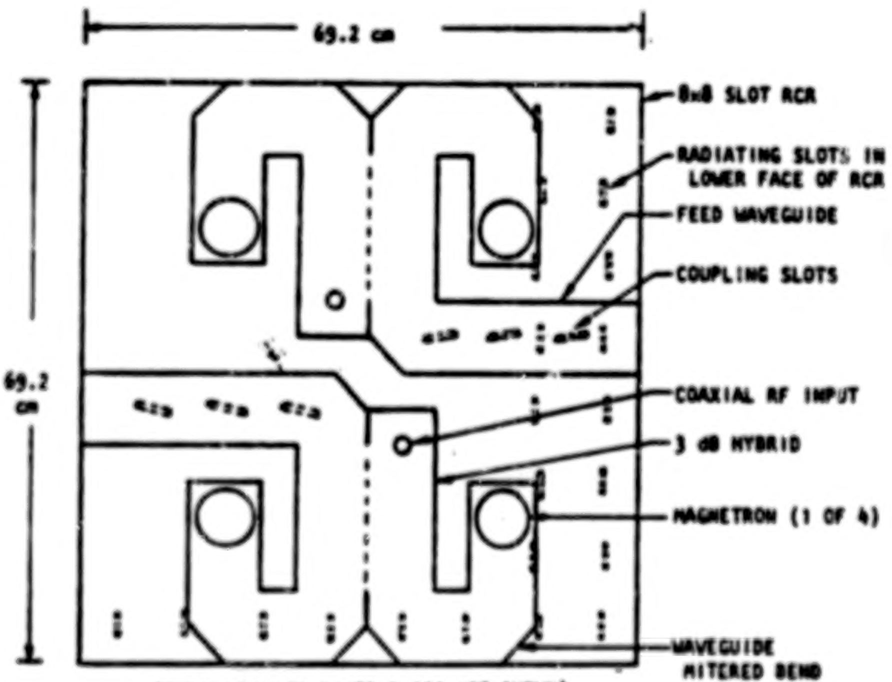
69.2 cm
69.2 cm
8x8 SLOT RCR
RADIATING SLOTS IN LOWER FACE OF RCR
FEED WAVEGUIDE
COUPLING SLOTS
COAXIAL RF INPUT
3 dB HYBRID
MAGNETRON (1 OF 4)
WAVEGUIDE MITERED BEND

(PYROLYTIC GRAPHITE DISCS NOT SHOWN)

Figure 3.1-60. Sectional View of Type 1 High Power Density Module

The magnetron tubes, to be described later, are coupled into the hybrid waveguide arms by means of coaxial probes. The reference (excitation signals to the hybrid input arms are also probe coupled through small coaxial connectors.

Lower Density Power Modules, Types 2 to 9

If the size of the 8×8 slot RCR shown in Figure 3.1-60 is increased to 8×12 slots and the same 4-magnetron excitation arrangement is used, the power module dimensions now become 69.2×103.8×2.0 cm. The separation between magnetron pairs will increase due to the increase from 69.2 to 103.8 cm in the one dimension. This type 2 module has an area of 0.718 m^2 and a theoretical power density of 19.5 kW/m^2.

A type 3 module is shown in Figure 3.1-61. In this case the 8×8 slot RCR is the same as that for the type 1 module, but only one pair of magnetrons is used for excitation, leading to a theoretical power density of one-half that of type 1, i.e., 14.6 kW/m . The feed waveguide now extends fully across the width of the RCR and has seven inclined coupling slots. The output of the hybrid combiner is fed to the feed waveguide by means of an H-plane T-junction.

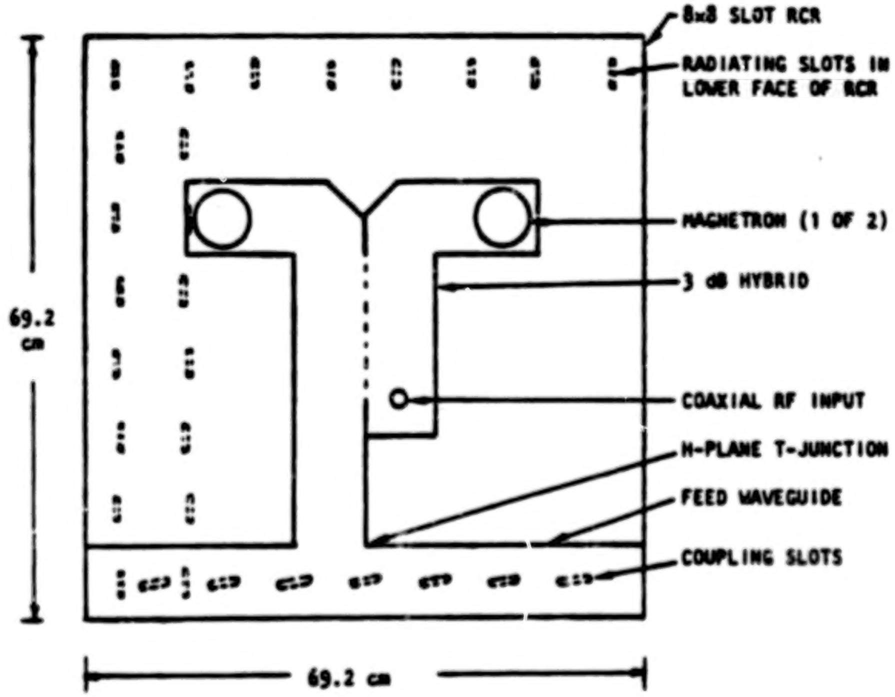
8x8 SLOT RCR
RADIATING SLOTS IN LOWER FACE OF RCR
MAGNETRON (1 OF 2)
3 dB HYBRID
COAXIAL RF INPUT
H-PLANE T-JUNCTION
FEED WAVEGUIDE
COUPLING SLOTS
69.2 cm
69.2 cm

(PYROLYTIC GRAPHITE DISCS NOT SHOWN)

Figure 3.1-61. Type 3, Lower Power Density Module

Type 4 to type 9 power modules all have a feed arrangement similar to that of type 3 and utilize only a single pair of magnetrons. The RCR dimensions, however, become progressively larger and therefore RF power density becomes progressively lower in going from type 4 to type 9.

Subarray Design

Corresponding to the nine different power modules there are nine standard subarrays, also designated types 1 to 9. These standard subarrays are all square, with identical dimensions, and differ only in numbers of tubes and therefore in power density levels. The way in which these subarrays are constructed from the various power modules is indicated in Table 3.1-30. The first column shows module dimensions (to nearest cm) and number of tubes. The second and third columns give the module type number and slot configuration. Column 5 indicates the number and arrangement of modules used to form a subarray of a given type. Column 5 lists the total number of magnetron tubes in the subarray. Since all subarrays have the same area, the number of tubes is proportional to the RF power density, and this relative level, in dB, is shown in the last column of the table.

Table 3.1-30. Nine Basic Power Module/Panel Configurations

MODULE CONFIGURATION, DIMENSIONS IN cm AND NO. OF TUBES	MODULE OR SUBARRAY TYPE NO.	NO. OF SLOTS PER MODULE	NO. OF MODULES PER SUBARRAY	NO. OF TUBES PER SUBARRAY	RELATIVE RF POWER DENSITY IN dB
69 4 69	1	8x8	6x6	144	0
69 4 104	2	8x12	6x4	96	-1.76
69 2 69	3	8x8	6x6	72	-3.01
69 2 104	4	8x12	6x4	48	-4.77
69 2 138	5	8x16	6x3	36	-6.02
104 2 104	6	12x12	4x4	32	-6.53
104 2 138	7	12x16	4x3	24	-7.78
138 2 138	8	16x16	3x3	18	-9.03
104 2 208	9	12x24	2x4	16	-9.54

Every subarray has 48x48 = 2304 slots and, if its component power modules were tightly packed, would have dimensions of 48x8.65 = 415.2 cm per side (neglecting RCR wall thicknesses). Some kind of mounting frame, however, is required in order to assemble and hold together the various RCR's which make up a subarray. The frame members will therefore force some separation between modules, so that overall subarray dimensions must be increased. For this reason a standard subarray size of 4.2 m^2 has been adopted. For the type 1 subarray the effective power density is then slightly reduced and, when rounded-off, becomes 28 kW/m^2. The gaps between adjacent power modules will vary from nearly 1 cm in a type 1 subarray to a maximum of about 2.5 cm in a type 9 subarray. This is not enough to cause a serious grating lobe problem.

Two examples of subarray formation are shown in Figure 3.1-62. The one at the left uses 16 modules of type 6 to form a complete type 6 subarray. The one at the right utilizes 8 type 9 modules arranged to fit into a standard subarray of type 9. At the center of each subarray a solid state amplifier is located which feeds the master phase reference signal through a corporate distribution network of coaxial cables (shown in dashed line) to the solid-state driver power amplifiers associated with each of the power modules.

Solid-state driver amplifiers, about which more will be said in the section on magnetron tube description, will be located in the gaps between adjacent RCR's and these spaces will also be utilized for location of pilot tone receiving antennas and amplifiers.

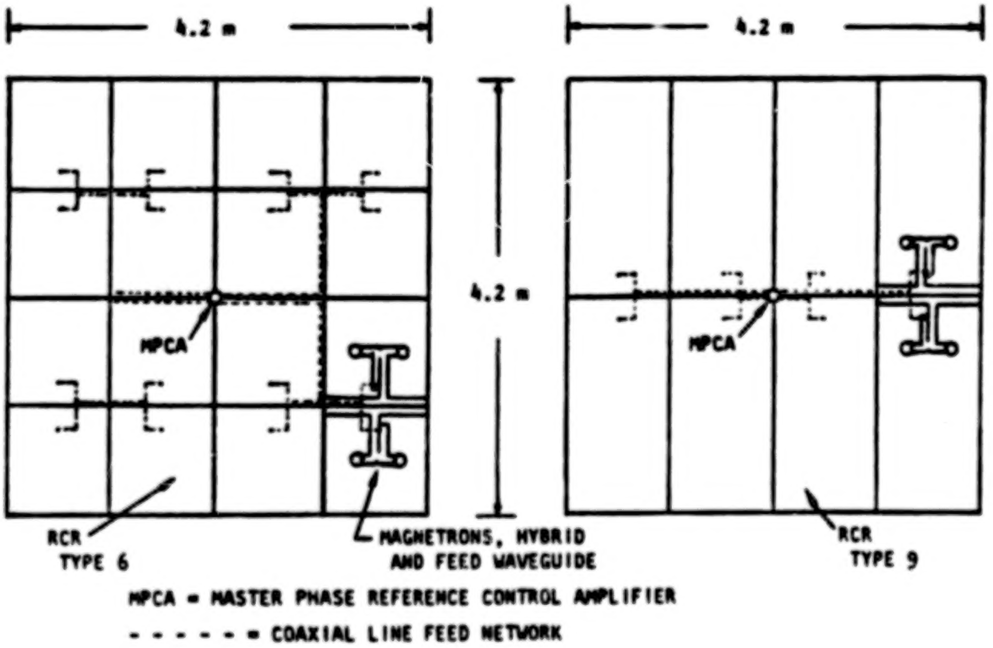
4.2 m
4.2 m
4.2 m
MPCA
MPCA
RCR
TYPE 6
MAGNETRONS, HYBRID
AND FEED WAVEGUIDE
RCR
TYPE 9
MPCA = MASTER PHASE REFERENCE CONTROL AMPLIFIER
- - - - - - = COAXIAL LINE FEED NETWORK

Figure 3.1-62. Two Examples of Subarray Formation
(Type 6 at Left, Type 9 at Right)

Nine-Step, -9.54 dB Aperture Distribution

During the analysis a comparison between Gaussian and Hansen aperture distributions, both truncated at -9.54 dB, revealed a slight superiority for the latter in terms of ability to radiate more total power. For this reason a 9-step approximation to the Hansen distribution has been chosen and is shown in Figure 3.1-63. The power densities at each level are, of course, those given in the last column of Table 3.1-30. The normalized radii at which the step changes occur are indicated on the figure. They have been chosen in such a way as to make the aperture power coefficient K the same for the stepped approximation as for the smooth Hansen curve, namely 0.436. Radiation pattern characteristics and microwave system performance resulting from this choice will be discussed in a later section.

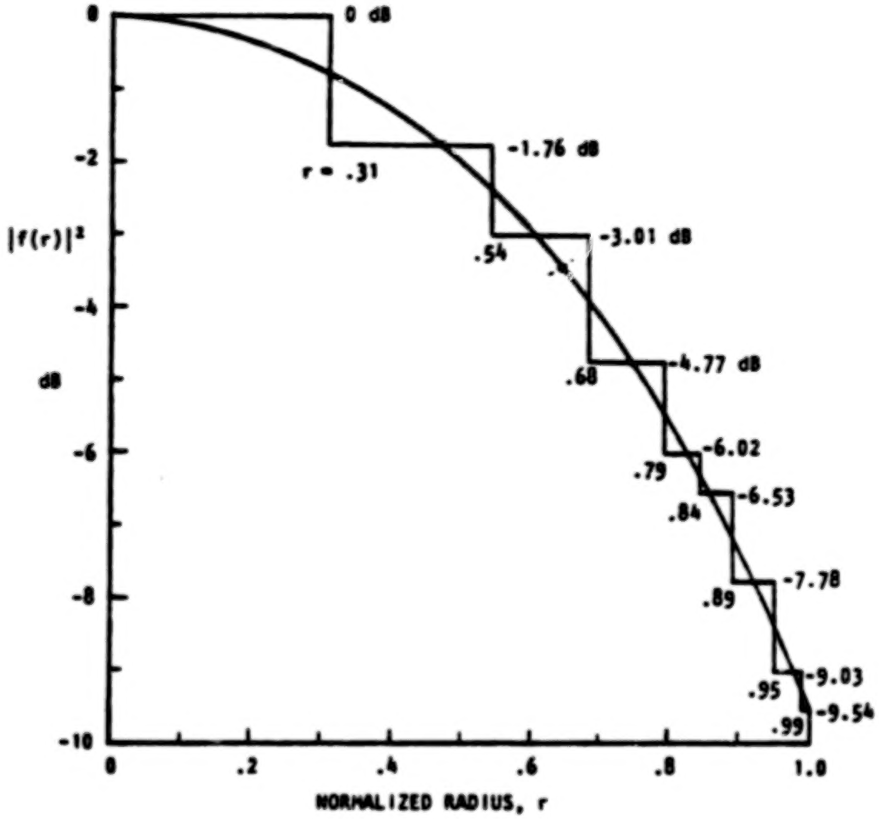

Figure 3.1-63. Nine-Step Approximation to Hansen Aperture Distribution Truncated at -9.54 dB

Ohmic Loss

The theoretical ohmic loss for the dominant mode in aluminum waveguide of dimensions a, b at 2450 MHz is

$$\alpha = \frac{3.7\times10^{-4}}{b}\left[1 + \frac{2b}{a}\left(\frac{\lambda}{\lambda c}\right)^{2}\right]\frac{\lambda g}{\lambda} \quad \text{dB/unit length.}$$

With $a = 8.65$ cm, $b = 2.0$ cm, the loss in the feed waveguide will be $\alpha = 3.2\ 10^{-4}$ dB per cm.

In the RCR the loss will be smaller because inner waveguide walls are eliminated; it turns out that this simply has the effect of making the second term within the square brackets above essentially negligible. As a result, loss in the RCR's is only about 2.6×10^{-4} dB/cm in the direction perpendicular to the feed waveguide.

For type 1 power modules the RCR length is 69.2 cm, hence loss within the RCR is only 0.018 dB. The total length of waveguide in the feed and hybrid network is also about 70 cm, so that feeder loss amounts to 0.022 dB. Thus the total theoretical loss in a type 1 power module is .040 dB or about 0.9%.

The losses are higher in other power modules, reaching .095 dB in the type 9 module. An integrated value for ohmic loss over the whole array can be calculated to be $\eta_H = 0.988 \approx 0.99$.

Magnetron Tube Description and Performance Characteristics

This section is a brief summary of pertinent magnetron tube characteristics. Physically the tube will be very much like the modified oven magnetron* shown in Figure 3.1-64 and mounted on a section of WR340 waveguide. Overall dimensions are expected to be about 8 cm in diameter by about 7 cm high, exclusive of pyrolytic graphite heat radiator. In the photograph of Figure 3.1-64 the heater leads are at the top, and the steel pole pieces, or shells, enclose the magnetron anode, the samarium-cobalt magnets and a buck-boost coil whose leads are brought out at the right. The tube has a coaxial output terminating in a probe coupler inside the waveguide. In the SPS version of the tube a pyrographite disc will replace the water-cooled copper tubing shown in the photograph. The heater/cathode is simply a helical coil of thoriated tungsten wire.

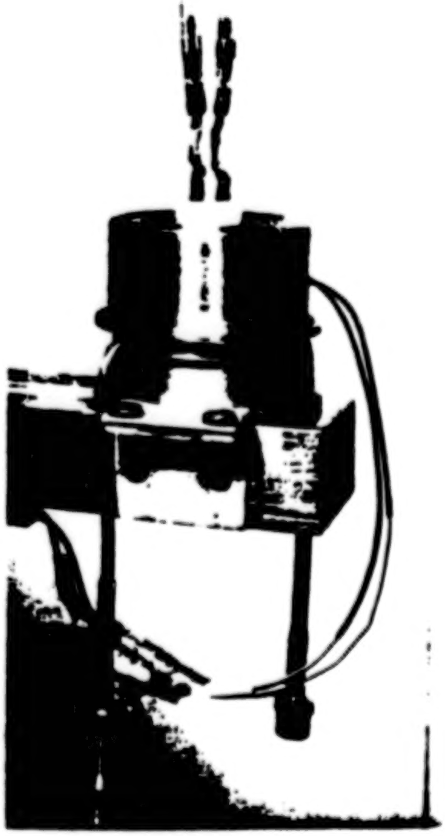

Figure 3.1-64. Typical Magnetron Mounted on WR340 Waveguide

---

*Photograph supplied by W. C. Brown, Raytheon Co.

Anode Voltage and Current

The operating anode voltage and current for a 3.5 kW tube have been determined to be almost 20 kV at nearly 0.2 A. This considers microwave circuit losses of 4%, and another 1% loss due to electron back bombardment to maintain cathode temperature after the heater power is turned off. To obtain an overall efficiency of 90% will require an electronic efficiency of 94.7%.

Alternatively, the anode voltage may be obtained from the equation

$$\eta_e = \frac{V-V_o}{V_o}$$

where V_o = 1038.3 volts and η_e is the electronic efficiency, .047. This gives V = 19,600 volts. The magnetic field, B, required to be supplied by the samarium-cobalt magnets can be found from the equation

$$V = V_o\left(\frac{2B}{B_o} - 1\right)$$

where B_o = 354.7 Gauss. It is found that B = 3524 Gauss.

Feedback Control of Output

Stability and control of the amplitude and phase of the magnetron's output is essential in the SPS application. Raytheon investigators have devised a technique in which a buck-boost coil is used to produce small variations around the mean or static level of magnetic field produced by the samarium-cobalt magnets in the tube itself. With an amplitude sensing device in the tube's output (e.g., directional coupler or lossely coupled probe, plus detector) and suitable feedback amplifiers and circuitry the output power level of the tube can be controlled over a considerable range (e.g., 3 to 4 dB) with little change in tube efficiency. The feedback control may also be applied to hold the output level constant to within tenths of a dB in the face of wide variations (15%) in applied anode voltage. In effect, this means that the magnetrons can always be operated optimally at close to maximum efficiency from an unregulated power supply. Thus the need for complex dc power conditioning is obviated; the magnetrons can run directly off the solar array buses.

Use of the feedback to control the magnetron's output phase has also been convincingly demonstrated in the course of Raytheon studies. For example, a normal output phase variation of 110° due to a change of 15% in applied anode voltage is reduced to about 2° by the application of feedback. In these demonstrations the output is sampled and compared to a fixed phase reference. In this way a dc error voltage is derived and is used to drive a motor-driven mechanical phase shifter in the magnetron input circuit. Clearly, this technique is somewhat cumbersome and undesirable in the SPS but there are at least two ways in which the motor-driven mechanical phase shifter may be eliminated. For example a varactor diode type of phase shifter could be used, preferably operating at low power level ahead of the magnetron's driver amplifier. Another technique has been suggested based upon the observation that the magnetron's free-running frequency is largely determined by its "cavity" dimensions. A change in these dimensions, or introduction of a tuning post, will cause a change in frequency. When operating as an injection locked amplifier the magnetron frequency cannot change in response to a change in "cavity" dimensions or introduction of a tuning device. What happens, instead, is that the magnetron's output phase undergoes a change in response to the "stimulus."

The concept is to utilize a tuning mechanism, which could be built into the tube itself, and whose very small movements are controlled by a small electromagnetic driving coil similar to the voice coil in a loudspeaker. The error signal from the phase sensing network would then be amplified and used to drive a restoring current through the driving coil. This phase-shifting technique turns out to have an additional benefit. Since the tuning mechanism acts in such a way as to cause the tube's free-running frequency to track the driving signal's frequency, the injection locking range is considerably increased. This appears to have important implications for gain and excitation requirements.

Startup, Heater Shutdown, and Lifetime

A startup procedure which makes use of the feedback amplitude control circuit has been devised and demonstrated experimentally by Raytheon. The procedure is as follows:

- Step 1. DC anode voltage is applied to the tube, but no heater power is present and the cathode is non-emitting.

- Step 2. A reference control voltage is applied to the amplitude feedback circuit that results in a relatively high current in the buck-boost coil. The resulting magnetic field, superimposed on the static field provided by the permanent magnets, results in a total magnetic field of a magnitude such that the tube cannot oscillate at the applied anode voltage even when the heater power is turned on and cathode emission occurs.

- Step 3. Heater power is turned on, the cathode heats up, and in about five seconds the normal emission level is reached.

- Step 4. After five seconds of cathode warm-up the heater power is removed entirely. At the same time the reference control voltage applied to the feedback circuit is changed to its operating level. At this point, the magnetic field in the tube assumes its proper operating value and the tube begins to function in the locked mode.

During the five-second cathode warm-up period, a heater input of 65 watts is needed for a 3.5-kW tube. When heater power is removed and the magnetic field is changing to its correct value, there is a buildup of oscillation in the tube. This transient condition lasts only for a few milliseconds before the tube settles into stable, controlled amplification.

The fact that external heater power is not required after the 5-second start-up period does not imply cold cathode operation of the tube. Parenthetically, it should be noted that heater and cathode are one and the same—a simple helical coil of carburized thoriated tungsten wire. The cathode surface is maintained at the required high electron-emitting temperature by back bombardment, in which some electrons, after acceleration by the field in the tube, actually return to the cathode where their kinetic energy is converted to heat. It is well established that the lifetime of such a cathode (operating in a high vacuum, of course) is a very sensitive function of its operating temperature. For example, a ten-fold increase in life occurs if this temperature is reduced from 2000 K to 1900 K. The back bombardment heating in a magnetron tube appears to be governed by a built-in regulatory mechanism which acts to hold cathode temperature to the lowest value that is sufficient to supply the necessary anode current. Thus the longest possible lifetime is assured.

Raytheon investigations indicate that an SPS magnetron tube could utilize a 50% carburized thoriated tungsten filament winding with wire diameter of 1 mm (0.040 in.) operating at a temperature that is possibly as low as 1900 K. Based on current life test data projections, a lifetime of from 30 to 50 years is anticipated.

Output Spectrum of Magnetron

Measurements of the noise power spectrum of any tube operating at high output power levels are difficult. In the case of the magnetron operating without external heater power the carrier to noise level is extremely high and, even with notch filter suppression of the carrier power by at least 49 dB in a 20 MHz band, measurements can be limited by the dynamic range of the spectrum analyzer. Observations by Raytheon investigators on a number of different tubes show considerable variability among the devices. Certain tubes have shown a carrier to noise level of at least 188 dB per Hertz at frequencies outside of a 60 MHz band centered on the 2450 MHz carrier. Refinements to the measurement technique may indicate even better performance on the part of selected tubes.

Little information on harmonic content in the output of high-power magnetrons is available. Some recent measurements on two tubes show the following levels of harmonic content, relative to the fundamental.

Harmonic	Level in dB Tube A	Tube B
1	-71	-69
2	-97	< -85
3	-86	-93
4	-62	-64

Overall System Description and Performance Summary

The complete spacetenna is constructed from the nine different subarrays described above. Type 1 arrays are used in the central region out to normalized radius $r = 0.31$, then type 2 arrays to radius $r = 0.54$, and so on, as indicated in Figure 3.1-63. Each subarray is a complete entity that includes a solid-state driver amplifier (~9 watts output) for each of its magnetrons, and a corporate feed network of RG141 or equivalent semi-rigid coaxial cables with appropriate power splitters. This corporate feed network branches from a master phase reference control amplifier (MPCA) as shown in Figure 3.1-62. Assuming that the solid state drivers have a gain of 25 dB, then input power per driver is about 30 mW. In a type 1 subarray there are 144 such drivers with a total input power requirement of 4.3 watts. Allowing for losses in the coaxial transmission lines of the feed network, an output level of 10 watts from the MPCA will suffice for the type 1 subarray. Because 144 is not an integral power of 2, simple binary division cannot be used in the corporate feed network. However, a combination of binary and ternary dividers will do the job; for example 4 binary levels plus 2 ternary levels. This is also true of type 2, 3, 4, 5, 7 and 8 subarrays except that the numbers of binary and ternary levels will change. The type 6 and type 9 subarrays require only binary dividers.

When the subarrays are put together to form a complete spacetenna, each will have to be provided with a source of high voltage (20 kV dc) power for the magnetron anodes, plus low-voltage power (presumably 10 V dc) for the feedback circuitry, buck-boost coils, solid state driver amplifiers, and master phase reference control amplifier (MPCA), as well as for heater power for the short, 5-second, startup period. In addition a 2450 MHz phase reference signal must be supplied to each subarray whose phase is controlled by suitable phase conjugation circuitry associated with a pilot tone antenna and receiver that are also a part of the subarray. No further description of this retrodirective control system will be given here; it is simply assumed that it is essentially identical to the system used with the klystron reference concept, with minor modifications as needed to suit the magnetron system.

In the klystron reference concept the subarray size is approximately 10×10 m^2, whereas it is only 4.2×4.2 m^2 for the magnetron system. It is therefore proposed that retrodirective phase control be applied to groups of $2\times2 = 4$ subarrays in the magnetron system. This will result in an effective subarray size of 8.4×8.4 m^2, which is closer, for comparative purposes, to that of the klystron system.

Spacetenna Performance Characteristics

The performance of this antenna when the central power density is limited to $S_T = 28$ kW/m^2 and received power density to $S_R = 230$ W/m^2. The rectenna characteristics are given in Table 3.1-32 on the assumption that the rectenna is located at latitude 40°, so that the range is R = 37,500 km.

Mass Estimate for Spacetenna

A careful estimate of the masses of all components comprising the spacetenna as described above has been made. Not included in this estimate are the masses of the 20 kV dc buses required for magnetron power, the 10 V dc buses for solid-state circuitry, the pilot tone antennas and receivers and the master phase reference distribution system.

Table 3.1-31. Spacetenna Characteristics

CHARACTERISTIC OR PARAMETER	VALUE
APERTURE FIELD	
AMPLITUDE DISTRIBUTION	9-STEP APPROX. TO -9.54 dB HANSEN
PHASE DISTRIBUTION	IDEAL UNIFORM
POWER COEFFICIENT	$K = .436$
APERTURE EFFICIENCY	$\eta_A = .914$
OHMIC EFFICIENCY	$\eta_H = .99$
FAR-FIELD PATTERN	
HPBW	1.138 λ/D RADIANS
BEAMWIDTH CONSTANT AT -13.6 dB	$B = 2.20$
BEAM EFFICIENCY AT -13.6 dB	$\eta_B = .937$
FULL WIDTH AT -23.6 dB	2.60 λ/D
FIRST SIDELOBE LEVEL	-23.2 dB

Table 3.1-32. Rectenna Characteristics
(Magnetron Transmitter)

• Spacetenna diameter	$D_T = 918$ km
• Total RF radiated power	$P_T = 8.00$ GW
• Rectenna minor diameter	$D_R = 11.0$ km
• Power incident on rectenna	$P_R = 7.50$ GW
• Safety fence minor diameter	$D_F = 13.0$ km

An estimate of magnetron tube mass is as follows:

Magnetic circuit	266 g
Copper anode and vanes	81
Ceramic insulators	30
Output RF line	30
Buck-boost coil	76
Heater/cathode	6
Tuner and drive coil	50
Miscellaneous	57
Tube mass	590 g

Each pyrolytic graphite heat radiator has an overall diameter of 34.6 cm and tapers from 0.3 cm thickness at the central hole to 0.05 cm at the edge. With density of 2.2 g/cm^3 the mass is found to be 310 g per disc. Thus, a single magnetron tube, complete with its heat radiator, will have a mass of 900 g or 0.90 kg.

The masses of each type of RCR and waveguide feeder have been calculated using previously noted dimensions and assuming they are fabricated of 0.25 mm (.010 in) thick aluminum. Then, the masses of RCR, tubes and heat radiators were combined to find the total mass for each of the nine kinds of power modules.

Standard subarray masses were next computed using the appropriate number and masses of subarrays. To this was added an allowance to account for the mass of the aluminum frame in which power modules are assembled and mounted. Finally, for each subarray type an estimate was made for the total masses of coaxial feed lines (assumed to be RG-141), solid-state drivers and feedback circuitry, etc. The resulting mass breakdown and totals for the nine different kinds of subarrays are summarized in Table 3.1-33.

Table 3.1-33. Mass Breakdown for Subarrays

ITEM	MASS IN kg									TOTAL
	SUBARRAY TYPE									
	1	2	3	4	5	6	7	8	9	
MAGNETRON TUBES	85.0	56.6	42.5	28.3	21.2	18.9	14.2	10.6	9.4	286.7
PG HEAT RADIATORS	44.6	29.8	22.3	14.9	11.2	9.9	7.4	5.6	5.0	150.7
RCR, W/G AND FRAME	34.4	31.7	32.5	30.4	29.5	29.8	28.8	28.4	27.8	273.3
COAX LINE AND SOLID-STATE ELECTRONICS	2.2	1.7	1.4	1.1	0.9	0.9	0.8	0.7	0.7	10.4
TOTAL	166.2	119.8	98.7	74.7	62.8	59.5	51.2	45.3	42.9	721.1

The number of a given type of subarray in the full spacetenna is obtained by dividing the area of one subarray (17.64 m^2) into the area of the appropriate zone (i.e., power density step) in the antenna. The areas of the various zones are calculated using the fractional radii indicated in Figure 3.1-63 along with a full diameter of 918 km.

Table 3.1-34 then shows the numbers of each kind of subarray, the total masses of all component sections (tubes, PG discs, RCR's, etc.) and finally the mass of the full spacetenna, namely 3.32×10^6 kg. The total number of magnetron tubes is 2.35×10^6 and the mass of PG is 729 metric tons.

Table 3.1-34. Mass Breakdown for Spacetenna

ITEM		SUBARRAY TYPE									TOTALS
		1	2	3	4	5	6	7	8	9	
NO. OF SUBARRAYS		3606	7335	6409	6067	3058	3246	4142	2912	747	37522
TOTAL MASSES IN kg × 10^3	TUBES	305.9	415.2	272.3	171.9	65.0	61.2	58.6	30.9	7.0	1388.0
	PYRO. GRAPHITE	160.7	218.1	143.1	90.3	34.1	32.1	30.8	16.2	3.7	729.1
	RCR'S & W/G	123.8	232.4	208.3	184.5	90.3	96.6	119.2	82.6	20.6	1158.3
	COAX AND SS ELECTRONICS	7.9	12.5	9.0	6.7	2.8	2.9	3.3	2.0	0.5	47.6
GRAND TOTALS IN kg×10^3		598.3	878.2	632.7	453.4	192.2	192.8	211.9	131.7	31.8	3323.0

3.1.5 STRUCTURE

Introduction

The satellite structure for the various configurations selected for analysis may be considered in two broadly differing categories. The first category, which applies only to the configurations utilizing a planar form factor, consists of the structure required to support the solar photovoltaic array, the rotary joint support structure, and the basic antenna yoke elements. A special variant of the first category is used to establish the special requirements associated with the reflector/concentrator support structure. The second category is the antenna itself. The primary structure assemblies are made up of the tribeam girders, tension cables, and joints. The fabrication and assembly of these structures are accomplished on orbit by beam machines and supporting auxiliary equipment.

Tribeam Girder

The general configuration and detailed breakout of the basic tribeam girder are illustrated in Figure 3.1-65.

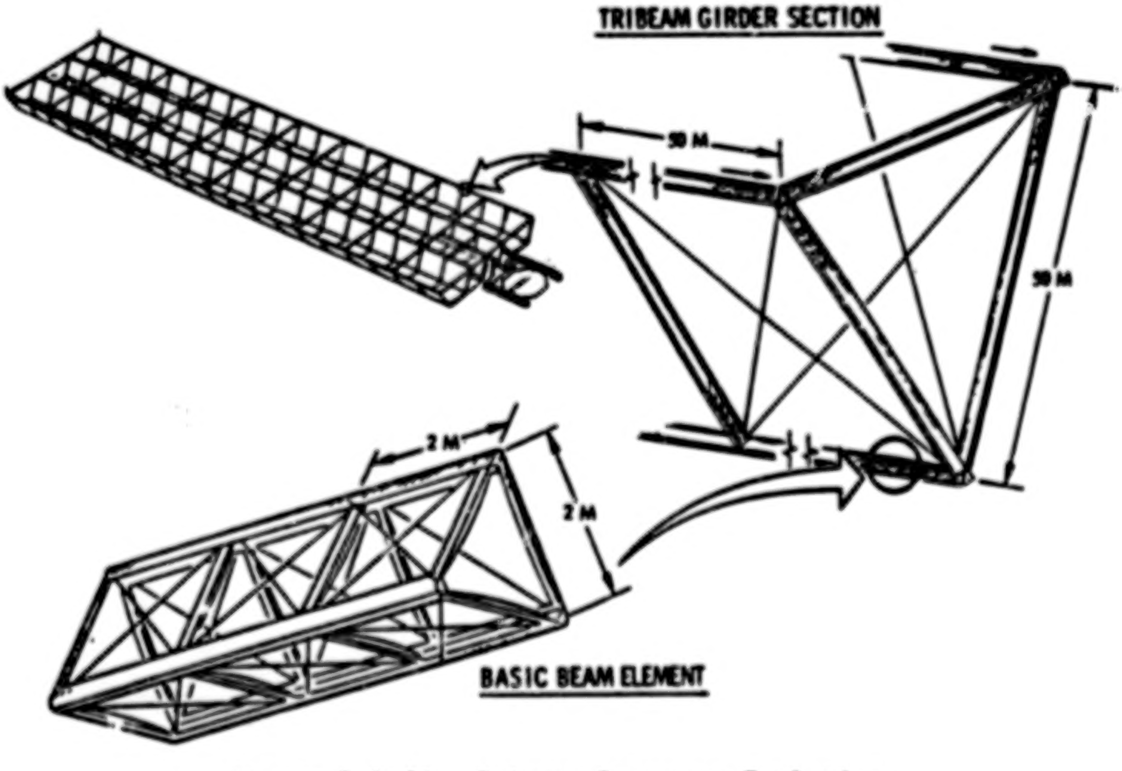

Figure 3.1-65. Primary Structure Evolution

The girder is 50 m on a side, and each bay is 50 m in length, stabilized by X-tension ties. Three longitudinal elements and the transverse struts are formed by basic beam elements fabricated on orbit by a beam machine. The basic beam element is 2 m on a side with transverse struts every 2 m and modified triangular cap sections at the vertices. The cap sections, transverse struts, and

X-tension braces are made from 60% graphite fiber composite sheets with approximately 88% cutouts, which are roll-formed, flanged, and welded by the beam machine to form a basic beam element 2 m on a side.

The pertinent physical properties of the tribeam girder basic beam element, cap section, and tension ties determined by this preliminary sizing analysis are listed in Table 3.1-35.

Table 3.1-35. Solar Array and Rotary Joint Tribeam Girder Characteristics

ITEM NO.	PARAMETER	CAP SECTION	BASIC BEAM ELEMENT	TRIBEAM GIRDER	TENSION TIE
1	A_{EM} = EFFECTIVE AREA FOR MASS CALCULATIONS IN m^2	0.035×10^{-3}	0.21×10^{-3}	0.63×10^{-3}	3.17×10^{-5}
2	A_{EI} = EFFECTIVE AREA FOR MOMENT-OF INERTIA CALCULATIONS IN m^2	0.064×10^{-3}	0.19×10^{-3}	0.57×10^{-3}	3.17×10^{-5}
3	ρ = RADIUS OF GYRATION (m)	28.28×10^{-3}	820.78×10^{-3}	20.23	1.59×10^{-3}
4	I = GEOMETRIC MOMENT OF INERTIA (m^4)	5.1×10^{-8}	0.128×10^{-3}	237.5×10^{-3}	7.9×10^{-11}
5	E = MODULUS OF ELASTICITY—P_a ††	9.65×10^{10}	9.65×10^{10}	9.65×10^{10}	2.34×10^{11}
6	α = COEFFICIENT OF THERMAL EXPANSION, M/M-°C	0.18×10^{-6}	0.18×10^{-6}	0.18×10^{-6}	0.4×10^{-6}
7	μ = POISSON'S RATIO	0.40	0.40	0.40	0.32
8	F_n = NATURAL FREQUENCY (Hz)	254	8.3	0.57†	8.4×10^{-3}

†TRIBEAM GIRDER LENGTH = 800 m
††MATERIAL IS GRAPHITE COMPOSITE, 60% FIBER, VOLUME, MADE UP AS (0, ◇ , 0)*

**0, ◇, 0 designator material ply orientation per Rockwell Space Division "Materials Properties Manual" (Jan. 1978)*

Solar Array

The basic layout for the planar configuration, the reference configuration (Figure 2.1-2), the solid-state dual end-mounted (Figure 2.1-3), and the magnetron configuration is identical except for the length and, in the case of the dual end-mounted configuration, the requirement for dual rotary joints. The following discussion, therefore, will concentrate on the reference concept with specific variations (if any) noted as required.

The Rockwell configuration (reference concept) for a coplanar satellite with end-mounted antenna was shown in Figure 2.1-2. The satellite has three troughs, each with 10 bays, and is 4200 m wide at the longeron points, and 16,000 m long (less antenna). Twenty-six solar blanket strips measuring 25 m by 730 m are installed in each bay along the bottom of the trough. The reflectors are attached to the inner diagonal sides of the troughs. The antenna with slip rings, support structure, and trunnion arms extends 1900 m from the basic satellite. The general arrangement of the space frame concept antenna is illustrated in Figure 3.1-66. The lower portion of the figure shows the

BLANK PAGE

BLANK PAGE

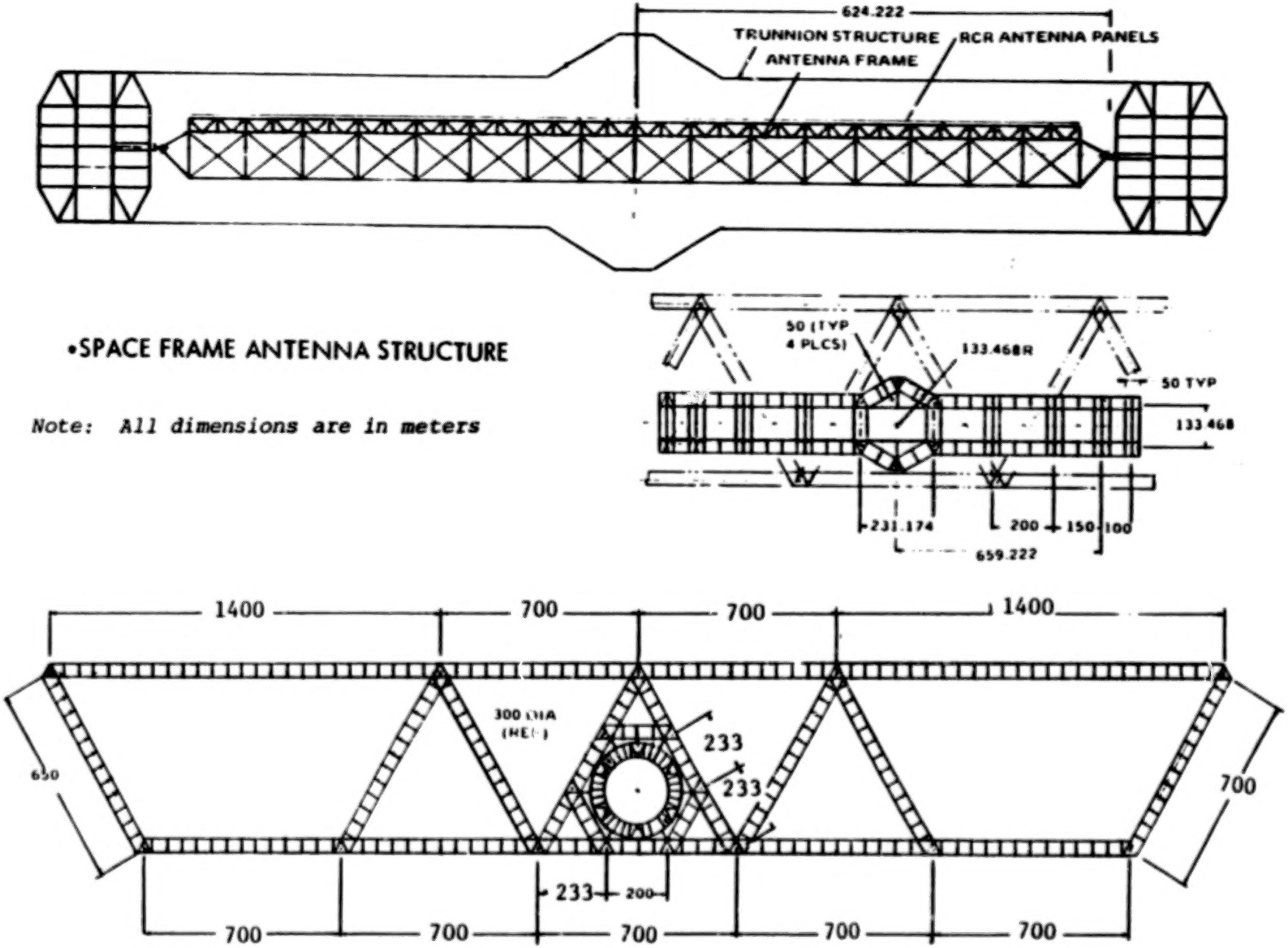
624.222
TRUNNION STRUCTURE
RCR ANTENNA PANELS
ANTENNA FRAME
50 (TYP
4 PLCS)
133.468R
50 TYP
133.468
231.174
200
150
100
659.222
1400
700
700
1400
300 DIA
(REF)
233
233
650
700
233
200
700
700
700
700
700

•SPACE FRAME ANTENNA STRUCTURE

Note: All dimensions are in meters

Figure 3.1-66. End-Mounted Antenna/Yoke—
Cross-Section 3-Trough Configuration

location of the slip rings, or rotary joint with relationship to the cross-section of the satellite structure. The support for the trunnion structure is attached to the rotary joint (middle illustration). The trunnion structure (upper view) extends about 625 m either side of the centerline and provides support for the two longitudinal arms upon which the antenna is mounted.

The satellite structure and solar converter are constructed in a single pass, utilizing an integrated space construction base (SCB). Construction of longitudinal members of the slip ring interface structure is initiated, and the members fabricated to a length permitting attachment to the SCB frame. The first satellite frame is then constructed, followed by additional fabrication of slip ring longitudinal members until the first triangular frame is positioned properly away from the SCB so that the second triangle can be completed. The SCB then proceeds to fabricate/install the remainder of the satellite structure. Concurrently, construction of the slip rings (rotary joint) takes place, utilizing free flying fabrication facilities. In Figure 3.1-67, the second satellite frame has been constructed and the slip ring structure has been completed.

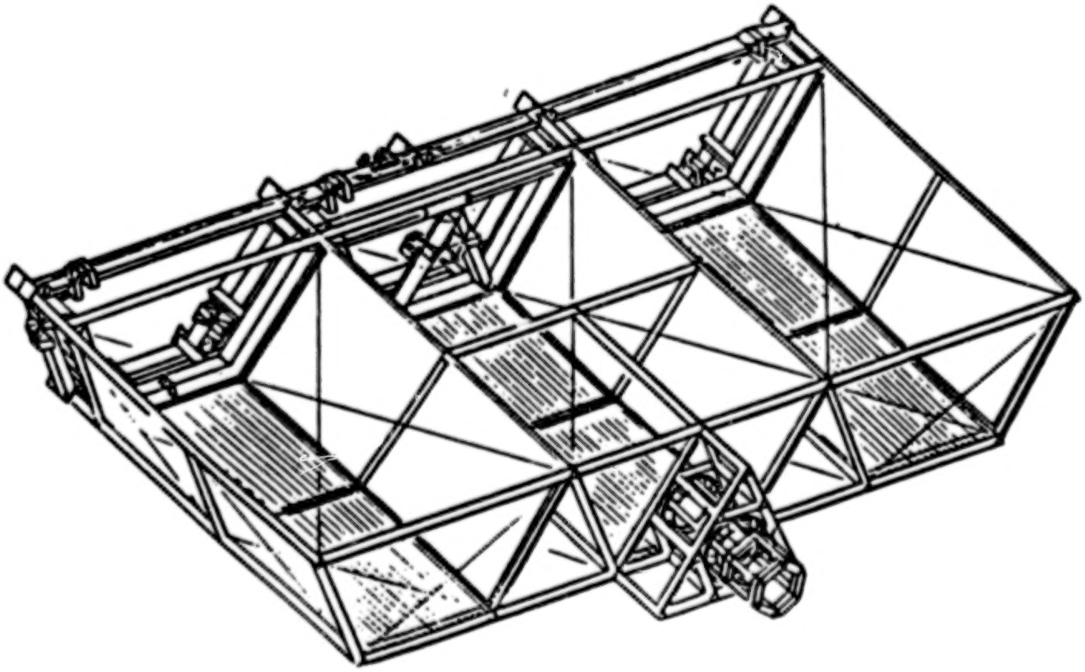

Figure 3.1-67. Slip Ring Structure
Independent Fabrication

Several concepts for attaching 2-m beams have been defined. All of these concepts require further study to identify the specific operations and equipment involved.

Figure 3.1-68 shows two views of the intersection of three 2-m tribeams. The concept entails use of special fittings which are inserted into the cap section of the beam, either at the end or at locations along the beam length, as required by the geometry of the intersection. The sections marked A and A' on the figure are detailed in Figure 3.1-69. In detail A, two end fittings

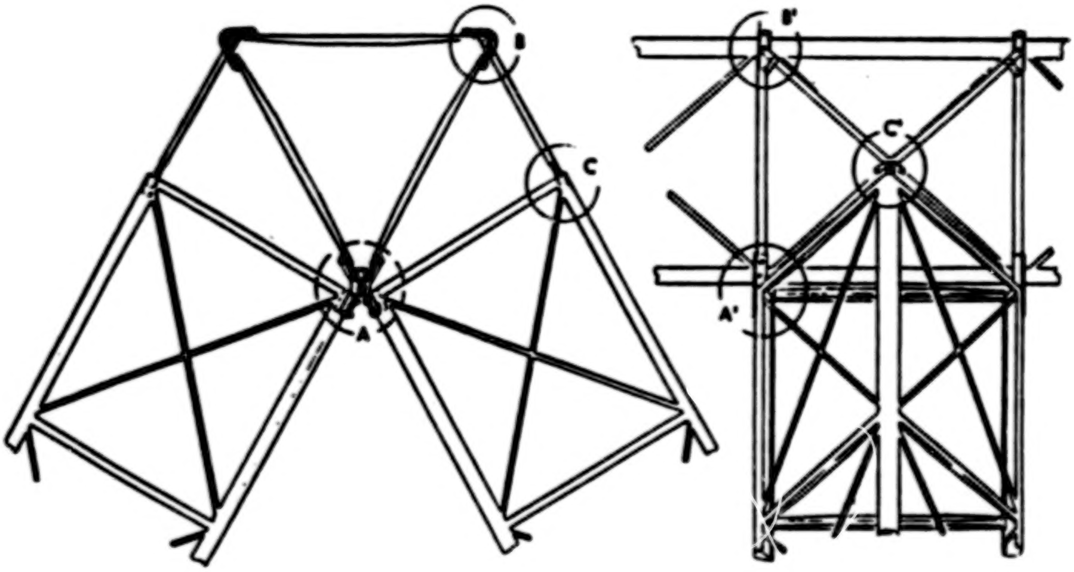

Figure 3.1-68. Reference Configuration Attach Fittings

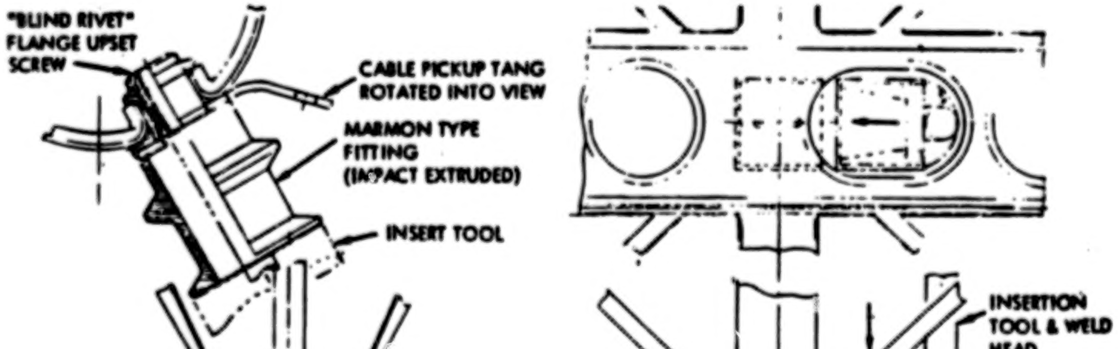
"BLIND RIVET" FLANGE UPSET SCREW
CABLE PICKUP TANG ROTATED INTO VIEW
MARMON TYPE FITTING (IMPACT EXTRUDED)
INSERT TOOL
INSERT SPOT WELDED TO STRUCTURE
CLAMP ROLL SWAGED
END FITTING TYP.
DETAIL A
INSERTION TOOL & WELD HEAD
DETAIL A'

Figure 3.1-69. Reference Configuration Details A and A'

have been inserted into the cap section of the two bottom beams and spot-welded in place. An insert fitting, capable of being inserted through lightening holes (Detail A') by a special tool, has been welded into the proper position on the third beam and two fittings inserted and secured as shown in the upper section of Detail A. These fittings are then mated to the two end fittings and secured by clamps.

Sandwich Concept Structural Configuration

The basic structure necessary to assemble the solid-state sandwich satellite is shown in Figure 3.1-70. The estimated tribeam structural characteristics for system weights analysis are tabulated in Table 3.1-36. These characteristics were determined to sustain the frame compression loads incurred with development of the in-plane tension loads necessary to limit the primary and secondary reflector surface deviations from flatness to no more than one meter.

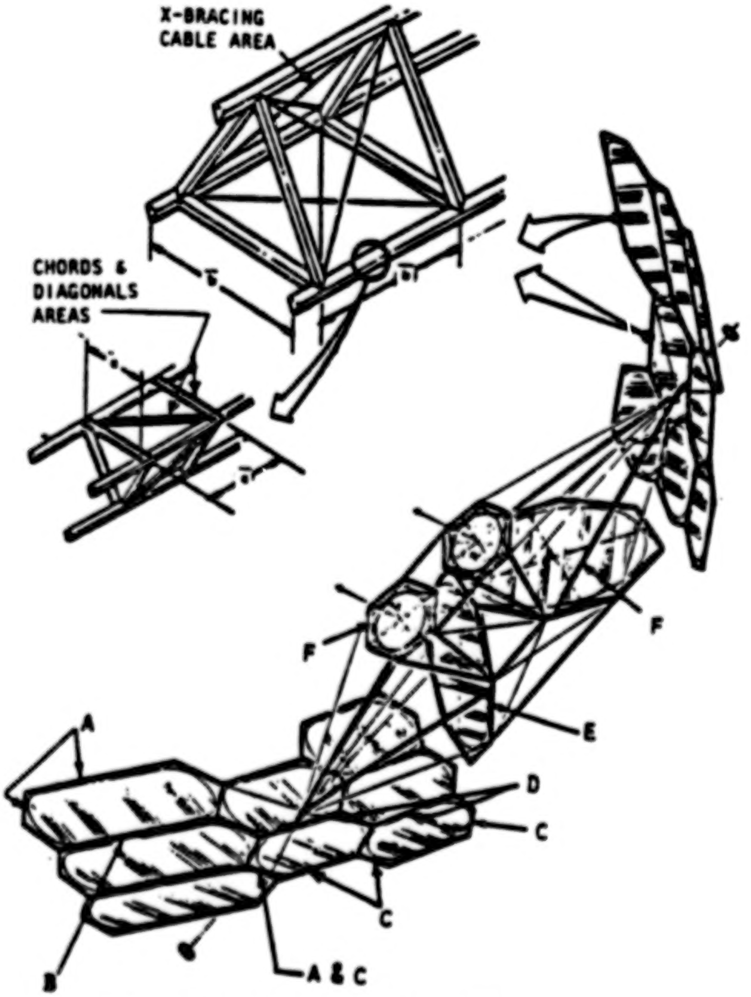

Refer to Table 3.1-36 for description of Elements A through F.

Figure 3.1-70. Solar Power Satellite Sandwich Configuration, Dual Solar Reflectors

Table 3.1-36. Frame Structural Characteristics

Element	Type	b (m)	c (m)	Unit Mass (kg/m)	Cross-Section Area (cm²)	Minimum Inertia, I (m⁴)
A	◁	122	2.0	12.5	13.9	3.45
B	◇	122	2.0	25.0	27.8	6.90
C	◁	97	1.6	8.3	8.0	1.26
D	◇	97	1.6	16.6	16.0	2.52
E	◁	140	2.3	15.8	18.5	6.0
F	◁	67	2.3	10.4	11.0	0.82

NOTE: GI/EI = 0.265 for all designs.

Refer to Figure 3.1-69.

The dimensions of each of the reflector compression frames are indicated on the NASTRAN plots shown in Figures 3.1-71, -72, and -73. The frame Buckling coefficients (η^*) utilized is indicated in Table 3.1-37.

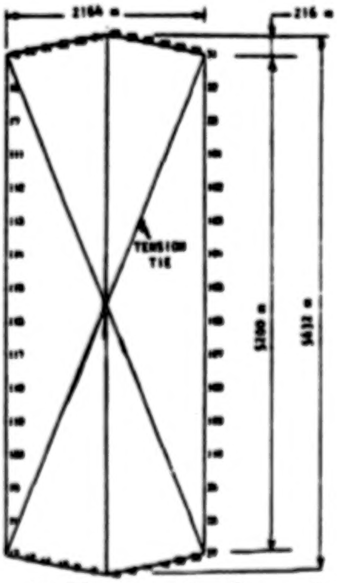

Figure 3.1-71. Primary Reflector Surface Compression Frame I

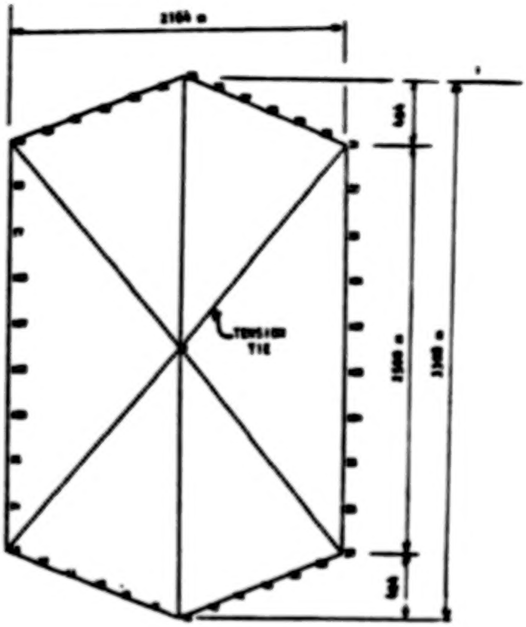
TENSION TIE

Figure 3.1-72. Primary Reflector Surface Compression Frame II

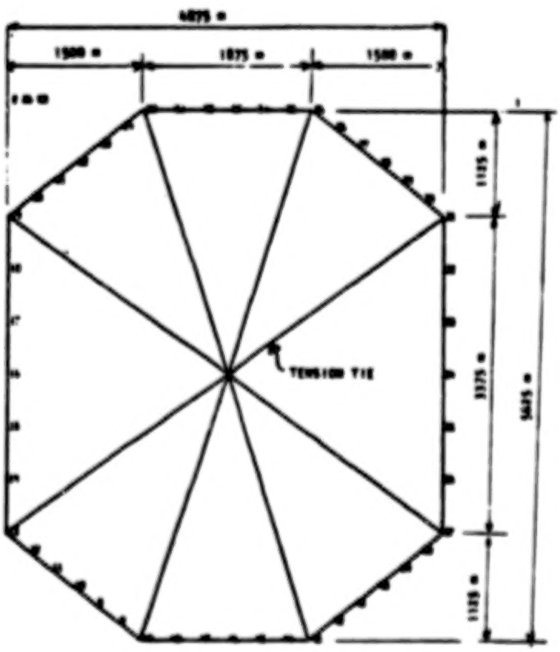
4875 m
1500 m
1875 m
1500 m
1125 m
TENSION TIE
3375 m
5625 m
1125 m

Figure 3.1-73. Secondary Reflector Surface Compression Frame III

Table 3.1-37. Frame Buckling Coefficient, η*
(Variation with Ratio of GI/EI)

Frame	Reference Figure	GI/EI = 0.053	GI/EI = 0.265	GI/EI = 0.53
I	3.1-70	0.193	0.873	0.984
II	3.1-71	0.072	0.31	0.52
III	3.1-72	0.097	0.286	0.365
$*\eta = \frac{P_1 \ell_2}{\pi^2 EI}$				

Antenna

Two alternate structural concepts for the antenna have been suggested. These are a rigid structure proposed for the NASA reference concept, and a tension-web/compression frame approach suggested by Rockwell International.

Space Frame

The space frame antenna structure concept is shown in Figure 3.1-74. This concept consists of two basic elements—the space frame primary structure, and the space frame secondary structure. The primary structure is an open-truss

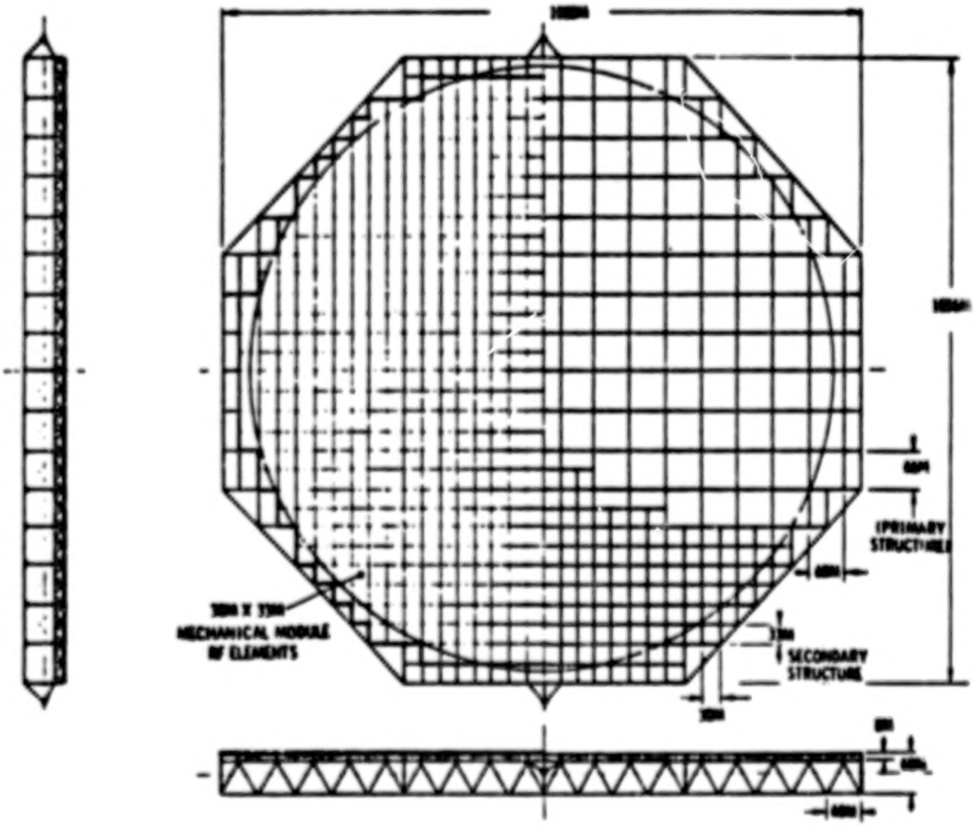

Figure 3.1-74. Space Frame Antenna Configuration

structure, 138 m deep, with a quasi-square shape approximately 60 m on a side. The secondary structure consists of an open-truss structure, 8 m deep, with a rectangular shape 30×33 m on the two sides. The material used on this concept is the same as that used on the compression frame approach.

Tension Web/Compression Frame

Antenna Structure

The tension-web/compression frame antenna structure concept, shown in Figure 3.1-27, consists of three major elements: (1) the tension web to which the dc-to-RF conversion and transmission hardware is attached, (2) a catenary rope system which is attached to the perimeter of the tension web, and (3) a hexagonal compression frame. The tension web resists the lateral pressure loading described in Figure 3.1-75. The loading is transmitted to the vertices of the hexagonal compression frame via the catenary rope system. The compression frame members are loaded in pure compression and can be analyzed as columns. Three of the six catenary-to-compression-frame vertice attachments are fixed. The other three attachments at every other intersection have lateral adjustment jacks. The three fixed attachments describe a plane perpendicular to the desired boresight and the adjustable attachments maintain the tension web as a flat surface. All six catenary rope/compression frame attachments have in-plane tensioning devices which maintain the tension web flat within the design limits. Antenna elevation (north-south) adjustments are accomplished by gimbals in the trunnion structure which attach the antenna to the rotary joint. Azimuth adjustments are made by the rotary joint.

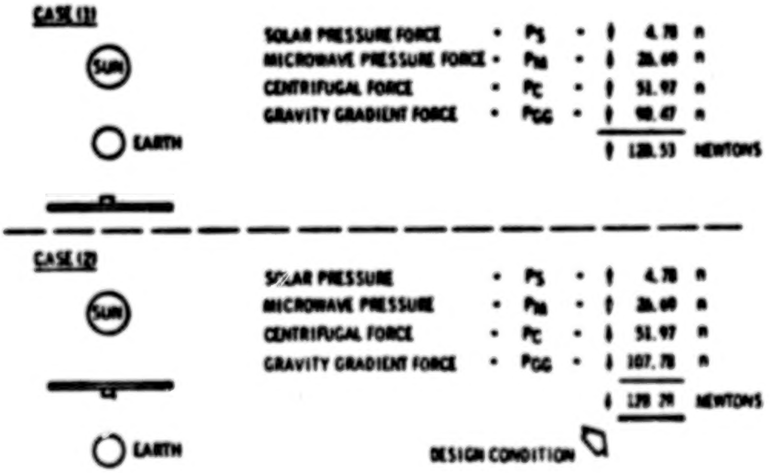
CASE (1)
SUN
EARTH
SOLAR PRESSURE FORCE = PS = 4.78 N
MICROWAVE PRESSURE FORCE = PM = 26.60 N
CENTRIFUGAL FORCE = PC = 51.97 N
GRAVITY GRADIENT FORCE = PGG = 40.47 N
128.53 NEWTONS
CASE (2)
SUN
EARTH
SOLAR PRESSURE = PS = 4.78 N
MICROWAVE PRESSURE = PM = 26.60 N
CENTRIFUGAL FORCE = PC = 51.97 N
GRAVITY GRADIENT FORCE = PGG = 107.78 N
179.79 NEWTONS
DESIGN CONDITION

Figure 3.1-75. Microwave Antenna Structure Design Condition

Reference Concept

The basic requirements for the reference concept compression frame tension web concept are as follows:

- 1-km-diameter surface (or equivalent)
- Web angular misalignment: ±0.08° under environmentally and operationally induced loads and temperature
- Optimize for light weight
- Compatible with on-orbit fabrication and assembly
- Compatible with operational equipment
- Service life: >30 years

The antenna structure was subjected to a sizing analysis based on the environmentally and internally induced loads and the pressure forces indicated in Figure 3.1-75, as well as the design requirements listed above. This resulted in the physical properties for each of the three structural elements listed in Table 3.1-38. The tribeam girder size dimension and bay length dimension are 30.57 m. The catenary cab les and tension-web cables are woven graphite, 0.0396 m (1.56 in.) and 0.0064 m (0.25 in.) in diameter, respectively.

Table 3.1-38. Antenna Structure Elements Physical and Mechanical Properties

ITEM NO.	PARAMETER	COMPRESSION FRAME			CATENARY CABLE	TENSION WEB CABLE
		CAP SECTION	BASIC BEAM ELEMENT	TRIBEAM GIRDER		
1	A_{EM} - EFFECTIVE AREA FOR MASS CALC. (M^2)	0.05×10^{-3}	0.3×10^{-3}	1.8×10^{-3}	1.2×10^{-3}	3.167×10^{-5}
2	A_{EI} - EFFECTIVE AREA FOR MOMENT-OF-INERTIA CALCULATIONS (M^2)	0.09×10^{-3}	0.27×10^{-3}	0.81×10^{-3}	1.2×10^{-3}	3.167×10^{-5}
3	ρ - RADIUS OF GYRATION (M)	23.68×10^{-3}	0.47	12.48	1.58×10^{-8}	1.53×10^{-11}
4	I - GEOMETRY MOMENT OF INERTIA (M^4)	5.15×10^{-6}	0.6×10^{-4}	0.126	1.2×10^{-7}	7.9×10^{-11}
5	E - MODULUS OF ELASTICITY (P_a)	9.65×10^{10}	9.65×10^{10}	9.65×10^{10}	13.79×10^{10}	13.79×10^{10}
6	α - COEFFICIENT OF THERMAL EXPANSION (M/M-°C)	0.18×10^{-6}	0.18×10^{-6}	0.18×10^{-6}	0	0
7	μ - POISSON'S RATIO	0.4	0.4	0.4	TBD	TBD
8	MATERIAL	*	*	*	**	**

*GRAPHITE COMPOSITE, 60% FIBER VOLUME, MADE UP AS (0, Φ, 0)
**WOVEN GRAPHITE

Solid-State Concept

A detailed analysis of the tension-web configuration for the solid-state microwave transmission concept was also performed to validate this approach. The resultant data confirmed the concept validity for the magnetron-based satellite as well as for the solid-state concepts.

The antenna frame will be constructed in geosynchronous orbit and consists of tribeams (Figure 3.1-76) built up from the individual machine-made beam elements shown, and connected by a pretensioned X-bracing system. Other constructions, such as a pentahedral truss utilizing union joints, are applicable but are not considered at this time. The machine-made beam element contains a closed-cap section fabricated of the same graphite composite material as that used in the cap of a General Dynamics design. The tension cables are graphite composite pultruded rods like those developed by McDonnell Douglas. The tribeam bay length is the same as the width, b.

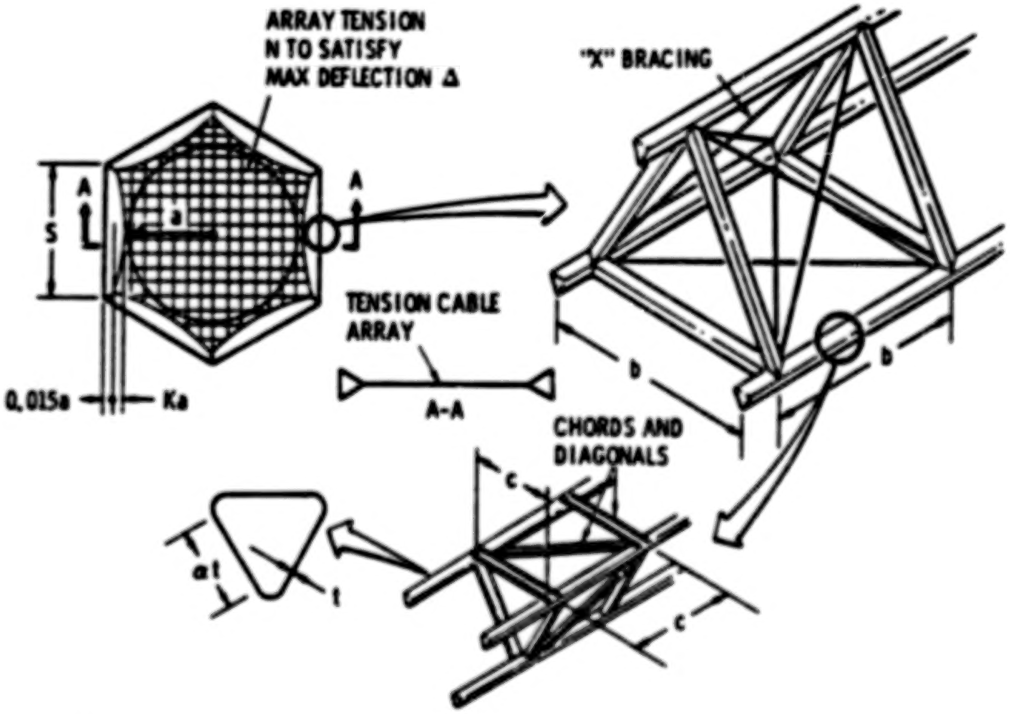

Figure 3.1-76. Analysis Model and Parameter Variations

Requirements

The operational scenario shown in Figure 3.1-77 illustrates the sources of the major structural requirements: (1) sustain the worst combination of "pretension closed forced system loads" in conjunction with structural temperature variation across the individual cap of 2-m beams—110°C, structural temperature differential between 30×30-m array cables and machine-made beam caps—±85°C, and structural temperature differential between tribeam X-bracing and machine-made beam caps—±55°C; (2) peak out-of-plane deflection 12 to 48 cm—during worst combination of solar pressure reflected—32.5×10^{-6} N/m^2, gravity-gradient load—32.5×10^{-6} N/m^2, microwave pressure—2.5×10^{-6} N/m^2, thermal gradient—24°C peak difference in average temperature of tribeam caps, 16°C sinβ difference in X-bracing cables, and gravity-gradient torque—negligible; (3) minimum modal frequency to be compatible with overall minimum of 0.0016 Hz; and (4) all materials to be compatible with temperatures of -170 to 200°C.

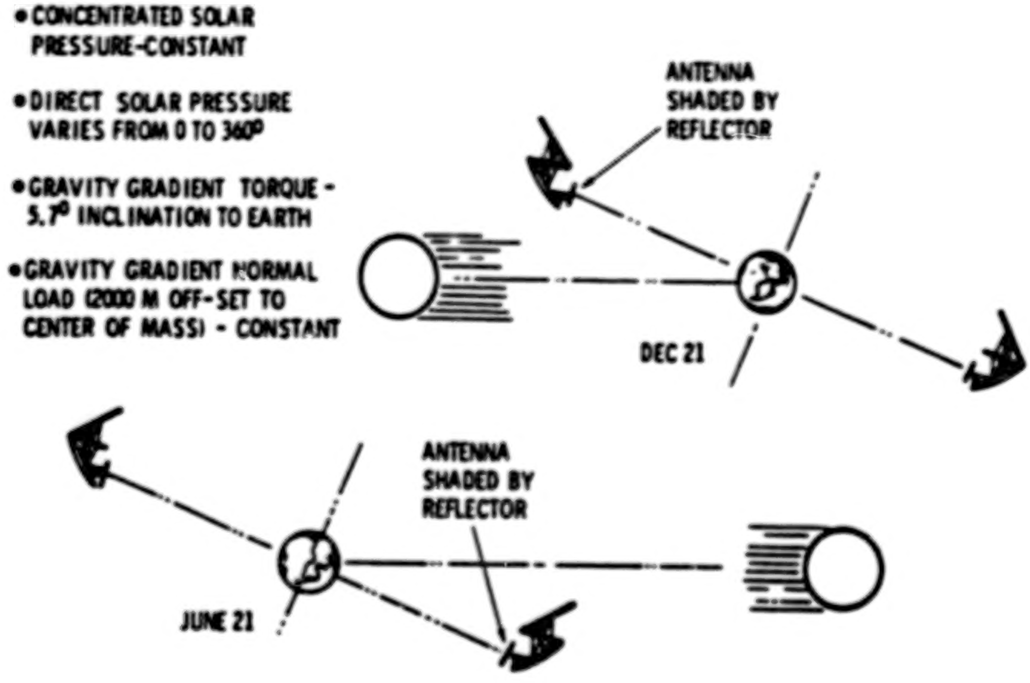
• CONCENTRATED SOLAR PRESSURE-CONSTANT
• DIRECT SOLAR PRESSURE VARIES FROM 0 TO 360°
• GRAVITY GRADIENT TORQUE - 5.7° INCLINATION TO EARTH
• GRAVITY GRADIENT NORMAL LOAD (2000 M OFF-SET TO CENTER OF MASS) - CONSTANT
ANTENNA SHADED BY REFLECTOR
DEC 21
ANTENNA SHADED BY REFLECTOR
JUNE 21

Figure 3.1-77. Microwave Antenna Operational Scenario

During operation, the concentrated solar pressure (CR = 5) is of constant intensity while the direct solar radiation varies from 0 to 360°. This is most significant to the initial contour adjustment and the thermal requirements stated above. Also of great signficance is the gravity-gradient loading resulting from the 2000-m offset between the antenna and total configuration center of mass. For the configuration shown, the concentrated solar pressure and gravity-gradient loading act in the same sense.

Despite exposure to these deterring sources, the antenna surface deviation from flatness must be compatible with the specific electronic efficiency requirements. The range of these requirements was 12 to 48 cm, as shown. Also, the integrated structure/control system must maintain the earth pointing accuracy of the antenna to within 0.05 degree. For that requirement, classical control techniques require the first modal frequency of this configuration (Figure 3.1-27) to be above 0.0016 Hz.

Structural Analysis Methodology

The general methodology of the structural analysis performed to parametrically describe the hexagonal frame's basic structural characteristics of mass and figure control quality is described in Figure 3.1-78. The basic closed-force system compression and tension loads (Figure 3.1-79) were derived parametrically in terms of the peak surface deflection Δ, antenna aperture radius a, and perimeter cable depth Ka. The interplay between the increased cable depth and frame perimeter with reduced compression load is shown in Figure 3.1-79. The frame compression stability criteria were obtained from NASTRAN stability analysis (Figure 3.1-80). For the first iteration, thermal loads were estimated

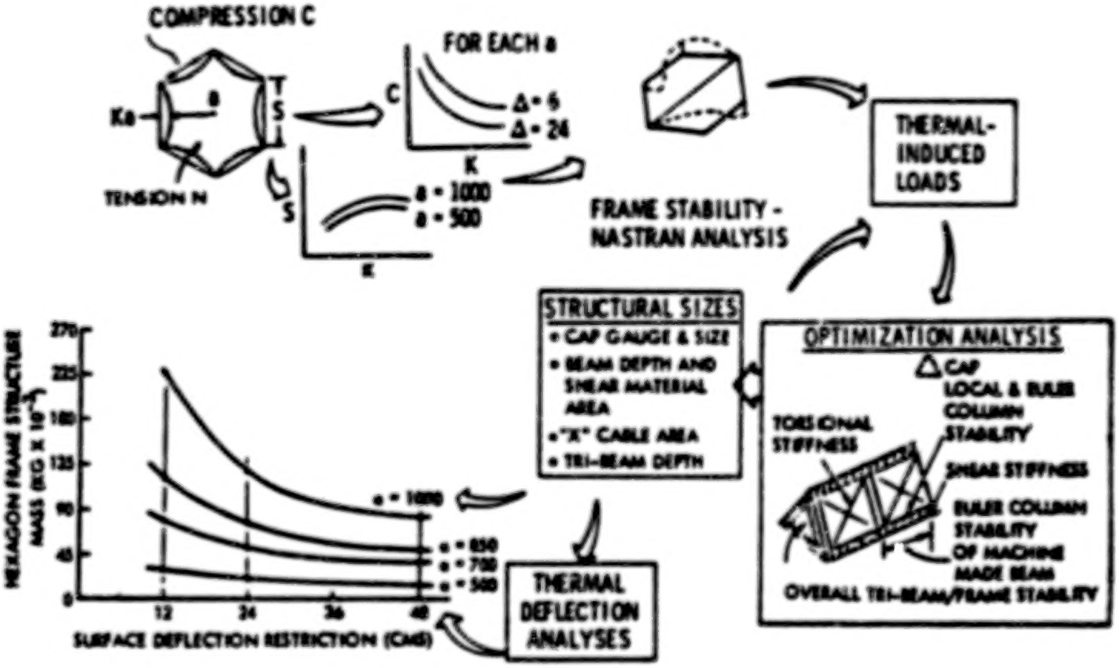
COMPRESSION C
Ka
a
T
S
TENSION N
FOR EACH a
C
Δ = 6
Δ = 24
K
S
a = 1000
a = 500
K
THERMAL-INDUCED LOADS
FRAME STABILITY - NASTRAN ANALYSIS
STRUCTURAL SIZES
• CAP GAUGE & SIZE
• BEAM DEPTH AND SHEAR MATERIAL AREA
• "X" CABLE AREA
• TRI-BEAM DEPTH
OPTIMIZATION ANALYSIS
Δ CAP
LOCAL & EULER COLUMN STABILITY
TORSIONAL STIFFNESS
SHEAR STIFFNESS
EULER COLUMN STABILITY OF MACHINE MADE BEAM
OVERALL TRI-BEAM/FRAME STABILITY
HEXAGON FRAME STRUCTURE MASS (KG X 10^-3)
270
225
180
135
90
45
0
12
24
36
48
SURFACE DEFLECTION RESTRICTION (CMS)
a = 1000
a = 850
a = 700
a = 500
THERMAL DEFLECTION ANALYSES

Figure 3.1-78. Structural Analysis Methodology

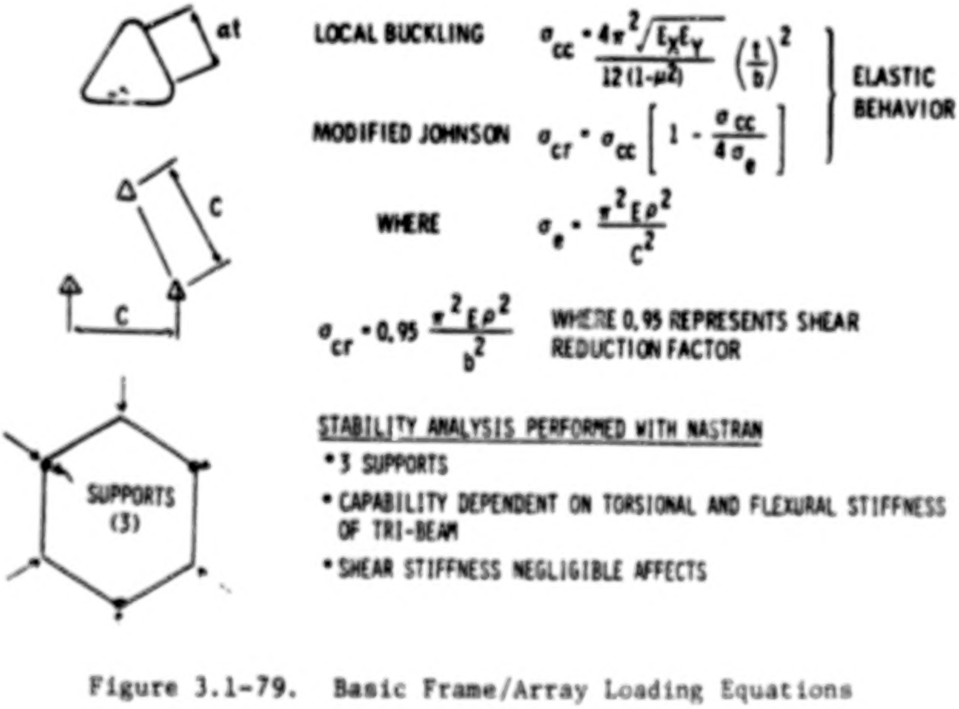
at
LOCAL BUCKLING
$\sigma_{cc} = \frac{4\pi^2\sqrt{E_X E_Y}}{12(1-\mu^2)}\left(\frac{t}{b}\right)^2$
ELASTIC BEHAVIOR
MODIFIED JOHNSON
$\sigma_{cr} = \sigma_{cc}\left[1 - \frac{\sigma_{cc}}{4\sigma_e}\right]$
C
WHERE
$\sigma_e = \frac{\pi^2 E\rho^2}{C^2}$
C
$\sigma_{cr} = 0.95\,\frac{\pi^2 E\rho^2}{b^2}$
WHERE 0.95 REPRESENTS SHEAR REDUCTION FACTOR
SUPPORTS (3)
STABILITY ANALYSIS PERFORMED WITH NASTRAN
• 3 SUPPORTS
• CAPABILITY DEPENDENT ON TORSIONAL AND FLEXURAL STIFFNESS OF TRI-BEAM
• SHEAR STIFFNESS NEGLIGIBLE AFFECTS

Figure 3.1-79. Basic Frame/Array Loading Equations

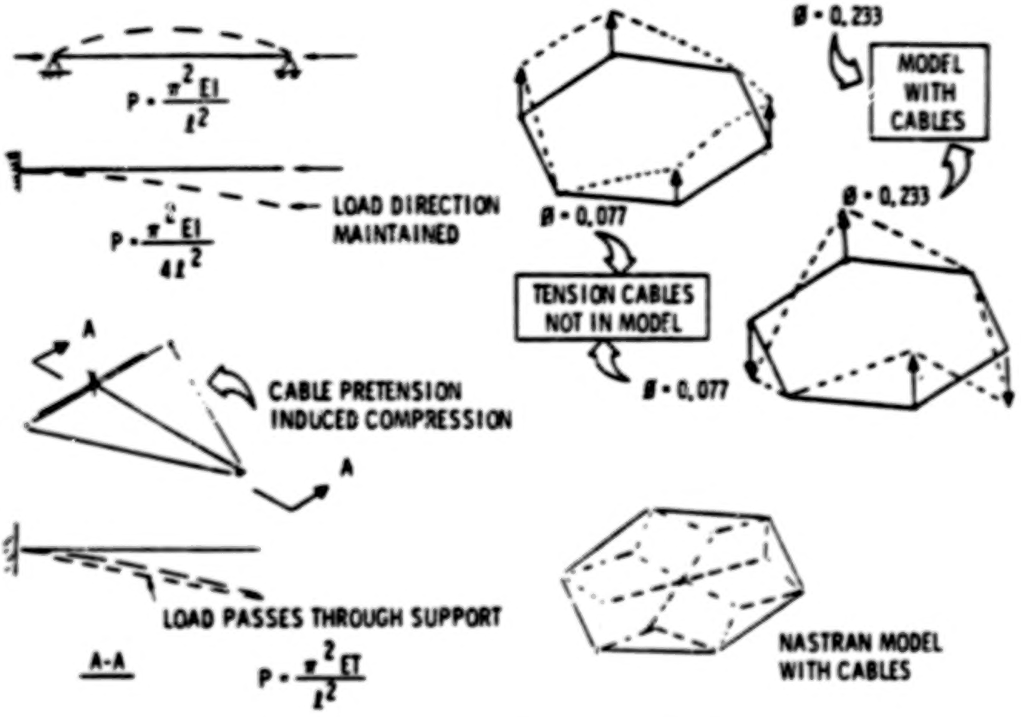
$P = \frac{\pi^2 EI}{\ell^2}$
LOAD DIRECTION MAINTAINED
$P = \frac{\pi^2 EI}{4\ell^2}$
A
CABLE PRETENSION INDUCED COMPRESSION
A
LOAD PASSES THROUGH SUPPORT
A-A
$P = \frac{\pi^2 EI}{\ell^2}$
Ø = 0,233
MODEL WITH CABLES
Ø = 0,233
Ø = 0,077
TENSION CABLES NOT IN MODEL
Ø = 0,077
NASTRAN MODEL WITH CABLES

Figure 3.1-80. Hexagon Frame Stability Considerations

to be negligible and confirmed in the subsequent analysis of the established designs. Through an optimization analysis that addressed the pertinent compression load stability requirements (Figures 3.1-80 and 3.1-81), the significant frame structural sizes and mass were determined in terms of the antenna

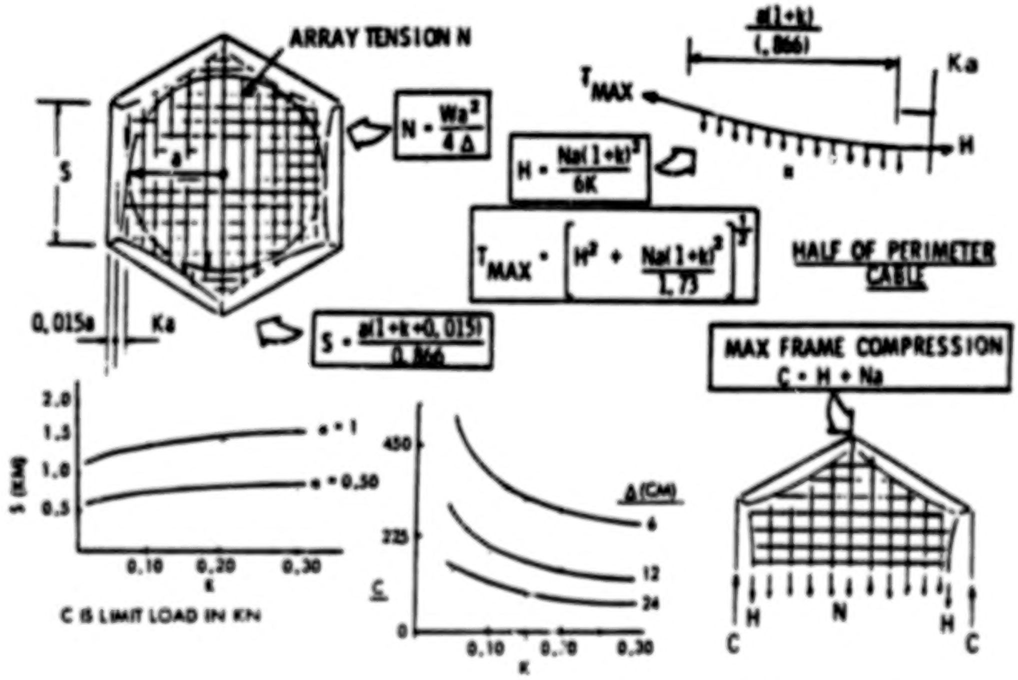
ARRAY TENSION N
a
S
0,015a
Ka
$N = \frac{Wa^2}{4\Delta}$
$S = \frac{a(1+k+0,015)}{0,866}$
$\frac{a(1+k)}{(,866)}$
Ka
T_{MAX}
H
a
$H = \frac{Na(1+k)^3}{6K}$
$T_{MAX} = \left[H^2 + \frac{Na(1+k)^2}{1,73}\right]^{\frac{1}{2}}$
HALF OF PERIMETER CABLE
MAX FRAME COMPRESSION
C = H + Na
2,0
1,5
1,0
0,5
S (KM)
a = 1
a = 0,50
0,10
0,20
0,30
K
C IS LIMIT LOAD IN KN
450
225
0
C
Δ(CM)
6
12
24
0,10
0,20
0,30
K
C
H
N
H
C

Figure 3.1-81. Hexagonal Frame Comparison Stability Criteria

aperture radius, a, and the deflection restriction Δ (Figure 3.1-82). At this stage, the additional surface deflection due to thermal distortions was determined with the appropriate adjustment of the final data (3.1-83). In all the foregoing analysis, the applied loading used was 62.5×10^{-6} N/m^2. The complete study is described in Volume II (Section 3.3).

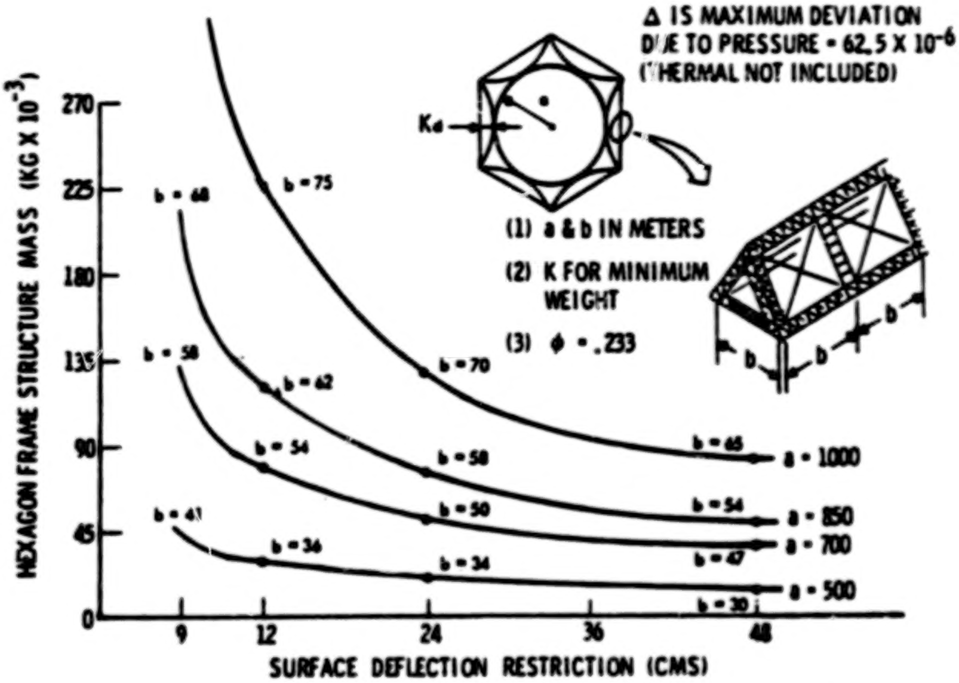

Figure 3.1-82. Hexagonal Frame Mass Variation (Size and Surface Deviation)

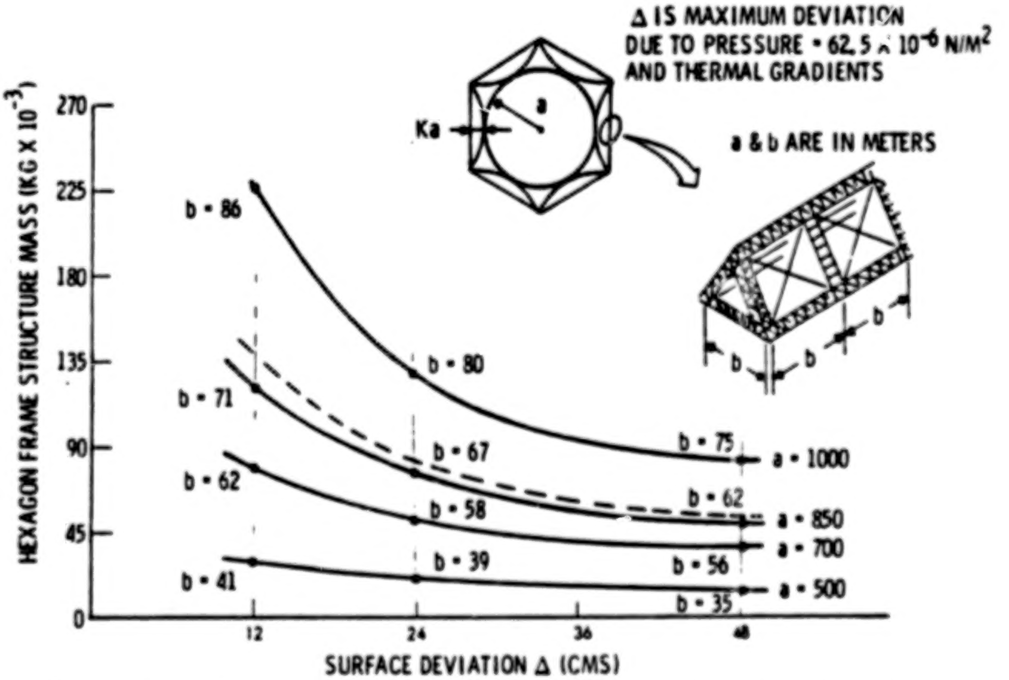

Figure 3.1-83. Hexagonal Frame Mass Vs. Surface Deviation Δ

Secondary Structure

The secondary structure consists of the various brackets, supports, fastening, cables, attachments, etc., required to attach, mount, support, control, or adjust the various primary support subsystems. Supported elements include solar panel suspension items, attitude precision mounting brackets, docking support, etc. As each of these secondary structural groups is unique, although generally well within the present technology, details are not included in this text.

Mass Properties

The contribution to total mass by primary and secondary structures is indicated in Table 3.1-39.

Table 3.1-39. Mass Properties—Structures

	GaAs				GaAlAs/GaAs			
	Reference	Magnetron	End Mounted	Sandwich	Klystron	Magnetron	End Mounted	Sandwich
SOLAR ARRAY								
Primary	0.928	0.904	1.077	3.026	0.804	0.565	0.902	2.138
Secondary	0.586	0.697	0.419	0.386	0.429	0.680	0.331	0.273
INTERFACE								
Primary	0.136	0.136	0.168	N/A	0.136	0.136	0.168	N/A
Secondary	0.034	0.121	0.068	N/A	0.034	0.121	0.068	N/A
ANTENNA								
Primary	0.023	0.023	0.094	0.161	0.023	0.023	0.094	0.143
Secondary	0.815	0.524	1.315	0.568	0.815	0.324	1.315	0.506
Total ($\times 10^6$ kg)	2.522	2.405	3.141	4.141	2.241	2.049	2.848	3.06
Sp. Density (kg/kW)	0.50	0.43	0.60	1.71	0.44	0.37	0.55	1.0

3.1.6 ATTITUDE CONTROL AND STATIONKEEPING SUBSYSTEM

Introduction

This section summarizes the SPS concept evolution trades that impact the attitude control and stationkeeping functions and develop requirements for the attitude control and stationkeeping subsystem (ACSS). The system trades considered a variety of control techniques appropriate to the application of very large SPS spacecraft. The factors considered in the trades included (1) orbit selection, (2) control techniques and spacecraft approaches to prevent unreasonable system implementation penalties, and (3) control system/structural dynamic interaction.

The ACSS requirements are then established for the planar configuration with an end-mounted antenna array and for the dual solid-state sandwich spacecraft.

Planar SPS Configuration

Orbit Selection Trades

The continuous earth visibility and near-continuous solar visibility afforded by the geosynchronous orbit make it highly desirable for SPS, and the only remaining issue was the selection of the inclination of the orbit plane. Three orbits which possess features attractive to SPS are illustrated in Figure 3.1-84. The equatorial orbit is the preferred orbit because it results in no increase in rectenna size.

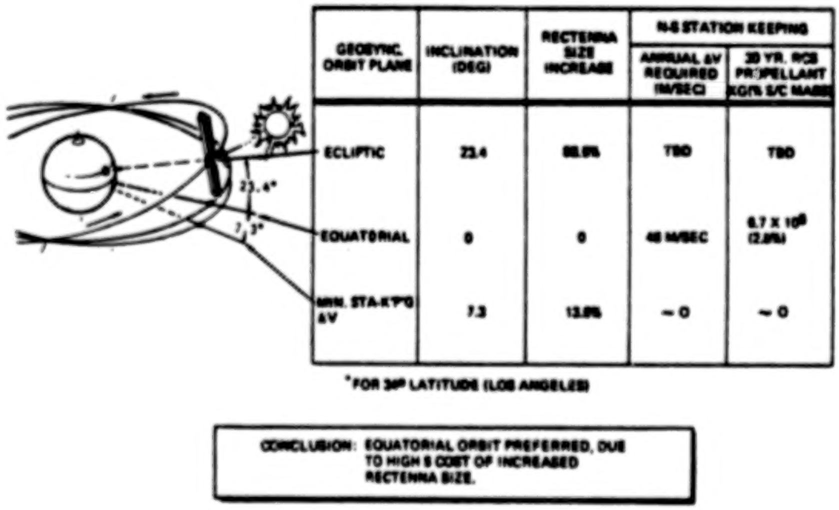

GEOSYNC. ORBIT PLANE	INCLINATION (DEG)	RECTENNA SIZE INCREASE*	N-S STATION KEEPING	
			ANNUAL ΔV REQUIRED (M/SEC)	30 YR. RCS PROPELLANT KG(% S/C MASS)
ECLIPTIC	23.4	88.5%	TBD	TBD
EQUATORIAL	0	0	48 M/SEC	8.7×10^{6} (2.8%)
MIN. STA-KP'G ΔV	7.3	13.8%	~0	~0

*FOR 34° LATITUDE (LOS ANGELES)

CONCLUSION: EQUATORIAL ORBIT PREFERRED, DUE TO HIGH $ COST OF INCREASED RECTENNA SIZE.

Figure 3.1-84. Orbit Selection Trade

Stationkeeping and Attitude Control

The sources of stationkeeping perturbations with associated RCS propellant requirements and control propellant penalty are summarized in Table 3.1-40. The dominant propellant penalty is for the correction of solar pressure induced perturbations. Several stationkeeping policies were considered that included

Table 3.1-40. Stationkeeping Perturbation Sources

FUNCTION	PROPELLANT REQUIRED* (% of S/C Mass Over 30 Years)
Attitude Control	
Gravity gradient torques	0.58
Stationkeeping	
Earth triaxility (E-W)	0.05
Solar/lunar pert. (N-S)	1.25
Solar Pressure (E-W)	
Complete Correction**	7.32
Eclipse effects only	0.05
MW radiation pressure (E-W)	-
Station change maneuvers (E-W)	0.03
TOTAL	9.28
TOTAL WITHOUT SOLAR PRESSURE CORRECTION	1.96

*Isp = 13,000 sec.

**Zero if ±5° longitude perturbations are acceptable

no correction, a Hohmman transfer correction policy, and a constant correction policy. To minimize SPS space requirements in GEO, to prevent satellite interference, and to minimize propellant consumption, the stationkeeping policy selected was one that provides a constant correction.

Because of the impact of the solar pressure force on the ACSS design, a more accurate model was developed to describe the solar pressure force for the planar configuration. The assumption was made that solar energy was reflected specularly off the reflectors and diffusely off the solar cell blankets in the derivation of the model. Figure 3.1-85 shows the major steps taken in the derivation.

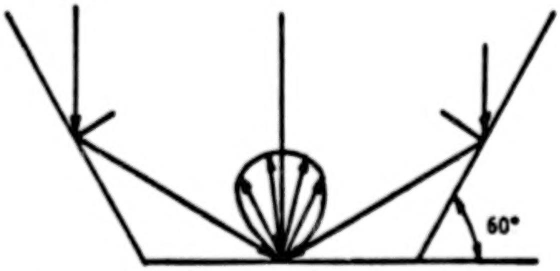

$A_b \overset{\Delta}{=}$ TOTAL AREA OF BLANKET

$A_c \overset{\Delta}{=}$ CAPTURE AREA OF BLANKET $= CR \cdot A_b$

$A_R \overset{\Delta}{=}$ TOTAL AREA OF REFLECTOR

$R_b \overset{\Delta}{=}$ REFLECTIVITY COEFFICIENT OF BLANKET $= 0.17$

$R_R \overset{\Delta}{=}$ REFLECTIVITY COEFFICIENT OF PEFLECTOR $= 0.90$

$$\Sigma F_{sp} = \underbrace{P_s A_b (1+R_b)}_{\text{FORCE ON BLANKET FROM DIRECT SUNLIGHT}} + \underbrace{P_s A_R \cos 60° [(1-R_R)\sin^2 60° + (1+R_R)\cos^2 60°]}_{\text{FORCE ON REFLECTORS FROM DIRECT SUNLIGHT}} + \underbrace{2(1+R_b) R_R P_s A_b \cos^2 60°}_{\text{FORCE ON BLANKET FROM REFLECTED SUNLIGHT}}$$

+ REFLECTIONS FROM BLANKET BACK ON REFLECTORS (NEGLECTED)

$$\Sigma F_{sp} = P_s [A_b (1+R_b)(1+R_R/2) + A_R/2(1-R_B/2)]$$

FOR $CR = 2$, $A_c = 2A_b$ AND SUBSTITUTING $R_b = 0.17$ & $R_R = 0.9$

$$\boxed{\Sigma F_{SP} = 1.125\ P_S\ A_C}$$

OVERALL COLLECTOR HAS EQUIVALENT REFLECTIVITY = 0.125

Figure 3.1-85. Solar Pressure Model

Attitude Control Techniques

Spacecraft Configurations

Since attitude control requirements for very large SPS vehicles are substantially different (at least in magnitude) from small contemporary spacecraft, various spacecraft configurations were considered and are shown in Figure 3.1-86. These include spin stabilization, gravity-gradient stabilization, and solar vanes to provide control torques for stability. Each of these concepts was rejected either for increased complexity or increased mass. The baseline planar SPS configuration is illustrated in Figure 3.1-87 along with the pertinent features of the baseline ACSS.

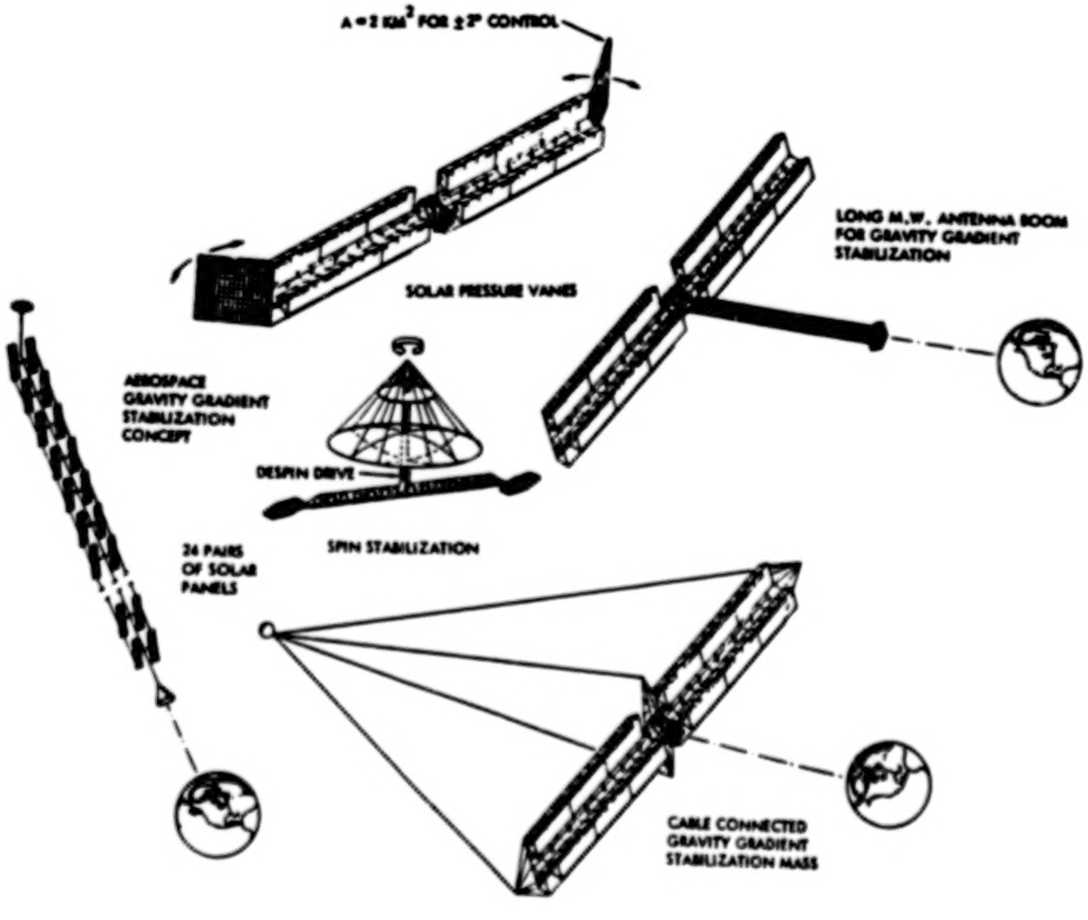
A = 2 KM² FOR ± 2° CONTROL
SOLAR PRESSURE VANES
LONG M.W. ANTENNA BOOM FOR GRAVITY GRADIENT STABILIZATION
AEROSPACE GRAVITY GRADIENT STABILIZATION CONCEPT
DESPIN DRIVE
SPIN STABILIZATION
24 PAIRS OF SOLAR PANELS
CABLE CONNECTED GRAVITY GRADIENT STABILIZATION MASS

Figure 3.1-86. Some Alternative Configurations Considered

Attitude Control Subsystem Approaches

Several attitude control techniques were investigated which included space-constructed momentum wheels, quasi-inertial free-drift mode, inertia balancing, and various reaction control propulsion types as well as reference orientation options. The trades are summarized in Figure 3.1-88 and Table 3.1-41. The selected baseline ACSS is an RCS system using argon as the propellant. The reference attitude is Y-POP, X-IOP orientation.

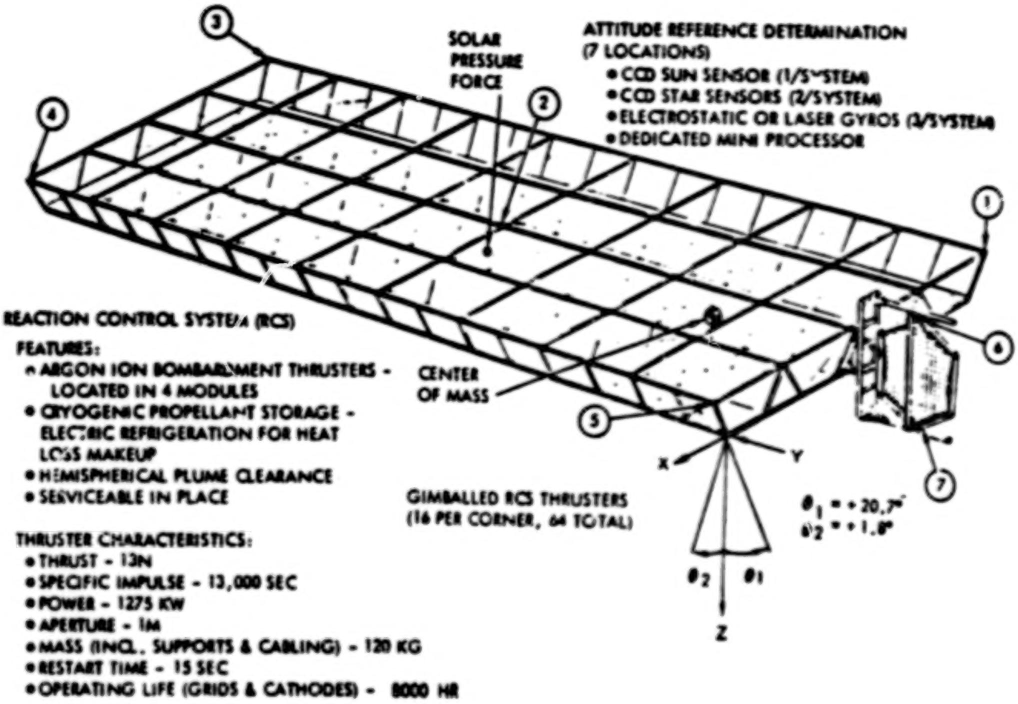
③
④
SOLAR PRESSURE FORCE
②
ATTITUDE REFERENCE DETERMINATION (7 LOCATIONS)
• CCD SUN SENSOR (1/SYSTEM)
• CCD STAR SENSORS (2/SYSTEM)
• ELECTROSTATIC OR LASER GYROS (3/SYSTEM)
• DEDICATED MINI PROCESSOR
①
REACTION CONTROL SYSTEM (RCS)
FEATURES:
• ARGON ION BOMBARDMENT THRUSTERS - LOCATED IN 4 MODULES
• CRYOGENIC PROPELLANT STORAGE - ELECTRIC REFRIGERATION FOR HEAT LOSS MAKEUP
• HEMISPHERICAL PLUME CLEARANCE
• SERVICEABLE IN PLACE
THRUSTER CHARACTERISTICS:
• THRUST - 13N
• SPECIFIC IMPULSE - 13,000 SEC
• POWER - 1275 KW
• APERTURE - 1M
• MASS (INCL., SUPPORTS & CABLING) - 120 KG
• RESTART TIME - 15 SEC
• OPERATING LIFE (GRIDS & CATHODES) - 8000 HR
CENTER OF MASS
⑤
⑥
⑦
X
Y
Z
GIMBALLED RCS THRUSTERS (16 PER CORNER, 64 TOTAL)
θ1 = + 20.7°
θ2 = + 1.8°
θ2
θ1

Figure 3.1-87. ACSS Equipment Locations

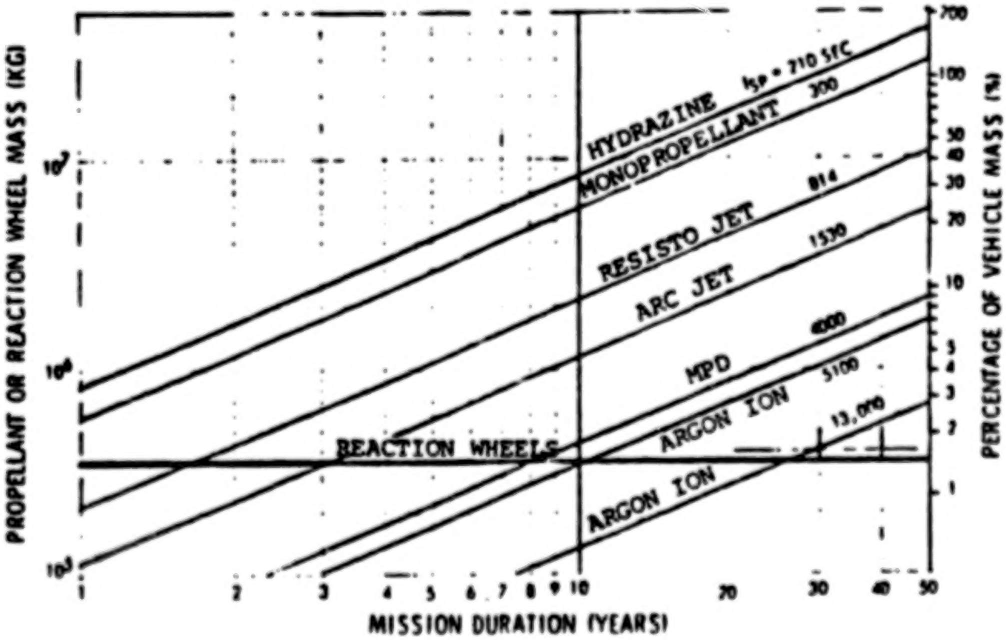

Figure 3.1-88. Attitude Control Propellant and Reaction Wheel Mass (Y-POP, X-IOP)

Table 3.1-41. Attitude Control System Concept Comparison

ATTITUDE	ATTITUDE CONTROL SYSTEM	30-YR RCS PROP REQMT^1 (% VEH MASS)^6	MOM. STORAGE SYSTEM MASS (% VEH MASS)^6	MASS COLLECTOR LOSS DUE TO PT ERROR (%)	COMMENTS
(A) -Z-SUN X-IOP	RCS ONLY	28.6	0	0	SECULAR DISTURBANCE TORQUES, PROP REQMTS CANNOT BE REDUCED WITH WHEELS OR FDAMS, NOT VIABLE
(B) Y-POP X-IOP	1. RCS ONLY (BASELINE)	4.27	0	8.2 (4.11% ANNUAL AVG)	BASELINE CONFIGURATION
	2. RCS + 2-D BAL^4	1.60^5	0	8.55	CANTING PAYS OFF, PREFERRED Y-POP OPTION
	3. RCS + FREE DRIFT	1.60^5	0	13.4 (CR = 1)	UNACCEPTABLE COLLECTOR LOSS FOR CR >1
	4. MOMENTUM STORAGE	NEGLIGIBLE^2	1.5	8.2	GOOD ALTERNATIVE IF HIGH I_{sp} RCS NOT ACHIEVABLE
(C) Z-SUN Y-IOP	1. RCS ONLY	44.1	-	0	EXCESSIVE RCS PROP RESUPPLY REQD, LARGE CYCLICAL DISTURBANCE TORQUES
	2. RCS + 2-D BAL^4	33.8	-	0.38	EXC. RCS RESUPPLY REQD
	3. RCS + 2-D BAL^4 + FREE DRIFT	1.52	-	5.7	FREE DRIFT REALLY PAYS OFF! PREFERRED Z-SUN OPTION
	4. MOM. STORAGE	NEGLIGIBLE^2	5.8 ^{3}	0	ACCEPTABLE ALTERNATIVE
	5. MOMENTUM STORAGE + 2-D BAL^4	NEGLIGIBLE^2	5.7 ^{3}	0	ACCEPTABLE ALTERNATIVE

[1] BASED ON ONE-DEGREE PRINCIPAL AXIS MISALIGNMENT, I_{sp} = 5100 SEC
[2] DUMP MOMENTUM WITH GRAVITY-GRADIENT TORQUES
[3] THREE MOMENTUM WHEELS
[4] TWO-DIMENSIONAL INERTIA BALANCING
[5] POTENTIAL FOR SIGNIFICANT PROPELLANT REDUCTION WITH SMART CONTROL POLICY
[6] SPACECRAFT MASS = 24.15×10^6 kg

ACSS Baseline Description

Referring to Figure 3.1-87, the baseline ACSS features an argon-ion bombardment thruster RCS whose characteristics are enumerated on the figure. The system operates an average of 36 thrusters. A total of 64 thrusters is included to provide the required redundancy. The redundancy was based on an annual maintenance/servicing interval, 5000-hour thruster grid lifetime, and five-year thruster MTBF. Sixteen thrusters are located on the lower portion of each corner of the spacecraft. Each thruster is gimbaled individually to facilitate thruster servicing, to permit operation of adjacent thrusters during servicing, and to provide the redundancy. The thrusters nominally establish a force vector approximately in the direction of the sun to counter the solar pressure force (stationkeeping) which is the dominant thruster requirement. The thrusters are gimbaled through small angles (as illustrated) and differentially throttled to provide the remaining forces and torques for attitude control and stationkeeping.

Also shown in Figure 3.1-87 are the locations and type of sensors that make up the attitude reference determination system (ARDS). The mass properties of the ACSS are summarized in Table 3.1-42. The summary includes the mass of the individual elements and propellant mass. The system average operating power, which is proportional to propellant mass, is 33.87 megawatts.

Table 3.1-42. ACSS Mass Summary

Item	Mass ($\times 10^{-3}$ kg)
Attitude reference determination systems (7)	0.32
Thrusters—including support structure, 64 @ 120 kg/thruster	7.68
Thruster gimals and mounting	1.00*
Tanks, lines, refrigeration	15.07
Power processing equipment (1.3 kg/kW)	43.93*
Solar array	48.00*
Argon propellant—annual requirement	85.39
Total (dry)	116.0
Total (with propellant)	201.39
*Estimated	

The ACSS is capable of permitting partial solar pointing with no increase in propellant and thruster penalty. A bank angle of up to 9.0 degrees can be realized with no loss of control authority and propellant penalty. For a bank angle of 9 degrees, the collector cosine loss is reduced to 3.2% from 8.2% for the Y-POP orientation. The reduction in cosine losses results in reducing the solar collector size requirement.

Control System/Structural Dynamic Interaction

Due to the large size and relatively small mass of the SPS structure, considerable concern was initially expressed that the structural frequencies would not be high enough to permit satisfactory control. As a result, an analysis was performed to define control system bandwidth and structural frequency requirements. Fortunately, the results indicate that the SPS operational control does not require wide bandwidth relative to some other satellites, and satisfactory structural frequencies are easily achievable through structural design concepts that have reasonable depth.

The control system must be capable of providing reasonable pointing accuracy in the presence of both constant and cyclical gravity-gradient torque which is the dominant operational disturbance torque the controller must accommodate. The control gains are selected to provide this stiffness. The bandwidth data are presented in Figure 3.1-89. A control bandwidth of 5.44 times the orbit frequency is found for a design point of 0.5-degree principal axis misalignment and a pointing error of 0.05 degree. A frequency separation exists between the control bandwidth and structural frequency. For LEO, this separation is small; however, it is quite large for the operational orbit—GEO.

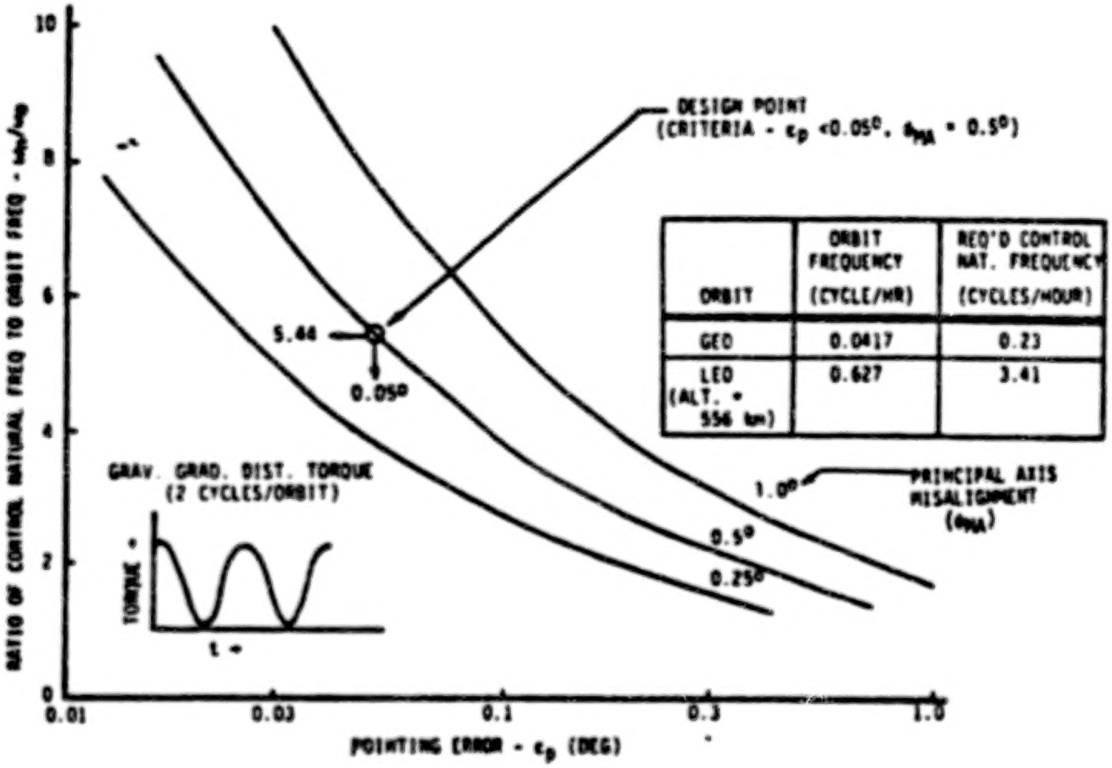

ORBIT	ORBIT FREQUENCY (CYCLE/HR)	REQ'D CONTROL NAT. FREQUENCY (CYCLES/HOUR)
GEO	0.0417	0.23
LEO (ALT. = 556 km)	0.627	3.41

Figure 3.1-89. Control Bandwidth Requirement

Stability analysis was performed using a model that included three bending modes in the flexible body dynamics. A controller employing a simple compensation network was found to meet the control bandwidth requirements and to provide stable operation for the first three bending modes. A second controller, using a Luenberger observer for estimation of bending characteristics, was synthesized and found to provide even better stability. A third concept, using multiple attitude sensors distributed along the spacecraft structure, was also synthesized and found to provide a powerful means for decoupling the control system and the dominant bending modes. Stability is achievable without employing such exotic techniques as distributed actuators.

Solid-State Configuration (Sandwich)

This section deals with the evolution of the ACSS requirements for the solid-state concepts. The single solid-state concept exhibits large gravity-gradient and solar pressure torques resulting from spacecraft asymmetry. The asymmetry reflects the large cp-cg offset of the primary mirror and the large mass c.g. offset of the sandwich antenna and primary mirror. Because of the symmetry of the dual solid-state configuration, the disturbance torques are reduced substantially. Each configuration has large solar pressure forces due to the large surfaces of the primary and secondary mirror systems. The solar pressure correction for stationkeeping has a large impact on the ACSS design.

The orbit selection and flight attitude remain the same as the planar configuration. The orbit is equatorial and the operational attitude is Y-POP. The main body which consists of the sandwich antenna, secondary mirror, and associated structure is in a local vertical attitude and the attitude of the primary mirror is solar inertial.

The solid-state configurations considered were (1) the concept that included the ring to provide the base of rotation for the primary mirror, and (2) the concept with a ball joint pivoted primary mirror. The ring concept was found to be undesirable because of complex construction problems. The emphasis is on the ACSS requirements for the ball joint pivoted primary mirror which includes a single solid-state sandwich and a dual solid-state sandwich concepts. The spacecraft are illustrated in Figure 3.1-90. In both spacecraft, the primary mirror system, which consists of eight mirrors mounted tangent to a parabola of revolution providing the concentration ratio, and the elliptical reflectors direct the solar energy to the solar cells.

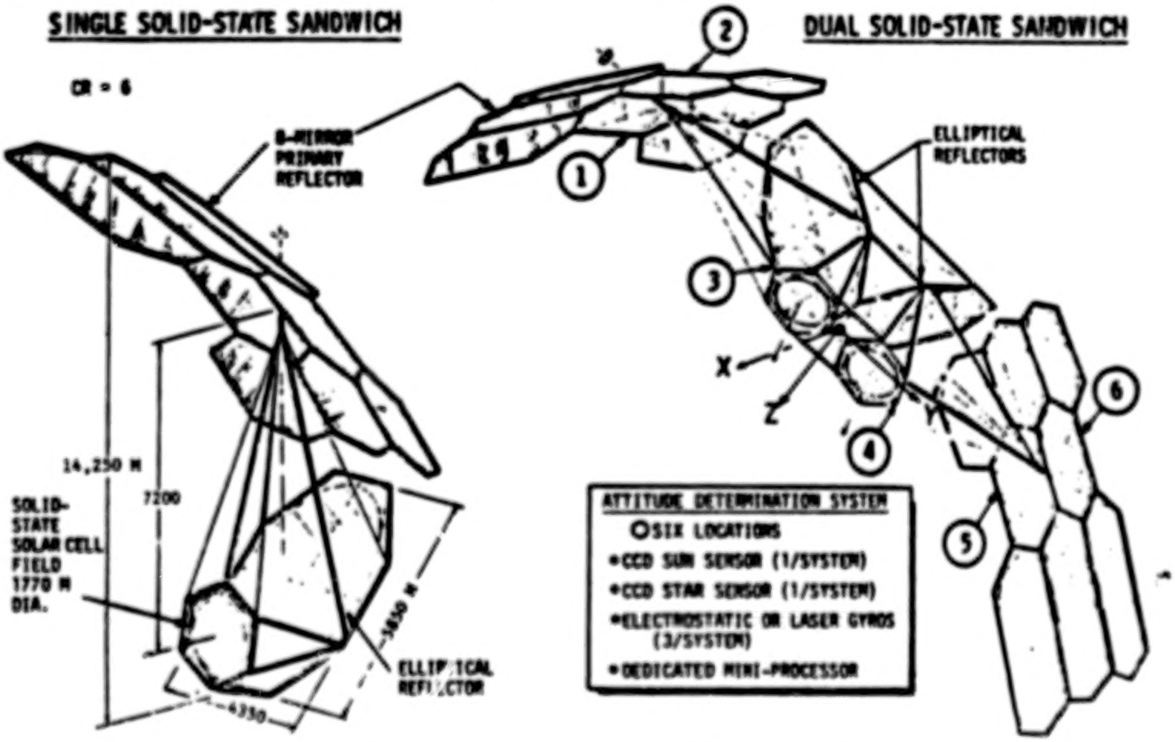
SINGLE SOLID-STATE SANDWICH
DUAL SOLID-STATE SANDWICH
CR = 6
8-MIRROR PRIMARY REFLECTOR
14,250 M
7200
SOLID-STATE SOLAR CELL FIELD 1770 M DIA.
5850 M
4330
ELLIPTICAL REFLECTOR
ELLIPTICAL REFLECTORS
①
②
③
④
⑤
⑥
X
Z
ATTITUDE DETERMINATION SYSTEM
○ SIX LOCATIONS
• CCD SUN SENSOR (1/SYSTEM)
• CCD STAR SENSOR (1/SYSTEM)
• ELECTROSTATIC OR LASER GYROS (3/SYSTEM)
• DEDICATED MINI-PROCESSOR

Figure 3.1-90. Solid-State Concepts

Impact of Solar Pressure

A major concern in an ACSS design is the propellant mass required over the lifetime of the spacecraft. For all SPS configurations, the stationkeeping of the solar pressure force is one of the dominant drivers affecting propellant consumption. As shown in Figure 3.1-91, the solar pressure force is directly proportional to the effective or capture area and, thus, the propellant mass is proportional to the area independent of spacecraft mass. The solid-state-type SPS have large area-to-mass ratio which drives up the percent of spacecraft mass over 30 years' number. This is clearly demonstrated in Figure 3.1-91. The effective areas of the planar and solid-state are essentially the same, but the area-to-mass ratio is 1.89 for the planar and 7.81 for the solid-state which directly reflects in the 6.3 and 26% of spacecraft mass requirements, respectively. Thus, for a solid-state-type SPS the expected minimum achievable propellant mass is in the range of approximately 22 to 27%, providing stationkeeping is a requirement.

- SOLAR PRESSURE FORCE: $F_S = P_S A^*$

  A = EFFECTIVE AREA OR CAPTURE AREA

- PROPELLANT CONSUMPTION

$$M_p = \left[\frac{P_S\ t\ SEC/YR}{g\ I_{SP}}\right] A$$

- PROPELLANT PROPORTIONAL TO AREA INDEPENDENT OF SPACECRAFT MASS

CONFIGURATION	AREA $(m^2 \times 10^6)$	PROPELLANT $(kg/yr \times 10^4)$	S/C MASS $(kg \times 10^6)$	% S/C MASS OVER 30 YR
PLANAR	69	7.67	36.6	6.3
SINGLE SOLID-STATE SANDWICH	64	7.12	8.19	26

*NOTE:

$$A \overset{\Delta}{=} \sum_i \left(\text{SURFACE GEOMETRY, ORIENTATION, REFLECTIVITY}\right)_i$$

Figure 3.1-91. Impact of Solar Pressure

ACSS Requirements

The RCS requirements for the single solid-state and dual solid-state spacecraft are presented in Table 3.1-43. Referring to the table, three approaches of thruster arrangements were considered for the single solid-state and only one for the dual solid-state because the disturbance torques were small.

In the first approach, the primary mirror is considered to be free-pivoted and the control torques result from thrusters located on the secondary mirror structure. The second and third options have servo motors to control the primary mirror relative to the main body, and the thrusters to control large disturbance torque along the X-axis (M_X) are located on the primary mirror.

In the latter two approaches, longer moment arms are available which results in propellant savings. The difference between the two options is that in the second M_x control, thrusters are radially fixed, and in the third the thrusters are inertially fixed. Inertially fixed thrusters are stationary with respect to the primary mirror, and radially fixed thrusters rotate once per orbit relative to the mirror to maintain a thrust direction along the radial Z-axis. The locations of the stationkeeping thrusters remained the same for the three solid-state thruster configurations.

Table 3.1-43. RCS Requirements

	PROPELLANT (KG/YRx10^4)	% S/C MASS OVER 30 YR	THRUSTERS REQUIRED*
SINGLE SOLID-STATE SANDWICH			
•FREE-PIVOTED PRIMARY MIRROR			
•M_x ATTITUDE CONTROL THRUSTERS MOUNTED ON SECONDARY MIRROR	15.5	56.9	73
•SERVO MOTORS CONTROL PRIMARY MIRROR WITH RESPECT TO MAIN BODY			
•M_x ATTITUDE CONTROL THRUSTERS MOUNTED ON PRIMARY MIRROR. RADIALLY FIXED	11.5	41.1	63
•M_x ATTITUDE CONTROL THRUSTERS MOUNTED ON PRIMARY MIRROR. INERTIALLY FIXED	13.5	48.6	111
DUAL SOLID-STATE SANDWICH	15.0	27.5	90

*SPARES NOT INCLUDED.

For the single solid-state spacecraft, the highest propellant penalty of 56.9% over the lifetime of the spacecraft resulted from the first approach, and the highest number of thrusters which total 111 (not including spares) resulted from the third arrangement. The second approach results in the lowest propellant and thruster requirements. A propellant penalty of 41.1% of spacecraft mass over 30 years was achieved, and an average of 63 thrusters is required to operate. Reductions of propellant mass of 15.8% and 7.5% were obtained relative to configurations one and three, respectively. Thus, the preferred approach is the second option.

The dual spacecraft has a propellant penalty of 27.5% of spacecraft mass over 30 years, which approaches the minimum achievable value for the solid-state sandwich concepts. A reduction in propellant penalty of 13.6% is realized compared to the preferred approach for the single solid-state vehicle. The dual spacecraft is an attractive concept.

The RCS which features an argon-ion bombardment thruster with $I_{sp} = 13,000$ seconds operates an average of 90 thrusters. A total of 146 is included to provide the necessary redundancy. The redundancy is based on the same criteria as the baseline planar ACSS. Referring to Figure 3.1-92, the thrusters are located on the centerline at the tips of the primary mirror and at opposite ends of the minor axis of the secondary mirror. The thrusters on the primary mirror are gimbaled ±11.75° to compensate for the mirror motion to track the sun travel of ±23.5° from the equinox position. The function of these thrusters is to provide (1) stationkeeping for the solar pressure which results from direct sunlight and reflected sunlight off the secondary mirror and solar-lunar perturbation, and (2) attitude control for the disturbance torque along the X-axis. Only two thrusters which are radially fixed are required for control about the X-axis. The thrusters mounted on the secondary mirror provide the stationkeeping of the solar pressure force resulting from direct sunlight on the mirror and control torques to correct the gravity-gradient disturbance torques about the Y and Z axes. The radial thrusters are differentially gimbaled to deliver control along these axes.

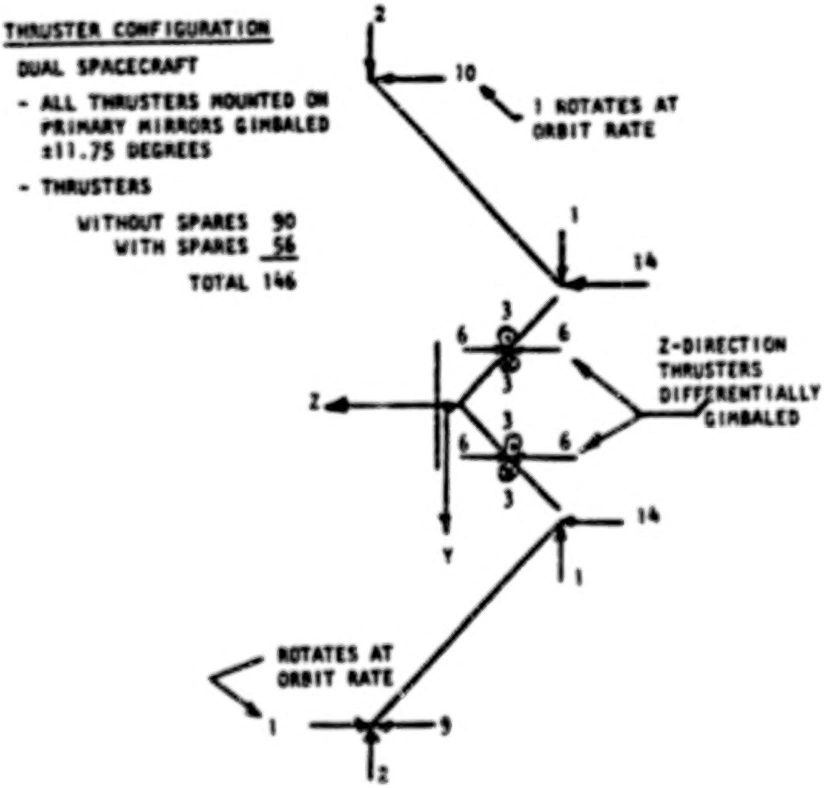
THRUSTER CONFIGURATION
DUAL SPACECRAFT
- ALL THRUSTERS MOUNTED ON PRIMARY MIRRORS GIMBALED ±11.75 DEGREES
- THRUSTERS
WITHOUT SPARES 90
WITH SPARES 56
TOTAL 146
2
10
1 ROTATES AT ORBIT RATE
1
14
3
6
6
3
Z
3
6
6
3
Z-DIRECTION THRUSTERS DIFFERENTIALLY GIMBALED
14
Y
1
ROTATES AT ORBIT RATE
1
9
2

Figure 3.1-92. Thruster Configuration

In Figure 3.1-90 are shown the locations of the attitude reference determination system (ARDS). The ARDS used in the dual spacecraft and the planar configuration is the same.

The mass properties are summarized in Table 3.1-44. The summary includes the mass of the individual elements and propellant mass. The average power required which is proportional to propellant consumption is 59.34 megawatts.

Table 3.1-44. ACSS Mass Summary

Item	Mass ($\times 10^3$ kg)
Attitude determination system	0.23
Thruster—including support structure —146 @ 120 kg	17.52
Tanks, lines, and refrigeration	25.45
Power processing equipment	-
Supporting solar arrays	60.0
Argon propellant (annual requirement)	149.88
Total (dry)	103.2
Total (with propellant)	253.08

3.1.7 THERMAL CONTROL

Introduction

The design of a solar power satellite is significantly influenced by thermal and thermal control considerations. The importance of this subsystem may extend well beyond the designation of the specific thermal control components inasmuch as it is a major contributing element in the selection of structural configuration, power generation and distribution network orientation, antenna power levels and layout, and the number and location of rotary joint slip rings.

The general discussion will center upon the Rockwell reference configuration. The other configurations, both planar and unique, will be discussed at appropriate points in this section.

A special note that must be made is that although the solar array structure modal configuration used in the NASTRAN is not the present reference configuration, the resulting conclusions remain valid.

Main Array

A model of the April 1978 baseline design was constructed to determine the adequacy of the design to meet blanket operating temperature specifications, and to identify the effect of coating optical properties on thermal gradients for incorporation in structural response analyses. The cross-sectional aspect of the modeled array is shown in Figure 3.1-93. Preliminary NASTRAN computations were based on the assumption that the basic material is anodized aluminum with values of $\alpha = 0.4$ and $\epsilon = 0.8$ for absorptivity and emissivity, respectively.

Several graphite fiber composites were also considered as candidates for the satellite. The thermal profile for the composite-based structure is shown in Figure 3.1-94. Table 3.1-45 summarizes the estimated maximum temperature (based upon General Dynamics quoted data and on Rockwell estimates) for the various candidates.

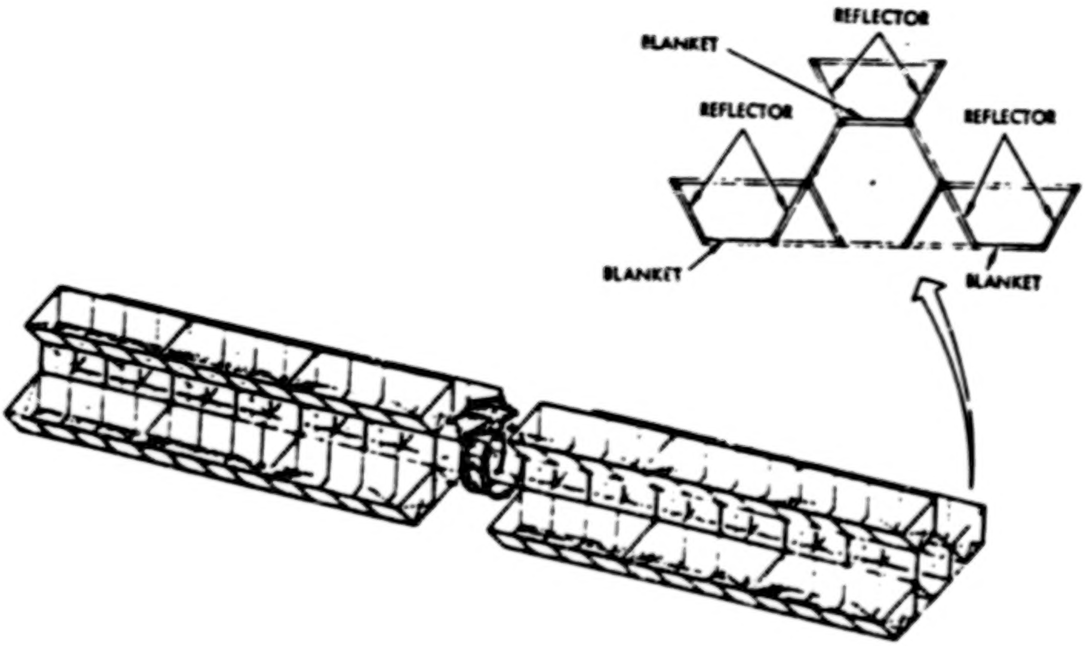
REFLECTOR
BLANKET
REFLECTOR
REFLECTOR
BLANKET
BLANKET

Figure 3.1-93. Photovoltaic Structure Model

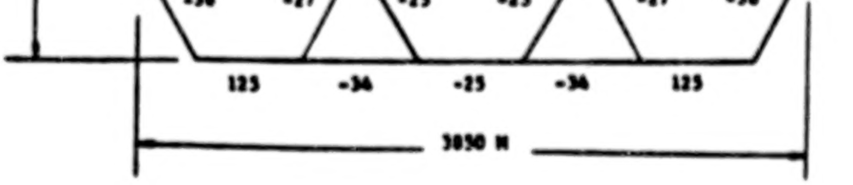
91
All temperatures
in degrees celsius
End of Life
Coated Graphite Composite
α = 0.89
ε = 0.86
7
7
125
1753.7 M
-37
-37
97
97
-36
-27
-25
-25
-27
-36
125
-34
-25
-34
125
3050 M

Figure 3.1-94. Photovoltaic Structural Configuration Temperatures (Graphite Composite)

Table 3.1-45. Maximum Estimated Temperatures
(Graphite Composite)

Material	Maximum Allowable Temperature (°K)
Thermosetting resins	
• Epoxy	395
• Phenolic	435
• Polyimide	
− Addition	475
− Condensation	560
Thermoplastic materials	
• Polysulfone	380
• Polyimide	590

The temperature of the solar blankets is 110°C to 112°C. As it is desired to operate at a temperature between 113-125°C to promote the GaAs self-annealing characteristic, some modification to the blanket design is expected. Because of the temperature uniformity of the three blanket sections, any changes introduced would be common to the array. The simplest approach is to reduce the rear surface emissivity from the design value of 0.68 to 0.36; this can be achieved at a negligible weight impact by the somewhat complex approach of vapor depositing a mosaic grid of several hundred angstroms of aluminum or, more simply, by adding approximately 1/4 mil of Kapton (or Mylar) rear-surface-coated aluminum to the blanket. The required emissivity reduction would be moderated if self-annealing could be satisfied by periodic shutdown of individual bays to increase thermal loads through elimination of electrical conversion. The selected approach was to add the thin aluminized plastic layer.

Switch Gear

At 99.9% efficiency, thermal losses per unit are 12,000 W, and this level is accommodated by appropriate sizing to permit passive rejection. Relative base dimension requirements as a function of design temperature are shown in Figure 3.1-95 for a cubic configuration. At a postulated allowable temperature of 60°C, a length of 2 m is adequate and, consequently, it is expected that any mass additions relative to the previous design concept of a 1-m cubed casing will be minimal.

The thermal impact on the main array of the dual solid-state sandwich configuration (Figure 2.1-4) differs primarily in that (1) separate solar photovoltaic cells are not of concern, and (2) the secondary mirror receives a thermal load equivalent of 6 to 7 suns during normal operation. The major concern in the latter case was that the surface temperature of the secondary mirror not exceed approximately 200°C.

The analysis was made on a steady-state basis, since thermal equilibration will take place in a few seconds. The secondary mirror is defined as aluminized Kapton with a baseline thickness of 12.5 μm (0.5 mil). A 25-μm (1.0-mil)

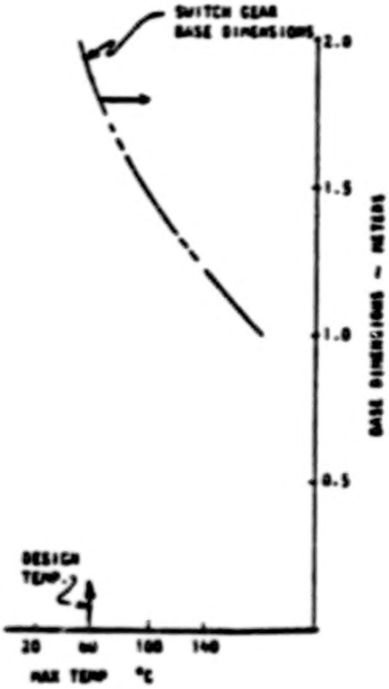

Figure 3.1-95. Power Distribution Component
Thermal Control—Switch Gear

thickness was also considered for comparison. The mirror is heated by the concentrated beam (6.35 suns) from the primary and also by direct sunlight in some orientations. It will also be heated by thermal radiation from the solar panel, assumed to be operating at 200°C. An average configuration factor of 0.2 was assumed between panel and secondary. The thermo-optical properties adopted for the mirror are summarized in Table 3.1-46.

Table 3.1-46. Reflector Thermo-Optical Properties

Property	First Surface	Second Surface (12.5-μm Kapton)	Second Surface (25-μm Kapton)
Reflectivity	0.83	--	--
Solar α	0.17	0.14	0.14
Thermal ϵ	0.10	0.58	0.63

Calculations were carried out, with and without direct sun on the second surface. Solar intensity was taken to be 1385 W/m^2 (winter solstice). The results of the analysis are shown in Table 3.1-47 and are predicted to be less than the 200°C limit.

Table 3.1-47. Reflector Predicted Temperatures

KAPTON THICKNESS	DIRECT SUN	TEMPERATURE (°C)
12.5 μ	YES	186
	NO	172
25.0 μ	YES	179
	NO	166

Microwave Antenna

Thermal control of the microwave antenna includes the protection of the power amplifiers, associated electronics, and the antenna structure.

Four variations of microwave power amplification will be considered in this section: (1) klystron, (2) magnetron, (3) decoupled solid-state, and (4) "sandwich." Because of the unique aspects of each approach, each will be discussed independently of the other although, by so doing, there will be some redundancy in the discussion.

Klystron

The antenna structure configuration can experience minimal distortions/deflections due to imposed thermal gradients/stresses. A thermal model of the hexagonal frame/web structure was developed for variable solar orientations to determine peak operating temperatures and thermal gradients, and to support dynamic structural response computations. The model, shown in Figure 3.1-96, assumed that the earth side of the web would be treated as an isothermal section at T = 200°C, and the space side of the web could be fixed at an isothermal temperature of 60°C. This represents a simplification because the hot side of the web will vary with time due to solar loading, and will vary with distance from the center due to antenna density and size variation. There may also be some influence by the higher temperature collector radiators (≈700°C) (klystrons) on structural temperature. The transmitting side of the antenna changes temperature with sun loading also, and will probably operate between 0°C and 60°C (effective temperature).

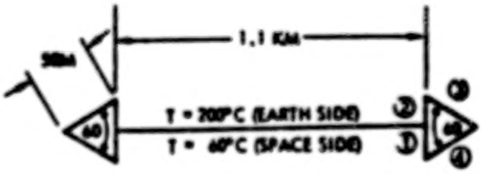

ENCIRCLED NUMBERS REPRESENT SECTION NODES

Figure 3.1-96. Antenna Frame/Web Model

Nodal points were selected as shown (Figure 3.1-96), and the thermal analysis was conducted assuming that each section was represented as a uniform node at a single temperature. View factors to space and from element to element were determined from an exact representation of the section by using the CONFAC computer code.

Due to variation in solar incidence during each orbit, the sections of the frame will experience time-varying temperature. Temperature profiles are shown in Figure 3.1-97 for a typical orbit representing the response of low α/ε anodized structural coating and, in Figure 3.1-98, for a degraded coating condition. (It could also represent a "dark" or high α/ε anodized structural coating.) For an eclipse condition, the minimum temperature levels and thermal profiles would markedly change. Temperature gradients during construction would also influence the structural design.

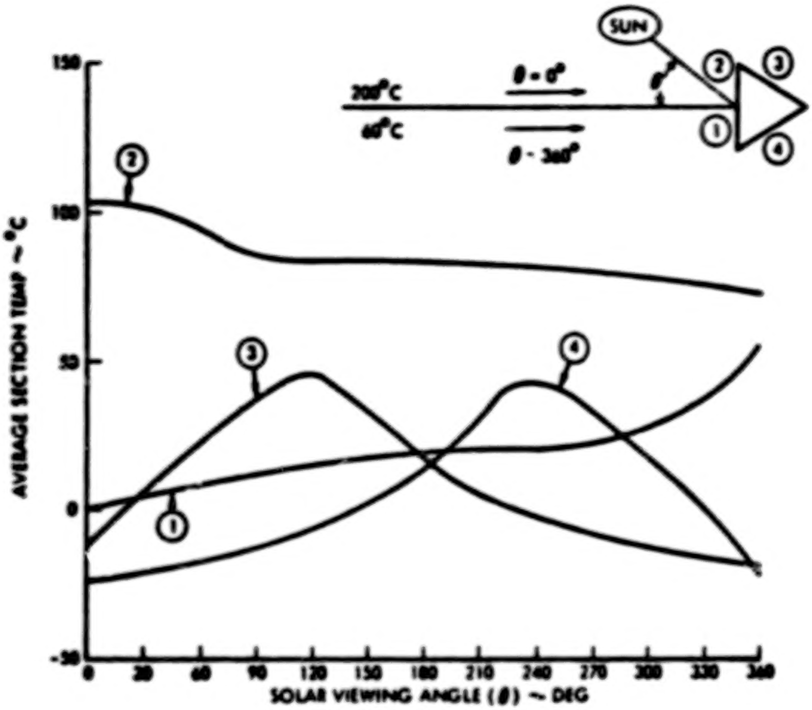

Figure 3.1-97. Frame Temperature Variation with Solar Orientation (BOL)

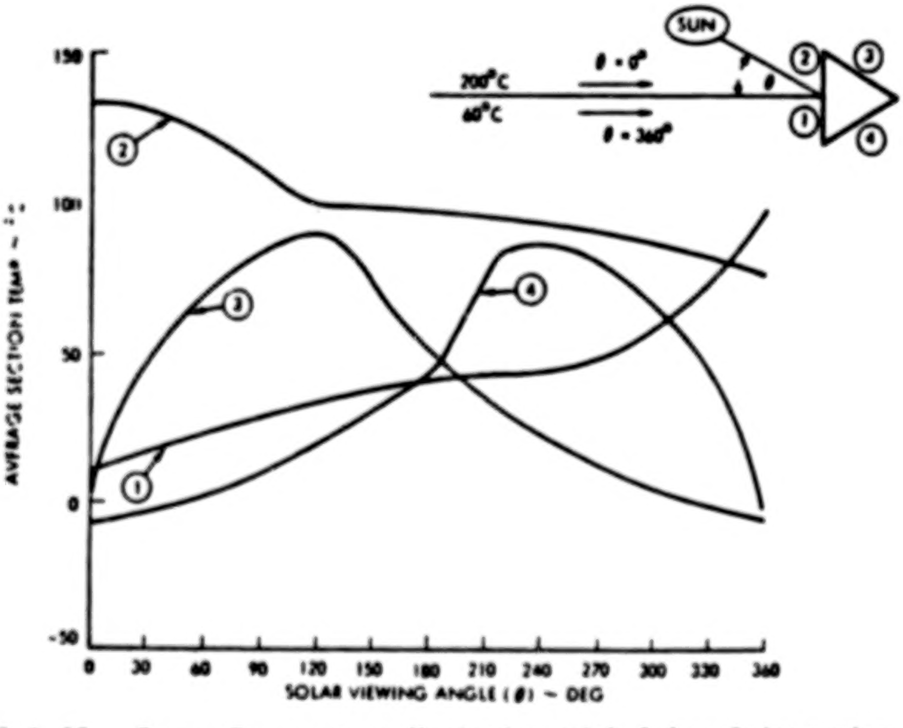

Figure 3.1-98. Frame Temperature Variation with Solar Orientation (EOL)

In the space frame configurations the primary structure is in close proximity to the high-temperature, heat-rejection surface of klystrons. Independent studies by Rockwell, General Dynamics, and Grumman have demonstrated that temperatures in the central region of the antenna will exceed allowables for low temperature composites. For beam machine concepts this can complicate the construction scenario by potentially requiring the substitution of a different machine at some point in the assembly sequence. This problem is illustrated in Table 3.1-48 for the candidate polysulfone resin, assuming a "worst case" condition. In this environment, the temperature could exceed the allowable maximum even if the klystron heating is neglected.

Table 3.1-48. Space Frame Configuration Limitations of Low-Temperature Composites

- Assume maximum allowable temperature = 380°K; $\alpha_s = 0.9$, $\varepsilon = 0.8$

  For these properties the maximum allowable effective antenna temperature is (approximately):

  $$(0.9)(1352) + 0.8\sigma(T_{max}^4 - 400^4) = 0.8\sigma \text{ or } T_{max} = 395°K$$

- For "worst case" solar loading on antenna (even if klystron emits zero power) assuming radiator has black coating and zero capacitance structure

  $$(0.93)(1352) = 0.85\sigma T^4 \text{ or } T_{max} = 402°K$$

∴ Under worst-case assumptions, low temperature composites may be marginal for zero power klystrons.

For compression frame/tension-web structures this situation cannot occur. The frame will experience relatively low temperatures and the secondary structure is sufficiently removed from the center of the antenna to permit application of low temperature composites. This represents a substantial thermal advantage for tension-web structures.

A thermal control design was developed for the klystron tubes to dissipate the waste heat levels and minimize interactions with the antenna structure and rotary joint. The thermal rejection study requirement included a cavity heat load of 3.267 kW and a collector heat load of 7.454 kW. Initial assumption was that the majority of the waste heat rejection could be from the "front" or RF radiating face of the antenna. It was determined that a heat pipe radiator for the cavity tube would provide a high-confidence/low-mass system. The relative orientation of the slots and the heat pipes in the baseline antenna is shown in Figure 3.1-99, along with the relative location of the insulation and electronics.

The initial Rockwell baseline power module was selected during Exhibit A/B of the contract because of thermal rejection considerations relative to potential overheating of the slip rings, temperature limitations on the electronics, and the postulated requirement (later deleted) for manned access to the antenna during operation. The alternate Rockwell concept, which has been adopted during Exhibit C eliminated the performance uncertainty and efficiency losses resulting from poking the klystron tube through the radiator.

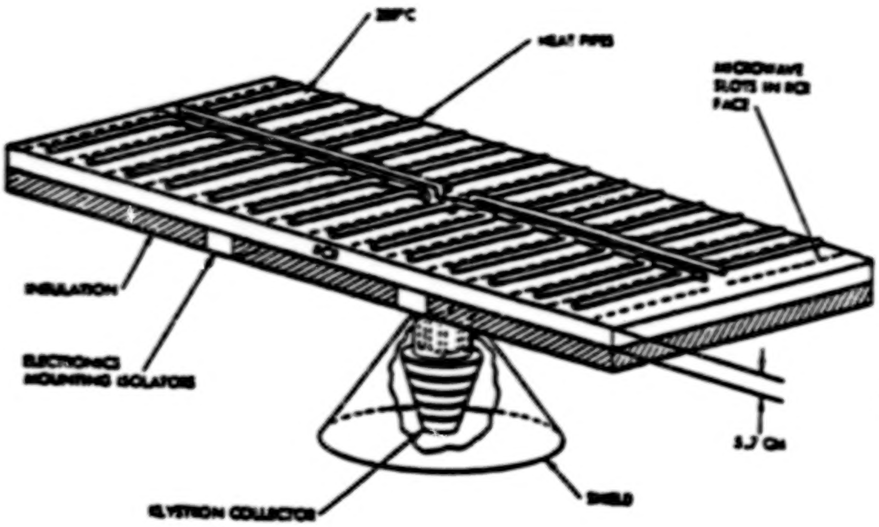

Figure 3.1-99.

Klystron Radiator Configuration (Rear Mounted)

The antenna as shown (Figure 3.1-99) is representative of a unit near the center of the antenna. Modules will vary in size and heat spacing/number throughout the antenna. The heat pipes all use water as a working fluid encased in a copper liner. The outer tube is aluminum to eliminate the single-point contact of dissimilar metals. The spacing of the axial groove heat pipes is 11.4 cm. Any one of the arterial wicked pipes can fail and the system will still reject the incident heat load and maintain allowable temperature limits, although the structural response for this mode must bb evaluated. There are four of these arterial wick pipes, each 1/2 inch O.D.; and 28 axial groove pipes, each 3/8 inch O.D. The layout of the pipes is dictated by the microwave slots which will not permit a more optimal radial distribution.

Thermal distortions may occur as a result of various temperature gradients occurring in the antenna as shown in Figure 3.1-100. The temperature drop across the fin length will be about 40°C. Thermal gradients from one face of the antenna to the other face are shown as a function of internal emissivity. The value of 0.9 corresponds to the use of a high emissivity coating (e.g., black anodize) and the lower limit of 0.1 is representative of bare aluminum. Gradients at the end of the antenna depend upon the fraction of the surface that is used for radiator, and the view factor variation to the collector radiator. The value shown (63°C) is an average value for the high-density portion of the antenna.

The collector radiator (Figure 3.1-101) is required to dissipate the 7.5 kW of waste heat dissipated due to beam inefficiencies. The pyrolytic graphite structure must have a relatively high fin efficiency to maintain local temperature below 700°C. If required, radiation shields can be used to isolate the collector from the cavity radiator. This would reduce the effective rejection capability and require higher temperature operation on thicker fins. The effect of fin efficiency on radiator temperature is shown in Table 3.1-49. It can be seen that the minimum possible operating temperature is only slightly below 700°C. This assumes that the waste heat distribution can be controlled and is rejected equally from the radiator segments.

Insulation is required for the back surface of the cavity radiator to restrict waste heat leaks which could increase temperature of the electronics

ΔT_1 • TEMP DROP BETWEEN HEAT PIPES

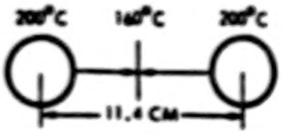
200°C
160°C
200°C
11.4 CM

ΔT_2 • TEMP DROP FROM TOP OF RADIATOR TO BOTTOM OF RADIATOR

EMISSIVITY OF OPPOSITE SURFACE	ε	ΔT °C
	0.9	3°
	0.5	5°
	0.1	21°

ΔT_3 • TEMP DROP FROM END OF HEAT PIPES TO END OF KLYSTRON RCR = 200°C ⟶ 137°C

Figure 3.1-100. Related Design Configurations

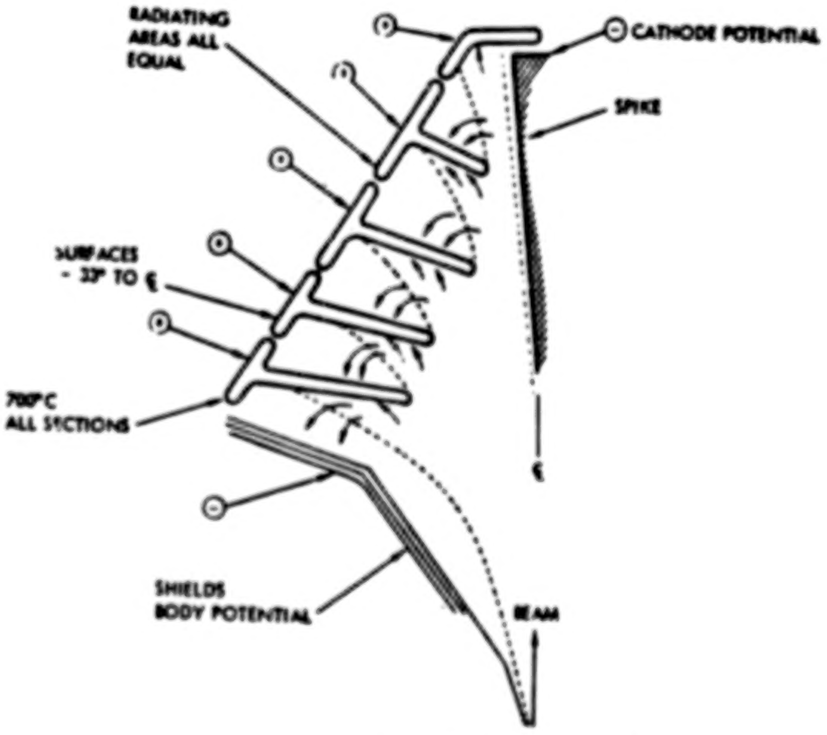
RADIATING AREAS ALL EQUAL
CATHODE POTENTIAL
SPIKE
SURFACES ~ 33° TO ℄
700°C ALL SECTIONS
℄
SHIELDS BODY POTENTIAL
BEAM

Figure 3.1-101. Collector Radiator

Table 3.1-49. Collector Radiator Analysis

- Assume rad. fin is pyrolytic graphite
- Collector area is 0.173 m^2
  (8-inch-high cone, $r_1 = 7$ in., $r_2 = 1.75$ in.)
- Assume all sections equal
- Assume $\alpha = \varepsilon = 0.9$
- Assume solar flux (eff.) = 35 watts

Fin Efficiency η	Temperature °C	
1.0	687	
0.9	712	← Baseline design
0.8	742	
0.7	776	
0.6	818	
0.5	868	
0.4	934	

to unacceptable levels. This insulation must be coated externally with low α/ε materials to limit the absorbed solar flux to which the surface is exposed during part of the orbit. Although many materials with low absorptivity/emissivity ratios are available, they typically experience substantial degradation as a function of solar exposure time. To limit the rear surface to 100°C (maximum allowable temperature of electronics), it is seen in Figure 3.1-102 that the maximum α/ε ratio is about 0.8, which is below values typically obtained for extended-life inexpensive insulations. If refurbishment of degraded blanket is not possible, the electronics could be protected by isolation in finned containers or by use of active cooling. Alternatively, advanced blankets using more expensive external surfaces (e.g., quartz microsheet) could be applied at some cost penalty.

Temperature extremes across the antenna (center to edge) are presented in Table 3.1-50 for the Exhibit A/B baseline and improved klystron concepts. The edge values assume that the total allowable radiator is used. Temperatures at the center were calculated for no rear surface insulation or collector shield. If the shield is used, then the maximum value would be approximately 100°C. The high proportion of waste heat that can be rejected from the earth side (≈30%) represents a significant advantage of this concept.

Additional sources of heat generation on the antenna are the high-voltage dc-dc converters. The 32 units on the antenna operate at 96% efficiency and dissipate 300 megawatts each. To maintain a 100°C design limit, active cooling must be provided. Figure 3.1-103 illustrates the required radiator area and associated system penalties at different temperature levels. For 60°C the antenna mass must be increased by about 1.0×10^6 kg for the proposed cooling system which utilizes an integrated heat pipe radiator design that incorporates optimized radial fin geometry.

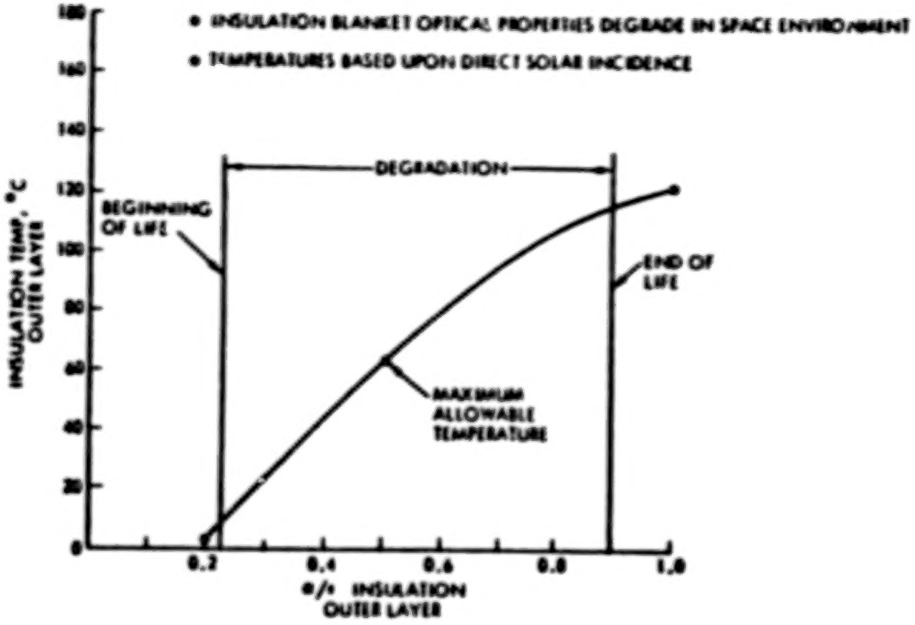

Figure 3.1-102. Rear Surface Cavity Radiator Thermal Response

Table 3.1-50. 50-kW Klystron Radiator Thermal Levels

		ANTENNA CENTER	ANTENNA EDGE
BASELINE KLYSTRON (TUBE POKED THROUGH) EARTH SIDE RADIATOR		152°C	-4°C
IMPROVED KLYSTRON (COLLECTOR RADIATES IN SPACE DIRECTION)	EARTH SIDE	129°C	-16°C
	SPACE SIDE	104°C	-29°C

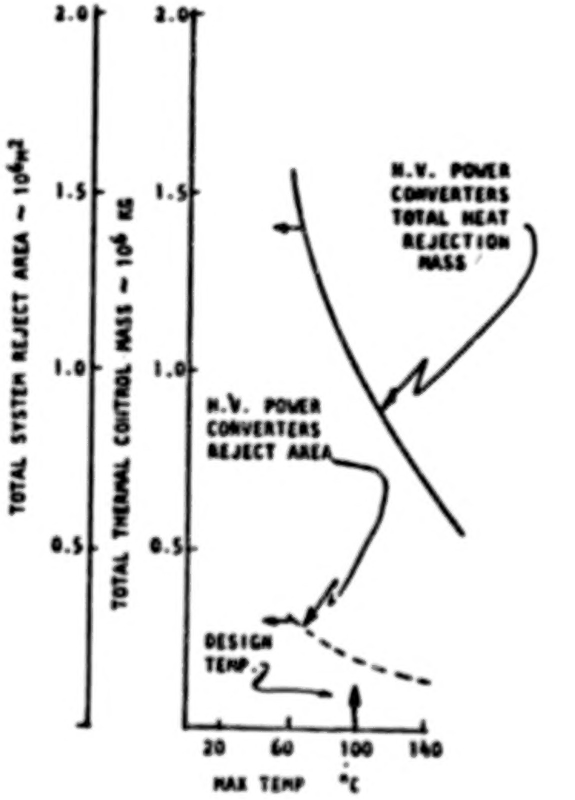

Figure 3.1-103. Power Distribution Component Thermal Control—HV Converters

The system power module was reanalyzed with the proviso that the control electronics could be located on insulated "islands" allowing minimum waste heat rejection from both sides of the antenna (Figure 3.1-104). The analysis considered the subarray located at the center of the array, and receiving power at a 74.5-kW input value at each klystron. The total heat load under the specified conditions was estimated to be 11.2 kW. The thermal profile of the antenna for these specified conditions is shown in Figure 3.1-105.

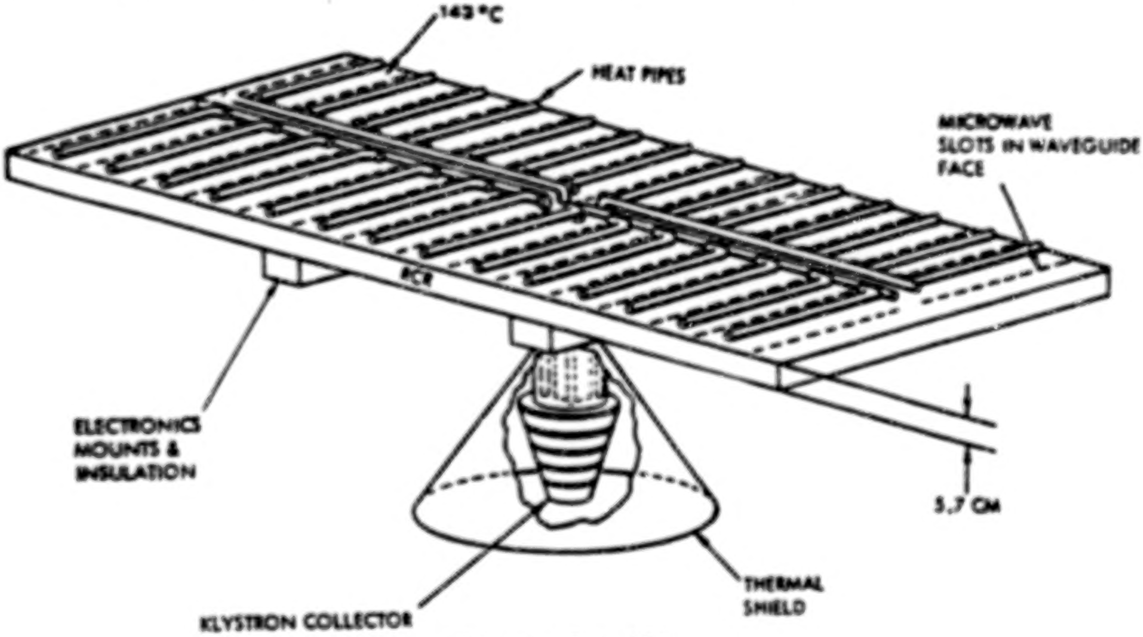
143°C
HEAT PIPES
MICROWAVE SLOTS IN WAVEGUIDE FACE
PCB
ELECTRONICS MOUNTS & INSULATION
5.7 CM
THERMAL SHIELD
KLYSTRON COLLECTOR

Figure 3.1-104.
Klystron Radiator Configuration—Radiation from Both Sides

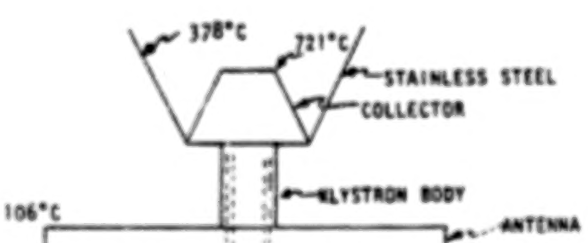
378°C
721°C
STAINLESS STEEL
COLLECTOR
KLYSTRON BODY
106°C
ANTENNA
143°C
HEAT PIPE

Figure 3.1-105. Revised Thermal Profile—Klystron Antenna

Magnetron

Thermal Analysis of Tube Heat Dissipation

The problem of getting rid of waste heat generated by the magnetron tubes is most severe for high-density (Type 1, Figure 3.1-59) power modules. The operating power level of the tubes, and ultimately the total amount of RF power radiated by the spacetenna, are governed by the amount of heat which can be dissipated while maintaining a safe operating temperature at the magnetron anodes.

Discussions with Raytheon investigators have established 300°C as the upper limit for magnetron anode block temperature. The temperature at the vane tips will be considerably higher than the 300°C at the anode block, and vapor pressure in the interaction region may become excessively high if this temperature is exceeded. Although the samarium-cobalt permanent magnets have a Curie temperature considerably above 300°C, the likelihood of metallurgical changes and increased mobility of lattice defects becomes a factor above this temperature. Finally, the thermal conductivity of pyrolytic graphite, selected as the heat radiating material, begins to decrease at temperatures above 300°C.

No doubt copper discs could dissipate waste tube heat, but the weight penalty would be excessive. Aluminum is another possibility, and a brief trade study of the use of this material is given later. For the present, pyrolytic graphite (PG) has been chosen for the radiating discs, following the recommendation of the Raytheon investigators. In the directions of its A-B axes, this material has a thermal conductivity greater than that of aluminum and about equal to that of copper, yet its density is only 2.2 g/cm^3 compared to 8.9 g/cm^3 for copper and 2.8 for aluminum.

The model used for thermal analysis is shown in Figure 3.1-106. The thickness of the pyrographite disc has been taken to be constant and equal to 3 mm. For Type 1 modules, adjacent discs are assumed to be touching, which limits disc diameter to 34.6 cm. Assumptions underlying use of the model shown schematically in the figure are listed below.

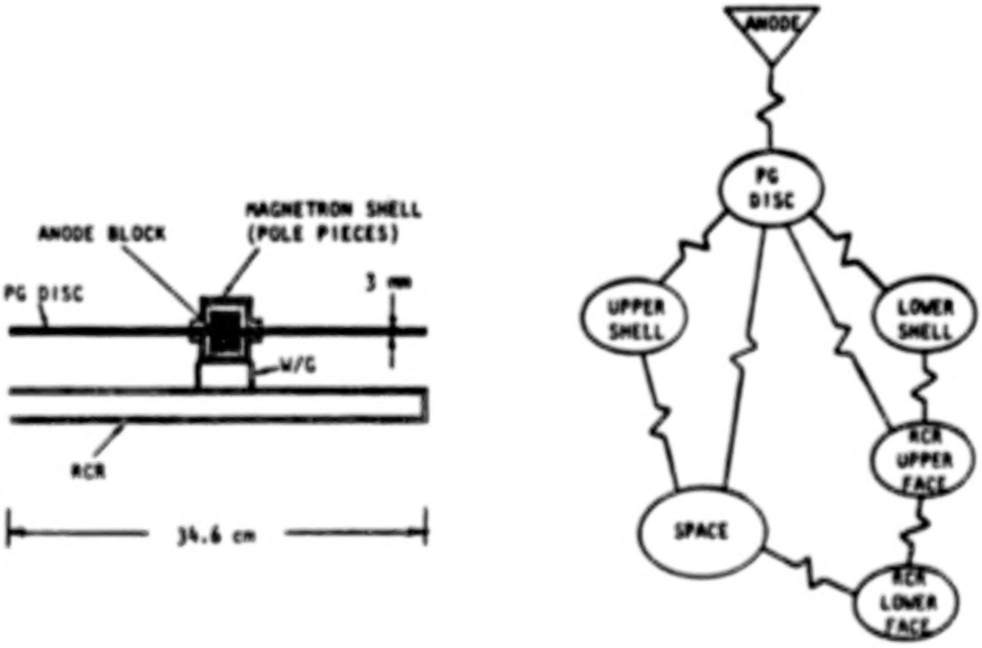

Figure 3.1-106. Model for Thermal Analysis of Magnetron Heat Dissipation

- Direct solar heating ignored
- Magnetron heat concentrated at anode and transferred by conduction to PG disc
- PG disc radiates to space and to upper face of antenna
- Other heat paths as shown
- Upper antenna surface is reflective with $\rho = 0.9$
- Inner and lower antenna surfaces treated to give $\alpha = \epsilon = 0.9$

The results of the analysis are given in Table 3.1-51, in which temperature at various locations are shown for four different values of waste heat dissipation.

Table 3.1-51. Results of Thermal Analysis

WASTE HEAT DISSIPATED (WATTS)	TEMPERATURE (°C) AND LOCATION				
	ANODE BLOCK	UPPER SHELL	LOWER SHELL	UPPER FACE RCR	LOWER FACE RCR
333	282	206	279	32	-2
444	324	242	320	55	0
529	350	265	346	70	12
706	397	305	393	95	33

After plotting these results for purposes of interpolation it is found that a temperature of 300°C at the anode block corresponds to a waste heat dissipation level of 390 W. Under these same conditions the upper face of the antenna is at 44°C while the lower face is at about -1°C.

In order to establish magnetron operating level, a tube conversion efficiency of 0.90 is projected. To justify this projection it is noted that the highest measured efficiency to date for a magnetron of the type required is 0.85. The improvement needed to reach the level 0.90 is 6% and is felt to be realistic by Raytheon investigators. By way of contract, the klystron reference concept assumes that tube efficiency, using depressed collector techniques, can be increased to 0.85, which is 14% above the best reported efficiency to date—namely, 0.744.

It follows at once that a tube having 90% efficiency and dissipating 390 W of heat will have an RF output level of 3.5 kW.

The weight of pyrographite in the disc of Figure 3.1-106 is 616 grams. It is clear that this could be halved if the disc thickness were tapered from 3 mm at the center to a sharp edge at the rim. Of course, this would entail a reduction in heat radiating efficiency but certainly not in proportion to the reduction in mass. At the time that this modification was incorporated into the thermal model it was learned from Raytheon that the thermal conductivity of pyrolytic graphite is significantly increased by heat treatment at 2900°C for two hours. The new value of conductivity is about 795 $W/m^{-1}K^{-1}$ at 300°C, compared to 380 $W/m^{-1}K^{-1}$ for copper. The net result is that the cooling efficiency of the tapered disc is not reduced at all if heat-treated PG is used. Thus, the mass of the PG disc is reduced to 310 grams.

It was noted above that a temperature difference of 45°C exists between the top and bottom faces of the antenna. This can cause the antenna to warp so that its faces become curved surfaces. The departure from planarity is approximately given by

$$\pm \frac{\alpha \ell^2 \Delta T}{16b}$$

where ℓ and b are the antenna dimensions (69.2 and 2.0 cm), α is the coefficient of linear expansion (2.4×10^{-5} per °C for aluminum) and $T = 45°C$. This turns out to be ±0.16 cm or ±4.7° in electrical phase angle. This small perturbation can be eliminated altogether by predistorting the antenna.

Solid-State End-Mounted

The solid-state end-mounted antenna concept utilizes solid-state power amplifiers located on the antenna as "replacements" for the reference concept klystrons. The amplifiers are distributed in a uniform manner over the entire face of the transmitting antenna, grouped about dipole microwave antenna, located on 7.81-cm centers. The amplifiers are clustered in groups of nine or less at the end of dipole antenna supports (see Figure 3.1-107). The amplifiers are bonded thermally to an aluminum closeout dish which acts as both fin and conductor. The closeout is attached around its perimeter to a doubled groundplane. The groundplane is separated from a bottom sheet by a honeycomb structure.

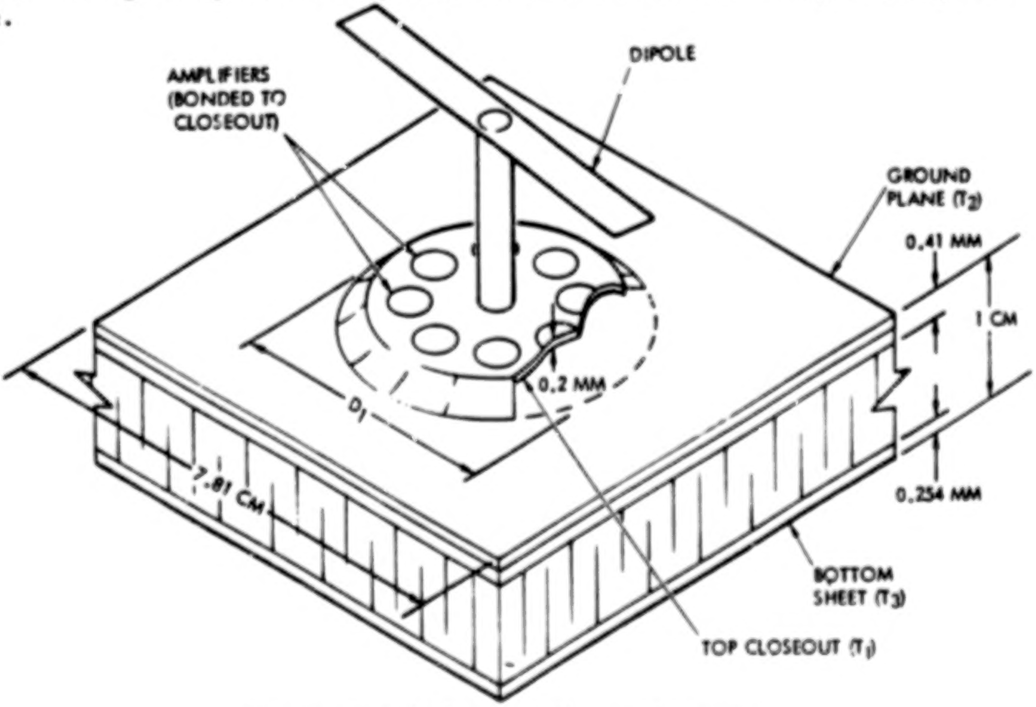

Figure 3.1-107. End-Mounted Concept

The thermal model employed is illustrated in Figure 3.1-108. Amplifier base temperature was held to the maximum allowable temperature of 125°C. Maximum amplifier dissipated power was calculated for two closeout sizes and two direct sun exposures—from the top (amplifier) side and from the bottom. Corresponding microwave power per unit area was calculated from component efficiencies and the module size (7.81 cm by 7.81 cm). Table 3.1-52 lists the assumptions employed in the thermal calculations.

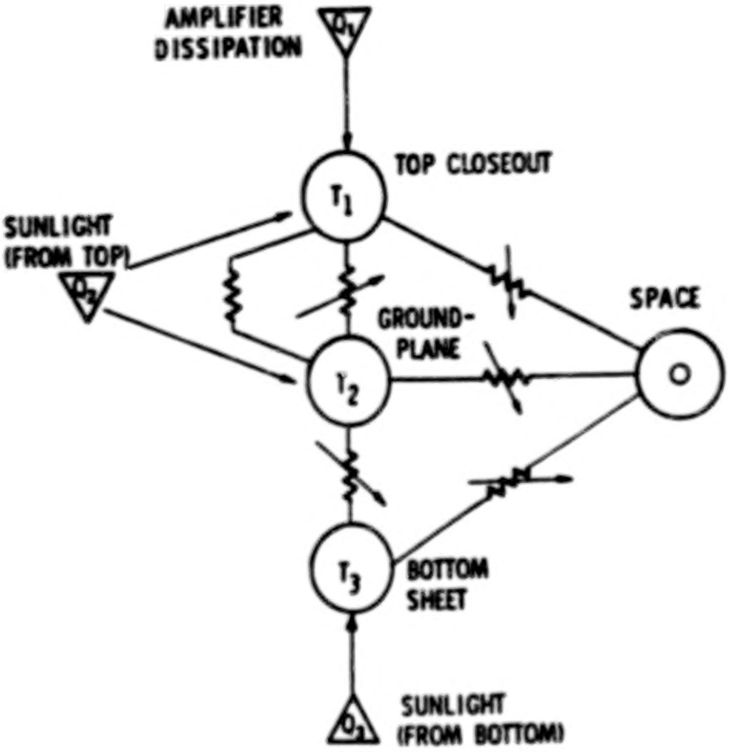
AMPLIFIER DISSIPATION
Q_1
TOP CLOSEOUT
T_1
SUNLIGHT (FROM TOP)
Q_2
GROUND-PLANE
T_2
SPACE
0
T_3
BOTTOM SHEET
Q_3
SUNLIGHT (FROM BOTTOM)

Figure 3.1-108. Thermal Model for End-Mounted Concept

Table 3.1-52. Thermal Calculation Assumptions

Component Efficiencies:	
Amplifier	0.80
Driver	0.99
Antenna	0.96
Fin (Close-out Disk)	0.75
Thermo-Optical Properties: (α/ϵ)	
Outer (Sun-Exposed) Surfaces	0.2/0.8
Inner Surfaces	0.9/0.9
Honeycomb Conductance (W/K)	
3 cm Diameter	0.27
4 cm Diameter	0.35

Maximum microwave output permitted under the 125°C amplifier temperature limitation is given in Table 3.1-53 for the cases considered.

Table 3.1-53. Maximum Microwave Output for End-Mounted Configuration

SUN	CLOSEOUT	TEMPERATURES (C)			MICROWAVE
(1385 W/M^2)	Diam D_1 (CM)	Amplifier	Groundplane	Bottom	Power (W/M^2)
TOP	3.0	125	104	33	3867
	4.0	125	109	37	4175
BOTTOM	3.0	125	102	58	4332
	4.0	125	108	62	4685

Sandwich Configuration

The sandwich configuration is characterized by dipole microwave antennas distributed over the back surface of the solar panel itself. Each atenna is supplied by a small solid-state amplifier. The antenna groundplane is separated from the solar panel by a honeycomb sandwich. The significant features from a thermal point of view are shown in Figure 3.1-109.

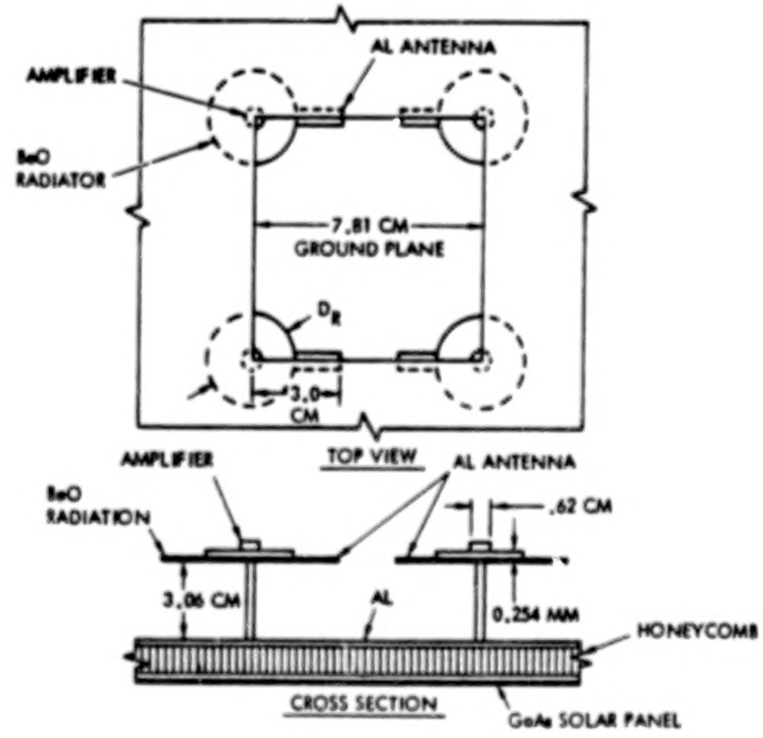
AL ANTENNA
AMPLIFIER
BeO
RADIATOR
7.81 CM
GROUND PLANE
D_R
3.0
CM
TOP VIEW
AMPLIFIER
AL ANTENNA
BeO
RADIATION
.62 CM
3.06 CM
AL
0.254 MM
HONEYCOMB
CROSS SECTION
GaAs SOLAR PANEL

Figure 3.1-109. Sandwich Configuration

The solar panel is exposed to a concentrated beam with an intensity of 5 to 6 suns. The solar cell temperature is limited to 200°C. On the opposite (antenna) side the antenna, amplifier, and groundplane are exposed to direct sunlight (one sun, worst case). In addition, they are heated by power dissipation in the amplifier and heat leaking through the honeycomb from the solar cells. Amplifier temperature is limited to 125°C.

Early calculations showed clearly that it would be very difficult to achieve the temperature limitations imposed on solar cells and amplifier at CR = 6 or higher. A number of design features were varied parametrically in order to approach this goal as closely as possible. Selective thermo-optical properties were assumed on surfaces exposed to direct sun. A circular disk radiator made of BeO (Berlox) was used to carry away heat from the amplifier. Berlox has a high thermal conductivity, but is dielectric and does not impair the functioning of the dipole radiator.

A final set of performance calculations was carried out for the optimized design. Solar cell and amplifier temperatures were assigned their limiting values. The calculation then determined the value of the solar concentration ratio which could be used, and the radiator diameter required. These parameters, in turn, determine the array output.

The thermal model employed is shown in Figure 3.1-110. It contains four nodes and three heat sources. Heat fransfer is primarily by radiation, but conduction through the honeycomb sandwich is also considered. Lateral temperature gradients in the radiator were taken into account by means of a radiator efficiency. Radiation exchange factors were estimated. Table 3.1-54 summarizes the assumptions employed.

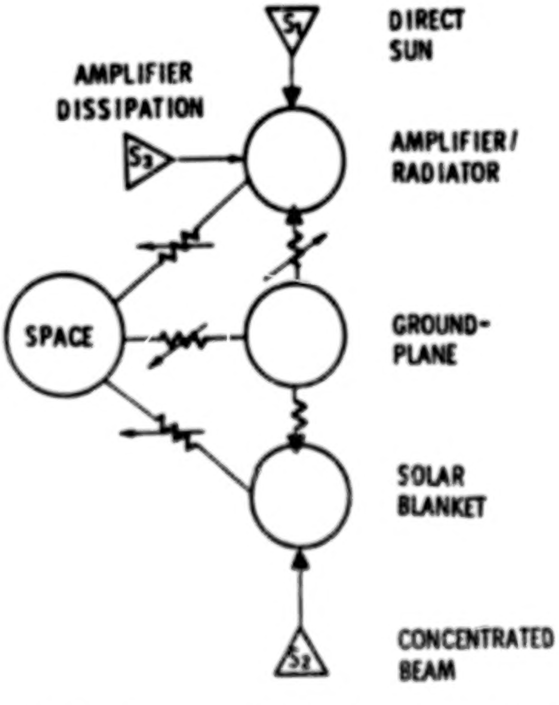

Figure 3.1-110. Thermal Model for Sandwich Configuration

Table 3.1-54. Sandwich Antenna Thermal Model Assumptions

Solar Constant, 1385 W/m^2 (Winter Solstice)

Solar Panel Characteristics	GaAs	Multi-Bandgap
Solar α	0.56	0.60
Emissivity ε	0.84	0.84
Efficiency (200°C)	1.151	0.2506
Array factor	0.94	0.94
Packing factor	0.95	0.95
Degradation (EOL)	0.96	0.96
Cell operating temperature	200°C	200°C

Honeycomb Structure

6.35-mm Hexcells with 50-μm walls
Inner surfaces blackened ($\varepsilon = 0.9$)

Groundplane Surface

Selective ($\alpha/\varepsilon = 0.2/0.8$)
View factor to space—fraction unblocked by radiator

Berlox Radiator

Selective ($\alpha/\varepsilon = 0.2/0.8$)
Operating temperature (inner radius), 125°C

Final calculations were made for two cases—one for advanced, single-junction GaAs and the other for a multi-bandgap solar cell. Node temperatures and steady-state power flows per amplifier are listed in Tables 3.1-55 and -56. The results show that, with a 4-1/2 cm radiator, the GaAs array can operate at about CR = 5-1/2. The multi-bandgap array can go to about CR = 5-3/4 by increasing the radiator diameter to 6 cm. The amplifier power is almost twice that for the GaAs array, however, because of the greater cell conversion efficiency.

Table 3.1-55. Node Temperatures and Energy Flow for Sandwich Configuration (GaAs Cells)

	ENERGY FLOW (W/AMPLIFIER)	
ENERGY BALANCE ON SOLAR BLANKET	BOL	EOL
CONCENTRATED INCIDENT BEAM	46.55 (CR = 5.51)	45.96 (CR = 5.44)
SUNLIGHT ABSORBED	26.07	25.74
NET POWER TO AMPLIFIER	6.28 ($\eta_E = 0.135$)	5.95 ($\eta_E = 0.129$)
RADIATED FROM CELL SURFACES	14.54 ($T_C = 200$°C)	14.54 ($T_C = 200$°C)
RADIATED/CONDUCTED TO GROUNDPLANE	5.25 ($T_G = 150$°C)	5.25 ($T_G = 150$°C
ENERGY BALANCE ON AMPLIF/RADIATOR		
HEAT DISSIPATED BY AMPLIFIER	1.25 ($\eta_A = 0.8$)	1.19 ($\eta_A = 0.8$)
DIRECT SUNLIGHT ABSORBED	0.45 ($D_R = 4.59$ CM)	0.43 ($D_R = 4.46$ CM)
RADIATION FROM GROUNDPLANE	0.13	0.12
RADIATION TO SPACE	1.84 ($T_R = 125$°C) ($\eta_R = 0.98$)	1.74 ($T_R = 125$°C) ($\eta_R = 0.98$)

Table 3.1-56. Node Temperature and Energy Flow for Sandwich Configuration (Multi-Bandgap Cells)

	ENERGY FLOW (W/AMPLIFIER)	
ENERGY BALANCE ON SOLAR BLANKET	**BOL**	**EOL**
CONCENTRATED INCIDENT BEAM	49.17 (CR = 5.82)	48.06 (CR = 5.69)
SUNLIGHT ABSORBED	29.50	28.83
NET POWER TO AMPLIFIER	11.01 (η_E = 0.224)	10.34 (η_E = 0.215)
RADIATED FROM CELL SURFACES	14.54 (T_C = 200°C)	14.54 (T_C = 200°C)
RADIATED/CONDUCTED TO GROUNDPLANE	3.95 (T_G = 163°C)	3.95 (T_G = 163°C)
ENERGY BALANCE ON AMPLIF/RADIATOR		
HEAT DISSIPATED BY AMPLIFER	2.20 (η_A = 0.8)	2.07 (η_A = 0.8)
DIRECT SUNLIGHT ABSORBED	0.86 (D_R = 6.28 CM)	0.81 (D_R = 6.09 CM)
RADIATION FROM GROUNDPLANE	0.39	0.37
RADIATION FROM SPACE	3.45 (T_R = 125°C) (η_R = 0.98)	3.25 (T_R = 125°C) (η_R = 0.98)

3.1.8 COMMUNICATIONS AND DATA MANAGEMENT

Introduction

The information management and control subsystem (IMCS) provides the interconnecting elements between and within all the various satellites and ground-based operational subsystems. The IMCS also provides operational control of both the satellite and ground systems as well as providing all subsystem processing support for all but very special functions.

The IMCS consists of the on-board and ground-based processing equipment [central processing units (CPU) and memories], the inter- and intra-subsystem data network (data buses), the man-machine interfaces (display/control), and inter-system communication links, including RF, but excepting those specifically provided for the control and transfer of primary power, and all elements provided to accommodate activities related to system security, safety, or any other operation necessary to the continuing operation of the SPS.

Because of the early stage of program analysis, only those requirements imposed upon the IMCS by a limited number of satellite operations have been identified. The identified requirements generally are limited to those associated with the immediate operations of an active satellite. Auxiliary functions such as ground/space communications, display/control, safety, security, etc., will be added when data become available.

Data Management

Design Approach

The IMCS design selected for the reference configuration is shown as a top-level block diagram in Figure 3.1-111. This diagram illustrates a simplex (non-redundant) system. Local computer centers are envisioned to be located at substations located at selected sites in each trough. The sites located at the end of the troughs would house attitude control support centers. Processing

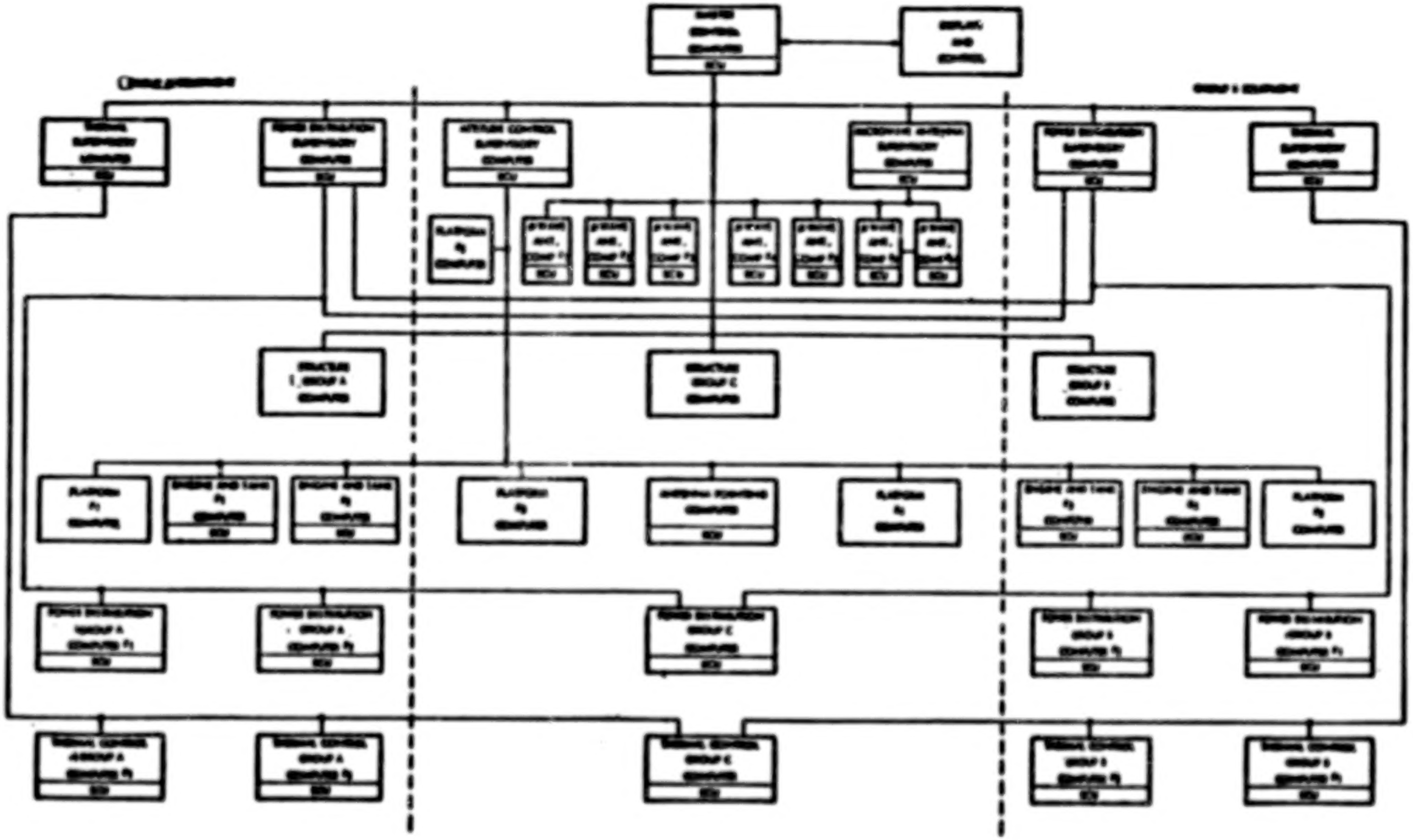

Figure 3.1-111. SPS IMCS Top-Level Block Diagram

support to structure alignment, microwave antenna beam pointing control, and additional attitude control functions would be housed in the sections near the antenna. The dual solid-state sandwich concept diagram would be similar, although with a slightly different distribution because of the different construction.

Three levels of data processing are illustrated in Figure 3.1-111—*master*, *supervisory*, and *remote*. Subtiered to this hierarchy are microprocessors, remote acquisition and control (RAC) units, and submultiplexers (SM). Microprocessors as stand-alone processors have only been identified for the microwave antenna beam pointing function.

The IMCS hierarchy applicable to the microwave antenna subsystem, attitude control and stationkeeping subsystem, and power distribution subsystems is presented in Figures 3.1-112 through 3.1-114, respectively. These hierarchies are established to the level at which the IMCS and the using subsystem interfaces are apparent (e.g., physical/electrical interface).

Table 3.1-57 summarizes the estimated number of data interfaces (not measurements) that must be accommodated by the reference concept IMCS. Note specifically that the microwave antenna subsystem is by far the major contributor to the determination of the complexity of the IMCS electrical interface. A very preliminary estimate of the control interface that must be accommodated by the IMCS is provided in Table 3.1-58, although the estimates are not supported by an in-depth analysis. Again, the microwave antenna system predominates.

The data processing requirements for the other configurations were not determined to any detail during this study, but rather were determined by estimating the relative complexity of the particular configuration with respect to the reference configuration. For example, the sandwich antenna—which does not require a means of switching or monitoring the individual microwave elements—is estimated to require only 20% of the reference IMCS subsystem. By the same reasoning, the IMCS on the reflector array is estimated at two-thirds of the reference solar array estimate. The others, the multi-bandgap solar cell variations and the magnetron concept, are adjusted according to either the plan-view area or by an estimate of the relative monitor/control complexity of the antenna.

Major Assemblies

Figure 3.1-115 identifies the major assemblies that form the IMCS. Six major assemblies have been identified at this time: (1) processors, (2) bus control units (BCU), (3) data bus, (4) remote acquisition and control units (RAC), (5) submultiplexers (SM), and (6) microprocessor (μP).

Processors

The satellite master control computer (Figure 3.1-112) will operate with a 16-32 bit word format and have a 64K-128K word activity memory plus a TBD billion word bulk storage facility. Second- and third-level processors (supervisory or local) will be 16-bit word assemblies and be limited to 16K-32K memories. In special cases, memory capacity may be increased to as much as

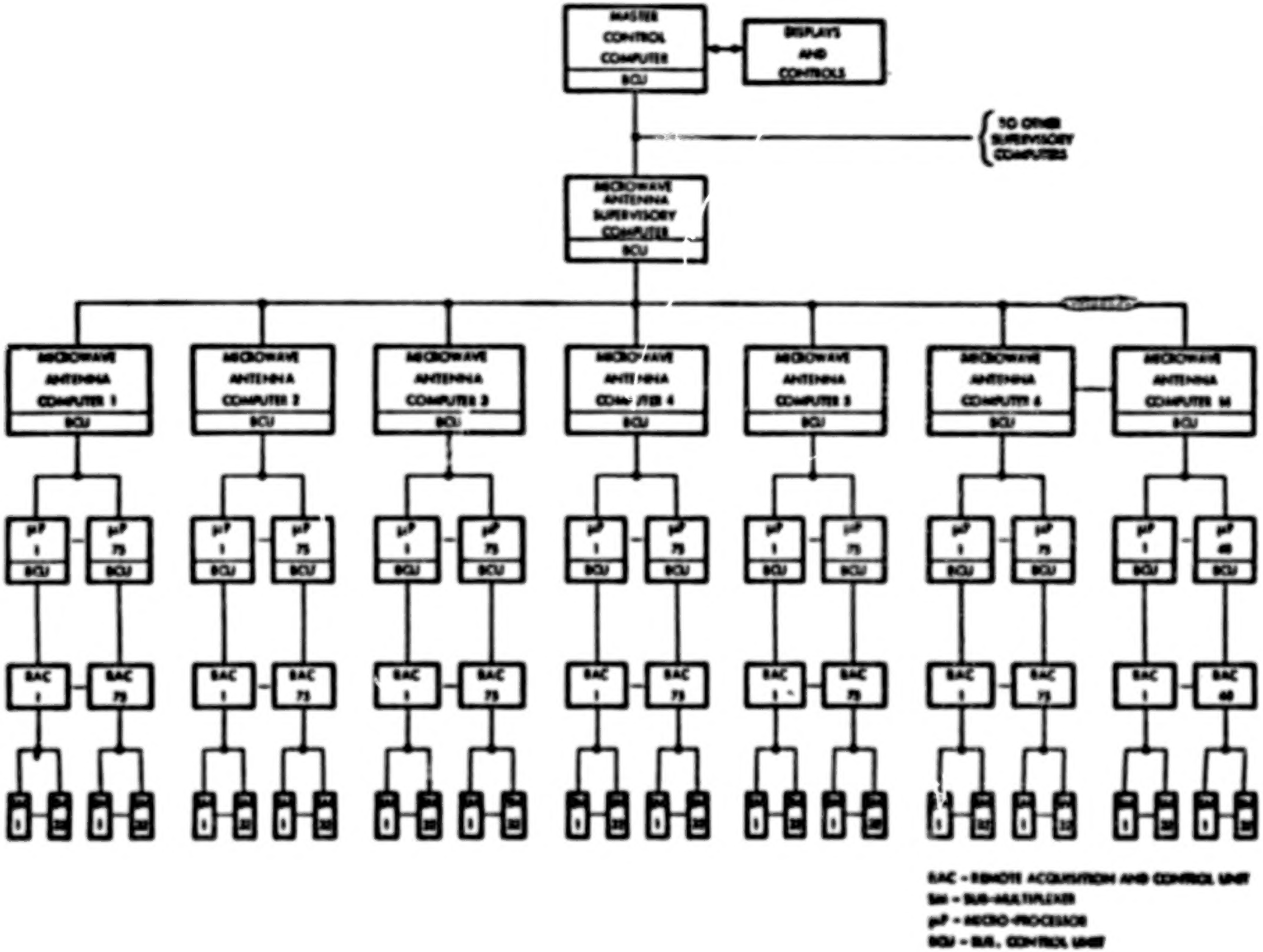
MASTER CONTROL COMPUTER
BCU
DISPLAYS AND CONTROLS
TO OTHER SUPERVISORY COMPUTERS
MICROWAVE ANTENNA SUPERVISORY COMPUTER
BCU
MICROWAVE ANTENNA COMPUTER 1
MICROWAVE ANTENNA COMPUTER 2
MICROWAVE ANTENNA COMPUTER 3
MICROWAVE ANTENNA COMPUTER 4
MICROWAVE ANTENNA COMPUTER 5
MICROWAVE ANTENNA COMPUTER 6
MICROWAVE ANTENNA COMPUTER 16
BCU
µP 1
µP 75
µP 40
BCU
RAC 1
RAC 75
RAC 40
SM 1
SM 32
RAC - REMOTE ACQUISITION AND CONTROL UNIT
SM - SUB-MULTIPLEXER
µP - MICRO-PROCESSOR
BCU - BUS CONTROL UNIT

Figure 3.1-112. IMCS—MW Antenna

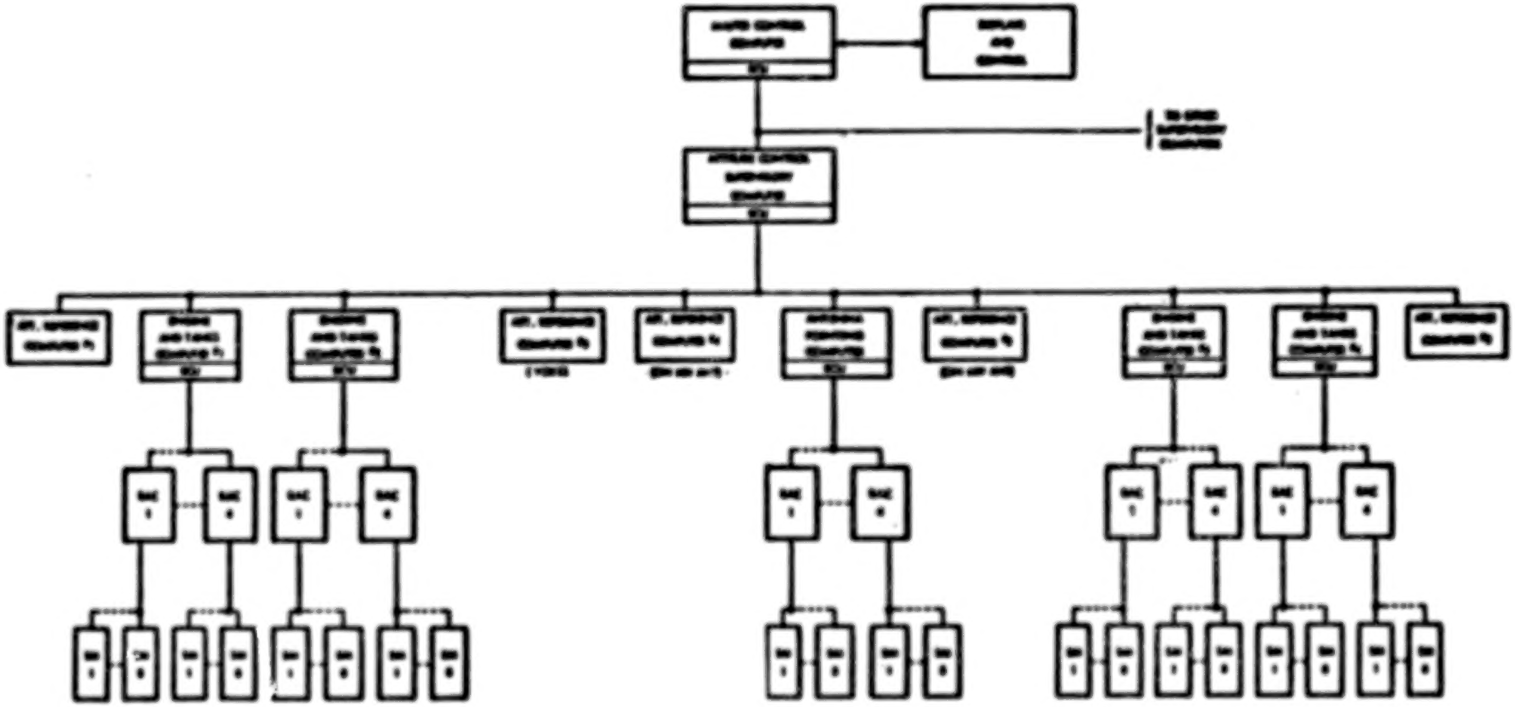

Figure 3.1-113. IMCS—Attitude Control

BLANK PAGE

BLANK PAGE

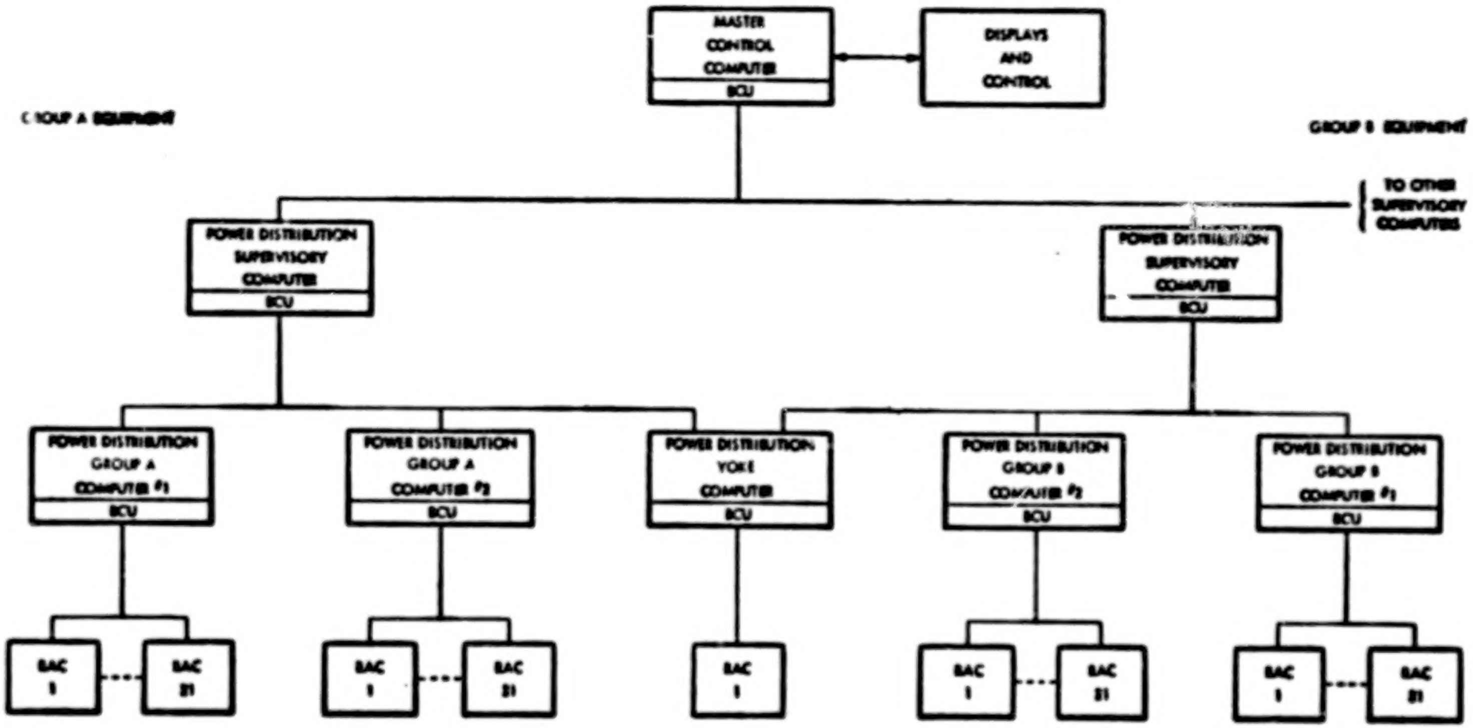
MASTER CONTROL COMPUTER
BCU
DISPLAYS AND CONTROL
GROUP A EQUIPMENT
GROUP B EQUIPMENT
TO OTHER SUPERVISORY COMPUTERS
POWER DISTRIBUTION SUPERVISORY COMPUTER
BCU
POWER DISTRIBUTION SUPERVISORY COMPUTER
BCU
POWER DISTRIBUTION GROUP A COMPUTER #1
BCU
POWER DISTRIBUTION GROUP A COMPUTER #2
BCU
POWER DISTRIBUTION YOKE COMPUTER
BCU
POWER DISTRIBUTION GROUP B COMPUTER #2
BCU
POWER DISTRIBUTION GROUP B COMPUTER #1
BCU
BAC 1
BAC 31
BAC 1
BAC 31
BAC 1
BAC 1
BAC 31
BAC 1
BAC 31

Figure 3.1-114. IMCS—Power Distribution (Solar Array and Yoke)

Table 3.1-57. Preliminary Data Interface Summary—Photovoltaic (CR-2) Configuration

	ANALOG	DIGITAL	EVENT	TOTAL
MICROWAVE ANTENNA	$6x10^6$	$1x10^6$	$2.1x10^6$	$>9x10^6$
OTHER SUBSYSTEMS				
STRUCTURE	35	35	35	>100
ATT. CONTROL & STATION-KEEPING	900	800	1000	~3000
POWER DISTRIBUTION	1000	100	2000	~3000
INFORMATION MANAGEMENT	-	~19,000	-	~19,000
THERMAL	16,000	-	-	16,000
LIFE SUPPORT	TBD	TBD	TBD	TBD
SAFETY AND SECURITY	TBD	TBD	TBD	TBD

Table 3.1-58. Preliminary Control Interface Summary—Photovoltaic (CR-2) Configuration

	PROPORTIONAL	EVENT	TOTAL
MICROWAVE ANTENNA	$<13.6x10^4$	$30x10^4$	$<44x10^4$
OTHER SUBSYSTEMS			
STRUCTURE	~35	-35	<100
ATTITUDE CONTROL & STATIONKEEPING	-100	>300	<500
POWER DISTRIBUTION	-	>300	>300
INFORMATION MANAGEMENT	-	>3000	>3000
THERMAL	-	-	-
LIFE SUPPORT	TBD	TBD	TBD
SAFETY AND SECURITY	TBD	TBD	TBD

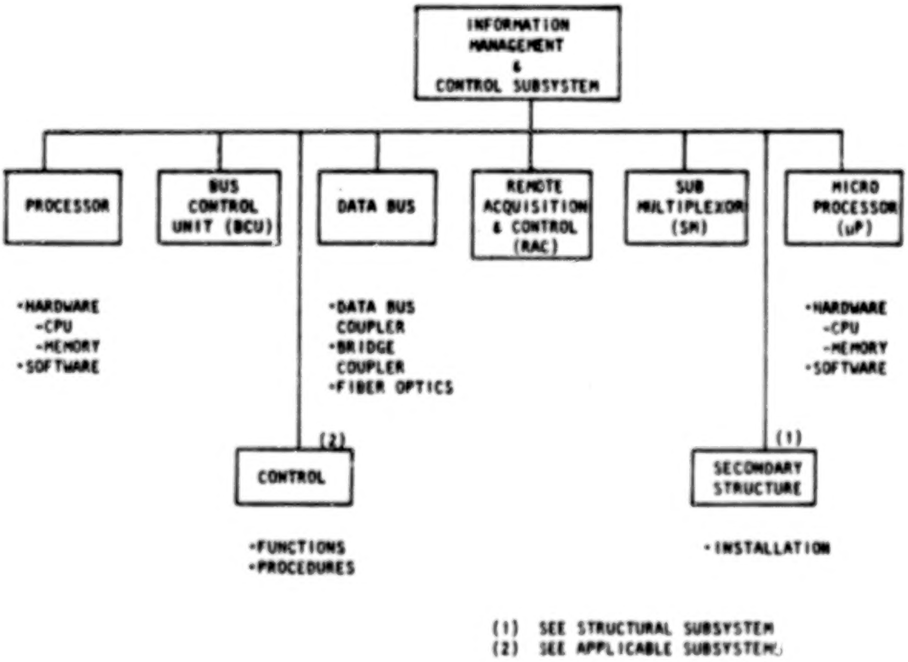
INFORMATION MANAGEMENT & CONTROL SUBSYSTEM
PROCESSOR
BUS CONTROL UNIT (BCU)
DATA BUS
REMOTE ACQUISITION & CONTROL (RAC)
SUB MULTIPLEXOR (SM)
MICRO PROCESSOR (uP)
•HARDWARE
-CPU
-MEMORY
•SOFTWARE
•DATA BUS COUPLER
•BRIDGE COUPLER
•FIBER OPTICS
•HARDWARE
-CPU
-MEMORY
•SOFTWARE
(2)
CONTROL
•FUNCTIONS
•PROCEDURES
(1)
SECONDARY STRUCTURE
•INSTALLATION
(1) SEE STRUCTURAL SUBSYSTEM
(2) SEE APPLICABLE SUBSYSTEMS

Figure 3.1-115. Assembly Tree—IMCS

128K words. Assemblies or subassemblies identified as microprocessors (normally those units incorporated directly within the associated electronics) will incorporate an 8-bit-word format and use active 8K-64K word memories.

Bus Control Unit

The bus control unit (BCU) provides the control necessary for data/command transfer over the subsystem data bus network. The BCU accepts instructions and data (or commands) from its associated processor and translates these data from a processor-compatible format to one compatible with the data network. It also accepts bus-compatible data and converts these data to processor formats. In addition, the BCU monitors the data traffic—performing bit and word checks as well as health/status checks.

In addition to data bus control, the BCU will provide computer-to-computer link where appropriate.

Data Bus

The data bus network accommodates multiplexed, digital data transmitted between the BCU and all other remotely located data acquisition and central devices associated with specific processor/BCU combinations. The bus link may utilize conventional wire techniques for short runs in low EMI areas or fiber-optic technology for long paths or through high EMI areas. Basic bit rate within the bus assembly is assumed to be 1.0 Mbps. Included in the data bus assembly are the data bus coupling devices used to connect the various remote units (one required per remote) as well as the bridge coupler required to transfer data across the microwave antenna rotary joints or the reflector ball joint; the latter elements are presently TBD.

Remote Acquisition and Control

The remote acquisition and control (RAC) assembly is the basic interface between the IMCS and the various operating subsystems. The RAC provides for data format conversion from the preconditioned analog, digital or event voltage/impedance levels, and converts these data into 8-bit digital, serial, equivalents. The RAC also accepts digital data words and outputs commands in a format compatible with the receiving subsystems.

Basic conversion (input/output) is assumed to be ±1% (e.g., 7-bit and sign). Voltage ranges and impedances are TBD.

Submultiplexers

The submultiplexer (SM) provides a means of expanding the capability of the RAC. The SM thus contains all of the capabilities of an RAC, but can only communicate with a single RAC rather than a given data bus. The number of SM's that can communicate with an RAC is presently TBD.

Microprocessors

The microprocessor (µP) elements provide local, front-end processing of data obtained from the various using systems. These processors will handle the bulk of the system's monitoring and control task, sending raw data up through the computer hierarchy only when the task levels exceed pre-established limits, or when detected out-of-tolerance conditions exceed local control boundaries. These devices are solid state and could normally be integrated within the user electronics. When necessary, the µP can be located within the RAC's or SM's to provide local performance monitoring and control.

Subsystem Summary

Table 3.1-59 summarizes the number of IMCS elements required for the reference configuration. Table 3.1-60 summarizes the estimated physical (mass, power, volume) requirements for this system. Table 3.1-61 summarizes the estimated IMCS mass for the other configurations.

Communications

While communications have not been specifically studied in this analysis, a number of implications have been drawn. The satellite must have the ability to maintain continuous contact with the ground receiving station (GRS) control center; this includes voice, data, and commands in both directions. In addition, the dual uplink pilot beams from the GRS are crucial to acquisition and fine pointing. The high EMI environment in the near vicinity of the satellite imposes difficult conditions for communications; this requires primary emphasis and special design considerations.

Intra-satellite communications are highly dependent upon optical data buses to avoid the EMI problems.

Space-ground communications may have to be encrypted to avoid command intrusions and interference. Data compression may be required if data traffic becomes too heavy due to large data base updates, significant amounts of video traffic, or excessive interference.

Table 3.1-59. Hardware Summary—IMCS

	FUNCTION							
HARDWARE ELEMENT	MASTER CONTROL COMPUTER	DISPLAY AND CONTROL	SUPERVISORY COMPUTER	REMOTE COMPUTER	MICRO-PROC.	BUS CONTROL UNIT	REMOTE ACQUIS. AND CONTROL	SUB-MUX
SATELLITE CONTROL	2X	1	-	-	-	2	-	-
THERMAL CONTROL	-	-	2	5	-	7	85	1,352
STRUCT. ALIGN.	-	-	-	3	-	3	-	-
ATTITUDE CONTROL	-	-	1	10	-	11	28	148
POWER DISTRIB.	-	-	2	5	-	7	85	-
MICROWAVE ANTENNA CONTROL	-	-	1	14	777	792	787	29,500
TOTAL	2X	1	6	37	777	822	985	31,000

Table 3.1-60. Mass/Power/Volume Summary—IMCS

HARDWARE ELEMENT	QUANTITY	UNIT MASS (Kg)	TOTAL MASS (Kg)	UNIT POWER (KW)	TOTAL POWER (KW)	UNIT VOLUME (m^3)	TOTAL VOLUME (m^3)
SOLAR ARRAY							
MASTER CONTROL COMPUTER	2	500	1,000	2	4	0.4	0.8
DISPLAY & CONTROL SET	1	200	200	0.9	0.9	0.72	0.72
SUPERVISORY COMPUTER	5	14	70	0.07	0.35	0.01	0.05
REMOTE COMPUTER	23	14	322	0.07	1.61	0.01	0.23
MICRO PROCESSOR	-	5	-	0.02	-	0.003	-
BUS CONTROL UNIT	38	5	150	0.02	0.6	0.005	0.15
REMOTE ACQUISITION & CONTROL	198	5	990	0.02	3.96	0.005	0.99
SUB MULTIPLEXOR	1500	3	4,500	0.01	15.0	0.003	4.5
SUBTOTAL			7,232		26.42		7.44
ANTENNA							
MASTER CONTROL COMPUTER	-	500	-	2	-	0.4	-
DISPLAY & CONTROL SET	-	200	-	0.9	-	0.72	-
SUPERVISORY COMPUTER	1	14	14	0.07	0.07	0.01	0.01
REMOTE COMPUTER	14	14	196	0.07	0.98	0.01	0.14
MICRO PROCESSOR	777	5	3,885	0.02	15.54	0.003	2.331
BUS CONTROL UNIT	792	5	3,960	0.02	15.84	0.005	3.96
REMOTE ACQUISITION & CONTROL	787	5	3,935	0.02	15.74	0.005	3.935
SUB MULTIPLEXOR	29500	3	88,500	0.01	295.0	0.003	88.5
SUBTOTAL			100,490		343.17		98.876
TOTAL			107,700		369.6		106.3
CABLE							
NON-ROTATING-WIRE (22GA) FIBER OPTICS	1,200 KM 90 KM	12.0/KM 0.14/KM	14,000 12			2x10^{5}/KM 2x10^{6}/KM	0.48
ROTATING-WIRE FIBER OPTICS	23,000 KM 350 KM		279,000 50				
TOTAL			293,000				0.48

Table 3.1-61. IMCS Mass Properties—Summary (Partial) (10^6 kg)

	Klystron	Magnetron	SS-End Mounted		Sandwich	
	GaAlAs/ GaAs	GaAs	GaAs	GaAlAs/ GaAs	GaAs	GaAlAs/ GaAs
SOLAR ARRAY						
Data Processing	0.021	0.021	0.024	0.024	0.014**	0.014**
Instrumentation	0.029	0.929	0.033	0.033	0.019**	0.019**
ANTENNA						
Data Processing	0.380	0.190	1.385	1.385	0.152***	0.152***
Instrumentation	0.260	0.130	0.237	0.237	0.104***	0.104***
Total	0.690	0.370	1.679	1.679	0.289	0.289

** 2/3 reference concept

*** 20% reference concept

3.2 GROUND RECEIVING STATION

3.2.1 INTRODUCTION

The microwave power transmission system (MPTS) is described as consisting of two major elements—the orbiting transmission antenna, and the ground receiving antenna (rectenna). The ground receiving station (GRS) consists of the ground element of the MPTS (the rectenna), and the power distribution, power conversion, data management, and other supporting subsystems required to collect, convert, and route power to the utility interface tie lines.

The following subsections address the rectenna and power distribution subsystems only for the reference system. The other satellite systems are different only as to scale, and are considered only in terms of land area, but may be further evaluated in future studies.

3.2.2 RECTENNA

Siting

The GRS site for the reference satellite requires approximately 35,000 acres. Figure 3.2-1 shows a layout of a typical site. The inner ellipse containing the rectenna panels (10×13 km) is about 25,200 acres or 72% of the total acreage.

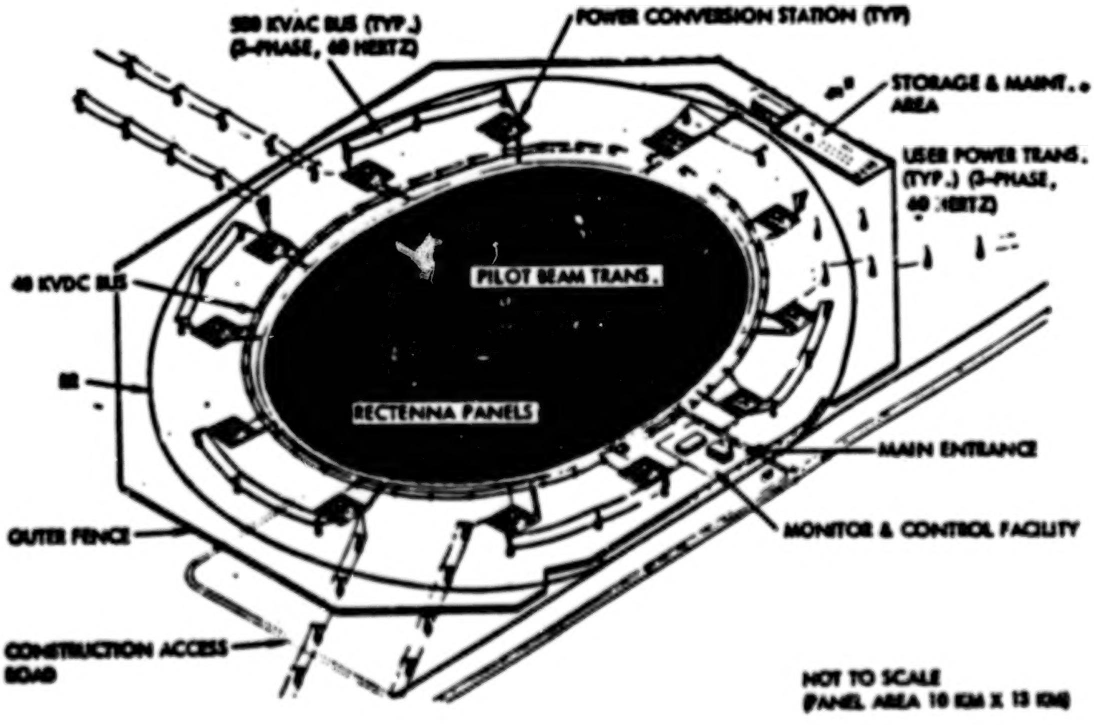
500 KVAC BUS (TYP.)
(3-PHASE, 60 HERTZ)
POWER CONVERSION STATION (TYP)
STORAGE & MAINT.
AREA
USER POWER TRANS.
(TYP.) (3-PHASE,
60 HERTZ)
40 KVDC BUS
PILOT BEAM TRANS.
RR
RECTENNA PANELS
MAIN ENTRANCE
OUTER FENCE
MONITOR & CONTROL FACILITY
CONSTRUCTION ACCESS
ROAD
NOT TO SCALE
(PANEL AREA 10 KM X 13 KM)

Figure 3.2-1. Operational Ground Receiving Facility (Rectenna)—Typical

The overall dimensions and area requirements for each of the suggested satellite configurations are summarized in Table 3.2-1.

Table 3.2-1. Ground Receiving Station Area Requirements

	Klystron (Reference)	Magnetron	Solid State (Dual End Mount)	Solid State GaAs	Sandwich GaAlAs/ GaAs
Dimensions (km)			← per Antenna →		
• Rectenna	10×13	10.95×14.3	7.45×9.76	4.87×6.38	5.47×7.16
• Perimeter	12×15	12.4 × 16.3	8.44×11.06	10.06×13.18	11.29×14.79
Land Area (km^2)					
• Rectenna	102.1	123.0	57.11	24.4	30.76
• Perimeter	141.4	158.7	73.31	104.13	131.15
Land Area (acres)					
• Rectenna	25,000	30,000	14,000	6,000	7,600
• Perimeter	35,000	39,000	18,000	26,000	32,000

The area surrounding the inner ellipse is utilized for maintenance facilities, access roads, converter stations, and the two peripheral rows of towers which support the 40-kV dc and 500-kV ac cables. The outer perimeter of the area is fenced for security reasons. The towers which support the 500-kV ac cables are constructed of steel girders footed in concrete and are approximately 70 m high. The inner towers are each comprised of four tapered steel columns 18.3 m tall. Fifty-four of the larger towers and 401 of the smaller towers are required; the latter figure translating into 1604 tubular members because of the configuration.

Receiving Antenna (Rectenna)

The rectenna is composed of many panels, each nominally 9×15 m, sloped so as to be perpendicular to the line of sight to the satellite as shown in Figure 3.2-2. In this section, the configuration of an individual panel and factors with respect to its location in the rectenna will be identified.

The portion of the panel initially under analysis is the structure of the microwave network that connects the individual antenna elements together and to a rectifier. The two major contenders for this network are stripline, for low cost; and waveguide, for low loss. However, there are other considerations in addition to the type of transmission line used. The main items among these are the rectifier operating point and the type of antenna elements comprising the panel; these will be discussed before comparing interconnect network types.

Rectifier Operating Point

Efficiency of a solid-state rectifier is a function of the power input level; this is illustrated in Figure 3.2-3.

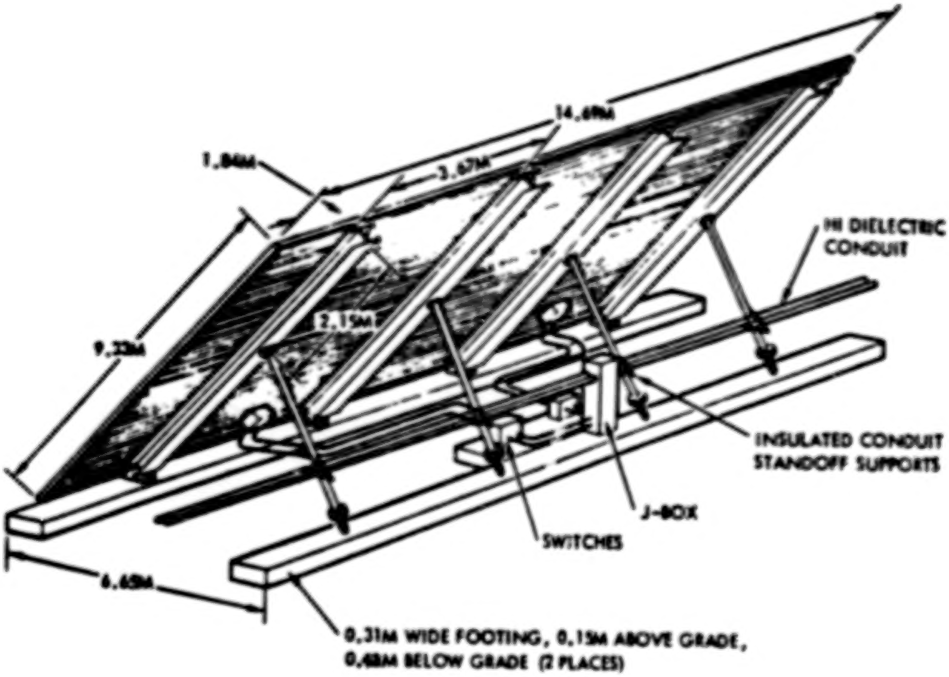
14,69M
1,84M
3,67M
9,33M
2,15M
HI DIELECTRIC CONDUIT
INSULATED CONDUIT STANDOFF SUPPORTS
J-BOX
SWITCHES
6,65M
0,31M WIDE FOOTING, 0,15M ABOVE GRADE, 0,48M BELOW GRADE (2 PLACES)

Figure 3.2-2. Rectenna Panel Assembly and Installation

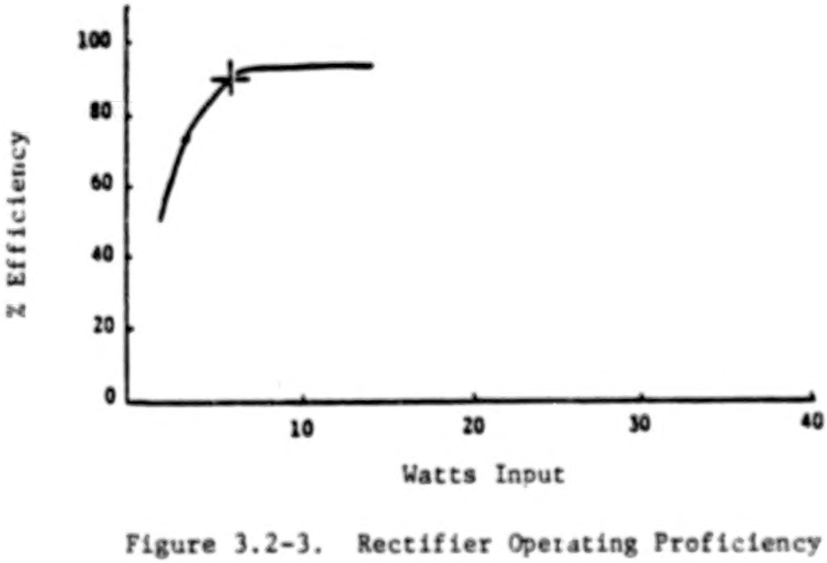

Figure 3.2-3. Rectifier Operating Proficiency

The curve shows that at 6 W RF input, the efficiency is about 90%. This establishes the benefit of operating the rectifier at a reasonably high power —for the purposes of this analysis, above 6 W. The maximum power handling capability of a rectifier is a function of many parameters encountered during its detailed design. Without pursuing these design problems further in this section, a maximum of about 45 W has been assumed. Thus, it is desired to keep the RF power input as high as possible, but no more than 45 W and no less than 6 W.

The incident microwave energy from the satellite is estimated to total 6.15 GW within an elliptical area with major- and minor-axis of 13 km and 10 km, respectively. The rectenna area is arbitrarily divided into five concentric zones, with power received per unit area diminishing from the center to the edge. Figure 3.2-4 shows these zones plotted for the 10×13 km (reference) rectenna, along with some of the other assumed rectenna characteristics. Table 3.2-2 shows the average power density in each zone, and also the power density at the center and edge.

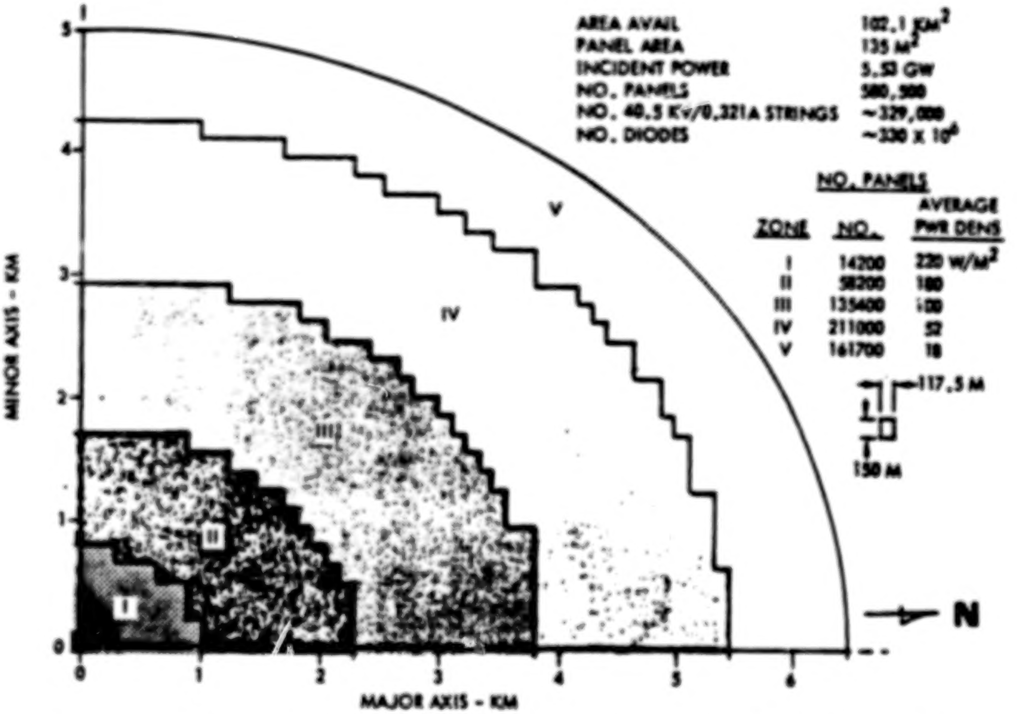
AREA AVAIL 102.1 KM²
PANEL AREA 135 M²
INCIDENT POWER 5.53 GW
NO. PANELS 580,500
NO. 40.5 Kv/0.321A STRINGS ~329,000
NO. DIODES ~330 X 10⁶
NO. PANELS
ZONE
NO.
AVERAGE PWR DENS
I 14200 220 W/M²
II 58200 180
III 135400 100
IV 211000 52
V 161700 18
117.5 M
150 M
I
II
III
IV
V
N
MINOR AXIS - KM
MAJOR AXIS - KM
0
1
2
3
4
5
6

Figure 3.2-4. Rectenna Power Density Pattern (34°N Latitude)

Table 3.2-2. Billboard Summary

.183 M²/CLUSTER

REGION	NOMINAL POWER DENSITY	WATTS PER CLUSTER	TYPICAL ALLOCATION CLUSTERS (49 ELEMENTS) PER DIODE	WATTS PER DIODE
CENTER	230 W/M²	42.1	1	42.1
I	220	40.3	1	40.3
II	180	33.0	1	33.0
III	100	18.3	1	18.3
IV	52	9.5	1	9.5
V	18	3.3	9 *	29.7
EDGE	10	1.8	9 *	16.2

* SATELLITE DRIFT < ± 0.2°

An area of 0.183 m^2 was taken as a unit power gathering area. (This will be shown to be equivalent to a 7×7-element array with $\lambda/2$ spacing between elements.) If one rectifier is allocated to each unit power gathering area—as shown by Table 3.2-2—for four out of five of the zones, the rectifier will have more than 6 W (but less than 45 W) input. For the fifth zone, a group of nine areas is assigned to each rectifier to maintain rectifier power in the efficient range.

By these choices of rectenna unit area, efficient rectifier operation is assumed, and a baseline established to compare microwave interconnecting networks.

Type of Antenna

The 9×15-m antenna panel can be anything between a dense ($\lambda/2$ spacing in both directions) array of radiating elements to a single antenna (9 15-m parabola or horn, center or offset fed). The single-element concept was discarded for a number of reasons—more power than could be handled by a single rectifier, too narrow a beam for ease in pointing and to accommodate satellite drift, and bulk that could cause complications in setting up the rectenna were the major ones.

It was suggested that under certain conditions the satellite might drift close to 3°. This is unlikely under most conditions, but the number provides a convenient unit for determining the fewest number of elements in a panel. If the beamwidth of an individual element is to be greater than 3°, and the pointing loss is to be held below 2%, the 3-dB beamwidth of that element must be broader than 19° or 20°, which is about 0.183 m^2.

Some general statements about antenna type and feed networks can be made at this point to illustrate trends in performance. Some of these statements can be modified through clever design; nevertheless, they are valid over large regions of the design range.

Uniform illumination is approached (a desirable characteristic for the rectenna is uniform illumination, meaning that the aperture efficiency is unity, all the energy impinging on the antenna is passed to the rectifier and none is scattered back into space) most closely by a dense array. As the number of elements is reduced, the aperture efficiency drops. However, the drop in efficiency is not linear with the inverse of the number of elements, but rapidly stabilizes at about 0.7 as the number of elements decreases, provided that the detailed design has as its objective the maximization of aperture efficiency.

As the number of elements increases, more interconnecting transmission lines and matching devices are required—increasing network losses. From the performance point of view (neglecting rectenna structure economics), the antenna design should be a tradeoff between aperture scattering loss and network loss.

The antenna configuration baseline has been bounded by adopting a 0.183-m^2 unit area, and allowing the design to range from a dense array of 7×7 elements spaced $\lambda/2$ to a square parabola of this same area with a single feed element. Configurations intermediate to these are a Yagi array of 12 elements, each with a capture area of about one square wavelength, a short backfire array either square or hexagonal with a capture area of about four square wavelengths, and a parabolic trough; these configurations are illustrated in Figure 3.2-5.

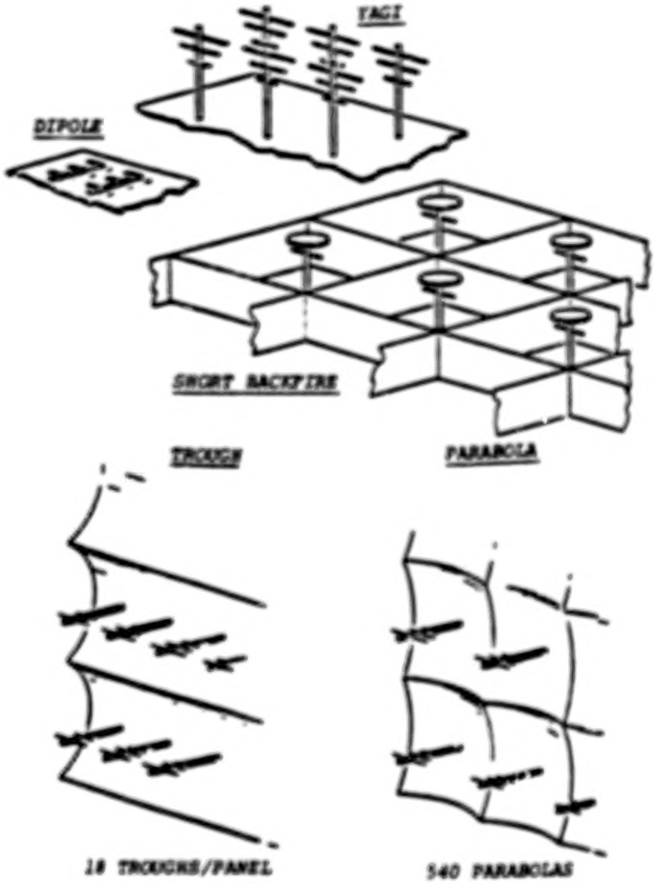

CONCEPT	NUMBER OF ELEMENTS (9 X 15 M PANEL)	DESCRIPTION	COMMENTS
→ DENSE ARRAY (BILLBOARD)	36044	DIPOLES, $\lambda/2$ SPACING SQUARE CLUSTERS OF 49 ELEMENTS	STRIPLINE INTERCONNECT MATCHING LOSS } NEEDS STUDY EDGE EFFECTS }
YAGI ARRAY	9011	λ SPACING, RECTANGULAR CLUSTERS OF 12 ELEMENTS	MUTUAL COUPLING EFFECT NEEDS STUDY
SHORT BACKFIRE ARRAY	2254	2λ SPACING, SQUARE CLUSTERS OF 4 ELEMENTS	BEAM WIDTH SLIGHTLY TOO NARROW, NEEDS STUDY
→ TROUGH	2205	18 PARABOLIC TROUGHS YAGI FEEDS SPACED λ	APERTURE EFFICIENCY $< .8$
SQUARE PARABOLAS	540	540 PARABOLAS YAGI FED	APERTURE EFFICIENCY $< .7$

Figure 3.2-5. Panel Alternative/Rectenna Concepts

Estimated characteristics are also shown in Figure 3.2-5, which also indicates the number of elements required for each rectenna panel, and some comments on aperture efficiency and unknown parameters that require further study.

Interconnecting Network

In comparing the losses in stripline with waveguide interconnecting networks, the approach taken was to interconnect 49 elements of a dense array arranged in a square, and show that the loss is tolerable. It is then assumed that any antenna configuration with a lesser number of elements will have less network loss. Following this, arrangements for interconnecting groups of 0.183-m^2 unit areas are examined, for use in the fifth or outer zone of the rectenna, without regard for the consequent beam barrowing that will be experienced.

A stripline configuration is shown in Figure 3.2-6. If the square 7×7 element array has its central element connected to a rectifier, and other elements connected in series parallel, the average transmission line length may be shown to be 3/2 λ_g. Figure 3.2-6 illustrates this method of connecting for one quarter of the 7×7-element array using connections λg long in serpentine form to fit the λ/2 spacing. A few places require 2 λg. This configuration appears to have the shortest average transmission line length, but has some severe matching problems. These could introduce losses that dominate the normal transmission line loss, taken here as 0.015 dB/λg, but much could be done in rectifier design to avoid matching networks. Both of these factors are unknown at present. Simple line loss amounts to 0.02 dB or 0.5% for stripline.

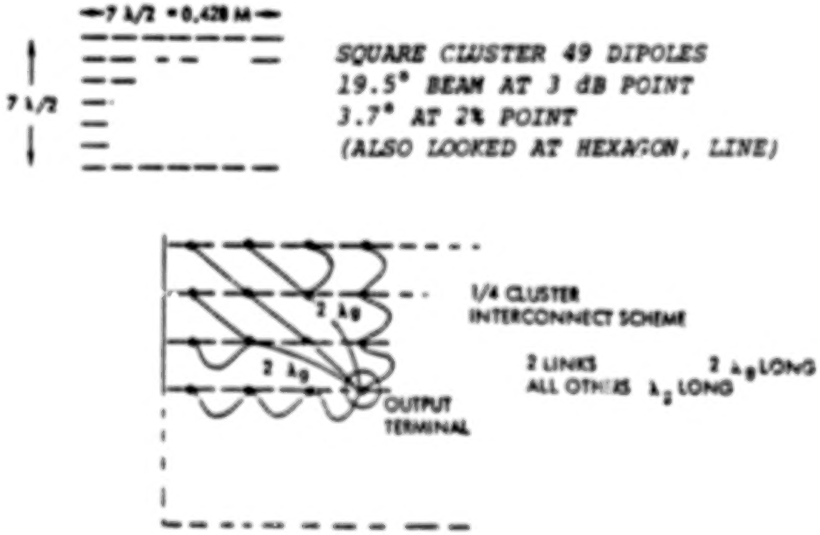
7 λ/2 = 0.428 M
7 λ/2
2 λ_g
2 λ_g
OUTPUT TERMINAL
1/4 CLUSTER INTERCONNECT SCHEME
2 LINKS 2 λ_g LONG
ALL OTHERS λ_g LONG

SQUARE CLUSTER 49 DIPOLES
19.5° BEAM AT 3 dB POINT
3.7° AT 2% POINT
(ALSO LOOKED AT HEXAGON, LINE)

DISTANCE - AVERAGE ELEMENT TO OUTPUT = 3/2 λ_g

- LOSS AT .015 DB/ λ_g = .0225 DB = 0.5%
- POTENTIAL DIFFICULTY - MATCHING LOSSES OF 17 PORT NETWORK

Figure 3.2-6. Billboard Feed—Stripline

In Zone V (Figure 3.2-4), several 0.183-m^2 (49-element) units are grouped to bring the power input to the rectifiers up to an efficient operating point. Figure 3.2-7 shows four possible groupings, including the grouping of nine indicated earlier. Average loss using stripline interconnect was computed for each of these groupings, this loss to be added to the transmission loss within each 0.183-m^2 unit. Loss for the grouping of nine is computed at 1.8%, while (because of the shortened path) the grouping of six has only half this loss. Because of the group interconnect loss, and possibly additonal matching losses, Zone V panels will have considerably more (estimated at four times) interconnection loss of ungrouped panels in other zones.

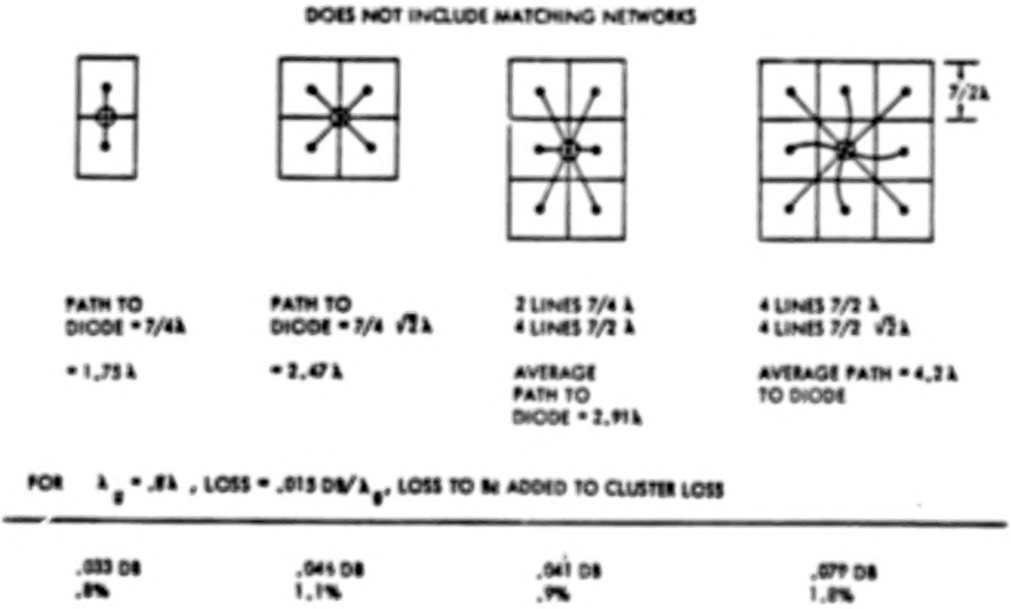
DOES NOT INCLUDE MATCHING NETWORKS
7/2λ
PATH TO DIODE = 7/4λ
= 1,75 λ
PATH TO DIODE = 7/4 √2 λ
= 2,47 λ
2 LINES 7/4 λ
4 LINES 7/2 λ
AVERAGE PATH TO DIODE = 2,91λ
4 LINES 7/2 λ
4 LINES 7/2 √2 λ
AVERAGE PATH = 4,2 λ TO DIODE
FOR λg = .8λ , LOSS = .015 DB/λg, LOSS TO BE ADDED TO CLUSTER LOSS
.033 DB
.8%
.045 DB
1,1%
.041 DB
.9%
.079 DB
1,8%

Figure 3.2-7. Cluster Interconnect

In considering the use of simple dipoles, the adequacy of linear polarization under Faraday rotation was examined. Typical values of diurnal variation at 100 MHz were extracted from the *Handbook of Geophysics and Space Environment*. The variation to be expected under average conditions is 450° to 3600°. Since variation is inversely proportional to the square of the frequency, these typical values may be extrapolated to 0.75° to 6° at 2.45 GHz. If linear polarization is used, this could result in 0.55% loss at 6°. This is summarized in Table 3.2-3. Should this problem be of concern, it should be estimated for the specific geometry of the locations under consideration, and also for the statistics on time that atypical conditions cause rotations greater than typical.

Panel Installation

Figure 3.2-2 showed a rectenna panel in the installed position. The panels are 9.33×14.69 m and are attached to continuous concrete footings at eight points as shown. A maximum wind force of 90 mph was assumed.

CONTENTS

Section Page

1.0 SCOPE/GENERAL REQUIREMENTS 1-1 1/B11
1.1 INTRODUCTION 1-1 1/B11
1.2 SATELLITE POWER SYSTEM CONCEPTS 1-3 1/B13
1.2.1 History of Study 1-3 1/B14
1.2.2 NASA Reference Satellite Concept 1-12 1/C9
1.2.3 Rockwell Alternative Satellite Concept (March 1979) 1-15 1/C12
1.2.4 Rockwell Reference Ground Receiving Station . 1-17 1/C14
1.2.5 Rockwell Concept Approaches (June 1980) . . 1-17 1/C14
1.2.6 Satellite Concept Summaries 1-22 1/D6
1.3 TRANSPORTATION SYSTEM 1-34 1/E9
1.4 PROGRAM GROUND RULES 1-35 1/E10
2.0 SYSTEM DESCRIPTION 2-1 1/E11
2.1 GENERAL 2-1 1/E11
2.1.1 System 2-1 1/E11
2.2 SATELLITE 2-9 1/F7
2.2.1 Reference System Definition 2-9 1/F7
2.2.2 Magnetron System Definition 2-16 1/G1
2.2.3 Solid State System Concepts 2-16 1/G1
2.3 GROUND RECEIVING STATION 2-26 2/A3
2.3.1 Introduction 2-26 2/A3
2.3.2 Rectenna 2-28 2/A5
2.3.3 Power Distribution 2-28 2/A5
2.4 OPERATIONS AND MAINTENANCE 2-29 2/A6
2.4.1 Satellite Operations 2-29 2/A6
2.4.2 Satellite Maintenance 2-46 2/B9
2.5 MASS PROPERTIES 2-51 2/B14
3.0 SUBSYSTEMS 3-1 2/C2
3.1 SATELLITE 3-1 2/C2
3.1.1 Introduction 3-1 2/C2
3.1.2 Power Generation 3-2 2/C3
3.1.3 Power Distribution 3-30 2/E8
3.1.4 Microwave Power Transmission 3-41 2/F8
3.1.5 Structure 3-84 3/B12
3.1.6 Attitude Control and Stationkeeping Subsystem . 3-101 3/D3
3.1.7 Thermal Control 3-112 3/D14
3.1.8 Communications and Data Management 3-131 3/F6
3.2 GROUND RECEIVING STATION 3-141 3/G7
3.2.1 Introduction 3-141 3/G7
3.2.2 Rectenna 3-141 3/G7
3.2.3 Power Distribution 3-150 4/A4
4.0 SUPPORT SYSTEMS 4-1 4/A5
4.1 GEO OPERATIONAL BASE 4-1 4/A5
4.2 MAINTENANCE AND REFURBISHMENT FACILITY 4-1 4/A5

Section Page

4.3 SPS TRANSPORTATION SYSTEM REQUIREMENTS (PRELIMINARY) . 4-1 4/A5
4.3.1 Configuration and Mission Requirements . . 4-1 4/A5
4.3.2 Heavy Launch Lift Vehicle(s) Requirements . . 4-2 4/A6
4.3.3 Cargo Transfer Vehicle (COTV) 4-5 4/A9
4.3.4 Personnel Orbital Transfer Vehicle (POTV) . . 4-6 4/A10
4.3.5 Personnel Module (PM) 4-7 4/A11

Table 3.2-3. Polarization Characteristics

- Faraday Rotation (*Handbook of Geophysics and Space Environment*)

Typical: Ω = 450° to 360° at 100 MHz—diurnal variation

$\Omega \propto \frac{1}{f^2}$

At 2.45 GHz

Typical Ω = 0.75° to 6°.

If uncorrected: Loss = 0.024 dB = 0.55%

Possibly larger under atypical conditions

Threaded inserts are placed in the concrete during the pouring process and provide the means for mounting the panel attach fittings which are capable of longitudinal and lateral adjustment. Screw jacks are installed at each of the four rear attach points to allow for panel adjustment and alignment.

Details of panel construction are shown in Figure 3.2-8. Four standard size eight-inch I-beams, to which the attach fittings are secured, are spaced in the lateral (14.69 m) direction. Galvanized steel hat sections (thin sheet, 0.020 in. thickness) of the dimensions as shown are mounted in the longitudinal direction (14.69 m) and provide the mounting for the substrate containing the electronic components. The substrate (with components) is delivered to the on-site assembly plant in strips of 9.33×0.74 m. The panels are supported in the inclined position by tubular steel members which provide an angle from the horizontal of 49° for this example (latitude = 34°N). Each panel weighs 2080 kg, of which approximately 85% is steel.

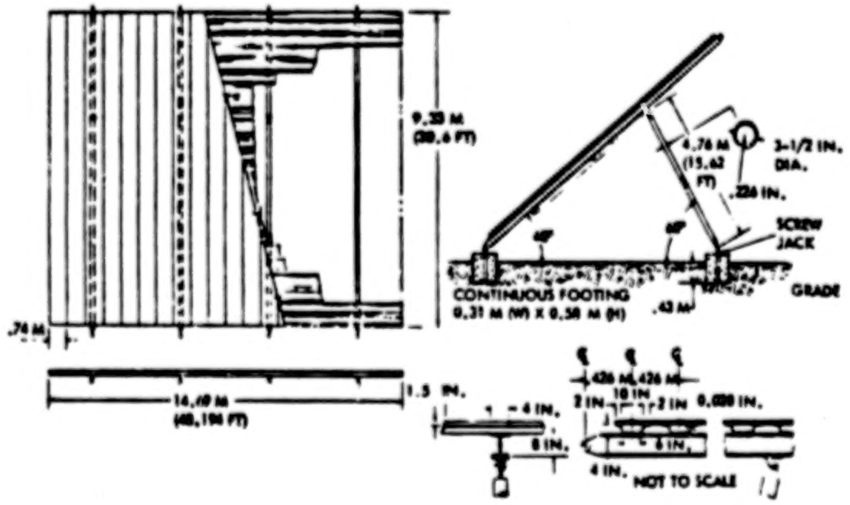
9.33 M
(30.6 FT)
4.76 M
(15.62
FT)
3-1/2 IN.
DIA.
.226 IN.
SCREW
JACK
CONTINUOUS FOOTING
0.31 M (W) X 0.58 M (H)
.43 M
GRADE
.74 M
14.69 M
(48.196 FT)
1.5 IN.
4 IN.
8 IN.
.426 M .426 M
2 IN
10 IN
2 IN
0.020 IN.
6 IN.
4 IN.
NOT TO SCALE

Figure 3.2-8. Rectenna Array Support Structure

Panel Hookup

From Figure 3.2-5 it can be calculated that each panel can require approximately 735 diodes (in Sectors I-IV; in Sector V there will be approximately 82). The total number of diodes required in the farm is estimated to be approximately 330×10^6. The output of each cluster/diode rectifier is series connected so as to provide 40.5 kV "voltage strings" (13 kW @ 0.321 A). It is estimated that the rectenna farm will have available approximately 329,000 strings. The number of diodes per string will vary, depending upon location in the rectenna farm area. The average number per string is estimated to be approximately 100+.

3.2.3 POWER DISTRIBUTION

The power available from each voltage string on the rectenna panels must now be collected and distributed to various feeders and buses. From there, the power is routed through interface converters and eventually converted to utility inter-ties. Figure 3.2-9 represents a simplified schematic of a typical station distribution subsystem.

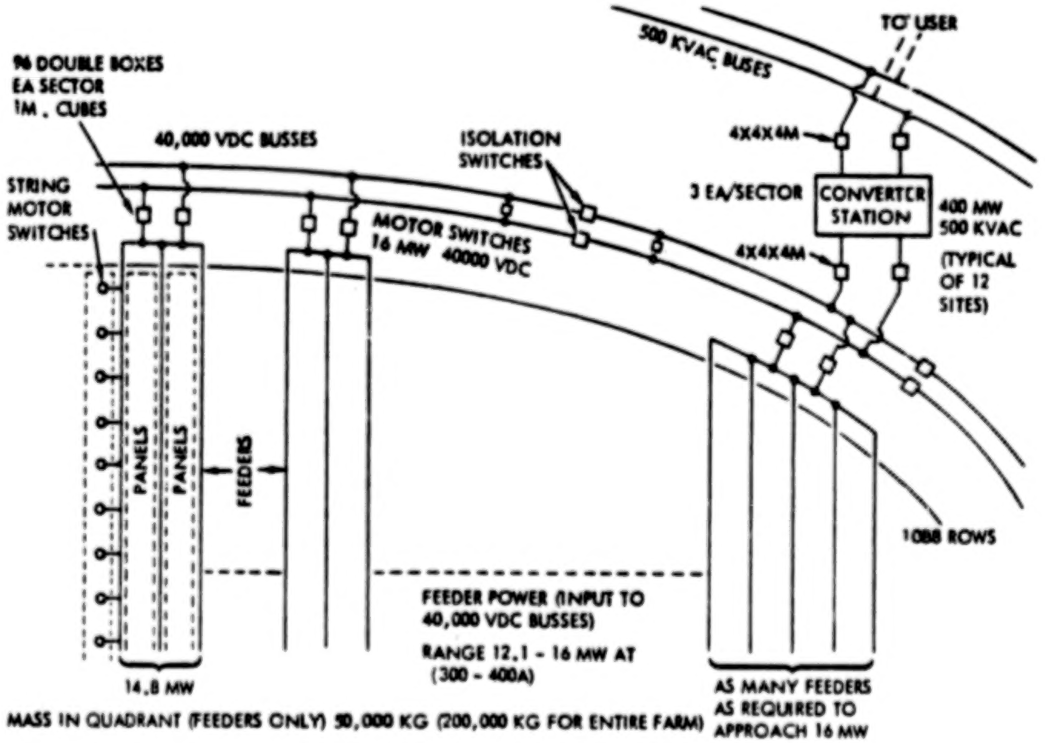
TO USER
500 KVAC BUSES
96 DOUBLE BOXES
EA SECTOR
1M . CUBES
40,000 VDC BUSSES
ISOLATION
SWITCHES
4X4X4M
3 EA/SECTOR
CONVERTER
STATION
400 MW
500 KVAC
STRING
MOTOR
SWITCHES
MOTOR SWITCHES
16 MW 40000 VDC
4X4X4M
(TYPICAL
OF 12
SITES)
PANELS
PANELS
FEEDERS
1088 ROWS
FEEDER POWER (INPUT TO
40,000 VDC BUSSES)
RANGE 12.1 - 16 MW AT
(300 - 400A)
14.8 MW
AS MANY FEEDERS
AS REQUIRED TO
APPROACH 16 MW
MASS IN QUADRANT (FEEDERS ONLY) 50,000 KG (200,000 KG FOR ENTIRE FARM)

Figure 3.2-9. Receiving Station Power Distribution Schematic—Preliminary

4.0 SUPPORT SYSTEMS

4.1 GEO OPERATIONAL BASE

(TBD)

4.2 MAINTENANCE AND REFURBISHMENT FACILITY

(TBD)

4.3 SPS TRANSPORTATION SYSTEM REQUIREMENTS (PRELIMINARY)

The primary driver in establishing transportation system requirements is the high density SPS mass flow requirements to LEO and GEO. The average expected number of earth launches required to support SPS construction ranges from 450/year to 1000/year dependent upon satellite configuration and launch vehicle payload capability. The requirements contained herein are for a Heavy Lift Launch Vehicle (HLLV) capable of delivering a payload from the selected launch site(s) to LEO; a high thrust Orbital Transfer Vehicle (OTV) and a low thrust OTV, both of which are required to deliver a payload from LEO to GEO; and an on-orbit shuttle craft (IOTV). The requirements as stated are based upon a mature program and may or may not be satisfied by a single transportation system configuration (i.e., a separate and distinct transportation system may be employed to satisfy personnel transfer requirements). Because the transportation system operations costs represent a significant percentage of overall SPS program costs, a primary objective is total system recovery/reusability with minimum maintenance, assembly and checkout requirements, consistent with the need for a high probability of mission completion and minimum risk of vehicle loss. Details of the vehicles proposed to comply with the identified requirements may be found in Volume III.

4.3.1 CONFIGURATION AND MISSION REQUIREMENTS

Although the selected satellite configuration may affect transportation system fleet size and launch rate requirements, it is not anticipated that the selection of an alternate SPS would lead to any significant changes in the overall approach to satisfying transportation system requirements (i.e., the total mass flow requirement is of sufficient magnitude that significant increases in mass flow would not be expected to change the transportation system concept).

Satellite Configuration

The reference SPS is a Solar Photovoltaic configuration with a CR of 2, a BOL power at the grid of 5 GW and an expected life of 30 years. The satellite mass is assumed to be 31×10^6 kg (GEO Assembly). The satellites are to be constructed at the rate of two per year (mature program) with a total requirement of 60 satellites. The satellite is to be constructed and/or assembled on-orbit. In addition to the satellite mass, the transportation system must also provide for the transfer of personnel and supplies to LEO and GEO. This requirement will lead to an additional average mass flow of approximately 200 men and 2,000,000 kg/month during the construction phase.

Satellite Orbital Requirements

The ultimate operational destination of the SPS is a Geosynchronous Orbit (~35,800 km equatorial). The LEO staging and/or construction orbit shall be selected to maximize operational flexibility (e.g., minimum radiation hazard and atmospheric drag with maximum opportunity for rendezvous by the HLLV and maximum opportunity of departure from LEO to GEO).

Flight Requirements

A primary transportation system objective is minimum earth and on-orbit operational requirements. Preferably methods of HLLV/OTV/payload handling would not require special orbital staging manpower/facilities. All elements of the transportation system should be sufficiently autonomous to require a minimum communication/data link between vehicle(s) and earth/orbital staging areas. For the purpose of analysis, it is assumed that at least 10% of the mass delivered to the satellite construction site will be structural mass required for satellite payload packaging and structural support; therefore, the transportation system shall provide a down-payload capability of at least 10% of the up-payload. Launch and reentry/recovery corridors shall be established to minimize restrictions and provide a maximum degree of flexibility in launch/recovery operations. All orbital elements of the transportation system shall be designed for a minimum orbital stay time commensurate with nominal turnaround requirements. All orbital elements of the transportation system shall have the capability of on-orbit propellant transfer to effect recovery in the event that the orbital stay-time exceeds the maximum allowed by system design.

Environmental Requirements

Specific environmental requirements are TBD. However, the overall impact on earth resources by transportation system materials and propellant selections must be considered. In addition, the overall levels of acoustic and toxic/noxious emissions must conform to generally accepted levels. The potential hazards of storing large quantities of propellants at the selected launch and orbital staging areas must be alleviated.

4.3.2 HEAVY LAUNCH LIFT VEHICLE(S) REQUIREMENTS

The HLLV must be capable of meeting the mass flow requirements of Section on Satellite Configuration. In addition, the HLLV must transport the OTV and/or OTV propellants to LEO. Since HLLV operations are the major contributor to SPS transportation costs, specific attention must be given toward minimizing handling, checkout and assembly equipment requirements; facility and manpower requirements; replacement and/or refurbishment hardware; and any other factors which affect overall turnaround time requirements. As in the case of the Space Shuttle Transportation System, a "spaceline" (airline) concept is required.

Payload and Interfaces

Since the efficient delivery of payloads to LEO is the primary objective of the HLLV, then payload mass, configuration and interface requirements may strongly influence HLLV design.

Payload Interface

For the purpose of HLLV synthesis, it may be assumed that all payloads will be prepackaged and self-contained. All payloads shall conform to a common HLLV mechanical interface and require minimum handling and installation equipment/operations. Those payloads requiring servicing (i.e., OTV propellant) shall be capable of servicing-deservicing after HLLV installation. The HLLV shall provide suitable launch and flight environmental protection for all payloads. The HLLV shall be capable of remote deployment of payloads in LEO and retrieval of empty payload modules and/or crew/OTV modules from LEO for return to Earth Base. All other HLLV/payload interfaces shall be avoided except where such interfaces will enhance mission accomplishment or are shown to be most cost-effective.

Payload Configuration

Specific payload weight and envelope requirements are dependent upon HLLV and OTV concept selection and potential environmental considerations. Because of the high mass flow requirement to support satellite construction, a minimum mix and manageable size of payload elements is desirable in order to reduce on-orbit operational requirements. The HLLV delivery concept and payload volume capability shall be such that a minimum payload density is required to meet maximum HLLV payload weight capability.

On-Orbit Docking Requirements

The HLLV will not require orbital docking provisions. However, docking provisions must be provided on all payload elements in order to effect their transfer by intra-orbit transfer vehicle.

Launch Site(s) Requirements

The predominant launch site requirement is in meeting the high launch/retrieval rates and mass flow requirements through the launch facility. Because of the high mass flow requirement, the launch site must be readily accessible by at least three of the four common means of earth transport (i.e., truck, rail, air and sea). In order to meet the high launch/retrieval rate requirement, launch site activities should be restricted to payload/HLLV mating, routine checkout/servicing and HLLV preparation for launch. The proximity of payload and transportation system maintenance and overhaul staging areas to the launch site must be compatible with accepted environmental and safety standards. Because of the high demand for propellants, it may be assumed that a propellant processing facility will be at or in close proximity to the launch site. A candidate launch site is the Kennedy Spaceflight Center. Owing to the high probability of suspension of launch/retrieval operations for periods of up to two weeks due to inclement weather (especially if sea recovery of the HLLV is planned), an alternate, geographically isolated launch/retrieval site is indicated. A possible alternate to another launch site would be to increase the launch rate capability to provide for a two-week inventory of satellite construction elements on-orbit. However, the emergency return of orbital crew members would be precluded.

HLLV/Launch Site Interface Requirements

Except for the potential requirement for specialized checkout/ maintenance equipment which might be employed in the HLLV staging area, physical launch site interfaces shall be restricted to consumables servicing and ground power requirements. Minimum communication and data interface requirements shall be required.

Launch Site/Recovery Site Interface

The recovery site shall be in as close proximity to the launch site as practicable. Launch and recovery site operations shall be autonomous and require a minimum of communication/data links between one another. Launch and recovery operations shall be capable of being conducted simultaneously on a non-interference basis. Should alternate launch/landing sites be employed, the HLLV shall be readily capable of transport from one launch/recovery site to the other. Recovery site and method of recovery shall be selected to assure intact recovery of the HLLV with minimum turnaround maintenance/checkout requirements.

HLLV Performance Requirements

The HLLV shall provide the delta-V required to deliver the desired payload to the selected LEO staging area. The HLLV shall have the capability of performing all necessary orbital maneuvers to effect rendezvous with the LEO staging base and/or with down-payload modules and all necessary deorbit/reentry/landing maneuvers. The HLLV shall have sufficient performance reserves to satisfy TBD error analyses.

Abort Requirements

Abort requirements are TBD.

Design Life Requirement

As a design goal, the HLLV shall have the capability of accomplishing 300 missions. Life-limited components and/or components requiring periodic overhaul shall meet line replaceable unit (LRU) accessability and maintenance requirements. Each LRU shall be capable of removal/replacement without materially affecting subsystem integrity, vehicle fleet size or turnaround requirements.

4.3.3 CARGO TRANSFER VEHICLE (COTV)

The COTV must be capable of meeting the satellite mass flow requirements of the section on Satellite Configuration. The COTV shall be capable of meeting the orbital transfer requirements defined in the section on Satellite Orbital Requirements and the flight requirements of the section on Flight Requirements. In addition, the COTV shall have the capability of self-test and monitoring in order to evaluate status and readiness for operation.

Payload and Interfaces

In addition to satellite construction/operation mass transfer requirements from LEO-to-GEO, the COTV shall be capable of meeting a down-payload requirement of 10% of the up-payload.

Payload Interface

All payloads shall be prepackaged and self-contained, and conform to a common COTV mechanical interface. All other COTV/payload interfaces shall be avoided except where such interfaces may be shown to enhance mission accomplishment or to be more cost-effective.

Payload Configuration

Except for the interface requirement of Payload Interface, above, there are no payload configuration restrictions.

On-Orbit Docking Requirements

The COTV shall be capable of autonomous rendezvous with the LEO and GEO bases. On-orbit docking of the COTV is not required.

COTV/HLLV Interface Requirements

The COTV shall conform to the interface equirements of the sections on Payload Interface, and Payload Configuration.

COTV/Orbital Base Interface Requirements

COTV/Orbital base interfaces are not required.

COTV/Launch Site Interfaces

The COTV SHALL BE SPACE BASED, therefore, there are no COTV/launch site interface requirements.

COTV Performance Requirements

The COTV shall provide the required delta-V capability to deliver the desired payload from the selected LEO staging base to the SPS GEO location and effect a return to the LEO staging base. The COTV shall provide a down-payload capability for crew supply and empty satellite payload containers.

The COTV shall have the capability of performing all necessary LEO/GEO rendezvous maneuvers and posses sufficient performance reserves to satisfy TBD error analysis.

Abort Requirements

Abort requirements are TBD.

Design Life Requirements

As a design goal, the COTV shall have a design life requirement of ten years with minimum maintenance.

4.3.4 PERSONNEL ORBITAL TRANSFER VEHICLE (POTV)

The personnel orbit transfer vehicle (POTV), as defined herein, consists of that propulsive element required to transfer the personnel module (PM) and its crew/construction personnel from LEO to GEO and return. The POTV must be capable of meeting the personnel mass flow requirements of the section on Satellite Configuration. In addition the POTV shall be capable of priority cargo transfer from LEO to GEO. The POTV shall utilize a chemical (LO_2/LH_2) propulsive stage capable of on-orbit maintenance/refueling. In addition, the POTV shall have provisions for self test and monitoring as required to evaluate status and operation readiness.

Payload and Interfaces

The POTV payload will consist of a self-contained personnel module (described below) or priority cargo module.

Payload/Interface

All payloads shall be prepackaged and self-contained, and conform to a common POTV mechanical and electrical interface. The payload module shall provide all required power, communication, guidance and navigation functions to accomplish orbital transfer.

Payload Configuration

Payload configuration restrictions are TBD.

On-Orbit Docking Requirements

The POTV shall be capable of rendezvous and docking with the LEO and GEO base facilities (when mated to the PM or Priority Cargo Module).

POTV/HLLV Interface Requirements

The POTV shall conform to the interface requirements of the section on Payload and Interfaces.

POTV/Orbital Base Interface Requirements

The POTV shall have provisions for refueling at both orbital bases, LEO and GEO. Orbital base mechanical and electrical interfaces shall be compatible with the common POTV mechanical and electrical interface.

POTV/Launch Site Interface Requirements

The POTV shall conform to the interface requirements of the section on Launch Site(s) Requirements.

POTV Performance Requirements

The POTV shall provide the required delta-V capability to deliver the desired payload from the LEO staging base to the SPS GEO construction facility. Following refueling in GEO the POTV shall provide the same down-payload capability. The POTV shall have the capability of performing all necessary LEO/GEO rendezvous and docking maneuvers and posses sufficient performance reserves to satisfy TBD error analysis. POTV accelerations shall be limited to that required to assure crew/personnel comfort during transit.

Abort Requirements

Abort requirements are TBD.

Design Life Requirements

As a design goal the POTV shall have a design life requirement of 100 missions with minimal on-orbit maintenance.

4.3.5 PERSONNEL MODULE (PM)

The personnel module (in conjunction with the POTV) shall be capable of meeting the personnel flow requirements of the section on Satellite Configuration. In addition, the PM shall be capable of crew personnel delivery to LEO by the Personnel Launch Vehicle or HLLV.

Payload and Interfaces

The PM constitutes a payload for the PLV/HLLV and POTV, and therefore must satisfy the payload interface requirements of the sections on Payload and Interfaces, and Launch Site(s) Requirements.

Payload Configuration

The PM shall be configured to satisfy the personnel flow requirements of the section on Satellite Configuration.

On-Orbit Docking Requirements

The PM shall provide common docking provisions at either end for mating with the POTV and docking with the LEO and GEO bases.

PM Performance Requirements

The PM shall provide all required power, communication, guidance and navigation functions to accomplish orbital transfer. In addition, the PM shall be capable of direct readout of POTV self-monitoring and status maintenance equipment. The PM shall provide a suitable habitat for crew/personnel transfer from Earth-to-LEO-to=GEO and return.

1. REPORT NO.
NASA CR-3399

2. GOVERNMENT ACCESSION NO.

3. RECIPIENT'S CATALOG NO.

4. TITLE AND SUBTITLE
Satellite Power Systems (SPS) Concept
Definition Study (Exhibit D)
Volume VII - System/Subsystems Requirements Databook

5. REPORT DATE
March 1981

6. PERFORMING ORGANIZATION CODE

7. AUTHOR(S)
G. M. Hanley

8. PERFORMING ORGANIZATION REPORT #
SSD-80-0108-7

9. PERFORMING ORGANIZATION NAME AND ADDRESS
Rockwell International
Space Operations and Satellite Systems Division
Downey, California

10. WORK UNIT NO.
M-340

11. CONTRACT OR GRANT NO.
NAS8-32475

12. SPONSORING AGENCY NAME AND ADDRESS
National Aeronautics and Space Administration
Washington, DC 20546

13. TYPE OF REPORT & PERIOD COVERED
Contractor Report

14. SPONSORING AGENCY CODE

15. SUPPLEMENTARY NOTES
Marshall Technical Monitor: Charles H. Guttman
Volume VII of the Final Report on Exhibit D

16. ABSTRACT

This volume summarizes the basic requirements used as a guide to system analysis, and is a basis for the selection of candidate SPS point designs. Initially, these collected data reflected the level of definition resulting from the evaluation of a broad spectrum of SPS concepts. As the various concepts matured, these requirements were updated to reflect the requirements identified for the projected satellite system/subsystem point designs.

Included in this volume is an updated version of earlier Rockwell concepts using klystrons as the specific microwave power amplification approach, as well as a more in-depth definition, analysis and preliminary point design on two concepts based on the use of advanced solid-state technology to accomplish the task of high power amplification of the 2.45 GHz transmitted power beam to the earth receiver. Finally, a preliminary definition of a concept using magnetrons as the microwave power amplifiers is presented. Included are the preliminary identification of system/subsystem requirements, alternative configurations considered, in-depth discussions of the selected (recommended) alternatives, as well as alternate approaches which may have potential for improved operation or fabrication/installation. The rectenna system described in this document essentially remains the same as described at the conclusion of previous study activity, although it was determined that variations due to alternate beam shaping techniques applied may cause a variation in the overall rectenna and ground receiving station dimensions. Where appropriate, the alternative rectenna dimensions have been noted, but the effects of the altered dimensions are not evaluated in detail.

17. KEY WORDS
Satellite power system
Microwave power amplifiers
Rectenna systems

18. DISTRIBUTION STATEMENT
Unclassified - Unlimited

Subject Category 44

19. SECURITY CLASSIF. (of this report)	20. SECURITY CLASSIF. (of this page)	21. NO. OF PAGES	22. PRICE
Unclassified	Unclassified	266	A12

For sale by National Technical Information Service, Springfield, Virginia 22161

4-9

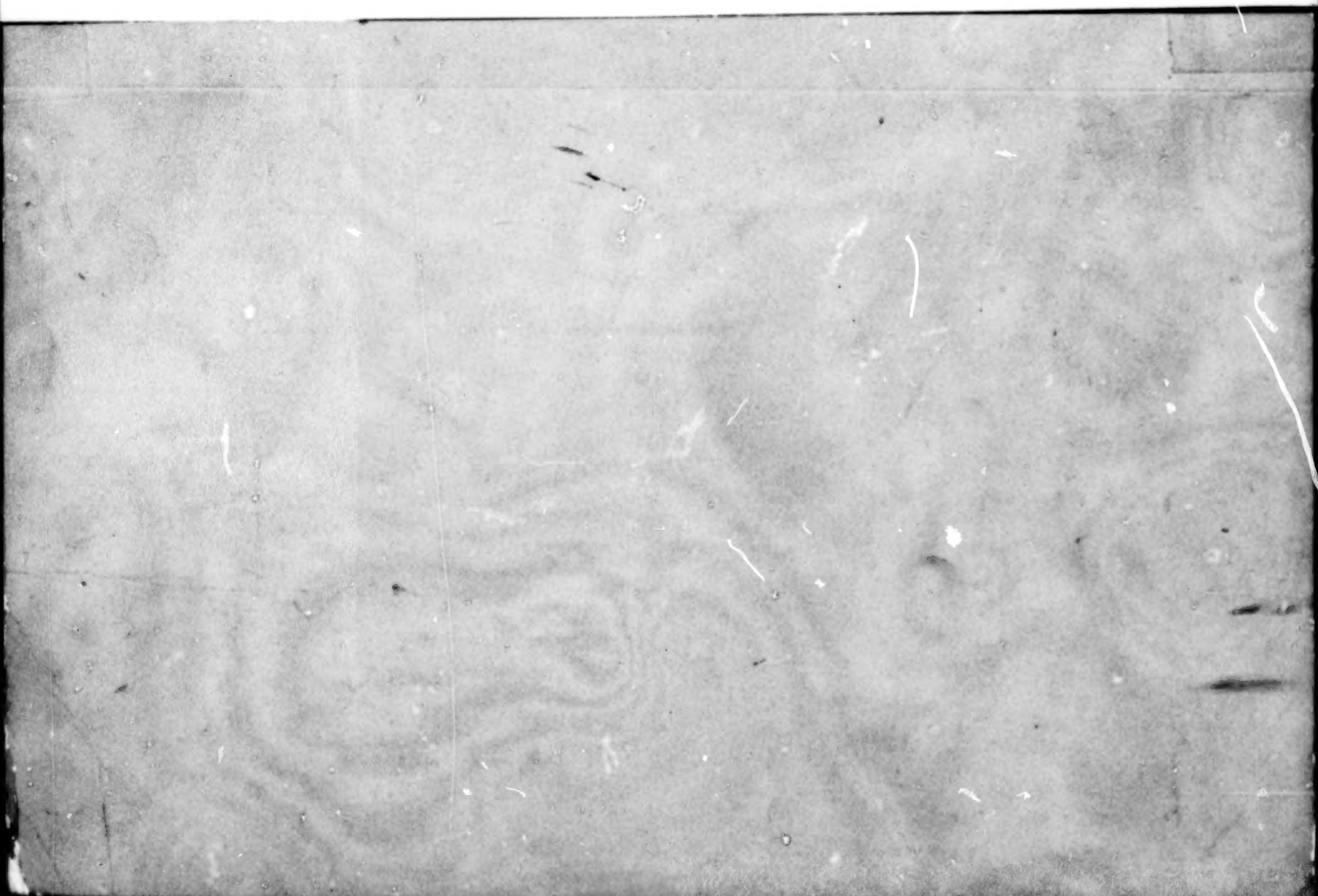

END

July 29, 1981